

NOVEL HETEROCYCLIC INHIBITORS FOR HUMAN AFRICAN TRYPANOSOMIASIS

**Lori Ferrins
B. Med. Chem. (Hons)**

A thesis submitted in fulfillment of the requirements for the degree of Doctor of Philosophy

**Department of Medicinal Chemistry
The Faculty of Pharmacy and Pharmaceutical Sciences
Monash University
2015**



MONASH University
Institute of Pharmaceutical Sciences

Copyright notices

Notice 1

Under the Copyright Act 1968, this thesis must be used only under the normal conditions of scholarly fair dealing. In particular no results or conclusions should be extracted from it, nor should it be copied or closely paraphrased in whole or in part without the written consent of the author. Proper written acknowledgement should be made for any assistance obtained from this thesis.

Notice 2

I certify that I have made all reasonable efforts to secure copyright permissions for third-party content included in this thesis and have not knowingly added copyright content to my work without the owner's permission.

Table of Contents

Abstract	v
Statement of Originality	vii
General Declaration.....	viii
Acknowledgements	x
Abbreviations and acronyms	xii
1. Introduction	1
1.1. Published manuscript	2
1.2. Post-script: updated literature surveillance	45
1.2.1. Natural products	60
1.2.2. Scaffold repurposing	63
1.3 SAR Rationale.....	76
1.4. Thesis Aims.....	80
1.5. General Experimental.....	81
1.5.1. Biological Experimental.....	81
1.5.2. Chemistry Experimental.....	84
1.5.3. Physicochemical Experimental	86
2. Investigation of the structure-activity relationships of the oxazolopyridines against <i>T.b. brucei</i>	88
2.1. Introduction	88
2.2. Aims	89
2.3. Synthesis of the oxazolopyridine analogues.....	89
2.4. Preliminary SAR	92

2.5.	Published manuscript.....	96
2.7.	Post-script: further development of SAR	116
2.7.1.	Core changes.....	116
2.7.2.	Northern heterocycle changes.....	120
2.7.	Metabolism analysis	122
2.8.	Biological analysis of compounds against <i>T. vivax</i> and <i>T. congolense</i>	124
2.9.	Target identification	125
2.10.	Competing work	125
2.11.	Future work.....	127
2.12.	Experimental.....	128
3.	Investigation of the structure-activity relationships of the pyrazine carboxamides against <i>T.b. brucei</i>	150
3.1.	Introduction	150
3.2.	Aims	151
3.3.	Historical work completed.....	152
3.3.1.	Analogues of the amide side chain	152
3.3.2.	Exploration of the SAR around the phenyl group	153
3.3.3.	Additive SAR	155
3.3.4.	Biological and pharmacokinetic analysis	156
3.4.	Optimisation of the synthesis of the pyrazine carboxamide core	159
3.5.	Analogues of the 6-position.....	160
3.5.1.	Substituted phenyl ring analogues	160
3.5.2.	5-Membered heterocyclic groups	161
3.5.3.	Replacement of the phenyl with 5-membered heterocyclic groups.....	163

3.6.	Selective <i>N</i> -alkylation of the amide -NH and free amine.....	165
3.7.	Synthesis of alternate core units to the pyrazine scaffold	171
3.8.	Biological analysis of compounds against <i>T. vivax</i> and <i>T. congolense</i>	175
3.9.	Physicochemical analysis of selected analogues	176
3.10.	Future work	179
3.11.	Experimental	180
4.	Investigation of the structure-activity relationships of the pyridyl benzamides against <i>T.b. brucei</i>	200
4.1.	Introduction	200
4.2.	Aims	201
4.3.	Synthesis of pyridylbenzamide core.....	201
4.4.	Preliminary SAR	202
4.5.	Published manuscript	205
4.6.	Post-script: further development of SAR	219
4.7.	Metabolism analysis	225
4.8.	Biological analysis of compounds against <i>T. vivax</i> and <i>T. congolense</i>	225
4.9.	Halonitrobenzamides as inhibitors of <i>T.b. brucei</i>	226
4.10.	Future work	228
4.11.	Experimental	229
5.	Investigation of the structure-activity relationships of the phenylthiazole amide against <i>T.b. brucei</i> ...	239
5.1.	Introduction	239
5.2.	Aims	240
5.3.	Historical work completed	240
5.4.	Biological analysis of compounds active against <i>T. vivax</i> and <i>T. congolense</i>	252

5.5.	Changes to the thiazole core	253
5.5.1.	2,6-Disubstituted pyridine core	253
5.5.2.	2,5-Disubstituted pyridine core	259
5.5.3.	Pyridazine core	261
5.6.	Linker modifications.....	267
5.6.1.	Methylation of the ethyl linker	267
5.6.2.	Cyclopropane linker.....	280
5.7.	Metabolism analysis	288
5.8.	Phenylthiazoles in the literature.....	290
5.9.	Future work.....	290
5.10.	Experimental.....	291
6.	References	328
7.	Appendix	337

Abstract

Human African trypanosomiasis (HAT), more commonly known as African sleeping sickness is caused by the protozoan *Trypanosoma brucei*. There are two subspecies of the parasite that are responsible for human infection; *T.b. rhodesiense* and *T.b. gambiense*. These parasites differ in that *T.b. rhodesiense* results in an acute infection whilst *T.b. gambiense* results in a chronic infection. HAT was recently named by the World Health Organisation in a list of 17 of the world's neglected tropical diseases.

HAT affects approximately 10,000 people in the remotest parts of Africa with the disease ultimately affecting the central nervous system, resulting in disrupted sleep patterns, brain damage and eventual death. The current treatments for this disease often involve complex therapeutic regimens, lead to the development of long term health issues, and even death in some patients. Reports of resistance developing to some of these treatment options are also becoming more frequent and as a result new treatments are urgently needed.

A whole organism high-throughput screen of 87,296 compounds from the WEHI/Bio21 Stage 1 screening library was conducted against *T.b. brucei* and led to the identification of a number of new compound series. This thesis describes the synthesis and structure-activity relationships (SAR) around four of these series.

The first body of work presented centres around the oxazolopyridines and details the initial SAR studies that were conducted. Whilst an increase in the potency of these analogues was achieved there were limiting physicochemical properties that hindered the progression of the series, namely metabolic stability and solubility. A number of analogues were designed and synthesised that particularly focused on improving the metabolic stability of the series.

The pyrazine carboxamides are the next series of compounds to be presented in this thesis. Much of the preliminary SAR had already been explored by previous researchers and a number of limitations were uncovered. Notably the metabolism of the series was rapid and the solubility was limiting. In order to

address the solubility issue a number of analogues were designed and synthesised with a greater percentage of sp³ carbons and these results are detailed. A number of analogues of the core pyrazine ring were also envisioned and synthesised in order to further probe the SAR around this series.

The pyridyl benzamides were chosen for progression as a result of their highly optimisable structure, despite their low micromolar activity against *T.b. brucei*. The work presented in this chapter demonstrates a significant boost in the activity of the series, down to low nanomolar inhibition as well as the identification of a related series, the thiazole benzamides.

Finally, a discussion around the phenyl thiazoles will be presented. A significant SAR exploration had already been conducted by other researchers and potent inhibitors of *T.b. brucei* had been identified, though the metabolism of the series was rapid and prevented progression of the series. As such a number changes to the core thiazole were envisioned and synthesised as well as modifications to the ethyl linker. The synthesis and results of this work has been detailed herein.

Statement of Originality

To the best of the authors knowledge and belief, this thesis contains no material which has been accepted for the award of any other degree or diploma in any University or other institution, and contains no material previously published or written, except where due reference is made. This thesis is based on joint research or publications, and the relative contributions of the other contributing authors has been disclosed at the commencement of each chapter in the ‘Declaration for Thesis Chapter.’



Lori Ferrins

June, 2015

General Declaration

Monash University

Declaration for thesis based or partially based on conjointly published or unpublished work

In accordance with Monash University Doctorate Regulation 17.2 Doctor of Philosophy and Research Master's regulations the following declarations are made:

I hereby declare that this thesis contains no material which has been accepted for the award of any other degree or diploma at any university or equivalent institution and that, to the best of my knowledge and belief, this thesis contains no material previously published or written by another person, except where due reference is made in the text of the thesis.

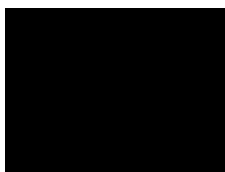
This thesis includes three original papers published in peer reviewed journals. The core theme of the thesis is the medicinal chemistry optimisation of a number of compounds as *Trypanosoma brucei* inhibitors. The ideas, development and writing up of all the papers in the thesis were the principal responsibility of myself, the candidate, working within Medicinal Chemistry under the supervision of Professor Jonathan B. Baell.

The inclusion of co-authors reflects the fact that the work came from active collaboration between researchers and acknowledges input into team-based research. The work conducted by myself is tabulated below, and attribution of the work contributed by others is described in detail in the preface to Chapters 2 and 4.

Thesis chapter	Publication title	Publication status	Nature and extent of candidate's contribution
1	Drug discovery and human African trypanosomiasis: a disease less neglected?	Published	Searched and analysed the literature, principal authorship of manuscript. 65% contribution.
2	3-(Oxazolo[4,5- <i>b</i>]pyridin-2-yl)anilides as a novel class of potent inhibitors for the kinetoplastid <i>Trypanosoma brucei</i> , the causative agent for human African trypanosomiasis.	Published	Synthesis of compounds 2, 5, 6, 10, 14-15, 18-19, 21-23, 26, 32-36, 38-41 , and synthetic intermediates, SAR analysis and principal authorship of manuscript. 50% contribution.
4	Pyridyl benzamides as a novel class of potent inhibitors for the kinetoplastid <i>Trypanosoma brucei</i> .	Published	Synthesis of compounds 28, 53-54, 59, 63, 66, 70, 77-78, 81-83, 94, 96-98, 100 , SAR analysis and principal authorship of manuscript. 40% contribution.

I have not renumbered sections of submitted or published papers in order to generate a consistent presentation within the thesis.

Signed:



Date: June, 2015

Acknowledgements

Firstly, I would like to thank my supervisor, Professor Jonathan Baell for his continued support in guiding my education and growth as a Medicinal Chemist. You have taught me invaluable skills which I will carry with me throughout the remainder of my career.

My thanks also go to Dr. Raphaël Rahmani who has worked with me on this project from the very beginning. You have provided me with valuable insights and you have made me a better chemist in the process. I cannot thank you enough for all of the assistance that you have given me.

This has truly been a collaborative project with chemistry collaborators at the University of Tasmania (Dr. Jason Smith and team), University of Western Australia (Associate Professor Matthew Piggott and team) and the University of Sydney (Professor Richard Payne and team). Many thanks to you all for your input in this project over the last few years.

To our biology collaborators at the Eskitis Institute, Griffith University who performed all of the biological assays against *T.b. brucei*; Professor Vicky Avery, Dr Melissa Sykes and, in particular Dr. Amy Jones. It has been a pleasure working with you and thank you for everything that you have done.

Thank you to Dr. Marcel Kaiser at the Swiss Tropical and Public Health Institute for providing us access to the parasite panel and running our samples.

To Professor Susan Charman and Dr. Karen White at the Centre for Drug Candidate Optimisation, my thanks to you and your team for your work on the determination of physicochemical properties of our compounds.

My thanks to Dr. Robert Gable at the University of Melbourne who undertook the crystallography study presented in this thesis.

To Dr. Jason Dang, I cannot thank you enough for everything that you have done for me throughout my PhD. The experiences that you have given me and the knowledge that I have gleaned from you will be with me throughout the remainder of my career.

To my fellow researchers in the Baell research group, both past present, Dr. David Leaver, Dr. Nghi Nguyen, Dr. Jitendra Harjani, Dr. Ryan Brady, Dr. Daniel Priebbenow, Kung Ban, Aaron DeBono, Ben Cleary, Silvia Teguh, Andrew Tang, Tamir Dingjan, Noel Pitcher, Sunil Banga, Julia Beveridge, Thuy Le, Mathilda Mesnard and Natacha Traffet. It has been a truly wonderful experience getting to know you all and I have learnt so much from each and every one of you.

To Swapna Johnson (née Varghese), I have found a friendship with you that will last a lifetime. Thank you for keeping me entertained in the lab, listening to all of my woes and generally doing your best to keep me sane. I will miss seeing you every day.

To my parents Pauline and Michael, and my brother John thank you for all of your love and support over the last eight years of university life. Despite the fact that you don't really know what it is I do every day your support has made this thesis possible. I love you all.

Finally, to my partner Daniel, thank you for being there with me on this journey over the last four years, encouraging me and keeping me sane along the way. You truly are an unreal chemist and you mean the world to me. I love you.

Abbreviations and acronyms

ADA	Adenosine deaminase
ADME	Absorption, distribution, metabolism and excretion
AGP	α_1 -acid glycoprotein
ATP	Adenosine triphosphate
aq	Aqueous
BBB	Blood-brain barrier
BOP	(Benzotriazol-1-yloxy)tris(dimethylamino)phosphonium hexafluorophosphate
CDI	Carbonyldiimidazole
CL _{int}	Intrinsic clearance
CNS	Central nervous system
CSF	Cerebrospinal fluid
d	Doublet
dd	Doublet of doublets
ddd	Doublet of doublet of doublets
DABAL-Me ₃	1,4-Diazabicyclo[2.2.2]octane-trimethylaluminium
DABCO	1,4-Diazabicyclo[2.2.2]octane
DBU	1,8-Diazabicycloundec-7-ene
DCM	Dichloromethane
DIPEA	<i>N,N</i> -Diisopropylethylamine
DMAP	Dimethylaminopyridine
DMF	<i>N,N</i> -Dimethylformamide
DMSO	Dimethylsulfoxide
DNA	Deoxyribose nucleic acid
DNDi	Drugs for neglected diseases initiative
EC ₅₀	Half maximal effective concentration
EDCI	1-Ethyl-3-(3-dimethylaminopropyl)carbodiimide
ee	Enantiomeric excess
E _H	Hepatic extraction
eq.	Equivalents

GALVmed	Global Alliance for Livestock Veterinary Medicine
gRNA	Guide ribonucleic acid
HAT	Human African trypanosomiasis
HATU	1-[Bis(dimethylamino)methylene]-1 <i>H</i> -1,2,3-triazolo[4,5- <i>b</i>]pyridinium 3-oxid hexafluorophosphate
HBTU	<i>O</i> -(Benzotriazol-1-yl)- <i>N,N,N',N'</i> -tetramethyluroniumhexafluorophosphate
HOBt	Hydroxybenzotriazole
HPLC	High-performance liquid chromatography
HRMS	High resolution mass spectrometry
HSA	Human serum albumin
HTS	High-throughput screen
IC ₅₀	Half maximal inhibitory concentration
kDNA	Kinetoplast DNA
LCMS	Liquid chromatography mass spectrometry
LDL	Low density lipoprotein
<i>L. donovani</i>	<i>Leishmania donovani</i>
<i>L. major</i>	<i>Leishmania major</i>
LRMS	Low resolution mass spectrometry
m	Multiplet
M	Molar
MD	Molecular dynamics
[M+H] ⁺	Singularly protonated molecular ion
MHz	Megahertz
mRNA	Messenger ribonucleic acid
MSD	Mean survival days
mTOR	Mammalian target of rapamycin
MPO score	Multiparameter optimisation score
MW	Molecular weight
m/z	Mass-to-charge ratio
NADPH	Nicotinamide adenine dinucleotide phosphate
NECT	Nifurtimox-eflornithine combination therapy

NMR	Nuclear magnetic resonance
PDB	Protein data bank
<i>P. falciparum</i>	<i>Plasmodium falciparum</i>
PFK	Phosphofructokinase
PI3K	Phosphoinositide 3-kinase
PPA	Polyphosphoric acid
PPB	Plasma protein binding
ppm	Parts per million
PSA	Polar surface area
q	Quartet
RBF	Round bottomed flask
RNA	Ribonucleic acid
RNAi	Ribonucleic acid interference
rRNA	Ribosomal ribonucleic acid
rt	Retention time
s	Singlet
SAR	Structure-activity relationships
SI	Selectivity index
TBAB	Tetra- <i>n</i> -butylammoniumbromide
TBAI	Tetra- <i>n</i> -butylammoniumiodide
THF	Tetrahydrofuran
TFA	Trifluoroacetic acid
TLC	Thin layer chromatography
<i>T.b. brucei</i>	<i>Trypanosoma brucei brucei</i>
<i>T.b. gambiense</i>	<i>Trypanosoma brucei gambiense</i>
<i>TbRET2</i>	<i>T. brucei</i> terminyl uridylyl transferase 2
<i>T.b. rhodesiense</i>	<i>Trypanosoma brucei rhodesiense</i>
<i>T. congolense</i>	<i>Trypanosoma congolense</i>
<i>T. cruzi</i>	<i>Trypanosoma cruzi</i>
<i>T. vivax</i>	<i>Trypanosoma vivax</i>
<i>TbPTR1</i>	<i>T. brucei</i> Pteridine Reductase 1

TUTase	Terminyl uridylyl transferase
UDPGA	Glucuronosyltransferase
UTP	Uridine triphosphate
WEHI	Walter and Eliza Hall Institute
WHO	World Health Organisation

1. Introduction

Human African trypanosomiasis (HAT) is one of 17 medical conditions that the World Health Organisation (WHO) lists as a neglected tropical disease. HAT is caused by the protozoan parasite *Trypanosoma brucei* and there are two subspecies responsible for human infection; *Trypanosoma brucei gambiense* and *Trypanosoma brucei rhodesiense*. The drugs that are currently available for the treatment of HAT have significant side effects, are part of complex treatment regimens, and the development of resistance has been reported. As such, there is considerable need to find novel compounds which could be utilised to treat this disease. This led to a high-throughput screen (HTS) of 87,296 compounds that formed the WEHI/Bio-21 Stage 1 screening library. The HTS was conducted against the whole parasite (specifically *T.b. brucei*) and utilised an Alamar Blue assay. This led to the identification of a number of compound series which have since entered a hit-to-lead medicinal chemistry optimisation program. This thesis will discuss the progress that has been made thus far in the optimisation of a number of these classes.

Initially an in depth investigation of the literature surrounding the drug development efforts in this area is presented in the form of a publication, followed by an updated literature surveillance. Finally, a summary of the work to be covered is presented and a rationale for the structure-activity relationship (SAR) exploration used throughout this thesis will be detailed.

Publication reproduced from Future Med. Chem. (2013) 5(15), 1801-1841 with permission of Future Medicine Ltd.

1.1. Published manuscript

Declaration by candidate

In the case of Chapter 1, the nature and extent of my contribution to the work was the following:

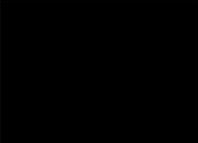
Nature of contribution	Extent of contribution
Searched and analysed the literature, principal authorship of manuscript	65%

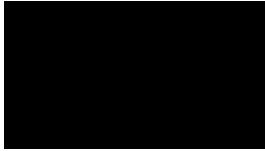
The following co-authors contributed to the work. If co-authors are students at Monash University, the extent of their contribution in percentage terms must be stated:

Name	Nature of contribution	Extent of contribution*
Raphaël Rahmani	Searched and analysed the literature, co-authorship of manuscript	
Jonathan B. Baell	Co-authored and edited the manuscript	

**Shown for Monash University students only*

The undersigned hereby certify that the above declaration correctly reflects the nature and extent of the candidate's and co-authors' contributions to this work.

Candidate's Signature		Date 18 th Feb, 2015
----------------------------------	---	---

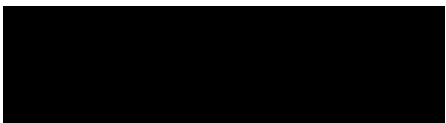
Main		Date
Supervisor's		18 th Feb, 2015
Signature		

Declaration by co-authors

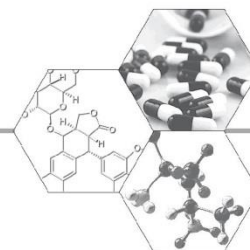
The undersigned hereby certify that:

- (1) The above declaration correctly reflects the nature and extent of the candidate's contribution to this work, and the nature of the contribution of each of the co-authors;
- (2) They meet the criteria for authorship in that they have participated in the conception, execution, or interpretation, of at least part of the publication in their field of expertise;
- (3) They take public responsibility for their part of the publication, except for the responsible author who accepts overall responsibility for the publication;
- (4) There are no other authors of the publication according to those criteria; and
- (5) Potential conflicts of interest have been disclosed to (a) granting bodies, (b) the editor or publisher of journal or other publications, and (c) the head of the responsible academic unit.

Signatures:

Signed:  Date: 03/05/2015

Signed:  Date: 18/02/2015



For reprint orders, please contact reprints@future-science.com

Drug discovery and human African trypanosomiasis: a disease less neglected?

Human African trypanosomiasis (HAT) has been neglected for a long time. The most recent drug to treat this disease, eflornithine, was approved by the US FDA in 2000. Current treatments exhibit numerous problematic side effects and are often ineffective against the debilitating CNS resident stage of the disease. Fortunately, several partnerships and initiatives have been formed over the last 20 years in an effort to eradicate HAT, along with a number of other neglected diseases. This has led to an increasing number of foundations and research institutions that are currently working on the development of new drugs for HAT and tools with which to diagnose and treat patients. New biochemical pathways as therapeutic targets are emerging, accompanied by increasing numbers of new antitrypanosomal compound classes. The future looks promising that this collaborative approach will facilitate eagerly awaited breakthroughs in the treatment of HAT.

Human African trypanosomiasis (HAT) is a disease caused by infection with *Trypanosoma brucei*, which is transmitted via the bite of the tsetse fly [1]. There are two subspecies of the parasite that can cause infection in humans: *Trypanosoma brucei rhodesiense*, which is primarily found within eastern and southern Africa and which causes an acute infection that can run its course in weeks to months; and *Trypanosoma brucei gambiense*, which causes a chronic infection that can last for years and is found in central and western Africa (FIGURE 1) [1,201,202]. There is a third subspecies, *Trypanosoma brucei brucei* that infects domestic and wild animals but not humans, although there have been some reports of humans infected with this parasite [2]. There are approximately 30,000 cases of HAT according to the WHO [203]. While this may seem a relatively insignificant number on a global scale, it is not possible to accurately determine the number of people infected with HAT, due to the remoteness of many populations, as well as the lack of effective monitoring and field-adapted diagnostics and treatments [3]. It has been estimated that less than 20% of those who are infected with HAT are currently being treated or are under surveillance [3].

The tsetse fly is responsible for the transmission of trypanosomes to humans. Humans themselves are the main reservoir for *T.b. gambiense*, although this parasite has been found in some other mammals, while wild game are the main reservoir for *T.b. rhodesiense* [4,202]. During a blood meal the tsetse fly injects metacyclic trypanosomes into the skin tissue and from here

the trypanosomes enter the lymphatic and blood systems of the mammalian host [5]. The trypanosomes multiply via binary fission to form trypomastigotes with a doubling time of approximately 6 h [5]. The transmission of the trypanosomes is a cyclic process. Once a mammal is infected, should an uninfected tsetse fly have a blood meal, the fly will then become infected with bloodstream trypomastigotes [5]. In the midgut of the tsetse fly the parasite transforms into procyclic trypomastigotes, which then leave the midgut, transforming into epimastigotes. Once in the salivary gland, the epimastigotes transform into infective metacyclic trypomastigotes [5]. The cycle in the tsetse fly takes approximately 3 weeks (FIGURE 2) [204].

Trypanosomes have a surface coat containing a variable surface glycoprotein which, in the case of *T.b. gambiense* and *T.b. rhodesiense*, is responsible for protecting the parasite against human lytic factors found in blood plasma [1,5]. There are approximately 2000 variant surface glycoprotein genes present in the genome of *T. brucei* and because of the potential for antigenic variation, development of a vaccine is not feasible [1].

Established chemotherapeutics

HAT is more commonly known as sleeping sickness and gets its name from the symptoms evident in the later stage of the disease process. The first stage is known as the hemolymphatic stage where the trypanosomes multiply within the subcutaneous tissue, blood and lymph. This is typically accompanied by intermittent fever, headaches, joint pain and itching [1]. The second

Lori Ferrins, Raphaël Rahman[#] & Jonathan B Baell^{*,#}

Medicinal Chemistry, Monash Institute of Pharmaceutical Sciences, Monash University (Parkville Campus), 381 Royal Parade, Parkville, VIC 3052, Australia

^{*}Author for correspondence: E-mail: jonathan.baell@monash.edu

[#]joint senior author

FUTURE SCIENCE part of **fsg**

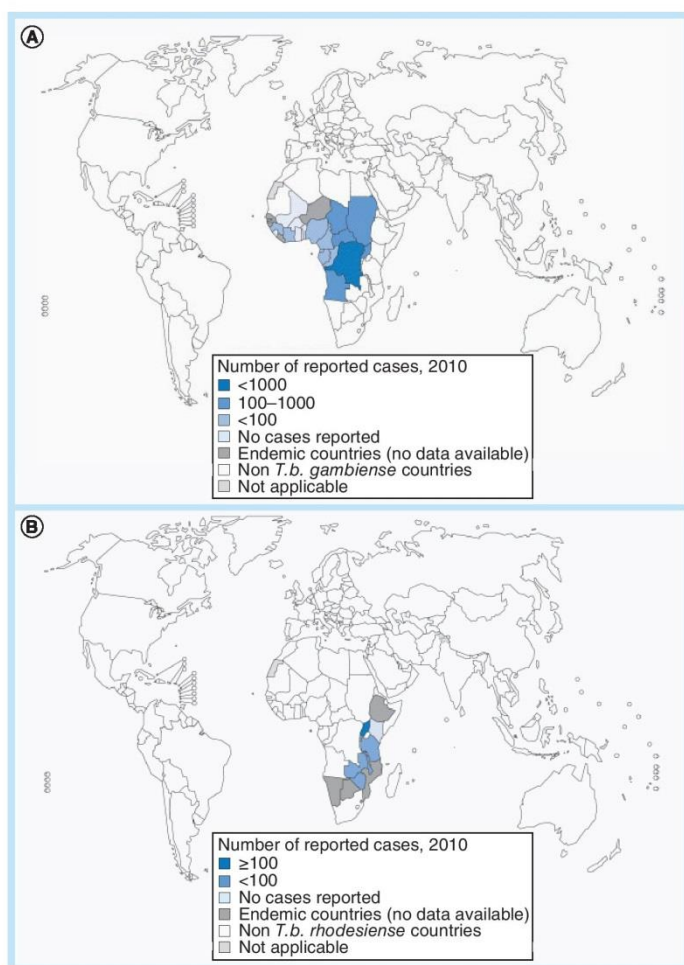


Figure 1. Distribution of human African trypanosomiasis worldwide as seen in 2010. (A) This map depicts the spread of infections caused by the subspecies *T. b. gambiense*, and **(B)** depicts cases caused by *T. b. rhodesiense*. *T. b. gambiense*: *Trypanosoma brucei gambiense*; *T. b. rhodesiense*: *Trypanosoma brucei rhodesiense*. Reproduced from [201,202].

stage occurs in the CNS and is known as the meningoencephalitic stage. The exact process involving the transport of the parasite across the blood–brain barrier (BBB) is still not fully understood although, once there, sleep disturbances, confusion and poor coordination dominate the clinical presentation (**FIGURE 3**) [1]. If left untreated, HAT is widely acknowledged as 100% fatal [1], although parasite clearance has been reported in a small number of untreated *T. b. gambiense* patients [6].

There are a number of drugs that are currently available for the treatment of HAT. However, there are significant side effects associated with the use of a number of them, as well as difficult and lengthy treatment regimens and increased incidences of resistance (**FIGURE 4**) [7].

■ Treatment of first-stage HAT: pentamidine (1) & suramin (2)

For the treatment of the hemolymphatic stage of the disease, while melarsoprol (3) and eflornithine (4) are effective [8], it is pentamidine (1) and suramin (2) that are predominantly used. Pentamidine (1) has been used in the treatment of HAT caused by *T. b. gambiense* for over 70 years [205]; it was originally developed after the effects of a structurally similar diamidine, synthalin, was observed to have antitrypanosomal activity [9]. Initially, it was formulated as a mesylate salt, although, in 1984 it was converted to the isethionate used today [205]. Diamidines are dicationic molecules that have slow diffusion rates across biological membranes and as such the drug is ineffective against stage two HAT, being unable to accumulate in sufficient concentrations in the cerebrospinal fluid [9]. Furthermore, patients treated with pentamidine (1) have reported a range of adverse reactions including nephrotoxicity, diabetes mellitus and hypotension [9].

On the other hand, suramin (2) is prescribed primarily to patients infected with *T. b. rhodesiense* and was first used to treat HAT in the 1920s [10,11]. It is a polysulfonated naphthylamine derivative of urea and was discovered after the antitrypanosomal activity of some symmetrical polysulfonated naphthylamine dyes such as trypan red and trypan blue was observed [10]. In addition to the large molecular size of suramin (2), it is also highly charged at physiological pH [9,10]. It is these two factors that are often attributed to its inability to cross the BBB rendering it ineffective against the second stage of HAT [9,10]. Furthermore, suramin (2) forms strong complexes with LDLs and many serum proteins, which results in the body's inability to absorb it from the GIT [10] and so it must be administered intravenously [205]. There are a number of observed adverse reactions to treatment, including nephrotoxicity and, in some cases, renal damage [10]. There have been an increasing number of reports of resistance developing to suramin (2) recently. It has been proposed that this resistance may arise due to changes in the drug target through mutation or expression levels, development of a parasite

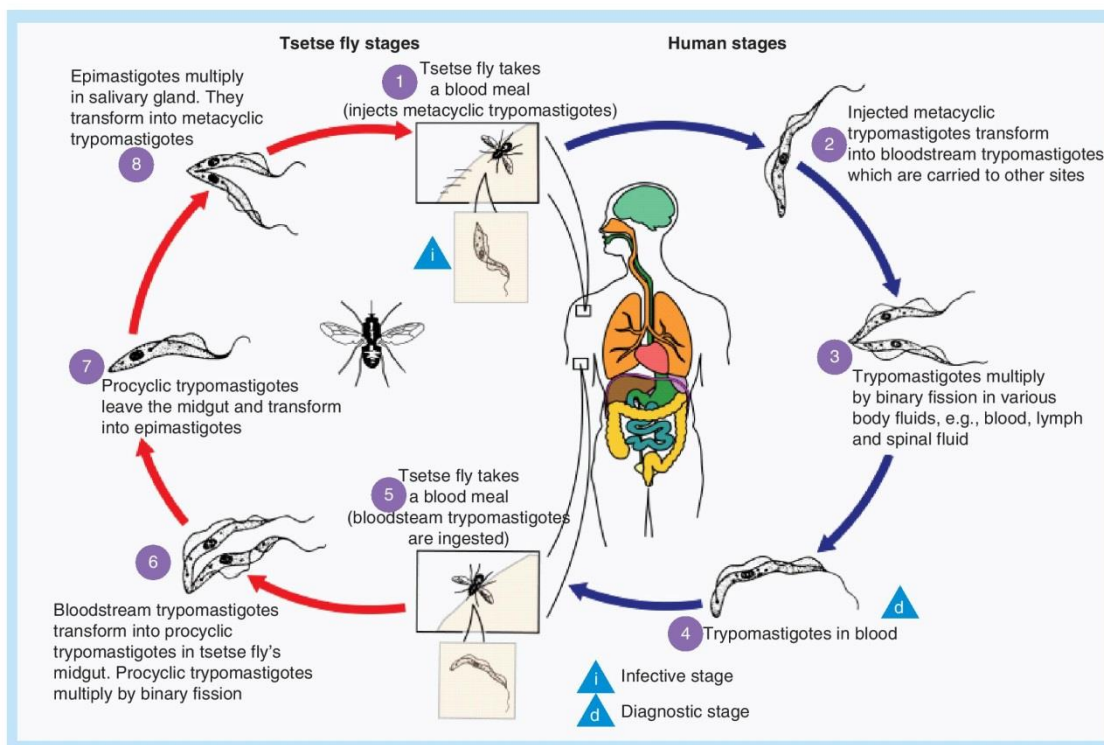


Figure 2. Life-cycle of the trypanosome in the tsetse fly and human. Reproduced from [204].

metabolizing mechanism or through the over-expression of parasite efflux pumps [11]. Recently, a genome-wide RNA interference screen was conducted in the hope of identifying the elements responsible for suramin (2) resistance [12]. The results of this screen suggest that suramin (2) resistance may be due to reduced expression of the major facilitator superfamily transporter [12], which are capable of transporting small solutes in response to chemiosmotic gradients [13]. The

authors propose that major facilitator superfamily transporters may deliver suramin (2) to the cytosol [12].

■ Treatment of second-stage HAT: melarsoprol (3) & eflornithine (4)

Once the parasite has crossed the BBB, only two treatments are available. Melarsoprol (3) was the first drug to be used in the treatment of stage two HAT and it is effective against both subspecies

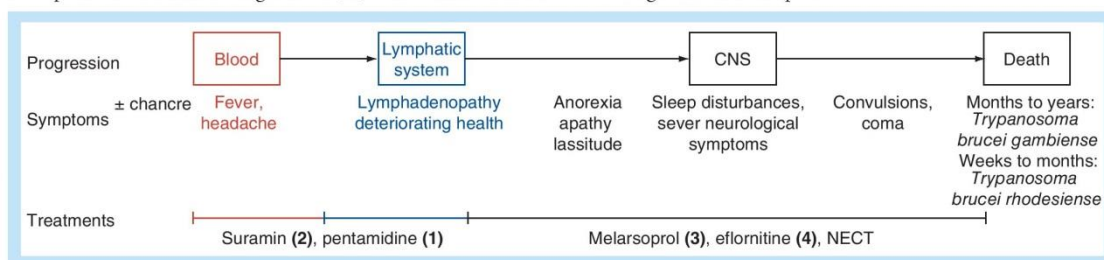


Figure 3. Progression of human African trypanosomiasis and the symptoms, as well as treatments associated with each stage of the disease.

of human infective trypanosomes [9,14]. The drug was introduced in 1947 and is still the first-choice therapy in patients with HAT [14]. The arsenoxide moiety appears to be responsible for the activity of melarsoprol (**3**); a number of analogs varying the arsenoxide moiety have been synthesized, which led to a significant decrease, or total loss of antiparasitic activity [9]. In order to minimize the clear potential for arsenic-related toxicity, the treatment regimen for melarsoprol (**3**) was shortened from 26 to 40 days (consisting of a series of three to four injections followed by a rest period of 7–10 days) [15] to only 10 days of consecutive treatment, resulting in a reduction of the drug required by 30% [14]. While efficacy in patients did not diminish neither did the observed side effects. Some of the major side effects reported include myocardial damage, hypotension and reactive encephalitis [14]. Reactive encephalitis is the most serious of these and occurs in 5–10% of patients [14]. It is fatal in 50% of cases [14]. While melarsoprol (**3**) has largely been one of the most successful treatments for HAT, there have been increasing reports of resistance over the last decade [14]. The precise reason behind this increase in resistance in the field is unknown, although plausible arguments can be formulated. Melarsoprol (**3**) is taken up in to the trypanosomes by the adenosine/adenine transport activity of P2 that is encoded by *TbAT1*, and subsequent loss

of this gene results in increased melarsoprol (**3**) resistance [16]. Melarsoprol (**3**) resistance has also been observed after overexpression of the ABC transporter *TbMPRA* *in vitro* [17].

Eflornithine (**4**) was the first new treatment for second stage HAT in over 30 years; however, it is only active against *T.b. gambiense* [14]. Further to this, the drug has a high cost, difficult therapeutic regimen and a number of side effects [14] including bone marrow toxicity and convulsions [1]. The treatment regimen for eflornithine (**4**) consists of an intravenous infusion of 100 mg/kg every 6 h over 14 days [14]. It is as a result of the short half-life of eflornithine (**4**) that such regular infusions are required in order to maintain a trypanostatic effect [18]. Eflornithine (**4**) acts as a suicide inhibitor towards ornithine decarboxylase. Inhibition of this enzyme disrupts polyamine homeostasis, which is necessary for cell survival [19]. There have been a number of reported failures when treated with eflornithine (**4**), although this has not yet been attributed to resistance, as it could be a result of patient age, disease progression at presentation to the clinic or co-infection with HIV [20]. Introduction of eflornithine (**4**) and nifurtimox (**5**) combination therapy (NECT) in recent years has led to a simplified administration regimen whilst still maintaining the efficacy observed with eflornithine monotherapy [18]. The study by Priotto

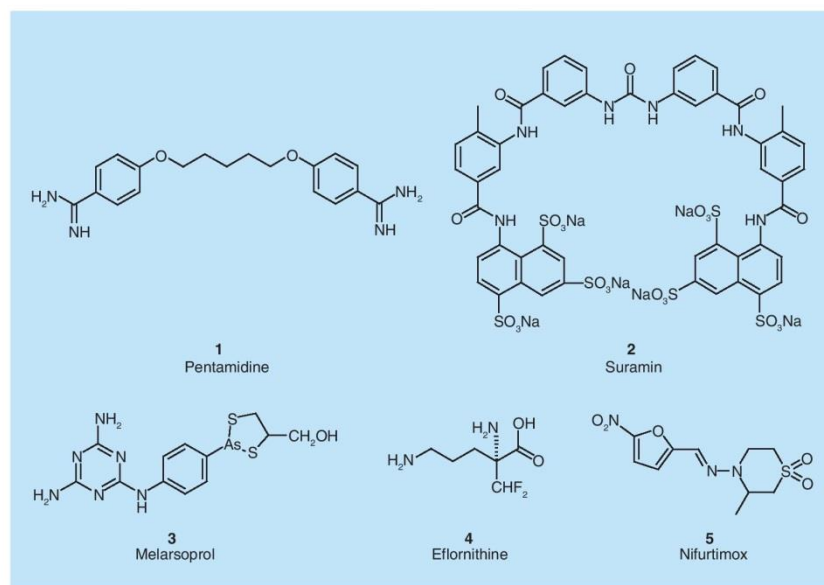


Figure 4. Traditional treatments for human African trypanosomiasis.

and co-workers in 2009 showed that eflornithine (**4**) could be administered every 12 h in combination with nifurtimox (**5**), making it more practical in sub-Saharan Africa and with added safety advantages [18]. The treatment regimen trialed consisted of intravenous eflornithine (**4**; 400 mg/kg per day, every 12 h) for 7 days combined with oral nifurtimox (**5**; 15 mg/kg per day, every 8h) for 10 days [18].

■ Current efforts towards antitrypanosomal compounds

Over the last 10 years there has been a resurgence in the number of investigations into possible novel treatments for HAT from a variety of sources. The first of these advances was seen with the introduction of NECT in 2009, as described previously. Novel inhibitors derived from known trypanosome inhibitors, including furamidine (**6**) and fexinidazole (**18**) have been successful and the latter is about to enter Phase II clinical trials [206]. There has also been significant interest in identifying natural products that could be inhibitors of trypanosomes. While there have been a large number of natural products with reported antitrypanosomal activity, to date there are none being trialed. With the advent of increasing access to high-throughput screening (HTS) technology, it has become possible to screen large libraries of compounds for potential antitrypanosomal activity. Two forms of HTS have been employed by groups in the search for inhibitors: target-based HTS and whole-organism HTS. All of these approaches to drug discovery are discussed.

Of the drugs currently in development, it is important to note that most of them are trypanosomacidal, that is, they kill the trypanosomes, as opposed to being trypanosomastatic where parasite growth is halted while treatment is occurring. There has been some debate about the value of one type of compound over the other but it appears that trypanosomacidal compounds constitute the vast majority of chemotherapeutics in

development to date. Whether a compound is classed as being trypanosomacidal or trypanosomastatic is primarily determined by performing time-to-kill assays, although a recent report described how real-time polymerase chain reaction was employed in order to assess this [21]. In this review we use the term antitrypanosomal to describe compounds that may be trypanosomacidal or trypanosomastatic. We have structured the review such that prominent advances in particular compound classes are described within their own section, immediately below, whereas other compounds are described by their method of discovery.

■ Diamidines

There are a number of recently developed diamidines, based on pentamidine (**1**), that have either entered or been assessed for entry into clinical trials. Furamidine (**6**) was initially identified in the 1980s as part of a screening campaign by the US government although, during initial tests it showed little clinical benefit over pentamidine (**1**) and so it was not taken through to clinical trials [7]. It was not until the methoxy prodrug, pafuramidine (**7**), became available that the benefit over pentamidine (**1**) was recognized and the drug entered clinical trials (**FIGURE 5**) [7]. This compound advanced to Phase III clinical trials against early-stage HAT and Phase II trials against malaria [22]. However, **7** displayed nephrotoxicity and hepatotoxicity in a recent expanded Phase I trial [7] and this led to suspension of the Phase III trials [23].

There were a number of aza analogs of pafuramidine (**7**) identified that have also been assessed for their activity against stage two HAT, these are DB829 (**8**), DB868 (**9**), DB1058 (**10**) and DB1284 (**11**; **FIGURE 6**) [24]. Compounds **9–11** showed similar CNS activity in a GVR35 mouse model, which mimics the CNS resident stage of HAT, and are considered candidates for oral treatment [24]. Given that DB829 (**8**) is also CNS-active but has poor oral

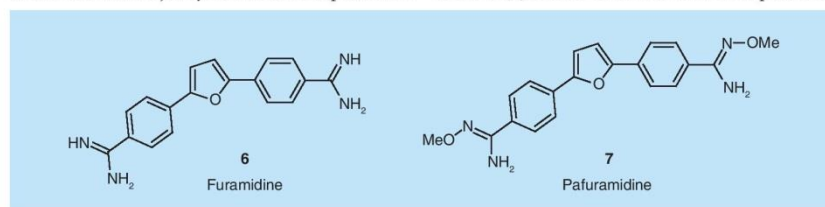


Figure 5. Recently developed diamidine compounds for potential treatment of human African trypanosomiasis.

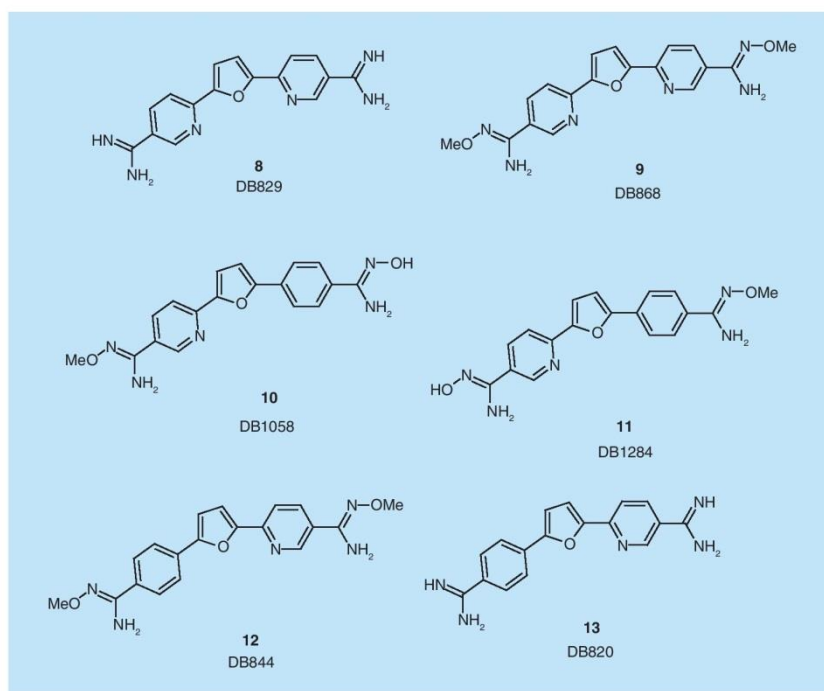


Figure 6. Aza analogs of pafuramidine (**7**) for the treatment of human African trypanosomiasis.

bioavailability its prodrug, DB868 (**9**) has been favored for progression into clinical trials [24]; although it appears that this has been delayed temporarily until the renal toxicity issues can be explained. In a vervet monkey model of first stage *T.b. rhodesiense*, infected monkeys were cured when treatment began 7 days post-infection [25]. Even at the lowest orally administered dose of 3 mg/kg once daily for 7 days, cure of the trypanosome infection was achieved [25]. DB844 (**12**), the prodrug of DB820 (**13**), has also been identified as a potential therapeutic treatment for stage two HAT [26]. The efficacy

data reported for these aza analogs are favorable when compared with both pentamidine (**1**) and pafuramidine (**7**) [26]. In a vervet monkey model DB844 (**12**) was administered orally at 5 mg/kg over 10 days and 6 mg/kg over 14 days [26]. These treatment regimens resulted in cure rates of 37.5 and 42.9%, respectively, during the 300 days of post-monitoring [26].

Most recently, the Tidwell group has reported on next-generation amidines, such as **14** and its prodrug **15** (Figure 7). In a stringent animal model for the acute stage of sleeping sickness, with an oral dose of 25 mg/kg daily for 4 days, **15** resulted in a 100% cure rate, with 4/4 mice surviving 60 days after infection [27]. Many of these next-generation amidines were also found to be highly potent against *Plasmodium falciparum* and *Leishmania donovani*. The exact mechanisms responsible for kinetoplastid toxicity and undesired mammalian toxicity remain ill-defined, and side effects such as hypoglycemia [28,29] and nephrotoxicity [24] may be unpredictable and cause for concern. Nevertheless, with careful monitoring, these next generation amidines may be usefully progressed.

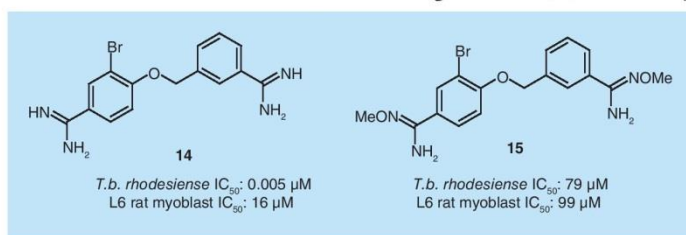


Figure 7. Next-generation diamidines reported by the Tidwell group. *T.b. rhodesiense*: *Trypanosoma brucei rhodesiense*.

■ Nitroaryls

A number of nitroheterocycles have been identified as potential inhibitors of trypanosomes although in all cases they have had significant issues with toxicity preventing their progression through the drug-development pipeline. Mid-20th century nitrofurazone (**16**) demonstrated activity against trypanosome infections, and in the 1990s, megazol (**17**), which has activity against *Trypanosoma cruzi*, showed genotoxicity issues [7]. Drugs for Neglected Diseases initiative (DNDi) screened over 700 nitroheterocycles for antitrypanosomal activity and they identified fexinidazole (**18**) as a potential treatment for both stages of HAT [3]. Fexinidazole (**18**) is orally bioavailable and is quickly metabolized into two oxidized sulfur metabolites with equivalent activity, the sulfoxide (**19**) and the sulfone (**20**; **FIGURE 8**) [3]. Furthermore, fexinidazole (**18**) has shown no genotoxicity issues in mammals and overall has an excellent safety profile [3]. It has so far successfully completed Phase I clinical trials in healthy members of the African population with no significant problems identified [3]. According to DNDi, fexinidazole (**18**) will be entering a Phase II/III clinical trial this year [207]. There is evidence to suggest that fexinidazole (**18**) is activated by nitroreductases (NTRs) [30]. These same enzymes are known to activate nifurtimox (**5**) [31]. It is thought that down-regulation of these NTRs is responsible for the resistance that has been observed for nifurtimox (**5**) and could potentially translate into resistance being observed for fexinidazole (**18**) even before the drug has been used [31].

The development of nifurtimox (**5**) as a drug for the treatment of HAT and the excellent results obtained with fexinidazole (**18**) as a nitroheterocycle with antitrypanosomal activity, has enhanced the interest of researchers in this field in investigating these compounds as inhibitors of *T. brucei*. Several studies in this sense have been published recently as well as some reviews on the topic. It has been demonstrated that nifurtimox (**5**) and benznidazole (**26**), an approved drug for the treatment of Chagas disease, could be reduced by type I or II NTRs. In the case of type I NTRs, the nitro group of nifurtimox (**5**) is reduced to a hydroxylamine product (**22**) through a nitroso intermediate, which can then promote DNA breakage by formation of a nitrenium ion (**23**), or it can generate a DNA-linked adduct, or it can open the heterocycle and form toxic nitriles (**24 & 25**). Alternatively, type II NTRs can reduce the nitro group leading to the formation of unstable nitro radicals, which can form superoxide anions in the presence of oxygen and may lead to the regeneration of the nitrofurans prodrug, although this does not necessarily result in a toxic mechanism. In the case of benznidazole (**26**), type I NTRs, reduce the nitroimidazole to dihydro-dihydroxylimidazole (**28**), which can then decompose to form glyoxal (**29**) and a guanidinoacetamide (**30**; **FIGURE 9**). Either **28** or **29** can then form adducts with a range of biomolecules, including DNA [32].

Modifications of nitrofurazone (**16**) have been studied and they have shown that the activity can be improved by making minor changes to its structure, such as introducing

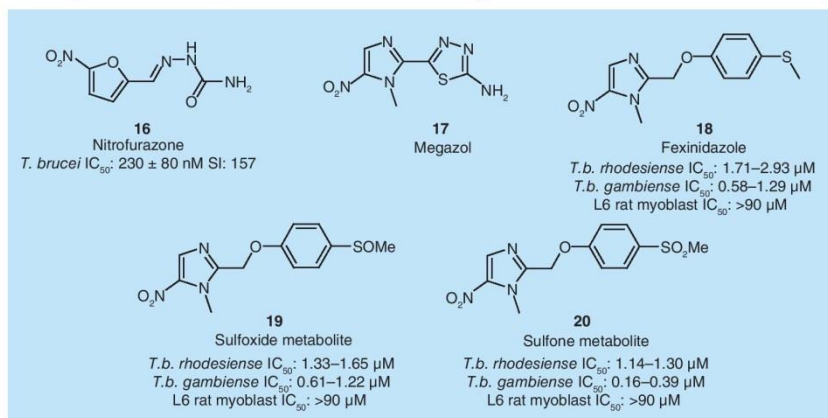


Figure 8. Nitroheterocycles identified as inhibitors of trypanosomes.

T. brucei: *Trypanosoma brucei*; *T. b. gambiense*: *Trypanosoma brucei gambiense*;
T. b. rhodesiense: *Trypanosoma brucei rhodesiense*.

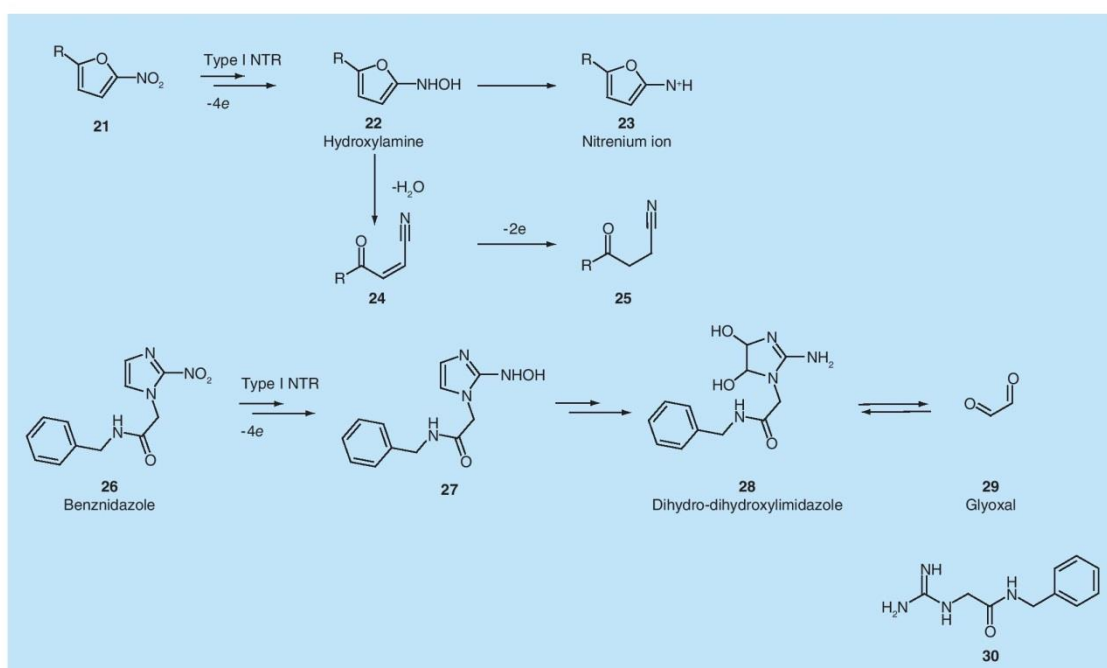


Figure 9. Mechanism of action of type I NTRs on nitroheterocycles.

a thiosemicarbazone (**31**) or a carbazate (**32**; **FIGURE 10**) [30]. These compounds were tested in a bloodstream form of *T. brucei*, which was overexpressing *TbNTR* [30]. It was observed that the cells were between four- and 15-fold more sensitive to the nitrofurans. The antiparasitic activity of these compounds was demonstrated to be *TbNTR*-dependent, as parasites with reduced levels of *TbNTR* to nitrofurans showed resistance to the compounds [30].

In this context, benznidazoles have been studied further. Changing the amide moiety of benznidazole (**26**) to an ether demonstrated that further improvement in the growth-inhibition of

T. brucei could be made (**FIGURE 11**) [33]. From this study, it is clear that the nitro group is required at the 5-position of the heterocycle such as in **33**, since moving it to the 4-position (**34**) resulted in a total loss of activity. While keeping the nitro in the 5-position, the addition of substituents at the 4-position was observed to be beneficial in some cases. In particular, the introduction of a sulfonate moiety (**35**) increased the solubility of these compounds but this was accompanied by a massive drop in selectivity. The mechanism of action of these compounds is not described, but their structures strongly suggest that they are likely to act similarly to benznidazole (**26**) being reduced by type I NTRs [33].

Alternative nitroimidazoles have been synthesized and tested. Here, the 2-position of the heterocycles has been left unsubstituted and the 1-position substituted by an aromatic ring instead of a methyl group (**FIGURE 12**) [34]. Interestingly, in an acute mouse model of infection **36** and **37** were administered once daily for 4 days with an oral dose of 50 mg/kg, the mean survival was over 60 days with a 100% cure rate for both compounds, demonstrating that **36** and **37** were orally bioavailable and active against the first stage of HAT [34]. Furthermore, in a chronic

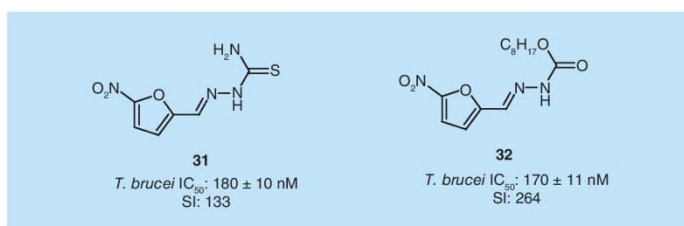


Figure 10. Modification of the hydrazone moiety of nitrofurazone (**16**) leading to improved activity against *Trypanosoma brucei*.
T. brucei: *Trypanosoma brucei*.

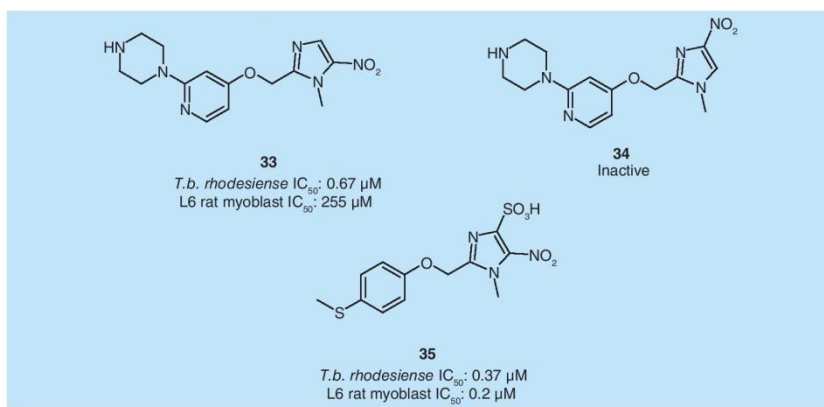


Figure 11. Nitroimidazoles as *Trypanosoma brucei* inhibitors demonstrating the requirement for the nitro group to be in the 5-position.
T. brucei: *Trypanosoma brucei rhodesiense*.

CNS mouse model **36** was shown to be 100% curative when 100 mg/kg was administered twice daily for 5 days [34], while **37** was 100% curative in a chronic mouse model when administered twice daily for 5 days with an oral dose of 50 mg/kg [34]. These results are comparable with fexinidazole (**18**), which requires administration twice daily with a dose of 100 mg/kg over 5 days to be curative in the chronic model for HAT [34]. The two compounds all tested negative in the human peripheral lymphocyte micronucleus test, a measure of genotoxicity [34].

Nitrobenzamides have also been reported to have good growth inhibition against *T. brucei* [35]. The initial phenotypic screening hit (**38**) of this study had good inhibition but poor selectivity against mammalian cells and the malaria parasite, *P. falciparum* [35]. Modifications around both aromatic rings (**39 & 40**) improved the selectivity of the compounds for *T. brucei* over *P. falciparum* and mammalian cells

whilst maintaining the inhibition of *T. brucei* (FIGURE 13). Although these compounds possess a nitroaromatic moiety, it is unclear if they are substrates for NTRs and are acting in the same way as nifurtimox (**5**) or whether some other mechanism is involved [35]. Certainly, there could be some concern about the potential reactivity of the relatively activated aryl halide.

Finally, nitronaphthoquinones have been studied [36]. Such compounds have shown good growth inhibition of *T. brucei*, associated with good selectivity for the trypanosome over mammalian cells (**41–43**; FIGURE 14). Here, the nitro is important but not crucial for the activity of these compounds since **44** and **45** are still active [36]. It is worth noting that the activity is almost unchanged whether the product is mono- or di-substituted with the trifluoromethylaniline, even the position of the monosubstituent does not seem to play a great role. Despite the compelling selectivity profile, these highly activated

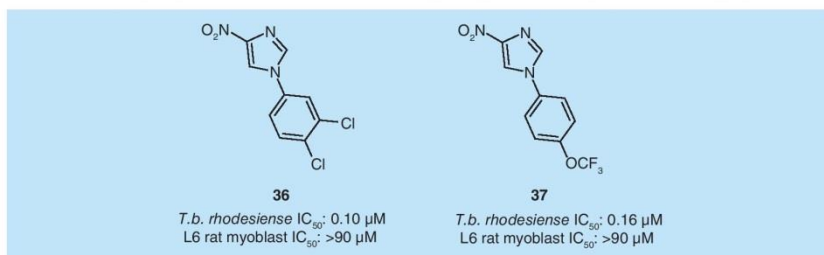


Figure 12. Nitroimidazoles with aromatic substituents active against *Trypanosoma brucei* rhodesiense and selective for trypanosome over mammalian cells.
T. brucei: *Trypanosoma brucei rhodesiense*.

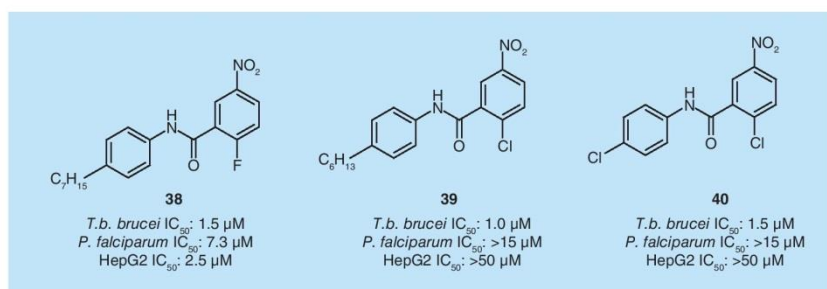


Figure 13. Halonitrobenzamides as inhibitors of *Trypanosoma brucei* showing improved selectivity for the trypanosome with varying aryl substituents.

P. falciparum: *Plasmodium falciparum*; *T.b. brucei*: *Trypanosoma brucei brucei*.

naphthoquinones would be potent electrophiles or redox-active and are unattractive compounds for further progression, especially considering the flat structure–activity relationship (SAR) [37,38]. It is quite possible that poor solubility registers as a false negative in the L6 rat myoblast assays.

In part, derived from the successful discovery of fexinidazole (**18**), a group in Spain recently screened its library of 76 nitroheterocycles and related compounds for activity against *T.b. rhodesiense* using the AlamarBlue™ growth

inhibition assay in collaboration with DNDi [39]. AlamarBlue is a solution of resazurin, which is a REDOX-sensitive dye that changes fluorescence properties upon reduction in living cells. Only living cells are capable of producing fluorescence as they are metabolically active [40]. As a result, five main compounds with IC₅₀ value of ≤10 μM against *T.b. rhodesiense* and selective over mammalian L6 cells were identified along with some important features that are necessary for *T. brucei* activity (FIGURE 15). A number

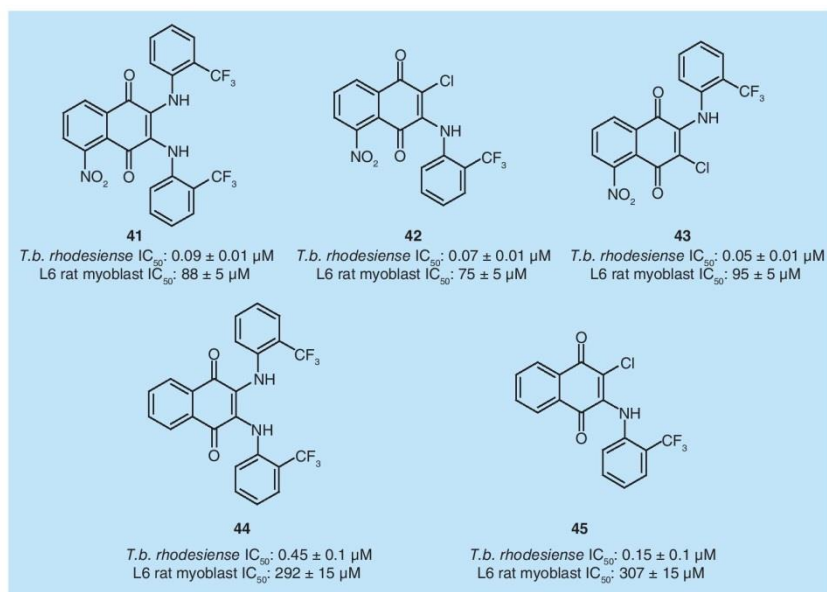


Figure 14. Nitronaphthoquinones as *Trypanosoma brucei rhodesiense* inhibitors demonstrating the importance of the nitro group for *T.b. rhodesiense* activity. Whether the compound is mono- or di-substituted does not seem to impinge upon activity.

T.b. rhodesiense: *Trypanosoma brucei rhodesiense*.

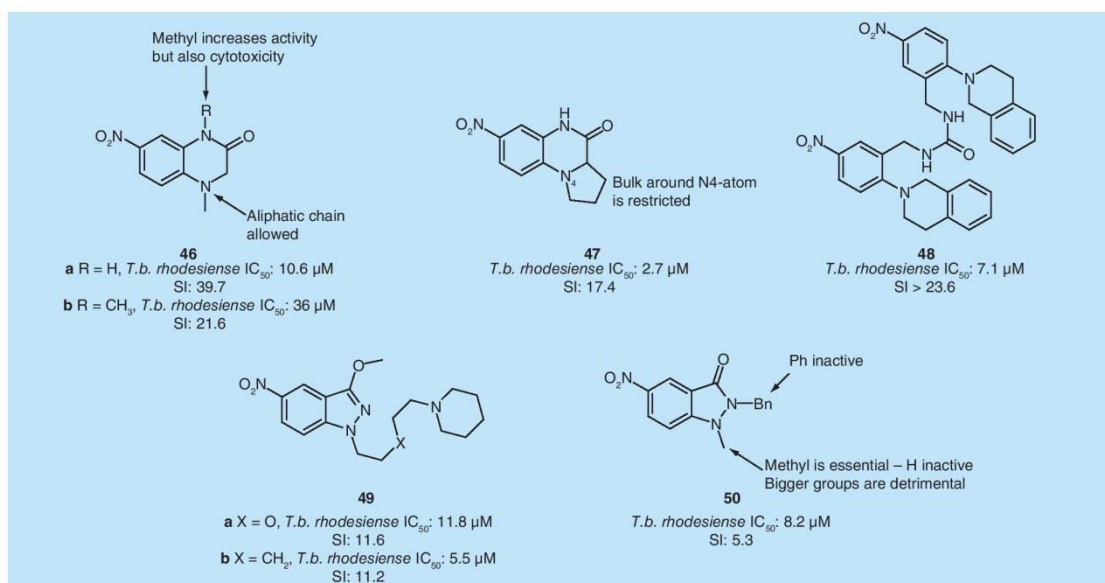


Figure 15. Hit compounds active against *Trypanosoma brucei rhodesiense* and some of the important features necessary for *T. brucei* activity, derived from whole-cell screening a library of 76 nitroheterocycles.
T.b. rhodesiense: *Trypanosoma brucei rhodesiense*.

of analogs of the quinoxalin-2-1 scaffold gave low- to mid-micromolar activity against *T.b. rhodesiense*, such as **46** and **47** [39]. The best result in this series was obtained with **47**, which has a fused pyrrolidine ring [39]. Further bulk around this nitrogen resulted in a loss of activity [39]. Of a small number of dimers in the nitroheterocycle library, only the urea-linked **48** displayed low micromolar inhibition of *T.b. rhodesiense* [39]. While 3-hydroxy-5-nitroindazole compounds were inactive, combining methylation of the 3-hydroxy with an alkyl sidechain in the 1-position that contained a basic nitrogen gave **49a** and **49b** as low- to mid-micromolar inhibitors [39]. Finally, the indazolinone (**50**) derivatives tended to be less active with only mid-micromolar activity against *T.b. rhodesiense* in most cases and poor selectivity [39].

This same group has previously tested two of these compounds in mouse models, confirming their oral bioavailability. Here, **49a** was evaluated (as the hydrochloride salt) *in vivo* in a murine model of acute Chagas disease with a dosage of 30 mg/kg/day where none of the treated animals died compared with a 60% survival fraction in the untreated group [41]. Compound **46b** was evaluated in a separate study using female NMRI mice infected with *T. cruzi* using a dose

of 50 mg/kg/day [42]. This resulted in a drop in parasite levels compared with the control group of 60.7% [42]. These compounds have been shown to be orally bioavailable. However, they would require significant medicinal chemistry optimization and in depth SAR studies in order to turn them into viable drug candidates, due to their low micromolar IC₅₀ values and their poor selectivity over mammalian L6 cells. Indeed, it is somewhat odd that such weak compounds can be orally efficacious.

■ Benzoxaborole benzanilides

There have been reports of a number of benzoxaborole benzanilides that are active against the second stage of HAT (**FIGURE 16**). This marks the first novel class of compound to show activity against the second stage of the disease in a number of years [208]. It has recently been announced that DNDi will also be taking SCYX-7158 (**51**) through to Phase I clinical trials in France [208]. Prior to entering Phase I clinical trial, SCYX-7158 (**51**), showed favorable ADMET properties indicating it was metabolically stable, orally available and CNS-permeable [43]. The benzoxaborole was sufficiently active to cure stage two HAT in a mouse model after treatment at 25 mg/kg for 7 days [43]. During this period the

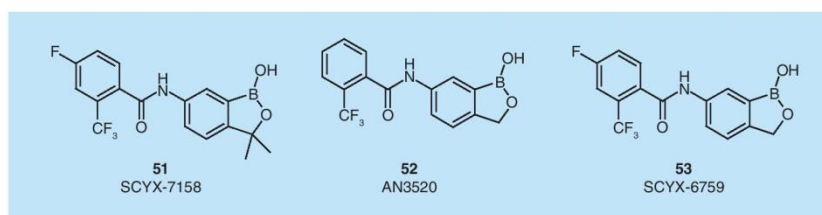


Figure 16. Selection of benzoxaboroles tested for activity against second-stage human African trypanosomiasis.

required concentration for therapeutic activity was maintained within the cerebrospinal fluid and suggests that, if in Phase I trials it behaves in the same way, it could potentially be administered once a day making it a practical drug choice for treatment of HAT [43]. SCYX-7158 (**51**) was evaluated in an array of *in vitro* receptor binding and enzyme inhibition assays; at the testing concentration of 10 μ M, SCYX-7158 (**51**) showed no inhibition of >100 biochemical targets [43]. AN3520 (**52**) and SCYX-6759 (**53**) were reported as inhibitors of *T.b. brucei* in mouse models at dosages between 2.5 and 10 mg/kg over just 4 days for stage one HAT and at 50 mg/kg twice daily for 7 days for stage two HAT [44]. There was also no evidence of toxicity commonly seen with the other drugs currently on the market [44].

■ Chemotherapeutics from target-based assays

Target-based HTS involves the screening of a library of compounds for activity against a specific enzyme or protein. There have been a number of target-based screening campaigns aimed at discovering a new starting point for medicinal chemistry optimization. Some of the targets that have been screened against include *N*-myristoyltransferase [45], ornithine decarboxylase [46], pteridine reductase 1 [47], the peroxidase cascade [48], inositol-3-phosphate synthase [49], trypanothione reductase [50–52] and trypanothione synthetase [53]. A disadvantage of this type of screening is that substantial medicinal chemistry optimization may be required before cell-based activity is observed. This is because serum binding and membrane penetration can limit effective intracellular concentrations. Furthermore, substantial inhibition of an intracellular target may be required before a phenotypic readout (i.e., viability) is obtained. Not only this, but competition with

high concentrations of an endogenous substrate or ligand may be involved in the mechanism of action. For all these reasons, cellular activity may be hundreds of times weaker than target-based activity [54]. In such cases, it is inappropriate to triage a micromolar target-based screening hit on the basis of the observation of micromolar cellular activity. Such observations are generally indicative of off-target effects yet many research groups triage screening hits on this basis, necessarily selecting for off-target compounds. This can often mean that on-target compounds can be overlooked if they are weakly active or inactive against parasites, even though all they require is optimization against the target first. The recommended way to progress a target-based screening hit is to therefore look for signs of clear SAR against the biological target protein and to not be too concerned with a lack of cellular activity. If clear SAR is obtained, aim to collate data on serum binding and permeability and to look for correlation of these with target-based IC_{50} and cellular readout as early as possible during optimization. Of course, active transport is a potential variable that could hinder interpretation of SAR. With a reasonable compound, significant target-based inhibition at 500 nM or lower might reasonably be expected to start to give a cell-based readout through passive transport. However, it is also the case that some biological targets simply do not validate. That is, potent intracellular inhibition with a small molecule does not inhibit parasite growth as expected. This is clearly a risk in target-based drug discovery after a lot of front-end investment in medicinal chemistry optimization. Because of this, strong prior target validation is highly recommended. To avoid waste of resource in such a case, it is therefore recommended to collate data on serum binding and permeability and to look for correlation of these with target-based IC_{50} and cellular readout as early as possible in any medicinal chemistry optimization program.

To date, the most successful target-based HTS was performed with the University of Dundee's general diverse screening library of 62,000 commercially available drug-like small molecules against *N*-myristoyltransferase [45]. From the initial hit, DDD64558 (**54**), a series of compounds was synthesized using crystal structures with inhibitors bound to the enzyme to guide the synthesis (FIGURE 17) [45]. In an impressive hit-to-lead medicinal chemistry effort, increasingly potent leads were obtained until DDD85646 (**55**) was synthesized and tested against *T. b. brucei* with an IC_{50} of 2 nM [45]. Further *in vivo* testing using female NMRI mice showed a 100% cure rate in the *T. b. brucei* acute mouse model of the disease [45]. In order to achieve this, a minimal oral dose of 12 mg/kg twice a day over 4 days was employed [45]. Similar results were observed when a shorter oral dosing schedule was implemented (100 mg/kg twice a day for 1 day and 25 mg/kg twice a day for 2 days) [45]. The efficacy observed for DDD85646 (**55**) in the *T. b. brucei* model was comparable with the response observed when pentamidine (**1**) and melarsoprol (**3**) were used [45]. In the more clinically relevant *T. b. rhodesiense* model of the disease, DDD85646 (**55**) also cured all animals when a dosing schedule of 50 mg/kg twice daily for 2 days was employed [45]. However, these compounds still require further optimization for CNS penetration and selectivity [45].

There have been a number of target-based HTS campaigns conducted against *TbTryR*, which is a validated enzyme involved in thiol metabolism in the protozoa [50–52]. Thiol metabolism by *TbTryR* is unique to the parasite as in humans the process is carried out by glutathione and glutathione reductase, which should

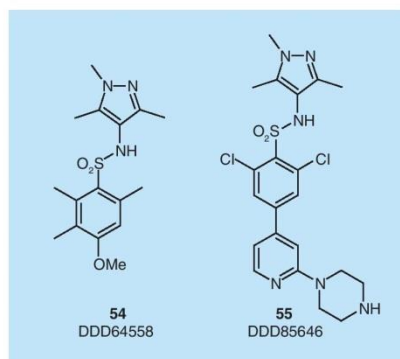


Figure 17. Potent inhibitor 55 derived from DDD64558 (54). Initially identified via targeted high-throughput screening against *N*-myristoyltransferase.

allow selective targeting of the parasite [52]. In 2009 a screen against *TbTryR* was conducted that tested the LOPAC1280 library; a library of 1280 pharmacologically active compounds that includes US FDA-approved drugs. As a selectivity counterscreen, the resultant hits were re-tested against human glutathione reductase, to give three new classes of selective inhibitors that might have potential for future development (FIGURE 18) [52]. BTCP (**56**), an analog of phencyclidine, which is an anesthetic drug, was identified as an inhibitor of *TbTryR* and was used as a starting point for medicinal chemistry optimization [55]. This compound was tested in bloodstream *T. b. brucei* and found to have an EC_{50} of 13.6 μ M. While medicinal chemistry optimization led to marginally improved compounds, it was concluded that as a target *TbTryR* may not be conducive to the discovery

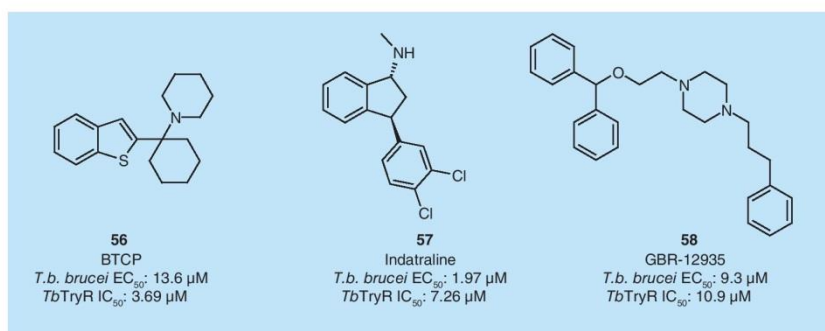


Figure 18. Selection of potential lead compounds identified via targeted high-throughput screening of *TbTryR*.

T. b. brucei: *Trypanosoma brucei brucei*.

of small-molecule drugs. Indatraline (**57**) is a nonselective monoamine reuptake inhibitor that has been identified as acting on the dopamine transporter with similar effects to cocaine [56]. This compound has an EC_{50} , which is approximately 3.5-fold greater than the IC_{50} observed against the enzyme. The authors have attributed this discrepancy to additional off-target activity or through the selective concentration or metabolic activation of this compound *in vivo*, or indeed a combination of these factors [52]. GBR-12935 (**58**) is described as a potent and selective inhibitor of dopamine reuptake [57]. Similarly, **58** has an EC_{50} , which is somewhat lower than anticipated, indicating some other mechanism is involved, as with **57**. Of course, the challenge with any hit arising from a known drug screen is to discern divergent SAR and engineer-out mammalian pharmacological activity, but there is good precedent for this type of approach [58].

In 2007, 2-iminobenzimidazoles were identified from a library of 100,000 compounds as a potential lead for medicinal chemistry optimization, targeting *TbTryR* [50]. Although the details were published two years later, this same campaign led to the identification of a further four classes, including aryl and alkyl piperidine-like compounds, benzhydryls, nitrogenous heterocycles and conjugated indole-like compounds [51]. All data were published on ChEMBL, from which an additional class (3,4-dihydroquinazolines; **59**) was later retrieved by another research group.

The 3,4-dihydroquinazolines (**59**) were further optimized by initially employing a chemistry-driven approach and subsequent structure-based inhibitor design (FIGURE 19) [59]. This led to the identification of a number of inhibitors with sub-micromolar activity against *T. brucei* (**60–63**) [59]. Crystal structures of selected inhibitors bound to *TbTryR* were also presented. This revealed a small hydrophobic pocket that was generated upon inhibitor binding and which lies within a ‘privileged’ region of the larger active site [59].

TbTryS has also been confirmed as a drug target with RNAi and gene knockout studies demonstrating it is essential for *T. brucei* growth in both bloodstream and procyclic forms of the parasite with no alternative bypass mechanism available [53]. With no equivalent pathway in humans, *TbTryS* is an ideal target for antiparasitic compounds. The University of Dundee’s general diverse screening library of 62,000 compounds was screened against *TbTryS* [53]. From the HTS there were six compounds (**64–69**) that were identified as potential inhibitors for *TbTryS* (FIGURE 20), which can be broadly clustered into two groups based upon common pharmacophoric features [53].

Initially work around **64–66** led to the identification of **70** and **71** as sub-micromolar inhibitors (FIGURE 21), while optimization of **67–69** was largely unsuccessful with only low micromolar

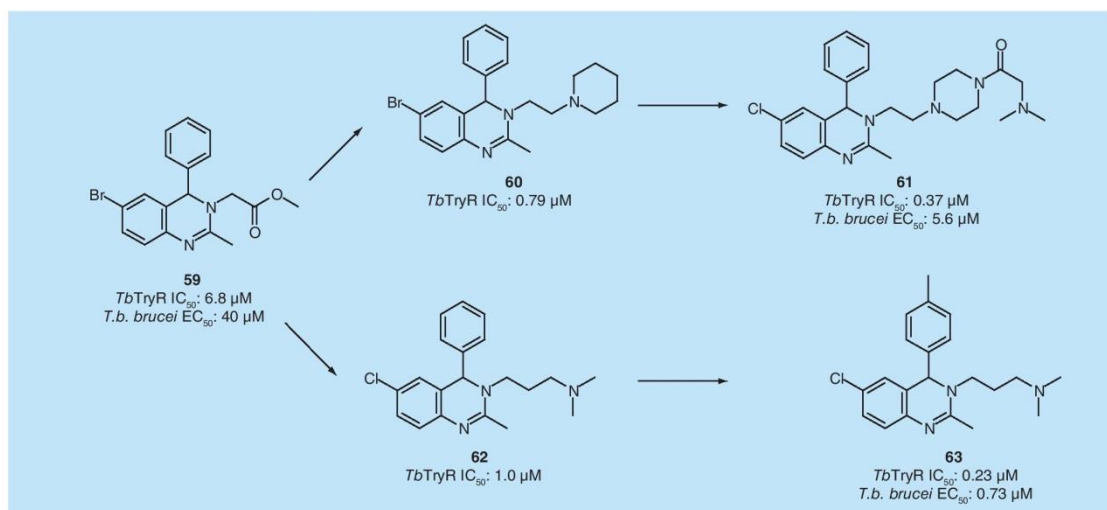


Figure 19. Optimization of the screening hit (**59**) against *TbTryR*, employing a chemistry-driven approach and subsequent structure-based inhibitor design.
T.b. brucei: *Trypanosoma brucei brucei*.

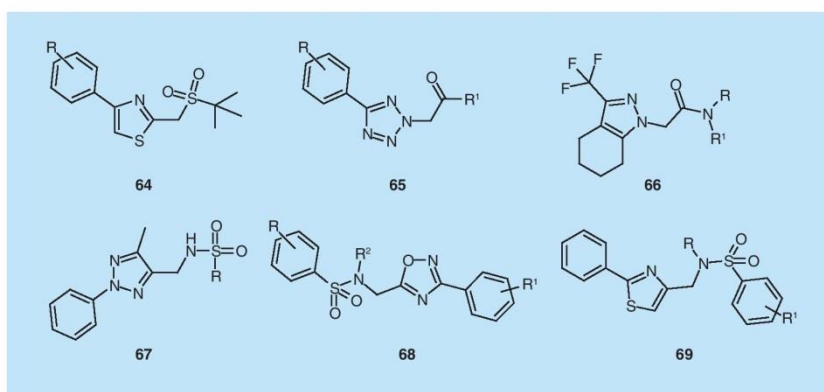


Figure 20. Putative hit series identified via high-throughput screening of *TbTryS*. These compounds can be broadly clustered into two distinct groups based on common pharmacophoric features. Compounds **64–66** each have two hydrogen bond-accepting groups in a 1,5 relationship with one of the hydrogen bond acceptors from a heterocyclic ring; there is also a region of hydrophobicity in each. Compounds **67–69** have a heteroatom of the heterocycles in a 1,6 relationship with the hydrogen bond-accepting sulfonamide. This second series was observed to be generally of higher molecular weight and lower potency.

inhibition obtained [53]. As a result of this, further optimization of the first series of compounds (**64–66**) was progressed by hybridizing the pharmacophoric features into a new scaffold (**73**) based around an indazole (**FIGURE 22**) [53]. This resulted in the breakthrough activity that was sought with a tenfold increase in potency against *TbTryS*. Testing against *T. brucei* revealed low micromolar EC_{50} values, while testing against human MRC5 cells revealed that **74** had good parasite selectivity while **75** required further optimization [53].

An alternative approach to identifying *T. brucei* inhibitors is to conduct a screen of the peroxidase pathway of the trypanosome. There are a number of enzymes that constitute the peroxidase pathway of *T. brucei* – trypanothione reductase, trypanedoxin and two types of trypanedoxin peroxidases [48]. The trypanothione/trypanedoxin system is responsible for delivering the reducing equivalents necessary for the synthesis of DNA precursors and, therefore, parasite replication [48]. Initially, 80,000 compounds were screened for activity against the *T. brucei* peroxidase pathway which led to the identification of 32 active compounds [48]. Of these, 12 were studied further and they could be broadly grouped in to five classes based upon common core structures (**76–80**; **FIGURE 23**). For each of these compounds, activity in an *in vitro* peroxidase assay and in the bloodstream form of *T. brucei* was obtained. For

most of the compounds the EC_{50} values were an order of magnitude lower (i.e., compounds were tenfold more potent) than the IC_{50} obtained from the *in vitro* assay [48], precisely the opposite of what would normally be expected. The authors attributed this apparent discrepancy to the fact that these compounds cause a time-dependent inactivation of the target protein [48]. It was shown that these compounds did apparently target trypanedoxin both *in vitro* and in the whole parasite [48]. The SI values were measured against HeLa cells, although this cancer cell line expresses thioredoxin in high levels [48]. This could potentially make the cells more susceptible to the compounds and lead to SI values that are lower than in reality [48]. Alternative cell lines, such as fibroblast MRC-5 cells, could have been utilized but they have been reported as having undetectable levels of the thioredoxin-1, which would have led to higher

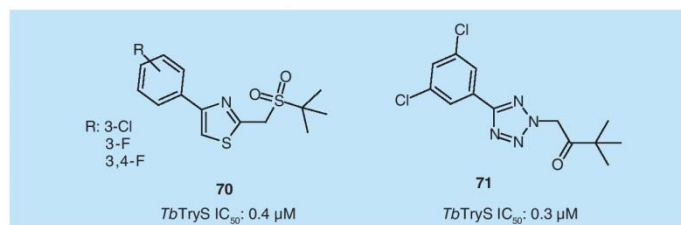


Figure 21. Selection of analogs leading to sub-micromolar inhibition against *TbTryS*.

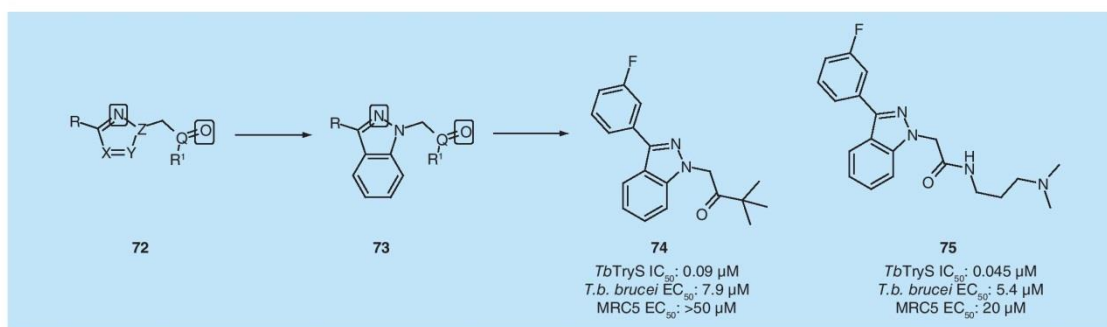


Figure 22. Generation of the indazole scaffold (**73**) and subsequent analogs demonstrating a tenfold increase in recorded inhibition against *TbTryS*.

T.b. brucei: *Trypanosoma brucei brucei*.

SI values being reported [48]. Time dependence is often associated with covalent binding, in line with the anticipated high electrophilicity of these alkyl halides which are unattractive candidates for further progression.

The largest target-based HTS that has been undertaken was against ornithine decarboxylase, which is a key enzyme in polyamine biosynthesis, the pathway eflornithine (**4**) has been demonstrated to inhibit [46]. A library of just over 316,000 compounds was screened and led to the identification of four unique families of inhibitors (**81–84**), one of which (**83**) was selective for

the parasite enzyme over the human ortholog [46]. The initial inhibitor identified was a bisguanidine (**81**), which was reasonably potent with a K_i of 2.7 μ M but unfortunately it inhibited both the trypanosome and human orthologues of the enzyme equally [46]. The benzothiazole (**82**) and indole (**84**) were also identified as inhibitors with a K_i 14.0 and 27.1 μ M, respectively [46]. Again both of these were nonselective for the parasitic enzyme [46]. Finally, dithioamides, such as **83**, were identified as being selective and potent inhibitors with the most potent having a K_i of 3.6 μ M (**Figure 24**) [46].

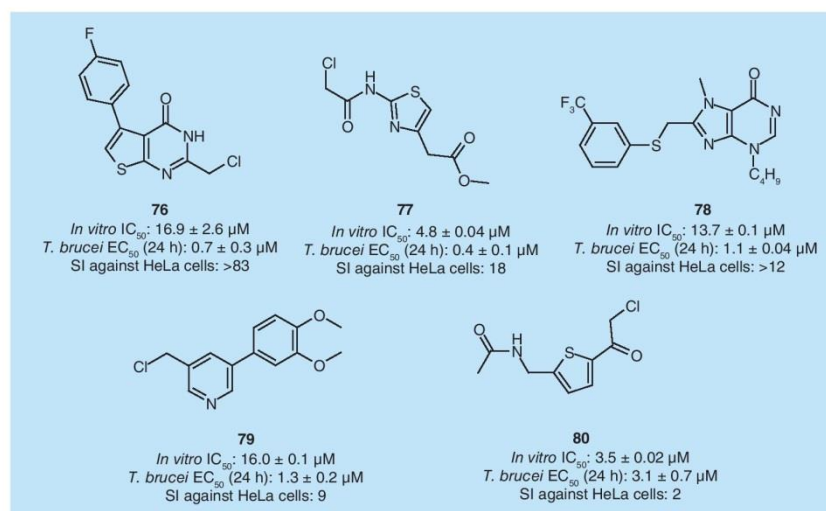


Figure 23. Representative compounds identified from high-throughput screening as exhibiting activity (IC_{50} listed) against an *in vitro* *Trypanosoma brucei* peroxidase pathway assay. Potent activity against *T. brucei* was also observed.

T. brucei: *Trypanosoma brucei*.

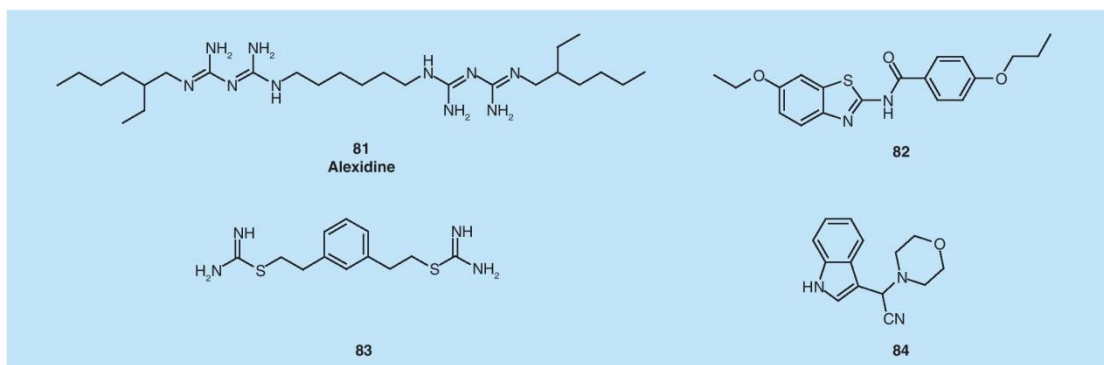


Figure 24. Representative structures of the four classes of compounds identified in the targeted high-throughput screening against ornithine decarboxylase.

Screening of the Institut de Chimie des Substances Naturelles (in France) library against the enzyme, farnesyltransferase (FTase) from yeast revealed arylthiophenes as sub-micromolar inhibitors [60]. This library is reported to contain approximately 53,000 molecules and 14,500 plant extracts from 29 French universities and research institutions [209]. An early SAR study was performed focusing on the alkyl chain, nitrile, thiophene and carboxylic acid of the initial compound, summarized in **85** (Figure 25). This early SAR was later assumed to apply to the trypanosome FTase although the reasoning for this was unclear especially as **86** is 100-fold less active against recombinant human and trypanosome FTase than it is against yeast FTase. While the SAR study against *T. brucei* around the substituted aryl is still valid, there remains the need to re-examine the previously established

SAR of these compounds around the other positions of the thiophene in order to determine the degree of translation from yeast to trypanosome FTase. The analogs generated of the aryl moiety have led to a tenfold increase in inhibition relative to *Tb*FTase (Figure 25) [60].

There is an unexpected difference between *Tb*FTase inhibition and *T. b. brucei* proliferation inhibition in that, the enzyme inhibition is much weaker than the whole parasite inhibition in some compounds such as the pyrogallol (**87**; Figure 26), which the authors acknowledge brings in to question the primary target of these compounds [60]. It was determined that the pyrogallol derivative (**88**) showed no cytotoxicity towards KB and MRC5 human cell lines at 10 μ M and on this basis it was suggested that potent effects observed against *T. b. brucei* did not arise through being nonspecifically toxic towards all cell types. Nevertheless, such polyphenolic

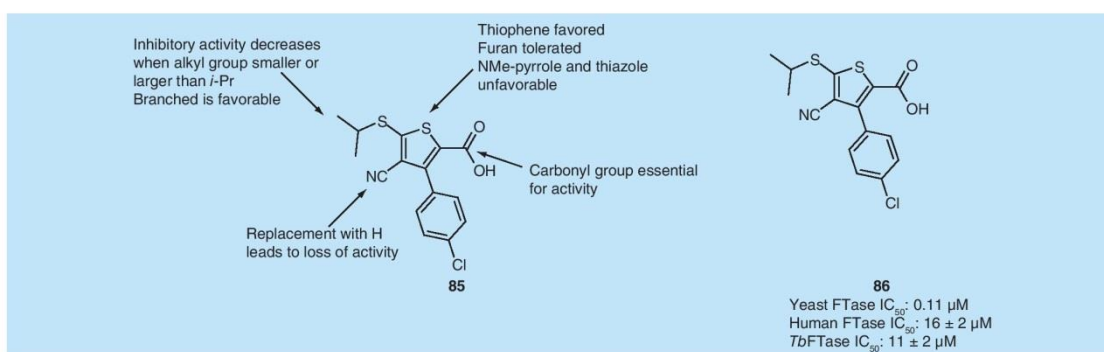


Figure 25. Structure–activity relationship study initially conducted around the hit compound (**85**) as well as the inhibitory activity of **86** against the yeast, human and *Trypanosoma brucei* orthologs of FTase.

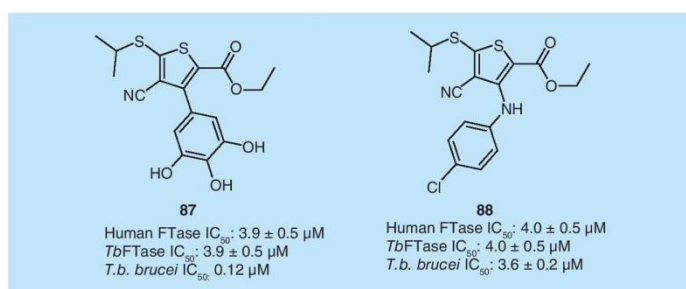


Figure 26. Analogs of the aryl moiety showing low micromolar activity against TbFTase and *Trypanosoma brucei*.
T. b. brucei: *Trypanosoma brucei brucei*.

compounds, in particular catechols should not be used in drug discovery given their propensity to hit very different screens (i.e., kinases, phosphatases and other enzymes) at low nanomolar concentration [37,38]. The target for these compounds appears to be unknown or, alternatively, polypharmacology could be responsible for the observed activity.

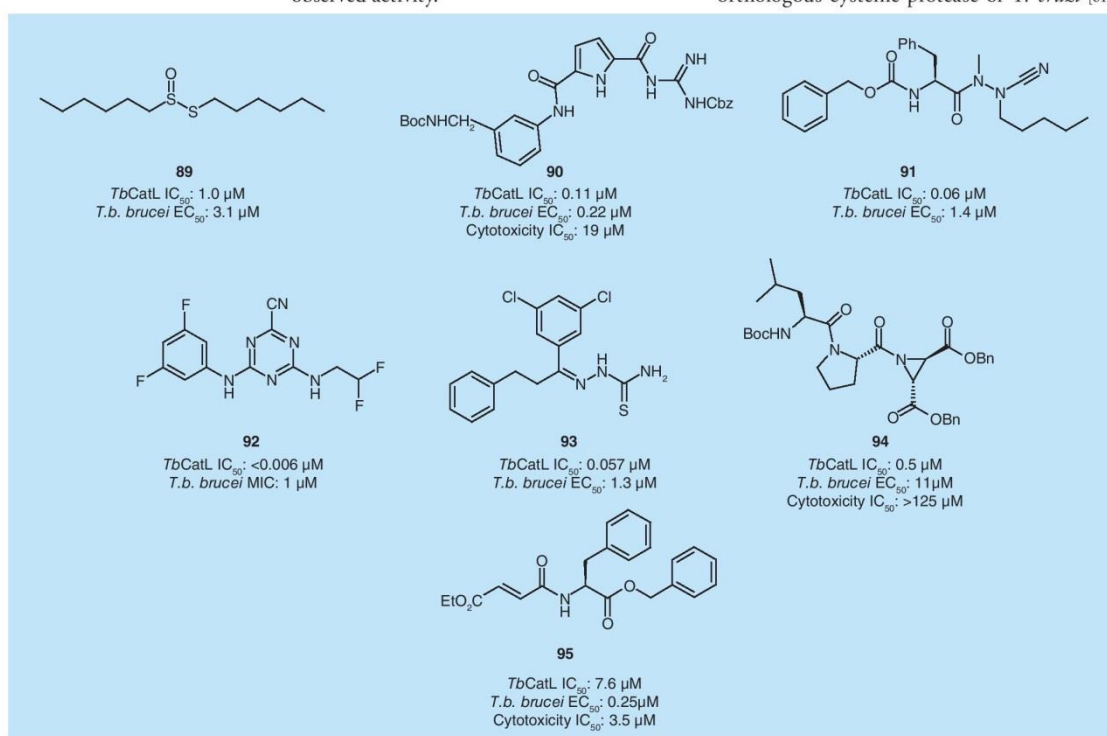


Figure 27. Examples of known *Trypanosoma brucei brucei* inhibitors acting through rhodesain inhibition.
T. b. brucei: *Trypanosoma brucei brucei*.

Focused screening

Cysteine proteases of the papain family, which are expressed in both humans and parasites, have been recognized as potential targets for the treatment of HAT. A review on this topic has been recently published, gathering all the recent efforts in the synthesis of new inhibitors for this pathway [61]. Proteases such as TbCatL, commonly known as rhodesain are essential to the metabolism of *T. brucei*. This protease is essential for the parasite to cross the BBB leading to the deadly second stage of the disease [61,62]. *In vitro* studies have shown that rhodesain activates protease-activated receptors (a G protein-coupled receptor), which facilitates transport of the parasite [61]. It is also believed that these proteases are involved in the turnover of variant surface glycoproteins that are densely coating/shielding the parasite from the mammalian host immune system [61,63]. Several studies using small molecules (including dipeptides) derived from previously known inhibitors of the cysteine proteases falcipain, cruzain (an orthologous cysteine protease of *T. cruzi*) [61]

and the disease-associated human cathepsins B and L have led to the identification of rhodesain inhibitors. Some diverse examples of such inhibitors are shown in **FIGURE 27**. These compounds inhibit the growth of *T. brucei* as well as inhibiting rhodesain. Prevalent among all cysteine protease inhibitors is the presence of warheads, designed to covalently react with active-site cysteine, and these are exhibited in compounds such as **89** [64], **91** [65], **92** [66], **93** [67], **94** [68] and **95** [69] in **FIGURE 27**. This can be a concern with respect to feasibility of progression of any such compound, but it needs to be pointed out that antiparasitic chemotherapy can tolerate unusual chemistries, and there is a vinyl sulfone cruzain inhibitor currently undergoing investigational new drug-enabling studies for the treatment of Chagas disease [70]. In such cases, it is recommended to optimize on noncovalent SAR before introducing a reactive center, and this approach could be deployed in the case of **90** [71]. Furthermore, unwanted activity at human cathepsin L should be monitored early on, as should cytotoxicity, for these sorts of compounds.

Another interesting target is the kinetoplast DNA-replication machinery. It has been demonstrated that topoisomerase II inhibitors such as ciprofloxacin (**96**) and other known molecules having the same dihydroquinolin-4-one moiety have antitrypanosomal activity (**FIGURE 28**) [72]. Further studies to improve selectivity and activity against *T. brucei* led to **97**, which showed

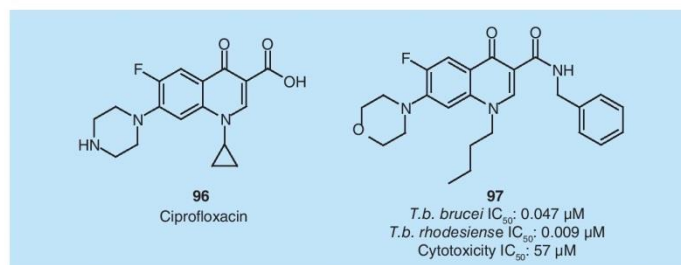


Figure 28. Ciprofloxacin (96) and a potent analog (97). While potent *in vitro* activity was observed for **96** it was inactive *in vivo*.
T. brucei: *Trypanosoma brucei brucei*; *T. brucei*: *Trypanosoma brucei rhodesiense*.

very good *in vitro* activity but was inactive *in vivo* when administered to *T. brucei*-infected NMRI mice at an oral dose of 50 mg/kg over 4 days [72]. There were no pharmacokinetic data available and so it was not possible to distinguish between a lack of *in vivo* efficacy or bioavailability of the compound, although further work targeting the optimization of water solubility has been identified [72]. Interestingly, it was not clear what intracellular targets were responsible for the *T. brucei* activity.

GSK3 is known to play a key role in the growth rate of *T. brucei*, but its precise function is yet to be determined [73,74]. After screening a focused kinase library against *Tb*GSK3, five series of *Tb*GSK3 inhibitors were identified (**98–102**; **FIGURE 29**) [75].

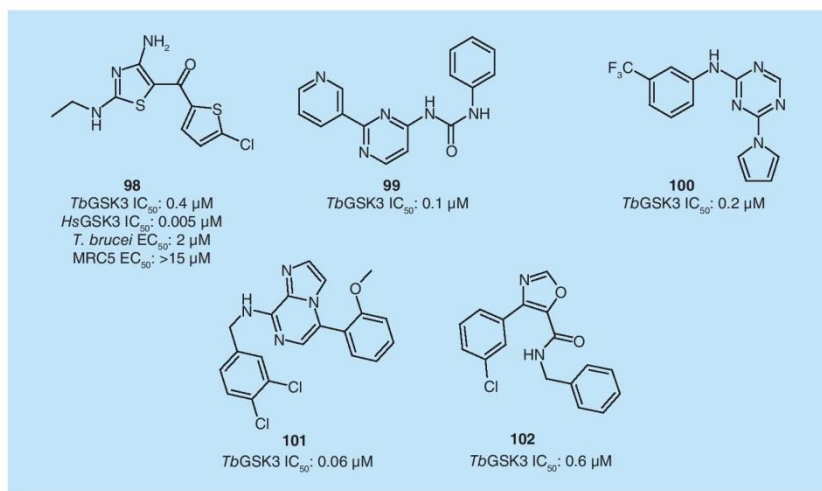


Figure 29. Compounds identified as inhibitors of *Tb*GSK3.
T. brucei: *Trypanosoma brucei*.

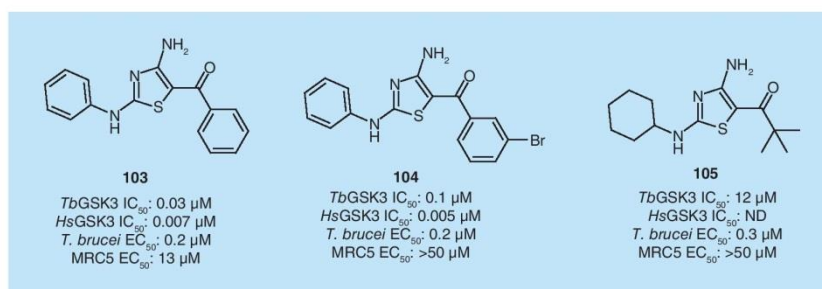


Figure 30. Optimization of 103 and subsequent analogs. In general the analogs were more active against *Hs*GSK3.
 ND: Not determined; *T. brucei*: *Trypanosoma brucei*.

A short SAR study focusing on **98** was conducted. Difficulty was encountered in trying to improve the selectivity of the compounds for *Tb*GSK3 over the human ortholog, *Hs*GSK3 (**FIGURE 30**) [75]. Indeed, all these analogs are much more potent against *Hs*GSK3 than against *Tb*GSK3, although, intriguingly, this is not reflected by activity against the mammalian cell line MRC5. Simultaneously increasing the hydrophobicity and bulk of the left-hand-side amine and replacing the thiophene with a phenyl (**103**) led to a tenfold increase in potency against *Tb*GSK3 while maintaining *Hs*GSK3 activity. Substitution of the right-hand-side phenyl with a bromine was tolerated (**104**); however, the introduction of bulky aliphatic groups on the right-hand-side while also replacing the left-hand-side phenyl with a cyclohexyl (**105**) led to a significant loss of activity against *Tb*GSK3. While mammalian cytotoxicity is especially diminished in **104** and **105**, it is highly concerning that **105** has potent cell activity but weak enzyme activity, suggesting off-target

sites of action. There are reports of substituted 2,4-diaminothiazoles being potent inhibitors of a number of cyclin-dependent kinases [76,77] and p25 [77].

Recently, several known EGFR tyrosine kinase inhibitors were tested against *T. brucei* [78]. The tyrosine kinase inhibitor lapatinib (**106**) was identified as a potential starting point for the development of new trypanosomastatic drugs since it showed inhibition of *T. brucei* growth (**FIGURE 31**) [78]. Based on this template, an elegant SAR study was conducted leading to an optimized structure (**107**) showing potent inhibition of *T. brucei* growth [78]. Compound **107** shows good selectivity for the parasite over mammalian cells [78]. Further to this, **107** has been identified as being orally bioavailable and it is stated as being moderately efficacious in a mouse model of HAT when a dose of 20 mg/kg is administered with survival post-infection extended approximately from 3 to 9 days although no further information is reported [78].

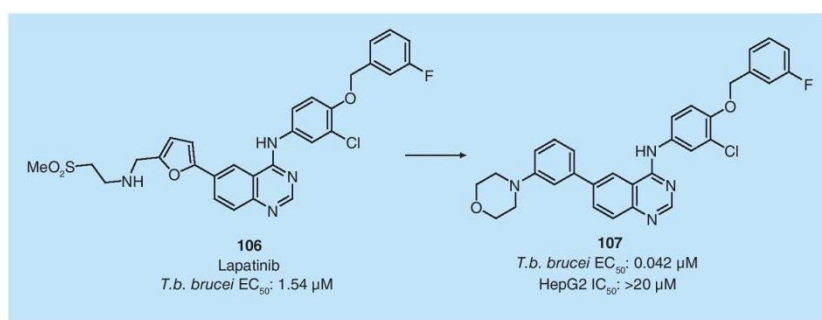


Figure 31. Optimization of lapatinib (106) by Pollastri's group [78].
T. brucei: *Trypanosoma brucei brucei*.

A selection of approved anticancer drugs and 15 known DNA topoisomerase inhibitors were tested for *in vitro* activity against bloodstream *T. brucei* and HL-60 cells [79]. All the tested compounds exhibited antitrypanosomal activities with ED₅₀ values from 3 nM to 30 μM. While the most active of these compounds (**108**, **109** & **111**) have comparable antitrypanosomal activity with that of commercial antitrypanosomal drugs, they have poor selectivity for the parasite over mammalian cells. In one instance, camptothecin (**110**) was identified as being more toxic to mammalian cells than the parasite (**FIGURE 32**).

Computer-assisted & *in silico* screening

It was reported that a series of benzoxaboroles, similar to the compound currently progressing through clinical trials (SCYX-7158; **51**) was optimized for their activity using an homology model against *TbLeuRS* [80]. However, the reported activity in the parasite was tenfold higher for **113**, while **112** shows similar activity against the supposed target as **113** (**FIGURE 33**) [80]. This suggests that *TbLeuRS* is not the primary target for the action of these benzoxaboroles (or a metabolite specific to **113** could be responsible) and their target is, as yet, unidentified.

While not yet clinically validated, *TbrPDEB1* represents an exciting new target for the treatment of HAT. Known inhibitors of the corresponding human ortholog have been successfully used as starting points for the development of compounds targeting *TbrPDEB1*, such as **114** and **115** in **FIGURE 34** [66]. However, from such starting points, it has been difficult to achieve inhibition of *TbrPDEB1* with the required selectivity. Recently, the crystal structure of *TbrPDEB1* was reported [81] revealing a parasite-specific pocket [81]. An *in silico* binding model predicted that both **114** and **115** will bind in this new parasite-specific pocket [81].

An *in silico* screen was then performed in order to identify selective *TbrPDEB1* inhibitors (**FIGURE 35**). A number of novel inhibitors were identified such as **116** and **117** with micromolar activity against *TbrPDEB1* and demonstrating some selectivity over *hPDE4B* [81]. These compounds may serve as starting points for future drug-discovery projects although it remains to be seen whether the selectivity can be maintained during this process. In particular, some of the compounds retrieved contain promiscuous substructures such as catechols and imides, as is often the case from both *in silico* screening

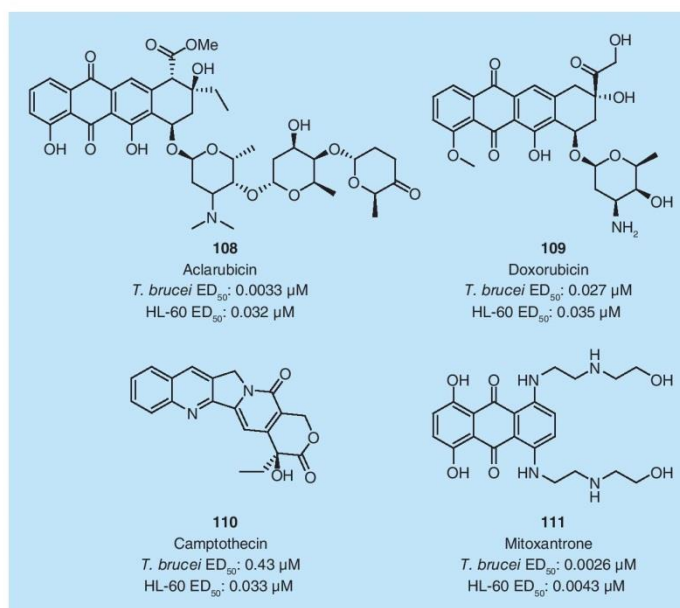


Figure 32. A range of potent DNA topoisomerase inhibitors for bloodstream *Trypanosoma brucei*.

T. brucei: *Trypanosoma brucei*.

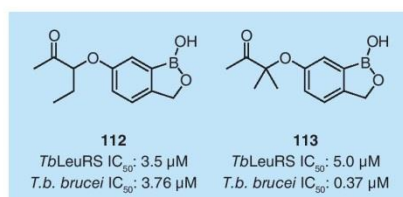


Figure 33. Benzoxaboroles identified as active against *TbLeuRS* however, the *Trypanosoma brucei* data suggest another target is involved.

T. b. brucei: *Trypanosoma brucei brucei*.

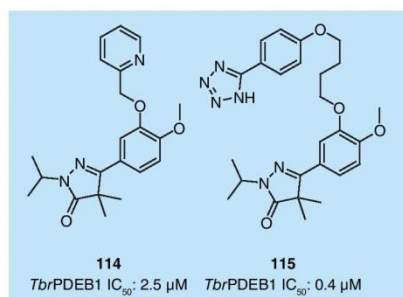


Figure 34. *TbrPDEB1* inhibitors with IC₅₀ values reported against *TbrPDEB1*.

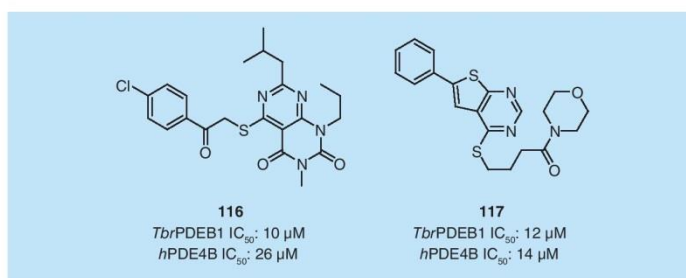


Figure 35. *Tbr*PDEB1 inhibitors identified through *in silico* screening with IC₅₀ values reported against *Tbr*PDEB1 and *h*PDE4B.

and HTS [82]. Even in **116** and **117**, the thioether linkages could be reactive and **116** resembles a known redox-active promiscuous core [82]. Caution should be exercised in progressing these compounds [83]. Trypanosomal inhibitory data were not reported.

Table 1. Pharmacological profile of compound **122**.

Enzymatic assay	IC ₅₀ (μM)	Cellular assay	IC ₅₀ (μM)
<i>Tbr</i> PDEB1	0.049	<i>T. b. brucei</i>	0.52
<i>Tbr</i> PDEB2	0.072	<i>T. b. rhodesiense</i>	0.06
<i>Tbr</i> PDEB1 catalytic domain	0.055	<i>T. cruzi</i>	7.6
<i>h</i> PDE4A1	0.0021	MRC5	> 64
<i>h</i> PDE4B1	0.0046	–	–
<i>h</i> PDE4C1	0.010	–	–
<i>h</i> PDE4D3	0.0012	–	–

T. b. brucei: *Trypanosoma brucei brucei*; T. cruzi: *Trypanosoma cruzi*; T. b. rhodesiense: *Trypanosoma brucei rhodesiense*.

Fragment-based drug discovery has attracted increasing interest over the past decade and the first drug discovered via fragment-based screening followed by intensive medicinal chemistry was Zelboraf™, which was FDA-approved in 2011 [210]. Trypanosomal phosphodiesterase B1 and B2 are known to have key roles in the division and lysis of *T. b. brucei* [84]. Initially, a HTS identified PPS54019 (**118**), a known human PDE inhibitor [84]. A follow-up of related chemotypes led to the identification of the veratrole pyrazolinone (**121**), which can be considered to be a fragment consisting of a merged scaffold from a known PDE4 inhibitor, rolipram (**120**), and a cardiotoxic *h*PDE3 inhibitor (**119**) [84]. Subsequent fragment-growing yielded **122**. Examination of the pharmacological profile of **122** revealed sub-micromolar activity against the enzyme *Tbr*PDEB1 and *Tbr*PDEB (**TABLE 1**); however, it is up to tenfold more active against the human PDEs. This unwanted target selectivity profile does not appear to translate to the cellular assays, with good selectivity seen for the parasite over MRC5 cells. Compound **122** displayed sub-micromolar activity against *T. b. brucei* and was tenfold more active against *T. b. rhodesiense* (**FIGURE 36**).

Mechanism-based design

6PGDH is essential to the growth of bloodstream *T. brucei*; part of the pentose phosphate pathway, it is key in the production of NADPH (which helps to protect the parasite from oxidative stress) and ribulose 5-phosphate

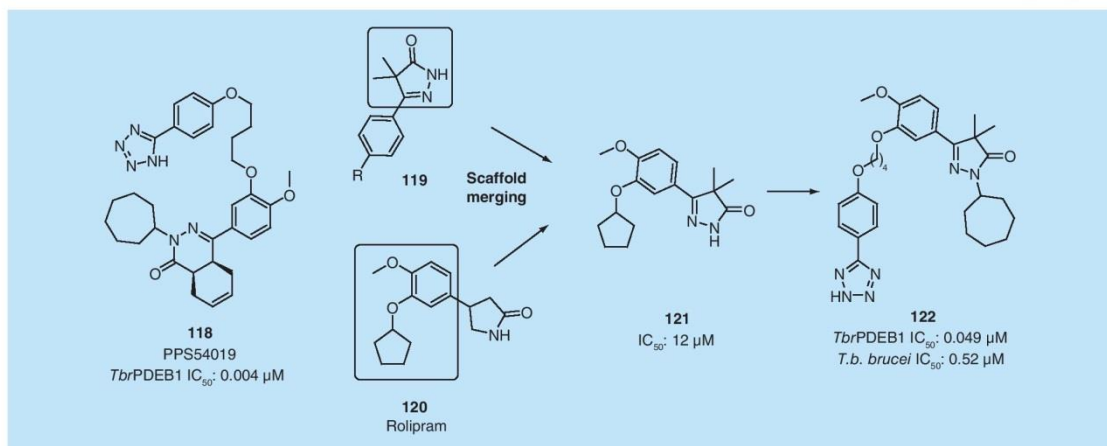


Figure 36. Identification of **122** with submicromolar activity in enzymatic and cellular assays as demonstrated in **TABLE 1**. The veratrole pyrazolinone (**121**) can be considered a product of scaffold merging between a known PDE4 inhibitor, rolipram (**120**), with a cardiotoxic *h*PDE3 inhibitor (**119**). Subsequent fragment growing of **121** yielded **122**.
T. b. brucei: *Trypanosoma brucei brucei*.

(carbohydrates are used in nucleotide and other biosynthetic pathways) [85]. In order to target 6PGDH, compounds designed to mimic the transition state and high energy intermediates were synthesized. This led to the identification of **123** (Figure 37), which was potent against the target and had good selectivity but had poor membrane permeability and so was inactive against the parasite [85]. A number of prodrugs were synthesized in order to overcome this issue, leading to the identification of improved compounds, such as **124** [86]. It was found that most of the prodrugs were active against the parasite although the activity was related to the stability of the prodrug in aqueous buffer [86]. It is likely that 6PGDH is the target, although this remains to be proven. Further optimization led to the identification of **125**, which is both potent and has a half-life ($T_{1/2}$) in mouse blood of 8 h indicating it is relatively stable to serum enzymes. Presumably, this allows passage of the prodrug into the parasite, where metabolism takes place and is critical to the conversion of the prodrug to the active species, which is cell-impermeable and which may accumulate in the parasite [87]. It is not at all obvious that this approach should either be straightforward or necessarily succeed, and this represents some very elegant work.

Chemotherapeutics from whole-organism assays

When conducting whole-parasite screening it is common to employ *T.b. brucei* as a surrogate for the human infective subspecies (*T.b. rhodesiense* and *T.b. gambiense*) as it is easier to culture and is devoid of the safety concerns that arise when working with human pathogenic organisms. Given that *T. brucei* is purely extracellular, it is

also much easier to work with than some other trypanosomes, such as *T. cruzi*, which requires mammalian cells to survive. In the latter case, one consequence of this is that intrinsically active compounds may give a negative readout, due to relative cellular impermeability. Additionally, compounds apparently active against *T. cruzi* may, in fact, merely be cytotoxic to the mammalian host cell, which under assay conditions is typically an L6 rat skeletal myoblast. This means that, when testing compounds against *T. cruzi*, a cytotoxicity value against the L6 cell line is required to ensure that the observed activity is due to the drug killing the parasite, rather than the drug killing the cells. This is not required when testing against *T. brucei* although of course it is still useful and indeed necessary to assess any compound for nonspecific cytotoxicity as part of compound progression criteria. For a comprehensive review on the small molecules and cell-based assays utilized to study infectious processes, see reference [88] and for a review around the development of whole-organism HTS assays for *T.b. brucei* and the advantages and disadvantages [89].

High-throughput whole-organism screening

A distinct disadvantage of target-based HTS is that it follows the notion that one drug must act solely on one target in order to obtain the observed therapeutic effect [7]. There is an increasing awareness and acceptance of poly-pharmacology whereby, better treatment of diseases may arise through the combination of drugs acting on a number of targets or through the ability of one drug to act on a number of targets [90]. Also, the advantage of whole-organism HTS is that screening hits are necessarily

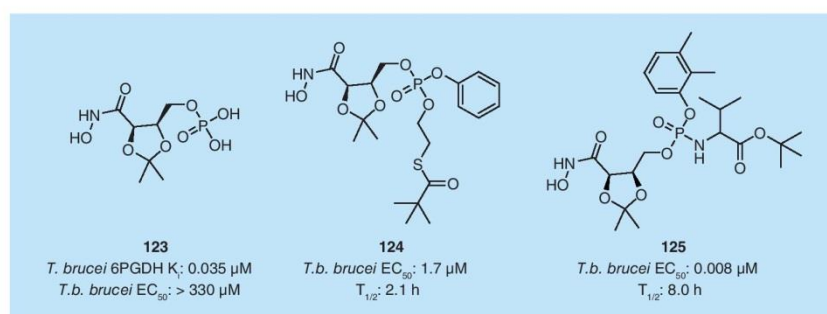


Figure 37. Biological activity for a substrate transition-state mimic for 6PGDH and the subsequent prodrugs synthesized. Compound **125** is both potent against *T.b. brucei* and has an excellent half-life in mouse blood.
T.b. brucei: *Trypanosoma brucei brucei*.

Table 2. Summary of compound classes identified in SCYNEXIS whole-organism high-throughput screening and the resultant outcome of hit-to-lead medicinal chemistry.

Compound Class	Best active [†]	Selectivity [‡]	Series outcome [§]
Aminoketones	15 μ M	47	Insufficient potency
Pyrimidoximes	70 nM	>143	Inactive in mouse serum
Arylazoles	200 nM	20	Limited selectivity
Aminooxazoles	3.8 μ M	>6	Insufficient potency
Sulfanilides	205 nM	>500	Poor properties
Heterocyclic ketones	5 nM	>2000	Active in mouse model [#]

[†]Most potent compound synthesized during hit-to-lead studies with the IC_{50} values against *Trypanosoma brucei brucei* parasites.
[‡]Measured against L929 fibroblast cells.
[§]Final decision was reached after compiling results from a variety of biological assays.
[#]Mice with an acute (stage 1) *Trypanosoma brucei brucei* infection were cured after treatment with a dose of 40 mg/kg/day for 4 days.

already active against the organism and so, the false negative issue associated with target-based HTS discussed earlier does not arise [7]. Another advantage is that if activity is indeed caused by interference in a number of different pathways, this could discourage the development of resistance. A disadvantage of whole-organism HTS is that pathway identification may be difficult, or that compounds with such polypharmacology may end up being promiscuous with respect to organism selectivity and hence non-progressable [7]. For *T. brucei*, whole-organism screening is essentially a subset of phenotypic screening, where the phenotypic readout in this case is

most commonly inhibition of parasite growth. This is becoming quite a common approach in the discovery of anti-infective and antiparasitic agents, where it is increasingly being seen that pathway-elucidation attempts can take place as late as during preclinical development.

A large screen was conducted by SCYNEXIS, whose primary screen involved approximately 48,000 compounds in a resazurin-based assay [40]. There were approximately 25 classes of compounds derived from the primary screen, which was narrowed down to just six after triage via a number of means. These include time-to-kill assays in order to determine compound-mediated killing of *T. brucei in vitro* over time, a test to establish the time required to cause persistent or irreversible antitrypanosomal effects by the compounds and a serum shift assay to assess any potential effects of protein binding on antitrypanosomal activity [40]. These classes have been summarized in **TABLE 2**. Unfortunately, no structures were available. Of these six classes the heterocyclic ketones were identified as having efficacy in a *T. brucei* mouse model of human infection and it was this class that was progressed through to lead optimization [40].

The most recent screen was conducted by the Avery group at the Eskitis Institute, in collaboration with DNDi and the Baell group [91]. The stage 1 HTS library [37,92] contains almost

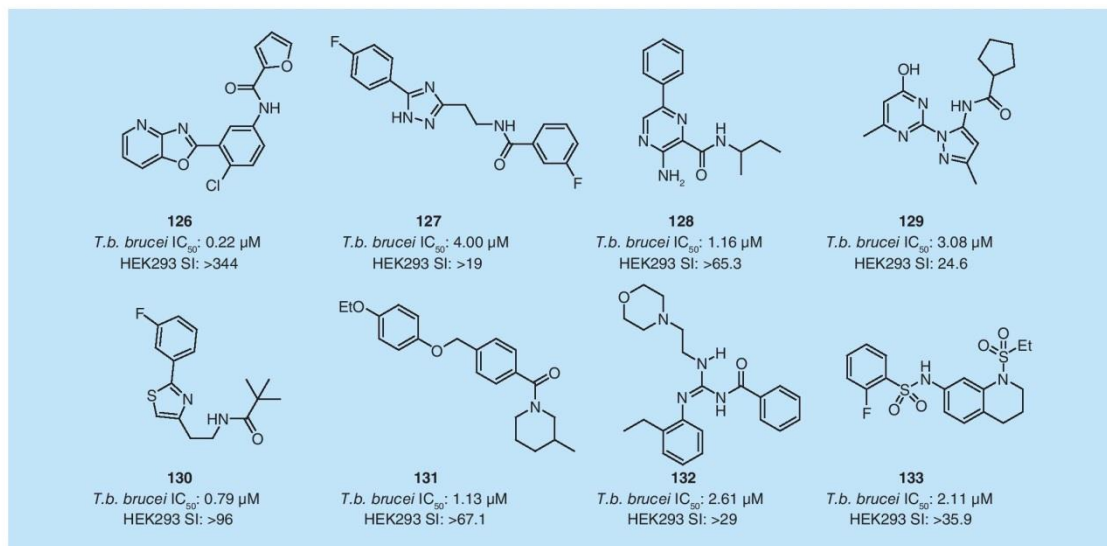


Figure 38. Summary of the compound classes identified in the Eskitis Institute whole-organism high-throughput screening with activity reported against *Trypanosoma brucei brucei*.
T. brucei: *Trypanosoma brucei brucei*.

88,000 compounds and was subjected to an AlamarBlue-based assay, which led to the identification of eight compound classes (FIGURE 38). These classes included pyridinoxazoles (126), 1,2,4-triazoles (127), pyrazines (128), pyrazolyl-pyridinyls (129), phenylthiazoles (130), benzamides (131), acyl-guanidines (132) and the sulfonyl amides (133). All the compounds have sub- to low-micromolar activity with SIs ranging from >19 to >344. Most were considered suitable for medicinal chemistry optimization, apart from 129 whose pyrazolyl-pyridinyl junction would be sensitive to nucleophilic attack.

An early SAR study (134) has recently been published on the optimization of 126, showing improvement in activity against *T.b. rhodesiense* and selectivity for the trypanosome over mammalian cells (135; FIGURE 39) [93]. Further work needs to be undertaken in order to optimize the solubility and metabolic stability of these compounds in the path to a preclinical program.

Phenotypic screening of drug libraries

This type of investigation is based on the screening and potential reuse of previously marketed drugs, known as repurposing. While target-based screening of FDA-approved drugs is sometimes undertaken, as was seen with the *TbTryR* section earlier, it is more traditional to screen such compounds against whole parasites. Such compounds are well described and may have favorable pharmacokinetic properties and can therefore represent promising starting points for development. This method might allow rapid access to a new drug at a relatively low development cost; this is attractive for small market diseases like HAT.

One of the first whole-cell HTS campaigns against *T.b. brucei* was conducted on a library of 2160 FDA-approved drugs and natural products (MicroSource Spectrum and Killer Collection) [94]. The assay utilized ATP-bioluminescence that was generated by the catalysis of luciferin to oxyluciferin by luciferase [94]. This process results in the generation of a fluorescent signal, the intensity of which can be measured and is proportional to the amount of ATP released from the trypanosomes and subsequently the number of viable parasites [94]. This initial screening campaign was considered a pilot screen and was utilized to test the efficacy of the luciferase assay in a high-throughput medium [94]. The advantage of this particular assay over the more common AlamarBlue assay is that it eliminates the time required for the parasite to chemically reduce the dye

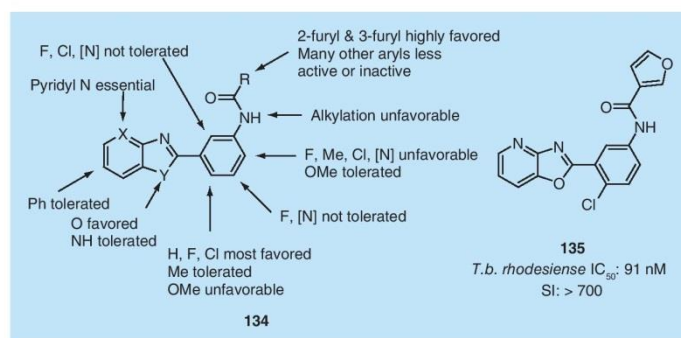


Figure 39. Summary of the medicinal chemistry optimization undertaken and the improvement in activity and selectivity obtained for 135.
T.b. rhodesiense: *Trypanosoma brucei rhodesiense*.

(which is variable between strains and so requires optimization) [94]. This would potentially result in a several-fold increase in the rate of throughput over the AlamarBlue assay [94]. This alternative ATP-detection screen was able to identify two of the current treatments for HAT, suramin (2) and pentamidine (1), as well as a number of other compounds [94]. Those compounds identified as being active in the assay exhibited >52% inhibition at 1 μ M, although to date there appears to have been no additional work undertaken in order to improve or investigate the activity of these compounds further.

The LOPAC 1280 library was subjected to a phenotypic screening campaign against *T. brucei* using a resazurin-based cell-viability assay [95]. The most potent and selective drugs to be identified as part of the screen were pentamidine (1) and suramin (2), which confirmed the robustness of this assay [95]. The most potent and selective novel inhibitor identified is a known κ -opioid agonist (136; FIGURE 40). Other structurally similar compounds had EC₅₀ values of approximately 5 μ M [95]. Pharmacokinetic

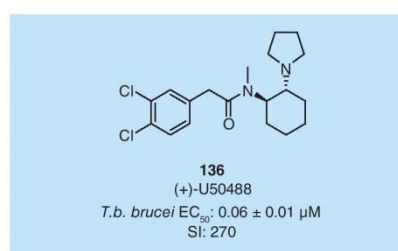


Figure 40. The novel, potent and selective κ -opioid agonist, (+)-U50488 (136).
T.b. brucei: *Trypanosoma brucei brucei*.

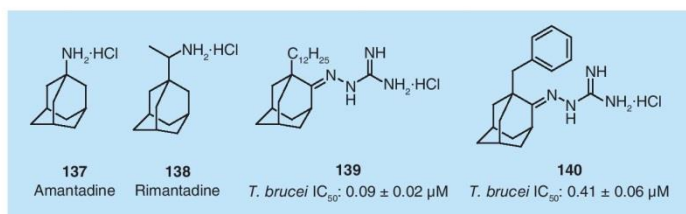


Figure 41. Adamantane derivatives discovered as part of a phenotypic screening against bloodstream *Trypanosoma brucei*.

T. brucei: *Trypanosoma brucei*.

studies on (+)-U50488 (**136**) were conducted on uninfected mice and revealed that the compound is not tightly bound to plasma protein and is well tolerated at a dose of 150 mg/kg orally [95]. Further to this, the brain to blood ratio was 8.2 indicating the potential for treatment of stage two HAT [95]. However, in a mouse model of *T. brucei* with a dosage of 150 mg/kg every 4 h for 32 h, the regimen was not curative with only one mouse showing a transient reduction in parasitemia followed by a relapse [95]. Further work is required in order to explore the SAR surrounding these compounds and improve the observed *in vivo* activity.

Focused phenotypic screening

Bloodstream *T. brucei* are known to be sensitive to amantadine (**137**) and rimantadine (**138**) [96]. As a result of this, a small library of adamantane derivatives was synthesized and the activity against bloodstream *T. brucei* reported (Figure 41) [96]. A number of compounds were identified with sub-micromolar activity including **139** and **140**. While the authors do not know the target of these compounds, it is suggested that these adamantane derivatives likely block or perturb an ion channel or transporter on the parasite membrane, as this is the only known mechanism by which these compounds are therapeutically effective [96].

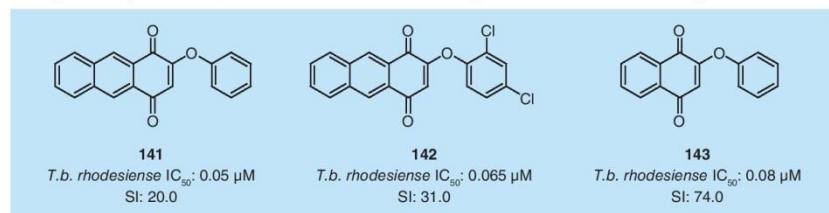


Figure 42. Quinone derivatives and their activity against bloodstream *Trypanosoma brucei rhodesiense* and SI values relative to L6 cells.

T. brucei rhodesiense: *Trypanosoma brucei rhodesiense*.

A library utilizing a quinone core was synthesized and tested for activity against *L. donovani*, *T. cruzi* and *T. b. rhodesiense* given the prominence of naphthoquinones and other related compounds that are often seen in natural products that are active against these parasites [97]. Compound **141** was the most active in the series, although it was only poorly selective over L6 cells [97]. Addition of halogen atoms to the phenyl ring (**142**) improved the selectivity somewhat, while still retaining potent activity [97]. However, removal of the left-hand-side phenyl group (**143**) led to a significant improvement in parasite selectivity, while still maintaining potent activity (Figure 42) [97]. However, toxicity would always be a concern when working with any quinone.

Bicyclic amines are common intermediates in the synthesis of a variety of natural substances [98]. A small library of bicyclic amines was synthesized and tested against a number of parasites including *L. donovani*, *T. cruzi*, *T. b. rhodesiense*, and *P. falciparum* K₁ and they demonstrated activity against the latter two organisms [98]. A number of sub-micromolar inhibitors were identified as in Figure 43. For the *in vivo* antitrypanosomal activity in *T. brucei* a dosage of 50 mg/kg four times a day by intraperitoneal (i.p.) administration was employed [98]. For the ester (**144**) it can be seen that only low *in vivo* activity was observed with no apparent change to the mean survival days (MSD) for mice treated with this compound [98]. The diamine (**145**) was slightly more active, extending the MSD by 2.25 days [98]. The most active compound reported was **146**, prolonging the mean survival time by 4.25 days [98]. A recent extension of this series has been reported [99], but good activity *in vivo* remains elusive.

A library of 1,4-benzodiazepin-2-ones was synthesized and evaluated for activity against bloodstream *T. brucei*. A preliminary SAR study was conducted, focusing on the R¹ and

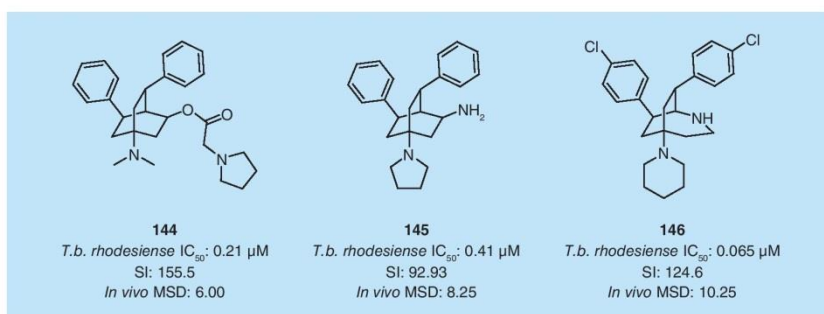


Figure 43. Activity of bicyclic amine derivatives against *Trypanosoma brucei rhodesiense* and the effect on the MSD in a mouse model of *Trypanosoma brucei brucei* where the control mean survival days was 6.00.

MSD: Mean survival days; *T.b. rhodesiense*: *Trypanosoma brucei rhodesiense*.

R² positions (summarized in **147**; **FIGURE 44**). The chirality at the R² position appears to be critical for the activity of these compounds [100]. This is exemplified by the activity observed for **148a**, which is eightfold more potent than **148b** [100]. Given the apparently large pocket around R³, a guanidine moiety was substituted onto the compound in order to try and improve cellular uptake by targeting the P2-transporter [100]. This proved successful, leading to the identification of a number of structurally similar compounds with a 100-fold increase over the lead compound (typified by **149**) [100]. Preliminary analysis of these compounds was performed in a number of cell lines, including: 427 wild-type, *TbAT1*^{-/-} (loss of P2- transporter) and B48 (loss of P2- transporter and high affinity pentamidine transporter) [100]. Compound **149** exhibits sub-micromolar activity in the wild-type strain and

diminution of the antitrypanosomal activity is observed as a result of the loss of the P2- transporter and a further loss is observed without the high-affinity pentamidine transporter [100]. This suggests that the guanidine moiety assists transport of the compound into the cell, although there appears to be an alternative route available given the reasonable IC₅₀ values still observed.

Chemical proteomics

A HTS of the SCYNEXIS library led to the identification of 2,4-diaminopyrimidines as inhibitors against *T. brucei* [101]. Further hit-to-lead and lead optimization activities led to the discovery of SCYX-5070 (**150**) [101]. Compound **150** has been tested *in vivo* and was shown to cure an acute mouse infection of *T. brucei* with a dosage regimen of 20 mg/kg twice daily for four days, either i.p. or orally (**FIGURE 45**) [101].

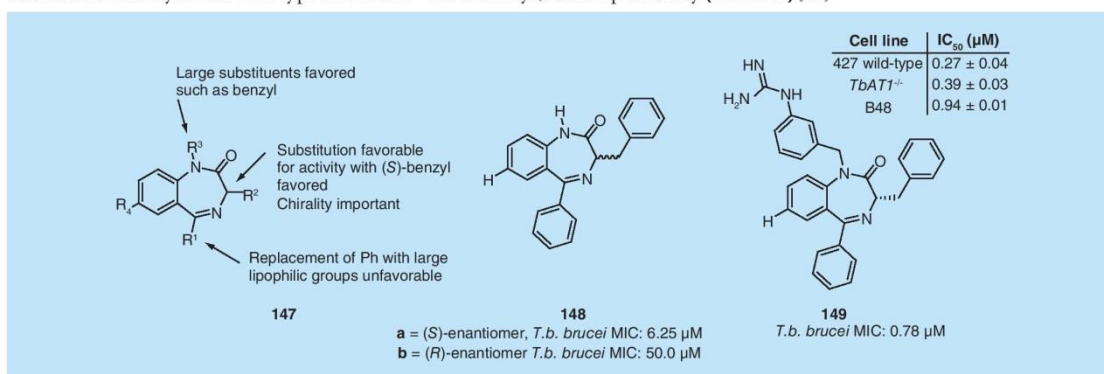


Figure 44. Preliminary structure–activity relationship around the 1,4-benzodiazepin-2-ones and the initial lead compound. Subsequent optimization gave **149**, which exhibited a 100-fold improvement in activity as well as sub-micromolar inhibition in a wild-type cell line of *Trypanosoma brucei*.
T.b. brucei: *Trypanosoma brucei brucei*.

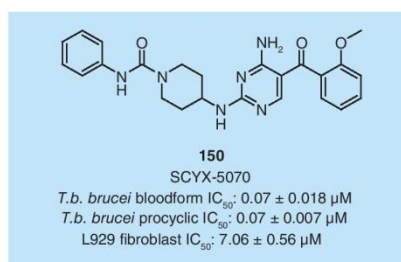


Figure 45. Optimized 2,4-diaminopyrimidine developed as a result of hit-to-lead medicinal chemistry after a high-throughput screening of the SCYNEXIS library. Chemical proteomics was employed to identify the target for these compounds.
T.b. brucei: *Trypanosoma brucei brucei*.

No toxicity was reported when this dose was increased to 50 mg/kg twice daily for four days, either i.p. or orally [101]. Utilization of chemical proteomics employing immobilized 2,4-diaminopyrimidine affinity chromatography and MS led to the identification of MAPKs and CRKs as potential targets for these compounds *in vivo* [101]. A brief SAR study has been performed, although only a slight improvement in overall activity was observed [102].

Natural products

Over the years drugs isolated from natural products have been instrumental in the fight against a variety of diseases. Perhaps the two most significant natural products relevant to this area were the identification and subsequent isolation of quinine and artemisinin for the treatment of malaria [103]. There have been a number of compounds that have been isolated from natural products and then tested against *T. brucei* [104–108]. Of the compounds described, many have inhibitory activity against trypanosome growth, typically in the mid- to low-micromolar

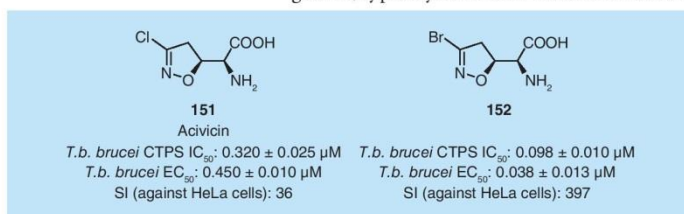


Figure 46. Acivicin and the most potent analog against *Trypanosoma brucei brucei* described in the literature.
T.b. brucei: *Trypanosoma brucei brucei*.

range, although only a small percentage have been assessed *in vivo* and no further drug optimization projects appear to have been performed on these compounds. There are a number of reviews on this area that illustrate the large number of natural products that have been screened and their varying sources [109–112].

Recently, a series of inhibitors derived from acivicin (**151**), an antibiotic isolated from the fermentable broths of *Streptomyces sviveus*, has been described (**FIGURE 46**) [113]. Acivicin (**151**) acts as a covalent inhibitor of a number of glutamine amidotransferases, including CTPS, which is responsible for the synthesis of CTP. Although expressed in both humans and the trypanosome, the latter organisms are more susceptible to inhibition of these enzymes, due to the low rate of synthesis and the lack of salvage pathways for cytidine [113]. Replacement of the chlorine with bromine (**152**) leads to a threefold improvement in activity against *T. brucei* CTPS with potent antitrypanosomal activity. However, some analogs were only very weakly antitrypanosomal while being potent CTPS inhibitors. It was not clear whether for such compounds, poor permeability was involved or indeed whether for compounds such as **152**, other targets may be involved in conferring potent antitrypanosomal activity.

Endoperoxide-containing molecules, merulin A (**153**), B and C have shown interesting inhibitory effects against *T.b. brucei* [114]. There are a number of other endoperoxide containing compounds that have been identified as antitrypanosomal compounds including artemisinin and sigmosceptrellin B [114]. An initial SAR study was conducted, which led to the identification of a number of key components in merulin A (**153**); including the endoperoxide bridge [114]. With this information, a second library of 20 compounds was synthesized, keeping the endoperoxide bridge intact, while also incorporating an acyl group to improve the drug-likeness of the merulin A core [114]. As a result of these investigations, several low- to mid- nanomolar inhibitory analogs (**154 & 155**) of merulin A were identified with high selectivity indices against HeLa and glioblastoma cells and good predicted BBB permeability (**FIGURE 47**) [114].

Azasterol (**156**) has been shown to inhibit *T.b. brucei* in micromolar concentrations [115]. This type of molecule is believed to inhibit the Δ²⁴-sterol methyltransferase enzyme. The sterol biosynthesis pathway has been identified as a target that could provide selectivity for the parasite over mammalian cells, due to a number of key

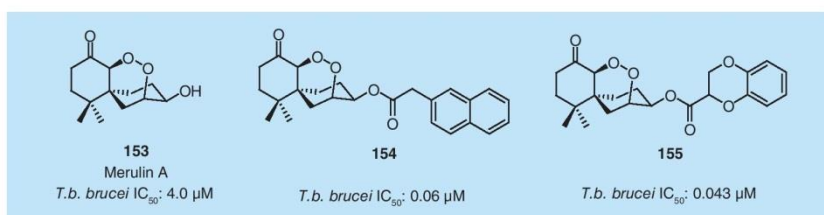


Figure 47. Merulin A (153) and the most potent derivatives against *Trypanosoma brucei brucei* with good predicted blood–brain barrier permeability.

T.b. brucei: *Trypanosoma brucei brucei*.

differences. The cell membranes of fungi, plants, *T. cruzi* and *L. donovani* consist of ergosterol and 24-alkylated sterols while mammalian plasma membranes consist of cholesterol [115]. The plasma membrane of procyclic *T. brucei* parasites has been shown to biosynthesize ergosterol and 24-alkylated sterols, while, in the bloodstream form, the parasite scavenges cholesterol from host cells [115]. A number of compounds, including **157**, were described as being potent against bloodstream form *T.b. rhodesiense* [115]. However, during the course of the investigation, it was shown that the biological target of these compounds was not Δ^{24} -sterol methyltransferase but another target. Proteomic studies and membrane-function assays were underway, but nothing has since been reported (**FIGURE 48**) [115].

An extensive study on the relationship between antiprotozoal activity and sesquiterpene lactones was described in 2012 [116], and 40 natural products bearing an exomethylene lactone were tested against several parasites (*T.b. rhodesiense*, *T. cruzi*, *L. donovani* and *P. falciparum*). Most of these showed potent inhibition of the parasite growth (low- to mid-micromolar range); unfortunately, this was associated with relatively high cytotoxicity in most cases (SIs from 1 to 10) [116]. This toxicity might be attributed to the presence of a Michael acceptor. The first natural product having *in vivo* activity against *T. brucei* was reported in 2012 [117]. Cynaropicrin (**158**) was isolated from the herb *Centaurea salmantica* L. (Asteraceae) and showed potent inhibition of *T.b. rhodesiense* and *gambiense* [117], also exhibiting activity against melarsoprol- and pentamidine-resistant strains (IC₅₀: 0.3 and 0.1 μM, respectively) with no cross-resistance [117]. Furthermore, i.p. administration of **158** into an acute mouse model of *T.b. rhodesiense* (10 mg/kg, twice-daily) led to a 92% reduction of parasitemia compared with untreated controls [117]. A deacylated derivative (**159**) was also identified in the plant extract although it was

found to be less active with poor selectivity for the parasite over L6 rat myoblast and murine peritoneal macrophages and with moderate selectivity against human colon adenocarcinoma cells [117]. The presence of a reactive α,β -unsaturated ester would also raise toxicity concerns with a low SI of 9.5. The furanone (**160**) showed reasonable inhibition against *T.b. rhodesiense* and *P. falciparum*; however, poor selectivity was observed [118]. 9 β -hydroxyparthenolide ester derivatives, such as **161**, were shown to be active against a panel of parasites including *T.b. rhodesiense*. Compound **161** only showed moderate selectivity for the parasite over L6 cells [119]. Other monoterpenes [120] and diterpenes [118,121,122], such as tetraprenylphenylacetic acid derivatives (**162**) and eleanolone (**163**), have also been described as potent inhibitors of *T. brucei* but have not been studied yet (**FIGURE 49**).

Recently, diketopiperazines isolated from deep water fungi have shown very interesting biological activities, including antitrypanosomal potential [123]. A short study on these disulfide-containing diketopiperazines have shown chaetocin (**164**) was very potent against *T. brucei*. Interestingly, its monomeric analog (commercially available), gliotoxin (**165**), is still very potent [123]. It is worth

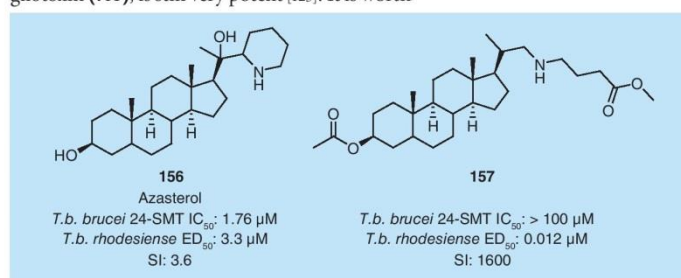


Figure 48. Azasterol derivative identified as a potent and selective inhibitor of *Trypanosoma brucei rhodesiense* although it is inactive against the proposed target, Δ^{24} -sterol methyltransferase.

T.b. brucei: *Trypanosoma brucei brucei*; *T.b. rhodesiense*: *Trypanosoma brucei rhodesiense*.

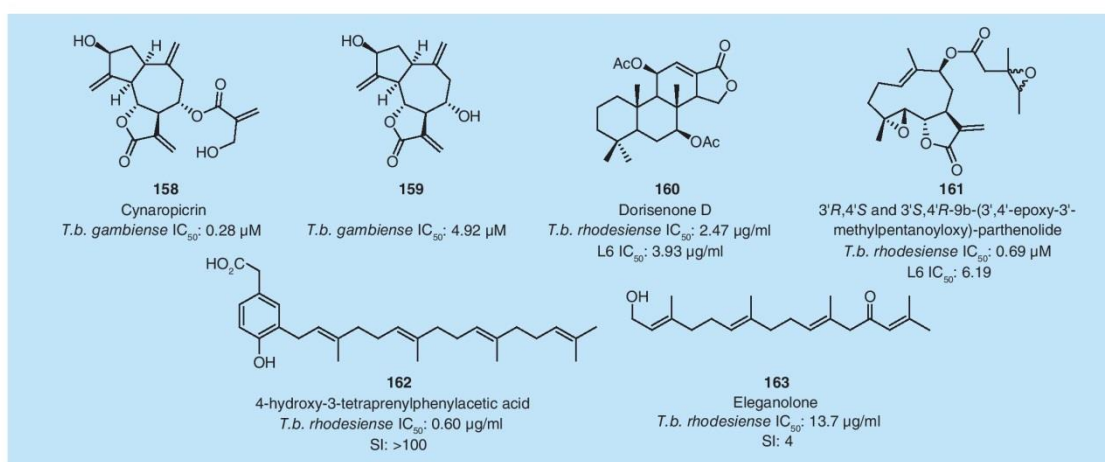


Figure 49. Cynaropicrin (**158**) and the deacylated derivative (**159**) identified in the plant extract from *Centaurea salmantica* L. (Asteraceae). Also shown are monoterpenes and diterpenes that have been described as *Trypanosoma brucei rhodesiense* inhibitors.
T.b. gambiense: *Trypanosoma brucei gambiense*; *T.b. rhodesiense*: *Trypanosoma brucei rhodesiense*.

noting that even less potent analogs without the disulfide moiety (**166**) are still active, but all these compounds suffer from a lack of selectivity for the trypanosome over mammalian cells (FIGURE 50).

A recent screen using extracts of *Carlina acaulis* (Asteraceae) showed carlina oxide (**167**) was able to inhibit the growth of *T. brucei* [123]. This natural product has been well known in Europe for several decades for its antimicrobial properties. Several other alkynoic acids (including **168**) have also been screened, although exhibiting only very weak inhibition against *T.b. rhodesiense* (FIGURE 51) [124]. Also, **168** has reportedly shown inhibition of *L. donovani* topoisomerase and is believed to inhibit a similar protein in *T. brucei* [124].

Nostocarboline (**169**), isolated from the cyanobacterium *Nostoc* 78-12A is a known inhibitor of hydrolytic enzymes, such as acetyl and butyryl cholinesterase and trypsin, while its toxicity is very low against the crustacean *Thamnocephalus platyurus* [125]. This template was therefore used as a starting point for an SAR study against several parasites, including *T. brucei* [125]. Compound **169** itself is only weakly active against *T.b. rhodesiense*, however, conversion into a symmetrical *bis* cationic dimer (**170**) resulted in a compound with submicromolar activity and showed an improved selectivity for the parasite over mammalian cells [125]. The structurally related cryptolepine (**171**) has also recently

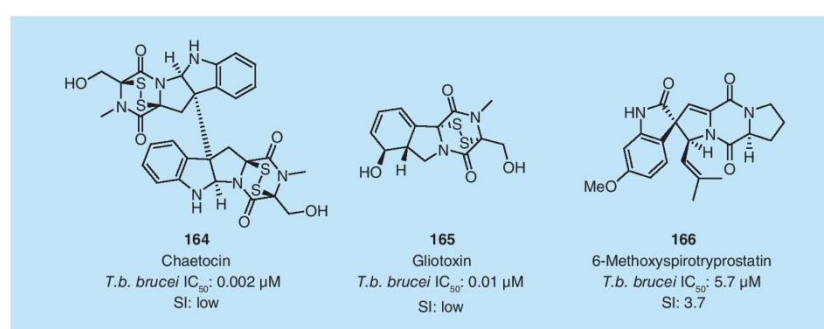


Figure 50. Diketopiperazine natural products and their activity against *Trypanosoma brucei*.
T.b. brucei: *Trypanosoma brucei brucei*.

been identified as a potential *T. brucei* inhibitor. This compound, isolated from *Cryptolepis sanguinolenta* (Lindl.) Schltr, showed antiparasitic activity but this was associated with cytotoxicity, due to its intercalative properties inhibiting the topoisomerase II [126]. Several analogs of this molecule were produced, resulting in products having low micromolar activity and good selectivity for the trypanosome over mammalian cells (Figure 52). Compound 172 showed a significant improvement in both activity and selectivity for the parasite over mammalian cells [126]. These molecules are presumably acting as cysteine protease inhibitors since they also show inhibition of rhodesain [126]. Ascididemine (173), another similar natural product has also been reported, which was isolated from *Polysyncrator achinatum* along with 174. No SAR study has been published, but both of these compounds have shown potent activity and reasonable selectivity toward

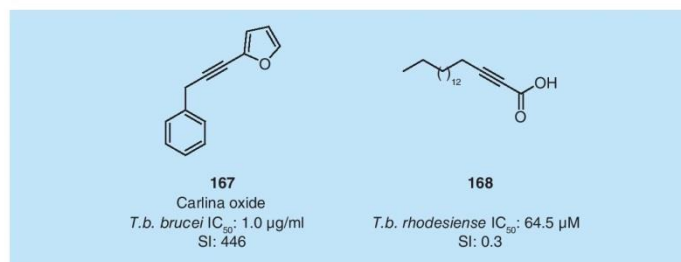


Figure 51. Alkyne containing natural products and their inhibitory activity against *Trypanosoma brucei*.

T. brucei: *Trypanosoma brucei brucei*; *T. brucei rhodesiense*: *Trypanosoma brucei rhodesiense*.

T. brucei over mammalian cells [127,128]. Ungeremine (175) and haemanthamine (176) have also been found to show antiparasitic activity against *T. brucei* [126]. Berberine (177) is known to be active against several parasites and was used as

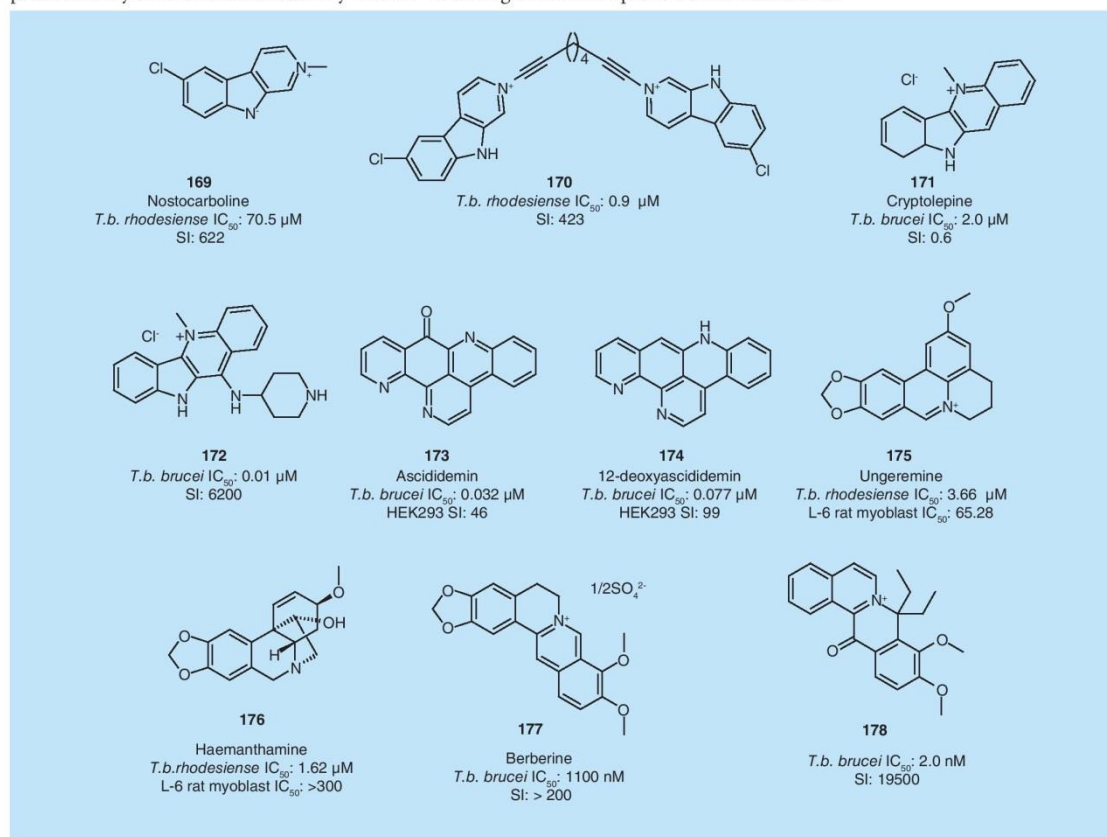


Figure 52. Pyridine- and pyridinium-containing natural products and related structures.

T. brucei: *Trypanosoma brucei brucei*; *T. brucei rhodesiense*: *Trypanosoma brucei rhodesiense*.

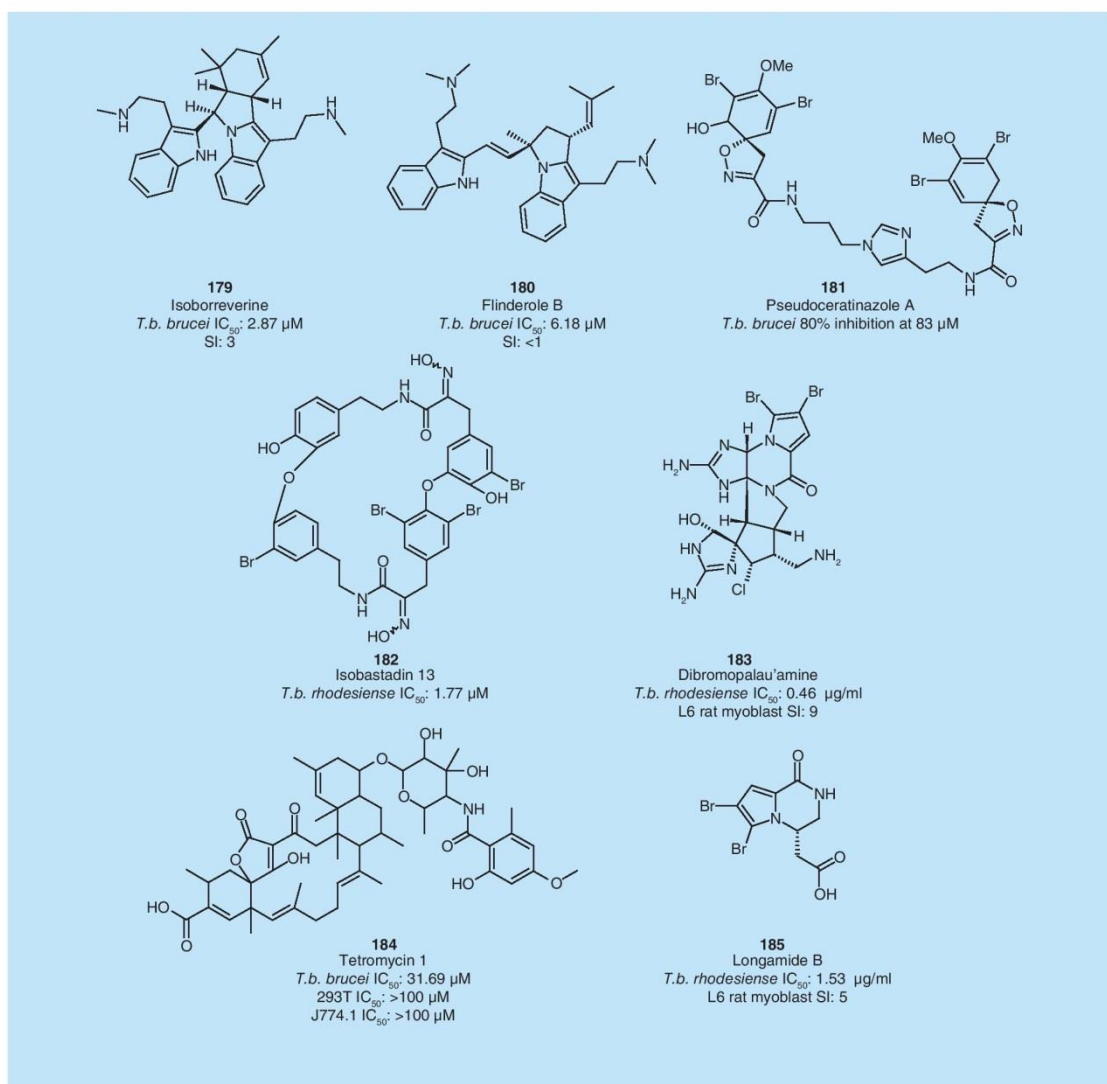


Figure 53. Alkaloids and secondary metabolites that have been identified as exhibiting activity against *Trypanosoma brucei brucei* or the human infective subspecies, *Trypanosoma brucei rhodesiense*.
T. b. brucei: *Trypanosoma brucei brucei*; *T. b. rhodesiense*: *Trypanosoma brucei rhodesiense*.

a starting point for an SAR study to discover new *T. brucei* inhibitors [129]. A few analogs have been prepared leading to another pyridinium type core (**178**) with a 500-fold increase in activity against *T. brucei* and a significant improvement in selectivity for the trypanosome over mammalian cells [130].

Some alkaloids and secondary metabolites have also been identified (**FIGURE 53**), such as

isoborreverine (**179**) and flinderoles (such as flinderole B, **180**). These products are shown to be reasonable inhibitors against *T. brucei* with IC₅₀ values in the low micromolar range, but they show poor selectivity for the trypanosome [131]. Bromopyrroles, such as dibromopalau'amine (**183**) and longamide B (**185**), were also tested with good inhibition of *T. b. rhodesiense*, but selectivity over mammalian cells was again an

issue [132]. Other compounds, such as pseudoceratinazole A (**181**) [133], isobastadin (**182**) [108] and tetracycline (**184**) [134] have also shown activity against the trypanosome. The general complexity of these molecules makes their use for SAR determination difficult and, therefore, a detailed exploration has not been performed around these compounds. In this regard, the relative simplicity of **185** could make it an interesting starting point for hit-to-lead optimization.

Phenolic type structures such as flavonoids (**186**), naphthoquinones (**187 & 188**), polyphenolics (**189–192**) and related natural products (**193**) were shown to be potential *T. brucei* inhibitors (**FIGURE 54**) [106,135–139]. These well-known structures often exhibit high toxicity and some (catechols and quinones) have been highlighted as pan-assay interference compounds, which are specific functional moieties that are responsible for producing false positive readings in a

variety of biological assays [37]. Unsurprisingly, these structures exhibit poor selectivity making their use for SAR difficult. Some toxicity concerns may arise during their study since some of these moieties are highly reactive similar to the nitronaphthoquinones described previously in **FIGURE 14**.

Ascofuranone (**194**) is a specific inhibitor of the trypanosome-alternative oxidase in *T. b. brucei* (*TbAO*), which is essential for the parasite survival in the host. Interestingly, compounds derived from ascofuranone (**194**) could potentially show excellent selectivity, since mammalian hosts lack this enzyme. Ascofuranone (**194**) has shown potent *in vitro* and *in vivo* activity against *T. b. brucei* [140,141]. A series of analogs were synthesized and their effect on *TbAO* investigated (**FIGURE 55**) [142]. The modifications around the furanone and linker led to **195**, which was more potent than the parent. The presence of a known toxicophore, such as an aldehyde,

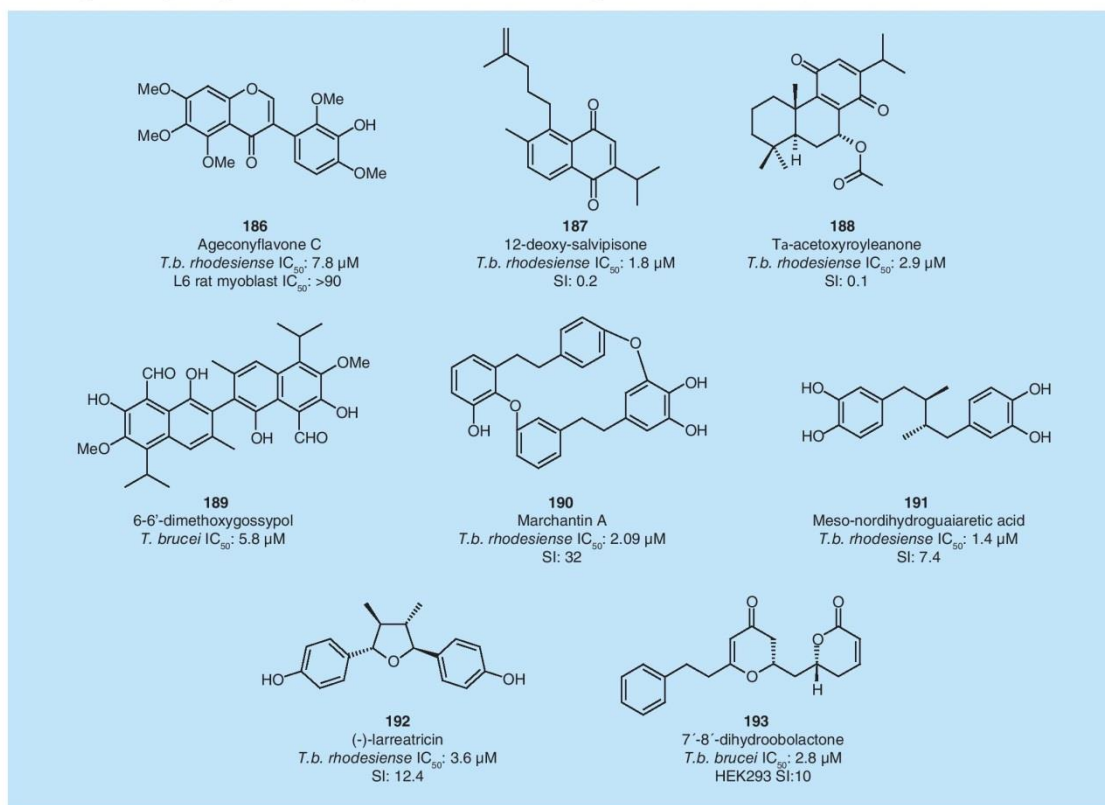


Figure 54. Flavonoid, naphthoquinones and related compounds with *Trypanosoma brucei* activity. *T. brucei*: *Trypanosoma brucei*; *T. b. brucei*: *Trypanosoma brucei brucei*; *T. b. rhodesiense*: *Trypanosoma brucei rhodesiense*.

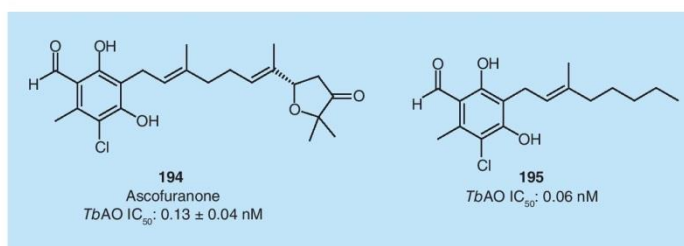


Figure 55. Ascofuranone (194) and its most potent derivative (195) synthesized to date.

may be a problem for the further development of these molecules as drugs. Unfortunately, no data on the selectivity of these compounds was described.

Clinical trials

Once a suitable candidate for HAT has been found, it can be progressed into clinical trials. However, this is no simple task. In addition to the standard regulations and problems associated with entering clinical trials, there are significant issues recruiting participants and identifying a suitable geographical area. In order to recruit just a single patient to a study, it is necessary to screen hundreds of people using mobile teams and a complex screening paradigm, including lumbar puncture for those people who are serologically and parasitologically positive, even although most are asymptomatic at the time of recruitment. In part, due to the relatively short flight range of the tsetse fly, HAT is a focal disease and over time a whole village can become heavily infected, while another nearby may be clear of the disease. Given this, once HAT has been cleared from an area, it may not return for many years. Since the introduction of NECT, most of the foci surrounding clinical research sites have been cleared, thus teams now have to look further afield for patients and new trial locations. Some of these sites can also be in countries or areas of civil unrest. Already this year, DNDi have had one site compromised [DON R, PERS. COMM.]. They were able to retrieve everything eventually and the patients will be treated, although they will not be recruited into the study [DON R, PERS. COMM.].

■ Path to market

There are a number of options available to register a new drug for the treatment of HAT.

- It may be possible to register a new drug through the FDA as an orphan drug. An

application under this banner may lead to a priority review being obtained. This is typically approved where the new drug would provide safe and effective therapy where no satisfactory alternative exists. As an orphan drug, many of the fees associated with registering a drug may be waived including the annual product and establishment fees;

- In Europe, the European Medicines Agency have created an Article 58 application. Under this type of application the European Medicines Agency provide advice during the clinical development process and allows the Committee for Medicinal Products for Human Use to provide ongoing feedback with regards to new drugs for neglected diseases. The advice is given with input and co-operation from WHO and regulators from the disease endemic countries;
- WHO prequalification is potentially available for some neglected diseases, including malaria, HIV/AIDS, tuberculosis and reproductive health. HAT is not specifically mentioned in this program. Under such an application a drug can be placed on to a prequalification list from which UN agencies, such as UNAIDS and UNICEF, can purchase drugs;
- A new initiative which is still evolving is centered around the idea of a pan-African regulator. This involves a number of African countries working together and combining their skills although many of these countries lack the critical mass to cover all the aspects of regulatory review.

The current option of choice centers around the European Medicines Agency, as this encourages engagement with WHO, Ministries of Health and regulators in the disease endemic countries. This helps guide the clinical development from a very early stage in the process. It is also likely that the continued distribution of new drugs for HAT will be carried out by WHO as part of their elimination program. As an alternative option WHO prequalification would be appealing for these same reasons if the scheme was to include HAT.

Conclusion

HAT has been neglected for a long time but is now receiving more and more interest from the scientific community. Sleeping sickness suffers from a lack of acceptable treatments, especially for chemotherapeutics, able to treat both

the hemolymphatic and neurological stages of the disease. Recent efforts are addressing these issues and molecules, such as fexinidazole (**18**) and SCYX-7158 (**51**), are being tested under Phase I/II clinical trials. Essentially, all known approaches to drug discovery are being applied. This has led to increasing reports of active compounds with new cores. A few show promise, but largely these compounds epitomize the difficulties of drug discovery. Compounds active against a target may not be active *in vitro* against the parasite. This could be due to a variety of causes such as compound instability, metabolic liability, or sub-optimal physicochemistry, which could negatively influence protein binding, solubility or membrane permeability. Compounding factors may include the requirement to inhibit the function of any intracellular target to a very large extent, as well as competition with cognate ligands or substrates that may exist in high local concentrations. This means that significant medicinal chemistry optimization to at least high nanomolar levels of target-based activity may be required before cellular activity is observed. Unfortunately, hits are often prematurely triaged on cell-based activity, and this can select for off-target compounds, leaving on-target compounds behind. One wonders how many such compounds, which may be intrinsically more likely to be successful in compound progression, have been overlooked due to inappropriate hit triage. Another barrier to observation of *in vitro* activity is that compounds could also be actively effluxed. Compounds that can overcome these obstacles to display *in vitro* activity may still not be active in animal models because related barriers exist *in vivo* but often to even greater degrees in the case of compound transport and metabolism, for example. Furthermore, compounds that are efficacious in animal models may not be efficacious in humans.

Publications in this area reflect an effort that is overall very front-ended. That is, compounds reported tend to be very early with very few progressing into promising *in vivo*, actives. This is plausibly attributable to the academic-heavy nature of the research effort, where early publication may be encouraged. Additionally, limited resources may hinder collection of downstream data useful for compound progression, such as ADMET properties and *in vivo* assessment of activity [143]. Animal models of HAT can be perceived to be relatively inaccessible, such that only the best compounds are likely

to be tested – compounds with more medicinal chemistry optimization than is often possible in an academic setting.

The attrition rate is likely to be very high for many of the compounds currently being reported with inhibitory activity towards *T. brucei* targets or *T. brucei* itself. This is because, while some new chemotypes are of high quality, many compounds are of poor structural quality, possessing reactive features and likely to be promiscuous and toxic. Indeed, it is quite remarkable how many of these compounds display inadequate selectivity for *T. brucei* over mammalian cells, or SAR against *T. brucei* that does not correlate with that against the intended target. Unfortunately, it is possible that the mere presence of a cell-based readout increases the chance of publication over a target-based active that is insufficiently developed to register on-target activity in the parasite. It is reassuring that observed disconnects between target-based and cellular activity are at least often commented on in such publications. The possibility of active uptake into the parasite is often evoked and, while this cannot be discounted, it seems unlikely that it would be so prevalent.

Among unattractive and reactive compounds frequently reported as *T. brucei* actives, quinones and catechols continue to be prevalent and highlight another complication in HAT drug discovery: that antiparasitics, like cytotoxic chemotherapeutics, can be useful even when containing promiscuous moieties and toxicophores. Quinones and catechols are prevalent in natural products. There is a developing notion that natural products have evolved to be useful in such cases and so much of the problematic medicinal chemistry optimization has been undertaken by nature. It is possible that a quinone-containing natural product with an excellent phenotypic and pharmacokinetic profile could be suitable for compound progression. It is also the case that promising HAT treatments such as fexinidazole (**18**) can contain the notoriously undrug-like toxicophore, the nitro group. Adding to the confusion is the successful clinical progression of a vinyl sulfone for the treatment of Chagas disease (although this is a nice example where target-based optimization and the contribution of significant benign SAR allows for subsequent incorporation of a warhead). Acceptance of the notion that reactive compounds may be useful antiparasitic agents may make it harder to reject

manuscripts reporting these. However, it is not clear that quinones or catechols or indeed any of the reactive compounds reported herein show promise as treatments for HAT. Instead, all the corresponding publications simply appear to add noise to the literature. On the whole, the acceptance of manuscripts reporting reactive, non-progressable compounds is still too lenient, and such work represents a significant waste of resources. What is not widely appreciated is that reactive, non-progressable compounds may furnish beguiling biological data, being potentially active towards a particular parasite and highly selective relative to mammalian cells. When we undertook both target-based and whole-organism HTS against *T. brucei* [51,91], many dozens of such compounds, including many quinones, were unearthed, from both approaches. That is, it is very easy to find compounds with this sort of profile. However, rather than attempt to progress them or to publish them, we chose to immediately remove such compounds from further consideration, in order to focus on those with benign chemotypes. It is not often appreciated that compounds can be usefully rejected based on structure alone even in the face of apparently acceptable early biological readouts.

While target-based drug discovery may be unfairly tarnished through limited ability to properly resource medicinal chemistry optimization, it is hard to argue against the worth of phenotypic screening in order to unearth the best possible starting points, with pathway identification coming later. The successes of bedaquiline [144] and NITD609 [145] attest to this approach. We are currently undertaking medicinal chemistry optimization of whole-cell HTS hits against *T. brucei* and understand that similar efforts are being undertaken elsewhere. We believe that, of the early compounds currently being reported, it is those arising from this approach that most likely will lead to new treatments for HAT, although resourcing hit-to-lead medicinal chemistry may be limiting. While there are now several initiatives worldwide with medicinal chemistry engines that could progress such compounds, this may not be beneficial to those outside such initiatives. Indeed, in our case, prior to successfully obtaining a competitive NHMRC project grant, we established an informal Australian Consortium of academic groups as the only way to progress medicinal chemistry. This comprised medicinal chemistry groups at the University of Western Australia, University of Wollongong, Sydney

University, Monash University, The Walter & Eliza Hall Institute of Medical Research and The University of Tasmania, with a key biology node at Griffith University. At each site, one or two students shared hit-to-lead medicinal chemistry progression, and this is largely continuing.

If target-based drug discovery is currently less likely to furnish new HAT treatments, this landscape may change as target validation information is further developed and if the importance of medicinal chemistry optimization and its resourcing is increasingly realized. The path for clinical progression of HAT treatments will not be easy and it is still relatively unexplored. Furthermore, attrition during downstream drug development remains very high. Overall success rates for 'first-in-human' to registration are around 11% (15% for infectious disease) [146]; most compounds will falter and fail, mainly due to lack of efficacy or to safety issues. For this reason, it is concerning that among funding bodies there appears to be a shift away from HAT and towards parasitic diseases, which are perceived to represent an even greater human burden and for which the pipeline is also poorly stocked, such as Chagas disease and the leishmaniasis. This is no doubt dictated by limited resources and it is hard to be critical of increased efforts in the latter two disease areas. Nevertheless, while HAT may today be a disease less neglected than it has been in the past, it is no time to relax efforts to discover new and better treatments. The product pipeline remains critically underpopulated.

Future perspective

As the academic research community becomes more experienced in drug discovery and hit quality continues to improve, the future pipeline for potential HAT treatments will increase significantly. As long as funding bodies maintain a certain commitment to supporting therapeutic development, then in partnership with academic collaborators and corporate goodwill, it may only be a matter of years before new and better treatments for HAT become available. However, the attrition rate in drug development is very high, and efforts towards HAT drug discovery should not be relaxed as soon as a new clinical candidate is reported. Research in this area, which is relatively poorly resourced, will benefit from continued collaboration, minimizing the duplication of work and accelerating the drug-discovery process.

Acknowledgements

The authors would like to acknowledge the contribution of R Don from DNDi for some useful comments in compiling the manuscript. This manuscript is dedicated to the memory of the late Ian Bathurst, a former employee of Medicines for Malaria Venture and a great champion for supporting Australasian research in tropical and neglected diseases.

Financial & competing interests disclosure

This research was supported by the NHMRC (NHMRC Senior Research Fellowship 1020411 (JB Baell), NHMRC Project Grant 1025581) and the Australian Government

for the Australian Postgraduate Award (L Ferrins). The authors acknowledge the Australian Federal Government Education Investment Fund Super Science Initiative and the Victorian State Government, Victoria Science Agenda Investment Fund for infrastructure support. The authors have no other relevant affiliations or financial involvement with any organization or entity with a financial interest in or financial conflict with the subject matter or materials discussed in the manuscript apart from those disclosed.

No writing assistance was utilized in the production of this manuscript.

Executive summary**Established chemotherapeutics**

- The current drugs available show unacceptable side effects and some drug resistance can be observed.
- No new drug has been brought to market in more than 10 years.

Current efforts towards antitrypanosomal compounds

- Two drugs are currently in Phase III clinical trials (fexinidazole and SCYX-7158).
- Many new chemotypes are being discovered as potential starting points for new treatments of HAT and a variety of approaches have been employed to identify these. Sources include target-based high-throughput screening, phenotypic high-throughput screening, focused screening, fragment-based drug discovery, *in silico* screening, natural products, modification of previously known actives and drugs.
- Some of the new chemotypes represent high-quality starting points, however there is still a number of compounds under investigation which contain undesirable functional groups known to be toxic and non-selective.

Conclusion

- A concerted effort has recently been made in this field and the major breakthrough appears to be on the horizon.

References

- 1 Brun R, Blum J, Chappuis F, Burri C. Human African trypanosomiasis. *Lancet* 375(9709), 148–159 (2010).
- 2 Deborggraeve S, Koffi M, Jamonneau V *et al.* Molecular analysis of archived blood slides reveals an atypical human trypanosoma infection. *Diagn. Microb. Infect. Dis.* 61(4), 428–433 (2008).
- 3 Torreele E, Bourdin Trunz B, Tweats D *et al.* Fexinidazole – a new oral nitroimidazole drug candidate entering clinical development for the treatment of sleeping sickness. *PLoS Negl. Trop. Dis.* 4(12), e923 (2010).
- 4 Kirchoff LV, Bacchi CJ, Machado FS *et al.* Trypanosomes. In: *Eukaryotic Microbes*. Schaechter M (Ed.). Academic Press, CA, USA, 744–757 (2009).
- 5 Vickerman K. Developmental cycles and biology of pathogenic trypanosomes. *Brit. Med. Bull.* 41(2), 105–114 (1985).
- 6 Jamonneau V, Ilboudo H, Kaboré J *et al.* Untreated human infections by *Trypanosoma brucei gambiense* are not 100% fatal. *PLoS Negl. Trop. Dis.* 6(6), e1691 (2012).
- 7 Barrett MP. Potential new drugs for human African trypanosomiasis: some progress at last. *Curr. Opin. Infect. Dis.* 23(6), 603–608 (2010).
- 8 Kuzoe FaS. Current situation of African trypanosomiasis. *Acta Tropica* 54(3–4), 153–162 (1993).
- 9 Nok AJ. Arsenicals (melarsoprol), pentamidine and suramin in the treatment of human African trypanosomiasis. *Parasitol. Res.* 90, 71–79 (2003).
- 10 Voogd TE, Vansterkenburg EL, Wilting J, Janssen LH. Recent research on the biological activity of suramin. *Pharmacol. Rev.* 45(2), 177–203 (1993).
- 11 De Koning HP. Transporters in African trypanosomes: role in drug action and resistance. *Int. J. Parasitol.* 31(5–6), 512–522 (2001).
- 12 Alford S, Eckert S, Baker N *et al.* High-throughput decoding of antitrypanosomal drug efficacy and resistance. *Nature* 482(7384), 232–236 (2012).
- 13 Pao SS, Paulsen IT, Saier MH. Major facilitator superfamily. *Microbiol. Mol. Biol. Rev.* 62(1), 1–34 (1998).
- 14 Seebeck T, Maser P. Drug resistance in african trypanosomiasis. In: *Antimicrobial Drug Resistance*. Mayers DL (Ed.). Humana Press, NY, USA, 589–604 (2009).
- 15 Burri C, Nkunku S, Merolle A, Smith T, Blum J, Brun R. Efficacy of new, concise schedule for melarsoprol in treatment of sleeping sickness caused by *Trypanosoma brucei gambiense*: a randomised trial. *Lancet* 355(9213), 1419–1425 (2000).
- 16 De Koning HP. Uptake of pentamidine in *Trypanosoma brucei brucei* is mediated by three distinct transporters: implications for cross-resistance with arsenicals. *Mol. Pharmacol.* 59(3), 586–592 (2001).
- 17 Shahi SK, Krauth-Siegel RL, Clayton CE. Overexpression of the putative thiol conjugate transporter *TbMRPA* causes melarsoprol resistance in *Trypanosoma brucei*. *Mol. Microbiol.* 43(5), 1129–1138 (2002).
- 18 Priotto G, Kasparian S, Mutombo W *et al.* Nifurtimox-eflornithine combination therapy for second-stage African *Trypanosoma brucei gambiense* trypanosomiasis: a multicentre, randomised, Phase III, non-inferiority trial. *Lancet* 374(9683), 56–64 (2009).

- 19 Wallace HM, Fraser AV, Hughes A. A perspective of polyamine metabolism. *Biochem. J.* 376(1), 1–14 (2003).
- 20 Balasegaram M, Young H, Chappuis F, Priotto G, Raguenaud M-E, Checchi F. Effectiveness of melarsoprol and eflornithine as first-line regimens for gambiense sleeping sickness in nine Médecins Sans Frontières programmes. *T. Roy. Soc. Trop. Med. H.* 103(3), 280–290 (2009).
- 21 Bahamontes-Rosa N, Rodríguez-Alejandre A, González-Del-Río R, García-Bustos JF, Mendoza-Losana A. A new molecular approach for cidal vs static antimalarial determination by quantifying mRNA levels. *Mol. Biochem. Parasitol.* 181(2), 171–177 (2012).
- 22 Yeramian P, Meshnick SR, Krudsood S *et al.* Efficacy of DB289 in Thai patients with *Plasmodium vivax* or acute, uncomplicated *Plasmodium falciparum* infections. *J. Infect. Dis.* 192(2), 319–322 (2005).
- 23 Goldsmith RB, Gray DR, Yan Z, Generaux CN, Tidwell RR, Reisner HM. Application of monoclonal antibodies to measure metabolism of an anti-trypanosomal compound *in vitro* and *in vivo*. *J. Clin. Lab. Anal.* 24(3), 187–194 (2010).
- 24 Wenzler T, Boykin DW, Ismail MA, Hall JE, Tidwell RR, Brun R. New treatment option for second-stage African sleeping sickness: *in vitro* and *in vivo* efficacy of aza analogs of DB289. *Antimicrob. Agents Chemother.* 53(10), 4185–4192 (2009).
- 25 Thuita JK, Wolf KK, Murilla GA *et al.* Safety, pharmacokinetic, and efficacy studies of oral DB868 in a first stage vervet monkey model of human African trypanosomiasis. *PLoS Negl. Trop. Dis.* 7(6), e2230 (2013).
- 26 Thuita JK, Wang MZ, Kagira JM *et al.* Pharmacology of DB844, an orally active aza analogue of pafuramidine, in a monkey model of second stage human African trypanosomiasis. *PLoS Negl. Trop. Dis.* 6(7), e1734 (2012).
- 27 Patrick DA, Bakunov SA, Bakunova SM *et al.* Synthesis and antiprotozoal activities of benzyl phenyl ether diamidine derivatives. *Eur. J. Med. Chem.* 67, 310–324 (2013).
- 28 Bouchard P, Sai P, Reach G, Caubarrere I, Ganeval D, Assan R. Diabetes mellitus following pentamidine-induced hypoglycemia in humans. *Diabetes* 31(1), 40–45 (1982).
- 29 Murphey SA, Josephs AS. Acute pancreatitis associated with pentamidine therapy. *Arch. Int. Med.* 141(1), 56–58 (1981).
- 30 Bot C, Hall BS, Álvarez G *et al.* Evaluating 5-nitrofurans as trypanocidal agents. *Antimicrob. Agents Chemother.* 57(4), 1638–1647 (2013).
- 31 Wilkinson SR, Taylor MC, Horn D, Kelly JM, Cheeseman I. A mechanism for cross-resistance to nifurtimox and benznidazole in trypanosomes. *Proc. Natl Acad. Sci. USA* 105(13), 5022–5027 (2008).
- 32 Wilkinson SR, Bot C, Kelly JM, Hall BS. Trypanocidal activity of nitroaromatic prodrugs: current treatments and future perspectives. *Curr. Top. Med. Chem.* 11(16), 2072–2084 (2011).
- 33 Samant BS, Sukhthankar MG. Compounds containing 2-substituted imidazole ring for treatment against human African trypanosomiasis. *Bioorg. Med. Chem. Lett.* 21(3), 1015–1018 (2011).
- 34 Trunz BB, Jedrysiak R, Tweats D *et al.* 1-Aryl-4-nitro-1H-imidazoles, a new promising series for the treatment of human African trypanosomiasis. *Eur. J. Med. Chem.* 46(5), 1524–1535 (2011).
- 35 Hwang JY, Smithson D, Connelly M, Maier J, Zhu F, Guy KR. Discovery of halo-nitrobenzamides with potential application against human African trypanosomiasis. *Bioorg. Med. Chem. Lett.* 20(1), 149–152 (2010).
- 36 Samant BS, Chakaingesu C. Novel naphthoquinone derivatives: synthesis and activity against human African trypanosomiasis. *Bioorg. Med. Chem. Lett.* 23(5), 1420–1423 (2013).
- 37 Baell JB, Holloway GA. New substructure filters for removal of pan assay interference compounds (PAINS) from screening libraries and for their exclusion in bioassays. *J. Med. Chem.* 53(7), 2719–2740 (2010).
- 38 Oprea TI, Bologa CG, Boyer S *et al.* A crowdsourcing evaluation of the NIH chemical probes. *Nat. Chem. Biol.* 5(7), 441–447 (2009).
- 39 Arán VJ, Kaiser M, Dardonville C. Discovery of nitroheterocycles active against African trypanosomes. *In vitro* screening and preliminary SAR studies. *Bioorg. Med. Chem. Lett.* 22(14), 4506–4516 (2012).
- 40 Bowling T, Mercer L, Don R, Jacobs R, Nare B. Application of a resazurin-based high-throughput screening assay for the identification and progression of new treatments for human African trypanosomiasis. *Int. J. Parasitol. Drugs Drug Resist.* 2, 262–270 (2012).
- 41 Boiani L, Gerpe A, Arán VJ *et al.* *In vitro* and *in vivo* antitrypanosomatid activity of 5-nitroindazoles. *Eur. J. Med. Chem.* 44(3), 1034–1040 (2009).
- 42 Vega MC, Montero-Torres A, Marrero-Ponce Y *et al.* New ligand-based approach for the discovery of antitrypanosomal compounds. *Bioorg. Med. Chem. Lett.* 16(7), 1898–1904 (2006).
- 43 Jacobs RT, Nare B, Wring SA *et al.* SCYX-7158, an orally-active benzoxaborole for the treatment of stage 2 human African trypanosomiasis. *PLoS Negl. Trop. Dis.* 5(6), e1151 (2011).
- 44 Nare B, Wring S, Bacchi C *et al.* Discovery of novel orally bioavailable oxaborole 6-carboxamides that demonstrate cure in a murine model of late-stage central nervous system African trypanosomiasis. *Antimicrob. Agents Chemother.* 54(10), 4379–4388 (2010).
- 45 Frearson JA, Brand S, Mcelroy SP *et al.* *N*-myristoyltransferase inhibitors as new leads to treat sleeping sickness. *Nature* 464(7289), 728–732 (2010).
- 46 Smithson DC, Lee J, Shelat AA, Phillips MA, Guy RK. Discovery of potent and selective inhibitors of *Trypanosoma brucei* ornithine decarboxylase. *J. Biol. Chem.* 285(22), 16771–16781 (2010).
- 47 Spinks D, Ong HB, Mpamhanga CP *et al.* Design, synthesis and biological evaluation of novel inhibitors of *Trypanosoma brucei* pteridine reductase 1. *ChemMedChem* 6(2), 302–308 (2011).
- 48 Fueller F, Jehle B, Putzker K, Lewis JD, Krauth-Siegel RL. High throughput screening against the peroxidase cascade of African trypanosomes identifies antiparasitic compounds that inactivate tryparedoxin. *J. Biol. Chem.* 287(12), 8792–8802 (2012).
- 49 Major LL, Smith TK. Screening the MayBridge rule of 3 fragment library for compounds that interact with the *Trypanosoma brucei* myo-inositol-3-phosphatase and/or show trypanocidal activity. *Mol. Biol. Int.* 2011, 389364 (2011).
- 50 Holloway GA, Baell JB, Fairlamb AH *et al.* Discovery of 2-iminobenzimidazoles as a new class of trypanothione reductase inhibitor by high-throughput screening. *Bioorg. Med. Chem. Lett.* 17(5), 1422–1427 (2007).
- 51 Holloway GA, Charman WN, Fairlamb AH *et al.* Trypanothione reductase high-throughput screening campaign identifies novel classes of inhibitors with antiparasitic activity. *Antimicrob. Agents Chemother.* 53(7), 2824–2833 (2009).
- 52 Richardson JL, Nett IRE, Jones DC, Abdille MH, Gilbert IH, Fairlamb AH. Improved tricyclic inhibitors of trypanothione reductase by screening and chemical synthesis. *ChemMedChem* 4(8), 1333–1340 (2009).
- 53 Spinks D, Torrie LS, Thompson S *et al.* Design, synthesis and biological evaluation of *Trypanosoma brucei* trypanothione synthetase inhibitors. *ChemMedChem* 7(1), 95–106 (2012).

- 54 Lessene G, Czabotar PE, Sleebs BE *et al.* Structure-guided design of a selective BCL-XL inhibitor. *Nat. Chem. Biol.* 9(6), 390–397 (2013).
- 55 Patterson S, Jones DC, Shanks EJ *et al.* Synthesis and evaluation of 1-(1-(benzo[*b*]thiophen-2-yl)cyclohexyl)piperidine (BTCP) analogues as inhibitors of trypanothione reductase. *ChemMedChem* 4(8), 1341–1353 (2009).
- 56 Kameyama M, Siqueira FA, Garcia-Mijares M, Silva LF Jr, Silva MTA. Indatraline: synthesis and effect on the motor activity of wistar rats. *Molecules* 16(11), 9421–9438 (2011).
- 57 Berger P, Janowsky A, Vocci F, Skolnick P, Schweri MM, Paul SM. [³H]GBR-12935: a specific high affinity ligand for labeling the dopamine transport complex. *Eur. J. Pharmacol.* 107(2), 289–290 (1985).
- 58 Wermuth CG. Selective optimization of side activities: the SOSA approach. *Drug Discov. Today* 11(3–4), 160–164 (2006).
- 59 Patterson S, Alphey MS, Jones DC *et al.* Dihydroquinazolines as a novel class of *Trypanosoma brucei* trypanothione reductase inhibitors: discovery, synthesis, and characterization of their binding mode by protein crystallography. *J. Med. Chem.* 54(19), 6514–6530 (2011).
- 60 Bosc D, Lethu S, Mouray E, Grellier P, Dubois J. Improvement of the trypanocidal activity of 3-arylthiophene farnesyltransferase inhibitors by modulation of their 3-aryl group. *MedChemComm* 3(12), 1512–1517 (2012).
- 61 Ettari R, Tamborini L, Angelo IC *et al.* Inhibition of rhodesain as a novel therapeutic modality for human African trypanosomiasis. *J. Med. Chem.* 56(14), 5637–5658 (2013).
- 62 Nikolskaia OV, De ALaP, Kim YV *et al.* Blood-brain barrier traversal by African trypanosomes requires calcium signaling induced by parasite cysteine protease. *J. Clin. Invest.* 116(10), 2739–2747 (2006).
- 63 Overath P, Chaudhri M, Steverding D, Ziegelbauer K. Invariant surface proteins in bloodstream forms of *Trypanosoma brucei*. *Parasitol. Today* 10(2), 53–58 (1994).
- 64 Waag T, Gelhaus C, Rath J, Stich A, Leippe M, Schirmeister T. Allicin and derivatives are cysteine protease inhibitors with antiparasitic activity. *Bioorg. Med. Chem. Lett.* 20(18), 5541–5543 (2010).
- 65 Yang P-Y, Wang M, Li L, Wu H, He CY, Yao SQ. Design, synthesis and biological evaluation of potent azadipeptide nitrile inhibitors and activity-based probes as promising anti-*Trypanosoma brucei* agents. *Chemistry* 18(21), 6528–6541 (2012).
- 66 Mott BT, Ferreira RS, Simeonov A *et al.* Identification and optimization of inhibitors of trypanosomal cysteine proteases: cruzain, rhodesain, and TbCatB. *J. Med. Chem.* 53(1), 52–60 (2009).
- 67 Mallari JP, Shelat A, Kosinski A *et al.* Discovery of trypanocidal thiosemicarbazone inhibitors of rhodesain and TbCatB. *Bioorg. Med. Chem. Lett.* 18(9), 2883–2885 (2008).
- 68 Vicik R, Hoerr V, Glaser M *et al.* Aziridine-2,3-dicarboxylate inhibitors targeting the major cysteine protease of *Trypanosoma brucei* as lead trypanocidal agents. *Bioorg. Med. Chem. Lett.* 16(10), 2753–2757 (2006).
- 69 Breuning A, Degel BR, Schulz F *et al.* Michael acceptor based antiplasmodial and antitrypanosomal cysteine protease inhibitors with unusual amino acids. *J. Med. Chem.* 53(5), 1951–1963 (2010).
- 70 Rogers KE, Keränen H, Durrant JD *et al.* Novel cruzain inhibitors for the treatment of Chagas' disease. *Chem. Biol. Drug Des.* 80(3), 398–405 (2012).
- 71 Langolf S, Machon U, Ehlers M *et al.* Development of antitrypanosomal and antiplasmodial nonpeptidic cysteine protease inhibitors based on *N*-protected-guanidino-furan and -pyrrole building blocks. *ChemMedChem* 6(9), 1581–1586 (2011).
- 72 Hiltensperger G, Jones NG, Niedermeier S *et al.* Synthesis and structure–activity relationships of new quinolone-type molecules against *Trypanosoma brucei*. *J. Med. Chem.* 55(6), 2538–2548 (2012).
- 73 Alsford S, Turner DJ, Obado SO *et al.* High-throughput phenotyping using parallel sequencing of RNA interference targets in the African trypanosome. *Genome Res.* 21(6), 915–924 (2011).
- 74 Ojo KK, Gillespie JR, Riechers AJ *et al.* Glycogen synthase kinase 3 is a potential drug target for African trypanosomiasis therapy. *Antimicrob. Agents Chemother.* 52(10), 3710–3717 (2008).
- 75 Woodland A, Grimaldi R, Luksch T *et al.* From on-target to off-target activity: identification and optimisation of *Trypanosoma brucei* GSK3 inhibitors and their characterisation as anti-*Trypanosoma brucei* drug discovery lead molecules. *ChemMedChem* 8(7), 1127–1137 (2013).
- 76 Lin R, Connolly PJ, Huang S *et al.* 1-acyl-1*H*-[1,2,4]triazole-3,5-diamine analogues as novel and potent anticancer cyclin-dependent kinase inhibitors: synthesis and evaluation of biological activities. *J. Med. Chem.* 48(13), 4208–4211 (2005).
- 77 Laha JK, Zhang X, Qiao L *et al.* Structure–activity relationship study of 2,4-diaminothiazoles as CDK5/p25 kinase inhibitors. *Bioorg. Med. Chem. Lett.* 21(7), 2098–2101 (2011).
- 78 Patel G, Karver CE, Behera R *et al.* Kinase scaffold repurposing for neglected disease drug discovery: discovery of an efficacious, Lapatanib-derived lead compound for trypanosomiasis. *J. Med. Chem.* 56(10), 3820–3832 (2013).
- 79 Deterding A, Dungey FA, Thompson K-A, Steverding D. Anti-trypanosomal activities of DNA topoisomerase inhibitors. *Acta Tropica* 93(3), 311–316 (2005).
- 80 Ding D, Meng Q, Gao G *et al.* Design, synthesis, and structure–activity relationship of *Trypanosoma brucei* leucyl-tRNA synthetase inhibitors as antitrypanosomal agents. *J. Med. Chem.* 54(5), 1276–1287 (2011).
- 81 Jansen C, Wang H, Kooistra AJ *et al.* Discovery of novel *Trypanosoma brucei* phosphodiesterase B1 inhibitors by virtual screening against the unliganded TbRPDEB1 crystal structure. *J. Med. Chem.* 56(5), 2087–2096 (2013).
- 82 Baell JB. Observations on screening-based research and some concerning trends in the literature. *Future Med. Chem.* 2(10), 1529–1546 (2010).
- 83 Baell JB. Redox-active nuisance screening compounds and their classification. *Drug Discov. Today* 16(17–18), 840–841 (2011).
- 84 Orling KM, Jansen C, Vu XL *et al.* Catechol pyrazolones as trypanocidals: fragment-based design, synthesis, and pharmacological evaluation of nanomolar inhibitors of trypanosomal phosphodiesterase B1. *J. Med. Chem.* 55(20), 8745–8756 (2012).
- 85 Dardonville C, Rinaldi E, Barrett MP, Brun R, Gilbert IH, Hanau S. Selective inhibition of *Trypanosoma brucei* 6-phosphogluconate dehydrogenase by high-energy intermediate and transition-state analogues. *J. Med. Chem.* 47(13), 3427–3437 (2004).
- 86 Ruda GF, Alibu VP, Mitsos C *et al.* Synthesis and biological evaluation of phosphate prodrugs of 4-phospho-D-erythronhydroxamic acid, an inhibitor of 6-phosphogluconate dehydrogenase. *ChemMedChem* 2(8), 1169–1180 (2007).
- 87 Ruda GF, Wong PE, Alibu VP *et al.* Aryl phosphoramidates of 5-phospho erythronhydroxamic acid, a new class of potent trypanocidal compounds. *J. Med. Chem.* 53(16), 6071–6078 (2010).
- 88 Muskavitch MAT, Barteneva N, Gubbels M-J. Chemogenomics and parasitology: small molecules and cell-based assays to study. *Comb. Chem. High Throughput Screen.* 11(8), 624–646 (2008).

- 89 Jones AJ, Avery VM. Whole-organism high-throughput screening against *Trypanosoma brucei brucei*. *Exp. Opin. Drug Discov.* 8(5), 495–507 (2013).
- 90 Boran AD, Iyengar R. Systems approaches to polypharmacology and drug discovery. *Curr. Opin. Drug Discov. Devel.* 13(3), 297–309 (2010).
- 91 Sykes ML, Baell JB, Kaiser M *et al.* Identification of compounds with anti-proliferative activity against *Trypanosoma brucei brucei* strain 427 by a whole cell viability based HTS campaign. *PLoS Negl. Trop. Dis.* 6(11), e1896 (2012).
- 92 Baell JB. Broad coverage of commercially available lead-like screening space with fewer than 350,000 compounds. *J. Chem. Inf. Model.* 53(1), 39–55 (2012).
- 93 Ferrins L, Rahmani R, Sykes ML *et al.* 3-(oxazol[4,5-*b*]pyridin-2-yl)anilides as a novel class of potent inhibitors for the kinetoplastid *Trypanosoma brucei*, the causative agent for human African trypanosomiasis. *Eur. J. Med. Chem.* 66, 450–465 (2013).
- 94 Mackey ZB, Baca AM, Mallari JP *et al.* Discovery of trypanocidal compounds by whole cell HTS of *Trypanosoma brucei*. *Chem. Biol. Drug Des.* 67(5), 355–363 (2006).
- 95 Jones DC, Hallyburton I, Stojanovski L, Read KD, Frearson JA, Fairlamb AH. Identification of a κ -opioid agonist as a potent and selective lead for drug development against human African trypanosomiasis. *Biochem. Pharmacol.* 80(10), 1478–1486 (2010).
- 96 Papanastasiou I, Tsotinis A, Kolocouris N, Prathalingam SR, Kelly JM. Design, synthesis, and trypanocidal activity of new aminoadamantane derivatives. *J. Med. Chem.* 51(5), 1496–1500 (2008).
- 97 Bolognesi ML, Lizzi F, Perozzo R, Brun R, Cavalli A. Synthesis of a small library of 2-phenoxy-1,4-naphthoquinone and 2-phenoxy-1,4-antraquinone derivatives bearing anti-trypanosomal and anti-leishmanial activity. *Bioorg. Med. Chem. Lett.* 18(7), 2272–2276 (2008).
- 98 Weis R, Seebacher W. New bicyclic amines: synthesis and SARs of their action against the causative organisms of malaria and sleeping sickness. *Curr. Med. Chem.* 16(11), 1426–1441 (2009).
- 99 Faist J, Seebacher W, Kaiser M, Brun R, Saf R, Weis R. Antiprotozoal activity of bicyclic diamines with a *N*-methylpiperazinyl group at the bridgehead atom. *Bioorg. Med. Chem.* 21(17), 4988–4996 (2013).
- 100 Spencer J, Rathnam RP, Harvey AL *et al.* Synthesis and biological evaluation of 1,4-benzodiazepin-2-ones with antitrypanosomal activity. *Bioorg. Med. Chem.* 19(5), 1802–1815 (2011).
- 101 Mercer L, Bowling T, Perales J *et al.* 2,4-diaminopyrimidines as potent inhibitors of *Trypanosoma brucei* and identification of molecular targets by a chemical proteomics approach. *PLoS Negl. Trop. Dis.* 5(2), e956 (2011).
- 102 Perales JB, Freeman J, Bacchi CJ *et al.* SAR of 2-amino and 2,4-diamino pyrimidines with *in vivo* efficacy against *Trypanosoma brucei*. *Bioorg. Med. Chem. Lett.* 21(10), 2816–2819 (2011).
- 103 Hannaert V. Sleeping sickness pathogen (*Trypanosoma brucei*) and natural products: therapeutic targets and screening systems. *Planta Med.* 77(06), 586–597 (2011).
- 104 Feng Y, Davis RA, Sykes ML, Avery VM, Quinn RJ. Iatrochamides A and B, antitrypanosomal compounds from the Australian marine sponge *Iatrochota* sp. *Bioorg. Med. Chem. Lett.* 22(14), 4873–4876 (2012).
- 105 Dua VK, Verma G, Dash AP. *In vitro* antiprotozoal activity of some xanthenes isolated from the roots of *Andrographis paniculata*. *Phytother. Res.* 23(1), 126–128 (2009).
- 106 Davis RA, Demirkiran O, Sykes ML *et al.* 7',8'-dihydroobolactone, a trypanocidal α -pyrone from the rainforest tree *Cryptocarya obovata*. *Bioorg. Med. Chem. Lett.* 20(14), 4057–4059 (2010).
- 107 Changtam C, De Koning HP, Ibrahim H, Sajid MS, Gould MK, Suksamrarn A. Curcuminoid analogs with potent activity against *Trypanosoma* and *Leishmania* species. *Eur. J. Med. Chem.* 45(3), 941–956 (2010).
- 108 Calcul L, Inman WD, Morris AA *et al.* Additional insights on the bastadins: isolation of analogues from the sponge *Ianthella* cf. *reticulata* and exploration of the oxime configurations. *J. Nat. Prod.* 73(3), 365–372 (2010).
- 109 Gehrig S, Efferth T. Development of drug resistance in *Trypanosoma brucei rhodesiense* and *Trypanosoma brucei gambiense*. Treatment of human African trypanosomiasis with natural products (Review). *Int. J. Mol. Med.* 22(4), 411–419 (2008).
- 110 Salem MM, Werbovetz KA. Natural products from plants as drug candidates and lead compounds against leishmaniasis and trypanosomiasis. *Curr. Med. Chem.* 13(21), 2571–2598 (2006).
- 111 Hoet S, Opperdoes F, Brun R, Quetin-Leclercq J. Natural products active against African trypanosomes: a step towards new drugs. *Nat. Prod. Rep.* 21(3), 353–364 (2004).
- 112 Ioset JR. Natural products for neglected diseases: a review. *Curr. Org. Chem.* 12(8), 643–666 (2008).
- 113 Tamborini L, Pinto A, Smith TK *et al.* Synthesis and biological evaluation of CTP synthetase inhibitors as potential agents for the treatment of African trypanosomiasis. *ChemMedChem* 7(9), 1623–1634 (2012).
- 114 Navarro G, Chokpaiboon S, De Muylder G *et al.* Hit-to-lead development of the chamigrane endoperoxide merulin A for the treatment of African sleeping sickness. *PLoS ONE* 7(9), e46172 (2012).
- 115 Ludovic Gros, Castillo-Acosta VM, Jiménez CJ *et al.* New azasterols against *Trypanosoma brucei*: role of 24-sterol methyltransferase in inhibitor action. *Antimicrob. Agents Chemother.* 50(8), 7 (2006).
- 116 Schmidt TJ, Nour AM, Khalid SA, Kaiser M, Brun R. Quantitative structure–antiprotozoal activity relationships of sesquiterpene lactones. *Molecules* 14(6), 2062–2076 (2009).
- 117 Zimmermann S, Kaiser M, Brun R, Hamburger M, Adams M. Cynaropicrin: the first plant natural product with *in vivo* activity against *Trypanosoma brucei*. *Planta Med.* 78, 553–556 (2012).
- 118 Orhan I, Sener B, Kaiser M, Brun R, Tasdemir D. Inhibitory activity of marine sponge-derived natural products against parasitic protozoa. *Marine drugs* 8(1), 47–58 (2010).
- 119 Gökbulut A, Kaiser M, Brun R, Särer E, Schmidt TJ. β -hydroxyphenolide esters from *Inula montbretiana* and their antiprotozoal activity. *Planta Med.* 78(03), 225–229 (2012).
- 120 Saeidnia S, Gohari AR. Chapter 6 – trypanocidal monoterpenes: lead compounds to design future trypanocidal drugs. In: *Studies in Natural Products Chemistry (Volume 37)*. Rahman AU (Ed.). Elsevier, The Netherlands 173–190 (2012).
- 121 Galle JB, Attioua B, Kaiser M, Rusig AM, Lobstein A, Vonthron-Senecheau C. Eleanolone, a diterpene from the French marine alga *Bifurcaria bifurcata* inhibits growth of the human pathogens *Trypanosoma brucei* and *Plasmodium falciparum*. *Mar. Drugs* 11(3), 599–610 (2013).
- 122 Li J, Lan J, Liu Z, Li Y. Studies on the synthesis of elean-type linear diterpenes: the efficient total syntheses of eleanolone, eleanolone acetate, eleanandiol, eleananonal, and epoxyeleanolone. *J. Nat. Prod.* 61(1), 92–95 (1998).
- 123 Watts KR, Ratnam J, Ang KH *et al.* Assessing the trypanocidal potential of natural and semi-synthetic diketopiperazines from two deep water marine-derived fungi. *Bioorg. Med. Chem.* 18(7), 2566–2574 (2010).

- 124 Carballeira NM, Cartagena M, Sanabria D *et al.* 2-alkynoic fatty acids inhibit topoisomerase IB from *Leishmania donovani*. *Bioorg. Med. Chem. Lett.* 22(19), 6185–6189 (2012).
- 125 Bonazzi S, Barbaras D, Patiny L *et al.* Antimalarial and antitubercular nostocarboline and eudistomin derivatives: synthesis, *in vitro* and *in vivo* biological evaluation. *Bioorg. Med. Chem.* 18(4), 1464–1476 (2010).
- 126 Lavrado J, Mackey Z, Hansel E, Mckerrow JH, Paulo A, Moreira R. Antitrypanosomal and cysteine protease inhibitory activities of alkyldiamine cryptolepine derivatives. *Bioorg. Med. Chem. Lett.* 22(19), 6256–6260 (2012).
- 127 Feng Y, Davis RA, Sykes ML *et al.* Antitrypanosomal pyridocridine alkaloids from the Australian ascidian *Polysyncrator echinatum*. *Tetrahedron Lett.* 51(18), 2477–2479 (2010).
- 128 Osorio EJ, Berkov S, Brun R *et al.* *In vitro* antiprotozoal activity of alkaloids from *Phaedranassa dubia* (Amaryllidaceae). *Phytochem. Lett.* 3(3), 161–163 (2010).
- 129 Merschjohann K, Sporer F, Steverding D, Wink M. *In vitro* effect of alkaloids on bloodstream forms of *Trypanosoma brucei* and *T. congolense*. *Planta Med.* 67(7), 623–627 (2001).
- 130 Endeshaw M, Zhu X, He S *et al.* 8,8-dialkyldihydroberberines with potent antiprotozoal activity. *J. Nat. Prod.* 76(3), 311–315 (2013).
- 131 Fernandez LS, Sykes ML, Andrews KT, Avery VM. Antiparasitic activity of alkaloids from plant species of Papua New Guinea and Australia. *Int. J. Antimicrob. Agents* 36(3), 275–279 (2010).
- 132 Scala F, Fattorusso E, Menna M *et al.* Bromopyrrole alkaloids as lead compounds against protozoan parasites. *Mar. Drugs* 8(7), 2162–2174 (2010).
- 133 Feng Y, Davis RA, Sykes ML, Avery VM, Camp D, Quinn RJ. Pseudoceratinazole A: a novel bromotyrosine alkaloid from the Australian sponge *Pseudoceratina* sp. *Tetrahedron Lett.* 51(37), 4847–4850 (2010).
- 134 Pimentel-Elardo SM, Buback V, Gulder TA *et al.* New tetrymycin derivatives with anti-trypanosomal and protease inhibitory activities. *Marine drugs* 9(10), 1682–1697 (2011).
- 135 Wang X, Beckham TH, Morris JC, Chen F, Gangemi JD. Bioactivities of gossypol, 6-methoxygossypol, and 6,6'-dimethoxygossypol. *J. Agric. Food Chem.* 56(12), 4393–4398 (2008).
- 136 Schmidt TJ, Rzeppa S, Kaiser M, Brun R. Larrea tridentata-absolute configuration of its epoxyignans and investigations on its antiprotozoal activity. *Phytochem. Lett.* 5(3), 632–638 (2012).
- 137 Ebrahimi SN, Zimmermann S, Zaugg J, Smiesko M, Brun R, Hamburger M. Abietane diterpenoids from *Salvia sabendica*-antiprotozoal activity and determination of their absolute configurations. *Planta Med.* 79(2), 150–156 (2013).
- 138 Jensen S, Omarsdottir S, Bwalya AG, Nielsen MA, Tasdemir D, Olafsdottir ES. Marchantin A, a macrocyclic bisbenzyl ether, isolated from the liverwort *Marchantia polymorpha*, inhibits protozoal growth *in vitro*. *Phytomedicine* 19(13), 1191–1195 (2012).
- 139 Nour AM, Khalid SA, Kaiser M, Brun R, Abdalla WE, Schmidt TJ. The antiprotozoal activity of methylated flavonoids from *Ageratum conyzoides* L. *J. Ethnopharmacol.* 129(1), 127–130 (2010).
- 140 Minagawa N, Yabu Y, Kita K *et al.* An antibiotic, ascofuranone, specifically inhibits respiration and *in vitro* growth of long slender bloodstream forms of *Trypanosoma brucei*. *Mol. Biochem. Parasitol.* 84(2), 271–280 (1997).
- 141 Yabu Y, Suzuki T, Nihei C-I *et al.* Chemotherapeutic efficacy of ascofuranone in *Trypanosoma vivax*-infected mice without glycerol. *Parasitol. Int.* 55(1), 39–43 (2006).
- 142 Saimoto H, Kido Y, Haga Y, Sakamoto K, Kita K. Pharmacophore identification of ascofuranone, potent inhibitor of cyanide-insensitive alternative oxidase of *Trypanosoma brucei*. *J. Biochem.* 153(3), 267–273 (2013).
- 143 Whitty A. Growing PAINS in academic drug discovery. *Future Med. Chem.* 3(7), 797–801 (2011).
- 144 Singh H, Natt NK, Garewal N, Pugazhenthana TA. Bedaquiline: a new weapon against MDR and XDR-TB. *Int. J. Basic Clin. Pharmacol.* 2(2), 96–102 (2013).
- 145 Van Pelt-Koops JC, Pett HE, Graumans W *et al.* The spiroindolone drug candidate NITD609 potently inhibits gametocytogenesis and blocks *Plasmodium falciparum* transmission to *Anopheles* mosquito vector. *Antimicrob. Agents Chemother.* 56(7), 3544–3548 (2012).
- 146 Kola I, Landis J. Can the pharmaceutical industry reduce attrition rates? *Nat. Rev. Drug Discov.* 3(8), 711–716 (2004).

■ Websites

- 201 WHO. Human African trypanosomiasis. http://gamapserver.who.int/maplibrary/files/maps/global_trypanosomiasis_gambiense_2010.png (Accessed 30 July 2013)
- 202 WHO. Human African trypanosomiasis. http://gamapserver.who.int/mapLibrary/Files/Maps/Global_trypanosomiasis_rhodiense_2010.png (Accessed 30 July 2013)
- 203 WHO. Human African trypanosomiasis. www.who.int/trypanosomiasis_african/en/ (Accessed 30 July 2013)
- 204 CDC: parasites – African trypanosomiasis (also known as sleeping sickness). www.cdc.gov/parasites/sleepingsickness/biology.html (Accessed 27 July 2013)
- 205 WHO: drugs. Human African Trypanosomiasis. www.who.int/trypanosomiasis_african/drugs/en/index.html (Accessed 27 July 2013)
- 206 DNDI: pivotal study of fexinidazole for human African trypanosomiasis in stage 2. www.clinicaltrials.gov/ct2/show/NCT01685827?term=fexinidazole&rank=3#wrapper (Accessed 23 November 2012)
- 207 DNDI: fexinidazole (human African trypanosomiasis). www.dndi.org/portfolio/fexinidazole.html (Accessed 27 July 2013)
- 208 DNDI: oxaborole SCYX-7158 (human African trypanosomiasis). www.dndi.org/portfolio/oxaborole-scyx-7158.html (Accessed 27 July 2013)
- 209 Chimiothèque Nationale. <http://chimiotheque-nationale.enscm.fr/?lang=en> Accessed 1 August 2013
- 210 FDA: FDA approves Zelboraf and companion diagnostic test for late-stage skin cancer 2013. www.fda.gov/NewsEvents/Newsroom/PressAnnouncements/ucm268241.htm (Accessed 30 July 2013)

1.2. Post-script: updated literature surveillance

A targeted screen of the Molecular Libraries Small Molecule Repository (MLSMR), which contains 330,683 compounds, was performed against both *T. brucei* and *T. cruzi* phosphofructokinase (PFK).¹ The initial hit (**1.01**, Figure 1.1) had an IC₅₀ against *T. brucei* PFK of 0.41 μM and investigations around the benzenesulfonamide core failed to yield an improvement in activity. Investigations of the left hand benzyl group showed that replacement of either chlorine with fluorine was well tolerated, though an increase in bulk or length of the alkyl chain resulted in a loss of activity. SAR of the right hand side heterocycle revealed that removal of the methyl from the isoxazole was well tolerated (**1.02**), while replacement with a thiadiazole (**1.03**) led to a two-fold improvement in activity with respect to *T. brucei* PFK. Compound **1.03** was also tested against rabbit PFK at a concentration of 1 μM and no appreciable inhibition was seen, suggesting that selectivity from parasitic PFK over mammalian PFK is possible. Examination of **1.01-1.03** against *T. brucei* (strain Lister 427) *in vitro* revealed moderate dose-dependent toxicity of **1.01** (ED₅₀ 26.8 μM) and **1.02** (ED₅₀ 16.3 μM), though the most potent analogue, **1.03**, showed no appreciable parasite toxicity. The authors have postulated that this lack of activity could be due to a lack of permeability of the compound to the cells though this requires further investigation.

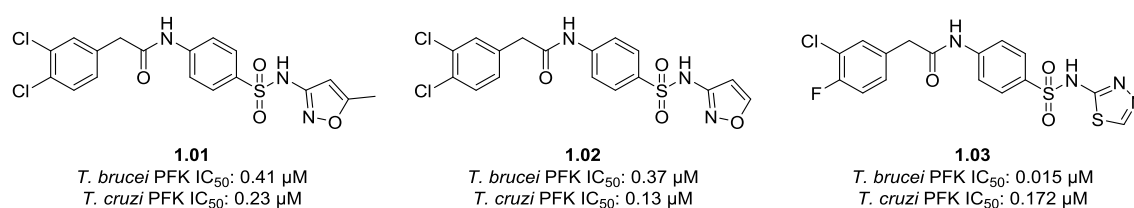


Figure 1.1 Identification of inhibitors of *T. brucei* PFK by screening of the Molecular Libraries Small Molecule Repository and subsequent SAR investigation to yield **1.02** and **1.03**.

Previously, the botulinum toxin inhibitor (**1.04**) was identified as a *T.b. brucei* inhibitor.² A group of 5 Swiss/Webster mice were infected with 5×10^5 trypanosomes (EATRO 110 – acute model of infection) and

the infection allowed to develop for 24 h before administration of **1.04** intraperitoneally with a dose of 1 mg/kg once daily for 3 days. This led to a 100% cure rate which was defined as > 30 day survival beyond death of the control mice. With a dose of 0.5 mg/kg once daily for 3 days an 80% cure rate was observed. Subsequent synthesis of a small number of analogues led to the identification of **1.05** and **1.06** as potent inhibitors of the human infective subspecies, *T.b. rhodesiense*.³ Interestingly, whilst **1.05** was identified as one of the most potent analogues in the SAR set it contains a reversed amide which led to a two-fold loss of activity against *T.b. rhodesiense* and L6 cells. A number of other analogues in the set displayed similar results and it was thought that having an aniline nitrogen *para* to the 2-imidazoline substituent was favourable. Replacement of one of the anilide functional groups with a pyrrole (**1.06**) led to a three-fold improvement in activity with good selectivity, though these analogues were generally more cytotoxic when compared with **1.04** and **1.05**.

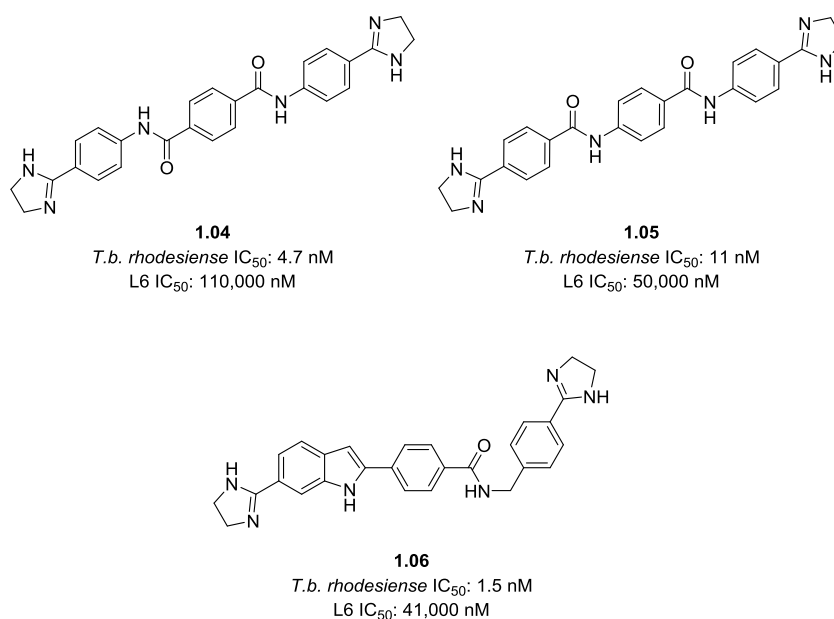


Figure 1.2 The botulinum toxin (**1.04**) previously identified as a *T.b. brucei* inhibitor and the subsequent analogues identified as *T.b. rhodesiense* inhibitors, **1.05** and **1.06**.

Examination of **1.04-1.06** in an acute mouse model of *T.b. rhodesiense* (STIB900) was performed with a dose of 50 mg/kg once daily (administered intraperitoneally on days 3-6 post infection) and the results are summarised in Table 1.1 where cure is defined as survival for > 60 days post infection without a parasitemia relapse.³ Compound **1.04** had a cure rate of 50% in the mouse model which is at odds with the data previously reported. Compound **1.05** was found to be completely curative in the model with no evidence of toxicity observed and **1.06** was ineffective and proved to be lethal to all mice after the first injection. In this instance the *in vitro* cytotoxicity appears to be an inadequate predictor of *in vivo* toxicity. None of these compounds were reported to be more effective than either pentamidine or furamidine which showed a 50% and 75% cure rate following the same experimental format with a dosage of 20 mg/kg daily over the four days.

Table 1.1 Anti-trypanosomal activity of **1.04-1.06** in an acute mouse model of *T.b. rhodesiense*.

Compound	Cures	Mean Survival Days
Control	-	6-10
1.4^a	2/4	39
1.5^a	4/4	> 60
1.6^a	0/4	Toxic ^b
Pentamidine^c	2/4	-
Furamidine^c	3/4	-

^a Four 50 mg/kg doses administered intraperitoneally on days 3-6.

^b Mice died following administration of first compound dose.

^c Four 20 mg/kg doses administered intraperitoneally on days 3-6.

A phenotypic screen of a library containing 700,000 compounds, with a focus on drug-like properties and structural diversity, led to the identification of **126** (Figure 38, FMC review pg 1824) with an EC₅₀ of 220 nM⁴ in a separate phenotypic screen to the one previously reported.⁵ As a result of investigations into the

SAR around this system, **1.07** was identified with improved anti-parasite activity with a reported EC₅₀ of 2 nM. One of the limitations of this system was identified as being metabolic stability though **1.07** demonstrated a significant improvement with an improvement in the half-life from 6.4 min to 31 min in human liver microsomes. In an acute mouse model of *T.b. rhodesiense* (STIB900) **1.07** was administered 48 h after infection by oral gavage for a total of 5 days (Table 1.2). With a dosage of 50 mg/kg and 20 mg/kg, a 100% cure rate was obtained with both once and twice daily dosing. At 5 mg/kg a 100% cure rate was obtained with twice daily administration though this dropped to 40% with once daily dosing, while a dose of 2.5 mg/kg twice daily resulted in a 40% cure rate and a dose of 1 mg/kg was ineffective. An extended treatment regimen with a dose of 50 mg/kg twice daily for 14 days showed no clinical toxicity indicating good tolerability of the compound above the fully efficacious dose. However, in a personal communication with Michael Gelb it was revealed that this series did not demonstrate a cure in the chronic mouse model of *T.b. gambiense* infection.⁶

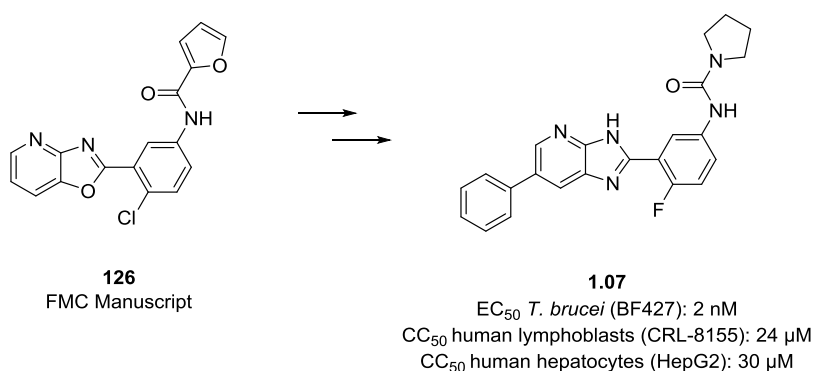


Figure 1.3 Optimisation of **126**, identified in two separate phenotypic screens, to give **1.07**.

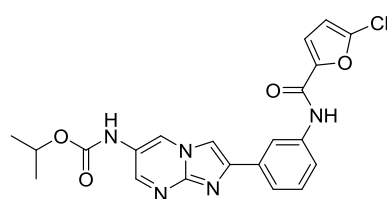
Researchers at Novartis have recently published data on a related series to that of Tatipaka *et al.*⁴ and our own hit-to-lead program.⁷ They have reported 42 compounds which exhibit a range of *in vitro* potencies against not only *T. brucei* but also *L. donovani* and *T. cruzi*, with compound **1.08** being their most potent *T. brucei* inhibitor disclosed.^{7, 8} To date, no data has been provided with respect to the selectivity of these compounds or on their performance in mouse models of the disease. As such, it is necessary to await the

release of further results to see whether they have been able to overcome the issues associated with demonstrating a cure in a chronic mouse model of *T.b. gambiense* as raised by Michael Gelb previously.

Table 1.2 Anti-trypanosomal activity of **1.07** in an acute mouse model of *T.b. rhodesiense*.

Dose (mg/kg)	Doses per day	Cures	Day of euthanasia ^a
50	2	5/5	60
50	1	5/5	60
20	2	5/5	60
20	1	5/5	60
5	2	5/5	60
5	1	2/5	13, 18, 27, 60, 60
2.5	2	2/5	16, 16, 20, 60, 60
1	2	0/5	4, 4, 9, 11, 13
Vehicle	2	0/5	4

^a Mice that cleared parasites and remained parasite free through day 60 after infection were declared cured.



1.08

L. donovani amastigotes EC₅₀: 0.41 uM

L. donovani macrophage EC₅₀: 0.17 uM

T. brucei EC₅₀: 0.057 uM

Figure 1.4 The most active compound against *T. brucei* from researchers at Novartis.

Bloodstream *T. brucei* derives all of its ATP by substrate-level phosphorylation.⁹ A number of regulators exist in order to carry out this process; one of these is RNA editing.⁹ *T. brucei* has mitochondrial DNA, referred to as kinetoplast DNA (kDNA), which consists of maxicircles and minicircles.^{9, 10} The maxicircles are homologues of eukaryotic mitochondrial DNA which encode for oxidative phosphorylation enzymes and mitochondrial rRNA.^{9, 10} The transcripts of 12 of the maxicircle protein-coding genes are edited post-transcriptionally through the insertion and deletion of uridine residues.¹⁰ This process is controlled by guide RNAs (gRNA), which are encoded by the minicircles, where a single gRNA can mediate the editing of a 'block' of 1-10 sites.¹⁰ An editing site occurs when there is a mismatch between the mRNA/gRNA sequence duplex which leads to either insertion or deletion of uridylylates by an exonuclease, terminyl uridylyl transferase (TUTase). The TUTase 2 of *T. brucei* (*TbRET2*) has previously been shown to be essential for the survival of both the insect and bloodstream parasites.

Recently, a computational study of *TbRET2* combined molecular dynamics (MD) in order to accommodate for flexibility in the receptor and virtual screening.¹¹ The authors initially used the static *TbRET2* crystal structure (PDB ID: 2B51) to conduct a virtual screen of the National Cancer Institute Diversity Set 2 (NCIDS2). The 1,324 compounds in the NCIDS2 were also docked into the most populated three cluster centroids of UTP-bound *TbRET2* which could be obtained from MD simulations. The screening process was performed twice, once in the presence of UTP in order to target the RNA-nucleotide binding site and once without UTP bound in order to target the UTP binding site. The resulting compounds were then ordered based on their docking scores and the top 100 were then filtered based on their ADME properties. This led to the identification of 24 unique compounds in total which were then tested against *T. brucei* and the human cell line, NCI60. NCI compounds 94600 (Camptothecin, **110**, Figure 32, FMC review pg 1821), 71881 (**1.09**), and 329249 (**1.10**) (Figure 1.5) were identified as inhibitors of *TbRET2*, corresponding to a 13% hit rate.¹¹ Had the authors not incorporated MD into their scoring of compounds, **1.10** would not have been tested against *T. brucei* based on a low docking score to the crystal structure.¹¹

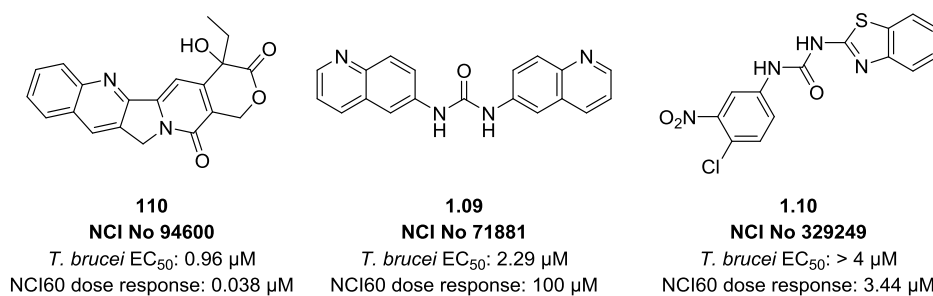


Figure 1.5 Compounds identified from the NCIDS2 screening collection as inhibitors of TbRET2 utilising a computational approach that combined MD simulations with virtual screening.¹¹

A second virtual screen of the NCI plated compounds was performed, which contained 805 compounds at the time of screening, consisting of the NCI's mechanistic set, natural products set, COMBO set and oncology approved set.¹¹ Of the 40 compounds that were submitted for testing against *T. brucei* 12 compounds were identified as having EC₅₀ values that were ≤ 4 μM which corresponded to a 30% hit rate. Of these, three were identified as having EC₅₀ values less than 30 nM (Figure 1.6). As with compound **1.10**, NCI compound 267461 (**1.13**) would not normally have been submitted for testing against *T. brucei* based on the crystal structure docking score. Finally, a similarity search of the full NCI database of NCI compounds with compounds 266535 (**1.11**), 132791 (**1.12**) and 267461 (**1.13**) led to the identification of a further 33 compounds with a 90% Tanimoto similarity. Of these, 10 compounds were tested and 2 compounds, 126765 (**1.14**) and 137443 (**1.15**), were identified as having EC₅₀ values of 23 and 51 nM respectively (Figure 1.6). Whilst a significant number of novel compound cores have been identified as potential therapeutics for HAT the authors acknowledge that in some of the compounds, reactive functionalities exist that would require attention early on in any drug discovery program, such as reactive alkenes. Many of the compounds that were identified also demonstrate selectivity issues against the NCI60 cell line, with **1.09** demonstrating one of the greatest selectivity margins.

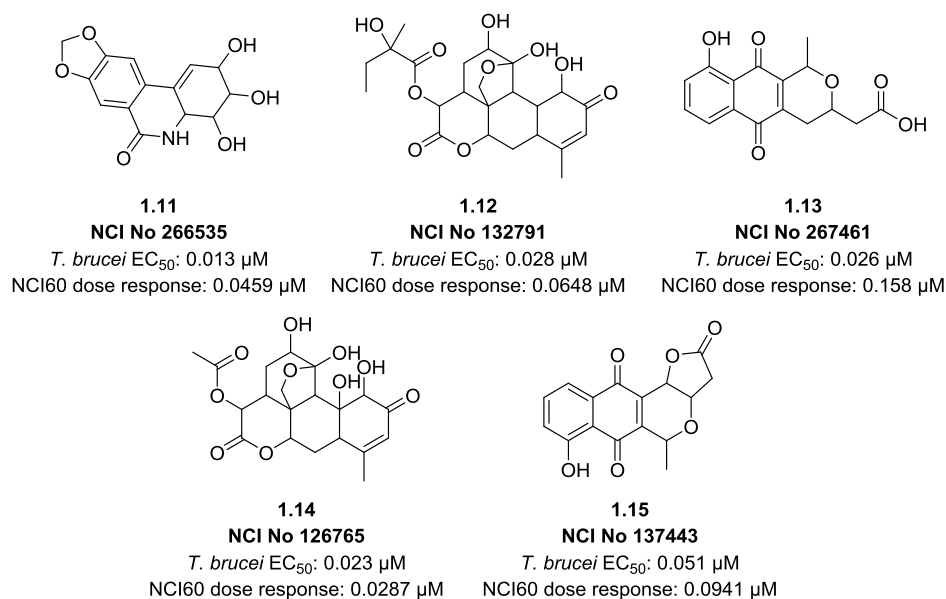


Figure 1.6 Compounds identified from the NCI plated compound collection consisting of the NCI's mechanistic set, natural products set, COMBO set and oncology approved set.¹¹

As discussed in the preceding review, the benzoxaboroles have been a target of great interest for identifying *T. brucei* inhibitors (FMC review, pg 1811).¹² Wu *et al.* initially incorporated the privileged indole scaffold into their design, however the indolebenzoxaborole and thioether derivatives failed to yield the desired activity with only one compound identified as being active, **1.16**.¹³ The authors proposed that this low activity could have been due to the added rigidity of the fused phenyl ring which would have resulted in a decrease in both solubility and permeability.¹³ As such, they moved to the pyrrolobenzoxaborole scaffold. Immediately they obtained active compounds such as **1.17**, the parent pyrrolobenzoxaborole compound.¹³ Introduction of a carboxylic acid at the 2-position led to a 15-fold improvement in potency of the series (IC₅₀ 0.13 μg/ml) highlighting the importance of a hydrogen bond acceptor and donor on the pyrrole ring whilst also enabling divergent synthesis.¹³ Investigations around the 2-acyl substitutions revealed compounds which exhibited a two- to ten-fold decrease in activity.¹³ However, movement of the acyl functionality to the 3-position saw a further improvement in the potency of these compounds and led to the identification of numerous inhibitors in the range of 30 μg/ml – 90 μg/ml, and **1.18** also exhibited excellent selectivity over L929 cells.¹³ Removal of the carboxyl group from the structure led to a 24-fold loss in the activity of these

compounds.¹³ Investigation of a number of these compounds (Figure 1.8) in a murine model of an acute blood stage infection was also performed with mixed results.¹³ Compounds **1.19**, **1.20**, **1.21**, **1.18** and **1.23** were studied and the mice were administered with a dose of 50 mg/kg twice daily, intraperitoneally, 24 h post infection, and the treatment was continued for 5 days.¹³ Compounds **1.20** and **1.21** demonstrated a moderate effect on the life expectancy of the mice though failed to eliminate the parasitemia infection, while compounds **1.19**, **1.18**, and **1.22** all demonstrated a 100% survival rate with no evidence of parasitemia on day 30.¹³ While compounds **1.18-1.22** are promising leads for further development, a close examination of their physicochemical properties would be required in order to determine the next step in the drug discovery process.

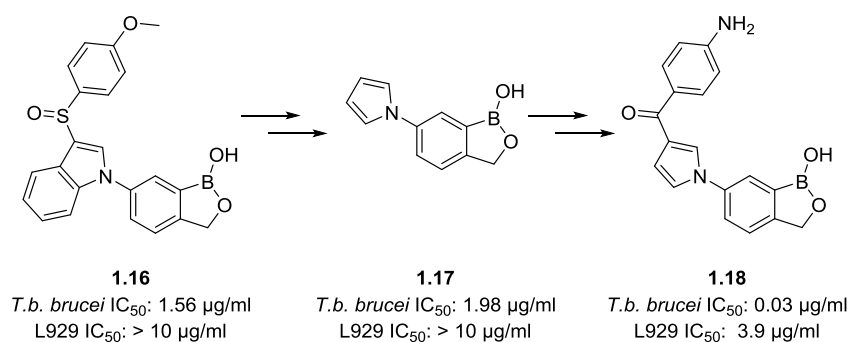


Figure 1.7 The development of the 6-pyrrolobenzoxaboroles from the 6-indoylbenzoxaboroles.

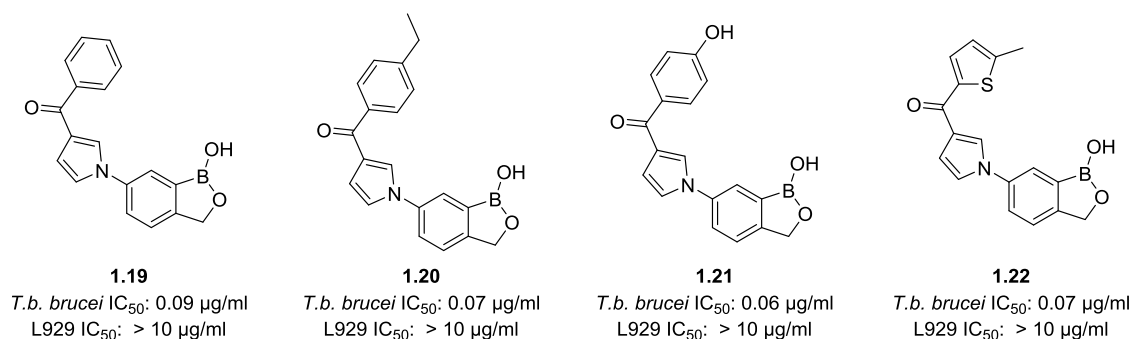


Figure 1.8 Compounds tested in an acute murine model of a blood stage infection with *T. brucei*.

Pyrrolopyrimidines have previously been identified as inhibitors of *T. brucei* Pteridine Reductase 1 (*TbPTR1*).^{14, 15} The pyrrolopyrimidine core carries a pharmacophore with structural similarity to the recognition motif of the P2 aminopurine transporter¹⁶ which is capable of accumulating substrates to internal levels at concentrations that exceed the external concentration > 1000-fold.¹⁷ Initial structure-based design focused on the pyrroloprimidine core (**1.23**) with substitution of the 4-amino or 4-oxo group by 4-alkylamino and 4-alkoxy groups.¹⁸ This gave no significant improvement in the *in vitro* activity of the compounds, suggesting the presence of a hydrophobic substituent on the pyrrole was necessary.¹⁸ Replacement of the nitrile with larger hydrophobically substituted alkynes, such as propargyl led to a compound with reasonable activity against the specific target and in the *in vitro* assay (0.19 μM and 0.65 μM respectively).¹⁸ Given only a three-fold difference in compound activity it is possible that there is an element of polypharmacology with this compound. However, this result led to the further exploration of the region with a variety of singly substituted phenyl groups. Whilst these modifications were generally well tolerated against *TbPTR1* these results did not translate into active compounds against *T.b. brucei*.¹⁸ Hydrophobic substituents at the 6-position were also trialled. These compounds showed improved affinity for *TbPTR1* though again lacked sufficient activity in the cellular assays.¹⁸ Upon introduction of two aryl substituents at the 5- and 6-positions there was an increase in the activity of the compounds in both the enzymatic and cellular assays, though there was also a decrease in the solubility of some compounds.¹⁸ An attempt at the introduction of a solubilising group off the 6-position led to a compound with only weak activity and the authors did not pursue this avenue further.¹⁸ Examination of the physicochemical properties of a selection of analogues revealed the compound series in general to have reasonable metabolic stability at 2-6 h and with cLogP in the range of 2-3.5.¹⁸ A number of compounds exhibited submicromolar activity against *TbPTR1* and *T.b. brucei* in addition to being relatively non-toxic when tested in HEK cells (Table 1.3).¹⁸ These compounds were progressed through to *in vivo* examination in three ICR mice which were infected with 1×10^5 bloodstream *T.b. brucei* strain 427.¹⁸ At 24 h post-infection the mice were injected intraperitoneally with the desired dose of compound daily over four consecutive days and parasitemia levels were monitored daily.¹⁸ In the first round of testing **1.25-1.27** from the 4-amino series, each showed severe toxicity issues at 100 mg/kg leading to some fatalities, some transient clinical signs at 30 mg/kg and no clinical signs at 10 mg/kg. As such, 30 mg/kg was utilised as the dose for the *in vivo* studies.¹⁸ During the experiments one mouse in each

group that was treated with compounds **1.25-1.27** survived long enough to demonstrate a reduction in parasitemia from $\sim 10^8$ to below detection limits, though surviving mice that were treated with **1.26** and **1.27** showed a relapse in parasitemia at day 10.¹⁸ The 4-oxo series was also evaluated using compounds **1.29** and **1.30**. When administered a dose of 30 mg/kg neither compound showed acute toxicity, however **1.30** was not curative in the mouse model and some toxicity was observed with **1.29** even though parasitemia levels were reduced.¹⁸ There are clearly still toxicity issues surrounding these which would need to be addressed before further progression of any of the compounds. In addition, the proposed enhanced mode of uptake of these compounds appears flawed with numerous compounds exhibiting submicromolar activity against *TbPTR1* and little or no activity against *T.b. brucei*.

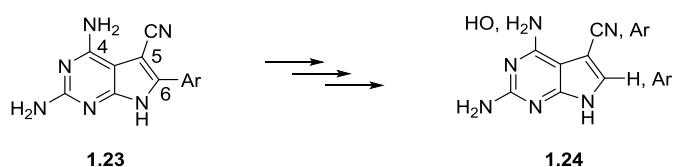
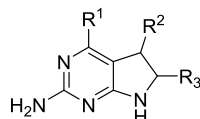


Figure 1.9 Pyrolopyrimidine template (**1.23**) used for structure-based design of drugs specific to *TbPTR1* and a summary of the SAR obtained.

In an effort to identify novel scaffolds for *TbPTR1* inhibitors, Dube *et al.* recently employed pharmacophore mapping coupled to *in silico* screening and molecular docking.¹⁹ A literature search revealed 45 compounds with known *TbPTR1* activity. These compounds represented four unique scaffolds with varying substitution patterns. When generating the pharmacophore map four parameters were considered: hydrogen bond donors, hydrogen bond acceptors, hydrophobic aromatics and ring aromatics. This led to the identification of the pharmacophore map of *TbPTR1* as one hydrogen bond donor, two aromatic rings and one hydrophobic aromatic.¹⁹ This information was then utilised to screen approximately 80,000 drug-like molecules from the ZINC database resulting in the filtering out of 284 compounds of interest.¹⁹ These compounds were further filtered for various ADME properties including toxicity, aqueous solubility, BBB penetration, plasma protein binding and adherence to Lipinski's rule of 5. The resulting compounds were then docked into the DX7

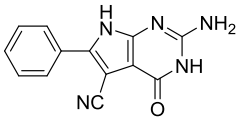
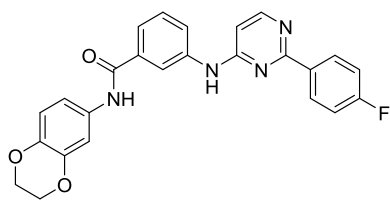
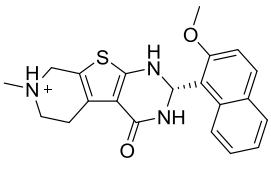
(**1.31**; a known inhibitor of *Tb*PTR1) binding site of the *Tb*PTR1 crystal structure. The predicted binding affinity of **1.31** was found to be in good agreement with the experimentally determined binding affinity.¹⁹ This led to the identification of ZINC33025157 (**1.32**) and ZINC20149815 (**1.33**), shown in Table 1.4, as two of the best inhibitors from the ZINC database. Both of these inhibitors occupied the binding pocket of the enzyme and interacted through numerous hydrogen bonding and stacking interactions.¹⁹ Whilst these compounds show potential to be lead compounds in the design of inhibitors of *Tb*PTR1 the predicted K_i values were not confirmed experimentally and this would need to be a priority before proceeding.

Table 1.3 In vitro results for selected pyrrolopyrimidines as inhibitors of *Tb*PTR1.¹⁸



ID	R ¹	R ²	R ³	<i>Tb</i> PTR1 (K_i^{app} μ M)	<i>T.b. brucei</i> (IC ₅₀ μ M)		HEK (IC ₅₀ μ M)
					HMI-9	CMM	
1.25	-NH ₂	C ₆ H ₅ -	4-F-C ₆ H ₄ -	0.24	0.59	0.15	49.19
1.26	-NH ₂	4-OCH ₃ -C ₆ H ₄ -	4-F-C ₆ H ₄ -	0.58	0.27	0.083	39.14
1.27	-NH ₂	C ₆ H ₅ -	4-Br-C ₆ H ₄ -	0.135	0.97	0.25	39.63
1.28	-NH ₂	3-Cl-C ₆ H ₄ -	4-F-C ₆ H ₄ -	0.29	0.39	0.19	34.59
1.29	-OH	C ₆ H ₅ -	4-Br-C ₆ H ₄ -	0.23	7.38	3.20	>100
1.30	-OH	C ₆ H ₅ -(CH ₂) ₂ -	C ₆ H ₅ -	0.95	0.40	0.14	33.18

Table 1.4 Virtual screening results of TbPTR1 inhibitors identified in the ZINC database.

ID	Structure	Predicted K_i
1.31		0.9 μ M
1.32		0.03 nM
1.33		0.01 nM

Both quinolinones and chalcones are prevalent in the literature as isolates from natural products. Roussaki *et al.* recently fused these two scaffolds to form a hybrid between the 4-hydroxy-2-quinolinone heterocycle and the chalcone moiety in order to investigate any synergistic effect of the two pharmacophores against *T. brucei*.²⁰ The authors focused their investigations on the amide moiety and the α,β -unsaturated carbonyl system. All of the active analogues contained an electron-donating substituent off the aromatic ring of the chalcone motif, though the position and number of these groups did affect the activity of the compounds.²⁰ For example, **1.34** has a methyl group at the 2-position, whilst its regioisomer, where the methyl is located at the 4-position was found to be completely inactive.²⁰ A similar situation is seen with compound **1.36** where it is substituted at the 3-position with a methoxy. Movement of the methoxy to the 4-position led to a complete loss in activity.²⁰ Disubstitution of the 3- and 4-positions with either two methoxy groups (**1.37**) or a methoxy and hydroxyl group respectively (**1.35**) was found to be detrimental to the activity of the compounds with a two-fold loss in activity against *T. brucei* observed.²⁰ Substitution of the phenyl with *tert*butyl and an alcohol as in **1.38** was one of the most potent compounds presented in this work with an IC_{50} of 3.3 μ M, though this particular compound also displayed high cytotoxicity (IC_{50} ~26 μ M) against THP1 cells.²⁰ However, modification of the α,β -unsaturated carbonyl system led to a two-fold increase in the

activity of the compounds (**1.39-1.40**), making these compounds more potent than the control, Nifurtimox.²⁰ Compound **1.39** in particular, not only showed potent trypanocidal activity but it was also exquisitely selective when compared with THP1 cells.²⁰

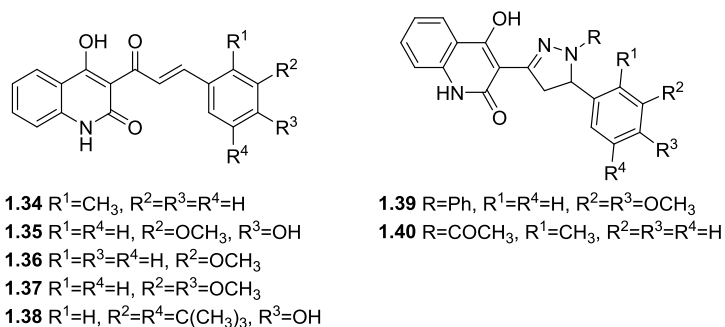


Figure 1.10 Quinolinone-chalcone hybrid scaffold analogues.

Table 1.5 In vitro activity of the quinolinone-chalcone hybrid scaffold against *T. brucei* and THP1 cells.

ID	IC ₅₀ (μM)	
	<i>T. brucei</i>	THP1
1.34	2.6 ± 0.1	> 50
1.35	4.9 ± 0.1	23.3 ± 1.4
1.36	6.5 ± 0.1	38.5 ± 2.1
1.37	4.9 ± 0.2	> 50
1.38	3.3 ± 0.1	26.2 ± 2.7
1.39	1.46 ± 0.1	> 50
1.40	1.43 ± 0.1	4.15 ± 0.19
Nifurtimox	2.9 ± 0.3	> 100

Most recently a HTS of 42,444 compounds from a kinase-targeted library was performed against *T. brucei*.²¹ 797 sub-micromolar hits were initially identified which had a selectivity index (SI) of > 100-fold relative to HepG2 cells.²¹ Of these hits, three were prioritised, based on their physicochemical and metabolism properties, for assessment in a murine bloodstream infection of *T.b. rhodesiense*.²¹ Female NMRI mice were infected with *T.b. rhodesiense* and three days post-infection they were administered with 10 mg/kg twice daily of NEU-1053 (**1.41**; Figure 1.11) for four days.²¹ A 4 day hiatus followed before **1.41** was administered for a further 4 days.²¹ In all mice rapid clearance of the parasitemia was observed between 24-48 h after the initial treatment. With only one mouse exhibiting a secondary peak of parasitemia on day 11, part way through the second round of treatment.²¹ Treatment with NEU-1053 led to a 100% cure rate of all mice.²¹

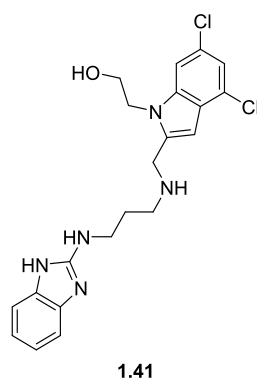


Figure 1.11 NEU-1053 (**1.41**), a putative *T. brucei* kinase inhibitor.

Table 1.6 Cure rate^a of a murine model of *T.b. rhodesiense* and *T.b. brucei* when mice treated with **1.41**.

ID	<i>T.b. rhodesiense</i>		<i>T.b. brucei</i>	
	Control	Treated	Control	Treated
1.41 ^b	0/5	5/5	0/4	3/4

^a Cure defined as no parasitemia detected after 90 days and the mouse still alive.

^b Dose of 10 mg/kg administered twice daily on days 3-6 and then again on days 11-14.

1.2.1. Natural products

A number of abruquinones were recently extracted from *Abrus precatorius*.²² The structures of the 5 isolated abruquinones can be found in Figure 1.12 and their *in vitro* activities are available in Table 1.7. Compounds **1.43-1.46** exhibit potent activity against *T.b. rhodesiense*, however examination of the structures of these compounds reveal liabilities in each of them; **1.42** contains a catechol moiety, which is known to be both protein and redox active, **1.43-1.44** are polyphenolic, and **1.45-1.46** contain a quinone moiety which is also known to be reactive.²³ As such, great caution would need to be taken if these compounds were to be progressed further, and removal of these reactive functionalities would need to be a priority in any subsequent work.

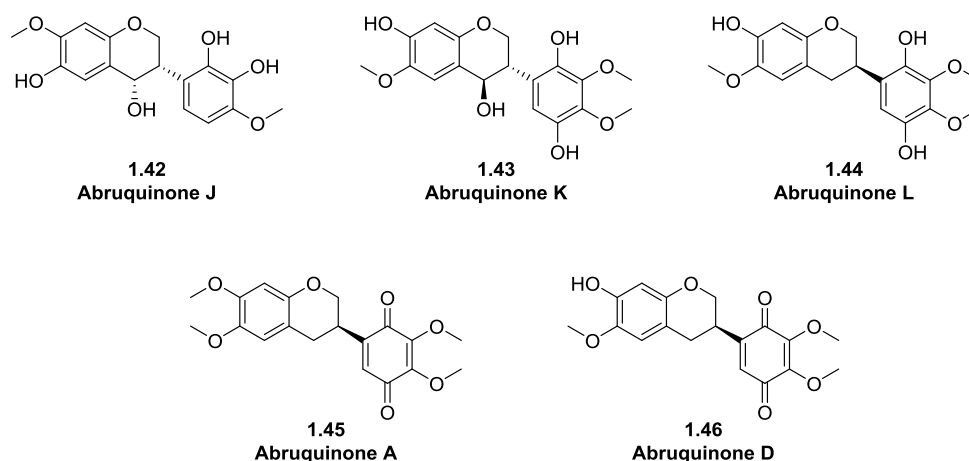


Figure 1.12 Structure of compounds **1.42-1.46**, isolated from *Abrus precatorius*.

Table 1.7 In vitro activity of **1.42-1.46** isolated from *Abrus precatorius*, against *T.b. rhodesiense* and L6 cells.

ID	IC ₅₀ (μM) ^a		SI
	<i>T.b. rhodesiense</i>	L6 cells	
1.42	11.2 ± 3.3	152.1 ± 7.8	13
1.43	0.11 ± 0.05	57.3 ± 4.3	508
1.44	0.02 ± 0.003	7.5 ± 1.2	374
1.45	0.02 ± 0.003	34.5 ± 16.3	1379
1.46	0.01 ± 0.001	4.8 ± 1.6	668
Melarsoprol	0.003 ± 0.002	-	-

^a Values are expressed as mean ± standard error of the mean.

Cordycepin (**1.47**; Figure 1.13) was isolated from the parasitic fungus *Cordyceps militaris*²⁴ and has since been examined for its activity against a range of parasites, including *T. brucei*.^{25, 26} However, whilst it exhibits potent *in vitro* activity against *T. brucei* (IC₅₀ 32 nM)²⁷ it is rapidly metabolised *in vivo* by adenosine deaminase (ADA).²⁶ As such, an investigation of the SAR around cordycepin was undertaken in order to improve the metabolic stability of the molecule.²⁵ It was quickly determined that the free amine and the 2'-hydroxyl group were both crucial for trypanocidal activity.²⁵ However, a previously known analogue of cordycepin with a fluorine at the 2-position on the pyrimidine (**1.48**)²⁸ appeared to have some resistance to ADA. Subsequent testing of **1.48** in an acute mouse model of *T.b. brucei* showed that a dose of 30 mg/kg over 6 days was sufficient to clear all parasitemia from the infected mouse.²⁵ However, *in vivo* pharmacokinetic evaluation shows that **1.48** still has a relatively short half-life of ~ 1h.²⁵ Whilst **1.48** was stable against ADA, there is another mechanism of inactivation which will require further optimisation if this compound was to progress further.

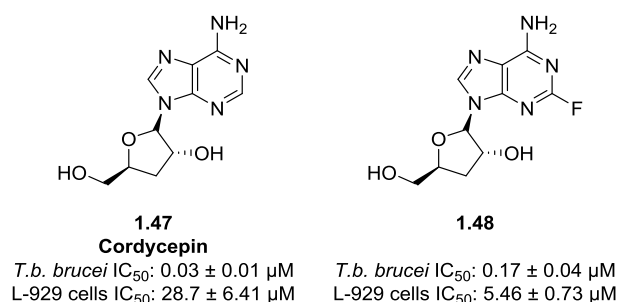


Figure 1.13 Structure of cordycepin (**1.47**) and **1.48** the ADA resistant analogue of cordycepin.

Table 1.8 In vivo study of **1.48** in an acute mouse model of *T. b. brucei*.

Dose (mg/kg)	Dosing	Day of relapse (post treatment)
1	10 doses twice daily	2
5	5 doses once daily	7
15	5 doses once daily	7
30	6 doses once daily	No relapse

Convolutamine I (**1.49**) was originally isolated from *Amathia tortusa*, *in vitro* analysis showed it to be potent against *T. brucei* (IC₅₀ 1.1 ± 0.2 μM) and relatively non cytotoxic with a selectivity index of 18 when measured against HEK293 cells.²⁹ To treat both stages of HAT the authors designed and synthesised a library of analogues that would lower the molecular weight, cLogP and PSA of the compounds, in order to improve CNS penetration.³⁰ The bromines at positions C-4 and C-6 were initially identified as important for anti-trypanostatic activity, yet loss of the bromine at C-2 led to a three-fold increase in the activity.³⁰ Attempted replacement or substitution of either of the basic nitrogen groups led to analogues with a complete loss of activity.³⁰ Similarly, replacement of the brominated phenyl group with functional groups such as naphthalene, pyridine or thiophene also led to a loss in activity, indicating the necessity of a phenyl group with bulky substituents.³⁰ However, having a singly substituted chlorine on the phenyl group at the 3-position (**1.51**) led to a compound with equipotent activity to **1.50**, but which had a lower molecular weight, cLogP and PSA.³⁰ The chloro could also be replaced by a trifluoromethyl (**1.52**) with similar results.³⁰ Other

trifluoromethyl substituted aryl compounds have been shown to have increased lipid solubility, thereby enhancing the rate of absorption and transport of the drug across the BBB.³¹ Whilst the authors have been able to demonstrate a modest improvement in the activity of these compounds there is no indication as to their selectivity and whether there may be cytotoxicity issues.

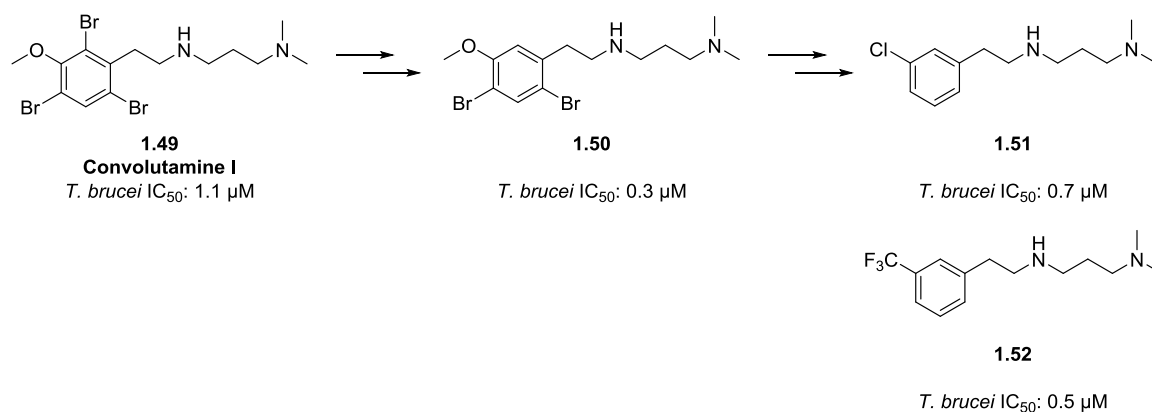


Figure 1.14 SAR investigation of convolutamine I (**1.49**) leading to compounds **1.51** and **1.52**.

1.2.2. Scaffold repurposing

The concept of repurposing current treatments in the effort to identify new treatments for other diseases is not a new one. A key aspect of this approach is to utilise any historical medicinal chemistry and structural biology information that would have been performed in the process of developing the clinical candidate.³² The success of this strategy also rests on selecting the ‘right’ compound. Ideally the compound will have gone through phase I clinical trials and will also be orally bioavailable.³³

Hesperadin (**1.53**), VX-680 (**1.54**) and danusertib (**1.55**) (Figure 1.15) were all tested in a parasite panel to determine if there was any activity against *T. brucei*, *T. cruzi*, *L. major* or *P. falciparum* (Table 1.14).³⁴ All of these drugs have previously been identified as inhibitors of human Aurora kinases, which are central

enzymes in cellular division;³⁴ controlling the assembly of the mitotic spindle, chromosomal separation and cytokinesis.³² There are three known Aurora kinase paralogs in the *T. brucei* genome.³⁵ However, RNAi has revealed that it is only *TbAUK1* that is required for mitotic progression, and not *TbAUK2* or *TbAUK3*.³⁶ It has also been shown that *TbAUK1* loss results in the inhibition of nuclear division, cytokinesis and growth in cultured, infectious bloodstream forms and insect stage procyclic forms.^{37, 38} It has also been shown that *TbAUK1* is required for the infection of mice.³⁸ *L. major* and *P. falciparum* have both previously been identified as containing Aurora kinases and inhibitors of Aurora kinase have been shown to be effective against both parasites and *T. brucei*.³⁴ Both hesperadin (**1.53**)³⁸ and danusertib (**1.55**) were shown to be submicromolar inhibitors of *T. brucei* and *P. falciparum*, while VX-680 (**1.54**)³⁹ showed some activity against *T. brucei* with an EC₅₀ of 10 μ M but not submicromolar activity against *P. falciparum*.

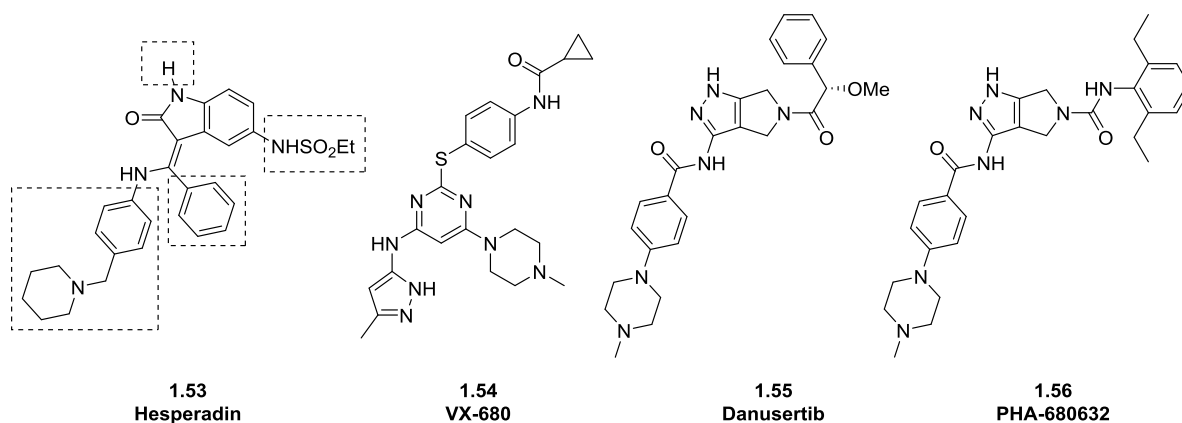


Figure 1.15 Known inhibitors of human Aurora kinase, hesperadin (**1.53**), VX-680 (**1.54**) and danusertib (**1.55**), along with the precursor analogue PHA-680632 (**1.56**) have been tested for activity against *T. brucei*. Highlighted are the regions explored during the SAR study of hesperadin.

Table 1.9 Results from screening of human Aurora kinase inhibitors against *T. brucei* and *L. major*.

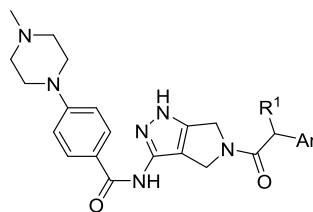
ID	EC ₅₀ (μM) ^a					TC ₅₀ (μM) ^a
	<i>T. brucei</i>	<i>T. cruzi</i>	<i>L. major</i> promastigotes	<i>L. major</i> amastigotes	<i>P. falciparum</i>	
						HepG2
1.53 ³⁸	0.06	39	0.12	2.37	0.01	<0.2
1.54 ³⁹	10	-	> 21	-	0.838	3.3
1.56 ³²	0.6	-	> 21	-	0.857	4

^a Results are the average of three experiments.

An exploration of the SAR surrounding hesperadin (**1.53**) was performed.³⁴ Initial investigations of the ethyl sulfonamide moiety revealed that the phenyl (EC₅₀ 0.01 μM) and methyl (EC₅₀ 0.02 μM) analogues were well tolerated as was the removal of the ethyl sulfonamide moiety (EC₅₀ 0.07 μM). Replacement with an amine or an acetamide led to a respective two-fold and 2.5-fold decrease in activity against *T. brucei*. Acetylation of the amide –NH led to a significant loss in activity across all the parasites tested, indicating the requirement of a hydrogen bond donating group at this position. Removal of the phenyl moiety led to a decrease in the observed activity (EC₅₀ 1.32 μM) as did replacement with either a methyl (EC₅₀ 3.36 μM), ethyl (EC₅₀ 1.79 μM) or *n*-butyl group (EC₅₀ 1.67 μM), highlighting the preference for a bulky hydrophobic group at this position. In addition to this, all of these analogues were found to be no longer active against *T. cruzi*. Removal of the phenyl ring from the phenyl-piperidine moiety led to a complete loss of observed activity against all the parasites tested. Removal of the piperidine moiety led to a six-fold loss in activity (EC₅₀ 0.37 μM) and removal of both the piperidine and the linker led to an analogue with a further diminished EC₅₀ of 1.44 μM. Replacement of the piperidine with a morpholine was reasonably well tolerated (EC₅₀ 0.1 μM) as was removal of the methylene linker. In general, the only positive modulation of the activity of these analogues was observed at the ethyl sulfonamide moiety.

An early SAR investigation around danusertib (**1.55**) has also been performed.⁴⁰ Development of a homology model for *TbAUK1* based on human and mouse Aurora A crystal structures allowed for close examination of any differences in the binding pockets of *TbAUK1* and human Aurora A. When **1.56** and danusertib (**1.55**) were docked into the homology model it was observed that **1.56** had a very similar binding pose to that of danusertib (**1.55**) in the Aurora A/danusertib complex.⁴⁰ The pyrazinylphenyl tail in both structures is oriented towards the solvent and the hydrogen bonding interactions between the kinase hinge region and the pyrazolopyrrole core were also preserved. The key difference concerned the position of the head group region. The head group region of **1.55** assumed a flipped orientation in the *TbAUK1* binding site with the phenyl group moving into a hydrophobic pocket. The authors proposed that the tetrahedral geometry of the carbon atom adjacent to the carbonyl of the **1.55** head group region would enable the head group flip. It was also proposed that lipophilic side chains around this region may drive potency. As a result 50 analogues were docked into the *TbAUK1* homology model and the results were ranked. The top 20 analogues were chosen for synthesis and then tested at 1 and 10 μM against *T.b. brucei*. Of these, 11 compounds showed greater than 60% inhibition and were selected for a full-dose response analysis in *T.b. rhodesiense* and MOLT-4 cells. A selection of these are shown in Table 1.10. MOLT-4 cells are acute myeloid leukemia cells that are known to overexpress Aurora kinases A and B when compared with uninduced peripheral blood mononuclear cells.⁴¹ When the racemate of **1.55** was tested (**1.57**) a decrease in the activity against both *T.b. rhodesiense* and MOLT-4 cells was observed. However, the loss in activity was greater in the mammalian cells leading to a 6.8-fold improvement in selectivity. Replacing the phenyl with the bulkier naphthyl group (**1.58**) led to a significant improvement in the selectivity of these compounds for the parasite, with a ~23-fold improvement. Whilst the authors have not been able to show any improvement in the potency of these compounds for *T.b. rhodesiense* they have successfully shown the ability to improve their selectivity over MOLT-4 cells. As the MOLT-4 cells are more susceptible to Aurora kinase inhibitors given the overexpression of Aurora kinases A and B, it is possible that the EC_{50} values against this cell line are not truly representative of the compounds mammalian toxicity levels and they would need to be re-examined in an alternative cell line.

Table 1.10 Dose-response results for a selection of analogues of danusertib (**1.55**).



ID	R ¹	Ar	EC ₅₀ (μM) ^b		Selectivity
			<i>T.b. rhodesiense</i> ^c	MOLT-4 ^d	
1.55	OCH ₃	Phenyl	0.15	0.15	1.0
1.57^a	OCH ₃	Phenyl	0.61	4.13	6.8
1.58	H	1-Naphthyl	0.61	14.25	23.4

^a Compound tested as a racemate.

^b EC₅₀ values calculated from inhibition curves at a minimum of 8 different drug concentrations tested in triplicate and using OriginPro 8.5 analysis software.

^c *T.b. rhodesiense* YTAT1.1 strain.

^d MOLT-4 acute myelogenous leukemia cell line.

A number of known human phosphoinositide 3-kinase (PI3K) and mammalian target of rapamycin (mTOR) inhibitors were recently screened against *T. brucei*, *T. cruzi* and *L. donovani* in an effort to identify any crossover activity (Table 1.11).⁴² Of particular note was compound NVP-BEZ235 (**1.59**) that has been in clinical trials for the treatment of a number of solid tumors.⁴³⁻⁴⁶ Compound **1.59** demonstrated subnanomolar activity against *T.b. brucei* which also translated into subnanomolar activity against the human infective *T.b. rhodesiense*; and was additionally shown to have potent activity against *T. cruzi* and *L. donovani*.

Table 1.11 Results from the screening of human PI3K and mTOR inhibitors against *T. brucei*, *T. cruzi* and *L. donovani*.⁴²

ID	EC ₅₀ (μM)				
	<i>T. cruzi</i> ^a	<i>T.b. brucei</i> ^b	<i>T.b. rhodesiense</i> ^b	<i>L. donovani</i> ^c	<i>L. donovani</i> ^d
PI-103		0.214 ±			
(1.59)	>25	0.036	0.105 ± 0.01	1.05 ± 0.28	0.62 ± 0.41
NVP-BEZ235					
(1.60)	0.12	<0.01	0.0073 ± 0.06	0.14 ± 0.08	0.07 ± 0.04
LY294002					
(1.61)	-	>2	-	-	>5
Pp242					
(1.62)	>10	0.48 ± 0.1	0.166 ± 0.015	0.42 ± 0.03	0.50 ± 0.09
WYE-354					
(1.63)	>10	0.58 ± 0.26	0.78 ± 0.08	5.95 ± 0.84	6.10 ± 1.73

^a trypomastigotes.

^b bloodstream form.

^c promastigotes.

^d axenic amastigotes.

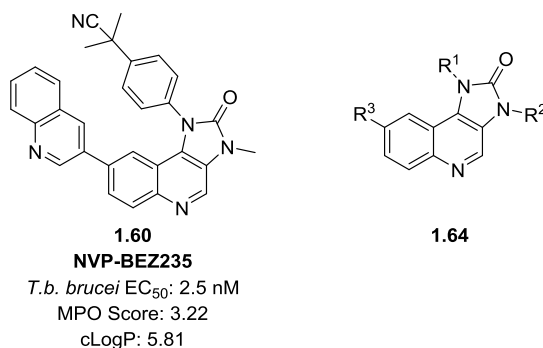
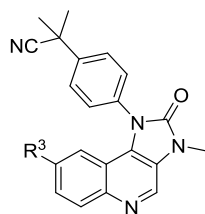


Figure 1.16 Structure of NVP-BEZ235 (**1.60**), a known inhibitor of human PI3K and mTOR, and the regions studied during the SAR investigation as denoted by R¹, R², and R³.

A SAR investigation around **1.60** was subsequently performed.⁴⁷ In addition to improving the potency and selectivity of these compounds, it was also necessary to address some of the physicochemical properties of **1.60**. It was identified as being lipophilic with a cLogP of 5.81 and also poorly soluble which could be partially due to the high number of aromatic rings that would contribute to favourable π -stacking interactions.⁴⁷ In addition to this, **1.60** has been calculated as having a CNS multiparameter optimisation (MPO) score of 3.2.⁴⁷ It had been previously shown that when **1.60** was docked into an homology model of PI3K γ the binding was largely due to three hydrogen bond interactions.⁴⁸ As a result of this, each of the regions responsible for forming a hydrogen bonding interaction were examined separately, as denoted by the R groups in **1.64** (Figure 1.16).

Initial investigations centered around the R³ region, highlighted in Table 1.12. Replacement of the quinolone (**1.60**) with a phenyl (**1.65**) moiety saw a 64-fold loss in the activity of the compound.⁴⁷ Replacement with a 4-pyridyl (**1.66**) also led to a significant decrease in the activity with a 54-fold loss, however there was a drastic reduction in the cLogP of this analogue.⁴⁷ Yet replacement with the 3-pyridyl (**1.67**), which ensured that the endocyclic nitrogen would be in the same spatial region, saw only a 6-fold decrease in the activity.⁴⁷ Insertion of an ethyne linker (**1.68**) resulted in a 3-fold loss in activity against the parasite, though there was a significant decrease in the selectivity of this compound.⁴⁷ The introduction of a trifluoromethyl in the *para* position (**1.69**) led to a complete loss of cytotoxicity whilst still maintaining potent *T.b. brucei* activity.⁴⁷ A number of other heterocycles, such as the benzothiophene (**1.70**), and cyclic or linear amines or amides including the acetylated amine (**1.71**) were also trialled, however, the pyridine substituents presented a more favourable profile.⁴⁷ In general, a heteroaromatic system at this position was found to be essential for potent anti-trypanosomal activity.

Table 1.12 Results of the SAR around the R³ position of NVP-BEZ235 (**1.60**).



ID	R ³	<i>T.b. brucei</i> EC ₅₀ (μM) ^a	HepG2 TC ₅₀ (μM) ^a	Selectivity	MPO Score
1.60		0.0025	-	-	3.2
1.65		0.159	1.82	11	3.6
1.66		0.136	3.43	25	3.9
1.67		0.016	0.575	36	3.9
1.68		0.008	0.14	17	3.4
1.69		0.053	> 25	> 470	3.1
1.70		0.054	> 25	> 460	3.2
1.71	-NHAc	9.02	> 50	> 5	4.6

^a Values are the average of two replicates.

At the R¹ position a *para* substituent was initially trialled (Table 1.13). Compounds **1.72-1.74** all demonstrated a 10- to 15-fold decrease in activity against *T.b. brucei*, though they all exhibited excellent selectivity profiles when compared with HepG2 cells.⁴⁷ When the R³ group is the 4-pyridyl the presence of a

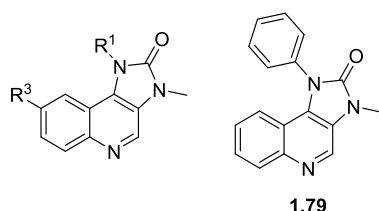
nitrile (**1.76**) or amine (**1.78**) is favourable for activity over the *para*-methyl (**1.75**) or methoxy (**1.77**).⁴⁷ There was also a complete loss of activity against both *T.b. brucei* and HepG2 cells when both the R¹ and R³ substituents were simultaneously eliminated as in **1.79**.⁴⁷

Exploration of the R² substituent via the des-methyl and original, methylated compounds was also performed. Though no clear trend in the data was evident, there was no observed difference in the solubility or permeability of the compounds.⁴⁷ As a result of this work, **1.77** was identified as the most promising lead for further development. With a significantly improved MPO score when compared with NVP-BEZ235 (**1.60**) as well as improved parasite selectivity, no further improvement in the solubility of this compound was observed.

A number of human tyrosine kinase inhibitors have been screened for activity against *T.b. brucei*, the results of which are in Table 1.14.³³ Previous pharmacological studies by the authors revealed that a tyrosine kinase, tryphostin A47, was responsible for the inhibition of diacylglycerol-stimulated endocytosis of transferrin, which is vital to the survival of bloodstream *T. brucei*.⁴⁹⁻⁵¹ During lead discovery the authors examined those drugs for which there was existing literature precedence of plasma concentrations equal to, or exceeding the previously measured GI₅₀ for efficacy in an acute mouse model of HAT (*T. brucei* CA427), Table 1.15.³³ Each mouse was inoculated with 10³ trypanosomes and treatment was started 1 day post infection and continued for 14 days.³³ The treatment was administered daily either orally or intraperitoneally. Administration of lapatinib (**1.83**) orally led to the reduction of parasitemia levels in the mice and exhibited a cure rate of 25% in three independent experiments, those mice that were not cured exhibited an extended MSD of 8 days.³³ Whilst intraperitoneal administration of lapatinib (**1.83**) failed to eliminate the parasitemia infection and all mice had died by day 8.³³ AEE788 (**1.84**) was equally able to reduce the parasitemia levels as lapatinib (**1.83**) though it was not successful in curing any mice and the authors failed to comment on the lower dosing given to the mice in the treatment regimen.³³ CI-1033 (**1.80**) demonstrated some cytotoxicity

issues above 30 mg/kg, hence the lower dosing in the mouse model, though it still failed to cure any of the mice and the MSD value is only marginally improved when compared with the control MSD.³³

Table 1.13 Results of the SAR around the R¹ position of NVP-BEZ235 (**1.60**).



ID	R ¹	R ³	<i>T.b. brucei</i> EC ₅₀ (μM) ^a	HepG2 TC ₅₀ (μM) ^a	Selectivity	MPO Score
1.60			0.0025	-	-	3.2
1.72			0.103	> 25	> 240	3.2
1.73			0.091	> 50	> 540	3.5
1.74			0.024	> 25	> 1000	3.7
1.75			0.202	4.78	24	4.1
1.76			0.072	-	-	4.8
1.77			0.166	11.2	67	4.6
1.78			0.082	2.34	28	4.2
1.79			18.5	> 50	> 3	5.0

^a Values are the average of two replicates.

Table 1.14 Effect of tyrosine kinase drugs on the replication of *T.b. brucei*.

Drug	<i>T.b. brucei</i> GI ₅₀ (mean ± SD) (μM)
CI-1033 (1.80)	1.4 ± 0.7
Erlotinib (1.81)	1.9 ± 0.1
PKI-166 (1.82)	1.3 ± 0.2
Lapatinib (1.83)	1.5 ± 0.1
AEE788 (1.84)	2.5 ± 0.1
Axitinib (1.85)	2.0 ± 0.5
Sunitinib (1.86)	1.3 ± 0.1
Imatinib (1.87)	> 10.0

Table 1.15 Efficacy of tyrosine kinase drugs in an acute mouse model of HAT.

ID	Administration	Dose	Cures ^a	MSD
Control	-		-	4.5-5.5
Lapatinib (1.83)	Oral	100 mg/kg every 12 h	1/4 ^b	8 ^{c,d}
AEE788 (1.84)	Oral	30 mg/kg every 24 h	0/4	10 ^e
CI-1033 (1.80)^f	Intraperitoneal	30 mg/kg every 24 h	0/4	5.8

^a Mice surviving 30 days after the death of the last control mouse and having no parasitemia.

^b Result replicated in three studies.

^c Value excludes those mice that were considered to be cured.

^d With intraperitoneal administration all mice had died by day 8 (data not shown in publication).

^e When administered intraperitoneally the mean survival time was similar to control mice (data not shown in publication).

^f Both oral and intraperitoneal administration produced similar results (data not shown in publication).

A subsequent SAR study around lapatinib (**1.83**; Figure 1.17) was performed in order to improve the potency and selectivity of these compounds for *T. brucei* over mammalian cells.⁵² Initial investigations centered

around the furan tail of lapatinib. The metabolic liability of furans has been well documented⁵³ and it appears that the authors have consciously moved away from this moiety leading to a series of compounds with modest activity against *T. brucei* with compound **1.88** showing good potency and selectivity.⁵² Whilst there were investigations around the northern head group there was no significant improvement in the activity or selectivity observed. Yet further examination of the tail region did lead the authors to identify **1.89** where the morpholine is directly connected to the phenyl ring in the *meta* position.⁵² Compound **1.89** exhibits potent activity against *T. brucei* and has an improved selectivity profile. In addition it has been shown to be an orally bioavailable inhibitor of trypanosome replication, blocking the duplication of the kinetoplast and arresting cytokinesis.⁵² The calculated MPO score for this compound is just 2.8, likely due to its high MW and high lipophilicity, which is well above the accepted guide of 4.0 for possible BBB penetration.⁵² The assessment of **1.89** in a mouse model of HAT showed a modest effect on parasitemia levels and led to an extension of life expectancy, though these effects were lower than expected, most likely due to the high plasma protein binding.⁵² Further work is required on this series if both stages of HAT are to be successfully treated.

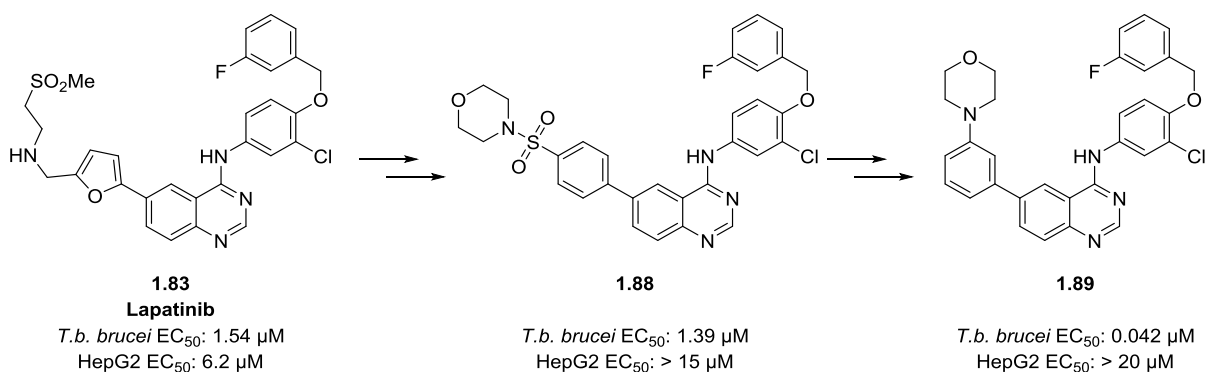


Figure 1.17 Lapatinib (**1.83**) and the subsequent modifications of the tail region to give compound **1.89**.

1.2 Introduction to the compounds addressed in this thesis

A whole organism, high-throughput phenotypic screen of 87,296 compounds was recently undertaken against bloodstream *T.b. brucei*.⁵ This led to the identification of 700 compounds with confirmed inhibition of $\geq 80\%$ against *T. brucei*. These compounds were subsequently tested against mammalian HEK293 cells in order to determine a SI value for each compound. This led to 205 compounds with a SI > 10 and an IC₅₀ against *T. brucei* of $< 10 \mu\text{M}$. Cluster analysis of the resulting hits and removal of pan-assay interference compounds (PAINS)²³ led to the identification of the compounds in Figure 1.18. These compounds were also screened in a parasite panel against *T.b. rhodesiense*, *T. cruzi*, *L. donovani* and *P. falciparum*. Of these compounds, four will be presented in this thesis, **126**, **130**, **1.90**, and **128**.

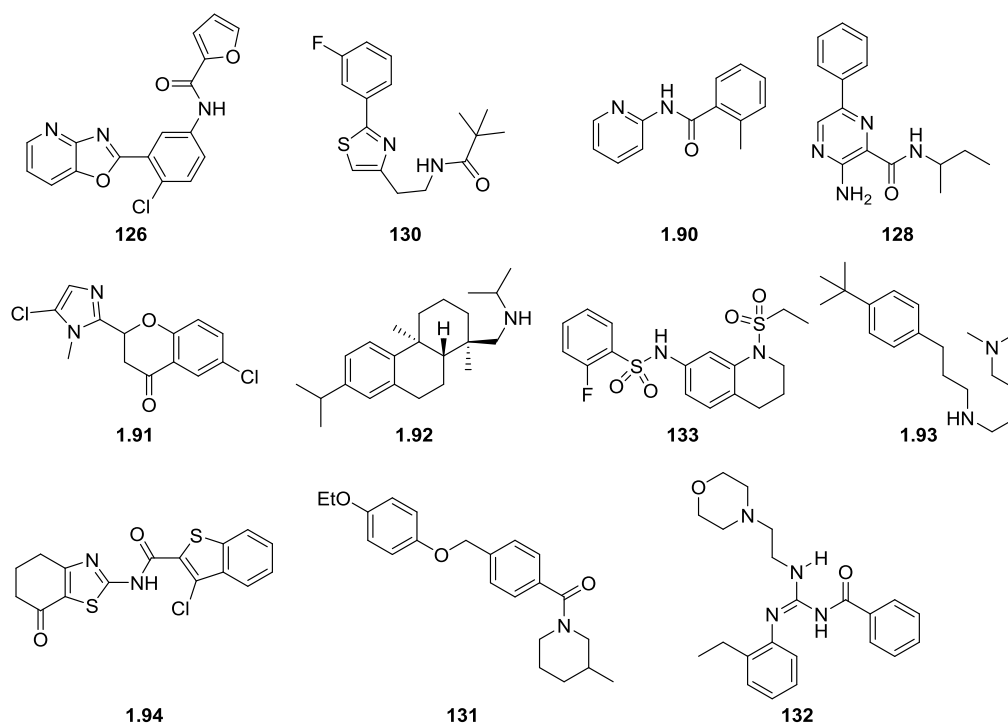


Figure 1.18 Compounds identified in the phenotypic screen against *T.b. brucei*.

1.3 SAR Rationale

During the investigation of the SAR around the core compounds in Figure 1.18, a number of substituents were chosen with which to probe the relevant positions. Substituents were chosen based on their hydrophobic, electronic, and steric properties in order to investigate each position fully. These are summarised in Table 1.16. The π value is representative of the hydrophobicity of a substituent and is a measure of the ratio of concentrations of a compound in a mixture of two phases, an octanol phase and an aqueous phase. A π value of 1.00 indicates a ten-fold increase in partitioning of a compound in to the octanol phase. Functional groups with a positive π value include bromine, chlorine, fluorine, iodine, methyl, trifluoromethyl and trifluoromethoxy. Correspondingly a value of -1.00 indicates a ten-fold increase in the partitioning of a compound in to the aqueous phase. Those functional groups with a negative π value include an alcohol, amine or nitrile. The inclusion of functional groups with hydrogen bond donors and acceptors has been accounted for with the alcohol and amine both able to accept and donate hydrogen bonds, while the nitrile, fluorine, methoxy and the trifluoromethoxy can act as hydrogen bond acceptors. The molar refractivity (MR) value is an indication of the steric bulk of a functional group, where larger numbers are indicative of increasingly bulky groups. A wide range of substituents have been selected based on their MR values, from the least bulky substituents, fluorine and hydrogen through to the very bulky phenyl group. Finally, compounds with varying electronic effects have been selected. A positive σ value indicated a group with an electron withdrawing effect while a negative σ value indicated an electron donating effect, at either the *meta* or *para* positions. The amine and alcohol are the most electron donating functional groups, while the nitrile and trifluoromethyl groups are strong electron withdrawing groups.

Endocyclic nitrogen is an additional functional group to those summarised in Table 1.16. It has a number of advantages in its use as it can decrease the hydrophobicity of a compound and improve its overall solubility. An endocyclic nitrogen can also act as a hydrogen bond acceptor which can turn a potentially unfavourable hydrophobic interaction into a favourable hydrophilic one.

The biological testing of these compounds was performed on the animal infective subspecies of the parasite, *T.b. brucei*, at the Eskitis Institute, Griffith University. This subspecies of the parasite is the safest to humans and also the easiest parasite with which to maintain a culture. For compounds that were of particular significance they were subjected to a wider parasite panel offered by the Swiss Tropical and Public Health Institute (STI). The panel includes the human infective parasite, *T.b. rhodesiense*, the causative agent of HAT and *T. cruzi*, the causative agent of Chagas disease.⁵⁴ The parasite panel also consists of *L. donovani* axenic amastigotes and *L. donovani* infective macrophages, which are the causative agent of Leishmaniasis, along with *P. falciparum*, the causative agent of malaria.⁵⁴ It was not possible to test these compounds against *T.b. gambiense* as it is a particularly difficult organism and culture to maintain.

T.b. brucei, *T. cruzi* and *L. donovani* all belong to the Trypanosomatidae family and they share many general characteristics including a number of subcellular structures though each has a unique complex life cycle, is transmitted by different vectors and targets different tissues in the mammalian host. *T.b. brucei*, *L. donovani* and *P. falciparum* are all able to survive extracellularly and, as such, are traditionally assayed in the bloodstream forms. However, *T. cruzi* cannot survive extracellularly and the trypomastigotes are allowed to infect erythrocytes prior to the biological analysis of compounds. This can make interpreting SAR for *T. cruzi* somewhat difficult as it needs to be clear that the compound being tested is indeed killing the parasite and not the host mammalian cell. Though in general, even for *T.b. brucei* membrane permeability is a factor for the interpretation of the SAR and more polar compounds may not be able to penetrate the membrane. This is an important consideration to be taken into account throughout this thesis when interpreting the SAR and this is emphasised throughout.

Table 1.16 Parameters used to probe the hydrophobic, electronic and steric properties of substituents typically employed in this SAR study.⁵⁵

Substituent	π	H-acceptor	H-donor	MR	Electronic	
					σ_m	σ_p
H	0.00	0	0	1.03	0.00	0.00
Br	0.86	0	0	8.88	0.39	0.23
Cl	0.71	0	0	6.03	0.37	0.23
F	0.14	1	0	0.92	0.34	0.06
I	1.12	0	0	13.94	0.35	0.18
OH	-0.67	1	1	2.85	0.12	-0.37
NH ₂	-1.23	1	1	5.42	-0.16	-0.66
CF ₃	0.88	0	0	5.02	0.43	0.54
OCF ₃	1.04	1	0	7.86	0.38	0.35
CN	-0.57	1	0	6.33	0.56	0.66
CH ₃	0.56	0	0	5.65	-0.07	-0.17
OCH ₃	-0.02	1	0	7.87	0.12	-0.27
CH ₂ CH ₃	1.02	0	0	10.30	-0.07	-0.15
C ₆ H ₆	1.96	0	0	25.36	0.06	-0.01

Further to the parasite panel, a number of compounds were subjected to further analysis of some key physicochemical properties and to determine *in vitro* metabolic stability. Initially the MW of the compounds were calculated. Ideally, the MW should be less than 500 Da for good intestinal membrane permeability and less than 450 Da for good BBB permeability.⁵⁶ The calculated polar surface area (PSA) of a molecule has been used to predict absorption and BBB permeability for drugs. A PSA of less than approximately 120 Å² indicates acceptable oral absorption and membrane permeability, while the PSA values for drugs destined for the CNS are much lower, typically within 60 - 70 Å² through to 90 Å².^{56, 57} Recently, researchers have begun reporting an MPO score for their compounds, which accounts for a number of factors (Table 1.17) when

trying to determine the potential of a compound to cross the BBB. On a scale of 0-6 any value ≥ 4 indicates the potential of a compound to penetrate the CNS.⁵⁸ As an MPO score is the culmination of a number of different factors it is thought that it provides a more accurate measure of a compounds potential to cross the BBB. The aqueous solubility of drugs is essential for delivery of a desired drug to a target within the body as any drug to be absorbed must be in the form of a solution at the site of absorption.⁵⁹ Typically, to be a successful CNS drug candidate aqueous solubility needs to be $> 60 \mu\text{g/ml}$.⁵⁶ The distribution co-efficient (logD) is a measure of the lipophilicity of a drug.⁵⁶ It is measured as a ratio of the concentration of ionised and un-ionised drug between two phases. It has previously been found that for optimal BBB permeability the lipophilicity of a drug needs to be in the range 1.5 – 2.7.⁵⁶ Plasma protein binding (PPB) values can be estimated using the human serum albumin (HSA) chromatographic method (cPPB); a measure of the degree to which drugs bind to HSA.⁵⁶ HSA is responsible for binding acidic drugs in the plasma while a second protein, α_1 -acid glycoprotein (AGP), is present and is responsible for binding basic drugs.^{60, 61} HSA serves as a transport protein, with a high capacity for binding but a low affinity while AGP has a low capacity and high affinity for binding.⁵⁶ Whilst HSA is the most predominantly found transport protein, the concentration of AGP in serum can be affected by disease, medications and pregnancy consequently affecting PPB values.⁶¹ A successful CNS drug should not be an efficient AGP binding drug nor a high-affinity HSA binder.⁵⁶ The half-life of the compounds may be measured in human liver microsomes providing an indication of the degree of first-pass metabolism by the liver and intestines experienced by the compound *in vivo*. Ideally this value should be as low as possible to ensure sufficient concentration of drug is circulating throughout the body to have an effect.⁵⁶ *In vitro* intrinsic clearance (CL_{int}) determined in human liver microsomes is determined as a predictor for clearance of the drug from the liver. The predicted hepatic extraction (E_{H}) ratio is calculated from *in vitro* data. Values range from 0.00-1.00 with 0.00 indicating the compound is not metabolised and 1.00 indicating complete metabolism of the compound.

Table 1.17 Desirable ranges for successful CNS penetration according to the MPO scoring system.

Property	Targeted value
Partition coefficient (cLogP)	≤ 3
Distribution coefficient (cLogD)	≤ 2
Polar surface area	$40 < X \leq 90$
Molecular weight	≤ 360
Hydrogen bond donors	≤ 0.5
pK _a	≤ 8

1.4. Thesis Aims

This thesis investigates the synthesis of novel, effective and safe inhibitors of *T. brucei*, and will focus on four unique structural classes (**126**, **130**, **1.90**, and **128**). Particular emphasis will be on improving the potency of these compounds into the therapeutically relevant range of single digit nanomolar EC₅₀ values against *T. brucei*. Given the toxicity issues observed with many of the current therapeutics, the selectivity of the synthesised analogues will also be measured against mammalian cells. All of the biological assays against *T.b. brucei* were performed by the Avery group at the Eskitis Institute. Furthermore, these compounds had their physicochemical properties assessed by collaborators at the Centre for Drug Candidate Optimisation. This is necessary in order to ensure a number of parameters are met, such as the PSA, solubility and metabolism, in order to effectively treat both stages of the disease. Finally, collaborators at the Swiss Tropical and Public Health Institute have tested selected analogues against the human infective subspecies, *T.b. rhodesiense*, along with *T. cruzi*, *L. donovani* and *P. falciparum*.

1.5. General Experimental

1.5.1. Biological Experimental

All *in vitro* assays were carried out *at least* twice independently in singleton.

***T.b. brucei* assay** Compound activity against *T.b. brucei* was assessed in an Alamar blue® viability assay as previously described by Sykes and Avery.⁶² Briefly, 55 µl of HMI-9 media +10% FCS⁶³ containing 1200 cells/ml of logarithmic phase *T.b. brucei* 427 bloodstream parasites were added to a 384-well microtiter plate (BD biosciences) and incubated for 24 h at 37 °C/5% CO₂. Serial drug concentrations were prepared in 100% DMSO and diluted 1:21 in DMEM media. 5 µl of this dilution was subsequently added to assay plates to give final compound concentrations ranging from 41.67 to 0.0004 µM. Plates were incubated for 48 h at 37°C/5% CO₂. 10 µl of 70% Alamar Blue® (Invitrogen) prepared in HMI-9 media +10% FCS was added to assay plates and plates incubated for a further 2 h at 37 °C/5% CO₂ followed by 22 h at room temperature. Assay plates were read at 535 nm excitation/590 nm emission on an Envision® multiplate reader (PerkinElmer, Massachusetts, USA). Data was analysed and EC₅₀ values calculated using the software GraphPad Prism 5. Pentamidine and suramin were used as controls.

HEK293 cytotoxicity assay 55 µl of DMEM +10% FCS media (Gibco) containing 72727 cells/ml of confluent HEK293 cells was added to a 384-well microtiter plate (BD biosciences) and incubated for 24 h at 37 °C/5% CO₂. Serial compound concentrations were prepared in 100% DMSO and diluted 1:21 in DMEM media. 5 µl of this dilution was subsequently added to assay plates to give final compound concentrations ranging from 83.34 to 0.0004 µM. Plates were incubated for 48 h at 37°C/5% CO₂. 10 µl of 70% Alamar Blue® (Invitrogen) prepared in DMEM media +10% FCS was added to assay plates and plates incubated for a further 5 h at 37 °C/5% CO₂ followed by 19 h at room temperature. Assay plates were read at 535 nm excitation/590 nm emission on an Envision® multiplate reader (PerkinElmer, Massachusetts, USA). Data

was analysed and EC₅₀ values calculated using the software GraphPad Prism 5. Puromycin was used as a control.

***P. falciparum* assay** *In vitro* activity against erythrocytic stages of *P. falciparum* was determined using a ³H-hypoxanthine incorporation assay,^{64, 65} using the drug sensitive NF54 strain⁶⁶ and the standard drug chloroquine (Sigma C6628). Compounds were dissolved in DMSO at 10 mg/ml and added to parasite cultures incubated in RPMI 1640 medium without hypoxanthine, supplemented with HEPES (5.94 g/l), NaHCO₃ (2.1 g/l), neomycin (100 U/ml), Albumax^R (5 g/L) and washed human red cells (type A⁺) at 2.5% haematocrit (0.3% parasitaemia). Serial drug dilutions of eleven 3-fold dilution steps covering a range from 100 to 0.002 µg/ml were prepared. The 96-well plates were incubated in a humidified atmosphere at 37 °C; 4% CO₂, 3% O₂, 93% N₂. After 48 h, 50 µl of ³H-hypoxanthine (0.5 µCi) was added to each well of the plate. The plates were incubated for a further 24 h under the same conditions. The plates were then harvested with a Betaplate™ cell harvester (Wallac, Zurich, Switzerland), and the red blood cells transferred onto a glass fibre filter and washed with distilled water. The dried filters were inserted into a plastic foil with 10 ml of scintillation fluid, and counted in a Betaplate™ liquid scintillation counter (Wallac, Zurich, Switzerland). EC₅₀ values were calculated from sigmoidal inhibition curves by linear regression⁶⁷ using Microsoft Excel. Chloroquine and artemisinin were used as controls.

***L. donovani* axenic amastigotes assay** Amastigotes of *L. donovani* strain MHOM/ET/67/L82 were grown in axenic culture at 37 °C in SM medium⁶⁸ at pH 5.4 supplemented with 10% heat-inactivated fetal bovine serum under an atmosphere of 5% CO₂ in air. 100 µl of culture medium with 10⁵ amastigotes from axenic culture with or without a serial drug dilution were seeded in 96-well microtitre plates. Serial drug dilutions of eleven three-fold dilution steps covering a range from 100 to 0.002 µg/ml were prepared. After 70 h of incubation the plates were inspected under an inverted microscope to assure growth of the controls and sterile conditions. 10 µl of Alamar Blue (12.5 mg resazurin dissolved in 100 ml distilled water)⁶⁹ were then added to each well and the plates incubated for another 2 h. The plates were read with a Spectramax Gemini XS microplate fluorometer (Molecular Devices Cooperation, Sunnyvale, CA, USA) using an excitation wavelength of 536 nm and an emission wavelength of 588 nm. Data were analysed using the software

Softmax Pro (Molecular Devices Cooperation, Sunnyvale, CA, USA). Decrease of fluorescence (i.e. inhibition) was expressed as percentage of the fluorescence of control cultures and plotted against the drug concentrations. From the sigmoidal inhibition curves the EC₅₀ values were calculated by linear regression.⁶⁷ Miltefosine was used as a control.

***T. cruzi* assay** Rat skeletal myoblasts (L6 cells) were seeded in 96-well microtitre plates at 2000 cells/well in 100 µl RPMI 1640 medium with 10% FBS and 2 mM l-glutamine. After 24 h, the medium was removed and replaced by 100 µl per well containing 5000 trypomastigote forms of *T. cruzi* Tulahuen strain C2C4 containing the β-galactosidase (Lac Z) gene.⁷⁰ After 48 h the medium was removed from the wells and replaced by 100 µl fresh medium with or without a serial drug dilution of eleven 3-fold dilution steps covering a range from 100 to 0.002 µg/ml. After 96 h of incubation the plates were inspected under an inverted microscope to assure growth of the controls and sterility and the substrate CPRG/Nonidet (50 µl) was added to all wells. A colour reaction developed within 2–6 h and could be read photometrically at 540 nm. Data were analysed with the graphic programme Softmax Pro (Molecular Devices), which calculated EC₅₀ values by linear regression⁶⁷ from the sigmoidal dose inhibition curves. Benznidazole was used as a control.

***Tb. rhodesiense* assay** This parasite stock was isolated in 1982 from a human patient in Tanzania and after several mouse passages cloned and adapted to axenic culture conditions.⁷¹ Minimum Essential Medium (50 µL) supplemented with 25 mM HEPES, 1 g/L additional glucose, 1% MEM non-essential amino acids (100x), 0.2 mM 2-mercaptoethanol, 1 mM Na-pyruvate and 15% heat inactivated horse serum was added to each well of a 96-well microtiter plate. Serial drug dilutions of eleven three-fold dilution steps covering a range from 100 to 0.002 µg/ml were prepared. Then 4x10³ bloodstream forms of *Tb. rhodesiense* STIB 900 in 50 µl was added to each well and the plate incubated at 37 °C under a 5% CO₂ atmosphere for 70 h. 10 µl Alamar Blue (resazurin, 12.5 mg in 100 ml double-distilled water) was then added to each well and incubation continued for a further 2–4 h.⁷² Then the plates were read with a Spectramax Gemini XS microplate fluorometer (Molecular Devices Cooperation, Sunnyvale, CA, USA) using an excitation wavelength of 536 nm and an emission wavelength of 588 nm. The EC₅₀ values were calculated by linear

regression⁶⁷ from the sigmoidal dose inhibition curves using SoftmaxPro software (Molecular Devices Cooperation, Sunnyvale, CA, USA). Melarsoprol was used as a control.

Rat skeletal myoblast cytotoxicity assay Assays were performed in 96-well microtiter plates, each well containing 100 μ l of RPMI 1640 medium supplemented with 1% L-glutamine (200 mM) and 10% foetal bovine serum, and 4000 L6 cells (a primary cell line derived from rat skeletal myoblasts).^{73, 74} Serial drug dilutions of eleven three-fold dilution steps covering a range from 100 to 0.002 μ g/ml were prepared. After 70 h of incubation the plates were inspected under an inverted microscope to assure growth of the controls and sterile conditions. 10 μ l of Alamar Blue was then added to each well and the plates incubated for another 2 h. The plates were then read with a Spectramax Gemini XS microplate fluorometer (Molecular Devices Cooperation, Sunnyvale, CA, USA) using an excitation wavelength of 536 nm and an emission wavelength of 588 nm. The EC₅₀ values were calculated by linear regression⁶⁷ from the sigmoidal dose inhibition curves using SoftmaxPro software (Molecular Devices Cooperation, Sunnyvale, CA, USA). Podophyllotoxine was used as a control.

1.5.2. Chemistry Experimental

All compounds tested had a purity of > 95% as measured by HPLC or LCMS.

Solvents were of analytical grade: ethyl acetate (EtOAc); dichloromethane (DCM); dimethyl formamide (DMF); methanol (MeOH); tetrahydrofuran (THF). Analytical TLC was performed on silica gel 60/F₂₅₄ pre-coated aluminium sheets (0.25 mm, Merck). Flash column chromatography was carried out with silica gel 60, 0.63–0.20 mm (70–230 mesh, Merck).

¹H and ¹³C NMR spectra were recorded at 400.13, and 100.62 MHz, respectively, on a Bruker Avance III Nanobay spectrometer with BACS 60 sample changer, using solvents from Cambridge Isotope Laboratories. Chemical shifts (δ , ppm) are reported relative to the solvent peak (CDCl₃: 7.26 [¹H] or 77.16 [¹³C]; DMSO-

d_6 : 2.50 [^1H] or 39.52 [^{13}C]; or CFCl_3 at 0.00 [^{19}F]). Proton resonances are annotated as: chemical shift (ppm), multiplicity (s, singlet; d, doublet; t, triplet; q, quartet; m, multiplet; v br, very broad), coupling constant (J , Hz), and number of protons.

Analytical HPLC was acquired on an Agilent 1260 Infinity analytical HPLC coupled with a G1322A degasser, G1312B binary pump, G1367E high performance autosampler, G4212B diode array detector. Conditions: Zorbax Eclipse Plus C18 Rapid resolution column (4.6 x 100 mm) with UV detection at 254 nm and 214 nm, 30 °C; sample was eluted using a gradient of 5 – 100% of solvent B in solvent A where solvent A: 0.1% formic acid in water, and solvent B: 0.1% formic acid in ACN (5 to 100% B [9 min], 100% B [1 min]; 0.5 ml/min).

Low resolution mass spectrometry was performed on an Agilent 6100 Series Single Quad LCMS coupled with an Agilent 1200 Series HPLC, G1311A quaternary pump, G1329A thermostatted autosampler, and G1314B variable wavelength detector (214 and 254 nm). LC conditions: Phenomenex Luna C8(2) column (100 Å, 5 µm, 50 × 4.6 mm), 30 °C; sample (5 µL) was eluted using a binary gradient (solvent A: 0.1% aq. HCO_2H ; solvent B: 0.1% HCO_2H in CH_3CN ; 5 to 100% B [10 min], 100% B [10 min]; 0.5 ml/min). MS conditions: quadrupole ion source with multimode-ESI; drying gas temperature, 300 °C; vaporizer temperature, 200 °C; capillary voltage, 2000 V (positive mode) or 4000 V (negative mode); scan range, 100–1000 m/z ; step size, 0.1 s over 10 min.

High resolution MS was performed on an Agilent 6224 TOF LCMS coupled to an Agilent 1290 Infinity LC. All data were acquired and reference mass corrected via a dual-spray electrospray ionisation (ESI) source. Each scan or data point on the total ion chromatogram (TIC) is an average of 13,700 transients, producing a spectrum every second. Mass spectra were created by averaging the scans across each peak and subtracting the background from first 10 s of the TIC. Acquisition was performed using the Agilent Mass Hunter Data Acquisition software ver. B.05.00 Build 5.0.5042.2 and analysis was performed using Mass Hunter Qualitative Analysis ver. B.05.00 Build 5.0.519.13. Acquisition parameters: mode, ESI; drying gas flow, 11 l/min; nebuliser pressure, 45 psi; drying gas temperature, 325 °C; voltages: capillary, 4000 V; fragmentor,

160 V; skimmer, 65 V; octapole RF, 750 V; scan range, 100–1500 m/z ; positive ion mode internal reference ions, m/z 121.050873 and 922.009798. LC conditions: Agilent Zorbax SB-C18 Rapid Resolution HT (2.1 × 50 mm, 1.8 μm column), 30 °C; sample (5 μl) was eluted using a binary gradient (solvent A: 0.1% aq. HCO_2H ; solvent B: 0.1% HCO_2H in CH_3CN ; 5 to 100% B [3.5 min], 0.5 ml/min).

1.5.3. Physicochemical Experimental

Solubility Estimates using Nephelometry Stock solutions of compound (10 mg/ml) prepared in DMSO were spiked into either pH 6.5 phosphate buffer or 0.01 M HCl (approximately pH 2.0) with the final DMSO concentration being 1% (v/v). Samples were then analysed by nephelometry to determine the solubility range as described previously.⁷⁵

Chromatographic LogD Measurement Partition coefficients (LogD) were estimated by comparing the chromatographic retention properties of each compound at pH 7.4 to the retention characteristics of a series of standard compounds with known partition coefficients. Data were collected using a Waters 2795 HPLC instrument with a Waters 2487 dual channel UV detector with a Synergy Hydro-RP 4 μm (30 mm x 2 mm) column. The mobile phase consisted of aqueous buffer (50 mM ammonium acetate, pH 7.4) and acetonitrile, with an acetonitrile gradient of 0 – 100% over 10 min. Compound elution was monitored at 220 and 254 nm. This method is a gradient HPLC method based on that originally described by Lombardo.⁷⁶

Chromatographic Protein Binding Estimation Plasma protein binding values were estimated using a chromatographic method whereby the retention characteristics on a human albumin column (Chromtech Chiral-HSA 50 mm x 3.0 mm, 5 μm , Sigma-Aldrich) were compared to the retention characteristics of a series of compounds with known human protein binding values. The method is a modification of a previously published method.⁷⁷ A Waters 2795 HPLC system equipped with a Waters 2487 dual channel UV detector (monitored at 220 and 254 nm) was used with a mobile phase comprised of aqueous buffer (25 mM

ammonium acetate buffer, pH 7.4) and 30% isopropyl alcohol in the same buffer. The isopropanol concentration gradient varied over 10 min and the column was reconditioned prior to the next injection.

***In Vitro* Metabolism in Human Liver Microsomes** A 10 mg/ml stock solution was prepared in DMSO and diluted in 50% acetonitrile/water to a spiking concentration of 500 μ M. This solution was then diluted 1 in 500 to give a final compound concentration of 1 μ M and incubated at 37 °C in the presence of human liver microsomes (XenoTech LLC, Lenexa, Kansas City) suspended in 0.1 M phosphate buffer (pH 7.4) at a final protein concentration of 0.4 mg/ml. An NADPH-regenerating system (1 mg/ml NADP, 1 mg/ml glucose-6-phosphate, 1 U/ml glucose-6-phosphate dehydrogenase and 0.67 mg/ml $MgCl_2$) were added to initiate the metabolic reactions, which were subsequently quenched with ice-cold acetonitrile at various time points over 60 min. Samples were centrifuged for 3 min at 10,000 rpm and the amount of parent compound remaining in the supernatant quantified by LCMS using a Waters Micromass ZQ coupled to a Waters Alliance 2975 HPLC. The first order rate constant for substrate depletion was determined by fitting the data to an exponential decay function and these values were used to calculate the *in vitro* intrinsic clearance (CL_{int}) and the predicted *in vivo* intrinsic clearance value ($CL_{int\ vivo}$) as described previously.⁷⁸ The predicted *in vivo* hepatic extraction ratio (E_H) was calculated using the following relationship: $E_H = CL_{int\ vivo} / (Q + CL_{int\ vivo})$ where Q is human liver blood flow (20.7 ml/min/kg).⁷⁹

2. Investigation of the structure-activity relationships of the oxazolopyridines against *T.b. brucei*

2.1. Introduction

As described in Chapter 1, a HTS screen of the WEHI/Bio-21 screening library yielded a number of hits that were progressed through to hit-to-lead medicinal chemistry optimisation.⁵ Of these the oxazolopyridine were a class of particular interest with **126** having an EC₅₀ of 0.22 μM against *T.b. brucei*. It also possesses a moderately low PSA of 81 Å² that indicated the potential for CNS penetration,⁵⁶ which is essential to treat stage two HAT, and a low cLogP of 2.6. There is a linear relationship between cLogP and the rate of metabolism of a drug, hence a value in the region of 2.0 is widely regarded as the optimum.⁸⁰

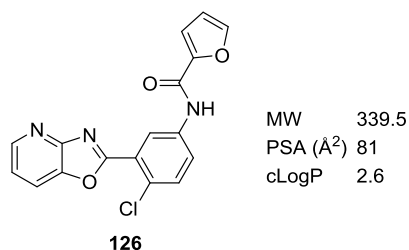


Figure 2.1 Structure and physicochemical profile of an initial screening hit with low cLogP, PSA and MW suitable for lead optimisation.

Furthermore, testing against a wider panel of parasites confirmed potent activity not only against *T.b. rhodesiense* (EC₅₀ 0.59 μM), but also against *T. cruzi* (EC₅₀ 0.23 μM). In both cases **126** was highly selective for these kinetoplastids compared with the L6 mammalian cell line, with respective selectivity indices of 39 and 99 (Table 2.1). Activity was significantly weaker against the unrelated protozoan *P. falciparum* (EC₅₀ 7.8 μM), a major causative agent of malaria.⁵⁴

Table 2.1 Biological activity profile of **126** against a number of parasites.^a

Parasite	EC ₅₀ (μM)	SI
<i>T.b. brucei</i>	0.22	> 345 ^b
<i>T.b. rhodesiense</i>	0.59	39 ^c
<i>T. cruzi</i>	0.23	99 ^c
<i>P. falciparum</i>	7.8	3 ^c

^a Values are the mean of 3 experiments, < ± 50%.

^b Selectivity relative to HEK293(human embryonic kidney) cells.

^c Selectivity relative to L6 (rat skeletal myoblast) cells.

2.2. Aims

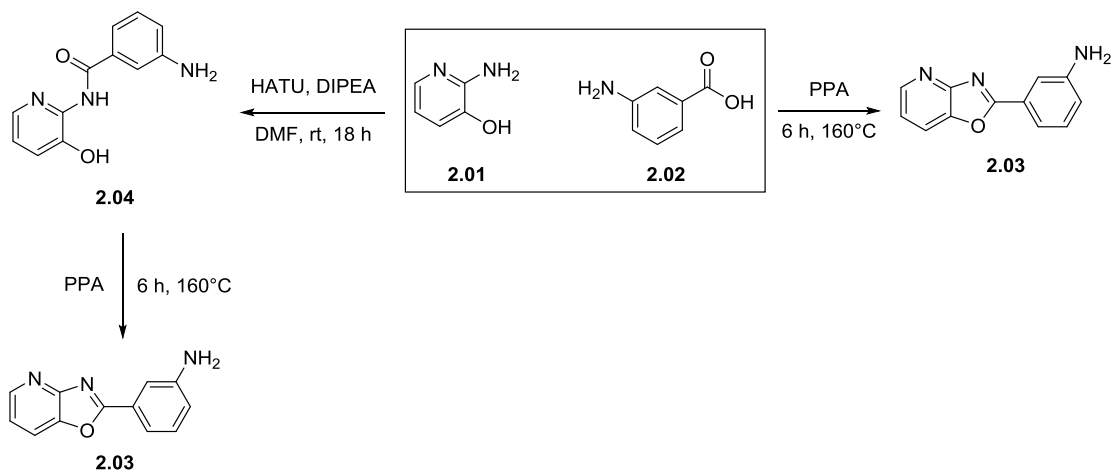
The aim for this section was to investigate alterations to the oxazolopyridine core. This included varying the northern heterocycle, substitutions around the central phenyl ring and making changes to the oxazolopyridine itself as previously outlined in the SAR rationale (Chapter 1, Section 1.4).

The work will be presented as an initial discussion of the synthesis of these derivatives, a number of analogues constituting the primary SAR for this series (presented as a publication), before concluding with additional follow up work.

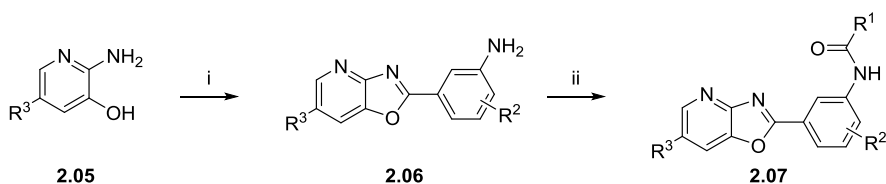
2.3. Synthesis of the oxazolopyridine analogues

There have been a number of reports of the synthesis of oxazolopyridines in the literature. The methods typically used consist of the formation of the amide followed by cyclisation (Scheme 2.1) or a one-pot cyclocondensation mediated by polyphosphoric acid (PPA).^{81, 82} According to the literature there appears to be no advantage in terms of overall yield with either route. As such, it was decided to pursue the targets in the least number of synthetic steps. In Scheme 2.2 it can be seen that initially the one-step cyclocondensation

reaction between 2-amino-3-hydroxypyridine and a substituted 3-aminobenzoic acid is mediated by PPA with a subsequent amide coupling reaction in order to install the northern heterocycle. For this latter step a variety of conditions could be utilised and are highlighted in Scheme 2.2.



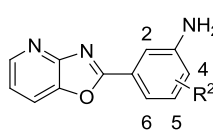
Scheme 2.1 Synthetic routes towards oxazolopyridine derivatives previously identified in the literature.



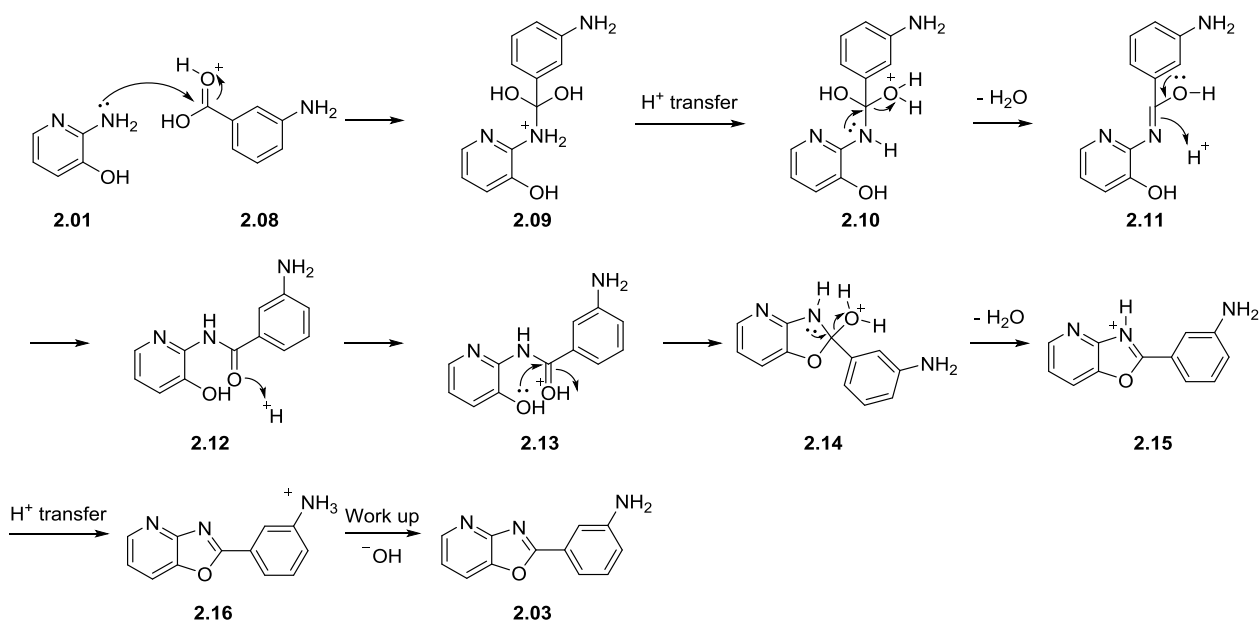
Scheme 2.2 Synthesis of oxazolopyridine derivatives. Reagents and conditions: **i**) substituted 3-aminobenzoic acid, PPA, 4 h, heating at 220 °C; **ii**) (a) EDCl, DMAP, R^1 -COOH, anhydrous DMF, overnight; (b) HBTU, DIPEA, R^1 -COOH, DMF, overnight; (c) HOBt, EDCl, DIPEA, R^1 -COOH, DMF, overnight.

The mechanism of the cyclocondensation reaction can be seen in Scheme 2.3. The reaction was performed utilising existing literature within the group and in accordance with literature procedures. However, it was found to give unreproducible yields (Table 2.2).

Table 2.2 Yields of product obtained from the synthesis of the oxazolopyridine core.^a

		R^2	Yield	R^2	Yield
		H	25%	4-OCH ₃	5%
		6-CH ₃	30%	2-CH ₃	20%
		6-F	34%		

^a Reaction conditions: substituted 3-aminobenzoic acid, PPA, 4 h, heating at 220 °C. Work-up consisted of neutralisation with an aqueous saturated sodium bicarbonate solution.



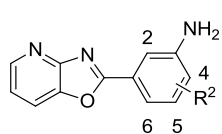
Scheme 2.3 Cyclocondensation mechanism between 2-amino-3-hydroxypyridine and 3-aminobenzoic acid, mediated by PPA.

The conditions required for the cyclocondensation were considered harsh given the need for heating at 220 °C for 4 h and the subsequent work up called for neutralisation of the PPA by slow addition of a 10% sodium bicarbonate solution. The neutralisation would result in a significant volume of aqueous phase from which to extract the desired product, which was not overly soluble in a wide range of organic solvents as well as a significant amount of effervescence and production of a black, tar-like substance. Analysis of this tar-like substance by Liquid Chromatography coupled to Mass Spectrometry (LCMS) showed no trace of starting materials or product, though a peak of 286.0 m/z was observed that corresponds to sodium triphosphate, thought to arise due to contamination by the aqueous phase. In an attempt to optimise the reaction conditions,

the length of time that the reaction was heated was decreased though this led to incomplete reaction with both starting materials and product being isolated. However, it was found that reducing the temperature from 220 °C to 180 °C and heating for 4 h gave complete conversion and significantly less tar-like substance.

For this reaction we also sought an alternative to the neutralisation with 10% aqueous sodium bicarbonate solution. Analysis of the literature revealed a variety of work up conditions had been employed. Typically the reaction mixture was poured onto iced water and neutralised by addition of solid sodium hydroxide^{81, 82} or solid potassium carbonate⁸³ followed by the extraction of the product. Alternatively, the reaction mixture was also neutralised by stirring in an iced 28% aqueous ammonium hydroxide solution followed by the filtration of the product and purification by column chromatography.⁸³ We found that employing an aqueous 5 M sodium hydroxide solution resulted in significantly less aqueous phase, without the problematic effervescence observed under the previous conditions. In many cases the desired product precipitated cleanly from the aqueous phase and was filtered and air dried. These changes led to drastic improvements in the yield obtained of the desired product as demonstrated in Table 2.3.

Table 2.3 Yields of product obtained using optimised conditions for the synthesis of the oxazolopyridine core.^a



R²	Yield	R²	Yield
H	81%	2-CH ₃	93%
4-OCH ₃	99%	2-F	72%

^a Reaction conditions: substituted 3-aminobenzoic acid, PPA, 4 h, heating at 180 °C. Work-up consisted of neutralisation with an aqueous 5M sodium hydroxide solution.

2.4. Preliminary SAR

Although oxazolopyridines have previously been described in the literature, they had not been identified or investigated for their potential activity against *T.b. brucei*. They have been investigated for their potential use

as sirtuin modulators,⁸² histone acetyl transferase inhibitors⁸⁴ and as inhibitors of lysophosphatidic acid acyltransferase β .⁸³

Workers at Sirtris have been investigating oxazolopyridines for their use as activators of NAD⁺-dependent deacetylase SIRT1, a sirtuin, the SAR for which has been summarised in Figure 2.2.⁸⁵ While sirtuins have been reported in trypanosomes,^{86, 87} it remains to be determined whether this is of value in the current project.

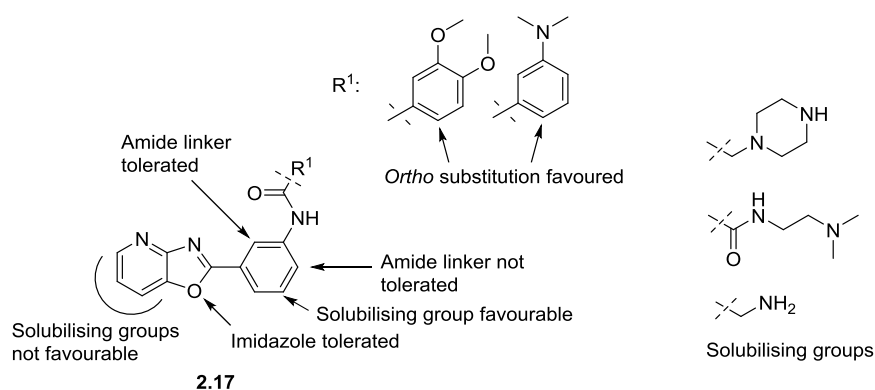


Figure 2.2 SAR of oxazolopyridine identified during HTS by Sirtris.⁸⁵

Our investigations into the preliminary SAR investigation began by studying the northern heterocycle through substituting the 2-furan for a range of alternative 5-membered heterocycles, including oxazoles, thiazoles, pyrazoles and furans with varying substitution patterns. A number of larger cycles were also examined, including pyridine, phenyl and substituted phenyl rings. These studies were performed by Elliott Teston and myself.

The next phase of SAR investigation focused on substitutions around the central phenyl ring. Each position around the ring was probed with a variety of functional groups in order to fully assess the effects of electronic, steric and hydrophobic properties at each position as discussed in Chapter 1. It is possible that “*ortho*” substitution at the 2- and 4- positions could conformationally influence the disposition of the amide group relative to the fused heterocycles and this was investigated. On examination of crystal structures from the Cambridge crystallographic database of compounds containing a benzamide with *ortho* substitution of

the respective functional groups (methyl, fluorine and methoxy) it became evident that there was a conformational shift in the compounds. These changes are depicted in Figure 2.3. Six compounds were identified in the database that had the fluoro substituted at the *ortho* position to the amide. Of these six compounds all were slightly twisted with the fluorine and amide –NH on the same side of the molecule (2.18). Of those compounds in the database where a methyl is substituted *ortho* to the amide, seven of the twelve experienced a large degree of twisting potentially due to the steric interaction between the methyl and carbonyl of the amide (2.19). Three compounds were identified with a methoxy functional group *ortho* to the amide (2.20) and in all cases the molecules were roughly planar with the methoxy and amide –NH on the same side of the molecule where there would be the potential for an electrostatic attraction between the δ^+ hydrogen of the amide and the δ^- oxygen of the methoxy.

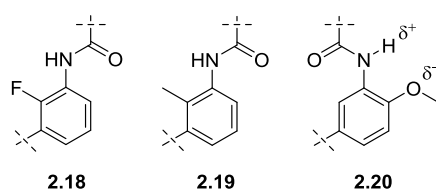


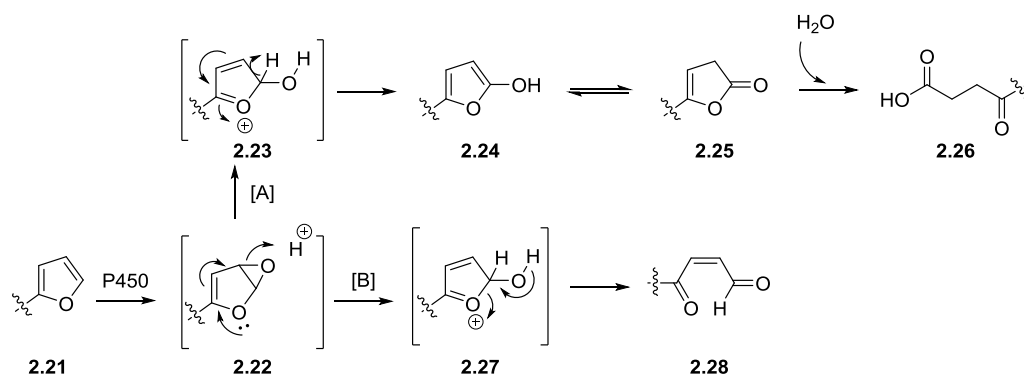
Figure 2.3 Conformational changes influenced by an *ortho* group substituent on the oxazolopyridine core exemplified by generic compounds found from a search of the Cambridge crystallographic database.

In addition, central core substitutions that returned favourable activity (6-fluoro, 6-methyl and 6-hydrogen) were combined with the most active northern heterocycles identified (2-furan, 3-furan, 3-methylfuran, oxazole and thiazole). This was done in an attempt to gain additive SAR in this series. This work was largely carried out by myself in conjunction with Elliott Teston and Raphaël Rahmani.

Some preliminary studies around the pyridine ring and the oxazolopyridine core were also performed by chemists at the University of Tasmania and Elliott Teston also studied the alkylation of the amide -NH.

ADME analysis revealed that in general this series has solubility and metabolism issues. Most compounds were degraded rapidly by human liver microsomes and each contained the metabolically labile furan

functionality. It seems likely that the furan is susceptible to cytochrome P450-mediated metabolism as demonstrated in Scheme 2.4. The most stable compound was the oxazolamide and the next most stable the thiazolamide, further lending support to the hypothesis that the furanyl group is the metabolic liability in this series.



Scheme 2.4 Bioactivation mechanism of the furan functional group (2.21) by the enzyme cytochrome P450. Pathway [A] involves hydrolysis of the lactone (2.25) to form the γ -ketocarboxylic acid (2.26). Pathway [B] arises as a result of ring opening of the epoxide (2.22) to give the γ -ketoenal (2.28).⁵³

These studies led to the identification of a compound with an EC₅₀ of 91 nM against *T.b. rhodesiense* and greater than 700 times selectivity for the parasite over mammalian cells, although further improvement to the solubility and metabolism of this series is required. These compounds also have potent activity against *T. cruzi*. The full details and conclusions of this preliminary SAR study follow in the published manuscript.

Reproduced from Ferrins, L.; Rahmani, R.; Sykes, M. L.; Jones, A. J.; Avery, V. M.; Teston, E.; Almohaywi, B.; Yin, J.; Smith, J.; Hyland, C.; White, K. L.; Ryan, E.; Campbell, M.; Charman, S. A.; Kaiser, M.; Baell, J. B. 3-(Oxazolo[4,5-*b*]pyridin-2-yl)anilides as a novel class of potent inhibitors for the kinetoplastid *Trypanosoma brucei*, the causative agent for human African trypanosomiasis. *European Journal of Medicinal Chemistry* **2013**, 66, 450-465. Copyright 2015 Elsevier Masson SAS. All rights reserved.

2.5. Published manuscript

Declaration for Thesis Chapter 2

Declaration by candidate

In the case of Chapter 2, the nature and extent of my contribution to the work was the following:

Nature of contribution	Extent of contribution
Synthesis of compounds 2, 5, 6, 10, 14-15, 18-19, 21-23, 26, 32-36, 38-41 , and synthetic intermediates, SAR analysis and principal authorship of manuscript	50%

The following co-authors contributed to the work. If co-authors are students at Monash University, the extent of their contribution in percentage terms must be stated:

Name	Nature of contribution	Extent of contribution*
Raphaël Rahmani	Synthesis of compounds 25, 27-28, 31 , and synthetic intermediates, SAR analysis and co-authorship of manuscript	
Melissa L. Sykes	Biological testing, data analysis	
Amy J. Jones	Biological testing, data analysis, editing of manuscript	
Vicky M. Avery	Data analysis, editing of manuscript	
Elliott Teston	Synthesis of compounds 1, 3-4, 7-9, 11-13, 16-17, 20, 29-30, 37, 48-49 , and synthetic intermediates	
Basmah Almohaywi	Synthesis of compounds 24, 42-47 , and synthetic intermediates	
JieXiang Yin		
Chris Hyland		

Jason Smith	Supervising chemistry program at UTAS	
Karen L. White	Data analysis, editing of manuscript	
Eileen Ryan	ADMET analysis	
Michael Campbell	ADMET analysis	
Susan A. Charman	Editing of manuscript	
Marcel Kaiser	Biological testing of compounds in a parasite panel	
Jonathan B. Baell	SAR analysis and co-authorship of manuscript	

**Shown for Monash University students only*

The undersigned hereby certify that the above declaration correctly reflects the nature and extent of the candidate's and co-authors' contributions to this work.

Candidate's Signature		Date 18/02/2015
----------------------------------	--	---------------------------

Main Supervisor's Signature		Date 18/02/2015
--	---	---------------------------

Declaration by co-authors

The undersigned hereby certify that:

- (6) The above declaration correctly reflects the nature and extent of the candidate's contribution to this work, and the nature of the contribution of each of the co-authors;
- (7) They meet the criteria for authorship in that they have participated in the conception, execution, or interpretation, of at least part of the publication in their field of expertise;
- (8) They take public responsibility for their part of the publication, except for the responsible author who accepts overall responsibility for the publication;
- (9) There are no other authors of the publication according to those criteria;

- (10) Potential conflicts of interest have been disclosed to (a) granting bodies, (b) the editor or publisher of journal or other publications, and (c) the head of the responsible academic unit; and
- (11) The original data are stored at the following location(s) and will be held for at least five years from the date indicated below:

Locations:

Department of Medicinal Chemistry, Monash Institute of Pharmaceutical Sciences, 381 Royal Pde, Parkville, Victoria, 3052, Australia.

Eskitis Institute for Cell and Molecular Therapies, Griffith University, Brisbane Innovation Park, Don Young Road, Nathan, Queensland, 4111, Australia.

The Walter and Eliza Hall Institute, 1G Royal Parade, Parkville, Victoria, 3052, Australia.

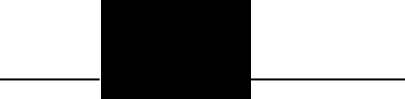
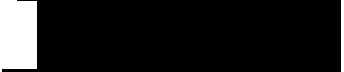
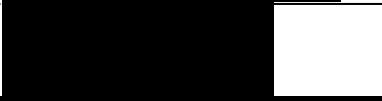
School of Chemistry, University of Tasmania, Private Bag 75, Hobart, 7001, Australia.

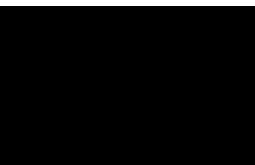
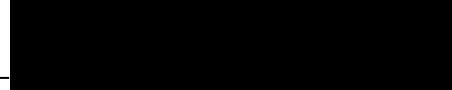
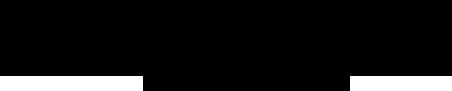
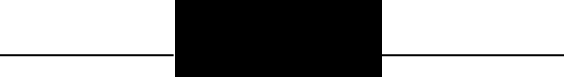
Centre for Drug Candidate Optimisation, Monash University, Parkville, Victoria, 3052, Australia.

Swiss Tropical and Public Health Institute, Socinstrasse 57, Basel, 4051, Switzerland.

University of Basel, Petersplatz 1, Basel, 4003, Switzerland.

Signatures:

Signed:		Date: 29/04/2015
Signed:		Date: 26/02/2015
Signed:		Date: 23/02/2015
Signed:		Date: 23/02/2015
Signed:		Date: 27/04/2015
Signed:		Date: 20/04/2015
Signed:		Date: 22/04/2015

Signed:		Date: 22/04/2015
Signed:		Date: 18/02/2015
Signed:		Date: 18/02/2015
Signed:		Date: 20/04/2015
Signed:		Date: 20/02/2015
Signed:		Date: 18/02/2015
Signed:		Date: 18/02/2015
Signed:		Date: 18/02/2015



Original article

3-(Oxazolo[4,5-*b*]pyridin-2-yl)anilides as a novel class of potent inhibitors for the kinetoplastid *Trypanosoma brucei*, the causative agent for human African trypanosomiasis



Lori Ferrins^a, Raphaël Rahmani^a, Melissa L. Sykes^b, Amy J. Jones^b, Vicky M. Avery^b, Elliott Teston^c, Basmah Almohaywi^d, JieXiang Yin^{d,1}, Jason Smith^d, Chris Hyland^{d,1}, Karen L. White^e, Eileen Ryan^e, Michael Campbell^e, Susan A. Charman^{a,e}, Marcel Kaiser^{f,g}, Jonathan B. Baell^{a,c,h,*}

^a Medicinal Chemistry, Monash Institute of Pharmaceutical Sciences, Monash University, Parkville, Victoria 3052, Australia

^b Eskitis Institute for Cell and Molecular Therapies, Griffith University, Brisbane Innovation Park, Don Young Road, Nathan, Queensland 4111, Australia

^c The Walter and Eliza Hall Institute, 1G Royal Parade, Parkville, Victoria 3052, Australia

^d School of Chemistry, University of Tasmania, Private Bag 75, Hobart 7001, Australia

^e Centre for Drug Candidate Optimisation, Monash University, Parkville, Victoria 3052, Australia

^f Swiss Tropical and Public Health Institute, Socinstrasse 57, Basel 4051, Switzerland

^g University of Basel, Petersplatz 1, Basel 4003, Switzerland

^h Department of Medical Biology, University of Melbourne, Parkville, Victoria 3010, Australia

ARTICLE INFO

Article history:

Received 17 February 2013

Received in revised form

1 May 2013

Accepted 7 May 2013

Available online 16 May 2013

Keywords:

3-(Oxazolo[4,5-*b*]pyridin-2-yl)anilides

Human African trypanosomiasis

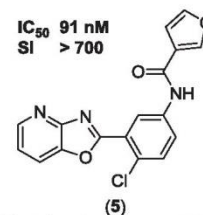
Sleeping sickness

Trypanosomacidal agent

Trypanosoma brucei

ABSTRACT

A whole organism high-throughput screen of approximately 87,000 compounds against *Trypanosoma brucei brucei* led to the recent discovery of several novel compound classes with low micromolar activity against this organism and without appreciable cytotoxicity to mammalian cells. Herein we report a structure–activity relationship (SAR) investigation around one of these hit classes, the 3-(oxazolo[4,5-*b*]pyridin-2-yl)anilides. Sharp SAR is revealed, with our most active compound (**5**) exhibiting an IC₅₀ of 91 nM against the human pathogenic strain *T.b. rhodesiense* and being more than 700 times less toxic towards the L6 mammalian cell line. Physicochemical properties are attractive for many compounds in this series. For the most potent representatives, we show that solubility and metabolic stability are key parameters to target during future optimisation.



© 2013 Published by Elsevier Masson SAS.

Abbreviations: BBB, blood–brain barrier; cPPB, chromatographic plasma protein binding; cytotox., cytotoxicity; DCM, dichloromethane; DMAP, *N,N*-dimethylamino-pyridine; DMEM, Dulbecco's modified Eagle's medium; DMF, *N,N*-dimethylformamide; EDCI, 1-ethyl-3-(3-dimethylaminopropyl)carbodiimide; E_H, hepatic extraction; FCS, foetal calf serum; HAT, human African trypanosomiasis; HBTU, *O*-(benzotriazol-1-yl)-*N,N,N',N'*-tetramethyluronium hexafluorophosphate; HEPES, 4-(2-hydroxyethyl)-1-piperazineethanesulfonic acid; STPHI, Swiss Tropical and Public Health Institute; TBAB, tetrabutylammonium bromide; *L. donovani*, *Leishmania Donovani*; *P. falciparum*, *Plasmodium falciparum*; *T.b. brucei*, *Trypanosoma brucei brucei*; *T.b. gambiense*, *Trypanosoma brucei gambiense*; *T.b. rhodesiense*, *Trypanosoma brucei rhodesiense*; WHO, World Health Organisation.

* Corresponding author. Medicinal Chemistry, Monash Institute of Pharmaceutical Sciences, Monash University, Parkville, Victoria 3052, Australia. Tel.: +61 9903 9044.

E-mail address: Jonathan.Baell@monash.edu (J.B. Baell).

¹ School of Chemistry, University of Wollongong, Wollongong, NSW 2522, Australia.

1. Introduction

Human African trypanosomiasis (HAT), more commonly known as sleeping sickness, is a vector-borne parasitic disease caused by infection of the host with either *Trypanosoma brucei gambiense* or *Trypanosoma brucei rhodesiense* [1]. The World Health Organisation (WHO) currently estimates that there are approximately 30,000 cases of HAT in Africa, which has a significant socioeconomic impact [2]. HAT is largely confined to the sub-Saharan continent where the vector, parasite and animal reservoirs co-exist [1]. The disease consists of two stages; the first involves the invasion of the haemolymphatic system by the parasite, and the second is associated with the transmission of the parasites across the blood–brain barrier (BBB) and into the central nervous system (CNS) [1]. Infection of the CNS leads to a number of symptoms including mental impairment, severe headaches, fever, chronic encephalopathy and eventual death. This stage of the disease is particularly in need of improved therapies [1].

There are a number of treatment options currently available for HAT, though none of them are ideal. Pentamidine and suramin are used to treat the first stage of HAT where *T. b. gambiense* and *T. b. rhodesiense* are the causative agents, respectively. However, neither of these drugs are able to cross the BBB making both ineffective against the second stage of HAT [3–5]. In addition, both treatments have significant side effects. Suramin has been linked to exfoliative dermatitis and renal failure [4], whilst pentamidine use is associated with diabetes mellitus and nephrotoxicity [6]. Melarsoprol is the primary treatment option available for second stage HAT being effective against both subspecies of trypanosome [6,7]. However, high failure rates have been reported even though resistance has not been proven [7]. Alternatively, eflornithine can also be used to treat second stage HAT [7]. It is a safer option but it is not effective against *T. b. rhodesiense* and the high costs may make it prohibitive [7]. Furthermore, administration requires four intravenous infusions daily for 14 days which is impractical in rural African facilities [8]. Recently nifurtimox has been introduced as a combination therapy with eflornithine (NECT) [8]. The combination therapy has the advantage of having a shorter and simplified regimen which has made it the current first line treatment for second stage HAT caused by *T. b. gambiense* [8]. Orally bioavailable oxaborole 6-carboxamides and orally active benzoxaboroles were identified and selected to enter pre-clinical studies in 2009 [9]. Also, fexinidazole has been progressed through phase 1 clinical trials and is currently recruiting for a phase 2 clinical trial [10]. However, there is still a great need for new trypanosomacidal compounds given the current chemotherapeutic options available, particularly for the CNS-resident second stage of this disease.

We recently screened approximately 87,000 compounds against *T. b. brucei* using an Alamar Blue® based 384-well viability assay [11]. Being the same species but just a different sub-species that is non-pathogenic to humans, *T. b. brucei* has a long history of useful and relevant application as a surrogate for *T. b. rhodesiense* and *T. b. gambiense* for early HAT drug discovery projects and comprises the mainstay of most primary animal models for HAT [12]. Indeed, *T. b. brucei* and *T. b. rhodesiense* differ in one gene – the serum resistance gene that allows *T. b. brucei* to survive in human serum – and there is recent strong evidence that *T. b. rhodesiense* is only a phenotypic variant of *T. b. brucei* [13]. Eight structurally unique compound classes were identified with IC₅₀ values of less than 10 μM against *T. b. brucei*, that were more than ten times selective for *T. b. brucei* over the mammalian cell line HEK293, and had favourable physicochemical properties. One compound of particular interest was an oxazolopyridine derivative with an IC₅₀ against *T. b. brucei* of 0.22 μM, shown in Fig. 1. This compound (**1**) had a moderately low molecular weight of 339.5, a reasonably low polar surface area of

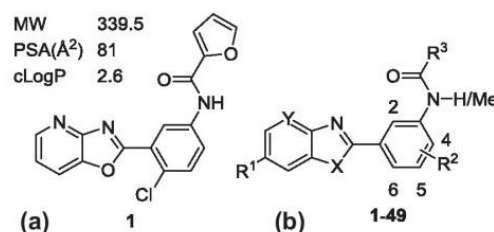


Fig. 1. (a) Structure and physicochemical profile of an initial screening hit; (b) numbering used herein.

81 Å² that could have potential for CNS penetration to treat stage two HAT [14], and an attractively low cLogP of 2.6.

Furthermore, testing against a wider panel of parasites confirmed potent activity not only against *T. b. rhodesiense* (IC₅₀ 0.59 μM), but also against *Trypanosoma cruzi* (IC₅₀ 0.23 μM). In both cases **1** was highly selective for these kinetoplastids compared with the L6 mammalian cell line, with respective selectivity indices of 39 and 99 (Table 1). Activity was significantly weaker against the unrelated protozoan *Plasmodium falciparum* (IC₅₀ 7.8 μM), a major causative agent of malaria [15].

As such, **1** was of interest as a starting point for drug development resulting in the initiation of an SAR study. Herein we report our discovery of a new class of compounds that are potent and specific against *T. b. brucei* and *T. b. rhodesiense*, as well as *T. cruzi*, the causative agent of Chagas' disease [16].

2. Chemistry

After mining our database for analogues, it was determined that directed synthesis was required to establish a focused SAR investigation. We have recently discussed the database mining results elsewhere [11]. Investigations initially centred around the “northern” heterocyclic group. As shown in Scheme 1, the synthesis was relatively straightforward requiring a one-step cyclocondensation reaction between 2-amino-3-hydroxypyridine and a substituted 3-aminobenzoic acid, mediated by PPA, followed by amide bond formation between the amino group and the relevant heteroaryl carboxylic acid using EDCI and DMAP. For selected compounds, amide *N*-methylation (c) was undertaken. This yielded the target compounds, which are listed in Table 2 along with their IC₅₀ values against *T. b. brucei*.

3. Results and discussion

Introduction of a 3-methyl group (**2**) into the furan ring leads to a slight loss of activity with an IC₅₀ of 0.65 μM relative to an IC₅₀ of 0.22 μM for **1** (Table 2). An isoxazole is less tolerated and **3** is more than 10-fold less active than **1** while the oxazole (**4**) is only slightly better than this with an IC₅₀ of 1.5 μM. On the other hand, a 3-furyl group (**5**) is well tolerated with an IC₅₀ of 0.3 μM. The thiazole (**6**) is about 10-fold less active than **1** while the corresponding pyrazole

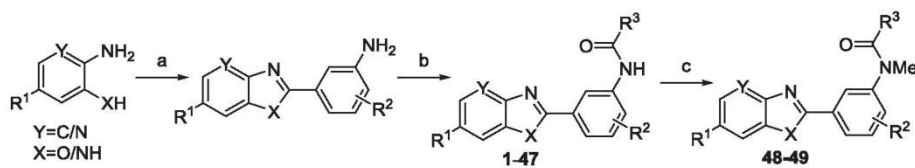
Table 1
Biological activity^a profile of **1** against a number of parasites.

Parasite	IC ₅₀ (μM)	SI
<i>T. b. brucei</i>	0.22	>345 ^b
<i>T. b. rhodesiense</i>	0.59	39 ^c
<i>T. cruzi</i>	0.23	99 ^c
<i>P. falciparum</i>	7.8	–

^a Values are the mean of 3 experiments, \pm 50%.

^b Selectivity relative to HEK293 cells.

^c Selectivity relative to L6 (rat skeletal myoblast) cells.

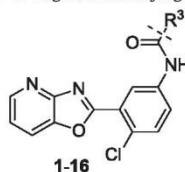


^a Reagents and conditions: (a) substituted 3-aminobenzoic acid, [PPA, 180 °C, 4 h]; (b) EDCl, DMAP, R³-COOH, [DMF, rt, 12 h]; (c) MeI, TBAB (cat.), K₂CO₃, [Acetone, rt, 12 h].

Scheme 1. Synthetic overview of oxazolopyridine derivatives.

(7) and imidazole (8) led to a loss of activity. Fusing a phenyl ring to the furan to give benzofuran (9) also gave rise to a loss of activity. Interestingly, while weaker, the phenyl analogue 10 has an IC₅₀ of 1.5 μM. It was hypothesized that a suitably placed ethereal oxygen atom could return potent activity like the furan, but substitution of a 2-methoxy (11) or 3-methoxy (12) on the phenyl ring only led to loss of activity. Introduction of endocyclic nitrogen atoms at the 2- and 4-positions in 13 and 14 respectively were not well tolerated with an IC₅₀ of 5.7 μM and 3.4 μM respectively while introduction of the nitrogen at the 3-position in 15 led to a complete loss of activity.

Table 2
T.b. brucei inhibitory activity^a of targets with varying amide groups.



ID	R ³	IC ₅₀ (μM)	SI ^b	ID	R ³	IC ₅₀ (μM)	SI ^b
1		0.22	>345	9		>10	–
2		0.65	>130	10		1.5	54
3		3.2	–	11		>10	–
4		1.5	>45	12		>10	–
5		0.30	160	13		5.7	15
6		1.8	39	14		3.4	–
7		>10	–	15		>10	–
8		>10	–	16	CH ₂ OMe	>10	–

^a Values are the mean of 3 experiments, <±50%.

^b Selectivity relative to HEK293 cells for selected potent compounds.

The aryl property of the furan appeared to be important because appropriate connectivity in the saturated ether (16) led to a loss of activity.

In summary, the requirements for the amide group are stringent, and 2- and 3-furans are highly favoured over other groups. As we are developing SAR in a whole cell assay, it is possible that negative SAR could be a reflection of poorer permeability rather than lower affinity to intracellular targets. However, apart from the pyrazole (7) and imidazole (8), it seems unlikely that permeability of this set of compounds would differ significantly from each other. Therefore we suggest steric hindrance in this region requires a small aryl group with one side being hydrophobic and the other containing a hydrogen-bond acceptor.

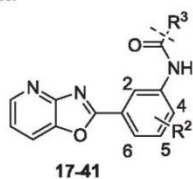
Following this, substitutions around the central ring were investigated. As shown in Table 3, removal of the 6-chloro (17) led to a compound with significant potency and selectivity. The 2-position appears to be unfavourable for substitution since methyl (22), fluoro (23) or chloro (24) led to a loss in activity. An endocyclic nitrogen (25) or chloro (29) at the 4-position led to a decrease in activity while a methyl (27) or fluoro (28) at the same position led to a loss of activity. Interestingly, a methoxy in the 4-position (26) retained some activity with an IC₅₀ of 1.1 μM. Substitutions at the 5-position with an endocyclic nitrogen (30) or fluoro (31), both led to loss of activity. Replacement of the 6-chloro with a 6-fluoro (37) was potent with an IC₅₀ of 0.29 μM and an SI of >288. Replacement with a methyl group (32) was somewhat less tolerated.

Thus, the central ring is remarkably intolerant of substitution at the 2-, 4- or 5-positions. However, the 6-chloro group can be removed or replaced with a 6-fluoro to give compounds that are essentially equally active with the 6-chloro parent compound but lower in both molecular weight and hydrophobicity. In most cases it appears unlikely that permeability would differ greatly amongst this set of compounds and so we attribute this SAR – at least at the 2-, 4- and 5-positions – to steric interactions with the intracellular target. It is possible that “ortho” substitution at the 2- and 4-positions could also conformationally influence the disposition of the amide group relative to the fused heterocycle.

We were then interested in whether crossover SAR could be observed in combining active heterocycles in Table 2 with the active central ring substituents just identified. The reason for this was two-fold. Firstly, furans are known to be potentially metabolically liable [17] and we reasoned that even though alternative heterocycles such as an oxazole may lead to less active compounds, other favourable metabolic and physicochemical properties such as solubility could counter such drawbacks during drug development. Secondly, we reasoned that it was not necessarily the case that these alternative heterocycles would stay correspondingly weaker with substitution changes in the central ring. Shown in Table 3 are the top central ring substitutions (17, 32, 37) which were combined with the 2- and 3-furans, 3-methylfuran, oxazole and thiazole heterocycles. An increase in trypanosomacidal activity for some of the heterocyclic amides was observed when the 6-substituent was

Table 3

T.b. brucei inhibitory activity^a of targets with substitutions around central ring system and with varying amides.



ID	R ²	R ³	IC ₅₀ (μM)	SI ^b
17	H		0.34	>245
18	H		0.17	115
19	H		2.9	29
20	H		0.60	89
21	H		1.3	63
22	2-Me		>10	–
23	2-F		>10	–
24	2-Cl		>10	–
25	4-[N] ^c		>10	–
26	4-OMe		1.1	74
27	4-Me		6.2	13
28	4-F		6.3	13
29	4-Cl		>10	–
30	5-[N] ^c		>10	–
31	5-F		>10	–
32	6-Me		0.94	>88
33	6-Me		0.57	145

(continued on next page)

Table 3 (continued)

ID	R ²	R ³	IC ₅₀ (μM)	SI ^b
34	6-Me		>10	–
35	6-Me		0.31	103
36	6-Me		2.6	32
37	6-F		0.29	290
38	6-F		0.10	840
39	6-F		2.0	43
40	6-F		0.12	680
41	6-F		0.76	110

^a Values are the mean of 3 experiments, $\leq \pm 50\%$.

^b Selectivity relative to HEK293 cells for selected potent compounds.

^c Endocyclic nitrogen.

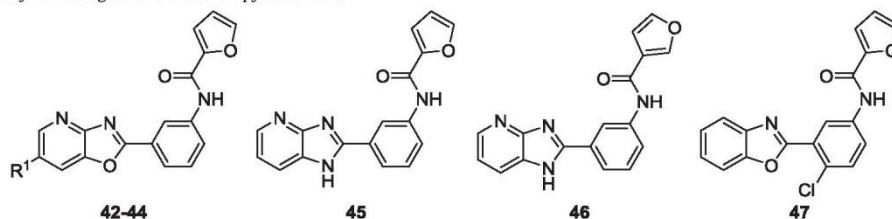
changed. For example, the combination of the 6-fluoro with the 3-methylfuran (**38**) and 3-furan (**40**) gave our most promising results to date with IC₅₀ values of 0.10 μM and 0.12 μM respectively, whilst the oxazole (**39**) and thiazole (**41**) were both less active. These trends were broadly emulated when the 6-fluoro was replaced with hydrogen (**18–21**) or 6-methyl (**33–36**), except that the former grouping was on the whole very slightly less active and the latter group marginally less active again.

While the focus of this work is on the central phenyl ring and northern amide group, some limited exploration was undertaken of the left hand side fused heterocycle, with interesting results. Shown in Table 4 are the results of installing a 6-phenyl group. When unsubstituted, the resulting compound (**42**) is potently inhibitory with an IC₅₀ of 0.12 μM. Substitution with a *p*-methoxy (**43**) or *p*-chloro (**44**) results in a slight loss of activity. While **42** is potent, it is not significantly more so than **17**, that has no 6-phenyl group, suggesting a null effect and lack of any interaction with intracellular targets. This position might therefore be useful to tailor other molecular properties such as solubility without loss of activity.

Also listed in Table 4 are the results of a core change where the oxazole is replaced by an imidazole and both compounds **44** and **45** retain significant activity with respective IC₅₀ values of 0.78 μM and 1.0 μM. It is possible that the slight loss of activity is contributed at least in part by poorer permeability, suggesting further investigation of this core heterocycle change is warranted. Interestingly, removal of the pyridine nitrogen leads to a complete loss of activity, suggesting it is essential for activity and there may be a hydrogen bond interaction with the receptor.

Finally, investigation of the effect of *N*-alkylation of the amide –NH was performed. In all cases the loss of the amide –NH led to a

Table 4
T.b. brucei inhibitory activity^a of analogues of the oxazolopyridine core.



ID	R ¹	IC ₅₀ (μM)	SI ^b
42	Ph	0.12	84
43	4-OMe-Ph	0.63	130
44	4-Cl-Ph	0.55	150
45	—	0.78	54
46	—	1.0	39
47	—	>10	—

^a Values are the mean of 3 experiments, <±50%.

^b Selectivity relative to HEK293 cells for selected potent compounds.

complete loss of activity, as seen in Table 5. This suggests that there may be an essential hydrogen bond interaction present between the compound and its putative receptor.

In order to investigate activity against the human pathogenic subspecies *T.b. rhodesiense*, selected compounds were tested against this organism as well as a small panel of parasites. As shown in Table 6, *T.b. rhodesiense* activity tracked well with *T.b. brucei* activity. The transfer of SAR was not linear and the 3-furylamide (**5**) was potent against *T.b. rhodesiense* with an IC₅₀ of 0.091 μM. Moreover, both **1** and **5** were potently active against *T.cruzi* and **5** in particular was active against *Leishmania donovani*, a causative agent of Leishmaniasis [18]. Furthermore, **5** exhibited low micromolar inhibitory activity towards *L. donovani* in infected macrophages, a pathogenically-relevant assay for which actives are extremely difficult to discover [18]. All compounds exhibited low micromolar activity against *P. falciparum*, but were relatively non-cytotoxic towards mammalian L6 cells. Indeed, the selectivity index for **5** was over 700 in this regard with respect to *T.b. rhodesiense* activity.

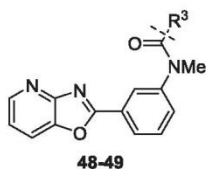
An assessment of drug-likeness was then made. Listed in Table 7 are various physicochemical and metabolic parameters for selected compounds. In general, all compounds are of relatively low molecular weight and in the range 319–340. Their polar surface areas are relatively low and within the range where acceptable CNS penetration is plausible [14]. This is important in order to treat the

CNS-resident second stage of HAT. Likewise, distribution coefficients were close to ideal and in the range 1.7–3.3 at pH 7.4. However, aqueous solubility for some compounds was poor and as low as 1.6–3.1 μg/mL for pH values of both 2 and 6.5 for several compounds. Plasma protein binding was moderate and would not likely limit distribution of the compound. However, most compounds were degraded rapidly by microsomes indicating that they are susceptible to cytochrome P450-mediated metabolism. The most stable compound was oxazolamide (**39**) and the next most stable thiazolamide (**41**), lending strong support to the hypothesis that the furanyl group is the metabolic hot spot.

4. Conclusion

We have described the discovery of 3-(oxazolo[4,5-*b*]pyridin-2-yl)anilides as a novel class of potent inhibitors for the kinetoplastid *Trypanosoma brucei*. Compound **5** exhibits an IC₅₀ of 0.091 μM against the human infective form, *T.b. rhodesiense*. As this is a whole cell readout, binding to intracellular targets must be extremely strong and with a tight fit with the receptor(s). We have discovered several key regions of this class with which we cannot interfere. Importantly, we have identified positions where activity can be modulated favourably. For example, replacement of the ring chloro with fluoro leads to improved activity and the 3-furyl is more active

Table 5
 Investigation of amide *N*-alkylation on activity against *T.b. brucei*^a for 3 selected compounds.



ID	R ³	IC ₅₀ (μM)
48		>10
49		>10

^a Values are the mean of 3 experiments, <±50%.

Table 6
 Biological activity profile of selected compounds against a parasite panel (IC₅₀, μM).^a

ID	<i>T.b. brucei</i>	<i>T.b. rhod.</i> ^b	<i>T. cruzi</i> ^c	<i>L. don. axe.</i> ^d	<i>L. don. inf. mac.</i> ^e	<i>P. falc. NF54</i> ^f	Cytotox. L6 ^g
1	0.22	0.59	0.23	1.8	—	7.8	23
5	0.30	0.091	0.26	0.34	12	4.9	65
6	1.8	1.1	2.3	4.8	>84	7.7	235
10	1.5	4.2	2.9	6.1	37	6.9	51

^a Values are the mean of 2 experiments, <±50%.

^b *T.b. rhodesiense* strain STIB 900, bloodstream form (trypomastigotes). Melaroprof (IC₅₀ 0.005 μM) was used as a control.

^c *T. cruzi* Tulahaen C4 strain, amastigote stage. Benznidazole was used as a control, EC₅₀ 1.46 μM.

^d *L. donovani* MHOM-ET-67/L82 strain, amastigote stage. Miltefosine was used as a control, EC₅₀ 0.49 μM.

^e *L. donovani* in infected macrophages. Miltefosine was used as a control, EC₅₀ 1.67 μM.

^f *P. falciparum* NF54 strain, erythrocytic stage. Chloroquine was used as a control, EC₅₀ 0.006 μM.

^g Rat skeletal myoblast cell L-6 strain. Podophyllotoxin was used as a control, EC₅₀ 0.017 μM.

Table 7
Key physicochemical parameters and *in vitro* metabolic stability of selected compounds.

ID	MW	PSA(Å ²) ^a	LogD ^b	Solubility (µg/mL) ^c		cPPB ^d (%)	Half-life (min)	<i>In vitro</i> Cl _{int} (µL/min/mg protein) ^e	Microsome-predicted E _H ^e
			pH 7.4	pH 2	pH 6.5				
1	340	81.2	2.7	1.6–3.1	1.6–3.1	93.9	7	258	0.91
18	319	81.2	2.9	6.3–12.5	3.1–6.3	94.2	10	181	0.88
33	333	81.2	3.3	1.6–3.1	<1.6	95.8	8	228	0.90
35	319	81.2	2.7	12.5–25.0	6.3–12.5	93.2	10	176	0.87
38	337	81.2	2.9	1.6–3.1	1.6–3.1	93.5	9	202	0.89
39	324	94.1	1.7	6.3–12.5	6.3–12.5	71.3	124	14	0.35
40	323	81.2	2.4	12.5–25.0	6.3–12.5	88.8	11	154	0.86
41	340	109.2	2.3	3.1–6.3	3.1–6.3	89.2	36	48	0.65

^a Calculated using ACD/Labs software, version 9.

^b Measured chromatographically.

^c Kinetic solubility determined by nephelometry.

^d Human plasma protein binding estimated using a chromatographic method.

^e *In vitro* intrinsic clearance determined in human liver microsomes and predicted hepatic extraction ratio calculated from *in vitro* data.

than the 2-furyl. Significantly, some of our compounds are also potent against *T. cruzi*, the causative agent of Chagas' disease [16], and low micromolar activity is also observed for **10** against *L. donovani* in infected macrophages. Despite this, these compounds are not at all appreciably toxic to mammalian cells. Assessment of predictive ADMET reveals these compounds to generally be drug-like and favourable for further investigation. Moving forward, key parameters to target for optimisation are aqueous solubility and metabolic stability and these will be interrogated during future refinement of SAR around the fused pyridyl ring and in looking at substituted furylamides.

The mechanism of action of these compounds is currently not known. However, a few structurally similar compounds have been reported by workers at Sirtris as being activators of NAD⁺-dependent deacetylase SIRT1, a sirtuin [19]. Such activity may be relevant to trypanosomes [20,21], but it remains to be determined if this is relevant to the compounds reported herein. For interested researchers, screening samples of compounds reported herein may be obtained by contacting the corresponding author.

5. Experimental protocol

Analytical TLC was performed on silica gel 60F₂₅₄ pre-coated aluminium sheets (0.25 mm, Merck) and visualized at 254 nm or by chemical staining with a solution ceric sulfate/phosphomolybdic acid followed by heating. Flash column chromatography was carried out using Merck silica gel 60, 0.63–0.20 mm (70–230 mesh).

Microwave reactions were performed on a CEM discovery fitted with an intelligent explorer unit. The temperature range of the unit is –80 °C to 300 °C, a pressure range of 0–27 bar, power range of 0–300 W and no pre stirring was required.

The purity of all compounds for biological testing was >95% in all cases, except where specified otherwise.

^a*Experimental conditions:* ¹H and ¹³C Nuclear Magnetic Resonance spectra were recorded at 300 MHz and 75 MHz respectively, on a Bruker UltraShield 300 MHz spectrometer running Bruker Topspin, version 1.3.

Low Resolution Mass Spectrometry analyses were performed on a Finnigan LCQ Advantage Max coupled with a Surveyor PDA detector and running XCalibur. Analysis was run on a Phenomenex column (Gemini, 5 µm, C18, 110 Å, 50 × 2 mm).

Preparative High Performance Liquid Chromatography was carried out on the Waters Alliance HT 2795 coupled with a Waters 2996 photodiode array detector and a Waters collector fraction III running Empower Pro. It was fitted with a Phenomenex, Luna, 5 µm, C18, 110 Å, 150 × 10 mm column.

^b*Experimental conditions:* Analytical reverse-phase HPLC was carried out on a Waters Millennium 2690 system, fitted with a

Phenomenex Luna C8 100 Å, 5 µm (150 × 4.6 mm I.D.) column. A binary solvent system was used (solvent A: 0.1% aqueous TFA, solvent B: 0.1% TFA/19.9% H₂O/80% ACN), with UV detection at 214 nm. A gradient of 0–80% buffer B over 10 min for a 20 min run time was used, with a flow rate of 1 mL/min.

¹H and ¹³C NMR spectra were recorded at 400.13 and 100.62 MHz, respectively, on a Bruker Avance III Nanobay spectrometer with BACS 60 sample changer, using solvents from Cambridge Isotope Laboratories. Chemical shifts (δ, ppm) are reported relative to the solvent peak (CDCl₃: 7.26 [¹H] or 77.16 [¹³C]; DMSO-*d*₆: 2.50 [¹H] or 39.52 [¹³C]). Proton resonances are annotated as: chemical shift (δ), multiplicity (s, singlet; d, doublet; t, triplet; q, quartet; m, multiplet; br, broad), coupling constant (J, Hz), and number of protons.

Low resolution mass spectrometry was performed on an Agilent 6100 Series Single Quad LC/MS coupled with an Agilent 1200 Series HPLC, G1311A quaternary pump, G1329A thermostatted autosampler, and G1314B variable wave length detector (214 and 254 nm). LC conditions: Phenomenex Luna C8(2) column (100 Å, 5 mm, 50 × 4.6 mm), 30 °C; sample (5 mL) was eluted using a binary gradient (solvent A: 0.1% aq. HCO₂H; solvent B: 0.1% HCO₂H in CH₃CN; 5–100% B [10 min], 100% B [10 min]; 0.5 mL/min). MS conditions: quadrupole ion source with multimode-ESI; drying gas temperature, 300 °C; vaporizer temperature, 200 °C; capillary voltage, 2000 V (positive mode) or 4000 V (negative mode); scan range, 100–1000 *m/z*; step size, 0.1 s over 10 min.

High resolution MS was performed on an Agilent 6224 TOF LC/MS coupled to an Agilent 1290 Infinity LC. All data were acquired and reference mass corrected via a dual-spray electrospray ionisation (ESI) source. Each scan or data point on the total ion chromatogram (TIC) is an average of 13,700 transients, producing a spectrum every second. Mass spectra were created by averaging the scans across each peak and subtracting the background from first 10 s of the TIC. Acquisition was performed using the Agilent Mass Hunter Data Acquisition software ver. B.05.00 Build 5.0.5042.2 and analysis was performed using Mass Hunter Qualitative Analysis ver. B.05.00 Build 5.0.519.13. Acquisition parameters: mode, ESI; drying gas flow, 11 L/min; nebuliser pressure, 45 psi; drying gas temperature, 325 °C; voltages: capillary, 4000 V; fragmentor, 160 V; skimmer, 65 V; octapole RF, 750 V; scan range, 100–1500 *m/z*; positive ion mode internal reference ions, *m/z* 121.050873 and 922.009798. LC conditions: Agilent Zorbax SB-C18 Rapid Resolution HT (2.1 × 50 mm, 1.8 mm column), 30 °C; sample (5 mL) was eluted using a binary gradient (solvent A: 0.1% aq. HCO₂H; solvent B: 0.1% HCO₂H in CH₃CN; 5–100% B [3.5 min], 0.5 mL/min).

^c*Experimental conditions:* ¹H and ¹³C NMR spectra were recorded at 300 MHz and 75 MHz respectively on a Varian Mercury 2000 spectrometer.

Infrared spectra were recorded on a Shimadzu FTIR 8400s spectrometer as thin films on NaCl plates or as solids using a Perkin Elmer Spectrum 100 FT-IR spectrometer fitted with a diamond window universal ATR sampling accessory.

5.1. General procedure A1: synthesis of the benzoxazole core

To 34 mL of polyphosphoric acid (1.5 g/mmol of limiting reagent) was added 2-amino-3-hydroxypyridine (1.0 eq) and the relevant benzoic acid (1.1 eq). The mixture was heated to 220 °C and stirred for 4 h, cooled and poured into 10% sodium bicarbonate solution. The suspension was stirred until gas evolution ceased, then filtered and washed with water. The aqueous medium was extracted three times with ethyl acetate. The combined organic layers were then washed with brine, dried with sodium sulphate and the solvent was removed *in vacuo*. Purification by column chromatography on silica gel, eluting cyclohexane/ethyl acetate 20–50% to give the desired benzoxazole core.

5.2. General procedure A2: synthesis of the benzoxazole core

To 34 mL of polyphosphoric acid (1.5 g/mmol of limiting reagent) was added 2-amino-3-hydroxypyridine (1.0 eq) and the relevant benzoic acid (1.1 eq). The mixture was heated to 180 °C and stirred for 4 h, cooled and poured into 5 M sodium hydroxide. The resulting precipitate was filtered and recrystallised from ethyl acetate to give the desired benzoxazole core.

5.3. General procedure B1: amide coupling

To a solution of the benzoxazole core (1.0 eq) in DCM (2 mL) was added the carboxylic acid (1.2 eq), EDCI (1.2 eq) and DMAP (0.1 eq). The solution was stirred under nitrogen at 45 °C overnight.

Work-up 1 (W1): The solution was extended with DCM, a saturated solution of sodium bicarbonate was added and the mixture was extracted three times with DCM. The combined organic layers were then washed with brine, dried with sodium sulphate and the solvent was removed *in vacuo*. Purification by column chromatography on silica gel, eluting ethyl acetate/cyclohexane 50:50 led to the desired carboxamide.

Work-up 2 (W2): Water (approximately 2 mL) was added to the reaction mixture and it was transferred to the fridge overnight. The resulting precipitate was filtered and gave the desired carboxamide.

5.4. General procedure B2: amide coupling

To a solution of the benzoxazole core (1.0 eq) in DMF (10 mL/mmol of limiting reagent) was added the carboxylic acid (1.2 eq), HBTU (1.2 eq) and triethylamine (5.0 eq). The solution was stirred under nitrogen at 45 °C overnight. The solution was extended with ethyl acetate, a saturated solution of sodium bicarbonate was added and the mixture was extracted three times with ethyl acetate. The combined organic layers were then washed with brine, dried with sodium sulphate and the solvent was removed *in vacuo*. Purification by column chromatography on silica gel, eluting ethyl acetate/cyclohexane 50:50 led to the desired carboxamide.

5.5. General procedure C1: Suzuki coupling

A solution of *N*-(3-(6-bromooxazolo[4,5-*b*]pyridin-2-yl)phenyl) furan-2-carboxamide (1.0 eq), boronic acid (3.3 eq) and Pd(PPh₃)₄ (0.1 eq) in toluene:ethanol:2 M aqueous sodium carbonate (10:1:1 15 mL total volume/0.1 mmol of limiting reagent) was refluxed for 10 h under an atmosphere of nitrogen. Ethyl acetate (20 mL) was added and the organic phase washed with saturated solution

sodium bicarbonate (2 × 10 mL). The organic extract was dried with sodium sulphate, filtered and evaporated to give the crude product which was purified by flash chromatography, eluting 1:1 ethyl acetate/hexane to give the desired compound.

5.6. General procedure D1: *N*-methylation

To a solution of *N*-(4-chloro-3-(oxazolo[4,5-*b*]pyridin-2-yl)phenyl)benzamide (0.029 mmol) in DMF (1 mL) was added methyl iodide (0.043 mmol) and caesium carbonate (0.086 mmol). The mixture was stirred at room temperature under a nitrogen atmosphere overnight. The reaction was diluted with ethyl acetate before washing with saturated sodium carbonate. The aqueous layer was extracted three times with ethyl acetate and the combined organic layers were washed with brine and dried with sodium sulphate. The solvent was removed *in vacuo* and the crude solid was purified on silica gel, eluting with *n*-heptane/ethyl acetate 1:2, to give the desired compound.

5.7. General procedure E1: oxidative addition

To a solution of oxazolo[4,5-*b*]pyridine (**52**) (1.0 eq) in dry DMF (30 mL/mmol of limiting reagent) was added the relevant bromo-furancarboxamide (2.0 eq), caesium carbonate (1.1 eq), tri-*tert*-butylphosphonium hexaboron salt (0.1 eq), palladium diacetate (0.05 eq) and copper bromide (0.2 eq). The mixture was stirred for 3 h at 150 °C in a sealed tube. After filtration and expansion with ethyl acetate, the solution was washed with saturated sodium bicarbonate. The combined organic layers were washed with brine and dried with sodium sulphate. The solvent was removed *in vacuo* and the crude material was purified on silica gel, eluting DCM. Further purification by preparative TLC was carried out with an eluent of *n*-heptanes/ethyl acetate 1:2 to give the desired compound.

5.8. Compound characterisation

5.8.1. 4-Chloro-3-(oxazolo[4,5-*b*]pyridin-2-yl)-aniline (**50**)^b

Title compound was prepared according to General procedure A1 to give a yellow powder (20%). LRMS [M + H]⁺ 246.1 *m/z*; HRMS [M + H]⁺ 246.0426 *m/z*, found 246.0431 *m/z*; ¹H NMR (DMSO, 300 MHz) δ 8.59 (dd, *J* = 4.9, 1.4 Hz, 1H), 8.27 (dd, *J* = 8.2, 1.4 Hz, 1H), 7.51 (dd, *J* = 8.2, 4.9 Hz, 1H), 7.41 (d, *J* = 2.8 Hz, 1H), 7.32 (d, *J* = 8.7 Hz, 1H), 6.83 (dd, *J* = 8.7, 2.8 Hz, 1H), 5.70 (s, 2H); ¹³C NMR (DMSO, 101 MHz) δ 164.0, 155.5, 148.6, 147.2, 142.2, 132.2, 125.2, 121.5, 119.7, 119.0, 118.1, 116.5.

5.8.2. *N*-(4-Chloro-3-(oxazolo[4,5-*b*]pyridin-2-yl)phenyl)furan-2-carboxamide (**1**)^b

Title compound was prepared from **50** according to General procedure B1 (W1) as a brown solid (51%). LRMS [M + H]⁺ 340.1 *m/z*; HRMS [M + H]⁺ 340.0483 *m/z*, found 340.0483 *m/z*; ¹H NMR (DMSO, 400 MHz) δ 10.62 (s, 1H), 8.75 (d, *J* = 2.6 Hz, 1H), 8.62 (dd, *J* = 4.8, 0.8 Hz, 1H), 8.32 (dd, *J* = 8.2, 0.8 Hz, 1H), 8.07 (dd, *J* = 8.8, 2.6 Hz, 1H), 8.03–7.93 (m, 1H), 7.72 (d, *J* = 8.8 Hz, 1H), 7.54 (dd, *J* = 8.2, 4.9 Hz, 1H), 7.41 (d, *J* = 3.5 Hz, 1H), 6.74 (dd, *J* = 3.5, 1.7 Hz, 1H); ¹³C NMR (DMSO, 101 MHz) δ 162.6, 156.5, 155.0, 147.0, 146.3, 142.6, 138.2, 131.9, 126.5, 124.8, 124.7, 122.9, 121.4, 119.4, 115.5, 112.4. Note: there is a quaternary carbon missing from the NMR which is assumed to be under one of the other peaks.

5.8.3. *N*-(4-Chloro-3-(oxazolo[4,5-*b*]pyridin-2-yl)phenyl)-3-methylfuran-2-carboxamide (**2**)^b

The title compound was prepared from **50** according to General procedure B1 (W1) except purification was performed by column chromatography, eluting 0–40% methanol in DCM. Further

purification was performed using the HPLC, to give the title compound as an off-white solid (21%). LRMS $[M + H]^+$ 354.1 *m/z*; HRMS $[M + H]^+$ 354.0640 *m/z*, found 354.0637 *m/z*; 1H NMR (DMSO, 400 MHz) δ 10.51 (s, 1H), 8.84 (d, *J* = 2.6 Hz, 1H), 8.61 (dd, *J* = 4.8, 1.4 Hz, 1H), 8.32 (dd, *J* = 8.2, 1.4 Hz, 1H), 8.03 (dd, *J* = 8.9, 2.7 Hz, 1H), 7.84 (d, *J* = 1.7 Hz, 1H), 7.68 (d, *J* = 8.8 Hz, 1H), 7.53 (dd, *J* = 8.2, 4.8 Hz, 1H), 6.62 (d, *J* = 1.6 Hz, 1H), 2.36 (s, 3H); ^{13}C NMR (DMSO, 101 MHz) δ 162.7, 157.6, 155.0, 146.9, 144.1, 142.5, 141.4, 138.3, 131.7, 128.8, 126.3, 124.8, 124.7, 122.8, 121.4, 119.4, 115.9, 11.1.

5.8.4. *N*-(4-Chloro-3-(oxazolo[4,5-*b*]pyridin-2-yl)phenyl)isoxazole-5-carboxamide (**3**)^d

Title compound was prepared from **50** according to General procedure B1 (W1) as an off-white solid (42%). LRMS $[M + H]^+$ 341.2 *m/z*; 1H NMR (DMSO, 300 MHz) δ 11.14 (br s, 1H), 8.83 (m, 1H), 8.75 (m, 1H), 8.61 (m, 1H), 8.32 (m, 1H), 8.07 (m, 1H), 7.70 (d, *J* = 8.8 Hz, 1H), 7.53 (m, 1H), 7.30 (m, 1H).

5.8.5. *N*-(4-Chloro-3-(oxazolo[4,5-*b*]pyridin-2-yl)phenyl)oxazole-5-carboxamide (**4**)^d

Title compound was prepared from **50** according to General procedure B1 (W1) as a brown solid (9%). LRMS $[M + H]^+$ 341.1 *m/z*; 1H NMR (DMSO, 300 MHz) δ 10.86 (br s, 1H), 8.68 (d, *J* = 2.6 Hz, 1H), 8.67 (m, 1H), 8.61 (dd, *J* = 4.9, 1.4 Hz, 1H), 8.32 (dd, *J* = 8.2, 1.5 Hz, 1H), 8.03 (dd, *J* = 8.9, 2.7 Hz, 1H), 8.02 (s, 1H), 7.73 (d, *J* = 8.8 Hz, 1H), 7.53 (dd, *J* = 8.2, 4.9 Hz, 1H).

5.8.6. *N*-(4-Chloro-3-(oxazolo[4,5-*b*]pyridin-2-yl)phenyl)furan-3-carboxamide (**5**)^b

Title compound was prepared from **50** according to General procedure B1 (W1) as a yellow solid (35%). LRMS $[M + H]^+$ 340.1 *m/z*; HRMS $[M + H]^+$ 340.0483 *m/z*, found 340.0483 *m/z*; 1H NMR (DMSO, 400 MHz) δ 10.32 (s, 1H), 8.67 (d, *J* = 2.6 Hz, 1H), 8.61 (dd, *J* = 4.8, 1.4 Hz, 1H), 8.43 (dd, *J* = 1.5, 0.8 Hz, 1H), 8.31 (dd, *J* = 8.2, 1.4 Hz, 1H), 8.06 (dd, *J* = 8.8, 2.7 Hz, 1H), 7.83 (t, *J* = 1.7 Hz, 1H), 7.71 (d, *J* = 8.8 Hz, 1H), 7.53 (dd, *J* = 8.2, 4.8 Hz, 1H), 7.03 (dd, *J* = 1.9, 0.8 Hz, 1H); ^{13}C NMR (DMSO, 101 MHz) δ 162.6, 160.8, 154.9, 147.0, 146.3, 144.5, 142.5, 138.4, 131.9, 126.3, 124.7, 124.4, 122.6, 122.6, 121.4, 119.4, 109.2.

5.8.7. *N*-(4-Chloro-3-(oxazolo[4,5-*b*]pyridin-2-yl)phenyl)thiazole-4-carboxamide (**6**)^b

Title compound was prepared from **50** according to General procedure B1 (W1) as a yellow solid (83%). LRMS $[M + H]^+$ 357.1 *m/z*; HRMS $[M + H]^+$ 357.0208 *m/z*, found 357.0207 *m/z*; 1H NMR (DMSO, 400 MHz) δ 10.87 (s, 1H), 9.31 (d, *J* = 2.0 Hz, 1H), 8.94 (d, *J* = 2.6 Hz, 1H), 8.63 (dd, *J* = 4.8, 1.4 Hz, 1H), 8.58 (d, *J* = 2.0 Hz, 1H), 8.34 (dd, *J* = 8.2, 1.4 Hz, 1H), 8.14 (dd, *J* = 8.9, 2.7 Hz, 1H), 7.74 (d, *J* = 8.8 Hz, 1H), 7.56 (dd, *J* = 8.2, 4.8 Hz, 1H); ^{13}C NMR (DMSO, 101 MHz) δ 164.8, 160.2, 155.4, 152.2, 152.2, 147.8, 143.4, 138.9, 137.0, 132.0, 131.6, 130.3, 130.0, 128.2, 126.6, 124.6.

5.8.8. *N*-(4-Chloro-3-(oxazolo[4,5-*b*]pyridin-2-yl)phenyl)-1H-pyrazole-3-carboxamide (**7**)^a

Title compound was prepared from **50** according to General procedure B1 (W1) as an off-white solid (79%). LRMS $[M + H]^+$ 340.1 *m/z*; 1H NMR (DMSO, 300 MHz) δ 10.54 (br s, 1H), 8.85 (d, *J* = 1.4 Hz, 1H), 8.60 (d, *J* = 4.8 Hz, 1H), 8.30 (m, 1H), 8.09 (m, 1H), 7.88 (s, 1H), 7.68 (dd, *J* = 8.8, 0.9 Hz, 1H), 7.52 (m, 1H), 6.84 (s, 1H), Note: the pyrazole –NH signal is presumed to be downfield of the sweep width used.

5.8.9. *N*-(4-Chloro-3-(oxazolo[4,5-*b*]pyridin-2-yl)phenyl)-1H-imidazole-4-carboxamide (**8**)^d

To a solution of **50** (0.204 mmol) in DMF (2 mL) was added 4-imidazole carboxylic acid (0.286 mmol), HBTU (0.286 mmol) and

triethylamine (0.612 mmol). The solution was stirred under nitrogen at room temperature overnight. A white solid precipitated out of the solution. Filtration and trituration of the precipitate solid led to the title compound as a white solid (20%). LRMS $[M + H]^+$ 340.1 *m/z*.

5.8.10. *N*-(4-Chloro-3-(oxazolo[4,5-*b*]pyridin-2-yl)phenyl)benzofuran-2-carboxamide (**9**)^a

To a solution of **50** (0.204 mmol) in DCM (2 mL) was added benzofuran-2-carboxylic acid (0.244 mmol), EDCI (0.244 mmol) and DMAP (0.0204 mmol). The solution was stirred under nitrogen at 45 °C overnight. A white solid precipitated out of the solution. Filtration and trituration with DCM led to the clean product as a purple solid (61%). LRMS $[M + H]^+$ 390.2 *m/z*; 1H NMR (CDCl₃, 300 MHz) δ 8.69 (br s, 1H), 8.65 (d, *J* = 4.8 Hz, 1H), 8.54 (d, *J* = 2.6 Hz, 1H), 8.11 (dd, *J* = 8.8, 2.9 Hz, 1H), 7.97 (d, *J* = 8.1 Hz, 1H), 7.71 (d, *J* = 7.9 Hz, 1H), 7.66 (s, 1H), 7.57 (m, 2H), 7.39 (dd, *J* = 8.1, 4.9 Hz, 1H), 7.33 (m, 2H).

5.8.11. *N*-(4-Chloro-3-(oxazolo[4,5-*b*]pyridin-2-yl)phenyl)benzamide (**10**)^b

Title compound was prepared from **50** according to General procedure B1 (W1) as an off-white solid (69%). LRMS $[M + H]^+$ 350.1 *m/z*; HRMS $[M + H]^+$ 350.0691 *m/z*, found 350.0686 *m/z*; 1H NMR (DMSO, 400 MHz) δ 10.66 (s, 1H), 8.81 (d, *J* = 2.6 Hz, 1H), 8.62 (dd, *J* = 4.8, 1.4 Hz, 1H), 8.33 (dd, *J* = 8.2, 1.4 Hz, 1H), 8.10 (dd, *J* = 8.8, 2.6 Hz, 1H), 8.05–7.95 (m, 2H), 7.74 (d, *J* = 8.8 Hz, 1H), 7.69–7.48 (m, 4H); ^{13}C NMR (DMSO, 101 MHz) δ 165.9, 162.7, 155.0, 147.0, 142.6, 138.7, 134.3, 132.0, 131.9, 128.5, 127.8, 126.4, 124.7, 124.7, 122.9, 121.4, 119.4.

5.8.12. *N*-(4-Chloro-3-(oxazolo[4,5-*b*]pyridin-2-yl)phenyl)-2-methoxybenzamide (**11**)^d

Title compound was prepared from **50** according to General procedure B1 (W1) as an orange solid (58%). LRMS $[M + H]^+$ 380.2 *m/z*; 1H NMR (CDCl₃, 300 MHz) δ 10.88 (br s, 1H), 8.80 (m, 2H), 8.77 (d, *J* = 2.3 Hz, 1H), 8.60 (dd, *J* = 4.7, 1.4 Hz, 1H), 8.32 (m, 1H), 8.07 (dd, *J* = 8.3, 2.5 Hz, 1H), 7.89 (d, *J* = 6.0 Hz, 2H), 7.75 (d, *J* = 8.7 Hz, 1H), 7.52 (m, 1H), 4.11 (s, 3H).

5.8.13. *N*-(4-Chloro-3-(oxazolo[4,5-*b*]pyridin-2-yl)phenyl)-3-methoxybenzamide (**12**)^d

Title compound was prepared from **50** according to General procedure B1 (W1) as a dark brown solid (52%). LRMS $[M + H]^+$ 380.2 *m/z*; 1H NMR (CD₃CN, 300 MHz) δ 9.02 (br s, 1H), 8.74 (d, *J* = 2.6 Hz, 1H), 8.59 (d, *J* = 4.9 Hz, 1H), 8.10 (d, *J* = 8.2 Hz, 1H), 7.96 (m, 1H), 7.63 (m, 1H), 7.53 (m, 1H), 7.47 (m, 3H), 7.16 (m, 1H), 3.88 (s, 3H).

5.8.14. *N*-(4-Chloro-3-(oxazolo[4,5-*b*]pyridin-2-yl)phenyl)picolinamide (**13**)^d

Title compound was prepared from **50** according to General procedure B2 as a yellow solid (34%). LRMS $[M + H]^+$ 351.1 *m/z*; 1H NMR (CD₃OD, 300 MHz) δ 7.06 (m, 2H), 6.66 (dd, *J* = 8.4, 1.5 Hz, 1H), 6.44 (m, 1H), 6.00 (m, 4H), 5.80 (m, 1H), 5.40 (m, 1H). Note: the amide proton can be seen in the 1H NMR when run in DMSO at 11.11 ppm.

5.8.15. *N*-(4-Chloro-3-(oxazolo[4,5-*b*]pyridin-2-yl)phenyl)isonicotinamide (**14**)^b

To a solution of **50** (0.204 mmol) in DCM (2 mL) and DMF (0.2 mL) was added isonicotinic acid (0.244 mmol), EDCI (0.244 mmol) and DMAP (0.0204 mmol). The solution was stirred under nitrogen at 45 °C. After 3 h a white solid precipitated out of the solution. The mixture was filtered and triturated with DCM, which led to the title compound as a white solid (35%). LRMS $[M + H]^+$ 351.1 *m/z*; HRMS $[M + H]^+$ 351.0643 *m/z*, found 351.0637

m/z ; ^1H NMR (DMSO, 400 MHz) δ 10.90 (s, 1H), 8.93–8.71 (m, 3H), 8.62 (dd, $J = 4.8, 1.4$ Hz, 1H), 8.33 (dd, $J = 8.2, 1.4$ Hz, 1H), 8.09 (dd, $J = 8.8, 2.6$ Hz, 1H), 7.91 (dd, $J = 4.5, 1.6$ Hz, 2H), 7.76 (d, $J = 8.8$ Hz, 1H), 7.55 (dd, $J = 8.2, 4.8$ Hz, 1H); ^{13}C NMR (DMSO, 101 MHz) δ 164.8, 163.0, 155.4, 150.9 (2C), 147.5, 143.0, 142.8, 141.8, 138.6, 132.5, 127.5, 125.3, 123.5, 122.1 (2C), 121.9, 119.9.

5.8.16. *N*-(4-Chloro-3-(oxazol[4,5-*b*]pyridin-2-yl)phenyl)nicotinamide (**15**)^b

Title compound was prepared from **50** according to General procedure B1 (W1) as a white solid (69%). LRMS $[\text{M} + \text{H}]^+$ 351.1 m/z ; HRMS $[\text{M} + \text{H}]^+$ 351.0643 m/z , found 351.0640 m/z ; ^1H NMR (DMSO, 400 MHz) δ 10.87 (s, 1H), 9.17 (dd, $J = 2.3, 0.7$ Hz, 1H), 8.80 (dd, $J = 4.5, 1.9$ Hz, 2H), 8.64 (dd, $J = 4.8, 1.4$ Hz, 1H), 8.40–8.30 (m, 2H), 8.10 (dd, $J = 8.8, 2.7$ Hz, 1H), 7.77 (d, $J = 8.8$ Hz, 1H), 7.62 (ddd, $J = 8.0, 4.8, 0.8$ Hz, 1H), 7.56 (dd, $J = 8.2, 4.8$ Hz, 1H); ^{13}C NMR (DMSO, 101 MHz) δ 164.5, 162.6, 154.9, 152.6, 142.6, 138.4, 135.7, 135.6, 132.0, 130.0, 126.8, 124.8, 124.8, 123.6 (2C), 121.4 (2C), 119.4.

5.8.17. *N*-(4-Chloro-3-(oxazol[4,5-*b*]pyridin-2-yl)phenyl)-2-methoxyacetamide (**16**)^a

Title compound was prepared from **50** according to General procedure B2 as a yellow solid (79%). LRMS $[\text{M} + \text{H}]^+$ 318.2 m/z ; ^1H NMR (DMSO, 300 MHz) δ 10.21 (br s, 1H), 8.67 (d, $J = 2.5$ Hz, 1H), 8.60 (dd, $J = 4.8, 1.3$ Hz, 1H), 8.30 (d, $J = 8.2$ Hz, 1H), 7.93 (dd, $J = 8.8, 2.6$ Hz, 1H), 7.66 (d, $J = 8.8$ Hz, 1H), 7.51 (dd, $J = 8.2, 4.8$ Hz, 1H), 4.04 (s, 2H), 3.38 (s, 3H).

5.8.18. 3-(Oxazol[4,5-*b*]pyridin-2-yl)aniline (**51**)^b

Title compound was prepared according to General procedure A1 as a pale-yellow solid (35%). LRMS $[\text{M} + \text{H}]^+$ 212.2 m/z ; ^1H NMR (DMSO, 400 MHz) δ 8.53 (dd, $J = 4.9, 1.4$ Hz, 1H), 8.22 (dd, $J = 8.1, 1.4$ Hz, 1H), 7.60–7.33 (m, 3H), 7.27 (t, $J = 7.8$ Hz, 1H), 6.85 (ddd, $J = 8.0, 2.3, 1.0$ Hz, 1H), 5.55 (s, 2H); ^{13}C NMR (DMSO, 101 MHz) δ 165.6, 155.6, 149.5, 146.3, 142.6, 129.8, 126.3, 120.5, 118.8, 118.0, 114.9, 112.3.

5.8.19. *N*-(3-(Oxazol[4,5-*b*]pyridin-2-yl)phenyl)furan-2-carboxamide (**17**)^b

To a solution of **51** (0.142 mmol) in DCM (2 mL) was added 2-furoic acid (0.199 mmol), EDCI (0.199 mmol) and DMAP (0.0142 mmol). The solution was stirred under nitrogen at 45 °C overnight. The solution was stirred under nitrogen at 45 °C overnight. A white solid precipitated from the solution. Filtration and trituration with DCM led to the title compound as a brown solid (51%). LRMS $[\text{M} + \text{H}]^+$ 306.1 m/z ; HRMS $[\text{M} + \text{H}]^+$ 306.0873 m/z , found 306.0871 m/z ; ^1H NMR (DMSO, 400 MHz) δ 10.62 (s, 1H), 8.80 (t, $J = 1.8$ Hz, 1H), 8.57 (dd, $J = 4.9, 1.4$ Hz, 1H), 8.30 (dd, $J = 8.2, 1.4$ Hz, 1H), 8.08 (ddd, $J = 8.2, 2.1, 1.0$ Hz, 1H), 8.02–7.89 (m, 2H), 7.61 (t, $J = 8.0$ Hz, 1H), 7.50 (ddd, $J = 6.6, 4.8, 4.0$ Hz, 2H), 6.72 (dd, $J = 3.5, 1.7$ Hz, 1H); ^{13}C NMR (DMSO, 101 MHz) δ 165.0, 156.6, 155.2, 147.2, 146.2 (2C), 143.1, 139.7, 129.9, 126.2, 124.3, 122.9, 121.0, 119.7, 119.1, 115.4, 112.3.

5.8.20. 3-Methyl-*N*-(3-(oxazol[4,5-*b*]pyridin-2-yl)phenyl)furan-2-carboxamide (**18**)^b

Title compound was prepared from **51** according to General procedure B1 (W2) as an off-white solid (48%). LRMS $[\text{M} + \text{H}]^+$ 320.1 m/z ; HRMS $[\text{M} + \text{H}]^+$ 320.1030 m/z , found 320.1040 m/z ; ^1H NMR (DMSO, 400 MHz) δ 10.42 (s, 1H), 8.89 (t, $J = 1.8$ Hz, 1H), 8.57 (dd, $J = 4.9, 1.4$ Hz, 1H), 8.29 (dd, $J = 8.2, 1.4$ Hz, 1H), 8.10–7.90 (m, 2H), 7.85 (d, $J = 1.5$ Hz, 1H), 7.61 (t, $J = 8.0$ Hz, 1H), 7.49 (dd, $J = 8.2, 4.9$ Hz, 1H), 6.64 (d, $J = 1.4$ Hz, 1H), 2.39 (s, 3H); ^{13}C NMR (DMSO, 101 MHz) δ 164.9, 157.7, 155.5, 146.6, 143.9, 142.8, 141.6, 139.6, 129.7, 128.4, 126.2, 124.2, 122.7, 120.8, 119.1, 119.0, 115.8, 11.7.

5.8.21. *N*-(3-(Oxazol[4,5-*b*]pyridin-2-yl)phenyl)oxazole-5-carboxamide (**19**)^b

Title compound was prepared from **51** according to General procedure B1 (W2) as a pale-orange solid (70%). LRMS $[\text{M} + \text{H}]^+$ 307.1 m/z ; HRMS $[\text{M} + \text{H}]^+$ 307.0826 m/z , found 307.0837 m/z ; ^1H NMR (DMSO, 400 MHz) δ 10.76 (s, 1H), 8.74 (dd, $J = 8.3, 6.6$ Hz, 2H), 8.58 (dd, $J = 4.8, 1.3$ Hz, 1H), 8.29 (dd, $J = 8.2, 1.3$ Hz, 1H), 8.12–7.94 (m, 3H), 7.66 (t, $J = 8.0$ Hz, 1H), 7.50 (dd, $J = 8.2, 4.9$ Hz, 1H); ^{13}C NMR (DMSO, 101 MHz) δ 164.6, 155.4, 155.2, 154.1, 146.6, 144.9, 142.8, 139.1, 130.5, 130.0, 126.4, 124.2, 123.2, 120.9, 119.1, 119.1.

5.8.22. *N*-(3-(Oxazol[4,5-*b*]pyridin-2-yl)phenyl)furan-3-carboxamide (**20**)^a

Title compound was prepared from **51** according to General procedure B1 (W1) as an off-white solid (79%). LRMS $[\text{M} + \text{H}]^+$ 305.0 m/z ; HRMS $[\text{M} + \text{H}]^+$ 305.08004 m/z , found 305.08019 m/z ; ^1H NMR (CDCl₃, 300 MHz) δ 8.54 (d, $J = 5.1$ Hz, 1H), 8.28 (s, 1H), 8.45 (s, 1H), 8.15 (d, $J = 0.9$ Hz, 1H), 8.00 (m, 2H), 7.82 (dd, $J = 8.1, 3.6$ Hz, 1H), 7.50–7.45 (m, 2H), 7.29 (t, $J = 4.8$ Hz, 1H), 6.83 (d, $J = 3.6$ Hz, 1H); ^{13}C NMR (CDCl₃, 75 MHz) δ 165.4, 161.3, 156.4, 146.9, 145.8, 144.3, 143.4, 138.8, 130.1, 127.2, 124.5, 124.1, 123.0, 120.5, 119.7, 118.6, 108.7.

5.8.23. *N*-(3-(Oxazol[4,5-*b*]pyridin-2-yl)phenyl)thiazole-4-carboxamide (**21**)^b

Title compound was prepared from **51** according to General procedure B2 as a pale-yellow solid (20%). LRMS $[\text{M} + \text{H}]^+$ 323.1 m/z ; HRMS $[\text{M} + \text{H}]^+$ 323.0597 m/z , found 323.0613 m/z ; ^1H NMR (DMSO, 400 MHz) δ 10.75 (s, 1H), 9.32 (d, $J = 2.0$ Hz, 1H), 8.97 (t, $J = 1.8$ Hz, 1H), 8.70–8.46 (m, 2H), 8.29 (dd, $J = 8.2, 1.4$ Hz, 1H), 8.11 (ddd, $J = 8.2, 2.1, 0.9$ Hz, 1H), 8.05–7.93 (m, 1H), 7.64 (t, $J = 8.0$ Hz, 1H), 7.50 (dd, $J = 8.2, 4.9$ Hz, 1H); ^{13}C NMR (DMSO, 101 MHz) δ 164.7, 159.5, 155.5, 155.2, 150.4, 146.6, 142.8, 139.5, 129.8, 126.3, 126.1, 124.5, 123.0, 120.8, 119.2, 119.1.

5.8.24. Oxazol[4,5-*b*]pyridine (**52**)^b

To a solution of 2-amino-3-hydroxypyridine (90.1 mmol) in triethylorthoformate (720.7 mmol) was added *p*-toluenesulphonic acid (4.50 mmol) and the mixture was stirred under nitrogen at 160 °C overnight. The triethylorthoformate was removed *in vacuo* and the crude material was purified by column chromatography, eluting with cyclohexane/ethyl acetate 5%–40% to give the title compound as a beige solid (68%). LRMS $[\text{M} + \text{H}]^+$ 121.1 m/z ; ^1H NMR (DMSO, 400 MHz) δ 9.04 (s, 1H), 8.58 (dd, $J = 4.8, 1.4$ Hz, 1H), 8.26 (dd, $J = 8.2, 1.4$ Hz, 1H), 7.50 (dd, $J = 8.2, 4.8$ Hz, 1H), 6.41 (s, 2H); ^{13}C NMR (DMSO, 101 MHz) δ 157.7, 154.5, 147.1, 142.0, 121.5, 120.1.

5.8.25. 2-Methyl-3-(oxazol[4,5-*b*]pyridin-2-yl)aniline (**53**)^b

Title compound was prepared according to General procedure A2 as a dark-red solid (48%). LRMS $[\text{M} + \text{H}]^+$ 226.2 m/z ; HRMS $[\text{M} + \text{H}]^+$ 226.0975 m/z , found 226.0975 m/z ; ^1H NMR (DMSO, 400 MHz) δ 8.54 (dd, $J = 4.9, 1.4$ Hz, 1H), 8.21 (dd, $J = 8.1, 1.4$ Hz, 1H), 7.45 (dd, $J = 8.1, 4.9$ Hz, 1H), 7.28 (dd, $J = 7.7, 1.0$ Hz, 1H), 7.12 (t, $J = 7.8$ Hz, 1H), 6.92 (dd, $J = 7.9, 0.9$ Hz, 1H), 5.26 (s, 2H), 2.48 (s, 3H); ^{13}C NMR (DMSO, 101 MHz) δ 166.1, 155.5, 148.1, 146.2, 142.1, 126.4, 125.7, 121.5, 120.6, 118.8, 117.9, 117.5, 14.3.

5.8.26. *N*-(2-Methyl-3-(oxazol[4,5-*b*]pyridin-2-yl)phenyl)furan-2-carboxamide (**22**)^b

Title compound was prepared from **53** according to General procedure B1 (W2) as a pale-yellow solid (68%). ^1H NMR (DMSO, 400 MHz) δ 10.13 (s, 1H), 8.59 (dd, $J = 4.9, 1.4$ Hz, 1H), 8.29 (dd, $J = 8.2, 1.4$ Hz, 1H), 8.10–8.02 (m, 1H), 7.97 (dd, $J = 1.7, 0.8$ Hz, 1H), 7.62 (d, $J = 6.8$ Hz, 1H), 7.55–7.44 (m, 2H), 7.35 (dd, $J = 3.5, 0.7$ Hz, 1H), 6.74 (dd, $J = 3.5, 1.8$ Hz, 1H), 2.63 (s, 3H).

5.8.27. 3-Amino-2-fluorobenzoic acid (**54**)^b

0.05 M Solution of 2-fluoro-3-nitrobenzoic acid (0.27 mmol) was made up in 50:50 ethyl acetate/ethanol (54 mL). This was loaded on to the ThalesNano H-Cube[®] with a 10% Pd/C CatCart[®]. The reaction was monitored by LRMS until no more starting material was present and the solvent was removed under reduced pressure to give the amine as a pale-yellow solid (95%). There was a small amount of starting material by ¹H NMR though it was not possible to separate the two compounds and so the material was used directly in the next reaction. LRMS [M + H]⁺ 156.1 m/z; ¹H NMR (DMSO, 400 MHz) δ 7.03–6.83 (m, 3H), 5.32 (s, 2H).

5.8.28. 2-Fluoro-3-(oxazolo[4,5-b]pyridin-2-yl)aniline (**55**)^b

Title compound was prepared using **53** according to General procedure A2 as a pale-brown solid (63%). LRMS [M + H]⁺ 230.1 m/z; HRMS [M + H]⁺ 230.0724 m/z, found 230.0723 m/z; ¹H NMR (DMSO, 400 MHz) δ 8.58 (dd, J = 4.9, 1.4 Hz, 1H), 8.26 (dd, J = 8.2, 1.4 Hz, 1H), 7.49 (dd, J = 8.2, 4.9 Hz, 1H), 7.35 (ddd, J = 7.8, 6.1, 1.8 Hz, 1H), 7.15–7.01 (m, 2H), 5.57 (s, 2H); ¹³C NMR (DMSO, 101 MHz) δ 162.3 (J_{C-F} = 4 Hz), 155.2, 148.5 (J_{C-F} = 252 Hz), 146.7, 142.4, 138.0 (J_{C-F} = 12 Hz), 124.9 (J_{C-F} = 4 Hz), 120.9, 119.95 (J_{C-F} = 5 Hz), 119.1, 116.2, 113.9 (J_{C-F} = 8 Hz).

5.8.29. N-(2-Fluoro-3-(oxazolo[4,5-b]pyridin-2-yl)phenyl)furan-2-carboxamide (**23**)^b

Title compound was prepared from **55** according to General procedure B1 (W2) as a pale-brown solid (44%). ¹H NMR (DMSO, 400 MHz) δ 10.27 (s, 1H), 8.61 (dd, J = 4.8, 1.4 Hz, 1H), 8.32 (dd, J = 8.2, 1.4 Hz, 1H), 8.19–8.08 (m, 1H), 8.00 (dd, J = 1.6, 0.7 Hz, 1H), 7.96–7.87 (m, 1H), 7.58–7.44 (m, 2H), 7.41 (dd, J = 3.5, 0.7 Hz, 1H), 6.75 (dd, J = 3.5, 1.8 Hz, 1H).

5.8.30. 2-(2-Chloro-3-nitrophenyl)oxazolo[4,5-b]pyridine (**56**)^c

Title compound was prepared according to General procedure A2 as a pale-yellow solid (60%) and used directly in the next reaction without further purification. ¹H NMR (CDCl₃, 300 MHz) δ 7.24 (dd, J = 8.4, 5.1 Hz, 1H), 7.61 (t, J = 8.1 Hz, 1H), 7.94 (ddd, J = 21.9, 8.1, 1.5 Hz, 2H), 8.43 (dd, J = 7.8, 1.5 Hz, 1H), 8.68 (J = 4.8, 1.5 Hz, 1H).

5.8.31. 2-Chloro-3-(oxazolo[4,5-b]pyridin-2-yl)aniline (**57**)^c

56 (1.45 mmol) was reduced by heating with iron powder (4.35 mmol) and concentrated hydrochloric acid (20.3 mmol) in refluxing ethanol (5 mL). The reaction mixture was diluted and basified with a saturated sodium bicarbonate solution. The aqueous phase was extracted with ethyl acetate (3 × 30 mL) and the extract was dried with sodium sulphate, filtered and evaporated to give the title compound as a brown solid (66%). LRMS M⁺ 245.0 m/z; HRMS M⁺ 245.03559 m/z, found 245.03559 m/z; ¹H NMR (CDCl₃, 300 MHz) δ 8.60 (s, 1H), 7.89 (d, J = 8.1 Hz, 1H), 7.70 (d, J = 7.5 Hz, 1H), 7.35–7.19 (m, 3H), 6.97 (d, J = 6.9 Hz, 1H).

5.8.32. N-(2-Chloro-3-(oxazolo[4,5-b]pyridin-2-yl)phenyl)furan-2-carboxamide (**24**)^c

Title compound was prepared from **57** according to General procedure B1 (W1) as a pale-brown solid (54%). LRMS M⁺ 339 m/z; HRMS M⁺ 339.04107 m/z, found 339.04141 m/z; ¹H NMR (CDCl₃, 300 MHz) δ 9.02 (s, 1H), 8.78 (dd, J = 8.4, 1.5 Hz, 1H), 8.64 (dd, J = 4.8, 1.5 Hz, 1H), 7.96 (J = 14.4, 8.1, 1.5 Hz, 2H), 7.60 (d, J = 2.7 Hz, 1H), 7.49 (t, J = 8.4 Hz, 1H), 7.37 (dd, J = 8.1, 4.8 Hz, 1H), 7.31 (d, J = 4.5 Hz, 1H), 6.6 (dd, J = 3.6, 1.8 Hz, 1H).

5.8.33. 4-(Oxazolo[4,5-b]pyridin-2-yl)pyridin-2-amine (**58**)^b

Title compound was prepared according to General procedure A1 as a pale-brown solid (36%). LRMS [M + H]⁺ 213.2 m/z; HRMS [M + H]⁺ 213.0771 m/z, found 213.0774 m/z; ¹H NMR (DMSO,

400 MHz) δ 8.85 (d, J = 5 Hz, 1H), 8.75 (dd, J = 5, 1 Hz, 1H), 7.83 (m, 1H), 7.65 (dd, J = 7, 5 Hz, 1H), 7.58 (d, J = 7 Hz, 1H), 7.38 (dd, J = 5, 2 Hz, 1H), 6.25 (s, 2H).

5.8.34. N-(4-(Oxazolo[4,5-b]pyridin-2-yl)pyridin-2-yl)furan-2-carboxamide (**25**)^b

Title compound was prepared from **58** according to General procedure B2 as a pale-brown solid (85%). LRMS [M + H]⁺ 307.1 m/z; HRMS [M + H]⁺ 307.0826 m/z, found 307.0826 m/z; ¹H NMR (DMSO, 400 MHz) δ 9.23 (s, 1H), 8.59 (dd, J = 4.8, 1.4 Hz, 1H), 8.31 (s, 1H), 8.28 (dd, J = 8.2, 1.4 Hz, 1H), 8.16 (d, J = 5.2 Hz, 1H), 7.52 (dd, J = 8.2, 4.8 Hz, 1H), 7.29–7.23 (m, 1H), 7.20 (dd, J = 5.2, 1.5 Hz, 1H), 6.42 (s, 2H); ¹³C NMR (DMSO, 101 MHz) δ 170.9, 162.6, 159.0, 157.4, 148.2, 147.5, 147.0, 146.0, 143.8, 142.6, 114.7, 114.4, 113.6, 112.8, 107.3, 102.1.

5.8.35. 2-Methoxy-5-(oxazolo[4,5-b]pyridin-2-yl)aniline (**59**)^b

Title compound was prepared according to General procedure A2 as a pale-brown solid (85%). LRMS [M + H]⁺ 242.2 m/z; ¹H NMR (DMSO, 400 MHz) δ 8.48 (dd, J = 4.9, 1.4 Hz, 1H), 8.15 (dd, J = 8.1, 1.4 Hz, 1H), 7.54 (d, J = 2.2 Hz, 1H), 7.48 (dd, J = 8.3, 2.2 Hz, 1H), 7.39 (dd, J = 8.1, 4.9 Hz, 1H), 7.02 (d, J = 8.4 Hz, 1H), 5.17 (s, 2H), 3.88 (s, 3H); ¹³C NMR (DMSO, 101 MHz) δ 165.8, 156.0, 150.0, 146.0, 142.5, 138.5, 120.0, 118.4, 118.2, 116.7, 111.9, 110.6, 55.6.

5.8.36. N-(2-Methoxy-5-(oxazolo[4,5-b]pyridin-2-yl)phenyl)furan-2-carboxamide (**26**)^b

Title compound was prepared from **59** according to General procedure B1 (W2) as a pale-brown solid (70%). LRMS [M + H]⁺ 336.1 m/z; HRMS [M + H]⁺ 336.0979 m/z, found 336.0976 m/z; ¹H NMR (DMSO, 400 MHz) δ 9.29 (s, 1H), 8.89 (d, J = 2.1 Hz, 1H), 8.52 (dd, J = 4.9, 1.4 Hz, 1H), 8.22 (dd, J = 8.1, 1.4 Hz, 1H), 8.08 (dd, J = 8.6, 2.2 Hz, 1H), 7.99 (dd, J = 1.7, 0.7 Hz, 1H), 7.44 (dd, J = 8.1, 4.9 Hz, 1H), 7.38 (dd, J = 4.7, 4.0 Hz, 2H), 6.75 (dd, J = 3.5, 1.7 Hz, 1H), 3.34 (s, 3H); ¹³C NMR (DMSO, 101 MHz) δ 164.8, 155.8, 155.7, 153.4, 147.0, 146.3, 146.0, 142.7, 127.1, 125.3, 120.9, 120.3, 118.7, 118.0, 115.4, 112.5, 112.0, 56.5.

5.8.37. 2-Methyl-5-(oxazolo[4,5-b]pyridin-2-yl)aniline (**60**)^b

Title compound was prepared according to General procedure A1 as a pale-brown solid (34%). LRMS [M + H]⁺ 226.2 m/z; HRMS [M + H]⁺ 226.0975 m/z, found 226.0979 m/z; ¹H NMR (DMSO, 400 MHz) δ 8.50 (d, J = 4.8 Hz, 1H), 7.95 (d, J = 7.7 Hz, 1H), 7.78 (dd, J = 7.7, 4.8 Hz, 1H), 7.75 (d, J = 8.4 Hz, 1H), 7.50 (s, 1H), 7.28 (d, J = 0.3 Hz, 1H), 5.45 (s, 2H), 2.30 (s, 3H); ¹³C NMR (DMSO, 101 MHz) δ 167.1, 155.3, 147.4, 145.0, 142.9, 126.5, 116.2, 126.5, 122.9 (2C), 117.6, 114.1, 18.1.

5.8.38. N-(2-Methyl-5-(oxazolo[4,5-b]pyridin-2-yl)phenyl)furan-2-carboxamide (**27**)^b

Title compound was prepared from **60** according to General procedure B2 as a pale-brown solid (54%). HPLC >85% purity at 254 nm. LRMS [M + H]⁺ 320.3 m/z; ¹H NMR (DMSO, 400 MHz) δ 10.12 (s, 1H), 8.61 (dd, J = 6.5, 1.8 Hz, 1H), 8.50 (dd, J = 1.7, 0.8 Hz, 1H), 7.95 (dd, J = 1.7, 0.9 Hz, 1H), 7.65–7.75 (m, 2H), 7.46 (dd, J = 8.5, 6.5 Hz, 1H), 7.40 (dd, J = 8.1, 0.8 Hz, 1H), 7.29 (dd, J = 3.4, 0.9 Hz, 1H), 6.72 (dd, J = 3.4, 1.7 Hz, 1H), 2.27 (3H); ¹³C NMR (DMSO, 101 MHz) δ 167.0, 161.9, 154.9, 148.2 (C2), 147.1, 142.6, 131.4, 133.1, 130.0, 123.6, 119.6 (C2), 119.6, 119.3, 115.3, 111.7, 17.3.

5.8.39. N-(2-Fluoro-5-(oxazolo[4,5-b]pyridin-2-yl)phenyl)furan-2-carboxamide (**28**)^b

Title compound was prepared according to General procedure B2 as a pale-brown solid (72%). LRMS [M + H]⁺ 324.1 m/z; HRMS [M + H]⁺ 324.0779 m/z, found 324.0779 m/z; ¹H NMR (DMSO,

400 MHz) δ 9.98 (s, 1H), 8.66 (m, 2H), 7.85–7.95 (m, 2H), 7.84 (d, $J = 8.2$ Hz, 1H), 7.57 (d, $J = 8.2$ Hz, 1H), 7.53 (dd, $J = 7.7, 5.3$ Hz, 1H), 7.29 (d, $J = 3.4$ Hz, 1H), 6.71 (dd, $J = 3.4, 1.8$ Hz, 1H); ^{13}C NMR (DMSO, 101 MHz) δ 167.0, 162.7, 158.3, 154.9, 148.2, 148.0, 143.8, 142.6, 124.7, 121.9, 121.1, 119.6, 119.9, 118.2, 116.2, 115.3, 111.7.

5.8.40. 2-(4-Chloro-3-nitrophenyl)oxazolo[4,5-b]pyridine (**61**)^c

Title compound prepared according to General procedure A1 as a grey solid (70%). ^1H NMR (CDCl₃, 300 MHz) δ 9.16 (d, $J = 2.7$ Hz, 1H), 8.70 (d, $J = 4.8$ Hz, 1H), 8.34 (dd, $J = 8.8, 2.7$ Hz, 1H), 8.02 (dd, $J = 8.2, 1.5$ Hz, 1H), 7.80 (d, $J = 8.8$ Hz, 1H), 7.44 (dd, $J = 8.2, 4.8$ Hz, 1H).

5.8.41. 2-Chloro-5-(oxazolo[4,5-b]pyridin-2-yl)aniline (**62**)^c

61 (1.45 mmol) was reduced by heating with iron powder (4.35 mmol) and concentrated hydrochloric acid (20.3 mmol) in refluxing ethanol (5 mL). The reaction mixture was diluted and basified with a saturated sodium bicarbonate solution. The aqueous phase was extracted with ethyl acetate (3 × 30 mL) and the extract was dried with sodium sulphate, filtered and evaporated to give the title compound as a pale yellow solid (66%). LRMS M⁺ 245.0 m/z; HRMS M⁺ 245.03559 m/z, found 245.03559 m/z; ^1H NMR (CDCl₃, 300 MHz) δ 8.59 (d, $J = 4.8$ Hz, 1H), 7.85 (d, $J = 8.1$ Hz, 1H), 7.74 (d, $J = 2.1$ Hz, 1H), 7.62 (dd, $J = 8.1, 1.8$ Hz, 1H), 7.41 (d, $J = 8.1$ Hz, 1H), 7.30 (dd, $J = 8.1, 5.1$ Hz, 1H). Note: The amine was observed as a broad peak and so was not assigned; ^{13}C NMR (CDCl₃, 75 MHz) δ 165.4, 156.5, 146.9, 143.7, 143.4, 130.3, 125.9, 123.7, 120.4, 118.5, 118.4, 114.9.

5.8.42. N-(2-Chloro-5-(oxazolo[4,5-b]pyridin-2-yl)phenyl)furan-2-carboxamide (**29**)^c

Title compound was prepared from **62** according to General procedure B1 (W1) as a pale-brown solid (47%). LRMS M⁺ 339.0 m/z; HRMS M⁺ 339.04107 m/z, found 339.04141 m/z; ^1H NMR (CDCl₃, 300 MHz) δ 9.45 (d, $J = 1.8$ Hz, 1H), 8.79 (s, 1H), 8.57 (dd, $J = 4.8, 1.2$ Hz, 1H), 8.09 (dd, $J = 8.4, 1.8$ Hz, 1H), 7.88 (dd, $J = 8.1, 1.5$ Hz, 1H), 7.58 (d, $J = 8.4$ Hz, 2H), 7.33 (d, $J = 4.2$ Hz, 2H), 6.60 ($J = 3.6, 1.8$ Hz, 1H); ^{13}C NMR (DMSO, 75 MHz) δ 164.7, 156.3, 156.1, 147.1, 146.8, 145.1, 143.4, 135.1, 127.0, 126.3, 124.7, 120.6, 120.2, 118.7, 116.5, 113.1, 112.6.

5.8.43. N-(5-Bromopyridin-3-yl)furan-2-carboxamide (**63**)^b

Title compound was prepared according to General procedure B1 (W1) to give the title compound as an orange solid (9% yield). LRMS [M + H, Br⁷⁹]⁺ 267.0 m/z, [M + H, Br⁸¹]⁺ 269.0 m/z; ^1H NMR (DMSO, 400 MHz) δ 10.59 (s, 1H), 8.90 (d, $J = 2.1$ Hz, 1H), 8.55–8.35 (m, 2H), 8.00 (dd, $J = 1.7, 0.8$ Hz, 1H), 7.39 (dd, $J = 3.5, 0.8$ Hz, 1H), 6.74 (dd, $J = 3.5, 1.7$ Hz, 1H); ^{13}C NMR (DMSO, 101 MHz) δ 156.6, 146.7, 146.4, 144.83, 140.2, 136.4, 129.2, 119.5, 115.9, 112.5.

5.8.44. N-(5-(Oxazolo[4,5-b]pyridin-2-yl)pyridin-3-yl)furan-2-carboxamide (**30**)^d

Title compound was prepared from **63** according to General procedure E1 as a brown solid (17% yield). LRMS [M + H]⁺ 307.2 m/z; ^1H NMR (CDCl₃, 300 MHz) : δ 9.80 (m, 2H), 9.74 (s, 1H), 9.29 (s, 1H), 8.69 (d, $J = 3.7$ Hz, 1H), 7.99 (d, $J = 8.7$ Hz, 1H), 7.66 (s, 1H), 7.62 (s, 1H), 7.43 (dd, $J = 8.1, 4.6$ Hz, 1H), 6.63 (m, 1H).

5.8.45. 3-Fluoro-5-(oxazolo[4,5-b]pyridin-2-yl)aniline (**64**)^b

Title compound was prepared according to General procedure A2 as a pale-brown solid (61%). HPLC >90% purity at 254 nm; LRMS [M + H]⁺ 230.1 m/z; HRMS [M + H]⁺ 230.0724 m/z, found 230.0725 m/z; ^1H NMR (DMSO, 400 MHz) δ 8.64 (d, $J = 5.1$ Hz, 1H), 7.72 (m, 2H), 7.52 (dd, $J = 7.6, 5.2$ Hz, 1H), 7.50 (br s, 1H), 7.44 (s, 1H), 5.62 (s, 2H); ^{13}C NMR (DMSO, 101 MHz) δ 106.9, 111.2, 118.3, 121.0 (2C), 129.0, 140.1, 148.0, 150.1, 155.2, 164.4, 167.0.

5.8.46. N-(3-Fluoro-5-(oxazolo[4,5-b]pyridin-2-yl)phenyl)furan-2-carboxamide (**31**)^b

Title compound was prepared from **64** according to General procedure B2 as a pale brown solid (61%). LRMS [M + H]⁺ 324.2 m/z; HRMS [M + H]⁺ 324.0779 m/z, found 324.0771 m/z; ^1H NMR (DMSO, 400 MHz) δ 9.65 (s, 1H), 8.69 (d, $J = 5.3$ Hz, 1H), 8.09 (s, 1H), 8.00 (d, $J = 1.9$ Hz, 1H), 7.85–7.95 (m, 3H), 7.57 (dd, $J = 8.1, 5.3$ Hz, 1H), 7.31 (d, $J = 3.4$ Hz, 1H), 6.74 (dd, $J = 3.4, 1.7$ Hz, 1H); ^{13}C NMR (DMSO, 101 MHz) δ 110.9, 112.3, 115.3 (2C), 116.4, 119.0, 120.1, 127.9, 139.6, 143.0, 143.5, 148.2 (2C), 161.0, 162.5, 163.9, 167.0.

5.8.47. 4-Methyl-3-(oxazolo[4,5-b]pyridin-2-yl)aniline (**65**)^b

Title compound was prepared according to General procedure A1 as a pale-yellow solid (30%). LRMS [M + H]⁺ 226.2 m/z; ^1H NMR (DMSO, 400 MHz) δ 8.54 (dd, $J = 4.9, 1.4$ Hz, 1H), 8.22 (dd, $J = 8.1, 1.4$ Hz, 1H), 7.52–7.41 (m, 2H), 7.11 (d, $J = 8.2$ Hz, 1H), 6.77 (dd, $J = 8.2, 2.5$ Hz, 1H), 5.30 (s, 2H), 2.59 (s, 3H); ^{13}C NMR (DMSO, 101 MHz) δ 165.70, 155.61, 147.01, 146.23, 141.96, 132.56, 125.45, 124.77, 120.51, 118.66, 117.96, 114.29, 20.85.

5.8.48. N-(4-Methyl-3-(oxazolo[4,5-b]pyridin-2-yl)phenyl)furan-2-carboxamide (**32**)^b

Title compound was prepared from **65** according to General procedure B2 as an off-white solid (7% yield). LRMS [M + H]⁺ 320.2 m/z; HRMS [M + H]⁺ 320.1030 m/z, found 320.1027 m/z; ^1H NMR (DMSO, 400 MHz) δ 10.44 (s, 1H), 8.70 (d, $J = 2.3$ Hz, 1H), 8.57 (dd, $J = 4.9, 1.4$ Hz, 1H), 8.28 (dd, $J = 8.1, 1.4$ Hz, 1H), 8.03–7.86 (m, 2H), 7.56–7.42 (m, 2H), 7.39 (dd, $J = 3.5, 0.6$ Hz, 1H), 6.73 (dd, $J = 3.5, 1.7$ Hz, 1H), 2.75 (s, 3H); ^{13}C NMR (DMSO, 101 MHz) δ 164.8, 156.3, 155.5, 147.3, 146.5, 146.0, 142.1, 137.0, 134.10, 132.4, 124.9, 123.7, 121.0, 120.9, 119.0, 115.0, 112.2, 21.4.

5.8.49. 3-Methyl-N-(4-methyl-3-(oxazolo[4,5-b]pyridin-2-yl)phenyl)furan-2-carboxamide (**33**)^b

Title compound was prepared from **65** according to General procedure B1 (W1) as a pale-orange solid (56%). LRMS [M + H]⁺ 334.2 m/z; HRMS [M + H]⁺ 334.1186 m/z, found 334.1195 m/z; ^1H NMR (DMSO, 400 MHz) δ 10.33 (s, 1H), 8.80 (d, $J = 2.3$ Hz, 1H), 8.58 (dd, $J = 4.9, 1.4$ Hz, 1H), 8.30 (dd, $J = 8.2, 1.4$ Hz, 1H), 7.90 (dd, $J = 8.3, 2.3$ Hz, 1H), 7.83 (d, $J = 1.7$ Hz, 1H), 7.60–7.37 (m, 2H), 6.62 (d, $J = 1.7$ Hz, 1H), 2.75 (s, 3H), 2.38 (s, 3H); ^{13}C NMR (DMSO, 101 MHz) δ 164.9, 157.5, 155.5, 146.5, 143.8, 142.1, 141.7, 137.1, 133.9, 132.3, 128.1, 124.7, 123.8, 121.0, 120.8, 118.9, 115.7, 21.3, 11.1.

5.8.50. N-(4-Methyl-3-(oxazolo[4,5-b]pyridin-2-yl)phenyl)oxazole-5-carboxamide (**34**)^b

Title compound was prepared from **65** according to General procedure B1 (W1) as an off-white solid (67%). LRMS [M + H]⁺ 321.1 m/z; HRMS [M + H]⁺ 319.0837 m/z, found 319.0834 m/z; ^1H NMR (DMSO, 400 MHz) δ 10.68 (s, 1H), 8.77–8.62 (m, 2H), 8.58 (dd, $J = 4.8, 1.4$ Hz, 1H), 8.28 (dd, $J = 8.1, 1.4$ Hz, 1H), 8.04 (s, 1H), 7.93 (dd, $J = 8.3, 2.3$ Hz, 1H), 7.61–7.40 (m, 2H), 2.76 (s, 3H); ^{13}C NMR (DMSO, 101 MHz) δ 164.7, 155.4, 155.0, 154.0, 146.5, 145.0, 142.1, 136.6, 134.5, 132.5, 130.2, 124.9, 123.7, 121.1, 120.9, 118.9, 21.4.

5.8.51. N-(4-Methyl-3-(oxazolo[4,5-b]pyridin-2-yl)phenyl)furan-3-carboxamide (**35**)^b

Title compound was prepared from **65** according to General procedure B1 (W1) as an off-white solid (79%). LRMS [M + H]⁺ 320.2 m/z; HRMS [M + H]⁺ 318.0884 m/z, found 318.0876 m/z; ^1H NMR (DMSO, 400 MHz) δ 10.18 (s, 1H), 8.77–8.49 (m, 2H), 8.43 (d, $J = 0.6$ Hz, 1H), 8.28 (dd, $J = 8.1, 1.4$ Hz, 1H), 7.94 (dd, $J = 8.3, 2.3$ Hz, 1H), 7.83 (t, $J = 1.7$ Hz, 1H), 7.58–7.36 (m, 2H), 7.04 (dd, $J = 1.8, 0.7$ Hz, 1H), 2.76 (s, 3H); ^{13}C NMR (DMSO, 101 MHz) δ 164.8, 160.5,

155.5, 146.5, 146.0, 144.3, 142.1, 137.3, 133.9, 132.4, 124.8, 123.5, 122.8, 120.9, 120.8, 118.9, 109.2, 21.3.

5.8.52. *N*-(4-Methyl-3-(oxazolo[4,5-*b*]pyridin-2-yl)phenyl)thiazole-4-carboxamide (**36**)^b

Title compound was prepared from **65** according to General procedure B1 (W1) as a pale-yellow solid (56%). LRMS [M + H]⁺ 337.1 *m/z*; HRMS [M + H]⁺ 337.0754 *m/z*, found 337.0768 *m/z*; ¹H NMR (DMSO, 400 MHz) δ 10.65 (s, 1H), 9.30 (d, *J* = 2.0 Hz, 1H), 8.89 (d, *J* = 2.3 Hz, 1H), 8.66–8.44 (m, 2H), 8.29 (dd, *J* = 8.1, 1.4 Hz, 1H), 7.98 (dd, *J* = 8.3, 2.3 Hz, 1H), 7.62–7.33 (m, 2H), 2.76 (s, 3H); ¹³C NMR (DMSO, 101 MHz) δ 164.8, 159.3, 155.5, 155.1, 150.5, 146.5, 142.1, 137.0, 134.3, 132.3, 125.8, 124.8, 124.0, 121.2, 120.9, 119.0, 21.4.

5.8.53. 4-Fluoro-3-(oxazolo[4,5-*b*]pyridin-2-yl)aniline (**66**)^b

Title compound was prepared according to General procedure A1 as a yellow solid (34%). LRMS [M + H]⁺ 230.2 *m/z*; ¹H NMR (DMSO, 400 MHz) δ 8.57 (dd, *J* = 4.9, 1.4 Hz, 1H), 8.27 (dd, *J* = 8.2, 1.4 Hz, 1H), 7.46 (ddd, *J* = 8.9, 7.1, 3.9 Hz, 2H), 7.16 (dd, *J* = 10.9, 8.9 Hz, 1H), 6.86 (ddd, *J* = 8.9, 4.1, 3.0 Hz, 1H), 5.42 (s, 2H); ¹³C NMR (DMSO, 101 MHz) δ 162.4 (*J*_{C-F} = 4 Hz), 155.1, 152.2 (*J*_{C-F} = 247 Hz), 146.67, 145.8 (*J*_{C-F} = 2 Hz), 142.45, 120.88, 119.5 (*J*_{C-F} = 8 Hz), 119.09, 117.6 (*J*_{C-F} = 22 Hz), 113.7 (*J*_{C-F} = 11 Hz), 113.5.

5.8.54. *N*-(4-fluoro-3-(oxazolo[4,5-*b*]pyridin-2-yl)phenyl)furan-2-carboxamide (**37**)^a

Title compound was prepared from **66** according to General procedure B1 (W1) as an off-white solid (4%). LRMS [M + H]⁺ 324.1 *m/z*; ¹H NMR (DMSO, 400 MHz) δ 10.55 (s, 1H), 8.77 (dd, *J* = 6.5, 2.7 Hz, 1H), 8.59 (dd, *J* = 4.8, 1.4 Hz, 1H), 8.39–8.23 (m, 1H), 8.07 (ddd, *J* = 9.0, 4.2, 2.8 Hz, 1H), 7.97 (ddd, *J* = 7.4, 1.7, 0.7 Hz, 1H), 7.51 (dt, *J* = 9.5, 3.4 Hz, 2H), 7.38 (ddd, *J* = 11.3, 3.5, 0.7 Hz, 1H), 6.79–6.63 (m, 1H); ¹³C NMR (DMSO, 101 MHz) δ 161.4, 156.4, 156.3 (*J*_{C-F} = 249 Hz), 147.1, 146.9, 146.1, 142.6, 135.6, 126.2 (*J*_{C-F} = 8 Hz), 121.4 (*J*_{C-F} = 26 Hz) (+1C identified by HSQC), 119.3, 117.7 (*J*_{C-F} = 22 Hz), 115.3, 114.0 (*J*_{C-F} = 11 Hz), 112.3, Note: 1 quaternary carbon is missing and is assumed to be overlapping with the other signals.

5.8.55. *N*-(4-Fluoro-3-(oxazolo[4,5-*b*]pyridin-2-yl)phenyl)-3-methylfuran-2-carboxamide (**38**)^b

Title compound was prepared from **66** according to General procedure B1 (W2) as a pale-orange solid (46%). LRMS [M + H]⁺ 338.1 *m/z*; HRMS [M + H]⁺ 338.0935 *m/z*, found 338.0952 *m/z*; ¹H NMR (DMSO, 400 MHz) δ 10.45 (s, 1H), 8.88 (dd, *J* = 6.5, 2.7 Hz, 1H), 8.60 (dd, *J* = 4.8, 1.4 Hz, 1H), 8.32 (dd, *J* = 8.2, 1.4 Hz, 1H), 8.04 (ddd, *J* = 9.0, 4.3, 2.8 Hz, 1H), 7.84 (d, *J* = 1.5 Hz, 1H), 7.59–7.42 (m, 2H), 6.63 (d, *J* = 1.5 Hz, 1H), 2.37 (s, 3H).

5.8.56. *N*-(4-Fluoro-3-(oxazolo[4,5-*b*]pyridin-2-yl)phenyl)oxazole-5-carboxamide (**39**)^b

Title compound was prepared from **66** according to General procedure B1 (W2) as a pale-yellow solid (93%). LRMS [M + H]⁺ 325.1 *m/z*; HRMS [M + H]⁺ 325.0731 *m/z*, found 325.0747 *m/z*; ¹H NMR (DMSO, 400 MHz) δ 10.79 (s, 1H), 8.84–8.67 (m, 2H), 8.61 (dd, *J* = 4.8, 1.2 Hz, 1H), 8.32 (dd, *J* = 8.2, 1.2 Hz, 1H), 8.15–7.96 (m, 2H), 7.64–7.43 (m, 2H).

5.8.57. *N*-(4-Fluoro-3-(oxazolo[4,5-*b*]pyridin-2-yl)phenyl)furan-3-carboxamide (**40**)^b

Title compound was prepared from **66** according to General procedure B1 (W2) as an off-white solid (80%). LRMS [M + H]⁺ 324.1 *m/z*; HRMS [M + H]⁺ 322.0633 *m/z*, found 322.0627 *m/z*; ¹H NMR (DMSO, 400 MHz) δ 10.27 (s, 1H), 8.70 (dd, *J* = 6.5, 2.7 Hz, 1H), 8.60 (dd, *J* = 4.8, 1.4 Hz, 1H), 8.43 (dd, *J* = 1.5, 0.8 Hz, 1H), 8.32 (dd,

J = 8.2, 1.4 Hz, 1H), 8.08 (ddd, *J* = 9.0, 4.2, 2.8 Hz, 1H), 7.83 (t, *J* = 1.7 Hz, 1H), 7.59–7.46 (m, 2H), 7.04 (dd, *J* = 1.9, 0.8 Hz, 1H).

5.8.58. *N*-(3-Fluoro-3-(oxazolo[4,5-*b*]pyridin-2-yl)phenyl)thiazole-4-carboxamide (**41**)^b

Title compound was prepared from **66** according to General procedure B1 (W2) as an off-white solid (77%). LRMS [M + H]⁺ 341.1 *m/z*; HRMS [M + H]⁺ 341.0503 *m/z*, found 341.0512 *m/z*; ¹H NMR (DMSO, 400 MHz) δ 10.80 (s, 1H), 9.31 (d, *J* = 2.0 Hz, 1H), 8.96 (dd, *J* = 6.5, 2.7 Hz, 1H), 8.69–8.47 (m, 2H), 8.32 (dd, *J* = 8.2, 1.4 Hz, 1H), 8.13 (ddd, *J* = 9.0, 4.2, 2.9 Hz, 1H), 7.64–7.42 (m, 2H); ¹³C NMR (DMSO, 101 MHz) δ 161.4, 161.4, 159.4, 155.2, 150.3, 146.9, 142.5, 135.6, 126.6, 126.5, 126.1, 121.7, 121.2, 119.3, 117.7, 117.4.

5.8.59. 3-(6-Bromooxazolo[4,5-*b*]pyridin-2-yl)aniline (**67**)^c

Title compound was prepared from 2-amino-5-bromo-3-hydroxypyridine [22] according to General procedure A1 as a grey solid (53%). LRMS [M + H]⁺ 289.0 *m/z*; ¹H NMR (CDCl₃, 300 MHz) δ 8.59 (d, *J* = 2.1 Hz, 1H), 7.98 (d, *J* = 2.1 Hz, 2H), 7.29 (t, 2H), 7.6 (m, 2H), 6.89 (dd, *J* = 8.1, 1.5 Hz, 1H); ¹³C NMR (CDCl₃, 101 MHz) δ 165.6, 154.6, 147.9, 147.6, 143.0, 130.0, 126.6, 121.2, 119.4, 117.6, 115.6, 113.8.

5.8.60. *N*-(3-(6-Bromooxazolo[4,5-*b*]pyridin-2-yl)phenyl)furan-2-carboxamide (**68**)^c

Title compound was prepared from **67** according to General procedure B1 (W1) as a pale-yellow solid (60%). LRMS [M + Na, Br⁷⁹]⁺ 406 *m/z*, [M + Na, Br⁸¹]⁺ 408 *m/z*; HRMS M⁺ 382.99055 *m/z*, found 382.99071 *m/z*; ¹H NMR (CDCl₃, 300 MHz) δ 8.64 (d, *J* = 2.1 Hz, 1H), 8.50 (d, *J* = 1.8 Hz, 1H), 8.30 (s, 1H), 8.03 (m, 3H), 7.55 (t, 2H), 7.3 (d, *J* = 4.2 Hz, 1H), 6.60 (dd, *J* = 3.6, 1.8 Hz, 1H); ¹³C NMR (CDCl₃, 75 MHz) δ 165.9, 156.4, 155.2, 148.2, 147.6, 144.8, 143.5, 138.5, 130.3, 127.0, 124.4, 124.2, 121.4, 119.3, 116.1, 113.0, Note: there is one carbon missing which is assumed to overlap with one of the other signals.

5.8.61. *N*-(3-(6-Phenyloxazolo[4,5-*b*]pyridin-2-yl)phenyl)furan-2-carboxamide (**42**)^c

Title compound was prepared from **68** according to General procedure C1 as a pale-yellow solid (90%). LRMS [M + H]⁺ 382.0 *m/z*; HRMS M⁺ 381.11134 *m/z*, found 381.11234 *m/z*; ¹H NMR (CDCl₃, 300 MHz): 8.56 (s, 1H), 8.54 (s, 1H), 8.31 (s, 1H), 8.10 (d, *J* = 8.1 Hz, 1H), 8.04 (m, 2H), 7.65 (m, 2H), 7.44–7.56 (m, 5H), 7.30 (d, *J* = 7.2 Hz, 1H), 6.6 (dd, *J* = 3.6, 1.8 Hz, 1H); ¹³C NMR (CDCl₃, 75 MHz): 165.7, 156.4, 155.7, 147.6, 146.3, 144.8, 138.4, 137.9, 130.3, 129.9, 129.5, 128.5, 127.8, 127.4, 124.3, 124.0, 119.3, 116.8, 116.1, 115.6, 113.0.

5.8.62. *N*-(3-(6-(4-Methoxyphenyl)oxazolo[4,5-*b*]pyridin-2-yl)phenyl)furan-2-carboxamide (**43**)^c

Title compound was prepared from **68** according to General procedure C1 as a pale-yellow solid (33%). LRMS [M + H]⁺ 412.0 *m/z*; HRMS [M + H]⁺ 412.1292 *m/z*, found 412.1292 *m/z*; ¹H NMR (CDCl₃, 300 MHz) δ 8.78 (d, *J* = 2.0 Hz, 1H), 8.53 (m, 1H), 8.28 (s, 1H), 8.12 (m, 1H), 7.98 (d, *J* = 2.0 Hz, 1H), 7.56 (m, 5H), 7.30 (dd, *J* = 3.6, 0.6 Hz, 1H), 7.05 (d, *J* = 8.7 Hz, 2H), 6.60 (dd, *J* = 3.3, 1.8 Hz, 1H), 3.89 (s, 3H); ¹³C NMR (CDCl₃, 75 MHz) δ 165.4, 160.1, 156.4, 155.2, 147.6, 146.0, 144.7, 143.8, 138.4, 134.5, 130.24, 128.9, 127.6, 124.3, 123.8, 119.1, 116.3, 116.1, 114.9, 113.0, 55.7, Note: there is one carbon missing which is assumed to overlap with another signal.

5.8.63. *N*-(3-(6-(4-Chlorophenyl)oxazolo[4,5-*b*]pyridin-2-yl)phenyl)furan-2-carboxamide (**44**)^c

Title compound was prepared from **68** according to General procedure C1 as a pale-yellow solid (69%). ¹H NMR (CDCl₃, 300 MHz) δ 8.79 (bs, 1H), 8.56 (s, 1H), 8.26 (s, 1H), 8.14 (d, *J* = 7.8 Hz,

1H), 8.01 (m, 2H), 7.60–7.48 (m, 6H), 7.31 (dd, $J = 3.3, 0.6$ Hz, 1H), 6.6 (dd, $J = 5.1, 1.5$ Hz, 1H).

5.8.64. 3-(1H-Imidazo[4,5-b]pyridin-2-yl)aniline (**69**) [23]^c

Title compound was prepared from 2,3-diaminopyridine according to General procedure A2 as a tan solid (80%) and was used without further purification. ¹H NMR (DMSO, 300 MHz) δ 8.29 (bs, 1H), 7.95 (bs, 1H), 7.46 (s, 1H), 7.33 (m, 1H), 7.19 (m, 2H), 6.71 (d, $J = 7.6$ Hz, 1H), 5.05 (bs, 2H). Note: imidazole –NH was not observed and is assumed to be downfield of 12 ppm; ¹³C NMR (DMSO, 75 MHz) δ 154.0, 149.8, 144.2, 136.2, 130.8, 130.1, 126.6, 119.7, 118.6, 116.9, 114.9, 112.7.

5.8.65. N-(3-(1H-Imidazo[4,5-b]pyridin-2-yl)phenyl)furan-2-carboxamide (**45**)^c

Title compound was prepared from **69** according to General procedure B1(W1) as a tan solid (48%). LRMS M^+ 305.0 m/z ; HRMS M^+ 304.09603 m/z , found 304.09490 m/z ; ¹H NMR (CDCl₃/DMSO, 300 MHz) δ 9.33 (s, 1H), 8.18 (s, 1H), 8.10 (bs, 1H) 7.77 (m, 3H), 7.37 (m, 1H), 7.25 (m, 1H), 7.07 (d, $J = 3.5$ Hz, 1H), 6.95 (dd, $J = 7.8, 4.8$ Hz, 1H), 6.34 (m, 1H); ¹³C NMR (CDCl₃/DMSO, 75 MHz) δ 156.8, 153.1, 147.8, 144.8, 144.1, 138.7, 130.5, 129.6, 122.9, 122.6, 118.9, 118.2, 115.2, 112.3. Note: there are three carbons missing which are assumed to overlap with the other signals.

5.8.66. N-(3-(1H-Imidazo[4,5-b]pyridin-2-yl)phenyl)furan-3-carboxamide (**46**)^c

Title compound was prepared from **69** according to General procedure B1 (W1) (44%). LRMS $[M + H]^+$ 305 m/z ; HRMS $[M + H]^+$ 305.1033 m/z , found 305.1031 m/z ; ¹H NMR (CDCl₃, 300 MHz) δ 10.15 (s, 1H), 8.63 (s, 1H), 8.36 (m, 2H), 8.05 (dd, $J = 8.1, 1.2$ Hz, 1H), 7.9 (dd, $J = 8.1, 1.8$ Hz, 1H), 7.80 (d, $J = 1.5$ Hz, 1H), 7.54 (t, $J = 7.8$ Hz, 1H), 7.27 (dd, $J = 8.1, 5.1$ Hz, 2H), 7.04 (dd, $J = 1.8, 0.9$ Hz, 1H); ¹³C NMR (DMSO, 75 MHz) δ 161.3, 146.8, 145.0, 144.4, 140.2, 130.7, 130.1, 123.5, 123.0, 122.4, 119.5, 118.9, 109.9. Note: there are four carbons missing which are assumed to overlap with other signals.

5.8.67. 3-(Benzo[d]oxazol-2-yl)-4-chloroaniline (**70**)^b

Title compound was prepared according to General procedure A2 as a pale-pink solid (74%). LRMS $[M + H]^+$ 245.1 m/z ; HRMS $[M + H]^+$ 245.0476 m/z , found 245.0474 m/z ; ¹H NMR (DMSO, 400 MHz) δ 7.93–7.71 (m, 2H), 7.55–7.38 (m, 2H), 7.35 (d, $J = 2.8$ Hz, 1H), 7.29 (d, $J = 8.7$ Hz, 1H), 6.79 (dd, $J = 8.7, 2.8$ Hz, 1H), 5.63 (s, 2H); ¹³C NMR (DMSO, 101 MHz) δ 160.9, 149.9, 148.1, 141.1, 131.5, 125.8, 125.3, 124.9, 120.0, 118.0, 117.5, 115.9, 110.9.

5.8.68. N-(3-(Benzo[d]oxazol-2-yl)-4-chlorophenyl)furan-2-carboxamide (**47**)^b

Title compound was prepared according to General procedure B1 (W1) except purification was performed on a silica coated glass plate, eluting with 5% methanol in DCM to give the title compound as a white solid (10%). LRMS $[M + H]^+$ 339.1 m/z ; ¹H NMR (DMSO, 400 MHz) δ 10.58 (s, 1H), 8.69 (d, $J = 2.6$ Hz, 1H), 8.04 (dd, $J = 8.8, 2.7$ Hz, 1H), 7.98 (dd, $J = 1.7, 0.8$ Hz, 1H), 7.92–7.87 (m, 1H), 7.87–7.81 (m, 1H), 7.69 (d, $J = 8.8$ Hz, 1H), 7.48 (dq, $J = 14.7, 7.4, 1.4$ Hz, 2H), 7.41 (dd, $J = 3.5, 0.8$ Hz, 1H), 6.73 (dd, $J = 3.5, 1.7$ Hz, 1H); ¹³C NMR (DMSO, 101 MHz) δ 160.0, 156.4, 150.0, 147.0, 146.2, 141.1, 138.1, 131.7, 126.2, 126.1, 125.3, 125.1, 124.1, 122.7, 120.3, 115.4, 112.3, 111.1.

5.8.69. N-(4-Chloro-3-(oxazolo[4,5-b]pyridin-2-yl)phenyl)-N-methylfuran-3-carboxamide (**48**)^a

Title compound was prepared from **5** according to General procedure D1 except purification was performed by column

chromatography, eluting cyclohexane/ethyl acetate 50:50. The fraction containing the compound was further purified using a silica coated glass plate eluting with cyclohexane/ethyl acetate 50:50 leading to the title compound as a white solid (64%). LRMS $[M + H]^+$ 354.2 m/z ; ¹H NMR (DMSO, 300 MHz) δ 8.61 (dd, $J = 4.7, 1.4$ Hz, 1H), 8.29 (d, $J = 8.2$ Hz, 1H), 8.15 (d, $J = 2.5$ Hz, 1H), 7.76 (d, $J = 8.6$ Hz, 1H), 7.6 (m, 3H), 6.20 (s, 1H), 5.33 (m, 1H), 3.37 (s, 3H).

5.8.70. N-(4-Chloro-3-(oxazolo[4,5-b]pyridin-2-yl)phenyl)-N-methylbenzamide (**49**)^a

Title compound was prepared from **10** according to General procedure D1 as a brown solid (46%). LRMS $[M + H]^+$ 364.2 m/z ; ¹H NMR (DMSO, 300 MHz) δ 8.61 (d, $J = 4.9$ Hz, 1H), 8.27 (d, $J = 8.3$ Hz, 1H), 8.08 (d, $J = 2.6$ Hz, 1H), 7.67 (m, 2H), 7.60 (d, $J = 8.6$ Hz, 1H), 7.51 (m, 1H), 7.42 (dd, $J = 8.7, 2.1$ Hz, 1H), 7.31 (m, 3H), 3.42 (s, 3H).

5.9. Physicochemistry

5.9.1. Solubility Estimates using Nephelometry

Stock solutions of compound prepared in DMSO were spiked into either pH 6.5 phosphate buffer or 0.01 M HCl (approximately pH 2.0) with the final DMSO concentration being 1% (v/v). Samples were then analysed by nephelometry to determine the solubility range as described previously [24].

5.9.2. Chromatographic logD measurement

Partition coefficients (logD) were estimated by comparing the chromatographic retention properties of each compound at pH 3 and pH 7.4 to the retention characteristics of a series of standard compounds with known partition coefficients. Data were collected using a Waters 2795 HPLC instrument with a Waters 2487 dual channel UV detector with a Synergy Hydro-RP 4 μ m (30 mm \times 2 mm) column. The mobile phase consisted of aqueous buffer (50 mM ammonium acetate, pH 7.4 or 50 mM ammonium formate, pH 3.0) and acetonitrile, with an acetonitrile gradient of 0–100% over 10 min. Compound elution was monitored at 220 and 254 nm. This method is a gradient HPLC based derivation of the method developed by Lombardo [25].

5.9.3. Chromatographic protein binding estimation

Plasma protein binding values were estimated using a chromatographic method whereby the retention characteristics on a human albumin column (Chromtech Chiral-HSA 50 mm \times 3.0 mm, 5 μ m, Sigma–Aldrich) were compared to the retention characteristics of a series of compounds with known human protein binding values. The method is a modification of a method published previously [26]. A Waters 2795 HPLC system equipped with a Waters 2487 dual channel UV detector (monitored at 220 and 254 nm) was used with a mobile phase comprised of aqueous buffer (25 mM ammonium acetate buffer, pH 7.4) and 30% isopropyl alcohol in the same buffer. The isopropanol concentration gradient varied over 10 min and the column was reconditioned prior to the next injection.

5.9.4. In vitro metabolism in human liver microsomes

A 10 mg/mL stock solution was prepared in DMSO which was diluted in 50% acetonitrile/water to a spiking concentration of 500 μ M. This was diluted 1 in 500 to give a final concentration of 1 μ M of compound which was incubated at 37 °C in human liver microsomes (XenoTech LLC, Lenexa, Kansas City) suspended in 0.1 M phosphate buffer (pH 7.4) at a final protein concentration of 0.4 mg/mL. An NADPH-regenerating system (1 mg/mL NADP, 1 mg/mL glucose-6-phosphate, 1 U/mL glucose-6-phosphate dehydrogenase) and MgCl₂ (0.67 mg/mL) was added to initiate the metabolic reactions, which were subsequently quenched with ice-cold

acetonitrile at various time points over 60 min. Samples were subjected to centrifugation and the amount of parent compound remaining in the supernatant was quantified by LC-MS using a Waters Micromass ZQ coupled to a Waters Alliance 2975 HPLC. The first order rate constant for substrate depletion was determined by fitting the data to an exponential decay function and these values were used to calculate the *in vitro* intrinsic clearance value (CL_{int}) and the predicted *in vivo* intrinsic clearance value ($CL_{int\ vivo}$) as described previously [27]. The predicted *in vivo* hepatic extraction ratio (E_H) was calculated using the following relationship: $E_H = CL_{int\ vivo} / (Q + CL_{int\ vivo})$ where Q is human liver blood flow (20.7 mL/min/kg) [28].

5.10. Biological assays

All *in vitro* assays were carried out at least twice independently in singleton. The IC_{50} values are the means of two independent assays and vary less than $\pm 50\%$.

5.10.1. *P. falciparum* assay

In vitro activity against erythrocytic stages of *P. falciparum* was determined using a 3H -hypoxanthine incorporation assay [29,30], using the drug sensitive NF54 strain [31] and the standard drug chloroquine (Sigma C6628). Compounds were dissolved in DMSO at 10 mg/mL and added to parasite cultures incubated in RPMI 1640 medium without hypoxanthine, supplemented with HEPES (5.94 g/L), $NaHCO_3$ (2.1 g/L), neomycin (100 U/mL), Albumax^R (5 g/L) and washed human red cells A^+ at 2.5% haematocrit (0.3% parasitaemia). Serial drug dilutions of eleven 3-fold dilution steps covering a range from 100 to 0.002 $\mu g/mL$ were prepared. The 96-well plates were incubated in a humidified atmosphere at 37 °C; 4% CO_2 , 3% O_2 , 93% N_2 . After 48 h 50 μL of 3H -hypoxanthine (=0.5 μCi) was added to each well of the plate. The plates were incubated for a further 24 h under the same conditions. The plates were then harvested with a BetaplateTM cell harvester (Wallac, Zurich, Switzerland), and the red blood cells transferred onto a glass fibre filter then washed with distilled water. The dried filters were inserted into a plastic foil with 10 mL of scintillation fluid, and counted in a BetaplateTM liquid scintillation counter (Wallac, Zurich, Switzerland). IC_{50} values were calculated from sigmoidal inhibition curves by linear regression [32] using Microsoft Excel. Chloroquine and artemisinin are used as control.

5.10.2. *L. donovani* axenic amastigotes assay

Amastigotes of *L. donovani* strain MHOM/ET/67/L82 were grown in axenic culture at 37 °C in SM medium [33] at pH 5.4 supplemented with 10% heat-inactivated foetal bovine serum under an atmosphere of 5% CO_2 in air. 100 μL of culture medium with 10^5 amastigotes from axenic culture with or without a serial drug dilution were seeded in 96-well microtitre plates. Serial drug dilutions of eleven 3-fold dilution steps covering a range from 100 to 0.002 $\mu g/mL$ were prepared. After 70 h of incubation the plates were inspected under an inverted microscope to assure growth of the controls and sterile conditions. 10 μL of Alamar Blue (12.5 mg resazurin dissolved in 100 mL distilled water) [34] were then added to each well and the plates incubated for another 2 h. Then the plates were read with a Spectramax Gemini XS microplate fluorometer (Molecular Devices Cooperation, Sunnyvale, CA, USA) using an excitation wave length of 536 nm and an emission wave length of 588 nm. Data were analysed using the software Softmax Pro (Molecular Devices Cooperation, Sunnyvale, CA, USA). Decrease of fluorescence (=inhibition) was expressed as percentage of the fluorescence of control cultures and plotted against the drug concentrations. From the sigmoidal inhibition curves the IC_{50} values were calculated by linear regression [32]. Miltefosine is used as control.

5.10.3. *L. donovani* intracellular amastigotes assay (infected macrophages)

Mouse peritoneal macrophages (4×10^4 in 100 μL RPMI 1640 medium with 10% heat-inactivated FBS) were seeded into wells of Lab-tek 16-chamber slides. After 24 h 1.2×10^5 amastigote *L. donovani* in 100 μL were added. The amastigotes were taken from an axenic amastigote culture grown at pH 5.4. 4 h later the medium containing free amastigote forms was removed and replaced by fresh medium. Next day the medium was replaced by medium containing different compound dilutions. Parasite growth in the presence of the drug was compared to control wells. After 96 h of incubation the medium was removed and the slides fixed with methanol for 10 min followed by a staining with a 10% Giemsa solution. Infected and non-infected macrophages were counted for the control cultures and the ones exposed to the serial drug dilutions. The infection rates were determined. The results were expressed as % reduction in parasite burden compared to control wells, and the IC_{50} calculated by linear regression analysis [32].

5.10.4. *T. cruzi* assay

Rat skeletal myoblasts (L-6 cells) were seeded in 96-well microtitre plates at 2000 cells/well in 100 μL RPMI 1640 medium with 10% FBS and 2 mM L-glutamine. After 24 h the medium was removed and replaced by 100 μL per well containing 5000 trypomastigote forms of *T. cruzi* Tulahuen strain C2C4 containing the β -galactosidase (Lac Z) gene [35]. After 48 h the medium was removed from the wells and replaced by 100 μL fresh medium with or without a serial drug dilution of eleven 3-fold dilution steps covering a range from 100 to 0.002 $\mu g/mL$. After 96 h of incubation the plates were inspected under an inverted microscope to assure growth of the controls and sterility. Then the substrate CPRG/Nonidet (50 μL) was added to all wells. A colour reaction developed within 2–6 h and could be read photometrically at 540 nm. Data were analysed with the graphic program Softmax Pro (Molecular Devices), which calculated IC_{50} values by linear regression [32] from the sigmoidal dose inhibition curves. Benznidazole is used as control.

5.10.5. *T. brucei rhodesiense* assay

This stock was isolated in 1982 from a human patient in Tanzania and after several mouse passages cloned and adapted to axenic culture conditions [36]. Minimum Essential Medium (50 μL) supplemented with 25 mM HEPES, 1 g/L additional glucose, 1% MEM non-essential amino acids (100 \times), 0.2 mM 2-mercaptoethanol, 1 mM Na-pyruvate and 15% heat inactivated horse serum was added to each well of a 96-well microtitre plate. Serial drug dilutions of eleven 3-fold dilution steps covering a range from 100 to 0.002 $\mu g/mL$ were prepared. Then 4×10^3 bloodstream forms of *T. b. rhodesiense* STIB 900 in 50 μL was added to each well and the plate incubated at 37 °C under a 5% CO_2 atmosphere for 70 h. 10 μL Alamar Blue (resazurin, 12.5 mg in 100 mL double-distilled water) was then added to each well and incubation continued for a further 2–4 h [37]. Then the plates were read with a Spectramax Gemini XS microplate fluorometer (Molecular Devices Cooperation, Sunnyvale, CA, USA) using an excitation wave length of 536 nm and an emission wave length of 588 nm. The IC_{50} values were calculated by linear regression [32] from the sigmoidal dose inhibition curves using Softmax Pro software (Molecular Devices Cooperation, Sunnyvale, CA, USA). Melarsoprol is used as control.

5.10.6. Rat skeletal myoblast cytotoxicity assay

Assays were performed in 96-well microtitre plates, each well containing 100 μL of RPMI 1640 medium supplemented with 1% L-glutamine (200 mM) and 10% foetal bovine serum, and 4000 L-6 cells (a primary cell line derived from rat skeletal myoblasts)

[38,39]. Serial drug dilutions of eleven 3-fold dilution steps covering a range from 100 to 0.002 $\mu\text{g}/\text{mL}$ were prepared. After 70 h of incubation the plates were inspected under an inverted microscope to assure growth of the controls and sterile conditions. 10 μL of Alamar Blue was then added to each well and the plates incubated for another 2 h. Then the plates were read with a Spectramax Gemini XS microplate fluorometer (Molecular Devices Cooperation, Sunnyvale, CA, USA) using an excitation wave length of 536 nm and an emission wave length of 588 nm. The IC_{50} values were calculated by linear regression [32] from the sigmoidal dose inhibition curves using Softmax Pro software (Molecular Devices Cooperation, Sunnyvale, CA, USA). Podophyllotoxine is used as control.

5.10.7. *T.b. brucei* assay

Compound activity against *T.b. brucei* was assessed in an Alamar blue[®] viability assay as previously described by Sykes and Avery [40]. Briefly, 55 μL of HMI-9 media +10% FCS [41] containing 1200 cells/mL of logarithmic phase *T.b. brucei* 427 bloodstream parasites were added to a 384-well microtiter plate (BD biosciences) and incubated for 24 h at 37 °C/5% CO_2 . Serial drug concentrations were prepared in 100% DMSO and diluted 1:21 in DMEM media. 5 μL of this dilution was subsequently added to assay plates to give final drug concentrations ranging from 41.67 to 0.0004 μM . Plates were incubated for 48 h at 37 °C/5% CO_2 . 10 μL of 70% Alamar Blue[®] (Invitrogen) prepared in HMI-9 media +10% FCS was added to assay plates and plates incubated for a further 2 h at 37 °C/5% CO_2 followed by 22 h at room temperature. Assay plates were read at 535 nm excitation/590 nm emission on an Envision[®] multiplate reader (PerkinElmer, Massachusetts, USA). Data was analysed and IC_{50} values calculated using the software GraphPad Prism 5.

5.10.8. HEK293 cytotoxicity assay

55 μL of DMEM +10% FCS media (Gibco) containing 72,727 cells/mL of confluent HEK293 cells was added to a 384-well microtiter plate (BD biosciences) and incubated for 24 h at 37 °C/5% CO_2 . Serial drug concentrations were prepared in 100% DMSO and diluted 1:21 in DMEM media. 5 μL of this dilution was subsequently added to assay plates to give final drug concentrations ranging from 83.34 to 0.0004 μM . Plates were incubated for 48 h at 37 °C/5% CO_2 . 10 μL of 70% Alamar Blue[®] (Invitrogen) prepared in DMEM media +10% FCS was added to assay plates and plates incubated for a further 5 h at 37 °C/5% CO_2 followed by 19 h at room temperature. Assay plates were read at 535 nm excitation/590 nm emission on an En vision[®] multiplate reader (PerkinElmer, Massachusetts, USA). Data was analysed and IC_{50} values calculated using the software GraphPad Prism 5.

Acknowledgements

This research was supported by the NHMRC (IRISS grant number 361646; NHMRC Senior Research Fellowship 1020411 (J.B.B.), NHMRC Project Grant 1025581); Victorian Stage Government OIS grant; Dr. Jason Dang for his assistance in obtaining some of our analytical data; Dr. Sebastian Marcuccio (Advanced Molecular Technologies Pty Ltd) for providing some of the chemicals used during the synthesis; the Australian Government for the Australian Postgraduate Award (L.F.) and DNDi for allowing access to their parasite screening platform at STPHI.

References

- [1] R. Brun, J. Blum, F. Chappuis, C. Burri, Human African trypanosomiasis, *Lancet* 375 (2010) 148–159.
- [2] WHO, Human African trypanosomiasis, http://www.who.int/trypanosomiasis_african/en/ (accessed 30.07.12).
- [3] WHO, Drugs, http://www.who.int/trypanosomiasis_african/drugs/en/index.html (accessed 27.07.12).
- [4] T.E. Voogd, E.L. Vansterkenburg, J. Wilting, L.H. Janssen, Recent research on the biological activity of suramin, *Pharmacol. Rev.* 45 (1993) 177–203.
- [5] H.P. de Koning, Transporters in African trypanosomiasis: role in drug action and resistance, *Int. J. Parasitol.* 31 (2001) 512–522.
- [6] A.J. Nok, Arsenicals (melarsoprol), pentamidine and suramin in the treatment of human African trypanosomiasis, *Parasitol. Res.* 90 (2003) 71–79.
- [7] T. Seebeck, P. Maser, Drug resistance in African trypanosomiasis, in: D.L. Mayers (Ed.), *Antimicrobial Drug Resistance*, Humana Press, 2009, pp. 589–604.
- [8] G. Priotto, S. Kasparian, W. Mutombo, D. Ngouama, S. Ghorashian, U. Arnold, S. Ghabri, E. Baudin, V. Buard, S. Kazadi-Kyanza, M. Ilunga, W. Mutangala, G. Pohl, C. Schmid, U. Karunakara, E. Torrelee, V. Kande, Nifurtimox-eflornithine combination therapy for second-stage African *Trypanosoma brucei gambiense* trypanosomiasis: a multicentre, randomised, phase III, non-inferiority trial, *Lancet* 374 (2009) 56–64.
- [9] DNDi, Oxaborole SCYX-7158 (HAT), <http://www.dndi.org/portfolio/oxaborole-scyx-7158.html> (accessed 27.07.12).
- [10] DNDi, Pivotal study of fexinidazole for human African trypanosomiasis in stage 2, <http://www.clinicaltrials.gov/ct2/show/NCT01685827?term=fexinidazole&rank=3#wrapper> (accessed 23.11.12).
- [11] M.L. Sykes, J.B. Baell, M. Kaiser, E. Chatelain, S.R. Moawad, D. Ganame, J.-R. Ioset, V.M. Avery, Identification of compounds with anti-proliferative activity against *Trypanosoma brucei brucei* strain 427 by a whole cell viability based HTS Campaign, *PLoS Negl. Trop. Dis.* 6 (2012) e1896.
- [12] L. Sanderson, M. Dogruel, J. Rodgers, B. Bradley, S.A. Thomas, The blood–brain barrier significantly limits eflornithine entry into *Trypanosoma brucei* infected mouse brain, *J. Neurochem.* 107 (2008) 1136–1146.
- [13] O. Balmer, J.S. Beadell, W. Gibson, A. Caccione, Phylogeography and taxonomy of *Trypanosoma brucei*, *PLoS Negl. Trop. Dis.* 5 (2011).
- [14] H. Pajouhesh, G.R. Lenz, Medicinal chemical properties of successful central nervous system drugs, *NeuroRx* 2 (2005) 541–553.
- [15] J.-R. Ioset, Natural products for neglected diseases: a review, *Curr. Org. Chem.* 12, 643–666.
- [16] E. Torrelee, B. Bourdin Trunz, D. Tweats, M. Kaiser, R. Brun, G. Mazué, M.A. Bray, B. Pécoul, Fexinidazole – a new oral nitroimidazole drug candidate entering clinical development for the treatment of sleeping sickness, *PLoS Negl. Trop. Dis.* 4 (2010) e923.
- [17] A.S. Kalgutar, I. Gardner, R.S. Obach, C.L. Shaffer, E. Callegari, K.R. Henne, A.E. Mutlib, D.K. Dalvie, J.S. Lee, Y. Nakai, J.P. O'Donnell, J. Boer, S.P. Harriman, A comprehensive listing of bioactivation pathways of organic functional groups, *Curr. Drug Metab.* 6 (2005) 161–225.
- [18] E. Handman, L. Kedzierski, A.D. Uboldi, J.W. Goding, Fishing for anti-leishmania drugs: principles and problems, *Adv. Exp. Med. Biol.* 625 (2008) 48–60.
- [19] J.E. Bemis, C.B. Vu, R. Xie, J.J. Nunes, P.Y. Ng, J.S. Disch, J.C. Milne, D.P. Carney, A.V. Lynch, L. Jin, J.J. Smith, S. Lavu, A. Iffland, M.R. Jirousek, R.B. Perni, Discovery of oxazol[4,5-*b*]pyridines and related heterocyclic analogs as novel SIRT1 activators, *Bioorg. Med. Chem. Lett.* 19 (2009) 2350–2353.
- [20] T.M. Kowieski, S. Lee, J.M. Denu, Acetylation-dependent ADP-ribosylation by *Trypanosoma brucei* Sir2, *J. Biol. Chem.* 283 (2008) 5317–5326.
- [21] S. Alsford, T. Kawahara, C. Isamah, D. Horn, A siruirtin in the African trypanosome is involved in both DNA repair and telomeric gene silencing but is not required for antigenic variation, *Mol. Microbiol.* 63 (2007) 724–736.
- [22] M.-C. Viaud, P. Jamoneau, L. Savelon, G. Guillaumet, Synthesis of 6-Substituted 2-phenyloxazol[4,5-*b*]pyridines, *Heterocycles* 41 (1995) 2799–2809.
- [23] P. Savarino, G. Viscardi, R. Carpignano, A. Borda, E. Barni, Aminophenyl-X-azolopyridines as precursors of heterocyclic azo dyes, *J. Heterocycl. Chem.* 26 (1989) 289–292.
- [24] C.D. Bevan, R.S. Lloyd, A high-throughput screening method for the determination of aqueous drug solubility using laser nephelometry in microtiter plates, *Anal. Chem.* 72 (2000) 1781–1787.
- [25] F. Lombardo, M.Y. Shalaeva, K.A. Tupper, F. Gao, ElogDoct: a tool for lipophilicity determination in drug discovery. 2. Basic and neutral compounds, *J. Med. Chem.* 44 (2001) 2490–2497.
- [26] K. Valko, S. Nunhuck, C. Bevan, M.H. Abraham, D.P. Reynolds, Fast gradient HPLC method to determine compounds binding to human serum albumin. Relationships with octanol/water and immobilized artificial membrane lipophilicity, *J. Pharm. Sci.* 92 (2003) 2236–2248.
- [27] R.S. Obach, Prediction of human clearance of twenty-nine drugs from hepatic microsomal intrinsic clearance data: an examination of *in vitro* half-life approach and nonspecific binding to microsomes, *Drug Metab. Dispos.* 27 (1999) 1350–1359.
- [28] B. Davies, T. Morris, Physiological parameters in laboratory animals and humans, *Pharm. Res.* 10 (1993) 1093–1095.
- [29] R.E. Desjardins, C.J. Canfield, J.D. Haynes, J.D. Chulay, Quantitative assessment of antimalarial activity *in vitro* by a semiautomated microdilution technique, *Antimicrob. Agents Chemother.* 16 (1979) 710–718.
- [30] H. Matile, J.R.L. Pink, *Plasmodium falciparum* malaria parasite cultures and their use in immunology, in: I. Lefkowitz, B. Pernis (Eds.), *Immunological Methods*, Academic Press, San Diego, 1990.
- [31] T. Ponnudurai, A.D. Leeuwenberg, J.H. Meuwissen, Chloroquine sensitivity of isolates of *Plasmodium falciparum* adapted to *in vitro* culture, *Trop. Geogr. Med.* 33 (1981) 50–54.

- [32] W. Huber, J.C. Koella, A comparison of three methods of estimating EC_{50} in studies of drug resistance of malaria parasites, *Acta Trop.* 55 (1993) 257–261.
- [33] M.L. Cunningham, A.H. Fairlamb, Trypanothione reductase from *Leishmania donovani*. Purification, characterisation and inhibition by trivalent antimonials, *Eur. J. Biochem.* 230 (1995) 460–468.
- [34] J. Mikus, D. Steverding, A simple colorimetric method to screen drug cytotoxicity against *Leishmania* using the dye Alamar Blue[®], *Parasitol. Int.* 48 (2000) 265–269.
- [35] F.S. Buckner, C.L. Verlinde, A.C. La Famme, W.C. Van Voorhis, Efficient technique for screening drugs for activity against *Trypanosoma cruzi* using parasites expressing beta-galactosidase, *Antimicrob. Agents Chemother.* 40 (1996) 2592–2597.
- [36] T. Baltz, D. Baltz, C. Giroud, J. Crockett, Cultivation in a semi-defined medium of animal infective forms of *Trypanosoma brucei*, *T. equiperdum*, *T. evansi*, *T. rhodesiense* and *T. gambiense*, *EMBO J.* 4 (1985) 1273–1277.
- [37] B. Ráz, M. Iten, Y. Grether-Bühler, R. Kaminsky, R. Brun, The Alamar Blue[®] assay to determine drug sensitivity of African trypanosomes (*T.b. rhodesiense* and *T.b. gambiense*) *in vitro*, *Acta Trop.* 68 (1997) 139–147.
- [38] B. Page, M. Page, C. Noel, A new fluorometric assay for cytotoxicity measurements *in vitro*, *Int. J. Oncol.* 3 (1993) 473–476.
- [39] S.A. Ahmed, R.M. Gogal, J.E. Walsh, A new rapid and simple non-radioactive assay to monitor and determine the proliferation of lymphocytes: an alternative to [³H]thymidine incorporation assay, *J. Immunol. Methods* 170 (1994) 211–224.
- [40] M.L. Sykes, V.M. Avery, Development of an Alamar Blue[™] viability assay in 384-well format for high throughput whole cell screening of *Trypanosoma brucei* bloodstream form strain 427, *Am. J. Trop. Med. Hyg.* 81 (2009) 665–674.
- [41] H. Hirumi, K. Hirumi, Continuous cultivation of *Trypanosoma brucei* bloodstream forms in a medium containing a low concentration of serum protein without feeder cell layers, *J. Parasitol.* 75 (1989) 985–989.

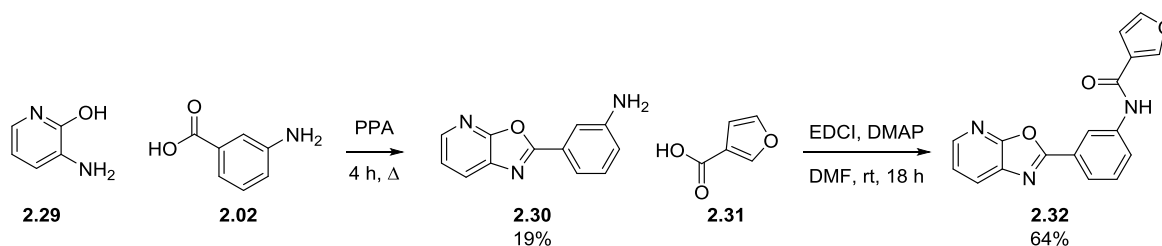
2.7. Post-script: further development of SAR

Since the publication of the preliminary SAR data a number of compounds have been synthesised with variations to the core oxazole and the northern heterocycle. These compounds were identified as targets of interest in order to overcome the issues with the series highlighted in the publication, namely the metabolic stability and the solubility.

2.7.1. Core changes

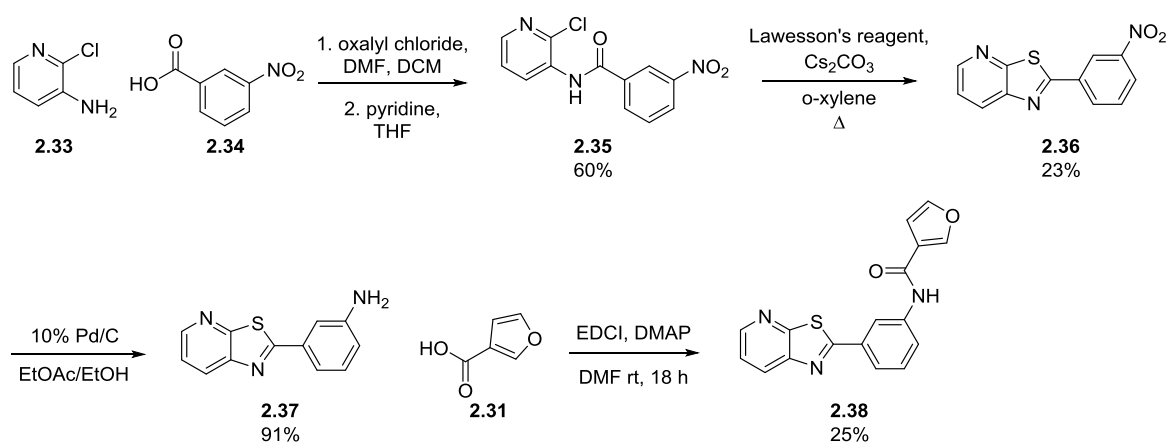
A number of analogues with changes to the oxazole core were identified and involved replacement by an inverted oxazole, the corresponding thiazole and both regioisomers of the methylated imidazole. The 3-furoic acid heterocycle was utilised moving forward as it was shown to convey greater activity against *T.b. rhodesiense* in previous studies whilst also having some improved pharmacokinetic properties, such as solubility. A discussion on the synthesis of these derivatives and their biological activity follows.

Synthesis of the inverted oxazole was performed following the same procedures previously described but instead of starting with 2-amino-3-hydroxypyridine, 3-amino-2-hydroxypyridine (**2.29**) was substituted (Scheme 2.5). The cyclocondensation was successfully achieved though there was a significant decrease in the yield. The subsequent amide formation with 3-furoic acid (**2.31**) was also performed as previously described and led to the desired product (**2.32**) in reasonable yield.



Scheme 2.5 Synthesis of the inverted oxazole core.

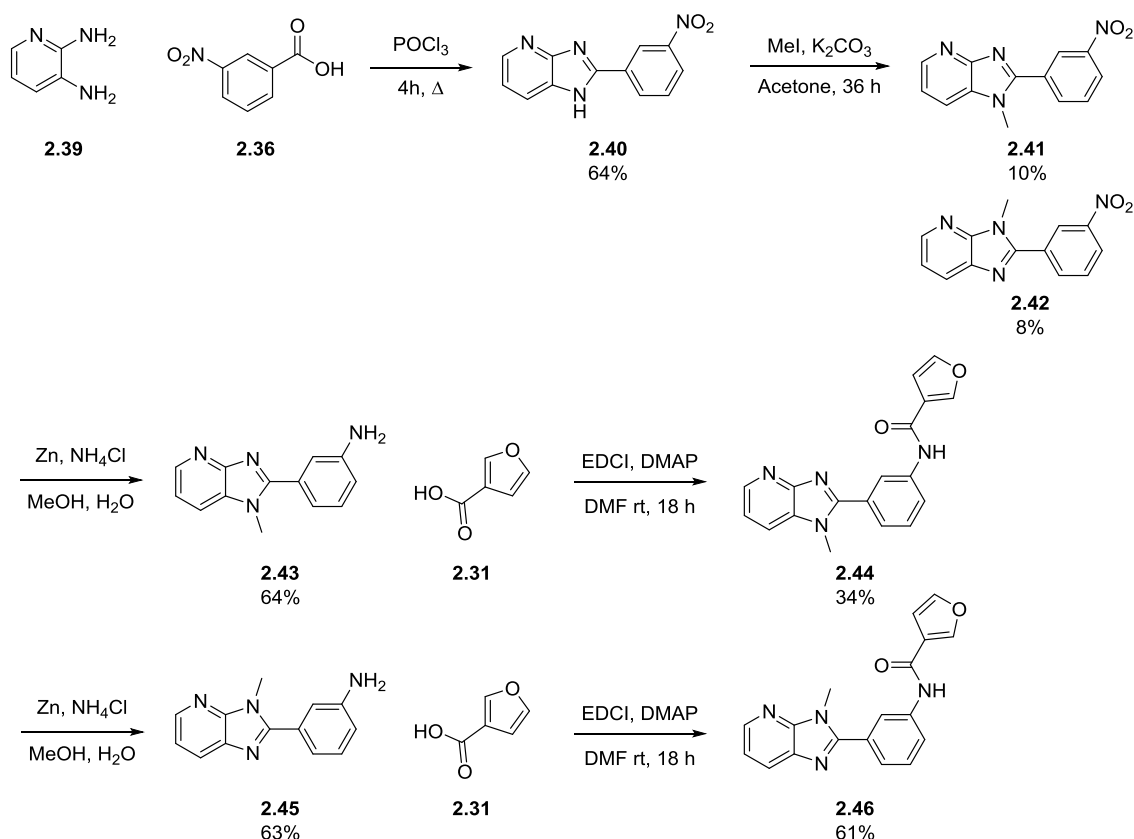
Synthesis of the thiazole analogue required the implementation of a different synthetic pathway. The amide was formed between 3-amino-2-chloropyridine (**2.33**) and 3-nitrobenzoic acid (**2.34**) via an acid chloride intermediate (Scheme 2.6). Treatment of **2.35** with Lawesson's reagent led to the desired thiazole core (**2.36**) being formed in low yields though sufficient material was obtained in order to proceed with the synthesis. Reduction of the nitro to the amine was performed on the H-cube[®] in excellent yields to give **2.37**. Finally, the installation of the 3-furan was achieved using EDCI, DMAP in DMF overnight to obtain the desired product (**2.38**).



Scheme 2.6 Synthesis of the thiazole core from 3-amino-2-chloropyridine and 3-nitrobenzoic acid.

Synthesis of the imidazole core was initially trialled using the previously established conditions for the cyclocondensation mediated by PPA between 2,3-diaminopyridine (**2.39**) and 3-aminobenzoic acid (**2.02**). However, multiple products were obtained and it was difficult to purify the desired product. As a result, an alternative route was identified which involved reaction between 2,3-diaminopyridine (**2.39**) and 3-nitrobenzoic acid (**2.34**) at reflux in phosphorous oxychloride led to the successful isolation of the desired product (**2.40**) in good yield. A methylation of the imidazole was then performed using methyl iodide and potassium carbonate in acetone. This led to both of the desired regioisomers being obtained, **2.41** and **2.42**, though in poor yields. It is possible that under these conditions the pyridyl nitrogen could have also been methylated and this material would have been lost in the aqueous work up. Sufficient material was obtained in order to progress the synthesis though further optimisation of these conditions is required. Reduction of the nitro to the amine was unsuccessful when using hydrogen gas and 5% Pd/C. However, reduction with

zinc powder, and ammonium chloride in methanol and water⁸⁸ was effective and the reaction completed in under 10 mins to give both of the desired products, **2.43** and **2.45**. The subsequent amide coupling was performed with 3-furoic acid (**2.31**) in order to obtain the desired products, **2.44** and **2.46**. This is summarised in Scheme 2.7.



Scheme 2.7 Synthesis of both regioisomers of the methylated imidazole core.

It was possible to differentiate **2.41** and **2.42** from one another through extensive 1D and 2D NMR studies. From the analyses of 2D heteronuclear NMR techniques (HMBC and HSQC), complete shift assignments were achieved for all protons and carbons. The HSQC NMR spectra revealed direct cross coupling peaks between numerous protons and carbons. The long-range correlations from the HMBC spectra identified the quaternary carbons (1', 2 and 4) as identified in Figure 2.4a between H_A, H_D, H_E and, H_G. The long-range correlations between the *N*-methyl and the quaternary carbons designated as 1' and 2 has confirmed the regioisomer shown in **2.42**.

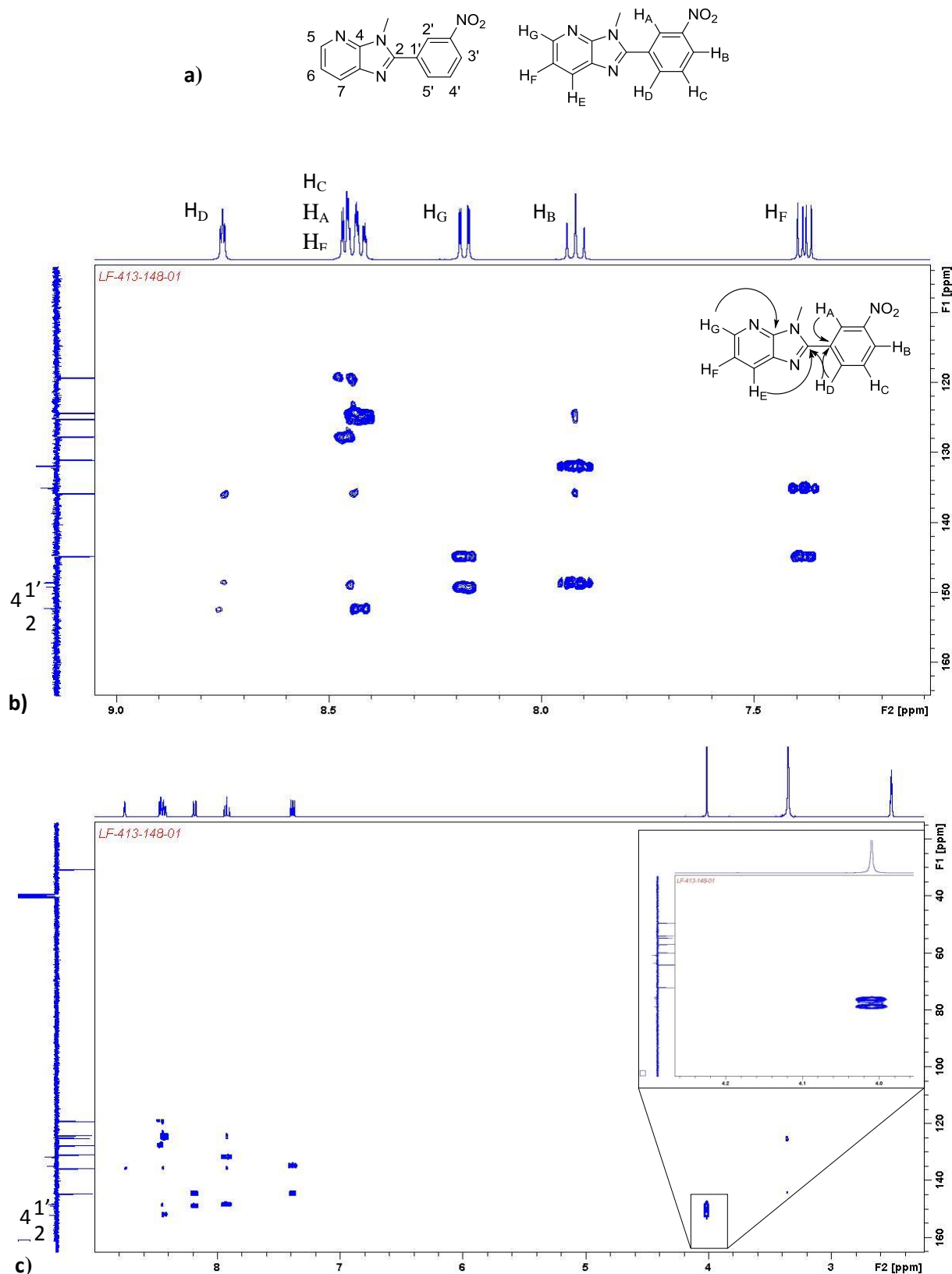
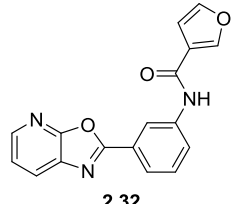
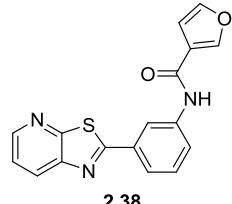
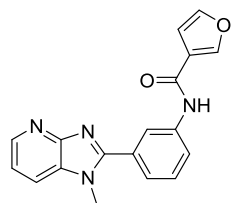
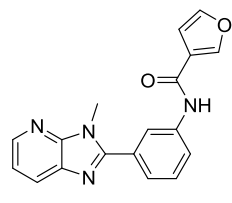


Figure 2.4a) Proton and carbon numbering of **2.42**; **b)** HSQC NMR confirmation of the quaternary carbons in the methylated imidazole regioisomer, **2.42**; **c)** HMBC NMR spectra which shows cross coupling peaks present between the methyl and the quaternary carbons **1'** and **2**, confirming the assigned regioisomer.

Table 2.4 summarises the results of the biological assays against *T.b. brucei* for these core changes. The inverted oxazole (**2.32**) maintained activity when compared with the initial hit (**126**, 0.22 μM) though the substitution of the oxygen atom for the more hydrophobic sulfur atom to give the corresponding thiazole (**2.38**) led to a complete loss of activity in this assay. This could be the result of the relative increase in size of the sulfur atom when compared with the oxygen atom, its longer bond lengths which would likely result in a conformational change affecting the interaction with the target, or the inability of the sulfur to accept a hydrogen bond. Whilst the unmethylated imidazole core (*Eur. J. Med. Chem.* manuscript, compound **46**) had an EC_{50} of 1.0 μM against *T.b. brucei*, the subsequent methylation led to a complete loss of activity in this assay suggesting that the hydrogen bond donor is a key feature in this core.

Table 2.4 *T.b. brucei* inhibitory activity of targets with varying core groups.

		ID	EC_{50} (μM)
	2.32	2.32	0.30 ± 0.08
	2.38	2.38	$> 10^a$
	2.44	2.44	$> 10^a$
	2.46	2.46	$> 10^a$

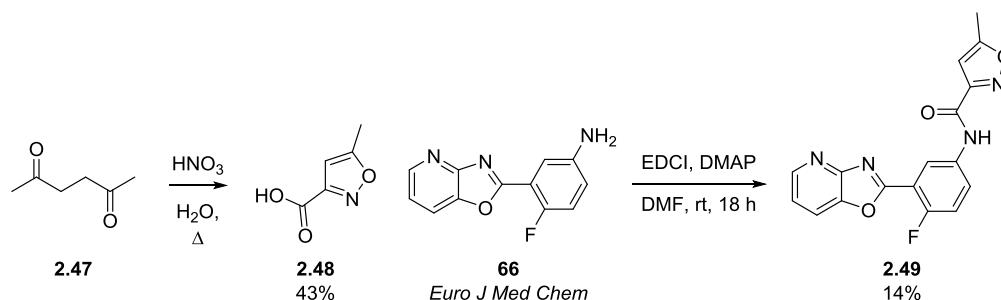
^a Compound found to have $< 50\%$ activity at 10.41 μM .

2.7.2. Northern heterocycle changes

The results of the ADME and metabolism analysis that were discussed in the *Eur. J. Med. Chem.* manuscript revealed that the oxazole heterocycle was the most metabolically stable whilst maintaining low micromolar inhibition of *T.b. brucei*. As a result a number of northern heterocycles were identified as synthetic targets. These oxazole analogues were all designed with the oxygen at the 3-position as the 3-furan was shown to convey greater activity against *T.b. rhodesiense* in previous studies whilst also having some improved

pharmacokinetic properties, such as solubility (compounds **20**, **35**, and **40** - Table 3 of the *Eur. J. Med. Chem.* paper). It was hoped that this would lead to an increase in the potency of these analogues whilst also maintaining the metabolic stability observed with the oxazoles previously tested. A variety of commercially available oxazole and isoxazole analogues were obtained while the 5-methylisoxazole-3-carboxylic acid (**2.48**) was synthesised.

Synthesis of the 5-methylisoxazole-3-carboxylic acid was performed in accordance with a procedure from Niemczyk (Scheme 2.8).⁸⁹ Nitric acid and water were heated to reflux prior to the gradual addition of acetylacetone (**2.47**) via a dropping funnel. This process was extremely exothermic and the addition was performed at a rate which maintained the reflux. This reaction was successfully performed on a multigram scale and led to the desired product in acceptable yields. An amide coupling was then performed with **66** (*Eur. J. Med. Chem.* manuscript) to obtain the desired product (**2.49**).

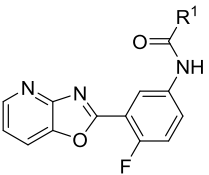


Scheme 2.7 Synthesis of 5-methylisoxazole-3-carboxylic acid (**2.48**) was successfully performed through reaction of acetylacetone (**2.47**) in a refluxing solution of nitric acid and water. Compound **2.48** could then be coupled to **66** using previously established amide coupling conditions.

Shown in Table 2.5 are the results of the biological assays against *T.b. brucei* of the oxazole analogues. These oxazole heterocycles gave analogues that were generally less active when compared with compound **40** (*Eur. J. Med. Chem.* manuscript; EC_{50} 0.12 μM), which had the 3-furan northern heterocycle. Compound **2.50** had an EC_{50} of 1.23 μM which was a 1.6-fold improvement in activity compared with **39**. This demonstrated a preference for the oxygen to be at the 3-position of the heterocycle. Further exploration of

this heterocycle with **2.51** (EC_{50} 0.68 μ M) saw a further ~3-fold improvement in the activity, yet **2.52** led to a 1.6-fold decrease in the activity with an EC_{50} 3.33 μ M. In an effort to gain a further increase in the activity of these isoxazole analogues compounds **2.49** and **2.53** were synthesised. The addition of the methyl group to both compounds led to a loss in activity against *T.b. brucei* in these assays. This was unexpected as there was SAR suggesting that a methyl and larger groups were tolerated, though it may be a combination of the methyl and the positioning of the heteroatoms in the ring.

Table 2.5 *T.b. brucei* inhibitory activity of compounds with varying amide groups.

	ID	R ^I	EC ₅₀ (μ M)	SI
	39^{a,b}		2.0	41
	2.50		1.23 \pm 0.22	68
	2.51		0.68 \pm 0.01	61
	2.52		3.33 \pm 0.64	25
	2.49		> 10 ^c	
	2.53		> 10 ^c	

^a Compound from the *Eur. J. Med. Chem.* manuscript.

^b Value is the mean of 3 experiments, \pm 50%.

^c Compound exhibited < 50% inhibition at 10.41 μ M.

2.7. Metabolism analysis

Analysis of the metabolism of these analogues (Table 2.6) revealed that methylation of the imidazole (**2.44** and **2.46**) led to an improvement in the metabolic stability of the compounds, with **2.44** defined as having

low clearance in human liver microsomes. The oxazole analogues in general showed no improvement to the metabolic stability of the compounds when compared with **39** (half-life of 124 mins, E_H 0.35). The dimethylated analogue, **2.53** displayed a similar metabolism profile to **39** though, as previously discussed, **2.53** demonstrated no activity against *T.b. brucei* in these assays.

Table 2.6 Metabolism evaluation of compounds using human or mouse liver microsomes.

ID	Species	Half-life (min)	<i>In vitro</i> CL _{int} ($\mu\text{l}/\text{min}/\text{mg}$ protein)	Microsome- predicted E_H	Clearance classification
2.44	Human	> 247 ^d	< 7	< 0.22	Low
	Mouse	59	30	0.39	Intermediate
2.46	Human	71	24	0.49	Intermediate
	Mouse	4 ^e	404	0.90	High
2.49	Human	15 ^b	118	0.82	High
	Mouse	< 2 ^{b,c}	> 875	> 0.95	Very high
2.50	Human	19 ^a	92	0.79	High
	Mouse	5 ^a	339	0.88	High
2.52	Human	30	58	0.7	Intermediate
	Mouse	2	881	0.95	High
2.53	Human	149	12	0.32	Intermediate
	Mouse	101	17	0.27	Low

^a Apparent non-NADPH mediated degradation in metabolism control samples. Hydrolysis products not detected.

^b Apparent non-NADPH mediated degradation in metabolism control samples. A putative amide hydrolysis product with m/z $[M+H]^+$ of 230 was detected.

^c Extensive degradation observed in the presence of absence of NADPH, hence, clearance parameters could not be determined and E_H was considered > 0.95.

^d Compound showed minimal microsomal degradation (< 15%) over the course of the incubation.

^e Apparent non-NADPH mediated degradation in metabolism control samples. A putative amide hydrolysis product with m/z $[M+H]^+$ of 225 was detected.

2.8. Biological analysis of compounds against *T. vivax* and *T. congolense*

A selection of compounds were analysed by researchers at the Swiss Tropical and Public Health Institute as part of the Global Alliance for Livestock Veterinary Medicine (GALVmed) project. The compounds were tested *ex vivo* against *T. vivax* and *in vivo* against *T. congolense*, which are both causative agents for animal trypanosomiasis in Western and Eastern Africa, respectively.⁹⁰ Table 2.7 summarises the results of these biological assays.

Table 2.7 *T. vivax* and *T. congolense* inhibitory activity of selected compounds.

ID	<i>T. vivax</i> EC ₅₀ (μM)	<i>T. congolense</i> EC ₅₀ (μM)
126 ^a	0.079	0.23
10 ^b	1.8	1.6
41 ^b	1.7	1.9
39 ^b	2.4	13
38 ^b	0.11	0.28
Diminazene ^c	0.34	0.25
Isometamidium ^c	0.0006	0.0006

^a Compound number from the Future Med. Chem. manuscript.

^b Compound number from the Eur. J. Med. Chem. manuscript.

^c Compound included as a standard control.

In general the compounds that were tested exhibited low micromolar activity against both *T. vivax* and *T. congolense*. The two notable exceptions are the hit compound, **126**, which proved to be the most potent in the *T. vivax* assay and was found to be four-fold more potent than diminazene against *T. vivax* and equipotent when tested against *T. congolense*. Compound **38** also demonstrated a 3-fold improvement in activity relative to diminazene and was equipotent when tested against *T. congolense*. Neither of these compounds were found to be as potent as Isometamidium in these assays. Diminazene and isometamidium are routinely

used in the treatment of animal trypanosomiasis though both have a multitude of side effects associated with their use.^{91, 92}

2.9. Target identification

Given that the initial hit was identified in a phenotypic, whole organism HTS no information is currently known about the potential target or targets of this series. Dr. Darren Creek in Drug Delivery, Disposition and Dynamics at the Monash Institute of Pharmaceutical Sciences employed an untargeted metabolomics approach to investigate the biochemical effects and the potential mode of action of this series. Analysis of the metabolite extracts with hydrophilic interaction chromatography coupled to HRMS revealed accumulation of ceramides in *T. brucei* that had been treated with **18** (*Eur. J. Med. Chem.* manuscript). In order to fully understand the drug-induced changes in lipid metabolism a new lipidomics method was developed which putatively identified > 500 lipids in *T. brucei* including glycerophospholipids, sphingolipids and fatty acyls. This method was used to confirm the drug-induced accumulation of ceramides. As a result of this work, the target for this series of compounds was putatively identified as sphingolipid synthase.

2.10. Competing work

As mentioned previously in Chapter 1, a second phenotypic screen of some 700,000 compounds also identified **126** (*Eur. J. Med. Chem.* manuscript) as a potential lead for medicinal chemistry optimisation.⁴ Given the limited commercially available screening space it is unsurprising that comprehensive libraries such as the screening libraries of Novartis and WEHI/Bio21 do have a degree of overlap. This can be challenging for academic drug discovery efforts to overcome if they are unknowingly beginning a project with the same starting point as a large pharmaceutical company given the resources that they will have to hand in order to progress their drug discovery efforts.

The study by researchers at Novartis revealed a similar SAR picture to the one observed throughout our studies, though there is some lack of correlation in the results, which is likely due to the different assay conditions used by the two groups.⁴ It was found by Tatipaka *et al.*⁴ that the replacement of the 2-furan with the *N*-pyrrolidinyl leads to a significant improvement in activity, particularly when coupled with the addition of the phenyl ring at the 6-position of the pyridinoxazole core. There was also a significant improvement in the metabolic stability of this compound with a half-life in human liver microsomes of 31 min compared with 6.1 min for **126**, though there was no indication as to whether the solubility was affected.⁴ As previously shown, **1.07** demonstrated a cure in a mouse model of the disease at doses of 50 mg/kg once and twice daily, 20 mg/kg once and twice daily and at 5 mg/kg when administered twice daily. There was also no clinical toxicity observed at a dose of 50 mg/kg twice daily over 14 days, indicating good tolerability of the compound.⁴

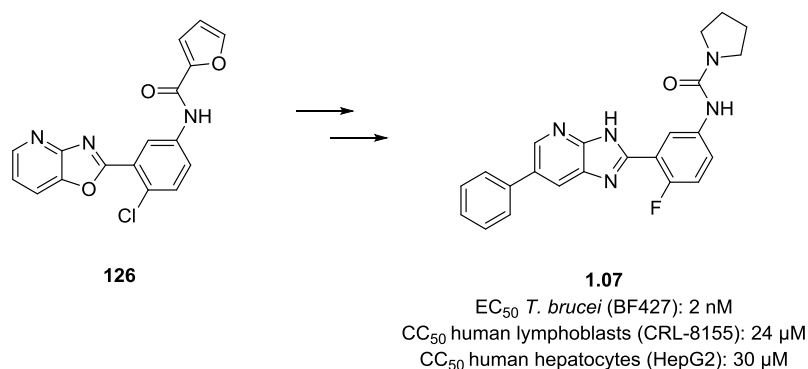
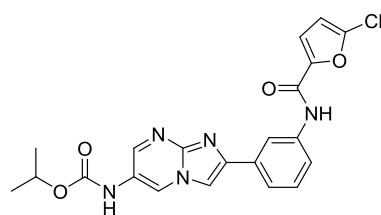


Figure 2.5 Optimisation of **126**, identified in a separate phenotypic screen of 700,000 compounds, to give **1.07** which exhibits nanomolar inhibition of *T. b. brucei* and has been demonstrated to cure mice infected with *T. brucei*.

Researchers at Novartis have also published data on a related series in the form of two patent applications.^{7, 8} They have reported some 42 compounds which exhibit a range of *in vitro* potencies against not only *T. brucei* but also *L. donovani* and *T. cruzi*, with compound **1.08** being their most potent *T. brucei* inhibitor disclosed.^{7, 8} To date, no data has been provided with respect to the selectivity of these compounds or on their performance in mouse models of the disease.



1.08

L. donovani amastigotes EC₅₀: 0.41 uM

L. donovani macrophage EC₅₀: 0.17 uM

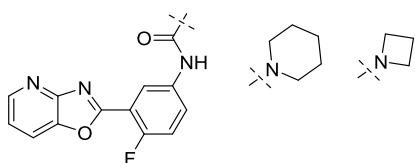
T. brucei EC₅₀: 0.057 uM

Figure 2.6 The most active compound against *T. brucei* identified in a hit-to-lead program by researchers at Novartis.

2.11. Future work

Given the work of Tatipaka and co-workers⁴ further exploration of the urea and various derivatives is warranted. Due to the solubility issues observed in the series and the tolerance to substitution at the 6-position of the pyridinoxazole core, the introduction of solubilising groups requires investigation. This could include substitution with morpholine, piperazine, or aliphatic substituents such as that introduced by researchers at Novartis in compound **1.08**. Further exploration of the 7- and 5-positions of the pyridinoxazole core is also warranted in order to determine the extent to which substitution can occur.

Modification and further probing of the urea



Probing around pyridine ring

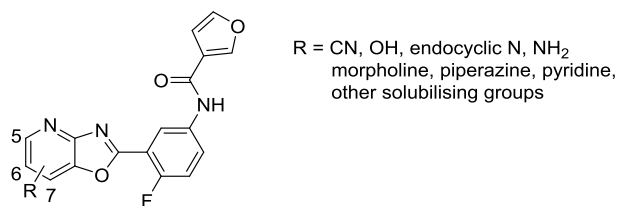


Figure 2.7 Concepts identified for consideration in future synthetic programs.

This series has been shown to have potent activity against *T. cruzi* when tested in the parasite panel, and this was also observed in the Novartis patents.^{7, 8} As a result our library of compounds is currently being tested against *T. cruzi* in order to develop an SAR picture for this series against this kinetoplastid. This may lead to further analogues being identified, though in pursuit of this series it is necessary to acknowledge the high risk of duplication associated with the interest shown by both Michael Gelb and Novartis.

2.12. *Experimental*

General Procedure 2-A1: Synthesis of the pyridinoxazole core

To polyphosphoric acid (1.5 g/mmol of limiting reagent) was added 2-amino-3-hydroxypyridine (1.0 eq.) and the relevant benzoic acid (1.1 eq.). The mixture was heated to 220 °C and stirred for 4 h prior to neutralisation.

Work-up 1 (2-W1): The reaction mixture was poured into 5 M sodium hydroxide and the resulting precipitate was filtered and recrystallised from ethyl acetate to give the desired pyridinoxazole core.

Work-up 2 (2-W2): The reaction mixture was poured into an aqueous 10% sodium bicarbonate solution. The suspension was stirred until gas evolution ceased, then filtered and washed with water. The aqueous medium was extracted three times with ethyl acetate. The combined organic layers were then washed with a saturated aqueous solution of sodium chloride, dried with sodium sulphate and the solvent was removed *in vacuo*. Purification by column chromatography on silica gel, eluting with 20-50% ethyl acetate/petroleum spirits gave the desired pyridinoxazole core.

General Procedure 2-B1: Amide coupling

To a solution of the pyridinoxazole core (1.0 eq.) in *N,N*-dimethylformamide (0.5 M final concentration) the carboxylic acid (1.2 eq.), EDCI (1.2 eq) and DMAP (0.1 eq.) was added. The solution was stirred under nitrogen at 45 °C for 18 h.

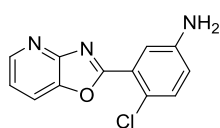
Work-up 1 (2-W1): Water (approximately 1 ml) was added to the reaction mixture and it was transferred to the fridge overnight. The resulting precipitate was filtered and gave the desired product.

Work-up 2 (2-W2): The reaction mixture was diluted with ethyl acetate, before a saturated aqueous solution of sodium bicarbonate was added and the mixture was extracted three times with ethyl acetate. The combined organic layers were washed with a saturated aqueous solution of sodium chloride, dried with magnesium sulphate and the solvent was removed *in vacuo*. The crude material was purified by column chromatography on silica gel, eluting with 50% ethyl acetate/cyclohexane to give the desired product.

General Procedure 2-B2: Amide coupling

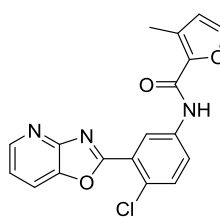
To a solution of the pyridinoxazole core (1.0 eq.) in *N,N*-dimethylformamide (0.5 M final concentration) the carboxylic acid (1.2 eq.), HBTU (1.2 eq.) and triethylamine (3.0 eq.) were added. The solution was stirred under nitrogen at 45 °C for 18 h. The reaction mixture was then diluted with ethyl acetate, before a saturated aqueous solution of sodium bicarbonate was added and the mixture was extracted three times with ethyl acetate. The combined organic layers were then washed with a saturated aqueous solution of sodium chloride, dried with magnesium sulphate and the solvent was removed *in vacuo*. The crude material was purified by column chromatography on silica gel, eluting with 50% ethyl acetate/petroleum spirits to give the desired carboxamide.

4-Chloro-3-(oxazolo[4,5-b]pyridin-2-yl)-aniline (**50**, Eur. J. Med. Chem. manuscript)



Title compound was prepared according to General Procedure 2-A1 using 2-W1 as a yellow powder (3.72 g, 20%). LRMS $[M+H]^+$ 246.1 m/z; HRMS $[M+H]^+$ 246.0426 m/z, found 246.0431 m/z; 1H NMR (DMSO, 300 MHz) δ 8.59 (dd, $J = 4.9, 1.4$ Hz, 1H), 8.27 (dd, $J = 8.2, 1.4$ Hz, 1H), 7.51 (dd, $J = 8.2, 4.9$ Hz, 1H), 7.41 (d, $J = 2.8$ Hz, 1H), 7.32 (d, $J = 8.7$ Hz, 1H), 6.83 (dd, $J = 8.7, 2.8$ Hz, 1H), 5.70 (s, 2H); ^{13}C NMR (DMSO, 101 MHz) δ 164.0, 155.5, 148.6, 147.2, 142.2, 132.2, 125.2, 121.5, 119.7, 119.0, 118.1, 116.5.

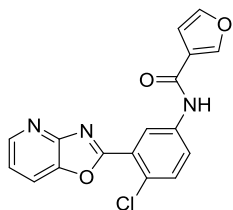
N-(4-Chloro-3-(oxazolo[4,5-b]pyridin-2-yl)phenyl)-3-methylfuran-2-carboxamide (**2**, Eur. J. Med. Chem. manuscript)



The title compound was prepared from **50** according to General Procedure 2-B1 using 2-W2. In addition the compound was purified by column chromatography, eluting with 0-40% methanol in dichloromethane before being further purified by preparatory HPLC, to give the title compound as an off-white solid (76 mg, 21%). LRMS $[M+H]^+$ 354.1 m/z; HRMS $[M+H]^+$ 354.0640 m/z, found 354.0637 m/z; 1H NMR (DMSO, 400 MHz) δ 10.51 (s, 1H), 8.84 (d, $J = 2.6$ Hz, 1H), 8.61 (dd, $J = 4.8, 1.4$ Hz, 1H), 8.32 (dd, $J = 8.2, 1.4$ Hz, 1H), 8.03 (dd, $J = 8.9,$

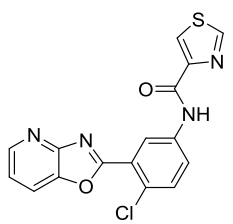
2.7 Hz, 1H), 7.84 (d, $J = 1.7$ Hz, 1H), 7.68 (d, $J = 8.8$ Hz, 1H), 7.53 (dd, $J = 8.2, 4.8$ Hz, 1H), 6.62 (d, $J = 1.6$ Hz, 1H), 2.36 (s, 3H); ^{13}C NMR (DMSO, 101 MHz) δ 162.7, 157.6, 155.0, 146.9, 144.1, 142.5, 141.4, 138.3, 131.7, 128.8, 126.3, 124.8, 124.7, 122.8, 121.4, 119.4, 115.9, 11.1.

N-(4-Chloro-3-(oxazolo[4,5-*b*]pyridin-2-yl)phenyl)furan-3-carboxamide (**5**, Eur. J. Med. Chem. manuscript)



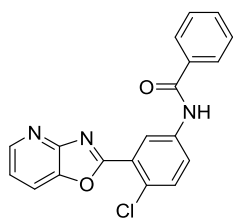
Title compound was prepared from **50** according to General Procedure 2-B1 using 2-W2 as a yellow solid (75 mg, 35%). LRMS $[\text{M}+\text{H}]^+$ 340.1 m/z; HRMS $[\text{M}+\text{H}]^+$ 340.0483 m/z, found 340.0483 m/z; ^1H NMR (DMSO, 400 MHz) δ 10.32 (s, 1H), 8.67 (d, $J = 2.6$ Hz, 1H), 8.61 (dd, $J = 4.8, 1.4$ Hz, 1H), 8.43 (dd, $J = 1.5, 0.8$ Hz, 1H), 8.31 (dd, $J = 8.2, 1.4$ Hz, 1H), 8.06 (dd, $J = 8.8, 2.7$ Hz, 1H), 7.83 (t, $J = 1.7$ Hz, 1H), 7.71 (d, $J = 8.8$ Hz, 1H), 7.53 (dd, $J = 8.2, 4.8$ Hz, 1H), 7.03 (dd, $J = 1.9, 0.8$ Hz, 1H); ^{13}C NMR (DMSO, 101 MHz) δ 162.6, 160.8, 154.9, 147.0, 146.3, 144.5, 142.5, 138.4, 131.9, 126.3, 124.7, 124.4, 122.6, 122.6, 121.4, 119.4, 109.2.

N-(4-Chloro-3-(oxazolo[4,5-*b*]pyridin-2-yl)phenyl)thiazole-4-carboxamide (**6**, Eur. J. Med. Chem. manuscript)



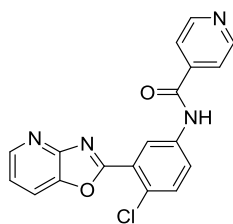
Title compound was prepared from **50** according to General Procedure B1 using 2-W2 as a yellow solid (181 mg, 83%). LRMS $[\text{M}+\text{H}]^+$ 357.1 m/z; HRMS $[\text{M}+\text{H}]^+$ 357.0208 m/z, found 357.0207 m/z; ^1H NMR (DMSO, 400 MHz) δ 10.87 (s, 1H), 9.31 (d, $J = 2.0$ Hz, 1H), 8.94 (d, $J = 2.6$ Hz, 1H), 8.63 (dd, $J = 4.8, 1.4$ Hz, 1H), 8.58 (d, $J = 2.0$ Hz, 1H), 8.34 (dd, $J = 8.2, 1.4$ Hz, 1H), 8.14 (dd, $J = 8.9, 2.7$ Hz, 1H), 7.74 (d, $J = 8.8$ Hz, 1H), 7.56 (dd, $J = 8.2, 4.8$ Hz, 1H); ^{13}C NMR (DMSO, 101 MHz) δ 164.8, 160.2, 155.4, 152.2, 152.2, 147.8, 143.4, 138.9, 137.0, 132.0, 131.6, 130.3, 130.0, 128.2, 126.6, 124.6.

N-(4-Chloro-3-(oxazolo[4,5-*b*]pyridin-2-yl)phenyl)benzamide (**10**, Eur. J. Med. Chem. manuscript)



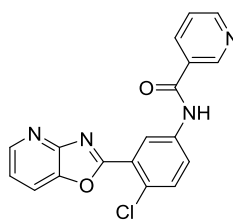
Title compound was prepared from **50** according to General Procedure 2-B1 using 2-W2 as an off-white solid (103 mg, 69%). LRMS [M+H]⁺ 350.1 m/z; HRMS [M+H]⁺ 350.0691 m/z, found 350.0686 m/z; ¹H NMR (DMSO, 400 MHz) δ 10.66 (s, 1H), 8.81 (d, *J* = 2.6 Hz, 1H), 8.62 (dd, *J* = 4.8, 1.4 Hz, 1H), 8.33 (dd, *J* = 8.2, 1.4 Hz, 1H), 8.10 (dd, *J* = 8.8, 2.6 Hz, 1H), 8.05 – 7.95 (m, 2H), 7.74 (d, *J* = 8.8 Hz, 1H), 7.69 – 7.48 (m, 4H); ¹³C NMR (DMSO, 101 MHz) δ 165.9, 162.7, 155.0, 147.0, 142.6, 138.7, 134.3, 132.0, 131.9, 128.5, 127.8, 126.4, 124.7, 124.7, 122.9, 121.4, 119.4.

N-(4-Chloro-3-(oxazolo[4,5-*b*]pyridin-2-yl)phenyl)isonicotinamide (**14**, Eur. J. Med. Chem. manuscript)



Title compound was prepared from **50** according to General Procedure 2-B1 using 2-W1 as a colourless solid (120 mg, 35%). LRMS [M+H]⁺ 351.1 m/z; HRMS [M+H]⁺ 351.0643 m/z, found 351.0637 m/z; ¹H NMR (DMSO, 400 MHz) δ 10.90 (s, 1H), 8.93 – 8.71 (m, 3H), 8.62 (dd, *J* = 4.8, 1.4 Hz, 1H), 8.33 (dd, *J* = 8.2, 1.4 Hz, 1H), 8.09 (dd, *J* = 8.8, 2.6 Hz, 1H), 7.91 (dd, *J* = 4.5, 1.6 Hz, 2H), 7.76 (d, *J* = 8.8 Hz, 1H), 7.55 (dd, *J* = 8.2, 4.8 Hz, 1H); ¹³C NMR (DMSO, 101 MHz) δ 164.8, 163.0, 155.4, 150.9 (2C), 147.5, 143.0, 142.8, 141.8, 138.6, 132.5, 127.5, 125.3, 123.5, 122.1 (2C), 121.9, 119.9.

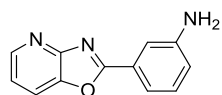
N-(4-Chloro-3-(oxazolo[4,5-*b*]pyridin-2-yl)phenyl)nicotinamide (**15**, Eur. J. Med. Chem. manuscript)



Title compound was prepared from **50** according to General Procedure B1 using 2-W2 as a colourless solid (148 mg, 69%). LRMS [M+H]⁺ 351.1 m/z; HRMS [M+H]⁺ 351.0643 m/z, found 351.0640 m/z; ¹H NMR (DMSO, 400 MHz) δ 10.87 (s, 1H), 9.17 (dd, *J* = 2.3, 0.7 Hz, 1H), 8.80 (dd, *J* = 4.5, 1.9 Hz, 2H), 8.64 (dd, *J* = 4.8, 1.4 Hz, 1H),

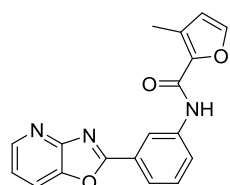
8.40 – 8.30 (m, 2H), 8.10 (dd, $J = 8.8, 2.7$ Hz, 1H), 7.77 (d, $J = 8.8$ Hz, 1H), 7.62 (ddd, $J = 8.0, 4.8, 0.8$ Hz, 1H), 7.56 (dd, $J = 8.2, 4.8$ Hz, 1H); ^{13}C NMR (DMSO, 101 MHz) δ 164.5, 162.6, 154.9, 152.6, 142.6, 138.4, 135.7, 135.6, 132.0, 130.0, 126.8, 124.8, 124.8, 123.6 (2C), 121.4 (2C), 119.4.

Oxazolo[4,5-b]pyridine (**52**, Eur. J. Med. Chem. manuscript)



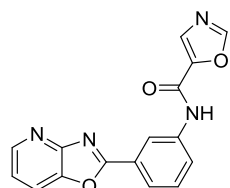
Title compound was prepared according to General Procedure 2-A1 using 2-W1 as an off-white solid (2.36 g, 25%). LRMS $[\text{M}+\text{H}]^+$ 121.1 m/z; ^1H NMR (DMSO, 400 MHz) δ 9.04 (s, 1H), 8.58 (dd, $J = 4.8, 1.4$ Hz, 1H), 8.26 (dd, $J = 8.2, 1.4$ Hz, 1H), 7.50 (dd, $J = 8.2, 4.8$ Hz, 1H), 6.41 (s, 2H); ^{13}C NMR (DMSO, 101 MHz) δ 157.7, 154.5, 147.1, 142.0, 121.5, 120.1.

3-Methyl-N-(3-(oxazolo[4,5-b]pyridin-2-yl)phenyl)furan-2-carboxamide (**18**, Eur. J. Med. Chem. manuscript)



Title compound prepared from **52** according to General Procedure 2-B1 using 2-W1 as an off-white solid (138 mg, 48%). HPLC – rt 9.57 min > 99% purity at 254 nm; LRMS $[\text{M}+\text{H}]^+$ 320.1 m/z; HRMS $[\text{M}+\text{H}]^+$ 320.1030 m/z, 320.1040 m/z; ^1H NMR (400 MHz, DMSO) δ 10.42 (s, 1H), 8.89 (t, $J = 1.8$ Hz, 1H), 8.57 (dd, $J = 4.9, 1.4$ Hz, 1H), 8.29 (dd, $J = 8.2, 1.4$ Hz, 1H), 8.10 – 7.90 (m, 2H), 7.85 (d, $J = 1.5$ Hz, 1H), 7.61 (t, $J = 8.0$ Hz, 1H), 7.49 (dd, $J = 8.2, 4.9$ Hz, 1H), 6.64 (d, $J = 1.4$ Hz, 1H), 2.39 (s, 3H); ^{13}C NMR (101 MHz, DMSO) δ 164.8, 157.7, 155.5, 146.6, 143.9, 142.8, 141.6, 139.6, 129.7, 128.4, 126.2, 124.2, 122.7, 120.8, 119.1, 119.0, 115.8, 11.1.

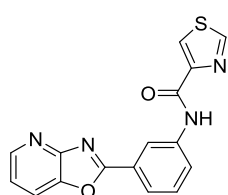
N-(3-(Oxazolo[4,5-b]pyridin-2-yl)phenyl)oxazole-5-carboxamide (**19**, Eur. J. Med. Chem. manuscript)



Compound **52** (European Journal of Medicinal Chemistry manuscript) (150 mg, 0.71 mmol), 5-oxazolecarboxylic acid (81 mg, 0.71 mmol) and hydroxybenzotriazole (134 mg, 0.85 mmol) were combined in anhydrous *N,N*-dimethylformamide (4 ml) and allowed to stir at ambient temperature for 5 min before addition of 1-ethyl-3-(3-

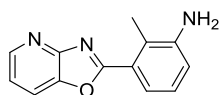
dimethylaminopropyl)carbodiimide hydrochloride (163 mg, 0.85 mmol) and diisopropylethylamine (320 μ l, 1.76 mmol). The suspension was stirred for 16 h under nitrogen at ambient temperature. The reaction mixture was quenched with the addition of water (1 ml) before being transferred to the fridge. The resulting precipitate was filtered and washed with water to obtain the title compound as a pale-orange solid (35 mg, 16%). HPLC – rt 8.30 min > 99% purity at 254 nm; LRMS $[M+H]^+$ 307.1 m/z; HRMS $[M+H]^+$ 307.0826 m/z, found 307.0837 m/z; ^1H NMR (400 MHz, DMSO) δ 10.76 (s, 1H), 8.74 (dd, $J = 8.3, 6.6$ Hz, 2H), 8.58 (dd, $J = 4.8, 1.3$ Hz, 1H), 8.29 (dd, $J = 8.2, 1.3$ Hz, 1H), 8.12 – 7.94 (m, 3H), 7.66 (t, $J = 8.0$ Hz, 1H), 7.50 (dd, $J = 8.2, 4.9$ Hz, 1H); ^{13}C NMR (101 MHz, DMSO) δ 164.6, 155.4, 155.2, 154.1, 146.6, 144.9, 142.8, 139.1, 130.5, 130.0, 126.4, 124.2, 123.2, 120.9, 119.1, 119.1.

N-(3-(Oxazolo[4,5-*b*]pyridin-2-yl)phenyl)thiazole-4-carboxamide (**21**, Eur. J. Med. Chem. manuscript)



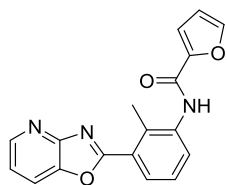
Title compound prepared from **52** according to General Procedure 2-B2 as a pale-yellow solid (50 mg, 20%). HPLC – rt 8.99 min 99% purity at 254 nm; LRMS $[M+H]^+$ 323.1 m/z; HRMS $[M+H]^+$ 323.0597 m/z, found 323.0613 m/z; ^1H NMR (400 MHz, DMSO) δ 10.75 (s, 1H), 9.32 (d, $J = 2.0$ Hz, 1H), 8.97 (t, $J = 1.8$ Hz, 1H), 8.70 – 8.46 (m, 2H), 8.29 (dd, $J = 8.2, 1.4$ Hz, 1H), 8.11 (ddd, $J = 8.2, 2.1, 0.9$ Hz, 1H), 8.05 – 7.93 (m, 1H), 7.64 (t, $J = 8.0$ Hz, 1H), 7.50 (dd, $J = 8.2, 4.9$ Hz, 1H); ^{13}C NMR (101 MHz, DMSO) δ 164.7, 159.5, 155.5, 155.2, 150.4, 146.6, 142.8, 139.5, 129.8, 126.3, 126.1, 124.5, 123.0, 120.8, 119.2, 119.1.

2-Methyl-3-(oxazolo[4,5-*b*]pyridin-2-yl)aniline (**53**, Eur. J. Med. Chem. manuscript)



Title compound prepared according to General Procedure 2-A1 using 2-W1 as a dark-red solid (647 mg, 48%). HPLC – rt 5.85 min > 99% purity at 254 nm; LRMS $[M+H]^+$ 226.2 m/z; HRMS $[M+H]^+$ 226.0975 m/z, found 226.0975 m/z; ^1H NMR (400 MHz, DMSO) δ 8.54 (dd, $J = 4.9, 1.4$ Hz, 1H), 8.21 (dd, $J = 8.1, 1.4$ Hz, 1H), 7.45 (dd, $J = 8.1, 4.9$ Hz, 1H), 7.28 (dd, $J = 7.7, 1.0$ Hz, 1H), 7.12 (t, $J = 7.8$ Hz, 1H), 6.92 (dd, $J = 7.9, 0.9$ Hz, 1H), 5.26 (s, 2H), 2.48 (s, 3H); ^{13}C NMR (101 MHz, DMSO) δ 166.1, 155.5, 148.1, 146.2, 142.1, 126.4, 125.7, 121.5, 120.6, 118.8, 117.9, 117.5, 14.3.

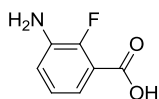
N-(2-Methyl-3-(oxazolo[4,5-*b*]pyridin-2-yl)phenyl)furan-2-carboxamide (**22**, Eur. J. Med. Chem. manuscript)



Title compound prepared from **53** according to General Procedure 2-B1 using 2-W1 as a pale-yellow solid (144 mg, 68%). HPLC – rt 5.98 min > 99% purity at 254 nm;

LRMS $[M+H]^+$ 320.2 m/z; HRMS $[M+H]^+$ 320.1030 m/z, found 320.1030 m/z; 1H NMR (400 MHz, DMSO) δ 10.13 (s, 1H), 8.58 (dd, $J = 4.9, 1.4$ Hz, 1H), 8.28 (dd, $J = 8.2, 1.4$ Hz, 1H), 8.05 (dd, $J = 7.8, 1.2$ Hz, 1H), 7.97 (dd, $J = 1.7, 0.8$ Hz, 1H), 7.61 (d, $J = 6.8$ Hz, 1H), 7.56 – 7.43 (m, 2H), 7.34 (dd, $J = 3.5, 0.7$ Hz, 1H), 6.73 (dd, $J = 3.5, 1.8$ Hz, 1H), 2.62 (s, 3H); ^{13}C NMR (101 MHz, DMSO) δ 164.9, 156.6, 155.4, 147.4, 146.5, 145.8, 142.3, 137.2, 135.4, 130.9, 128.1, 126.4, 126.4, 121.0, 119.1, 114.8, 112.2, 16.0.

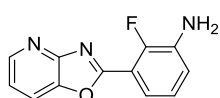
3-Amino-2-fluorobenzoic acid (**54**, Eur. J. Med. Chem. manuscript)



A 0.05 M solution of 2-fluoro-3-nitrobenzoic acid (510 mg, 0.27 mmol) made up in 50:50 ethyl acetate/ethanol (54 ml). This was loaded on to a ThalesNano H-Cube[®] with a 10% Pd/C

CatCart[®]. The reaction was monitored by LCMS until no more starting material was present and the solvent was removed under reduced pressure to give the amine as a pale-yellow solid (418 mg, 95%), which was used directly in the next reaction. LRMS $[M+H]^+$ 156.1 m/z; 1H NMR (400 MHz, DMSO) δ 7.03 – 6.83 (m, 3H), 5.32 (s, 2H).

2-Fluoro-3-(oxazolo[4,5-*b*]pyridin-2-yl)aniline (**55**, Eur. J. Med. Chem. manuscript)

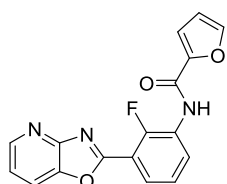


Title compound prepared from **54** according to General Procedure 2-A1 using 2-W1 as a pale-brown solid (330 mg, 63%). LRMS $[M+H]^+$ 230.1 m/z; HRMS $[M+H]^+$

230.0724 m/z, found 230.0723 m/z; 1H NMR (400 MHz, DMSO) δ 8.57 (dd, $J = 4.9, 1.4$ Hz, 1H), 8.26 (dd, $J = 8.2, 1.4$ Hz, 1H), 7.48 (dd, $J = 8.2, 4.9$ Hz, 1H), 7.35 (ddd, $J = 7.8, 6.1, 1.8$ Hz, 1H), 7.21 – 6.98 (m, 2H), 5.56 (s, 2H); ^{13}C NMR (101 MHz, DMSO) δ 162.3 ($J_{C-F} = 4$ Hz), 155.2, 148.5 ($J_{C-F} = 252$ Hz), 146.7,

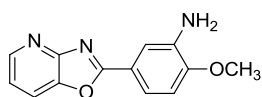
142.4, 138.0 ($J_{\text{C-F}} = 12$ Hz), 124.9 ($J_{\text{C-F}} = 4$ Hz), 120.9, 120.0 ($J_{\text{C-F}} = 5$ Hz), 119.1, 116.2, 113.9 ($J_{\text{C-F}} = 8$ Hz).

N-(2-Fluoro-3-(oxazol[4,5-*b*]pyridin-2-yl)phenyl)furan-2-carboxamide (**23**, Eur. J. Med. Chem. manuscript)



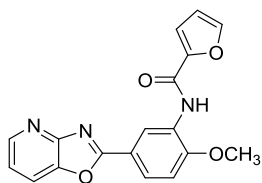
Title compound prepared from **55** according to General Procedure 2-B1 using 2-W1 as a pale-brown solid (92 mg, 44%). HPLC – rt 6.16 min > 97% purity at 254 nm; LRMS $[M+H]^+$ 324.1 m/z; HRMS $[M+H]^+$ 324.0779 m/z, found 324.0785 m/z; ^1H NMR (400 MHz, DMSO) δ 10.27 (s, 1H), 8.61 (dd, $J = 4.8, 1.4$ Hz, 1H), 8.31 (dd, $J = 8.2, 1.4$ Hz, 1H), 8.12 (ddd, $J = 8.0, 6.5, 1.7$ Hz, 1H), 8.00 (dd, $J = 1.7, 0.8$ Hz, 1H), 7.96 – 7.84 (m, 1H), 7.59 – 7.44 (m, 2H), 7.41 (dd, $J = 3.5, 0.7$ Hz, 1H), 6.74 (dd, $J = 3.5, 1.8$ Hz, 1H); ^{13}C NMR (101 MHz, DMSO) δ 161.4, 156.6, 155.1, 154.1 ($J_{\text{C-F}} = 263$ Hz), 147.1, 147.0, 146.3, 142.7, 131.3, 127.5, 126.7 ($J_{\text{C-F}} = 12$ Hz), 125.1 ($J_{\text{C-F}} = 5$ Hz), 121.4, 119.5, 115.6, 115.0 ($J_{\text{C-F}} = 9$ Hz), 112.5.

N-(2-methoxy-5-(oxazol[4,5-*b*]pyridin-2-yl)aniline) (**59**, Eur. J. Med. Chem. manuscript)



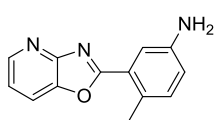
Title compound prepared according to General Procedure 2-A1 using 2-W1 as a pale-brown solid (1.11 g, 85%). HPLC – rt 6.19 min > 92% purity at 254 nm. LRMS $[M+H]^+$ 242.2 m/z; HRMS $[M+H]^+$ 242.0924 m/z, found 242.0926 m/z; ^1H NMR (400 MHz, DMSO) δ 8.48 (dd, $J = 4.9, 1.4$ Hz, 1H), 8.15 (dd, $J = 8.1, 1.4$ Hz, 1H), 7.54 (d, $J = 2.2$ Hz, 1H), 7.48 (dd, $J = 8.3, 2.2$ Hz, 1H), 7.39 (dd, $J = 8.1, 4.9$ Hz, 1H), 7.02 (d, $J = 8.4$ Hz, 1H), 5.17 (s, 2H), 3.88 (s, 3H); ^{13}C NMR (101 MHz, DMSO) δ 165.8, 156.0, 150.0, 146.0, 142.5, 138.5, 112.0, 118.4, 118.2, 116.7, 111.9, 110.6, 55.6.

N-(2-Methoxy-5-(oxazolo[4,5-*b*]pyridin-2-yl)phenyl)furan-2-carboxamide (**26**, Eur. J. Med. Chem. manuscript)



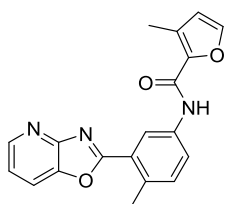
Title compound prepared from **59** according to General Procedure 2-B1 using 2-W1 as a pale-brown solid (85 mg, 70%). HPLC – rt 9.29 min \geq 95% purity; LRMS [M+H]⁺ 336.1 m/z; HRMS [M+H]⁺ 336.0979 m/z, found 336.0976 m/z; ¹H NMR (400 MHz, DMSO) δ 9.29 (s, 1H), 8.89 (d, *J* = 2.1 Hz, 1H), 8.52 (dd, *J* = 4.9, 1.4 Hz, 1H), 8.22 (dd, *J* = 8.1, 1.4 Hz, 1H), 8.08 (dd, *J* = 8.6, 2.2 Hz, 1H), 7.99 (dd, *J* = 1.7, 0.7 Hz, 1H), 7.44 (dd, *J* = 8.1, 4.9 Hz, 1H), 7.38 (dd, *J* = 4.7, 4.0 Hz, 2H), 6.75 (dd, *J* = 3.5, 1.7 Hz, 1H), 3.34 (s, 3H); ¹³C NMR (101 MHz, DMSO) δ 164.8, 155.8, 155.7, 153.4, 147.0, 146.3, 146.0, 142.7, 127.1, 125.3, 120.9, 120.3, 118.7, 118.0, 115.4, 112.5, 112.0, 56.5.

4-Methyl-3-(oxazolo[4,5-*b*]pyridin-2-yl)aniline (**65**, Eur. J. Med. Chem. manuscript)



Title compound prepared according to General Procedure 2-A2 using 2-W2 as a pale-yellow solid (810 mg, 30%). HPLC – rt 5.94 min > 99% purity at 254 nm; LRMS [M+H]⁺ 226.2 m/z; HRMS [M+H]⁺ 226.0975 m/z, found 226.0976 m/z; ¹H NMR (400 MHz, DMSO) δ 8.54 (dd, *J* = 4.9, 1.4 Hz, 1H), 8.22 (dd, *J* = 8.1, 1.4 Hz, 1H), 7.52 – 7.41 (m, 2H), 7.11 (d, *J* = 8.2 Hz, 1H), 6.77 (dd, *J* = 8.2, 2.5 Hz, 1H), 5.30 (s, 2H), 2.59 (s, 3H); ¹³C NMR (101 MHz, DMSO) δ 165.7, 155.6, 147.0, 146.2, 142.0, 132.6, 125.5, 124.8, 120.5, 118.7, 118.0, 114.3, 20.9.

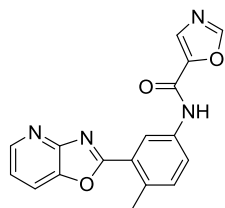
3-Methyl-N-(4-methyl-3-(oxazolo[4,5-*b*]pyridin-2-yl)phenyl)furan-2-carboxamide (**33**, Eur. J. Med. Chem. manuscript)



Title compound prepared from **65** according to General Procedure 2-B1 using 2-W1 as a pale-orange solid (124 mg, 56%). HPLC – rt 9.94 min > 98% purity at 254 nm; LRMS [M+H]⁺ 334.2 m/z; HRMS [M+H]⁺ 334.1186 m/z, found 334.1195 m/z; ¹H NMR (400 MHz, DMSO) δ 10.33 (s, 1H), 8.80 (d, *J* = 2.3 Hz, 1H), 8.58 (dd, *J* = 4.9, 1.4 Hz, 1H), 8.30 (dd, *J*

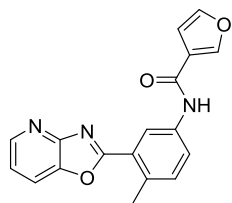
= 8.2, 1.4 Hz, 1H), 7.90 (dd, $J = 8.3, 2.3$ Hz, 1H), 7.83 (d, $J = 1.7$ Hz, 1H), 7.60 – 7.37 (m, 2H), 6.62 (d, $J = 1.7$ Hz, 1H), 2.75 (s, 3H), 2.38 (s, 3H); ^{13}C NMR (101 MHz, DMSO) δ 164.9, 157.5, 155.5, 146.5, 143.8, 142.1, 141.7, 137.1, 133.9, 132.3, 128.1, 124.7, 123.8, 121.0, 120.8, 118.9, 115.7, 21.3, 11.1.

N-(4-Methyl-3-(oxazol[4,5-*b*]pyridin-2-yl)phenyl)oxazole-5-carboxamide (**34**, Eur. J. Med. Chem. manuscript)



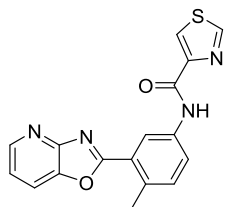
Title compound prepared from **65** according to General Procedure 2-B1 using 2-W1 as an off-white solid (106 mg, 67%). HPLC – rt 8.68 min > 98% purity at 254 nm; LRMS $[\text{M}+\text{H}]^+$ 321.1 m/z; HRMS $[\text{M}-\text{H}]^-$ 319.0837 m/z, found 319.0834 m/z; ^1H NMR (400 MHz, DMSO) δ 10.68 (s, 1H), 8.77 – 8.62 (m, 2H), 8.58 (dd, $J = 4.8, 1.4$ Hz, 1H), 8.28 (dd, $J = 8.1, 1.4$ Hz, 1H), 8.04 (s, 1H), 7.93 (dd, $J = 8.3, 2.3$ Hz, 1H), 7.61 – 7.40 (m, 2H), 2.76 (s, 3H); ^{13}C NMR (101 MHz, DMSO) δ 164.7, 155.4, 155.0, 154.0, 146.5, 145.0, 142.1, 136.6, 134.5, 132.5, 130.2, 124.9, 123.7, 121.1, 120.9, 118.9, 21.4.

N-(4-Methyl-3-(oxazol[4,5-*b*]pyridin-2-yl)phenyl)furan-3-carboxamide (**35**, Eur. J. Med. Chem. manuscript)



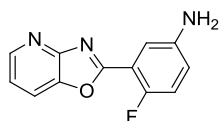
Title compound prepared from **65** according to General Procedure 2-B1 using 2-W1 as an off-white solid (169 mg, 79%). HPLC – rt 9.27 min > 99% purity at 254 nm; LRMS $[\text{M}+\text{H}]^+$ 320.2 m/z; HRMS $[\text{M}-\text{H}]^-$ 318.0884 m/z, found 318.0876 m/z; ^1H NMR (400 MHz, DMSO) δ 10.18 (s, 1H), 8.77 – 8.49 (m, 2H), 8.43 (d, $J = 0.6$ Hz, 1H), 8.28 (dd, $J = 8.1, 1.4$ Hz, 1H), 7.94 (dd, $J = 8.3, 2.3$ Hz, 1H), 7.83 (t, $J = 1.7$ Hz, 1H), 7.58 – 7.36 (m, 2H), 7.04 (dd, $J = 1.8, 0.7$ Hz, 1H), 2.76 (s, 3H); ^{13}C NMR (101 MHz, DMSO) δ 164.8, 160.5, 155.5, 146.5, 146.0, 144.3, 142.1, 137.3, 133.9, 132.4, 124.8, 123.5, 122.8, 120.9, 120.8, 118.9, 109.2, 21.3.

N-(4-Methyl-3-(oxazolo[4,5-*b*]pyridin-2-yl)phenyl)thiazole-4-carboxamide (**36**, Eur. J. Med. Chem. manuscript)



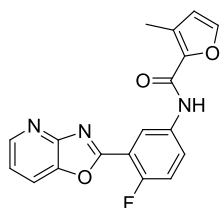
Title compound prepared from **65** according to General Procedure 2-B1 using 2-W1 as a pale-yellow solid (70 mg, 56%). HPLC – rt 9.38 min > 98% purity at 254 nm; LRMS [M+H]⁺ 337.1 m/z; HRMS [M+H]⁺ 337.0754 m/z, found 337.0768 m/z; ¹H NMR (400 MHz, DMSO) δ 10.65 (s, 1H), 9.30 (d, *J* = 2.0 Hz, 1H), 8.89 (d, *J* = 2.3 Hz, 1H), 8.66 – 8.44 (m, 2H), 8.29 (dd, *J* = 8.1, 1.4 Hz, 1H), 7.98 (dd, *J* = 8.3, 2.3 Hz, 1H), 7.62 – 7.33 (m, 2H), 2.76 (s, 3H); ¹³C NMR (101 MHz, DMSO) δ 164.8, 159.3, 155.5, 155.1, 150.5, 146.5, 142.1, 137.0, 134.3, 132.3, 125.8, 124.8, 124.0, 121.2, 120.9, 119.0, 21.4.

4-Fluoro-3-(oxazolo[4,5-*b*]pyridin-2-yl)aniline (**66**, Eur. J. Med. Chem. manuscript)



Title compound prepared according to General Procedure 2-A1 using 2-W1 as a yellow solid (838 mg, 34%). HPLC – rt 5.65 min > 96% purity at 254 nm; LRMS [M+H]⁺ 230.2 m/z; HRMS [M+H]⁺ 230.0724 m/z, found 230.0727 m/z; ¹H NMR (DMSO, 400 MHz) δ 8.57 (dd, *J* = 4.9, 1.4 Hz, 1H), 8.27 (dd, *J* = 8.2, 1.4 Hz, 1H), 7.46 (ddd, *J* = 8.9, 7.1, 3.9 Hz, 2H), 7.16 (dd, *J* = 10.9, 8.9 Hz, 1H), 6.86 (ddd, *J* = 8.9, 4.1, 3.0 Hz, 1H), 5.42 (s, 2H); ¹³C NMR (DMSO, 101 MHz) δ 162.4 (*J*_{C-F} = 4 Hz), 155.1, 152.2 (*J*_{C-F} = 247 Hz), 146.67, 145.8 (*J*_{C-F} = 2 Hz), 142.45, 120.88, 119.5 (*J*_{C-F} = 8 Hz), 119.09, 117.6 (*J*_{C-F} = 22 Hz), 113.7 (*J*_{C-F} = 11 Hz), 113.5.

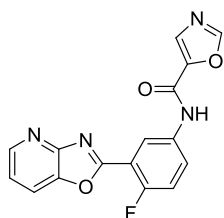
N-(4-Fluoro-3-(oxazolo[4,5-*b*]pyridin-2-yl)phenyl)-3-methylfuran-2-carboxamide (**38**, Eur. J. Med. Chem. manuscript)



Title compound prepared from **66** according to General Procedure 2-B1 using 2-W1 as a pale-orange solid (54 mg, 46%). HPLC – rt 9.52 min > 99% purity at 254 nm; LRMS [M+H]⁺ 338.1 m/z; HRMS [M+H]⁺ 338.0952 m/z; ¹H NMR (400 MHz, DMSO) δ 10.45 (s, 1H), 8.88 (dd, *J* = 6.5, 2.7 Hz, 1H), 8.60 (dd, *J* = 4.8, 1.4 Hz, 1H), 8.32 (dd, *J* = 8.2, 1.4 Hz, 1H), 8.04

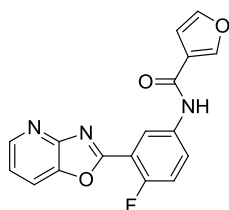
(ddd, $J = 9.0, 4.3, 2.8$ Hz, 1H), 7.84 (d, $J = 1.5$ Hz, 1H), 7.59 – 7.42 (m, 2H), 6.63 (d, $J = 1.5$ Hz, 1H), 2.37 (s, 3H); ^{13}C NMR (101 MHz, DMSO) δ 161.4 ($J_{\text{C-F}} = 6$ Hz), 157.6, 156.2 ($J_{\text{C-F}} = 256$ Hz), 155.1, 146.9, 144.0, 142.6, 141.5, 135.7, 128.5, 126.3 ($J_{\text{C-F}} = 8$ Hz), 121.3 ($J_{\text{C-F}} = 25$ Hz), 119.3, 117.5 ($J_{\text{C-F}} = 22$ Hz), 115.8, 113.8 ($J_{\text{C-F}} = 11$ Hz), 11.1. *Note: There is 1 carbon missing from the spectrum which is assumed to be overlapping with another signal.

N-(4-Fluoro-3-(oxazol[4,5-*b*]pyridin-2-yl)phenyl)oxazole-5-carboxamide (**39**, Eur. J. Med. Chem. manuscript)



Title compound prepared from **66** according to General Procedure 2-B1 using 2-W1 as a pale-yellow solid (82 mg, 93%). HPLC – rt 8.28 min > 97% purity at 254 nm; LRMS $[\text{M}+\text{H}]^+$ 325.1 m/z; HRMS $[\text{M}+\text{H}]^+$ 325.0747 m/z; ^1H NMR (400 MHz, DMSO) δ 10.79 (s, 1H), 8.84 – 8.67 (m, 2H), 8.61 (dd, $J = 4.8, 1.2$ Hz, 1H), 8.32 (dd, $J = 8.2, 1.2$ Hz, 1H), 8.15 – 7.96 (m, 2H), 7.64 – 7.43 (m, 2H); ^{13}C NMR (101 MHz, DMSO) δ 161.3 ($J_{\text{C-F}} = 5$ Hz), 156.4 ($J_{\text{C-F}} = 258$ Hz), 155.1, 155.0, 154.1, 146.9, 144.9, 142.6, 135.1 ($J_{\text{C-F}} = 3$ Hz), 130.5, 126.2 ($J_{\text{C-F}} = 9$ Hz), 121.6, 121.2, 119.3, 117.8 ($J_{\text{C-F}} = 23$ Hz), 114.1 ($J_{\text{C-F}} = 11$ Hz).

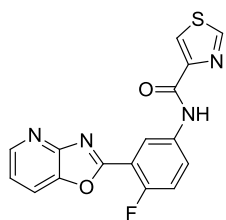
N-(4-Fluoro-3-(oxazol[4,5-*b*]pyridin-2-yl)phenyl)furan-3-carboxamide (**40**, Eur. J. Med. Chem. manuscript)



Title compound prepared from **66** according to General Procedure 2-B1 using 2-W1 as an off-white solid (79 mg, 80%). HPLC – rt 8.95 min > 99% purity at 254 nm; LRMS $[\text{M}+\text{H}]^+$ 324.1 m/z; HRMS $[\text{M}-\text{H}]^-$ 322.0627 m/z; ^1H NMR (400 MHz, DMSO) δ 10.27 (s, 1H), 8.70 (dd, $J = 6.5, 2.7$ Hz, 1H), 8.60 (dd, $J = 4.8, 1.4$ Hz, 1H), 8.43 (dd, $J = 1.5, 0.8$ Hz, 1H), 8.32 (dd, $J = 8.2, 1.4$ Hz, 1H), 8.08 (ddd, $J = 9.0, 4.2, 2.8$ Hz, 1H), 7.83 (t, $J = 1.7$ Hz, 1H), 7.59 – 7.46 (m, 2H), 7.04 (dd, $J = 1.9, 0.8$ Hz, 1H); ^{13}C NMR (101 MHz, DMSO) δ 161.4 ($J_{\text{C-F}} = 5$ Hz), 160.6, 156.1 ($J_{\text{C-F}} = 255$ Hz), 155.0, 146.9, 146.2, 144.4, 142.6, 135.9 ($J_{\text{C-F}} = 3$ Hz), 125.9 ($J_{\text{C-F}} = 8$ Hz), 122.6, 121.2, 119.3, 117.7 ($J_{\text{C-F}} = 22$ Hz), 114.0 ($J_{\text{C-F}} = 11$ Hz), 109.2.

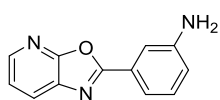
N-(4-Fluoro-3-(oxazolo[4,5-*b*]pyridin-2-yl)phenyl)thiazole-4-carboxamide (**41**, Eur. J. Med. Chem.

manuscript)



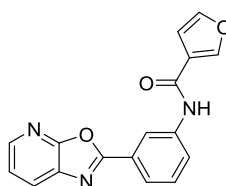
Title compound prepared from **66** according to General Procedure 2-B1 using 2-W1 as an off-white solid (170 mg, 77%). HPLC – rt 8.92 min > 99% purity at 254 nm; LRMS $[M+H]^+$ 341.1 m/z; HRMS $[M+H]^+$ 341.0512 m/z; 1H NMR (400 MHz, DMSO) δ 10.79 (s, 4H), 9.30 (d, $J = 2.0$ Hz, 3H), 8.96 (dd, $J = 6.5, 2.7$ Hz, 4H), 8.70 – 8.46 (m, 7H), 8.31 (dd, $J = 8.2, 1.4$ Hz, 4H), 8.13 (ddd, $J = 9.0, 4.3, 2.8$ Hz, 4H), 7.68 – 7.41 (m, 8H); ^{13}C NMR (101 MHz, DMSO) δ 161.4 ($J_{C-F} = 5$ Hz), 159.5, 156.4 ($J_{C-F} = 259$ Hz), 155.2, 155.1, 150.3, 146.9, 142.5, 135.6, 126.6 ($J_{C-F} = 9$ Hz), 126.1, 121.7, 121.2, 119.3, 117.6 ($J_{C-F} = 22$ Hz), 113.9 ($J_{C-F} = 11$ Hz).

3-(Oxazolo[5,4-*b*]pyridin-2-yl)aniline (**2.30**)



Title compound prepared according to General Procedure 2-A1 using 2-W1 as an off-white solid (371 mg, 19%). HPLC rt – 4.40 min > 98% purity at 254 nm; LRMS $[M+H]^+$ 212.1 m/z; HRMS $[M+H]^+$ 212.0818 m/z, found 212.0818 m/z; 1H NMR (400 MHz, DMSO) δ 8.36 (dd, $J = 4.9, 1.5$ Hz, 1H), 8.23 (dd, $J = 7.8, 1.6$ Hz, 1H), 7.54 – 7.41 (m, 2H), 7.41 – 7.31 (m, 1H), 7.25 (t, $J = 7.8$ Hz, 1H), 6.83 (ddd, $J = 8.0, 2.3, 1.0$ Hz, 1H), 5.53 (s, 2H); ^{13}C NMR (101 MHz, DMSO) δ 162.9, 159.2, 149.5, 144.4, 133.3, 129.9, 128.4, 126.4, 121.5, 117.9, 114.7, 112.1.

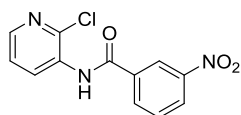
N-(3-(Oxazolo[5,4-*b*]pyridin-2-yl)phenyl)furan-3-carboxamide (**2.32**)



Title compound prepared according to General Procedure 2-B1 using 2-W1 as an off-white solid (230 mg, 64%). HPLC rt – 6.79 min > 99% purity at 254 nm; LRMS $[M+H]^+$ 306.1 m/z; HRMS $[M+H]^+$ 306.0873 m/z, found 306.0873 m/z; 1H NMR (400 MHz, DMSO) δ 10.22 (s, 1H), 8.69 (t, $J = 1.8$ Hz, 1H), 8.45 (dd, $J = 1.5, 0.8$ Hz, 1H), 8.40 (dd, $J = 4.9, 1.6$ Hz, 1H), 8.29 (dd, $J = 7.8, 1.6$ Hz, 1H), 8.05 (ddd, $J = 8.2, 2.2, 1.0$ Hz, 1H), 7.95 (ddd, $J = 7.8, 1.6, 1.0$ Hz, 1H), 7.83 (t, $J = 1.7$ Hz, 1H), 7.62 (t, $J = 8.0$ Hz, 1H), 7.52 (dd, $J = 7.9, 4.9$ Hz, 1H), 7.05 (dd, $J = 1.9, 0.8$

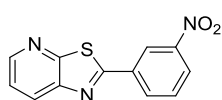
Hz, 1H); ¹³C NMR (101 MHz, DMSO) δ 162.0, 160.7, 159.3, 146.2, 144.9, 144.4, 139.9, 133.3, 129.9, 128.8, 126.4, 123.6, 122.8, 122.4, 121.7, 118.6, 109.2.

N-(2-Chloropyridin-3-yl)-3-nitrobenzamide (**2.35**)



3-Nitrobenzoic acid (1.0 g, 5.98 mmol) was added to anhydrous dichloromethane (10 ml) under nitrogen and the suspension was cooled to 0 °C. A catalytic amount of anhydrous *N,N*-dimethylformamide was added followed by the gradual addition of oxalyl chloride (0.56 ml, 6.58 mmol). The reaction mixture was left to stir at 0 °C until no further effervescence was observed. All of the volatiles were removed *in vacuo* and the resulting residue was re-suspended in anhydrous tetrahydrofuran. The reaction mixture was again cooled to 0 °C before the addition of 3-amino-2-chloropyridine (769 mg, 5.98 mmol) and pyridine (963 μl, 11.96 mmol). Once the addition was complete the reaction mixture was allowed to gradually warm to ambient temperature and stirred for 18 h. The reaction mixture was neutralised by addition of saturated aqueous ammonium chloride and extracted with ethyl acetate. The organic layers were collected, dried with magnesium sulphate and the solvent removed. The crude material was purified by column chromatography, eluting with 25%-50% ethyl acetate/petroleum spirits to yield the title product as an off-white solid (1.00 g, 60%). HPLC *rt* – 6.39 min > 99% purity at 254 nm; LRMS [M+H]⁺ 278.0 m/z; HRMS [M+H]⁺ 278.0327 m/z, found 278.0331 m/z; ¹H NMR (400 MHz, DMSO) δ 10.68 (s, 1H), 8.83 (t, *J* = 1.9 Hz, 1H), 8.49 (ddd, *J* = 8.2, 2.3, 1.0 Hz, 1H), 8.42 (ddd, *J* = 7.8, 1.6, 1.1 Hz, 1H), 8.36 (dd, *J* = 4.7, 1.8 Hz, 1H), 8.08 (dd, *J* = 7.9, 1.8 Hz, 1H), 7.88 (t, *J* = 8.0 Hz, 1H), 7.54 (dd, *J* = 7.9, 4.7 Hz, 1H); ¹³C NMR (101 MHz, DMSO) δ 163.7, 147.8, 147.2, 146.6, 137.4, 135.0, 134.2, 131.7, 130.5, 126.7, 123.6, 122.6.

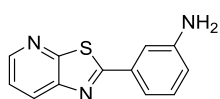
2-(3-Nitrophenyl)thiazolo[5,4-*b*]pyridine (**2.36**)



N-(2-Chloropyridin-3-yl)-3-nitrobenzamide (0.50 g, 1.80 mmol) and Lawesson's reagent (0.44 g, 1.08 mmol) were added to *ortho*-xylene (5 ml) under nitrogen. The suspension was heated to 110 °C and after 10 mins all of the solid had dissolved, the reaction was heated for

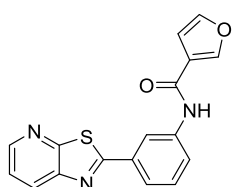
a further 2.5 h. After this time cesium carbonate (1.17g, 3.60 mmol) was added and the reaction was then refluxed for 5 h. The reaction mixture was diluted with ethyl acetate and washed with water. The organic layers were dried with magnesium sulphate and the solvent was removed *in vacuo*. The crude material was then purified by column chromatography, eluting with 15%-25% ethyl acetate/petroleum spirit to yield the title compound as an off-white solid (107 mg, 23%). HPLC *rt* – 7.69 min > 96% purity at 254 nm; LRMS $[M+H]^+$ 258.1 m/z; HRMS $[M+H]^+$ 258.0332 m/z, found 258.0334 m/z; 1H NMR (400 MHz, DMSO) δ 8.85 (t, J = 2.0 Hz, 1H), 8.69 (dd, J = 4.6, 1.5 Hz, 1H), 8.54 (ddd, J = 5.0, 2.6, 1.3 Hz, 2H), 8.45 (ddd, J = 8.2, 2.3, 0.9 Hz, 1H), 7.90 (t, J = 8.0 Hz, 1H), 7.68 (dd, J = 8.3, 4.6 Hz, 1H); ^{13}C NMR (101 MHz, DMSO) δ 165.0, 157.6, 148.5, 148.3, 146.4, 134.0, 133.7, 131.3, 130.9, 126.2, 122.6, 121.3.

3-(Thiazolo[5,4-b]pyridin-2-yl)aniline (**2.37**)



A 0.005 M solution of **2.36** (0.42 mmol) was dissolved in a 50:50 ethyl acetate/ethanol (20 ml) mixture. This was loaded on to a ThalesNano H-Cube[®] with a 10% Pd/C CatCart[®]. The reaction was monitored by LCMS until no more starting material was present and the solvent was removed under reduced pressure to give the title compound as a yellow solid (86 mg, 91%) which was used directly in the next reaction. LRMS $[M+H]^+$ 228.1 m/z; 1H NMR (400 MHz, DMSO) δ 8.60 (dd, J = 4.6, 1.4 Hz, 1H), 8.40 (dd, J = 8.2, 1.4 Hz, 1H), 7.60 (dd, J = 8.2, 4.6 Hz, 1H), 7.36 (d, J = 1.0 Hz, 1H), 7.27 – 7.15 (m, 2H), 6.78 (dt, J = 6.1, 2.4 Hz, 1H), 5.50 (s, 2H).

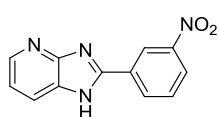
N-(3-(Thiazolo[5,4-b]pyridin-2-yl)phenyl)furan-3-carboxamide (**2.38**)



Title compound prepared according to General Procedure 2-B1 using 2-W1 as a pale-orange solid which was further purified by recrystallisation from ethyl acetate (30 mg, 25%). HPLC – *rt* 6.84 min > 99% purity at 254 nm; LRMS $[M+H]^+$ 322.1 m/z; HRMS $[M+H]^+$ 322.0645 m/z, found 322.0647 m/z; 1H NMR (400 MHz, DMSO) δ 10.22 (s, 1H), 8.64 (dd, J = 4.6, 1.5 Hz, 1H), 8.57 (t, J = 1.9 Hz, 1H), 8.46 (ddd, J = 4.9, 2.3, 1.2 Hz, 2H), 8.02 (ddd, J = 8.2, 2.0, 0.8 Hz, 1H), 7.83 (tdd, J = 2.7, 1.7, 1.0 Hz, 2H), 7.63 (dd, J = 8.2, 4.6 Hz, 1H), 7.58 (t, J = 8.0 Hz, 1H), 7.05 (dd, J =

1.9, 0.8 Hz, 1H); ^{13}C NMR (101 MHz, DMSO) δ 167.3, 160.7, 157.4, 147.6, 146.6, 146.2, 144.4, 139.9, 133.1, 130.3, 130.0, 123.2, 122.8, 122.5, 122.3, 118.3, 109.2.

2-(3-Nitrophenyl)-1H-imidazo[4,5-b]pyridine (2.40)

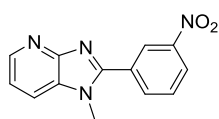


Synthesis based upon the previously reported procedure by Picard *et al.*⁹³

2,3-Diaminopyridine (1.0 g, 9.16 mmol) and 3-nitrobenzoic acid (1.53 g, 9.16 mmol) were combined before being added portion wise to phosphorous oxychloride (20 ml) at ambient temperature. Once the addition was complete the reaction mixture was heated to reflux for 4 h before being cooled to ambient temperature and left to stir for 18 h. The reaction mixture was then quenched by slow addition to a saturated aqueous solution of sodium bicarbonate. The resulting precipitate was filtered and air dried before being transferred to the vacuum oven overnight. The title compound was obtained as a grey solid (1.40 g, 64%). LRMS $[\text{M}+\text{H}]^+$ 241.1 m/z; ^1H NMR (400 MHz, DMSO) δ 9.20 – 9.01 (m, 1H), 8.69 (d, $J = 7.8$ Hz, 1H), 8.38 (ddd, $J = 9.6, 5.9, 2.5$ Hz, 2H), 8.09 (s, 1H), 7.88 (t, $J = 8.0$ Hz, 1H), 7.30 (dd, $J = 8.0, 4.7$ Hz, 1H).

*Note: there is 1 proton missing from the NMR spectrum.

1-Methyl-2-(3-nitrophenyl)-1H-imidazo[4,5-b]pyridine (2.41)

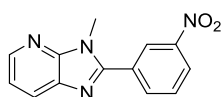


Synthesis based upon the previously reported procedure by Chai *et al.*⁹⁴

Compound (**2.40**) (1.0 g, 4.16 mmol), potassium carbonate (1.72 g, 12.48 mmol) and acetone (25 ml) were combined in a round bottom flask under an atmosphere of nitrogen. The methyl iodide (390 μl , 6.24 mmol) was added to a further 25 ml of acetone before being added gradually to the reaction mixture. The subsequent mixture was then stirred at ambient temperature for 36 h. The reaction mixture was filtered and purified by column chromatography, eluting with 5-50% ethyl acetate/petroleum spirits to give the title compound as a grey solid (105 mg, 10%). HPLC – rt 4.62 min > 96% purity at 254 nm; LRMS $[\text{M}+\text{H}]^+$ 255.1 m/z; HRMS $[\text{M}+\text{H}]^+$ 255.0877 m/z, found 255.0877 m/z; ^1H NMR (400 MHz, DMSO) δ 9.09 (dd, $J = 2.1, 1.6$ Hz, 1H), 8.81 – 8.70 (m, 1H), 8.33 (dd, $J = 7.7, 0.6$ Hz, 1H), 8.31 – 8.25 (m, 2H), 7.79 (dd, J

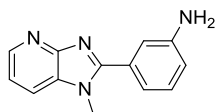
= 11.9, 4.0 Hz, 1H), 7.27 (dd, $J = 7.7, 6.2$ Hz, 1H), 4.35 (s, 3H); ^{13}C NMR (101 MHz, DMSO) δ 164.8, 153.5, 148.2, 144.2, 136.4, 133.6, 133.4, 130.4, 129.1, 123.9, 121.6, 113.4, 40.5.

3-Methyl-2-(3-nitrophenyl)-3H-imidazo[4,5-b]pyridine (2.42)



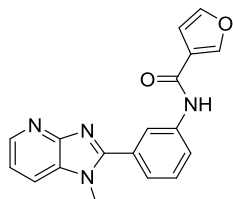
The title compound was isolated as a product of the previous reaction as a grey solid (88 mg, 8%). LRMS $[\text{M}+\text{H}]^+$ 255.1 m/z; HRMS $[\text{M}+\text{H}]^+$ 255.0877 m/z, found 255.0877 m/z; ^1H NMR (400 MHz, DMSO) δ 8.81 – 8.68 (m, 1H), 8.53 – 8.35 (m, 3H), 8.17 (dd, $J = 8.0, 1.5$ Hz, 1H), 7.98 – 7.84 (m, 1H), 7.37 (dd, $J = 8.0, 4.7$ Hz, 1H), 4.00 (s, 3H); ^{13}C NMR (101 MHz, DMSO) δ 151.8, 148.7, 148.1, 144.3, 135.3, 134.5, 131.4, 130.6, 127.2, 124.7, 123.9, 118.8, 30.3.

3-(1-Methyl-1H-imidazo[4,5-b]pyridin-2-yl)aniline (2.43)



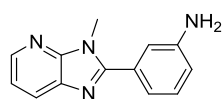
Compound **2.41** (80 mg, 0.31 mmol) was dissolved in methanol (4 ml) and zinc powder (203 mg, 3.10 mmol) was added. An aqueous solution of ammonium chloride was prepared by dissolving 166 mg of ammonium chloride (3.10 mmol) in 0.8 ml of water. This solution was then added dropwise to **2.41** and the progress of the reaction monitored by TLC and LCMS. After 10 min the reaction was complete and the reaction mixture was filtered through celite. All of the volatiles were removed *in vacuo*. The residue was then re-dissolved in ethyl acetate (10 ml) and washed with water (three times) and an aqueous saturated solution of sodium chloride. The organic layers were then dried with magnesium sulphate and the solvent removed to give the title compound as an orange oil (41 mg, 59%). LRMS $[\text{M}+\text{H}]^+$ 225.1 m/z; ^1H NMR (400 MHz, DMSO) δ 8.13 (t, $J = 6.5$ Hz, 2H), 7.74 – 7.60 (m, 1H), 7.58 – 7.46 (m, 1H), 7.22 – 7.02 (m, 2H), 6.62 (ddd, $J = 7.9, 2.4, 1.0$ Hz, 1H), 5.17 (s, 2H), 4.28 (s, 3H).

N-(3-(1-Methyl-1H-imidazo[4,5-b]pyridin-2-yl)phenyl)furan-3-carboxamide (**2.44**)



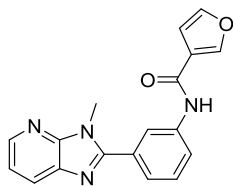
Title compound prepared according to General Procedure 2-B1 using 2-W1. The only modification to this procedure was that the crude material was purified by column chromatography, eluting with 0-10% methanol/dichloromethane. The title compound was isolated as a yellow oil which crystallised upon standing (14 mg, 34%). HPLC – rt 4.80 min > 91% purity at 254 nm; LRMS [M+H]⁺ 319.1 m/z; HRMS [M+H]⁺ 319.1190 m/z, found 319.1192 m/z; ¹H NMR (400 MHz, DMSO) δ 10.10 (s, 1H), 8.70 – 8.58 (m, 1H), 8.44 (dd, *J* = 1.5, 0.8 Hz, 1H), 8.24 – 8.16 (m, 2H), 8.13 – 8.07 (m, 1H), 7.95 (dd, *J* = 5.1, 4.1 Hz, 1H), 7.81 (t, *J* = 1.7 Hz, 1H), 7.45 (t, *J* = 7.9 Hz, 1H), 7.20 (dd, *J* = 7.7, 6.3 Hz, 1H), 7.06 (dd, *J* = 1.9, 0.8 Hz, 1H), 4.32 (s, 3H); ¹³C NMR (101 MHz, DMSO) δ 167.3, 160.5, 153.9, 146.0, 144.5, 144.3, 139.1, 135.2, 132.6, 128.8, 127.7, 123.1, 122.8, 121.2, 119.3, 112.8, 109.3, 40.3.

N-(3-(3-Methyl-3H-imidazo[4,5-b]pyridin-2-yl)aniline) (**2.45**)



Compound **2.42** (80 mg, 0.31 mmol) was dissolved in methanol (4 ml) and zinc powder (203 mg, 3.10 mmol) was added. An aqueous solution of ammonium chloride was prepared by dissolving ammonium chloride (166 mg, 3.10 mmol) in water (0.8 ml). This solution was then added dropwise to **2.42** and the progress of the reaction monitored by TLC and LCMS. After 10 min the reaction was complete and the reaction mixture was filtered through celite. All of the volatiles were removed *in vacuo*. The residue was then re-dissolved in ethyl acetate (10 ml) and washed with water (three times) and an aqueous saturated solution of sodium chloride. The organic layers were then dried with magnesium sulphate and the solvent removed to give the title compound as an orange oil (28 mg, 40%). LRMS [M+H]⁺ 225.1 m/z; ¹H NMR (400 MHz, DMSO) δ 8.36 (dd, *J* = 4.8, 1.5 Hz, 1H), 8.06 (dd, *J* = 7.9, 1.5 Hz, 1H), 7.30 (dd, *J* = 7.9, 4.8 Hz, 1H), 7.22 (t, *J* = 7.8 Hz, 1H), 7.14 – 7.09 (m, 1H), 7.02 (ddd, *J* = 7.6, 1.6, 1.0 Hz, 1H), 6.75 (ddd, *J* = 8.1, 2.3, 1.0 Hz, 1H), 5.38 (s, 2H), 3.90 (s, 3H).

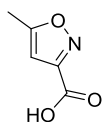
N-(3-(3-Methyl-3H-imidazo[4,5-b]pyridin-2-yl)phenyl)furan-3-carboxamide (**2.46**)



Title compound prepared according to General Procedure 2-B1 using 2-W1. The only modification to this procedure was that the crude material was purified by column chromatography, eluting 0-10% methanol/dichloromethane. The title compound was

isolated as a colourless solid (35 mg, 61%). HPLC – 4.85 min > 99% purity at 254 nm; LRMS [M+H]⁺ 319.1 m/z; HRMS [M+H]⁺ 319.1190 m/z, found 319.1193 m/z; ¹H NMR (400 MHz, DMSO) δ 10.17 (s, 1H), 8.43 (dd, *J* = 1.5, 0.8 Hz, 1H), 8.41 (dd, *J* = 4.8, 1.4 Hz, 1H), 8.35 (t, *J* = 1.8 Hz, 1H), 8.11 (dd, *J* = 8.0, 1.4 Hz, 1H), 7.95 (ddd, *J* = 8.1, 2.0, 1.0 Hz, 1H), 7.82 (t, *J* = 1.7 Hz, 1H), 7.71 – 7.65 (m, 1H), 7.58 (t, *J* = 7.9 Hz, 1H), 7.33 (dd, *J* = 8.0, 4.8 Hz, 1H), 7.04 (dd, *J* = 1.9, 0.8 Hz, 1H), 3.98 (s, 3H); ¹³C NMR (101 MHz, DMSO) δ 160.7, 153.7, 148.8, 146.1, 144.4, 143.6, 139.3, 134.6, 130.2, 129.2, 126.7, 124.1, 122.9, 121.6, 120.8, 118.5, 109.3, 30.5.

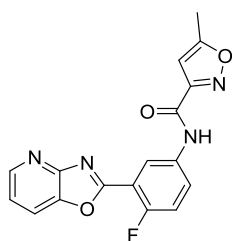
5-Methylisoxazole-3-carboxylic acid (**2.48**)



The title compound was synthesised based on a procedure from Niemczyk, 2002.⁸⁹

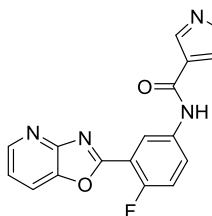
Nitric acid (43 ml, 1.03 mol) was added to a 3N-RBF containing water (77 ml). This solution was heated to reflux prior to the gradual addition of acetonylacetone (26 ml, 0.22 mol) via a dropping funnel. This process was extremely exothermic and the addition was performed at a rate which maintained the reflux. Once the addition was complete the reaction mixture was refluxed for a further 2 h. The reaction mixture was cooled to ambient temperature and left with no stirring for 18 h. The resultant precipitate was filtered and washed with water before being air dried. This gave the title compound as a pale-yellow solid (12.03 g, 43%). LRMS [M+Na]⁺ 172.0 m/z, [2M+Na]⁺ 321.0 m/z, [3M+Na]⁺ 470.0 m/z; ¹H NMR (400 MHz, DMSO) δ 6.56 (d, *J* = 0.9 Hz, 1H), 2.46 (d, *J* = 0.9 Hz, 3H); ¹³C NMR (101 MHz, DMSO) δ 171.7, 161.1, 157.1, 102.4, 11.9. *Note: the –OH peak was not visible in the ¹H NMR.

N-(4-Fluoro-3-(oxazolo[4,5-*b*]pyridin-2-yl)phenyl)-5-methylisoxazole-3-carboxamide (**2.49**)



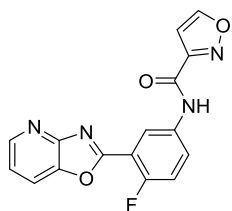
Title compound prepared according to General Procedure 2-B1 using 2-W1. The resultant material required further purification and was subjected to column chromatography, eluting with 10-50% ethyl acetate/petroleum spirits, to give the title compound as a colourless solid (53 mg, 14%). HPLC – rt 6.66 min > 99% purity at 254 nm; LRMS [M+H]⁺ 339.2 m/z; HRMS [M+H]⁺ 339.0888 m/z, found 339.0892 m/z; ¹H NMR (400 MHz, DMSO) δ 11.03 (s, 1H), 8.85 (dd, *J* = 6.5, 2.7 Hz, 1H), 8.60 (dd, *J* = 4.8, 1.4 Hz, 1H), 8.32 (dd, *J* = 8.2, 1.4 Hz, 1H), 8.05 (ddd, *J* = 9.0, 4.2, 2.8 Hz, 1H), 7.67 – 7.39 (m, 2H), 6.71 (d, *J* = 0.9 Hz, 1H), 2.52 (d, *J* = 0.7 Hz, 3H); ¹³C NMR (101 MHz, DMSO) δ 171.8, 161.3 (*J*_{C-F} = 5 Hz), 159.0, 157.8, 156.6 (*J*_{C-F} = 254 Hz), 155.0, 147.0, 142.6, 135.1 (*J*_{C-F} = 3 Hz), 126.6 (*J*_{C-F} = 9 Hz), 121.8, 121.3, 119.4, 117.9 (*J*_{C-F} = 23 Hz), 114.1 (*J*_{C-F} = 12 Hz), 101.7, 11.9.

N-(4-Fluoro-3-(oxazolo[4,5-*b*]pyridin-2-yl)phenyl)isoxazole-4-carboxamide (**2.50**)



Title compound prepared according to General Procedure 2-B1 using 2-W1 as a pale-brown solid (90 mg, 32%). HPLC rt – 6.00 min > 95% purity at 254 nm; LRMS [M+H]⁺ 325.1 m/z; HRMS [M+H]⁺ 325.0731 m/z, found 325.0736 m/z; ¹H NMR (400 MHz, DMSO) δ 10.53 (s, 1H), 9.59 (s, 1H), 9.08 (s, 1H), 8.58 (ddd, *J* = 6.1, 5.6, 2.0 Hz, 2H), 8.27 (dd, *J* = 8.2, 1.3 Hz, 1H), 8.10 – 7.92 (m, 1H), 7.58 – 7.34 (m, 2H); ¹³C NMR (101 MHz, DMSO) δ 161.3 (*J*_{C-F} = 5 Hz), 161.2, 158.1, 156.3 (*J*_{C-F} = 254 Hz), 155.0, 148.8, 147.0, 142.6, 135.5 (*J*_{C-F} = 3 Hz), 125.9 (*J*_{C-F} = 8 Hz), 121.3, 119.4, 118.0, 117.8, 117.8, 114.1 (*J*_{C-F} = 12 Hz).

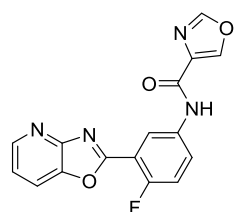
N-(4-Fluoro-3-(oxazolo[4,5-*b*]pyridin-2-yl)phenyl)isoxazole-3-carboxamide (**2.51**)



Title compound prepared according to General Procedure 2-B1 using 2-W1 as a colourless solid (88 mg, 62%). HPLC – rt 6.19 min > 99% purity at 254 nm; LRMS

$[M+H]^+$ 325.1 m/z; HRMS $[M+H]^+$ 325.0731 m/z, found 325.0729 m/z; 1H NMR (400 MHz, DMSO) δ 11.11 (s, 1H), 9.21 (d, $J = 1.6$ Hz, 1H), 8.86 (dd, $J = 6.4, 2.7$ Hz, 1H), 8.61 (dd, $J = 4.8, 0.8$ Hz, 1H), 8.33 (dd, $J = 8.2, 0.8$ Hz, 1H), 8.15 – 7.99 (m, 1H), 7.65 – 7.43 (m, 2H), 7.08 (d, $J = 1.6$ Hz, 1H); ^{13}C NMR (101 MHz, DMSO) δ 161.9, 161.3 ($J_{C-F} = 6$ Hz), 158.0, 157.4, 156.6 ($J_{C-F} = 257$ Hz), 155.0, 146.9, 142.6, 135.0, 126.6 ($J_{C-F} = 8$ Hz), 121.9, 121.2, 119.4, 117.8 ($J_{C-F} = 22$ Hz), 114.1 ($J_{C-F} = 11$ Hz), 104.6.

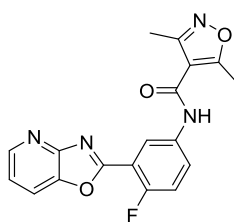
N-(4-Fluoro-3-(oxazol[4,5-*b*]pyridin-2-yl)phenyl)oxazole-4-carboxamide (**2.52**)



Title compound prepared according to General Procedure 2-B1 using 2-W1 as a pale-brown solid (60 mg, 42%). HPLC – rt 5.78 min > 99% purity at 254 nm; LRMS

$[M+H]^+$ 325.1 m/z; HRMS $[M+H]^+$ 325.0731 m/z, found 325.0730 m/z; 1H NMR (400 MHz, DMSO) δ 10.60 (s, 1H), 8.94 – 8.79 (m, 2H), 8.66 (s, 1H), 8.60 (dd, $J = 4.8, 1.2$ Hz, 1H), 8.31 (dd, $J = 8.2, 1.2$ Hz, 1H), 8.10 (ddd, $J = 9.0, 4.1, 2.9$ Hz, 1H), 7.58 – 7.42 (m, 2H); ^{13}C NMR (101 MHz, DMSO) δ 161.4 ($J_{C-F} = 6$ Hz), 158.9, 156.4 ($J_{C-F} = 254$ Hz), 155.0, 152.5, 146.9, 143.3, 142.5, 135.4, 135.3 ($J_{C-F} = 3$ Hz), 126.5 ($J_{C-F} = 9$ Hz), 121.8, 121.2, 119.3, 117.6 ($J_{C-F} = 22$ Hz), 113.9 ($J_{C-F} = 11$ Hz).

N-(4-Fluoro-3-(oxazol[4,5-*b*]pyridin-2-yl)phenyl)-3,5-dimethylisoxazole-4-carboxamide (**2.53**)



Title compound prepared according to General Procedure 2-B1. The reaction mixture was quenched through the addition of water and the product was then extracted with ethyl acetate three times. The organic layers were combined and dried with magnesium sulphate and all of the volatiles were removed *in vacuo*. The crude

material was purified by column chromatography eluting with 10-50% ethyl acetate/petroleum spirits, to give the title compound as a pale-brown solid (52 mg, 23%). HPLC – rt 6.14 min > 99% purity at 254 nm; LRMS $[M+H]^+$ 353.1 m/z; HRMS $[M+H]^+$ 353.1044 m/z, found 353.1048 m/z; 1H NMR (400 MHz, DMSO) δ 10.36 (s, 1H), 8.70 (dd, $J = 6.5, 2.7$ Hz, 1H), 8.60 (dd, $J = 4.8, 1.4$ Hz, 1H), 8.32 (dd, $J = 8.2, 1.4$ Hz, 1H), 7.94 (ddd, $J = 9.0, 4.2, 2.8$ Hz, 1H), 7.57 – 7.49 (m, 2H), 2.59 (s, 3H), 2.37 (s, 3H); ^{13}C NMR (101 MHz, DMSO) δ 170.1, 161.3 ($J_{C-F} = 5$ Hz), 160.4, 158.5, 156.3 ($J_{C-F} = 255$ Hz), 155.0, 147.0, 142.6, 135.7 ($J_{C-F} = 2$

Hz), 125.9 ($J_{\text{C-F}} = 9$ Hz), 121.2 ($J_{\text{C-F}} = 14$ Hz), 119.4, 117.8 ($J_{\text{C-F}} = 22$ Hz), 114.1 ($J_{\text{C-F}} = 11$ Hz), 113.2, 12.3, 10.5. *Note: there is 1 carbon missing from the spectrum.

3. Investigation of the structure-activity relationships of the pyrazine carboxamides against *T.b. brucei*

3.1. Introduction

The pyrazine carboxamides were another class of compounds identified in the whole organism HTS as a potential target for lead optimisation.⁵ Compound **128** had an EC₅₀ of 0.43 μM and a SI of > 98 against *T.b. brucei*. In conjunction with this **128** also possesses a number of key physicochemical properties that make it favourable for such a study. It has a low molecular weight of 270 g mol⁻¹, a moderately low PSA that could indicate potential for CNS penetration⁵⁶ and a low cLogP which could further aid with CNS penetration.⁸⁰

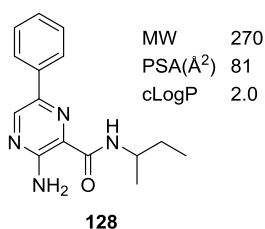


Figure 3.1 Structure and physicochemical properties of **128** with a low cLogP, PSA and MW making it a suitable candidate for lead optimisation.

Testing of this compound against a wider parasite panel showed that it had potent activity against the human infective *T.b. rhodesiense* (EC₅₀ 0.97 μM). However, it showed only weak activity against the closely related *T. cruzi* (EC₅₀ 19.1 μM) though this could be due to the cytotoxicity of the compound to L6 cells, a result of the *T. cruzi* assay conditions. When performing *T. cruzi* assays the trypomastigotes are allowed to infect erythrocytes as the parasite is unable to survive extracellularly. Given the low selectivity index in this assay it is not possible to attribute the observed EC₅₀ as a result of killing the L6 cells or as a result of directly killing the parasite. This could suggest a high degree of selectivity for *T.b. rhodesiense*. The activity was also significantly weaker for the unrelated kinetoplastids *L. donovani* and *P. falciparum*. These results are

summarised in Table 3.1. It is important to acknowledge that **128** contains a chiral centre and it would be interesting to separate and re-test the enantiomers as it is possible that the observed activity is due to just one enantiomer or both could be equally active.

Table 3.1 Biological activity^a profile of **128** against a number of parasites.

Parasite	EC ₅₀ (μM)	SI
<i>T.b. brucei</i>	0.43	>98 ^b
<i>T.b. rhodesiense</i>	0.97	18 ^c
<i>T. cruzi</i>	19.1	0.93 ^c
<i>L. donovani</i> axenic	34	0.52 ^c
<i>P. falciparum</i>	11.5	1.6 ^c

^a Values are the mean of 3 experiments, < ± 50%.

^b Selectivity relative to HEK293 (human embryonic kidney) cells.

^c Selectivity relative to L6 (rat skeletal myoblast) cells.

3.2. Aims

The aim for this section was to initially analyse the existing SAR literature within the group. From here, a number of analogues were identified that required exploration in order to determine additive SAR that may be obtained based upon identified active phenyl substitutions and amide side chains. The work was then expanded to include further exploration of the northern heterocycle, by replacement with solubilizing groups and non-aromatic ring systems. Finally, a variety of modifications to the core structure were identified including methylation of the amine and amide –NH, respectively, as well as a variety of changes to the pyrazine ring.

This work will be presented as a summary of a number of early analogues that constituted the primary SAR for this series. This initial analysis was performed in collaboration with a post-doctoral researcher in the lab,

Raphaël Rahmani. A discussion around the development of an optimised synthetic route for these derivatives will follow, before a detailed explanation of the analogues that were made as part of this PhD and the relevant synthetic pathways that were applied in order to obtain them.

3.3. Historical work completed

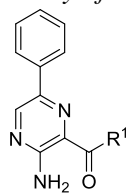
A number of analogues have previously been generated on this class of compounds by previous research chemists. Despite this, no comprehensive analysis of this data had been undertaken in order to identify new SAR probes that were needed to complete the primary SAR. This was performed in collaboration with Raphaël Rahmani.

3.3.1. Analogues of the amide side chain

Initially the amide side chain was examined and the results of this work are presented in Table 3.2.

As shown in Table 3.2, a range of bulky alkyl groups were tolerated including the 2-butyl (**128**, EC₅₀ 0.43 μM) and *n*-pentyl (**3.05**, EC₅₀ 1.7 μM) side chains. Substitution with 1-ethylpropyl (**3.03**, EC₅₀ 0.32 μM), cyclopentyl (**3.08**, EC₅₀ 0.26 μM), 2-pentyl (**3.06**, EC₅₀ 0.36 μM) and cyclohexyl groups (**3.07**, EC₅₀ 0.20 μM) each led to an improvement in the activity between 1.5- and 2-fold. Bulkier groups such as the 1-methylethyl (**3.01**, EC₅₀ 2.5 μM), and *tert*-butyl groups (**3.02**, EC₅₀ 3.0 μM) showed only moderate activity while smaller alkyl groups such as the methyl (**3.04**) led to a complete loss of activity in this assay. These results suggest that a hydrophobic side chain is required on the amide. This is confirmed by the loss of activity against *T.b. brucei* when hydrophilic groups such as a hydroxyl (**3.09** and **3.10**, EC₅₀ 7.4 and >10 μM) or basic nitrogen (**3.11** and **3.12**, EC₅₀ > 10 and > 10 μM) were introduced on the amide side chain. It was also observed that a benzyl group (**3.14**, EC₅₀ 2.6 μM) was well tolerated but the addition of a methylene as in **3.13** led to a complete loss of activity, suggesting there is a relatively tight binding pocket in the putative target in this region.

Table 3.2 T.b. brucei inhibitory activity of targets with varying amide groups.



ID	R ¹	EC ₅₀ (μM)	SI ^a	ID	R ¹	EC ₅₀ (μM)	SI ^a
3.01		2.5 ± 0.4	33	3.08		0.26 ± 0.01	368
3.02		3.0 ± 0.4	14	3.09		7.4 ± 0.5	11
3.03		0.32 ± 0.09	263	3.10		> 10 ^b	
3.04		> 10 ^b		3.11		> 10 ^b	
3.05		1.7 ± 0.2	50	3.12		> 10 ^b	
3.06		0.36 ± 0.07	228	3.13		> 10 ^b	
3.07		0.20 ± 0.02	423	3.14		2.6 ± 0.5	32

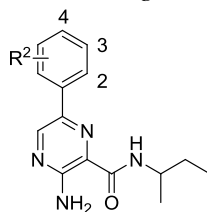
^a Selectivity relative to HEK293 (human embryonic kidney) cells.

^b Compound found to have < 50% activity at 10.41 μM.

3.3.2. Exploration of the SAR around the phenyl group

Following on from the investigations of the amide, substitutions around the northern aromatic group were explored. The results of these investigations are summarised in Table 3.3.

Table 3.3 T.b. brucei inhibitory activity of racemic targets with singularly substituted aromatic groups.



ID	R ²	EC ₅₀ (μM)	SI ^a	ID	R ²	EC ₅₀ (μM)	SI ^a
3.15	2-F	0.73 ± 0.3	111	3.29	3-NH ₂	1.1 ± 0.1	78
3.16	2-Cl	1.1 ± 0.4	76	3.30	3-COCH ₃	> 10 ^b	
3.17	2-Br	> 10 ^b		3.31	3-CH ₃	0.17 ± 0.01	495
3.18	2-OCH ₃	5.4 ± 0.4	15	3.32	3-CN	2.7 ± 0.6	31
3.19	2-NO ₂	0.89 ± 0.2	94	3.33	4-F	0.40 ± 0.04	206
3.20	2-NH ₂	> 10 ^b		3.34	4-Cl	0.68 ± 0.05	123
3.21	2-COCH ₃	> 10 ^b		3.35	4-Br	2.2 ± 0.6	38
3.22	2-CH ₃	1.2 ± 0.1	71	3.36	4-OCH ₃	1.3 ± 0.1	64
3.23	2-CN	0.35 ± 0.1	239	3.37	4-NO ₂	4.5 ± 2.1	19
3.24	3-F	0.45 ± 0.07	186	3.38	4-NH ₂	2.9 ± 0.06	28
3.25	3-Cl	0.48 ± 0.04	175	3.39	4-COCH ₃	4.7 ± 1.0	9
3.26	3-Br	0.57 ± 0.02	147	3.40	4-CH ₃	3.7 ± 1.1	22
3.27	3-OCH ₃	> 10 ^b		3.41	4-CN	2.7 ± 0.98	30
3.28	3-NO ₂	0.45 ± 0.03	185				

^a Selectivity relative to HEK293 (human embryonic kidney) cells.

^b Compound found to have < 50% activity at 10.41 μM.

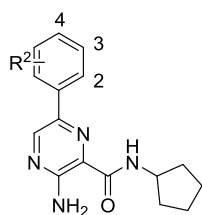
Initially small lipophilic groups were introduced at the *ortho*-position such as, the fluorine (**3.15**, EC₅₀ 0.73 μM), chlorine (**3.16**, EC₅₀ 1.1 μM), methyl (**3.22**, EC₅₀ 1.2 μM) and nitro (**3.19**, EC₅₀ 0.89 μM) groups, and all were equally active with the parent molecule. Yet introduction of the larger bromine group (**3.17**) at the *ortho*-position led to a complete loss of activity in this assay. Furthermore, introduction of a more hydrophilic substituent, such as a methoxy group (**3.18**, EC₅₀ 5.4 μM) led to a decrease in activity while introduction of an acetyl (**3.21**) or amine group (**3.20**) led to a complete loss of activity. Introduction of a

nitrile group (**3.23**) gave promising results with an EC₅₀ of 0.35 μM. The *meta*-position was substituted with similar lipophilic groups and in this instance favourable results were obtained with the small alkyl methyl (**3.31**, EC₅₀ 0.17 μM) being the most active followed by the fluorine (**3.24**, EC₅₀ 0.45 μM), chlorine (**3.25**, EC₅₀ 0.48 μM) and bromine (**3.26**, EC₅₀ 0.57 μM) analogues. Substitution with polar groups such as the nitrile (**3.32**, EC₅₀ 2.7 μM) or amine groups (**3.29**, EC₅₀ 1.1 μM) led to a decrease in activity, whilst the nitro group (**3.28**, EC₅₀ 0.45 μM) was found to be equally active with the parent compound. Yet introduction of an acetyl or methoxy group at this position (**3.30** and **3.27**) led to a complete loss of activity in this assay. The *para*-position when substituted with either a fluorine (**3.33**, EC₅₀ 0.40 μM) or a chlorine group (**3.34**, EC₅₀ 0.68 μM) led to analogues that were equally active when compared with the parent compound. However, as the size of the group increased there was a decrease in the activity, as seen with the methoxy (**3.36**, EC₅₀ 1.3 μM), bromine (**3.35**, EC₅₀ 2.2 μM) and methyl groups (**3.40**, EC₅₀ 3.7 μM). Whilst these compounds were tested as racemates it would be interesting to re-test each enantiomer in order to confirm the biological activity observed; though this work was outside the scope of this thesis. As such, the *ortho*-nitrile, *meta*-methyl and chloro and *para*-fluoro derivatives were identified as the top aromatic substituents.

3.3.3. Additive SAR

Once the most active amide sidechains and aromatic substituents had been identified, some second generation SAR was undertaken as shown in Table 3.4.

Table 3.4 *T.b. brucei* inhibitory activity of targets with active aromatic and amide substituents.



ID	R ²	EC ₅₀ (μM)	SI ^a
3.42	2-CN	0.20 ± 0.04	417
3.43	4-F	1.2	68
3.44	2-CN, 4-F	0.43	194
3.45	3-CH ₃	0.013 ± 0.01	1505

^a Selectivity relative to HEK293 (human embryonic kidney) cells.

Substitution with the *ortho*-nitrile group (**3.42**, EC₅₀ 0.20 μM) was equally active compared with **3.08**, while substitution with the *para*-fluoro (**3.43**, EC₅₀ 1.2 μM) led to a decrease in the activity when compared with **3.08** (EC₅₀ 0.26 μM). The combination of the *ortho*-nitrile and *para*-fluoro groups did not yield a significant improvement in the overall activity of **3.44** (EC₅₀ 0.43 μM). Introduction of the *meta*-methyl group led to a significant boost in the activity of **3.45** (EC₅₀ 0.013 μM).

3.3.4. Biological and pharmacokinetic analysis

To examine the activity of these compounds against the human pathogenic subspecies *T.b. rhodesiense*, selected compounds were tested against a small parasite panel offered by STI. The results of this have been summarised in Table 3.5.

From Table 3.5 it could be seen that *T.b. rhodesiense* activity tended to track well with the *T.b. brucei* activity as previously reported, with some exceptions (**3.23**, **3.25** and **3.34**). Broadly, these compounds were reasonably selective for *T.b. rhodesiense* with only **3.34** and **3.42** showing low micromolar activity against *P. falciparum*. However, closer analysis of the activity against *T.b. rhodesiense* did reveal some interesting information. Compound **3.31** is substituted at the 3-position of the aromatic ring and, while this compound didn't show an increase in potency, it appears to be less cytotoxic to mammalian cells. Further investigation

would need to be carried out in order to confirm if this is a trend for substituents at the 3-position. Meanwhile, compound **3.23** has an *ortho*-nitrile and it appears that this substitution was unfavourable for activity against *T.b. rhodesiense*, having gone from an EC₅₀ of 0.35 μM against *T.b. brucei* to 2.9 μM against *T.b. rhodesiense*.

Table 3.5 Biological activity profile of selected compounds against a parasite panel (EC₅₀, μM).^a

ID	<i>T.b. brucei</i>	<i>T.b. rhodesiense</i> ^b	<i>T. cruzi</i> ^b	<i>L. don. axe</i> ^d	<i>P. falc. K1</i> ^e	Cytotox. L6 ^f
3.01	2.5	0.97	19	34	11	18
3.08	0.26	0.14	14	16	6.1	20
3.23	0.35	2.9	32	19	6.6	21
3.25	0.48	2.0	25	28	11	39
3.31	0.17	0.13	26	12	19	43
3.33	0.40	0.32	18	20	6.8	20
3.34	0.68	1.9	23	18	3.6	20
3.42	0.20	0.57	5	-	2.5	11

^a Values are the mean of 2 experiments, < ± 50%.

^b *T.b. rhodesiense* strain STIB 900, bloodstream form (trypomastigotes). Melarsoprol was used as a control, EC₅₀ 0.005 μM.

^c *T. cruzi* Tulahaen C4 strain, amastigote stage. Benznidazole was used as a control, EC₅₀ 1.46 μM.

^d *L. donovani* MHOM-ET-67/L82 strain, amastigote stage. Miltefosine was used as a control, EC₅₀ 0.49 μM.

^e *P. falciparum* K1 strain, erythrocytic stage. Chloroquine was used as a control, EC₅₀ 0.006 μM.

^f Rat skeletal myoblast cell L6 strain. Podophyllotoxin was used as a control, EC₅₀ 0.017 μM.

An assessment of drug-likeness was made and the results are summarised in Table 3.6. A variety of physicochemical and metabolic parameters were examined and, in general, all of the compounds had low molecular weights in the range 282-307 g mol⁻¹. Their PSA values were relatively low and suitable for CNS penetration,⁵⁶ with the exception of **3.23** and **3.42**. It has been shown through analysis of small drug-like molecules that a logD value in the range of 0-3 can lead to improved ability to cross the BBB⁹⁵ and for improved intestinal permeability.⁹⁶ These compounds were shown to have moderate distribution coefficients

in the range of 3.6-4.5, which may hinder their ability to cross the BBB and limit their intestinal permeability. The majority of the compounds were poorly soluble (1.6-3.1 $\mu\text{g/ml}$), though **3.33** and **3.08** had good solubility at pH 6.5 of between 50-100 $\mu\text{g/ml}$ and 25-50 $\mu\text{g/ml}$ respectively. The compounds were generally highly protein bound with values in the range of 94.2-97.2%. Metabolism of these compounds was generally rapid, though **3.34** was relatively stable with an *in vitro* clearance value of 48 $\mu\text{l/min/mg}$ protein and a microsome predicted hepatic extraction of 0.65. Given the only difference between **3.33** and **3.34** is the halogen at the 4-position (a fluorine and chlorine respectively) it is difficult to explain these observations.

Table 3.6 Key physicochemical parameters and *in vitro* metabolic stability of selected compounds.

ID	MW	PSA (\AA^2) ^a	logD ^b			cPPB ^d (%)	<i>In vitro</i> CL _{int} ($\mu\text{l/min/mg}$ protein) ^e	Microsome- Predicted E _H ^e
			pH 7.4	pH 2	pH 6.5			
3.08	282	81	4.1	6.3-12.5	25-50	95.8	198	0.88
3.23	295	105	3.6	1.6-3.1	1.6-3.1	95.0	122	0.82
3.25	305	81	4.4	1.6-3.1	1.6-3.1	97.2	147	0.85
3.33	288	81	4.0	6.3-12.5	50-100	94.2	119	0.82
3.34	305	81	4.5	3.1-6.3	1.6-3.1	97.0	48	0.65
3.42	307	105	3.9	3.1-6.3	<1.6	96.2	165	0.86

^a Calculated using ACD/Labs software, version 9.

^b Measured chromatographically.

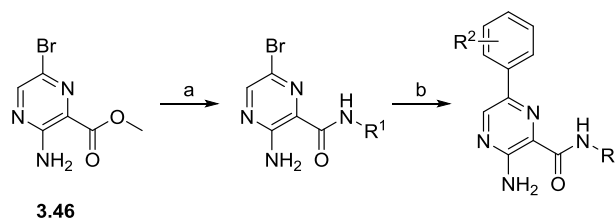
^c Kinetic solubility determined by nephelometry.

^d Human plasma protein binding estimated using a chromatographic method.

^e *In vitro* intrinsic clearance determined in human liver microsomes and predicted hepatic extraction ratio calculated from *in vitro* data.

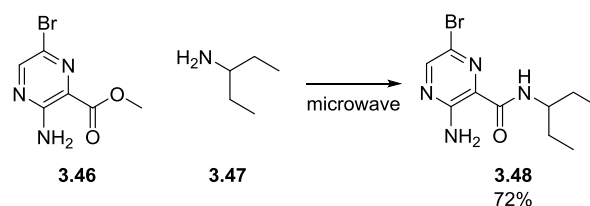
3.4. Optimisation of the synthesis of the pyrazine carboxamide core

The synthesis of derivatives required a two-step process with the initial synthesis developed by previous chemists, though the yields were often low and the reactions produced numerous products. As such it was necessary to optimise the synthetic procedures utilised to access the derivatives and this will now be discussed. The first step involved an amide bond formation between methyl 3-amino-6-bromopyrazine-2-carboxylate (**3.46**) and the relevant amine. This was followed by a Suzuki coupling with a substituted phenyl boronic acid as outlined in Scheme 3.1.



Scheme 3.1 Synthesis of pyrazine carboxamide derivatives. Reagents and conditions (a) methyl 3-amino-6-bromopyrazine-2-carboxylate, R^1 -amine, DBU, microwave; (b) R^2 - $B(OH)_2$, K_2CO_3 , TBAB, $PdCl_2$, dppf, dioxane:water, microwave.

The conditions previously utilised for the amide coupling employed DBU and the reaction was warmed to 60 °C for 18 h under nitrogen. However, with such a sterically hindered substrate as 1-ethylpropyl amine it was found that there were issues forming the desired product. As an alternative the reaction mixture was heated in a CEM microwave at 100 °C for 30 mins. This led to the formation of the desired product though there appeared to be a number of unidentified side products forming simultaneously. In an effort to overcome this, DBU was removed and the reaction mixture was heated under solventless conditions with a large excess of the amine. This led to a cleaner reaction with only the desired product being formed (Scheme 3.2).



Scheme 3.2 Optimised synthesis of the pyrazine carboxamide intermediate, **3.48**, prior to Suzuki coupling.

The subsequent step called for a Suzuki coupling and initially the conditions that were trialled entailed 1 eq bromopyrazineamide intermediate, 4 eq potassium carbonate, 1.2 eq substituted phenylboronic acid, 0.1 eq TBAI, 0.05 eq $\text{PdCl}_2(\text{PPh}_3)_2$ in the microwave. However, instead of forming the product it was observed by LCMS analysis that the major product of the reaction corresponded to the loss of bromine from the starting material, which could arise through reduction of the bromine. There were trace amounts of the product evident in the LCMS though the reaction was largely starting material. Switching the phase transfer catalyst from TBAI to TBAB yielded product though the yield was low (~10%) and the conditions were not universally applicable to a variety of substituted phenylboronic acids. Changing the catalyst to PdCl_2 and introducing the ligand 1,1'-bis(diphenylphosphino)ferrocene led to significant increase in the yields of product obtained (~75-80%). For the *ortho*-nitrile substituted phenylboronic acids the yields were typically lower (~20%) even with these optimised conditions. However, introducing the 2-cyanophenylboronic acid as its pinacol ester led to a significant increase in the yield of desired product (93%) due to the ability of the pinacol ester to stabilise the boronic acid.

3.5. Analogues of the 6-position

3.5.1. Substituted phenyl ring analogues

The initial focus of this PhD project was centred around completion of the second generation SAR analysis previously started by other researchers in the group. The results from this are outlined in Table 3.7.

The 1-ethylpropylamine side chain appears to give better activity when the results are compared with the compounds in Table 3.4. Substitution of the 3-position with a methyl group (**3.50**, EC₅₀ 0.11 μM) led to a three-fold improvement in the activity compared with **3.03** (EC₅₀ 0.32 μM). Yet, substitution with a 3-chloro group (**3.51**, EC₅₀ 0.39 μM) led to an analogue with essentially equipotent activity to the parent compound. The 4-fluoro analogue (**3.52**, EC₅₀ 0.085 μM) exhibited a four-fold improvement in activity over **3.03**. Combination of the 2-nitrile and 4-fluoro substituents revealed no additive SAR between these groups as evidenced by the activities of the 2-nitrile, 4-fluoro (**3.53**, EC₅₀ 0.10 μM) analogue and the individually substituted 2-nitrile (**3.49**, EC₅₀ 0.17 μM) and 4-fluoro (**3.52**, EC₅₀ 0.085 μM) analogues. Both **3.52** and **3.53** have such similar activities that any difference may be attributed to experimental error.

Table 3.7 T.b. brucei inhibitory activity of further analogues with top aromatic substitutions and the 1-ethylpropylamine side chain as shown.



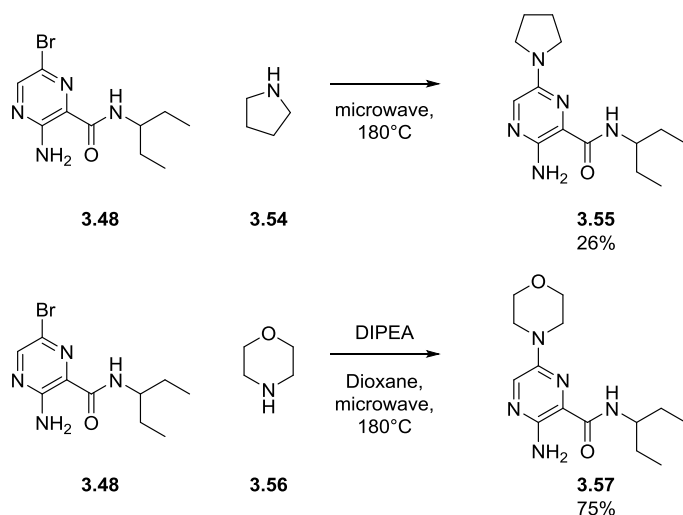
ID	R ²	EC ₅₀ (μM)	SI ^a
3.49	2-CN	0.17 ± 0.0	488
3.50	3-CH ₃	0.11 ± 0.01	775
3.51	3-Cl	0.39 ± 0.04	214
3.52	4-F	0.085 ± 0.03	1024
3.53	2-CN, 4-F	0.10 ± 0.0	850

^a Selectivity relative to HEK293 (human embryonic kidney) cells.

3.5.2. 5-Membered heterocyclic groups

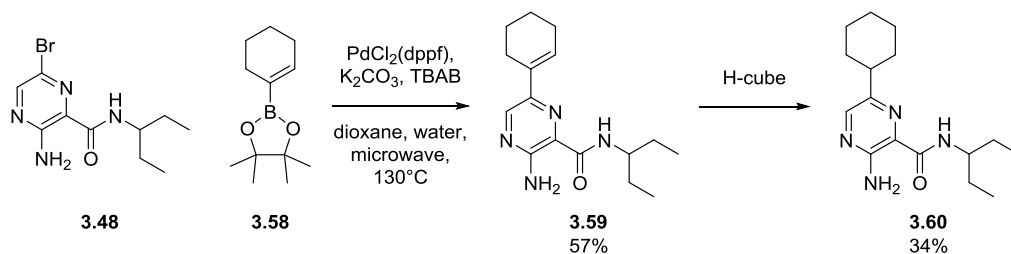
It was evident from the data in Table 3.6 that solubility was an issue with this class and the introduction of sp³ carbons may lead to an improvement in the solubility of the analogues.⁹⁷ As such, a number of saturated heterocycles were identified as targets of interest. In order to synthesise the pyrrolidine derivative, **3.55**, a Buchwald coupling was initially attempted between **3.48** and pyrrolidine. Both PdCl₂(dppf) in the presence of cesium carbonate in dioxane, and Pd₂(dba)₃ with potassium carbonate and SPhos in *tert*-butanol at 100 °C

in a CEM microwave were trialled, however no reaction was observed under these conditions. Instead, it was found that heating **3.48** in a CEM microwave at 180 °C in neat pyrrolidine led to the isolation of the desired product (**3.55**) in 26% yield after purification (Scheme 3.3). The morpholine derivative, **3.57**, could be accessed in a similar fashion; though the addition of diisopropylethylamine and using 1,4-dioxane as the solvent improved the yield of the reaction to 75%.



Scheme 3.3 Synthesis of the pyrrolidine and morpholine derivatives, **3.55** and **3.57** respectively.

In order to access the partially saturated 1-cyclohexene derivative (**3.59**) a Suzuki coupling between **3.48** and 1-cyclohexen-yl-boronic acid pinacol ester (**3.58**) led to the isolation of **3.59** in moderate yields. This could then be reduced using the H-cube[®] and a 10% Pd/C CatCart[®] to give the fully saturated analogue, **3.60**, as shown in Scheme 3.4.



Scheme 3.4 Synthesis of the partially saturated 1-cyclohexene and the fully saturated cyclohexyl derivatives, **3.59** and **3.60** respectively.

The biological activity of these analogues against *T.b. brucei* is summarised in Table 3.8.

Table 3.8 *T.b. brucei* inhibitory activity of analogues of the 6-position.



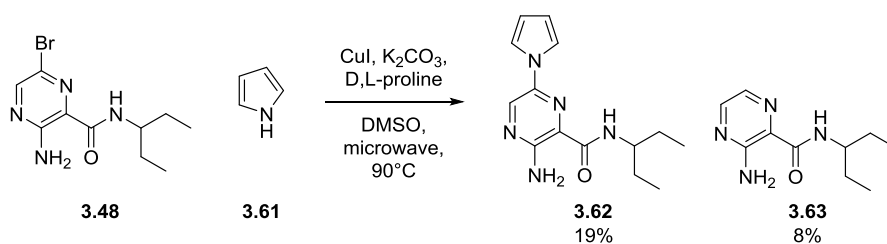
ID	R	EC ₅₀ (μM)	SI ^a
3.55		0.31 ± 0.1	268
3.57		0.93 ± 0.31	45
3.59		0.78 ± 0.14	54
3.60		0.95 ± 0.15	22

^a Selectivity relative to HEK293 (human embryonic kidney) cells.

Replacement of the phenyl with a pyrrolidine ring led to **3.55**, which was equipotent with the unsubstituted phenyl analogue, **3.03** (EC₅₀ 0.30 μM). The introduction of the larger morpholine group (**3.57**, EC₅₀ 0.93 μM), the partially saturated 1-cyclohexene group (**3.59**, EC₅₀ 0.78 μM) and, the fully reduced cyclohexyl group (**3.60**, EC₅₀ 0.95 μM) led to a series of compounds with essentially equipotent activity against *T.b. brucei* though they were generally less active than **3.03**.

3.5.3. Replacement of the phenyl with 5-membered heterocyclic groups

Given that the activity of the pyrrolidine analogue (**3.55**) was comparable to the unsubstituted phenyl (**3.03**), further investigation of this system was warranted. As such, a number of 5-membered heterocycles were synthesised from the previously prepared intermediate, **3.48**, using copper(I) iodide, with potassium carbonate and D,L-proline in a CEM microwave. This led to the successful isolation of the desired product in low to moderate yields (Table 3.9) as well as the isolation of the des-bromo side-product, **3.63**, in some instances as demonstrated in Scheme 3.5.



Scheme 3.5 Synthesis of analogues of the phenyl ring with 5-membered heterocyclic groups, such as the pyrrole (**3.62**) as shown.

Table 3.9 summarises the biological activity for these compounds against *T.b. brucei*. Whilst the pyrrole (**3.62**) was well tolerated with an EC_{50} of $0.21 \mu\text{M}$ against *T.b. brucei*, the activity quickly dropped off as the number of nitrogens increased. Only the pyrazole analogue, **3.64**, showed low micromolar activity with an EC_{50} of $6.14 \mu\text{M}$. The imidazole (**3.65**) and triazoles (**3.66-3.68**) were all found to be completely inactive against *T.b. brucei*.

Table 3.9 *T.b. brucei* inhibitory activity of the 5-membered heterocyclic analogues of the 6-position.

ID	R	Yield	EC_{50} (μM)	SI ^a
3.62		19%	0.21 ± 0.03	189
3.64		71%	6.14 ± 0.90	
3.65		55%	$> 10^b$	
3.66		48%	$> 10^b$	
3.67		17%	$> 10^b$	
3.68		54%	$> 10^b$	

^a Selectivity relative to HEK293 (human embryonic kidney) cells

^b Compound found to have $< 50\%$ activity at $10.41 \mu\text{M}$

3.6. Selective *N*-alkylation of the amide -NH and free amine

The selective *N*-alkylation of the exocyclic amine and the amide -NH was then attempted. It was anticipated that the amide -NH would be more acidic than the exocyclic amine. This is evident when the resonance structures are examined for the amide, Figure 3.2a, when in carboximidic acid form the -NH would be more readily deprotonated by base. The pK_a values of similar amides⁹⁸ (**3.69**) and anilines⁹⁹ (**3.70**) have been examined and are shown in Figure 3.2b. It can be seen that the amide has a pK_a two orders of magnitude lower than that of the amine, in reality there would likely be an even greater difference given there is a pyrazine ring attached to the carbonyl and not just a methyl. The pyrazine is not only electron-withdrawing but its aromaticity, allowing for conjugation, should stabilize a negative charge on the amide anion.

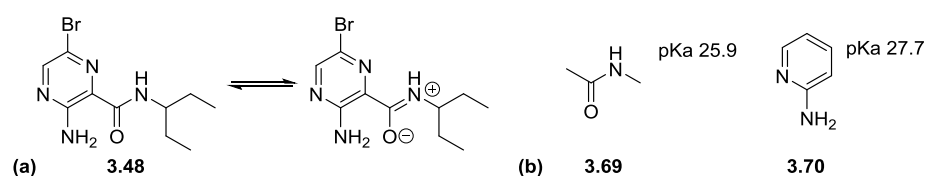


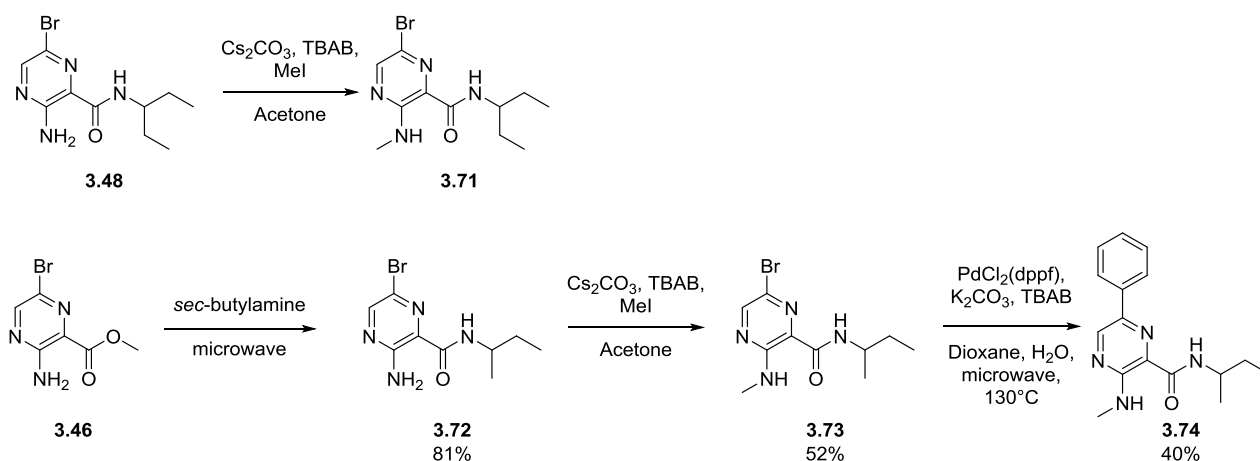
Figure 3.2 (a) Resonance structures of the amide; (b) pK_a of structurally similar compounds.

A review of the literature revealed that *N*-alkylation of the amide -NH was typically performed via deprotonation with sodium hydride and addition of methyl iodide.¹⁰⁰ While the literature shows that *N*-alkylation of the exocyclic amine could be performed by a number of routes. Organosilane reagents were commonly reported,^{101, 102} as was a combination of strong base (either sodium hydride or potassium *tert*-butoxide) and alkylhalide.^{103, 104} However, there was no literature where both of these functionalities were present on the same molecule.

As a result of the literature survey, milder conditions were chosen in order to attempt the synthesis of the amide *N*-alkylated analogue (**3.78**). Given the more acidic nature of the amide -NH, it was hypothesised that a mild base such as potassium carbonate may deprotonate the amide -NH to allow alkylation with minimal deprotonation of the exocyclic amine. However, under these conditions only starting material was recovered from the reaction mixture, indicating that the base was not strong enough to deprotonate the amide -NH.

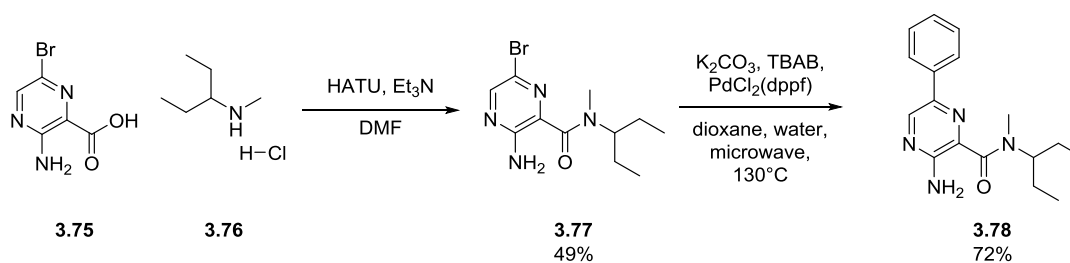
Given that only starting material was recovered, none of the nitrogens in the system were seen to be nucleophilic enough for alkylation to occur directly. Yet employing a stronger base by way of cesium carbonate or sodium hydride led instead to alkylation of the exocyclic amine (**3.71**). There are a number of possible mechanistic explanations for this. The stronger base could deprotonate the exocyclic amine, or it could deprotonate the amide resulting in electrons being pushed into the ring making the amine more nucleophilic and enabling alkylation. Alternatively, the anionic amide could pull a hydrogen off of the amine thereby increasing the nucleophilicity of the amine. Due to the sterically hindered nature of the amide it is likely that this would have been alkylated second. It is possible to confirm the alkylation of the free amine through ^1H NMR analysis. In Figure 3.3a) a peak for the amide $-\text{NH}$ is clearly seen at 8.10 ppm and a broad stretch for the exocyclic amine at 7.70 ppm. However, in the ^1H NMR of the methylated amine there is no longer a peak corresponding to the exocyclic amine and a second $-\text{NH}$ peak is present.

As it was hypothesised that the bulky amide side chain could be influencing the selectivity by sterically hindering the amide position the methylation was attempted on **3.72**. Compound **3.72** could be obtained from the reaction of **3.46** with *sec*-butylamine in good yields (Scheme 3.6). Given that the *sec*-butylamine side chain is less hindered and has been shown to be active against *T.b. brucei* it was thought that it may help facilitate *N*-alkylation. Utilising cesium carbonate as the base in the presence of TBAB and methyl iodide the methylation was determined to have taken place on the exocyclic amine again by the presence of diagnostic ^1H NMR signals to give **3.73**. Given this it appeared that the *sec*-butylamine side chain was still too hindered for the methylation to occur.



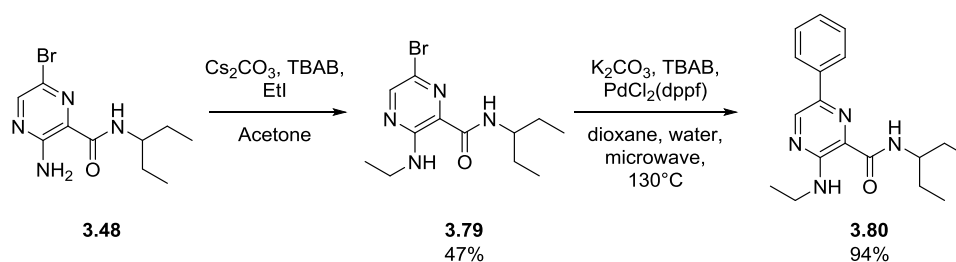
Scheme 3.6 Attempted synthesis of the amide N-alkylated analogue led instead to the alkylation of the free amine under a number of different conditions.

Therefore, an alternative synthesis was designed which involved the coupling of methyl-(3-pentyl)-amine hydrochloride (**3.76**) directly to the carboxylic acid (**3.75**) as shown in Scheme 3.7. Initially, conditions utilising EDCI, DMAP, triethylamine in *N,N*-dimethylformamide were trialed however the reaction was unsuccessful. As an alternative, an amide coupling with HATU was employed. It is well reported that HATU gives faster and more efficient couplings when secondary amines are involved given the hydrogen bond that forms with the amine -NH .¹⁰⁵ The amide coupling utilising HATU, with triethylamine in *N,N*-dimethylformamide did lead to the successful isolation of the desired intermediate (**3.77**) though the reaction was very slow and did not go to completion. This could then be coupled with phenylboronic acid via a Suzuki reaction to give the final product (**3.78**) in good yield.



Scheme 3.7 Selective synthesis of the amide N-alkylated analogue via amide coupling.

Utilising cesium carbonate, TBAB and ethyl iodide in acetone it was also possible to synthesise the ethylated amine intermediate, **3.79** (Scheme 3.8). This could then be coupled with phenylboronic acid using the previously established conditions for the Suzuki reaction to obtain the ethylated analogue, **3.80**, in good yields.



Scheme 3.8 Synthesis of the ethylated amine analogue, 3.80.

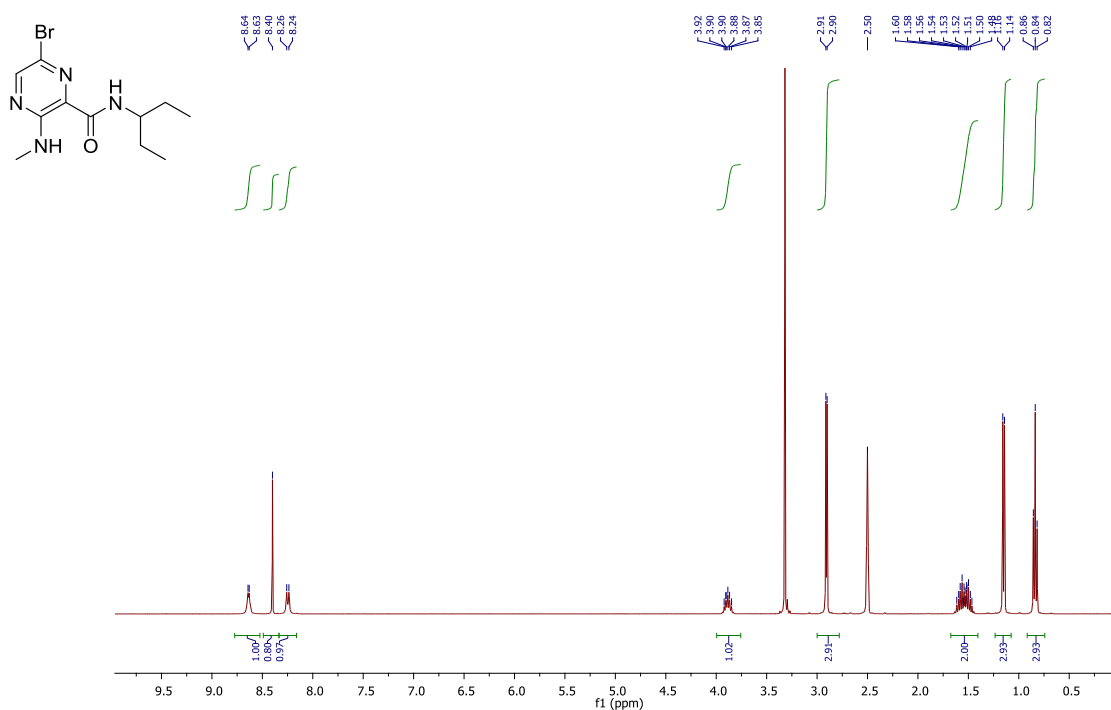
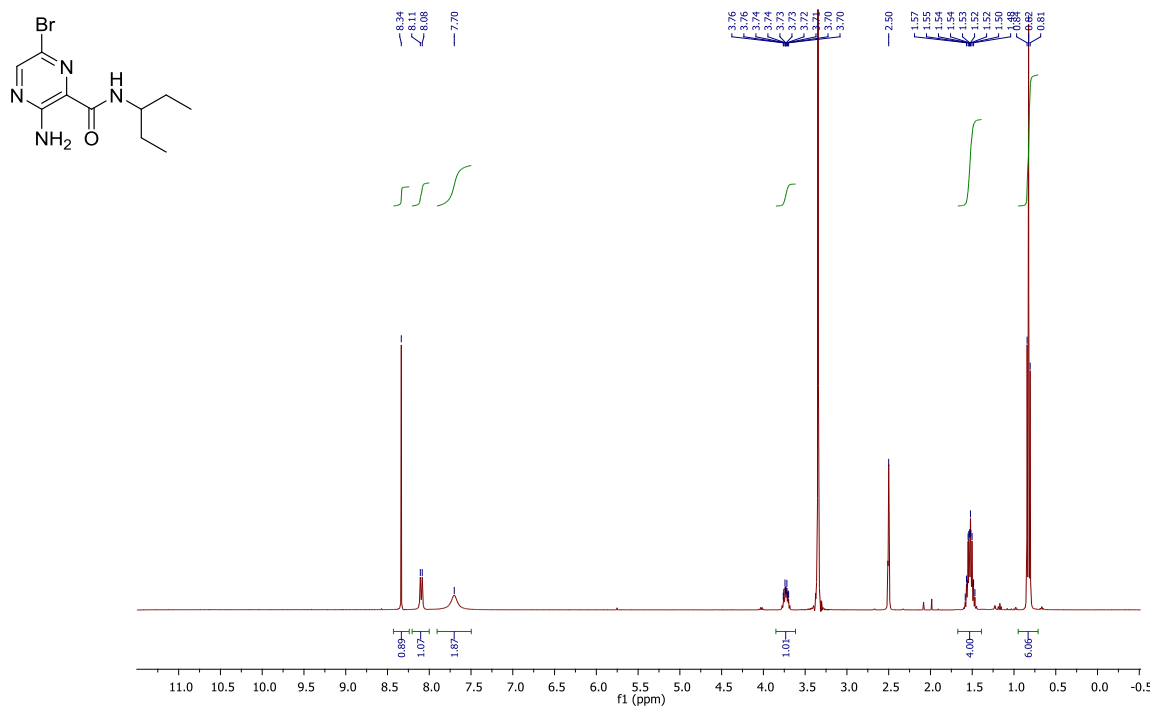
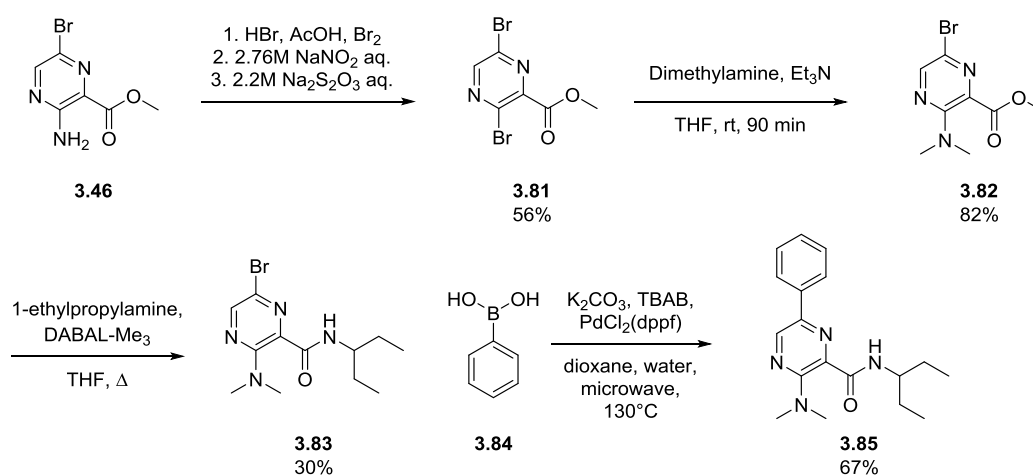


Figure 3.3a) ¹H NMR of **3.48** where a peak for the amide –NH and a broad stretch belonging to the exocyclic amine are clearly seen at 8.10 ppm and 7.70 ppm respectively; **b)** ¹H NMR confirming methylation occurs on the exocyclic amine. The presence of two –NH peaks at 8.63 ppm and 8.25 ppm and the absence of a –NH₂ broad stretch in the spectrum.

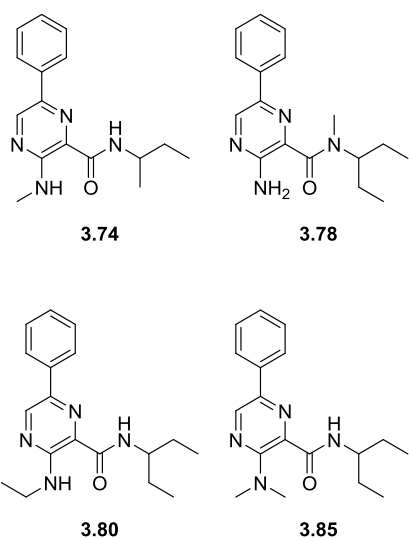
In order to synthesise the dimethylated amine analogue it was necessary to first perform a Sandmeyer reaction to convert the free amine into the bromine, **3.81**, Scheme 3.9. Combining **3.81** with dimethylamine gave exclusively the desired product, **3.82** in good yield. However, the previously established amide conditions to install the 1-ethylpropylamine side chain were unsuccessful due to the relative unreactivity of the starting material. Direct amide formation from unactivated esters can be achieved through the generation of aluminium amides through treatment of an amine with trimethylaluminium. However, due to the pyrophoric nature of trimethylaluminium, an adduct of trimethylaluminium and DABCO, DABAL-Me₃, was employed. This aluminium amide could then react with the ester to give the desired amide product, **3.83** in moderate yields. Once the desired intermediate had been obtained the Suzuki coupling was performed and led to the desired analogue, **3.85** in good yield.



Scheme 3.9 Synthesis of the dimethylated amine analogue, **3.85**.

Table 3.10 summarises the biological activity for these compounds against *T.b. brucei*.

Table 3.10 *T.b. brucei* inhibitory activity of *N*-alkylated derivatives.



ID	EC ₅₀ (μM)	SI ^a
3.74	1.3 ^b	
3.78	> 10 ^c	
3.80	> 10 ^c	
3.85	3.38 ± 0.31	12

^a Selectivity relative to HEK293 (human embryonic kidney) cells.

^b Experiment performed as *n*=1.

^c Compound found to have < 50% activity at 10.41 μM.

It could be seen that *N*-alkylation of the amide -NH (**3.78**) led to a significant loss in activity suggesting the amide is involved in a critical interaction, such as hydrogen bonding, within the receptor of the putative target. Whereas *N*-alkylation of the free amine (**3.74**) was equally as active as the parent compound (**128**, EC₅₀ 0.43 μM), extension to the ethyl (**3.80**) led to an approximately two-fold loss in activity and dimethylation led to a complete loss in activity (**3.85**, EC₅₀ >10 μM). This suggests that at least one hydrogen bond donor is required at this position in order to maintain activity against *T.b. brucei*.

3.7. Synthesis of alternate core units to the pyrazine scaffold

A number of analogues of the pyrazine core were also identified that were of interest (Figure 3.4). It was thought that alterations to the pyrazine core may lead to an improvement in the metabolic stability of these compounds in human liver microsomes.

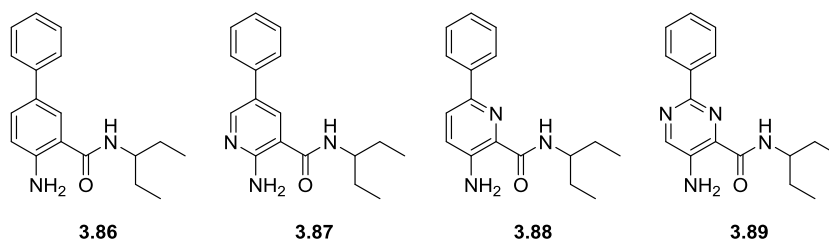
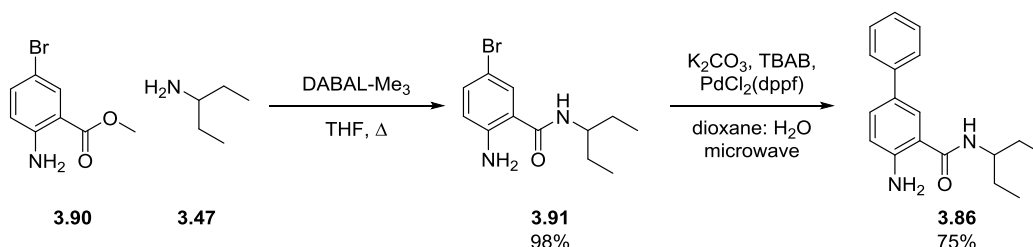


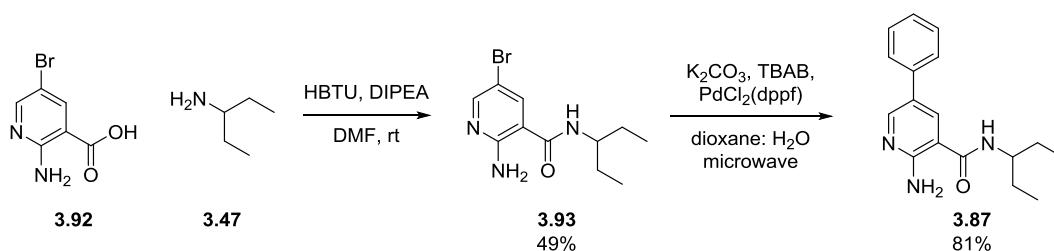
Figure 3.4 Pyrazine core analogues.

Initially, the focus was on removing both of the nitrogens from the pyrazine core and then re-introducing them one by one. In order to access **3.86**, methyl 2-amino-5-bromobenzoate (**3.90**) was combined with 1-ethylpropylamine in a CEM microwave, however no reaction was observed. Replacement of the pyrazine with an electron rich phenyl group resulted in the carbonyl being less electrophilic and not as reactive towards the nucleophile under these conditions. As a result the methyl 2-amino-5-bromobenzoate (**3.90**) was instead refluxed with DABAL-Me₃ and **3.47** in order to obtain the desired intermediate, **3.91** (Scheme 3.10). A Suzuki reaction to install the phenyl group was then performed in accordance with the previously established conditions to give the desired product, **3.86** in good yields.



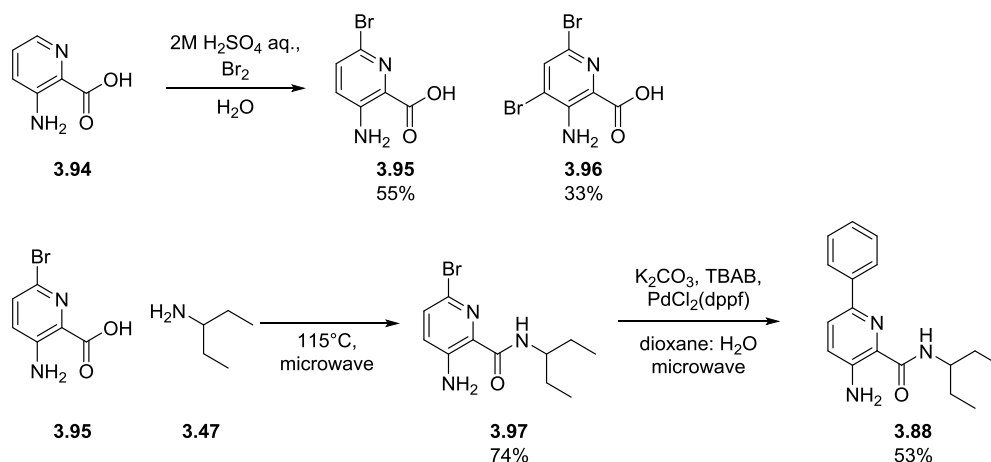
Scheme 3.10 Synthesis of the phenyl core analogue.

Synthesis of the nicotinamide analogue (**3.87**) was performed as shown in Scheme 3.11. 2-Amino-5-bromonicotinic acid (**3.92**) was coupled to 1-ethylpropylamine (**3.47**) in a reaction mediated by HBTU and DIPEA in *N,N*-dimethylformamide. This was then followed by a Suzuki coupling to achieve the desired product, **3.87** in good yields.



Scheme 3.11 Synthesis of the nicotinamide regioisomer of the central core.

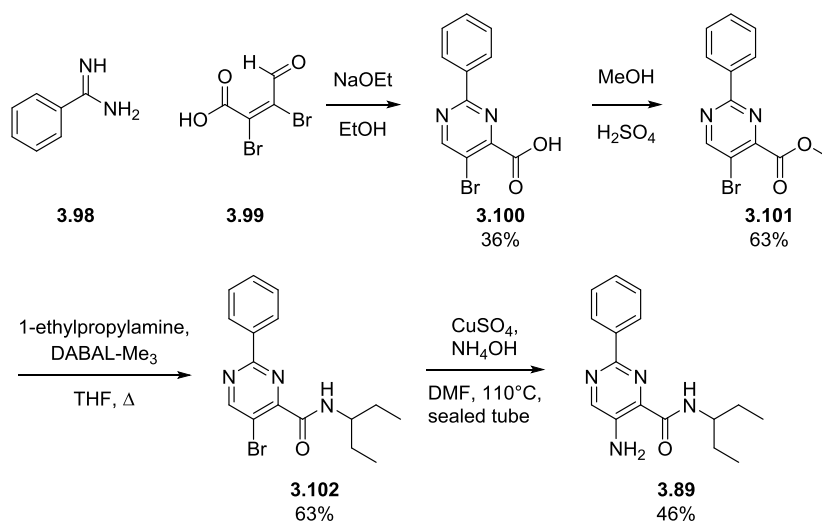
Synthesis of the picolinamide analogue (**3.88**) could be performed as shown in Scheme 3.12. Methyl 3-aminopicolinate (**3.94**) was initially brominated to give **3.95** in moderate yield. In addition to the isolation of **3.95**, there was an additional 33% of methyl 3-amino-4,6-dibromopicolinate (**3.96**) recovered. A NOESY experiment was performed and no cross-coupling was observed between the free amine and the aromatic proton. This was taken as confirmation of the 4,6-dibromination substitution pattern as shown. It was then possible to form the amide (**3.97**) using the previously established conditions in good yield, prior to the Suzuki coupling which gave the desired product (**3.88**) in good yields.



Scheme 3.12 Synthesis of the picolinamide regioisomer of the central core.

In order to obtain the pyrimidine core (**3.89**), benzamidine (**3.98**) and mucobromic acid (**3.99**) were reacted to give the resultant pyrimidinecarboxylic acid (**3.100**) (Scheme 3.13). The proposed mechanism for this reaction can be seen in Figure 3.5. A subsequent amide coupling with EDCI, DMAP and 1-ethylpropylamine was attempted, however this reaction failed. As such, the acid was esterified with methanol and sulphuric

acid to give **3.101**. This was then used in a reaction with DABAL-Me₃ and 1-ethylpropylamine to form the amide (**3.102**) before subsequent conversion of the aryl bromide to the free amine to obtain the desired product, **3.89**.



Scheme 3.13 Synthesis of the pyrimidine central core analogue.

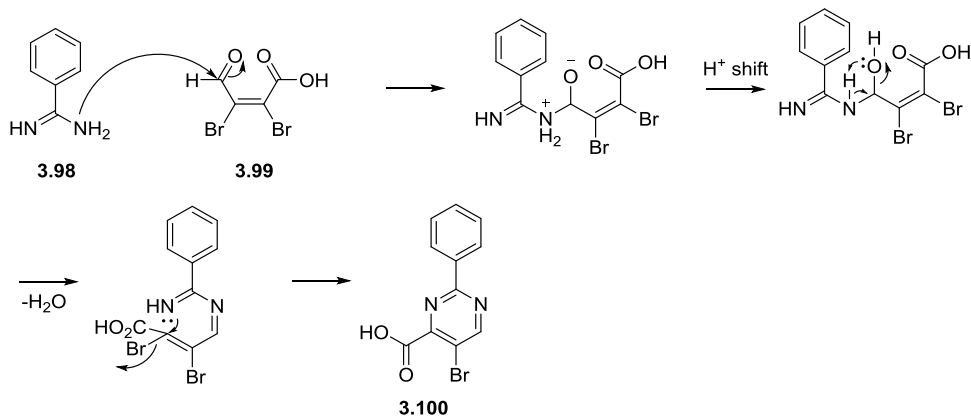
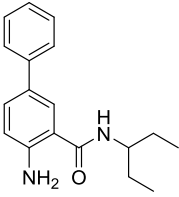
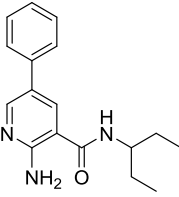
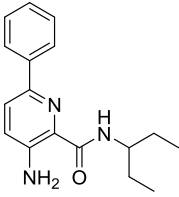
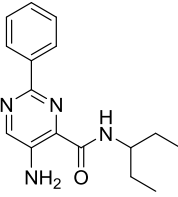


Figure 3.5 Mechanism for the formation of the pyrimidine core from benzamidine hydrochloride and mucobromic acid.

Biological analysis of these compounds for their activity against *T.b. brucei* was performed and the results summarised in Table 3.11.

Table 3.11 *T.b. brucei* inhibitory activity of pyrazine core derivatives.

	ID	EC ₅₀ (μM)
	3.86	> 10 ^a
	3.87	> 10 ^a
	3.88	> 10 ^a
	3.89	> 10 ^a

^a Compound found to have < 50% activity at 10.41 μM.

From this data it is clear that removal of one or both of the nitrogens from the pyrazine ring leads to a complete loss of activity against *T.b. brucei* in this assay (**3.86-3.89**). This indicates that the pyrazine ring is essential for the activity of this series and it is likely that the nitrogen atoms are involved in critical interactions with the putative target.

3.8. Biological analysis of compounds against *T. vivax* and *T. congolense*

A selection of compounds were analysed by researchers at the Swiss Tropical and Public Health Institute as part of the GALVmed project. The compounds were tested *ex vivo* against *T. vivax* and *in vivo* against *T. congolense*, both of which are causative agents for animal trypanosomiasis in Western and Eastern Africa, respectively.⁹⁰ Diminazene and isometamidium are routinely used in the treatment of animal trypanosomiasis though both have a multitude of side effects associated with their use.^{91, 92} They have both been included as standards in these assays. Table 3.12 summarises the results of the biological assays.

Table 3.12 *T. vivax* and *T. congolense* inhibitory activity of selected compounds.

ID	<i>T. vivax</i> EC ₅₀ (μM)	<i>T. congolense</i> EC ₅₀ (μM)
3.74	39	165
3.52	19	15
3.45	24	14
Diminazene^a	0.34	0.25
Isometamidium^a	0.0006	0.0006

^a Compound included as a standard control.

In general the compounds that were tested exhibited micromolar activity against both *T. vivax* and *T. congolense*. None of the compounds were found to be as potent as diminazene or isometamidium in these assays.

3.9. Physicochemical analysis of selected analogues

Assessment of the drug-likeness of a selection of analogues was again made and the results summarised in Table 3.13. The MW of these analogues were still, in general, quite low ranging from 284-327 g mol⁻¹. The PSA values were also relatively low with the exception of **3.53**, which was somewhat higher than the upper limit of 90 Å² that is the generally acknowledged cut off value for potential CNS penetration.⁵⁶ In general, the distribution coefficients were slightly higher than the earlier analogues being in the range of 4.2-5.3. Solubility was again an issue with all of the analogues exhibiting poor solubility. The plasma protein binding of these compounds was quite high with values in the range of 96.4-98.2%, which could adversely affect the ability of the compounds to dissociate and cross the BBB.⁵⁶ The MPO score, first introduced in Chapter 1, was used to assess and balance the effects of several variables (the lipophilicity, distribution coefficient, MW, PSA, number of hydrogen bond donors and pK_a) on a compounds potential to cross the BBB.⁵⁸ The MPO calculations (seen in Table 3.14) demonstrated that in all cases the high cLogD of these compounds was detrimental to the overall MPO score obtained. Despite being inactive against *T.b. brucei* in the assay,

3.78 exhibited the highest MPO score of 4.6 which can be attributed to the removal of the hydrogen bond donating amide –NH. Despite compound **3.85** having the lowest PSA value in the series it had an MPO score of 4.0 due to the much higher LogD value.

The compounds were still generally susceptible to metabolism by human liver microsomes, though an improvement was observed upon alkylation of the free amine, **3.85**. There was also a benefit observed with multiple substitutions on the phenyl ring (2-nitrile, 4-fluoro; **3.53**) and also the 4-fluoro substituted phenyl (**3.52**), which may indicate that substitutions in this region block some sites of metabolism.

Table 3.13 Key physicochemical parameters and in vitro metabolic stability of selected compounds.

ID	MW	PSA (Å ²) ^a	LogD ^b			Solubility (µg/ml) ^c	cPPB ^d (%)	In vitro CL _{int} (µl/min/mg protein) ^e	Microsome- Predicted E _H ^e	MPO
			pH 7.4	pH 2	pH 6.5					
3.51	318.8	80.9	4.8	<1.6	<1.6	98.2	102	0.80	4.1	
3.52	302.4	80.9	4.4	3.1-6.3	3.1-6.3	96.4	84	0.77	4.3	
3.53	327.4	104.7	4.2	<1.6	<1.6	96.6	66	0.72	3.9	
3.78	284.4	72.1	4.8	6.3-12.5	1.6-3.1	96.4	155	0.86	4.6	
3.85	312.4	66.9	>5.3 ^f	1.6-3.1	<1.6	98.1	55	0.68	4.0	

^a Calculated using ACD/Labs software, version 9.

^b Measured using the chromatographic gLogD technique.

^c Kinetic solubility determined by nephelometry.

^d Human plasma protein binding estimated using a chromatographic method.

^e In vitro intrinsic clearance determined in human liver microsomes and predicted hepatic extraction ratio calculated from in vitro data.

^f Measured using the chromatographic cPPB technique.

Figure 3.14 CNS MPO composite score calculations^a for compounds 3.51-3.53 and 3.78 and 3.85.

3.51

CNS MPO Calculator		
Property	Value	T0
cLogP	3.87	0.565
cLogD	4.8	0
PSA	80.9	1
MW	318.8	1
HBD	2	0.5
pK _a	0.81	1
CNS MPO		4.1

3.52

CNS MPO Calculator		
Property	Value	T0
cLogP	3.41	0.795
cLogD	4.4	0
PSA	80.9	1
MW	302.4	1
HBD	2	0.5
pK _a	0.83	1
CNS MPO		4.3

3.53

CNS MPO Calculator		
Property	Value	T0
cLogP	3.26	0.87
cLogD	4.2	0
PSA	104.7	0.51
MW	327.4	1
HBD	2	0.5
pK _a	0.73	1
CNS MPO		3.9

3.78

CNS MPO Calculator		
Property	Value	T0
cLogP	3.49	0.755
cLogD	4.8	0
PSA	72.1	1
MW	298.4	1
HBD	1	0.833
pK _a	0.81	1
CNS MPO		4.6

3.85

CNS MPO Calculator		
Property	Value	T0
cLogP	3.92	0.54
cLogD	5.3	0
PSA	66.9	1
MW	312.4	1
HBD	2	0.5
pK _a	0.64	1
CNS MPO		4.0

^a An active CNS MPO calculator is available to download from Wager, T. T. et al. Moving beyond rules: The development of a central nervous system multiparameter optimization (CNS MPO) approach to enable alignment of druglike properties. ACS Chem. Neurosci. **2010**, 1, 435-449.

^b Where green indicates a physicochemical property which is in the optimal range, yellow indicates a physicochemical property which is considered to be less optimal and red indicates a physicochemical property which is in an undesirable range.

3.10. Future work

There is a clear SAR picture emerging for this series of compounds and the assessment of predictive ADME and MPO scores reveals these compounds to be generally drug-like and favourable for further development. A number of areas have been identified where changes were not well tolerated though there is still much investigation required to definitively identify the pharmacophore. The priority must be to address the solubility and metabolic stability of these compounds.

There are a number of core changes that could still be attempted in order to try and improve the solubility and metabolism of this series as a whole as shown in Figure 3.6. For instance, it is possible to replace each of the pyrazine nitrogens with a nitrile group, which has been shown to act as an isostere of an endocyclic nitrogen, replacing the water-mediated hydrogen-bond bridges.¹⁰⁶ It may also be interesting to synthesise a bicyclic core, such as **3.105**, which may lead to an improvement in the metabolic stability of the series. However, the SAR indicates that the presence of one hydrogen bond donor from the amine is required for activity and this would need to be taken into account when designing future analogues.

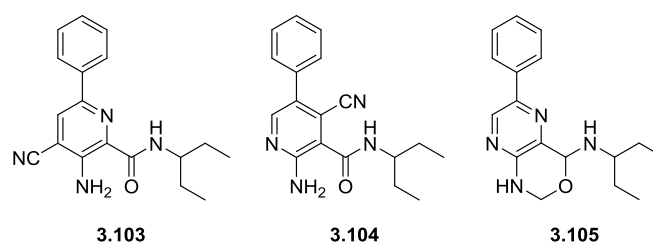


Figure 3.6 Analogues which could be targeted in order to improve the metabolic stability and solubility of this series.

3.11. Experimental

General Procedure 3-A1: Suzuki coupling

The relevant carboxamide (1.0 eq.), potassium carbonate (4.0 eq.), phenylboronic acid (1.2 eq.) and TBAB (0.1 eq.) were combined in a microwave reactor vessel with a 4:1 mix of 1,4-dioxane and water (0.5 M final concentration). The reaction mixture was de-gassed by bubbling nitrogen through for 2 min prior to the addition of either PdCl₂ (0.05 eq.) and dppf (0.055 eq.) or PdCl₂(dppf) (0.05 eq.). The reaction mixture was irradiated in a CEM microwave at 130 °C for the time specified. The reaction was diluted with ethyl acetate and filtered through celite and the filtrate collected. The solvent was removed to give the crude product which was purified by column chromatography, eluting with 15% ethyl acetate/petroleum spirits to give the desired product.

General Procedure 3-B1: Coupling of secondary aromatic amines

3-Amino-6-bromo-*N*-(pentan-3-yl)pyrazine-2-carboxamide (1.0 eq.), copper (I) iodide (0.15 eq.), potassium carbonate (2.0 eq.) and D,L-proline (0.3 eq.) were added to DMSO (0.5 M final concentration). To the reaction mixture was added the relevant secondary aromatic amine (8.0 eq.) before the reaction was transferred to a CEM microwave and heated to 90 °C for the time specified. The reaction mixture was poured into a saturated aqueous solution of sodium bicarbonate and the product was extracted with ethyl acetate three times. The organic layers were combined and washed once with a saturated aqueous solution of sodium chloride before being dried with magnesium sulphate. The crude material was purified by column chromatography, eluting with 10% ethyl acetate/petroleum spirits to give the desired product.

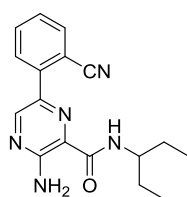
3-Amino-6-bromo-*N*-(pentan-3-yl)pyrazine-2-carboxamide (3.48)



Methyl 3-amino-6-bromopyrazine-2-carboxylate (500 mg, 2.15 mmol) was combined with 1-ethylpropylamine (2.5 ml, 21.50 mmol) in a microwave reactor vessel and irradiated in a CEM microwave for 4 h at 115 °C. The reaction mixture was transferred to a RBF and the solvent removed under reduced pressure to give the crude material which was recrystallised from acetic acid

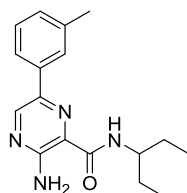
and water to give the carboxamide as a pale-yellow solid (445 mg, 72%). HPLC – rt 11.59 min > 99% purity at 254 nm; LRMS $[M+H]^+$ 287 m/z (^{79}Br), 289 m/z (^{81}Br); HRMS $[M+H]^+$ 287.0502 m/z, found 287.0502 m/z (^{79}Br), 289.0482 m/z, found 289.0483 m/z (^{81}Br); ^1H NMR (400 MHz, DMSO) δ 8.34 (s, 1H), 8.10 (d, $J = 9.3$ Hz, 1H), 7.70 (s, 2H), 3.82 – 3.65 (m, 1H), 1.65 – 1.37 (m, 4H), 0.83 (t, $J = 7.4$ Hz, 6H); ^{13}C NMR (101 MHz, DMSO) δ 164.7, 154.2, 148.5, 125.7, 121.5, 52.0, 26.8 (2C), 10.7 (2C).

3-Amino-6-(2-cyanophenyl)-N-(pentan-3-yl)pyrazine-2-carboxamide (**3.49**)



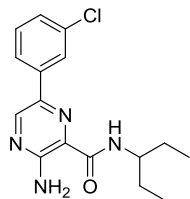
The title compound was prepared according to General Procedure 3-A1 and was irradiated for 2 h and 30 min. Title compound was isolated as a pale-yellow solid (22 mg, 20%). HPLC – rt 8.38 min > 97% purity at 254 nm; LRMS $[M+H]^+$ 310.3 m/z; HRMS $[M+H]^+$ 310.1662 m/z, found 310.1664 m/z; ^1H NMR (400 MHz, DMSO) δ 8.89 (s, 1H), 8.15 (d, $J = 7.6$ Hz, 1H), 8.07 (d, $J = 9.3$ Hz, 1H), 7.96 (dd, $J = 7.8, 1.1$ Hz, 1H), 7.79 (td, $J = 7.8, 1.4$ Hz, 1H), 7.57 (td, $J = 7.6, 1.1$ Hz, 1H), 3.90 – 3.63 (m, 1H), 1.73 – 1.34 (m, 4H), 0.86 (t, $J = 7.4$ Hz, 6H); ^{13}C NMR (101 MHz, DMSO) δ 165.5, 154.4, 145.5, 138.3, 135.5, 135.4, 133.5, 128.6, 127.5, 123.5, 120.5, 107.8, 51.8, 26.9 (2C), 10.4 (2C). *Note: The amine peak appears as a broad stretch under the aromatic protons, as such it has not been reported.

3-Amino-N-(pentan-3-yl)-6-(m-tolyl)pyrazine-2-carboxamide (**3.50**)



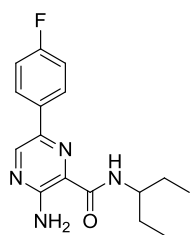
The title compound was prepared according to General Procedure 3-A1 and was irradiated for 30 min. Title compound was isolated as a pale-yellow solid after recrystallisation from acetic acid/water (38 mg, 37%). HPLC – rt 11.28 min 100% purity at 254 nm. LRMS $[M+H]^+$ 299.3 m/z; HRMS $[M+H]^+$ 299.1866 m/z, found 299.1868 m/z; ^1H NMR (400 MHz, DMSO) δ 8.81 (s, 1H), 8.22 (d, $J = 9.3$ Hz, 1H), 7.97 – 7.82 (m, 2H), 7.62 (s, 2H), 7.37 (t, $J = 7.6$ Hz, 1H), 7.20 (d, $J = 7.5$ Hz, 1H), 3.91 – 3.68 (m, 1H), 2.40 (s, 3H), 1.71 – 1.47 (m, 4H), 0.89 (t, $J = 7.4$ Hz, 6H); ^{13}C NMR (101 MHz, DMSO) δ 165.8, 154.0, 143.8, 138.4, 137.8, 135.9, 128.7, 128.7, 125.8, 124.4, 122.7, 51.8, 26.9 (2C), 21.2, 10.6 (2C).

3-Amino-6-(3-chlorophenyl)-N-(pentan-3-yl)pyrazine-2-carboxamide (3.51)



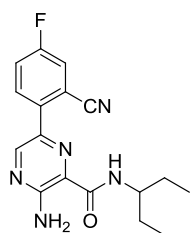
The title compound was prepared according to General Procedure 3-A1 and was irradiated for 30 min. Title compound was isolated as a yellow solid after recrystallisation from acetic acid/water (46 mg, 41%). LRMS $[M+H]^+$ 319.2 m/z; HRMS $[M+H]^+$ 319.132 m/z, found 319.1334 m/z; 1H NMR (400 MHz, DMSO) δ 8.88 (s, 1H), 8.32 (d, $J = 9.3$ Hz, 1H), 8.18 (t, $J = 1.7$ Hz, 1H), 8.10 (d, $J = 7.9$ Hz, 1H), 7.73 (s, 2H), 7.50 (t, $J = 7.9$ Hz, 1H), 7.47 – 7.35 (m, 1H), 3.90 – 3.71 (m, 1H), 1.70 – 1.47 (m, 4H), 0.88 (t, $J = 7.4$ Hz, 6H); ^{13}C NMR (101 MHz, DMSO) δ 165.7, 154.3, 144.1, 138.2, 136.6, 133.8, 130.5, 127.7, 125.0, 124.7, 124.0, 38.9, 26.9 (2C), 10.7 (2C).

3-Amino-6-(4-fluorophenyl)-N-(pentan-3-yl)pyrazine-2-carboxamide (3.52)



The title compound was prepared according to General Procedure 3-A1 and was irradiated for 30 min. Title compound was isolated as a yellow solid after recrystallisation from acetic acid/water (54 mg, 51%). HPLC – rt 10.95 min > 99% purity at 254 nm. LRMS $[M+H]^+$ 303.2 m/z; HRMS $[M+H]^+$ 303.1616 m/z, found 303.1622 m/z; 1H NMR (400 MHz, DMSO) δ 8.82 (s, 1H), 8.26 (d, $J = 9.3$ Hz, 1H), 8.21 – 8.09 (m, 2H), 7.63 (s, 2H), 7.30 (t, $J = 8.9$ Hz, 2H), 3.90 – 3.69 (m, 1H), 1.70 – 1.43 (m, 4H), 0.87 (t, $J = 7.4$ Hz, 6H); ^{13}C NMR (101 MHz, DMSO) δ 165.8, 162.2 ($J_{C-F} = 244$ Hz), 153.9, 143.6, 137.4, 132.5 ($J_{C-F} = 3$ Hz), 127.5 ($J_{C-F} = 8$ Hz), 124.4, 115.5 ($J_{C-F} = 21$ Hz), 51.9, 26.9 (2C), 10.7 (2C). *Note: there are multiple equivalent carbons in the ^{13}C NMR spectrum.

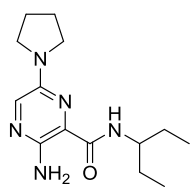
3-Amino-6-(2-cyano-4-fluorophenyl)-N-(pentan-3-yl)pyrazine-2-carboxamide (3.53)



The title compound was prepared according to General Procedure 3-A1 and was irradiated for 3 h. Title compound was isolated as a yellow solid after recrystallisation from acetic acid/water (10 mg, 10%). LRMS $[M+H]^+$ 328.2 m/z; HRMS $[M+H]^+$ 328.1568 m/z, found

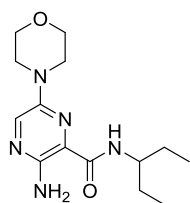
328.1574 m/z; ^1H NMR (400 MHz, DMSO) δ 8.86 (s, 1H), 8.20 (dd, $J = 9.0, 5.4$ Hz, 1H), 8.04 (d, $J = 9.3$ Hz, 1H), 7.98 (dd, $J = 8.7, 2.7$ Hz, 1H), 7.82 – 7.64 (m, 1H), 3.91 – 3.67 (m, 1H), 1.66 – 1.40 (m, 4H), 0.87 (t, $J = 7.4$ Hz, 6H); ^{13}C NMR (101 MHz, DMSO) δ 165.4, 161.0 ($J_{\text{C-F}} = 248$ Hz), 154.4, 145.5, 135.4 ($J_{\text{C-F}} = 3$ Hz), 134.8, 130.0 ($J_{\text{C-F}} = 8$ Hz), 123.5, 122.0 ($J_{\text{C-F}} = 25$ Hz), 121.1 ($J_{\text{C-F}} = 21$ Hz), 119.1 ($J_{\text{C-F}} = 9$ Hz), 109.5 ($J_{\text{C-F}} = 10$ Hz), 51.8, 26.9 (2C), 10.4 (2C). *Note: the amine peak is a broad peak under the aromatic protons and, as such it has not been reported.

3-Amino-N-(pentan-3-yl)-6-(pyrrolidin-1-yl)pyrazine-2-carboxamide (3.55)



3-Amino-6-bromo-N-(pentan-3-yl)pyrazine-2-carboxamide (100 mg, 0.35 mmol) was combined with pyrrolidine (2 ml, 24.35 mmol) and placed in a CEM microwave for 2 h at 180 °C. The excess pyrrolidine was removed under reduced pressure and the crude material was purified by column chromatography, eluting with 10% ethyl acetate/petroleum spirits. The title compound was isolated as an orange solid (58 mg, 60%) which could be further purified by recrystallisation with acetic acid/water to give an orange solid (25 mg, 26%). HPLC – rt 7.69 min > 98% purity at 254 nm; LRMS $[\text{M}+\text{H}]^+$ 278.3 m/z; HRMS $[\text{M}+\text{H}]^+$ 278.1975 m/z, found 278.1974 m/z; ^1H NMR (400 MHz, DMSO) δ 7.82 (s, 1H), 7.77 (d, $J = 9.3$ Hz, 1H), 6.52 (s, 2H), 3.85 – 3.58 (m, 1H), 3.38 (t, $J = 6.6$ Hz, 4H), 1.93 (td, $J = 6.7, 3.4$ Hz, 4H), 1.62 – 1.41 (m, 4H), 0.85 (t, $J = 7.4$ Hz, 6H); ^{13}C NMR (101 MHz, DMSO) δ 166.2, 147.5, 145.5, 133.6, 119.8, 51.2, 46.4 (2C), 26.9 (2C), 24.8 (2C), 10.4 (2C).

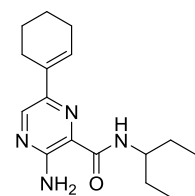
3-Amino-6-morpholino-N-(pentan-3-yl)pyrazine-2-carboxamide (3.57)



3-Amino-6-bromo-N-(pentan-3-yl)pyrazine-2-carboxamide (200 mg, 0.70 mmol) was dissolved in 1,4-dioxane (700 μl) prior to the addition of morpholine (120 μl , 1.40 mmol) and diisopropylethylamine (245 μl , 1.40 mmol). The reaction mixture was placed in a CEM microwave for 24 h at 180 °C. The reaction was incomplete by TLC, so additional morpholine (485 μl , 5.6 mmol) and diisopropylethylamine (975 μl , 5.6 mmol) was added before the reaction was returned to a CEM microwave for a further 6 h at 180 °C. By TLC the reaction was complete so all of

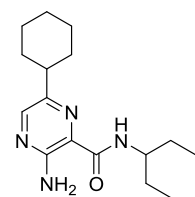
the volatiles were removed under reduced pressure and the crude material was purified by column chromatography, eluting with 20-50% ethyl acetate/petroleum spirits as a yellow oil (153 mg, 75%). HPLC – rt 6.69 min > 98% purity at 254 nm; LRMS $[M+H]^+$ 294.3 m/z; HRMS $[M+H]^+$ 294.1925 m/z, found 294.1924 m/z; ^1H NMR (400 MHz, DMSO) δ 8.11 (s, 1H), 7.81 (d, $J = 9.3$ Hz, 1H), 6.80 (s, 2H), 3.86 – 3.60 (m, 5H), 3.33 (d, $J = 9.3$ Hz, 4H), 1.68 – 1.37 (m, 4H), 0.84 (t, $J = 7.4$ Hz, 6H); ^{13}C NMR (101 MHz, DMSO) δ 166.0, 149.2, 146.9, 134.8, 120.0, 65.9, 51.5, 46.0, 26.9 (2C), 10.6 (2C). *Note: the doublet at 3.33ppm in the ^1H NMR is overlapping with the water signal and is assumed to account for 4 protons.

3-Amino-6-(cyclohex-1-en-1-yl)-N-(pentan-3-yl)pyrazine-2-carboxamide (3.59)



The title compound was prepared according to General Procedure 3-A1 and was irradiated for 30 min. Title compound was isolated as a yellow oil (142 mg, 57%). LRMS $[M+H]^+$ 289.2 m/z; ^1H NMR (400 MHz, DMSO) δ 8.39 (s, 1H), 7.98 (d, $J = 9.4$ Hz, 1H), 7.43 (s, 2H), 3.87 – 3.62 (m, 1H), 2.48 – 2.38 (m, 2H), 2.20 (dt, $J = 5.8, 3.7$ Hz, 2H), 1.71 (ddd, $J = 8.3, 5.8, 2.7$ Hz, 2H), 1.65 – 1.43 (m, 7H), 0.85 (t, $J = 7.4$ Hz, 6H); ^{13}C NMR (101 MHz, DMSO) δ 165.9, 153.5, 142.7, 140.4, 133.1, 125.1, 123.3, 51.6, 26.9 (2C), 25.2, 24.7, 22.3, 21.8, 10.6 (2C).

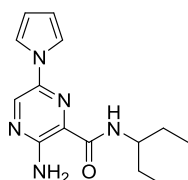
3-Amino-6-(cyclohexyl)-N-(pentan-3-yl)pyrazine-2-carboxamide (3.60)



3-Amino-6-(cyclohex-1-en-1-yl)-N-(pentan-3-yl)pyrazine-2-carboxamide (70 mg, 0.24 mmol) was dissolved in a 50% solution of ethyl acetate in ethanol (20 ml). This was loaded on to a ThalesNano H-Cube[®] with a 10% Pd/C CatCart[®]. The reaction was monitored by LCMS until no more starting material was present (~1 h) and the solvent was removed under reduced pressure to give the title compound as a yellow solid (24 mg, 34%). HPLC – rt 8.97 min > 99% purity at 254 nm; LRMS $[M+H]^+$ 291.3 m/z; HRMS $[M+H]^+$ 291.2179 m/z found 291.2180 m/z; ^1H NMR (400 MHz, DMSO) δ 8.14 (s, 1H), 7.98 (d, $J = 9.3$ Hz, 1H), 7.28 (s, 2H), 3.89 – 3.59 (m, 1H), 1.92 – 1.74 (m, 4H), 1.69 (d, $J = 12.1$ Hz, 1H), 1.65 – 1.20 (m, 9H), 0.84 (t, $J = 7.4$ Hz, 6H); ^{13}C NMR (101

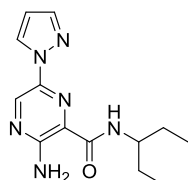
MHz, DMSO) δ 165.8, 153.6, 146.9, 144.7, 123.7, 51.5, 41.8, 32.1 (2C), 26.9 (2C), 26.0 (2C), 25.5, 10.6 (2C).

3-Amino-N-(pentan-3-yl)-6-(1H-pyrrol-1-yl)pyrazine-2-carboxamide (3.62)



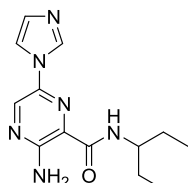
The title compound was prepared according to General Procedure 3-B1 and was irradiated for 150 min. The title compound was obtained as a yellow solid (18 mg, 19%). HPLC – rt 8.11 min 95% purity at 254 nm; LRMS $[M+H]^+$ 274.2 m/z; HRMS $[M+H]^+$ 274.1662 m/z, found 274.1663 m/z; 1H NMR (400 MHz, DMSO) δ 8.71 (s, 1H), 8.24 (d, $J = 9.3$ Hz, 1H), 7.84 – 7.69 (m, 2H), 7.47 (s, 2H), 6.39 – 6.17 (m, 2H), 3.79 (ddq, $J = 11.7, 7.7, 5.9$ Hz, 1H), 1.70 – 1.43 (m, 4H), 0.86 (t, $J = 7.4$ Hz, 6H); ^{13}C NMR (101 MHz, DMSO) δ 165.5, 152.9, 136.6, 136.5, 121.3, 118.3 (2C), 110.5 (2C), 52.0, 26.7 (2C), 10.8 (2C).

3-Amino-N-(pentan-3-yl)-6-(1H-pyrazol-1-yl)pyrazine-2-carboxamide (3.64)



The title compound was prepared according to General Procedure 3-B1 and was irradiated for 6 h. The title compound was obtained as a yellow solid (68 mg, 71%). HPLC – rt 7.28 min 94% purity at 254 nm; LRMS $[M+H]^+$ 275.2 m/z; HRMS $[M+H]^+$ 275.1615 m/z, found 275.1616 m/z; 1H NMR (400 MHz, DMSO) δ 8.97 (dd, $J = 2.5, 0.5$ Hz, 1H), 8.80 (s, 1H), 8.35 (d, $J = 9.3$ Hz, 1H), 7.84 – 7.73 (m, 1H), 7.73 – 7.46 (m, 2H), 6.59 (dd, $J = 2.4, 1.8$ Hz, 1H), 3.79 (qt, $J = 8.5, 5.6$ Hz, 1H), 1.73 – 1.43 (m, 4H), 0.86 (t, $J = 7.4$ Hz, 6H); ^{13}C NMR (101 MHz, DMSO) δ 165.3, 153.6, 141.4, 136.7, 136.4, 127.8, 120.9, 107.4, 52.1, 27.0 (2C), 10.9 (2C).

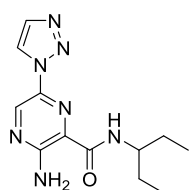
3-Amino-6-(1H-imidazol-1-yl)-N-(pentan-3-yl)pyrazine-2-carboxamide (3.65)



The title compound was prepared according to General Procedure 3-B1 and was irradiated for 1 h. The crude material was purified by column chromatography, eluting with 85%

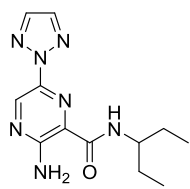
ethyl acetate/petroleum spirits to give the title compound as a yellow solid (26 mg, 55%). HPLC – rt 4.85 min 100% purity at 254 nm; LRMS $[M+H]^+$ 275.2 m/z; HRMS $[M+H]^+$ 275.1615 m/z, found 275.1615 m/z; ^1H NMR (400 MHz, DMSO) δ 8.74 (s, 1H), 8.68 (t, $J = 1.0$ Hz, 1H), 8.31 (d, $J = 9.3$ Hz, 1H), 8.08 (t, $J = 1.3$ Hz, 1H), 7.65 (s, 2H), 7.12 (t, $J = 1.3$ Hz, 1H), 3.88 – 3.65 (m, 1H), 1.71 – 1.45 (m, 4H), 0.86 (t, $J = 7.4$ Hz, 6H); ^{13}C NMR (101 MHz, DMSO) δ 165.2, 153.8, 137.4, 135.1, 134.0, 129.6, 121.7, 116.7, 52.1, 27.0 (2C), 10.8 (2C).

3-Amino-N-(pentan-3-yl)-6-(1H-1,2,3-triazol-1-yl)pyrazine-2-carboxamide (3.66)



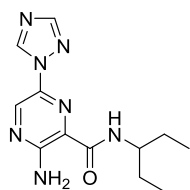
The title compound was prepared according to General Procedure 3-B1 and was irradiated for 10 h. The crude material was then purified by column chromatography, eluting 15% ethyl acetate/petroleum spirits to give the title compound as a yellow solid (46 mg, 48%). HPLC – rt 6.47 min 100% purity at 254 nm; LRMS $[M+H]^+$ 276.2 m/z; HRMS $[M+H]^+$ 276.1567 m/z, found 276.1568 m/z; ^1H NMR (400 MHz, DMSO) δ 9.22 (d, $J = 1.2$ Hz, 1H), 8.93 (s, 1H), 8.37 (d, $J = 9.3$ Hz, 1H), 8.02 (d, $J = 1.1$ Hz, 1H), 3.91 – 3.70 (m, 1H), 1.57 (qdd, $J = 13.7, 7.9, 6.5$ Hz, 4H), 0.86 (t, $J = 7.4$ Hz, 6H); ^{13}C NMR (101 MHz, DMSO) δ 164.9, 154.8, 138.0, 133.9, 133.6, 122.6, 121.7, 52.2, 27.0 (2C), 10.9 (2C). *Note: the free amine appeared as a very broad stretch under the aromatic protons and as such, has not been reported.

3-Amino-N-(pentan-3-yl)-6-(2H-1,2,3-triazol-2-yl)pyrazine-2-carboxamide (3.67)



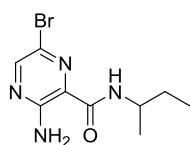
The title compound was isolated as a side product in the previous reaction as a yellow solid (16 mg, 17%). HPLC – rt 6.55 min 100% purity at 254 nm; LRMS $[M+H]^+$ 276.2 m/z; HRMS $[M+H]^+$ 276.1567 m/z, found 276.1569 m/z; ^1H NMR (400 MHz, DMSO) δ 8.81 (s, 1H), 8.17 (s, 2H), 7.98 (d, $J = 9.3$ Hz, 1H), 7.87 (d, $J = 9.3$ Hz, 2H), 3.93 – 3.66 (m, 1H), 1.70 – 1.40 (m, 4H), 0.86 (t, $J = 7.4$ Hz, 6H); ^{13}C NMR (101 MHz, DMSO) δ 164.9, 154.6, 139.4, 136.6 (2C), 136.0, 121.8, 51.9, 26.8 (2C), 10.6 (2C).

3-Amino-N-(pentan-3-yl)-6-(1H-1,2,4-triazol-1-yl)pyrazine-2-carboxamide (3.68)



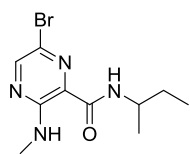
The title compound was prepared according to General Procedure 3-B1 and was irradiated for 8 h. The crude material was then purified by column chromatography, eluting with 20-30% ethyl acetate/petroleum spirits to give the title compound as a pale-yellow solid (52 mg, 54%). HPLC – rt 6.17 min 100% purity at 254 nm; LRMS $[M+H]^+$ 276.2 m/z; HRMS $[M+H]^+$ 276.1567 m/z, found 276.1570 m/z; ^1H NMR (400 MHz, DMSO) δ 9.72 (s, 1H), 8.71 (s, 1H), 8.38 (d, $J = 9.3$ Hz, 1H), 8.27 (s, 1H), 7.76 (d, $J = 57.8$ Hz, 2H), 3.79 (pd, $J = 8.7, 5.3$ Hz, 1H), 1.73 – 1.41 (m, 4H), 0.86 (t, $J = 7.4$ Hz, 6H); ^{13}C NMR (101 MHz, DMSO) δ 164.9, 154.5, 152.6, 142.3, 137.2, 133.9, 121.5, 52.2, 27.0 (2C), 10.9 (2C).

3-Amino-6-bromo-N-(sec-butyl)pyrazine-2-carboxamide (3.72)



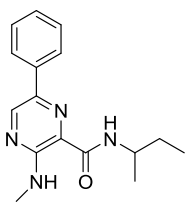
Methyl 3-amino-6-bromopyrazine-2-carboxylate (1.0 g, 4.31 mmol) was combined with *sec*-butylamine (4.35 ml, 43.10 mmol) in a microwave reactor vessel and irradiated in a CEM microwave for 6 h at 100 °C. The reaction mixture was transferred to a RBF and the solvent removed under reduced pressure to give the crude material which was purified by column chromatography, eluting with 10% ethyl acetate/petroleum spirits. The title compound was isolated as a yellow solid (950 mg, 81%). HPLC – rt 9.22 min > 96% purity at 254 nm; LRMS $[M+H]^+$ 273.1 m/z (^{79}Br), 275.1 m/z (^{81}Br); HRMS $[M+H]^+$ 273.0346 m/z, found 273.0346 m/z (^{79}Br), 275.0326 m/z, found 275.0326 m/z (^{81}Br); ^1H NMR (400 MHz, DMSO) δ 8.33 (s, 1H), 8.18 (d, $J = 8.8$ Hz, 1H), 7.70 (s, 2H), 3.89 (dt, $J = 21.7, 7.2$ Hz, 1H), 1.67 – 1.39 (m, 2H), 1.14 (d, $J = 6.6$ Hz, 3H), 0.84 (t, $J = 7.4$ Hz, 3H); ^{13}C NMR (101 MHz, DMSO) δ 164.1, 154.2, 148.5, 125.7, 121.5, 46.2, 28.6, 20.0, 10.8.

6-Bromo-N-(sec-butyl)-3-(methylamino)pyrazine-2-carboxamide (3.73)



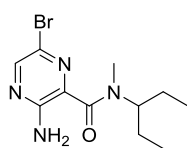
3-Amino-6-bromo-N-(sec-butyl)pyrazine-2-carboxamide (400 mg, 1.46 mmol) was dissolved in acetone (3 ml) prior to addition of cesium carbonate (1.43 g, 4.38 mmol), tetra-*n*-butylammonium bromide (94 mg, 0.29 mmol) and methyl iodide (275 μ l, 4.38 mmol). The resulting suspension was stirred for 72 h at ambient temperature before the reaction mixture was diluted with ethyl acetate and washed twice with water and brine. The resulting oil was purified by column chromatography, eluting with 10% ethyl acetate/petroleum spirits to give the title compound as a pale-yellow solid (220 mg, 52%). HPLC – rt 10.44 min > 95% purity at 254 nm; LRMS [M+H]⁺ 287.1 m/z (⁷⁹Br), 289.1 m/z (⁸¹Br); HRMS [M+H]⁺ 287.0502 m/z, found 287.0503 m/z (⁷⁹Br), 289.0482 m/z, found 289.0482 m/z (⁸¹Br); ¹H NMR (400 MHz, DMSO) δ 8.64 (d, *J* = 4.8 Hz, 1H), 8.40 (s, 1H), 8.25 (d, *J* = 8.7 Hz, 1H), 3.89 (dt, *J* = 21.6, 7.2 Hz, 1H), 2.91 (d, *J* = 4.9 Hz, 3H), 1.66 – 1.40 (m, 2H), 1.15 (d, *J* = 6.6 Hz, 3H), 0.84 (t, *J* = 7.4 Hz, 3H); ¹³C NMR (101 MHz, DMSO) δ 164.2, 153.7, 126.7, 120.4, 46.3, 28.5, 27.5, 20.0, 10.8. *Note: there is 1 carbon missing from the ¹³C NMR which is assumed to be overlapping with another signal.

N-(sec-Butyl)-3-(methylamino)-6-phenylpyrazine-2-carboxamide (3.74)



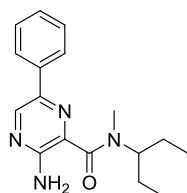
The title compound was prepared according to General Procedure 3-A1 and was irradiated for 30 min. Title compound was isolated as a yellow solid (40 mg, 40%). LRMS [M+H]⁺ 285.2 m/z; HRMS [M+H]⁺ 285.1710 m/z, found 285.1716 m/z; ¹H NMR (400 MHz, DMSO) δ 8.90 (s, 1H), 8.69 (d, *J* = 4.8 Hz, 1H), 8.39 (d, *J* = 8.7 Hz, 1H), 8.11 (d, *J* = 7.9 Hz, 2H), 7.48 (t, *J* = 7.6 Hz, 2H), 7.38 (t, *J* = 7.0 Hz, 1H), 4.07 – 3.82 (m, 1H), 2.99 (d, *J* = 4.8 Hz, 3H), 1.61 (dtq, *J* = 27.3, 13.6, 7.0 Hz, 2H), 1.22 (d, *J* = 6.6 Hz, 3H), 0.89 (t, *J* = 7.4 Hz, 3H); ¹³C NMR (101 MHz, DMSO) δ 165.4, 153.6, 143.3, 136.7, 136.0, 128.7, 127.9, 125.4, 125.3, 46.2, 28.7, 27.3, 20.1, 10.8.

3-Amino-6-bromo-N-(sec-butyl)-N-methylpyrazine-2-carboxamide (3.77)



3-Amino-6-bromopyrazine-2-carboxylic acid (100 mg, 0.46 mmol) was dissolved in *N,N*-dimethylformamide (1 ml) and to this was added HATU (192 mg, 0.51 mmol) and, trimethylamine (212 μ l, 1.52 mmol). The reaction mixture was stirred at ambient temperature for 10 min after which the methyl-(3-pentyl)-amine hydrochloride (70 mg, 0.51 mmol) was added and the reaction mixture was heated to 80 $^{\circ}$ C. After 18 h there was a trace amount of desired product evident by TLC so further methyl-(3-pentyl)-amine hydrochloride (250 mg, 1.84 mmol) and triethylamine (260 μ l, 1.84 mmol) were added and the reaction mixture heated to 120 $^{\circ}$ C. After 1 week of heating the reaction mixture there was approximately 50% conversion by TLC. The reaction mixture was cooled to ambient temperature and concentrated *in vacuo* prior to extraction twice with ethyl acetate. The organic layers were combined, and washed with a saturated aqueous solution of sodium chloride, dried with magnesium sulphate and all of the volatiles were removed. The crude material was purified by column chromatography, eluting with 5-20% ethyl acetate/petroleum spirits to give the title compound as a pale-yellow solid (68 mg, 49%). HPLC – rt 7.42 min > 98% purity at 254 nm; LRMS $[M+H]^+$ 301.1 m/z (^{79}Br), 303.1 m/z (^{81}Br); HRMS $[M+H]^+$ 301.0659 m/z, found 301.0662 m/z (^{79}Br), 303.0368 m/z, found 303.0643 m/z (^{81}Br); ^1H NMR (400 MHz, DMSO) rotamer 1 δ 8.16 (s, 1H), 6.61 (s, 2H), 3.39 (ddd, $J = 14.4, 9.2, 5.4$ Hz, 1H), 2.78 (s, 3H), 1.53 - 1.51 (m, 4H), 0.77 (t, $J = 7.4$ Hz, 6H); ^1H NMR (400 MHz, DMSO) rotamer 2 δ 8.20 (s, 1H), 6.57 (s, 2H), 4.37 (dq, $J = 9.1, 6.1$ Hz, 1H), 2.70 (s, 3H), 1.46 – 1.37 (m, 4H), 0.84 (t, $J = 7.4$ Hz, 6H). *Note: rotamer 1 and 2 are in a 2:1 relationship respectively. ^{13}C NMR (101 MHz, DMSO) δ 166.0, 152.4, 145.2, 144.8, 133.3, 121.8, 121.4, 60.9, 55.5, 29.5, 25.6, 24.9, 24.0, 10.7.*Note rotamers present in ^{13}C NMR.

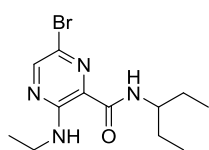
3-Amino-N-(sec-butyl)-N-methyl-6-phenylpyrazine-2-carboxamide (3.78)



The title compound was prepared according to General Procedure 3-A1 and was irradiated for 30 min. Title compound was isolated as an oily yellow solid (21 mg, 72%). HPLC – rt

7.90 min > 98% purity at 254 nm; LRMS [M+H]⁺ 299.2 m/z; HRMS [M+H]⁺ 299.1866 m/z, found 299.1869 m/z; ¹H NMR (400 MHz, DMSO) rotamer 1 δ 8.68 (s, 1H), 7.93 (t, *J* = 7.6 Hz, 2H), 7.45 (dd, *J* = 14.9, 7.5 Hz, 2H), 7.34 (dt, *J* = 13.4, 6.6 Hz, 1H), 6.48 (s, 2H), 4.46 (dt, *J* = 15.2, 7.6 Hz, 1H), 2.80 (s, 3H), 1.45 (dt, *J* = 21.2, 7.0 Hz, 4H), 0.90 (t, *J* = 7.3 Hz, 6H); ¹H NMR (400 MHz, DMSO) rotamer 2 δ 8.64 (s, 1H), 7.93 (t, *J* = 7.6 Hz, 2H), 7.45 (dd, *J* = 14.9, 7.5 Hz, 2H), 7.34 (dt, *J* = 13.4, 6.6 Hz, 1H), 6.45 (d, *J* = 9.3 Hz, 2H), 3.52 (td, *J* = 8.9, 4.4 Hz, 1H), 2.83 (s, 3H), 1.67 – 1.49 (m, 4H), 0.78 (t, *J* = 7.4 Hz, 6H). *Note rotamer 1 and 2 occur in a 2:3 relationship respectively; ¹³C NMR (101 MHz, DMSO) δ 167.5, 152.5, 152.1, 140.3, 139.8, 137.9, 137.7, 136.4, 133.1, 132.2, 128.9, 128.8, 127.9, 127.8, 124.8, 124.8, 60.6, 55.4, 29.8, 25.7, 24.8, 24.2, 10.8, 10.7. *Note: rotamers present in ¹³C NMR.

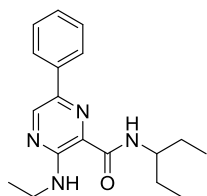
6-Bromo-3-(ethylamino)-N-(pentan-3-yl)pyrazine-2-carboxamide (3.79)



3-Amino-6-bromo-*N*-(pentan-3-yl)pyrazine-2-carboxamide (400 mg, 1.40 mmol) was dissolved in acetone (3 ml) prior to the addition of cesium carbonate (1.37 g, 4.20 mmol), tetrabutylammoniumbromide (90 mg, 0.28 mmol) and ethyl iodide (336 μl, 4.20 mmol).

The reaction was left to stir at ambient temperature until no further starting material was observed, ~ 72 h. The reaction mixture was extracted with ethyl acetate three times and the organic layers combined and washed once with water and once with an aqueous saturated solution of sodium chloride. The organic phase was then dried with magnesium sulphate and all of the volatiles were removed. The crude material was purified by column chromatography, eluting with 5% ethyl acetate/petroleum spirits to give the title compound as a yellow solid (207 mg, 47%). HPLC – rt 9.66 min > 99% purity at 254 nm; LRMS [M+H]⁺ 315.1 m/z (Br⁷⁹), 317.1 m/z (Br⁸¹); HRMS [M+H]⁺ 315.0815 m/z, found 315.0815 m/z (Br⁷⁹), 317.0795 m/z, found 317.0796 m/z (Br⁸¹); ¹H NMR (400 MHz, DMSO) δ 8.75 (t, *J* = 5.4 Hz, 1H), 8.39 (s, 1H), 8.16 (d, *J* = 9.3 Hz, 1H), 3.86 – 3.62 (m, 1H), 3.46 – 3.35 (m, 2H), 1.68 – 1.39 (m, 4H), 1.16 (t, *J* = 7.2 Hz, 3H), 0.82 (t, *J* = 7.4 Hz, 6H); ¹³C NMR (101 MHz, DMSO) δ 164.9, 153.1, 148.1, 126.2, 120.5, 52.1, 35.1, 26.8 (2C), 14.4, 10.8 (2C).

3-(Ethylamino)-N-(pentan-3-yl)-6-phenylpyrazine-2-carboxamide (3.80)



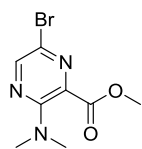
The title compound was prepared according to General Procedure 3-A1 and was irradiated for 30 min. Title compound was isolated as a yellow oil (94 mg, 94%). HPLC – rt 4.94 min > 92% purity at 254 nm; LRMS [M+H]⁺ 313.3 m/z; HRMS [M+H]⁺ 313.2023 m/z, found 313.2023 m/z; ¹H NMR (400 MHz, DMSO) δ 8.88 (s, 1H), 8.78 (t, *J* = 5.5 Hz, 1H), 8.30 (d, *J* = 9.3 Hz, 1H), 8.10 (d, *J* = 8.1 Hz, 2H), 7.47 (t, *J* = 7.7 Hz, 2H), 7.37 (dd, *J* = 10.6, 4.0 Hz, 1H), 3.78 (dt, *J* = 13.9, 6.8 Hz, 1H), 3.59 – 3.39 (m, 2H), 1.59 (p, *J* = 7.3 Hz, 4H), 1.20 (t, *J* = 7.2 Hz, 3H), 0.87 (t, *J* = 7.4 Hz, 6H); ¹³C NMR (101 MHz, DMSO) δ 166.0, 153.0, 143.4, 136.8, 136.0, 128.8 (2C), 127.9, 125.3 (2C), 124.9, 52.0, 34.9, 26.9 (2C), 14.6, 10.8 (2C).

Methyl 3,6-dibromopyrazine-2-carboxylate (3.81)



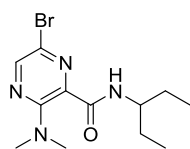
Methyl 3-amino-6-bromopyrazine-2-carboxylate (1.0 g, 4.31 mmol) was suspended in a mixture of hydrobromic acid (2.5 ml) and acetic acid (0.5 ml) and the reaction was cooled to -10 °C. Bromine (250 μl, 4.89 mmol) was gradually added over ~ 30 min. Once the addition was complete a 2.76 M aqueous solution of sodium nitrite (2 ml) was added in portions over 1 h. The reaction mixture was stirred for 30 min after completion of the addition. A 2.2 M aqueous solution of sodium thiosulphate (3.6 ml) was then added over 30 min and the resultant precipitate was filtered and washed with water. The solid was then collected and purified by column chromatography, eluting with 10-25% ethyl acetate/petroleum spirits to give the title compound as a colourless solid (706 mg, 56%). HPLC – rt 6.50 min > 99% purity at 254 nm; LRMS [M+H]⁺ 294.9 m/z (Br⁷⁹Br⁷⁹), 296.9 m/z (Br⁷⁹Br⁸¹), 299.0 m/z (Br⁸¹Br⁸¹); ¹H NMR (400 MHz, DMSO) δ 8.93 (s, 1H), 3.95 (s, 3H); ¹³C NMR (101 MHz, DMSO) δ 162.9, 149.9, 145.2, 137.9, 136.1, 53.5.

Methyl 6-bromo-3-(dimethylamino)pyrazine-2-carboxylate (3.82)



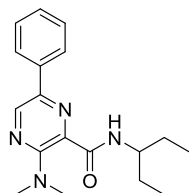
Dimethylamine hydrochloride salt (813 mg, 9.97 mmol), triethylamine (1.3 ml, 9.97 mmol) and tetrahydrofuran (5 ml) were combined. Methyl 3,6-dibromopyrazine-2-carboxylate (507 mg, 1.69 mmol) was then added and the reaction mixture was stirred at ambient temperature for 90 min, the reaction mixture went from colourless to yellow during this time. By TLC the reaction was complete and all of the volatiles were removed *in vacuo*. The crude material was purified by column chromatography, eluting with 10-20% ethyl acetate/petroleum spirits to give the title compound as a yellow solid (361 mg, 82%). HPLC – 6.55 min > 99% purity at 254 nm; LRMS $[M+H]^+$ 260.0 m/z (Br^{79}), 262.0 m/z (Br^{81}); HRMS 260.0030 m/z, found 260.0029 m/z (Br^{79}), 262.0009 m/z, found 262.0008 m/z (Br^{81}); 1H NMR (400 MHz, DMSO) δ 8.37 (s, 1H), 3.87 (s, 3H), 2.98 (s, 6H); ^{13}C NMR (101 MHz, DMSO) δ 165.1, 152.4, 145.2, 127.6, 121.8, 52.7, 39.7 (2C).

6-Bromo-3-(dimethylamino)-N-(pentan-3-yl)pyrazine-2-carboxamide (3.83)



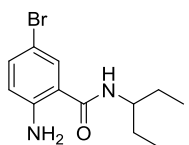
DABAL- Me_3 (790 mg, 3.08 mmol) was added to anhydrous THF (4 ml) under nitrogen prior to the addition of 1-ethylpropylamine (310 μ l, 3.08 mmol) and methyl 3,6-dibromopyrazine-2-carboxylate (400 mg, 1.54 mmol). The reaction mixture was then heated to reflux for 18 h. After this time there was a 50:50 mixture of starting material and product, as such the reaction was refluxed for an additional 8 h. After this time there was a 50:50 mixture of the des-bromo starting material and the desired product. As such, the reaction mixture was filtered through celite and the filtrate was collected, and all of the volatiles were removed. The crude material was purified by column chromatography, eluting with 5-20% ethyl acetate/petroleum spirits to give the title compound as an off-white solid (145 mg, 30%). HPLC – 7.56 min > 99% purity at 254 nm; LRMS $[M+H]^+$ 315.1m/z (Br^{79}), 317.1 m/z (Br^{81}); HRMS $[M+H]^+$ 315.0815 m/z, found 315.0814 m/z (Br^{79}), 317.0795 m/z, found 317.0794 m/z (Br^{81}); 1H NMR (400 MHz, DMSO) δ 8.40 (d, J = 8.7 Hz, 1H), 8.26 (s, 1H), 3.80 – 3.56 (m, 1H), 3.00 (s, 6H), 1.65 – 1.32 (m, 4H), 0.87 (t, J = 7.4 Hz, 6H); ^{13}C NMR (101 MHz, DMSO) δ 165.8, 151.6, 143.3, 135.0, 121.4, 52.0, 39.2 (2C), 26.7 (2C), 10.5 (2C).

3-(Dimethylamino)-N-(pentan-3-yl)-6-phenylpyrazine-2-carboxamide (3.85)



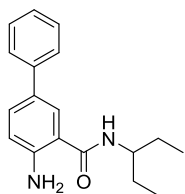
The title compound was prepared according to General Procedure 3-A1 and was irradiated for 45 min. Title compound was isolated as a yellow solid (66 mg, 67%). HPLC – rt 8.04 min 100% purity at 254 nm; LRMS $[M+H]^+$ 313.2 m/z; HRMS $[M+H]^+$ 313.2023 m/z, found 313.2023 m/z; 1H NMR (400 MHz, DMSO) δ 8.72 (s, 1H), 8.37 (d, $J = 8.9$ Hz, 1H), 8.01 (dt, $J = 8.3, 1.6$ Hz, 2H), 7.56 – 7.41 (m, 2H), 7.35 (ddd, $J = 7.3, 4.0, 1.2$ Hz, 1H), 3.89 – 3.60 (m, 1H), 3.06 (s, 6H), 1.69 – 1.37 (m, 4H), 0.93 (t, $J = 7.4$ Hz, 6H); ^{13}C NMR (101 MHz, DMSO) δ 167.3, 151.5, 138.4, 137.2, 136.2, 133.8, 128.8 (2C), 127.9, 125.1 (2C), 51.8, 39.2 (2C), 26.9 (2C), 10.5 (2C).

2-Amino-5-bromo-N-(pentan-3-yl)benzamide (3.91)



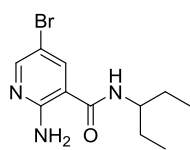
DABAL- Me_3 (836 mg, 3.26 mmol) was added to anhydrous THF (16 ml) under nitrogen prior to the addition of 1-ethylpropylamine (380 μ l, 3.76 mmol). The reaction mixture was heated to 40 $^\circ C$ for 1 h. Methyl 2-amino-5-bromobenzoate (390 mg, 1.69 mmol) was then added which resulted in a yellow solution. The reaction mixture was then heated to reflux for 18 h. Once the reaction was complete by TLC it was quenched by addition of aqueous 2M hydrochloric acid dropwise. The product was extracted with diethyl ether and passed through a silica plug to yield the title compound as a pale-yellow solid (472 mg, 98%). HPLC – rt 7.46 min > 98% purity at 254 nm; LRMS $[M+H]^+$ 285.1 m/z (Br^{79}), 287.1 m/z (Br^{81}); HRMS $[M+H]^+$ 285.0598 m/z, found 285.0604 m/z (Br^{79}), 287.0577 m/z, found 287.0584 m/z (Br^{81}); 1H NMR (400 MHz, DMSO) δ 7.95 (d, $J = 8.5$ Hz, 1H), 7.65 (d, $J = 2.4$ Hz, 1H), 7.25 (dd, $J = 8.8, 2.4$ Hz, 1H), 6.66 (d, $J = 8.8$ Hz, 1H), 6.47 (s, 2H), 3.86 – 3.59 (m, 1H), 1.63 – 1.32 (m, 4H), 0.84 (t, $J = 7.4$ Hz, 6H); ^{13}C NMR (101 MHz, DMSO) δ 167.4, 148.7, 133.8, 130.1, 118.3, 116.9, 104.9, 51.6, 26.9 (2C), 10.7 (2C).

4-Amino-N-(pentan-3-yl)-[1,1'-biphenyl]-3-carboxamide (3.86)



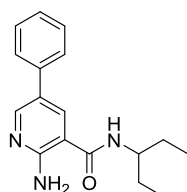
The title compound was prepared according to General Procedure 3-A1 and was irradiated for 30 min. Title compound was isolated as a yellow solid (148 mg, 75%). HPLC – rt 7.61 min > 96% purity at 254 nm; LRMS $[M+H]^+$ 283.2 m/z; HRMS $[M+H]^+$ 283.1805 m/z, found 283.1807 m/z; 1H NMR (400 MHz, DMSO) δ 7.99 (d, $J = 8.7$ Hz, 1H), 7.77 (d, $J = 2.1$ Hz, 1H), 7.69 – 7.56 (m, 2H), 7.47 (dd, $J = 8.5, 2.2$ Hz, 1H), 7.44 – 7.37 (m, 2H), 7.32 – 7.17 (m, 1H), 6.78 (d, $J = 8.5$ Hz, 1H), 6.43 (s, 2H), 3.79 (qd, $J = 8.5, 3.3$ Hz, 1H), 1.70 – 1.31 (m, 4H), 0.88 (t, $J = 7.4$ Hz, 6H); ^{13}C NMR (101 MHz, DMSO) δ 168.7, 149.0, 140.3, 129.7, 128.7 (2C), 126.5, 126.2, 126.0, 125.7 (2C), 116.7, 115.8, 51.5, 27.0 (2C), 10.8 (2C).

2-Amino-5-bromo-N-(pentan-3-yl)nicotinamide (3.93)



2-Amino-5-bromopyridine carboxylic acid (100 mg, 0.46 mmol) was dissolved in *N,N*-dimethylformamide (2 ml) prior to the addition of 1-ethylpropylamine (93 μ l, 0.92 mmol), HBTU (175 mg, 0.46 mmol) and diisopropylethylamine (160 μ l, 0.92 mmol). The reaction mixture was stirred for 18 h at ambient temperature. Once the reaction was complete the reaction mixture was extracted with ethyl acetate three times. The organic layers were combined and washed twice with water and once with a saturated aqueous solution of sodium chloride. The organic layers were dried with magnesium sulphate and all of the volatiles were removed. The crude material was purified by column chromatography, eluting with 15% ethyl acetate/petroleum spirits to give the title compound as a colourless solid (65 mg, 49%). HPLC – rt 5.83 min > 95% purity at 254 nm; LRMS $[M+H]^+$ 286.1 m/z (Br^{79}), 288.1 m/z (Br^{81}); HRMS $[M+H]^+$ 286.0550 m/z, found 286.0554 m/z (Br^{79}), 288.0530 m/z, found 288.0534 m/z (Br^{81}); 1H NMR (400 MHz, DMSO) δ 8.26 – 7.96 (m, 3H), 7.20 (s, 2H), 3.88 – 3.61 (m, 1H), 1.65 – 1.31 (m, 4H), 0.85 (t, $J = 7.4$ Hz, 6H); ^{13}C NMR (101 MHz, DMSO) δ 166.1, 157.6, 151.1, 138.0, 111.4, 104.0, 51.9, 26.8 (2C), 10.6 (2C).

2-Amino-N-(pentan-3-yl)-5-phenylnicotinamide (3.87)



The title compound was prepared according to General Procedure 3-A1 and was irradiated for 30 min. Title compound was isolated as a colourless solid (39 mg, 81%). HPLC – rt 6.32 min > 96% purity at 254 nm; LRMS $[M+H]^+$ 284.2 m/z; HRMS $[M+H]^+$ 284.1757 m/z, found 284.1760 m/z; 1H NMR (400 MHz, DMSO) δ 8.42 (d, $J = 2.4$ Hz, 1H), 8.19 (d, $J = 2.4$ Hz, 2H), 7.68 (dd, $J = 8.3, 1.2$ Hz, 2H), 7.59 – 7.39 (m, 2H), 7.39 – 7.23 (m, 1H), 7.14 (s, 2H), 3.81 (dq, $J = 8.4, 3.3$ Hz, 1H), 1.69 – 1.35 (m, 4H), 0.88 (t, $J = 7.4$ Hz, 6H); ^{13}C NMR (101 MHz, DMSO) δ 167.4, 158.1, 148.8, 137.5, 134.4, 128.9 (2C), 126.7, 125.8 (2C), 123.6, 109.8, 51.8, 26.9 (2C), 10.7 (2C).

Methyl 3-amino-6-bromopicolinate (3.95)



Synthesis based upon the previously reported procedure by Bell *et al.*¹⁰⁷

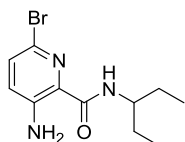
Methyl 3-aminopicolinate (590 mg, 3.88 mmol) was added to water (10 ml). 2 ml of an aqueous 2 M solution of sulphuric acid was added and the reaction stirred for 5 min until all of the solid had dissolved. To this was added a solution of bromine (200 μ l, 3.88 mmol) in acetic acid (1.5 ml). A precipitate was observed and after 30 min there was no evidence of starting material by TLC. The reaction mixture was neutralised to pH ~ 6 through the addition of aqueous 5 M sodium hydroxide. The product was extracted with ethyl acetate three times before the organic layers were combined, dried with magnesium sulphate and all of the volatiles were removed. The crude material was purified by column chromatography, eluting with 15-25% ethyl acetate/petroleum spirits as an orange solid (489 mg, 55%). The material was further purified by recrystallisation with ethyl acetate/petroleum spirit to give the title compound as an orange solid (328 mg, 37%). HPLC – rt 5.48 min > 98% purity at 254 nm; LRMS $[M+H]^+$ 231.1 m/z (Br^{79}), 233.0 m/z (Br^{81}); 1H NMR (400 MHz, DMSO) δ 7.45 (d, $J = 8.8$ Hz, 1H), 7.21 (d, $J = 8.8$ Hz, 1H), 6.89 (s, 2H), 3.81 (s, 3H); ^{13}C NMR (101 MHz, DMSO) δ 166.4, 147.6, 132.5, 128.7, 125.4, 124.4, 51.8.

Methyl 3-amino-4,6-dibromopicolinate (**3.96**)



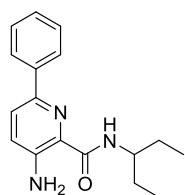
The title compound was isolated as a side product in the previous reaction as a pale-yellow solid (299 mg, 33%). ^1H NMR (400 MHz, DMSO) δ 8.03 (s, 1H), 3.85 (s, 3H). A NOESY experiment was performed and no cross-coupling was observed between the amine and the aromatic proton. This was taken as confirmation of the bromination substitution pattern shown. *Note: the amine peak was not clearly seen in the ^1H NMR spectrum.

3-Amino-6-bromo-N-(pentan-3-yl)picolinamide (**3.97**)



Methyl 3-amino-6-bromopicolinate (250 mg, 1.08 mmol) was combined with 1-ethylpropylamine (1.26 ml, 10.80 mmol) in a microwave reactor vessel and irradiated in a CEM microwave for 34 h at 115 °C. All volatiles were removed and the crude material was purified by column chromatography, eluting with 10% ethyl acetate/petroleum spirits to give the title compound as an orange oil (230 mg, 74%). HPLC – rt 8.17 min > 98% purity at 254 nm; LRMS $[\text{M}+\text{H}]^+$ 286.1 m/z (Br^{79}), 288.1 m/z (Br^{81}); HRMS $[\text{M}+\text{H}]^+$ 286.0550 m/z, found 286.0556 m/z (Br^{79}), 288.0530 m/z, found 288.0536 m/z (Br^{81}); ^1H NMR (400 MHz, DMSO) δ 7.78 (d, $J = 9.4$ Hz, 1H), 7.40 (d, $J = 8.7$ Hz, 1H), 7.14 (d, $J = 8.7$ Hz, 1H), 6.99 (s, 2H), 3.79 – 3.59 (m, 1H), 1.66 – 1.39 (m, 4H), 0.83 (t, $J = 7.4$ Hz, 6H); ^{13}C NMR (101 MHz, DMSO) δ 166.0, 146.0, 131.2, 128.8, 128.6, 123.2, 51.4, 26.9 (2C), 10.7 (2C).

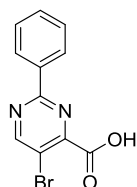
3-Amino-N-(pentan-3-yl)-6-phenylpicolinamide (**3.88**)



The title compound was prepared according to General Procedure 3-A1 and was irradiated for 30 min. Title compound was isolated as a dark yellow oil (60 mg, 53%). HPLC – rt 8.85 min > 99% purity at 254 nm; LRMS $[\text{M}+\text{H}]^+$ 284.2 m/z; HRMS $[\text{M}+\text{H}]^+$ 284.1757 m/z, found 284.1760 m/z; ^1H NMR (400 MHz, DMSO) δ 8.13 (d, $J = 9.4$ Hz, 1H), 8.02 (d, $J = 7.8$ Hz, 2H), 7.86 (d, $J = 8.7$ Hz, 1H), 7.46 (t, $J = 7.6$ Hz, 2H), 7.34 (t, $J = 7.2$ Hz, 1H), 7.26 (d, $J = 8.7$ Hz, 1H), 6.96 (s, 2H), 3.89 – 3.66 (m, 1H), 1.73 – 1.44 (m, 4H), 0.89 (t, $J = 7.4$ Hz, 6H); ^{13}C NMR (101

MHz, DMSO) δ 167.2, 145.4, 142.1, 138.3, 128.7 (2C), 128.0, 127.7, 125.7, 125.5 (2C), 124.1, 51.2, 27.0 (2C), 10.6 (2C).

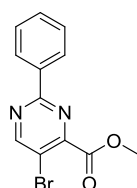
5-Bromo-2-phenylpyrimidine-4-carboxylic acid (**3.100**)



Synthesis based upon the previously reported procedure by Burger *et al.*¹⁰⁸

The hydrochloride salt of benzamidine (1.21 g, 7.76 mmol) was added to anhydrous ethanol (76 ml) and cooled to 0 °C. A 2.68 M solution of sodium ethoxide was made by dissolving sodium (268 mg, 11.64 mmol) in anhydrous ethanol. The sodium ethoxide solution was then added dropwise to the benzamidine solution. The resulting mixture was allowed to warm to ambient temperature and stirred under nitrogen for 30 min. Mucobromic acid (1.0 g, 3.88 mmol) was dissolved in anhydrous ethanol with shaking before gradual addition to the reaction mixture. The resulting solution was then heated to 50 °C for 2.5 h. The reaction mixture was concentrated *in vacuo* before an aqueous 2 M sodium hydroxide solution was added to the reaction mixture. The aqueous phase was extracted once with ethyl acetate. The aqueous phase was then acidified to pH ~ 4 by the addition of an aqueous 1 M hydrochloric acid solution. The product was then extracted with ethyl acetate three times and the organic layers were combined, washed once with a saturated aqueous solution of sodium chloride and then dried with magnesium sulphate. All volatiles were removed to give the title compound as an orange solid (392 mg, 36%). LRMS $[M+H]^+$ 279.0 m/z (Br^{79}), 281.0 m/z (Br^{81}); 1H NMR (400 MHz, DMSO) δ 9.22 (s, 1H), 8.49 – 8.24 (m, 2H), 7.69 – 7.43 (m, 3H).

Methyl 5-bromo-2-phenylpyrimidine-4-carboxylate (**3.101**)



5-Bromo-2-phenylpyrimidine-4-carboxylic acid (263 mg, 1.22 mmol) was dissolved in methanol (0.5 ml) and concentrated sulphuric acid (10 μ l) was added. The reaction mixture was heated to reflux and the reaction monitored by TLC for completion (~18 h). Once complete all volatiles were removed *in vacuo* and the crude material was dissolved in ethyl acetate and washed with a saturated aqueous solution of sodium bicarbonate. The organic phase was then washed with a

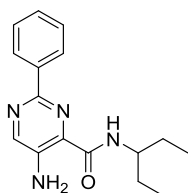
saturated aqueous solution of sodium chloride before being dried with magnesium sulphate. All of the volatiles were removed and the crude material was purified by column chromatography, eluting with 10% ethyl acetate/petroleum spirits to yield the title compound as a yellow solid (139 mg, 63%). HPLC – rt 7.91 min > 99% purity at 254 nm; LRMS [M+H]⁺ 293.0 m/z (Br⁷⁹), 295.0 m/z (Br⁸¹); HRMS [M+H]⁺ 292.9921 m/z, found 292.9920 m/z (Br⁷⁹), 294.9900 m/z, found 294.9906 m/z (Br⁸¹); ¹H NMR (400 MHz, CDCl₃) δ 8.97 (s, 1H), 8.50 – 8.33 (m, 2H), 7.48 (qdd, *J* = 6.0, 3.1, 1.3 Hz, 3H), 4.04 (s, 3H); ¹³C NMR (101 MHz, CDCl₃) δ 164.5, 163.3, 161.1, 156.4, 135.8, 131.7, 128.9 (2C), 128.6 (2C), 114.9, 53.5.

5-Bromo-N-(pentan-3-yl)-2-phenylpyrimidine-4-carboxamide (3.102)



DABAL-Me₃ (223 mg, 0.87 mmol) was added to anhydrous THF (1 ml) under nitrogen prior to the addition of 1-ethylpropylamine (90 μl, 0.87 mmol). The reaction mixture was heated to 40 °C for 1 h. Methyl 5-bromo-2-phenylpyrimidine-4-carboxylate (100 mg, 0.44 mmol) was then added and the reaction mixture was heated to reflux for 18 h. Once the reaction was complete by TLC the reaction mixture was filtered through celite. The filtrate was collected, and all volatiles removed. The crude material was purified by column chromatography, eluting with 10% ethyl acetate/petroleum spirits to give the title compound as an off-white solid (79 mg, 63%). HPLC – rt 8.64 min > 95% purity at 254 nm; LRMS [M+H]⁺ 348.1 m/z (Br⁷⁹), 350.1 m/z (Br⁸¹); HRMS [M+H]⁺ 348.0706 m/z, found 348.0709 m/z (Br⁷⁹), 350.0686 m/z, found 350.0691 m/z (Br⁸¹); ¹H NMR (400 MHz, DMSO) δ 9.18 (s, 1H), 8.54 (d, *J* = 8.8 Hz, 1H), 8.37 (dd, *J* = 7.5, 2.1 Hz, 2H), 7.57 (dd, *J* = 4.9, 2.4 Hz, 3H), 3.89 – 3.64 (m, 1H), 1.59 (ddd, *J* = 12.5, 7.4, 5.0 Hz, 2H), 1.52 – 1.36 (m, 2H), 0.95 (t, *J* = 7.4 Hz, 6H); ¹³C NMR (101 MHz, DMSO) δ 164.2, 161.7, 161.2, 160.5, 135.7, 131.6, 129.0 (2C), 127.9 (2C), 114.3, 52.0, 26.9 (2C), 10.5 (2C).

5-Amino-N-(pentan-3-yl)-2-phenylpyrimidine-4-carboxamide (3.89)



5-Bromo-*N*-(pentan-3-yl)-2-phenylpyrimidine-4-carboxamide (30 mg, 0.086 mmol), copper sulphate (2 mg, 0.014 mmol) and 28% ammonium hydroxide solution (2 ml) were combined in a sealed tube. The reaction mixture was heated to 110 °C and the progress of the reaction was monitored by LCMS until the reaction was complete. The reaction mixture was concentrated *in vacuo* and then an aqueous 1 M hydrochloric acid solution was added until pH ~ 7. The product was extracted with ethyl acetate three times and the subsequent organic layers were combined, washed once with a saturated aqueous solution of sodium chloride, and dried with magnesium sulphate. All of the volatiles were removed and the crude material was purified by column chromatography, eluting with 10% ethyl acetate/petroleum spirits to give the title compound as a yellow oil (11 mg, 46%). HPLC – rt 8.62 min > 99% purity at 254 nm; LRMS [M+H]⁺ 285.2 m/z; HRMS [M+H]⁺ 285.1710 m/z, found 285.1707 m/z; ¹H NMR (400 MHz, DMSO) δ 8.55 (s, 1H), 8.46 – 8.24 (m, 3H), 7.48 (t, *J* = 7.4 Hz, 2H), 7.42 (dd, *J* = 8.4, 6.0 Hz, 1H), 6.96 (s, 2H), 3.93 – 3.67 (m, 1H), 1.61 (p, *J* = 7.3 Hz, 4H), 0.89 (t, *J* = 7.4 Hz, 6H); ¹³C NMR (101 MHz, DMSO) δ 166.3, 150.1, 148.6, 141.1, 137.1, 132.6, 129.0, 128.5 (2C), 126.6 (2C), 51.7, 26.9 (2C), 10.8 (2C).

4. Investigation of the structure-activity relationships of the pyridyl benzamides against *T.b. brucei*

4.1. Introduction

The pyridyl benzamides were identified as a class that was well suited to lead optimisation. The initial screening hit (**1.92**) had an EC₅₀ of 12 μM against *T.b. brucei* (Figure 4.1). Under the conditions for the HTS this compound was initially categorised as inactive. However, **1.92** is a very small molecule, having a MW of only 212 gmol⁻¹, making it a highly optimisable lead compound. Additionally, **1.92** also possesses a low PSA that has potential for CNS penetration, and a low cLogP that could further aid CNS penetration.⁵⁶

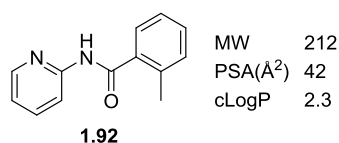


Figure 4.1 Structure and physicochemical profile of the initial screening hit with a low cLogP, PSA and MW suitable for lead optimisation.

The initial lead compound (**1.92**) was subjected to a parasite panel the results of which are summarised in Table 4.1. Subsequent re-testing of the initial hit against *T.b. brucei* led to a revision of the activity and it was identified as having an EC₅₀ of 3 μM. The activity observed in *T.b. brucei* was indicative of activity in the human subspecies, *T.b. rhodesiense*. However, **1.92** showed little activity for the related kinetoplastid, *T. cruzi* (EC₅₀ 180 μM) and only weak activity against the unrelated *L. donovani* (EC₅₀ 56.1 μM) and *P. falciparum* (EC₅₀ 42.2 μM).⁵⁴

Table 4.1 Biological activity profile of **1.92** against a number of parasites.

Parasite	EC₅₀ (μM)	SI
<i>T.b. brucei</i>	3.0 ± 0.7	28 ^a
<i>T.b. rhodesiense</i>	11.5	16 ^b
<i>T. cruzi</i>	180	1 ^b
<i>L. donovani</i> axenic	56.1	3 ^b
<i>P. falciparum</i>	42.2	4 ^b

^a Selectivity relative to HEK293 mammalian cells.

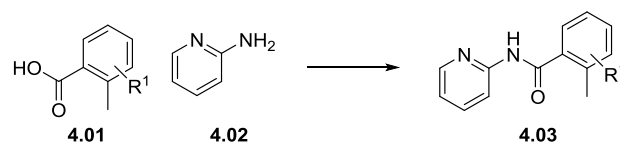
^b Selectivity relative to L6 (rat skeletal myoblast) cells.

4.2. Aims

The aim for this section of work was to investigate alterations to the pyridylbenzamide core. This included, varying the substitutions around the pyridine and tolyl rings as well as amide *N*-alkylation. The work will be presented as an initial discussion of the synthesis of these derivatives, a number of analogues constituting the primary SAR for this series (presented as a publication), before concluding with some additional follow up work.

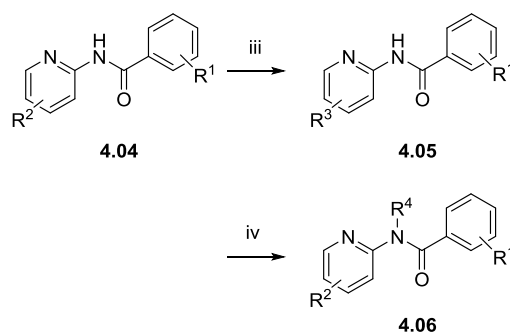
4.3. Synthesis of pyridylbenzamide core

As shown in Scheme 4.1, the synthetic versatility of this scaffold allowed ready access to all compounds targeted. Core assembly was constructed via coupling of an appropriately substituted 2-aminopyridine with an appropriately substituted benzoic acid or benzoyl chloride. There are numerous conditions for amide couplings published in the literature though in the course of this project three sets of conditions were employed depending upon the amines and acids that were being utilised.



Scheme 4.1 Synthesis of pyridyl benzamide derivatives via an amide coupling. There are numerous methods by which to form an amide bond though three have been employed throughout this chapter: *i*) R^1 -PhCOOH, DIPEA, HBTU, DMF, 18 h, 60 °C; *ii*) R^1 -PhCOCl, pyridine, 18 h, 25 °C; *iii*) R^1 -PhCOOH, EDCI, DMAP, DMF, 18 h, 30 °C.

Once the pyridyl benzamide had been obtained it was possible to further derivatise these analogues. Typical variations are highlighted in Scheme 4.2 and consisted of Suzuki and Sonogashira coupling reactions in order to access analogues similar to **4.05**. It was also possible to alkylate the amide –NH using potassium carbonate and TBAB in acetone, such as with **4.06**.



Scheme 4.2 Further derivatisation of pyridyl benzamide analogues *iii*) Suzuki: R^3 -B(OH)₂, K₂CO₃, TBAB, Pd(PPh₃)₂Cl₂, 1,4-dioxane, H₂O, microwave 130 °C, 15 min; Sonogashira: R^3 -H, CuI, PPh₃, Pd(PPh₃)₂Cl₂/Pd(PPh₃)₄, DMF, Et₃N, microwave 120 °C, 10-40 min; *iv*) N-alkylation: X-R⁴, K₂CO₃, TBAB, acetone, 18 h, 25 °C.

4.4. Preliminary SAR

There were three concurrent approaches employed in trying to establish SAR for this series of compounds. The first involved identification of close analogues in the literature with reported biological activity,

especially where that activity might have some relevance to trypanosomes (such as targeting succinate dehydrogenase and other enzymes known to be present in trypanosomes). It was determined that little is known on the biological activity of **1.92** although it has been reported to have a low level of antifungal activity against a strain of corn-smut (*Ustilago maydis*).¹⁰⁹ More potent and wide-ranging antifungal activity was evident in the closely related 2-methylbenzanilide system.¹⁰⁹ Such compounds appeared to act through inhibition of succinate dehydrogenase (Complex II in mitochondria)¹⁰⁹ and this enzyme has been found in trypanosomes.¹¹⁰ There is known to be crossover activity between fungicides and trypanocides in the examples of the lanosterol 14 α -demethylase inhibitors fenarimol¹¹¹ and posaconazole.¹¹² This work was performed by Michelle Gazdik.

The second approach that was adopted involved searching databases of compound biological activities such as the TCAMS set¹¹³ and PubChem. The latter revealed around a dozen analogues of **1.92** with a variety of biological activities. This work was largely performed by Michelle Gazdik with assistance from Raphaël Rahmani.

The third approach was to utilise traditional medicinal chemistry techniques and began by focusing on modifications and substitutions around the pyridine ring, including removal and isosteric replacement of the pyridyl nitrogen and *N*-alkylation of the amide. This work was followed by investigating substitutions around the tolyl ring and modification, either removal or extension, of the methyl. This work was largely performed by myself and Michelle Gazdik with assistance from Raphaël Rahmani.

Finally, evidence of additive SAR was sought to see if further increases in potency could be engineered in a rational way by combining the most active substitutions around the tolyl and pyridinyl moieties. This work was largely carried out by myself in conjunction with Raphaël Rahmani.

Assessment of predictive ADME parameters revealed that these low MW compounds have favourable properties for further optimisation. In particular, they have relatively low LogD values, good aqueous solubility, and low plasma protein binding. Most of the analogues were predicted to have good CNS

penetration, a key feature for the treatment of second stage HAT. Microsomal degradation was moderate to quite high across all of the compounds tested. In general, those compounds that had moderate degradation were substituted at the 4- or 5-position on the pyridine ring. It is possible that the effect of this substitution pattern is to hinder metabolic oxidation of the adjacent electron rich 6-position. This work was carried out by collaborators at the Centre for Drug Candidate Optimisation, Monash Institute of Pharmaceutical Sciences.

These studies led to the identification of a compound with an EC₅₀ of 45 nM against the human pathogenic, *T.b. rhodesiense*. These compounds appear to be highly selective for *T. brucei* over other parasites, including *T. cruzi*, and they do not display any significant activity against mammalian L6 cells. These analyses were performed by collaborators at the Swiss Tropical and Public Health Institute.

The full details and conclusions of this preliminary SAR study follow in the form of a published manuscript. Reprinted with permission from Ferrins, L.; Gazdik, M.; Rahmani, R.; Varghese, S.; Sykes, M. L.; Jones, A. J.; Avery, V. M.; White, K. L.; Ryan, E.; Charman, S. A.; Kaiser, M.; Bergström, C. A. S.; Baell, J. B. Pyridyl Benzamides as a Novel Class of Potent Inhibitors for the Kinetoplastid Trypanosoma brucei. *Journal of Medicinal Chemistry* **2014**, *57*, 6393-6402. Copyright 2015 American Chemical Society. The complete supplementary information for this publication can be viewed in Appendix 1.

4.5. Published manuscript

Declaration for Thesis Chapter 4

Declaration by candidate

In the case of Chapter 4, the nature and extent of my contribution to the work was the following:

Nature of contribution	Extent of contribution
Synthesis of compounds 28, 53-54, 59, 63, 66, 70, 77-78, 81-83, 94, 96-98, 100 , SAR analysis and principal authorship of manuscript	40%

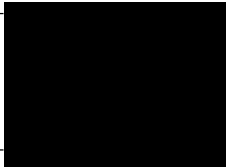
The following co-authors contributed to the work. If co-authors are students at Monash University, the extent of their contribution in percentage terms must be stated:

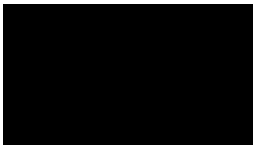
Name	Nature of contribution	Extent of contribution*
Michelle Gazdik	Synthesis of compounds 8-16, 18-21, 23-27, 29-34, 36-52, 62, 64-65, 67-69, 73, 75-76, 79-80, 85, 88, 91 and proof-reading of manuscript	
Raphaël Rahmani	Synthesis of compounds 17, 22, 35, 57, 71-72, 74, 84, 86-87, 89-90, 92-93, 95, 99 , SAR analysis and co-authorship of manuscript	
Melissa L. Sykes	Biological testing, data analysis	
Swapna Varghese	Synthesis of compounds 55-56, 58, 60-61	
Amy J. Jones	Biological testing, data analysis, editing of manuscript	
Vicky M. Avery	Data analysis, editing of manuscript	
Karen L. White	Data analysis, editing of manuscript	
Eileen Ryan	ADMET analysis	
Susan A. Charman	Data analysis, editing of manuscript	

Marcel Kaiser	Biological testing of compounds in a parasite panel	
Christel A. S. Bergstrom	<i>In silico</i> prediction of CNS exposure, editing of manuscript	
Jonathan B. Baell	SAR analysis, co-authorship of manuscript	

**Shown for Monash University students only*

The undersigned hereby certify that the above declaration correctly reflects the nature and extent of the candidate's and co-authors' contributions to this work.

Candidate's Signature		Date 24/04/2015
----------------------------------	---	---------------------------

Main Supervisor's Signature		Date 24/04/2015
--	---	---------------------------

Declaration by co-authors

The undersigned hereby certify that:

- (12) The above declaration correctly reflects the nature and extent of the candidate's contribution to this work, and the nature of the contribution of each of the co-authors;
- (13) They meet the criteria for authorship in that they have participated in the conception, execution, or interpretation, of at least part of the publication in their field of expertise;
- (14) They take public responsibility for their part of the publication, except for the responsible author who accepts overall responsibility for the publication;
- (15) There are no other authors of the publication according to those criteria;
- (16) Potential conflicts of interest have been disclosed to (a) granting bodies, (b) the editor or publisher of journal or other publications, and (c) the head of the responsible academic unit; and

- (17) The original data are stored at the following location(s) and will be held for at least five years from the date indicated below:

Locations:

Department of Medicinal Chemistry, Monash Institute of Pharmaceutical Sciences, 381 Royal Pde, Parkville, Victoria, 3052, Australia.

Eskitis Institute for Cell and Molecular Therapies, Griffith University, Brisbane Innovation Park, Don Young Road, Nathan, Queensland, 4111, Australia.

The Walter and Eliza Hall Institute, 1G Royal Parade, Parkville, Victoria, 3052, Australia.

School of Chemistry, University of Tasmania, Private Bag 75, Hobart, 7001, Australia.

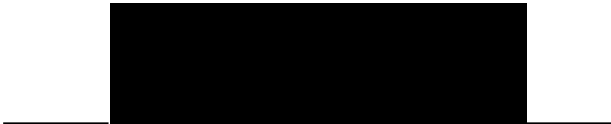
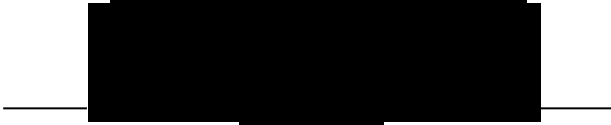
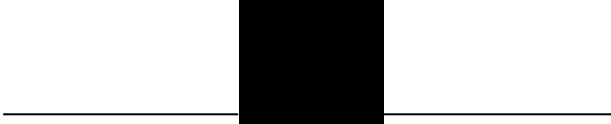
Centre for Drug Candidate Optimisation, Monash University, Parkville, Victoria, 3052, Australia.

Swiss Tropical and Public Health Institute, Socinstrasse 57, Basel, 4051, Switzerland.

University of Basel, Petersplatz 1, Basel, 4003, Switzerland.

Department of Pharmacy, Uppsala University, Biomedical Centre P.O. Box 580, SE-751 23 Uppsala, Sweden

Signatures:

Signed:		Date: 20 /05/2015
Signed:		Date: 13/05/2015
Signed:		Date: 04/05/2015
Signed:		Date: 30/04/2015
Signed:		Date: 30/04/2015
Signed:		Date: 06/05/2015

Signed: _____  _____ Date: 30/04/2015

Signed: _____  _____ Date: 18/05/2015

Signed: _____  _____ Date: 30/04/2015

Signed: _____  _____ Date: 04/05/2015

Signed: _____  _____ Date: 04/05/2015

Signed: _____  _____ Date: 24/04/2015

Pyridyl Benzamides as a Novel Class of Potent Inhibitors for the Kinetoplastid *Trypanosoma brucei*

Lori Ferrins,^{†,□} Michelle Gazdik,^{||,⊥,□} Raphaël Rahmani,[†] Swapna Varghese,^{||} Melissa L. Sykes,[#] Amy J. Jones,[#] Vicky M. Avery,[#] Karen L. White,[‡] Eileen Ryan,[‡] Susan A. Charman,^{†,‡} Marcel Kaiser,^{∇,○} Christel A. S. Bergström,^{§,◆} and Jonathan B. Baell^{*,†,⊥,||}

[†]Medicinal Chemistry, [‡]Centre for Drug Candidate Optimisation, and [§]Drug Delivery, Disposition and Dynamics, Monash Institute of Pharmaceutical Sciences, Monash University, Parkville, Victoria 3052, Australia

^{||}Department of Chemistry, La Trobe Institute for Molecular Science, La Trobe University, Melbourne, Victoria 3086, Australia

[⊥]The Walter and Eliza Hall Institute, 1G Royal Parade, Parkville, Victoria 3052, Australia

[#]Eskitis Institute for Drug Discovery, Griffith University, Brisbane Innovation Park, Don Young Road, Nathan, Queensland 4111, Australia

[∇]Swiss Tropical and Public Health Institute, Socinstrasse 57, Basel, 4051, Switzerland

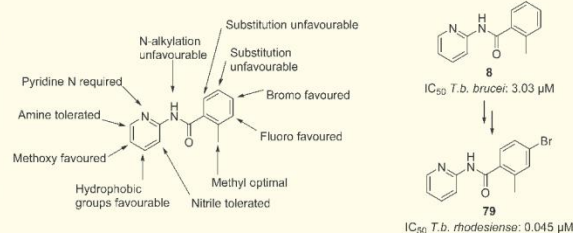
[○]University of Basel, Petersplatz 1, Basel, 4003, Switzerland

[◆]Department of Pharmacy, Uppsala University, Biomedical Center P.O. Box 580, SE-751 23 Uppsala, Sweden

^{*}Department of Medical Biology, University of Melbourne, Parkville, Victoria 3010, Australia

Supporting Information

ABSTRACT: A whole-organism screen of approximately 87000 compounds against *Trypanosoma brucei brucei* identified a number of promising compounds for medicinal chemistry optimization. One of these classes of compounds we termed the pyridyl benzamides. While the initial hit had an IC_{50} of 12 μ M, it was small enough to be attractive for further optimization, and we utilized three parallel approaches to develop the structure–activity relationships. We determined that the physicochemical properties for this class are generally favorable with particular positions identified that appear to block metabolism when substituted and others that modulate solubility. Our most active compound is 79, which has an IC_{50} of 0.045 μ M against the human pathogenic strain *Trypanosoma brucei rhodesiense* and is more than 4000 times less active against the mammalian L6 cell line.



INTRODUCTION

Human African trypanosomiasis (HAT) currently affects more than 20000 people according to the latest report published by the World Health Organization.¹ HAT is caused by the transmission of *Trypanosoma brucei* spp. by the tsetse fly to humans, and, as a result, this disease is largely restricted to Africa where the vector, parasite, and animal reservoirs coexist.² Infection is with either *Trypanosoma brucei gambiense* or *Trypanosoma brucei rhodesiense*, and the rate of progression of the disease is subspecies-dependent, with *T. b. gambiense* being accountable for 95% of cases and causing a chronic infection, while *T. b. rhodesiense* presents as an acute infection.² The disease has two stages: the first stage is the hemolymphatic phase where trypanosomes multiply in subcutaneous tissue, blood, and the lymphatic system, and is accompanied by fever, headaches, joint pain, and itching.² Stage two is the neurological phase and occurs when the parasites cross the blood brain barrier (BBB) and infect the central nervous system (CNS). This typically results in behavioral change, confusion,

poor coordination, and sleep disturbances.² Without treatment HAT is eventually fatal. There are currently few treatment options, making this disease a key target for drug discovery.

For treatment of the first stage of HAT, there are currently two drugs registered for use, as shown in Figure 1: pentamidine (1) and suramin (2). Pentamidine is used to treat infection with *T. b. gambiense*,³ while suramin is prescribed to patients infected with *T. b. rhodesiense*.^{4,5} Neither of these drugs can cross the BBB, and they both have significant side effects. Pentamidine has been associated with nephrotoxicity and diabetes mellitus,⁶ while suramin can lead to renal failure and exfoliative dermatitis.⁴ Melarsoprol (3) was the first drug used to treat stage two HAT.^{6,7} It is effective against both pathogenic subspecies, although recently resistance to the drug has been observed.⁷ There are also significant side effects associated with its use including reactive encephalopathy, which can be fatal in

Received: February 4, 2014

Published: June 30, 2014

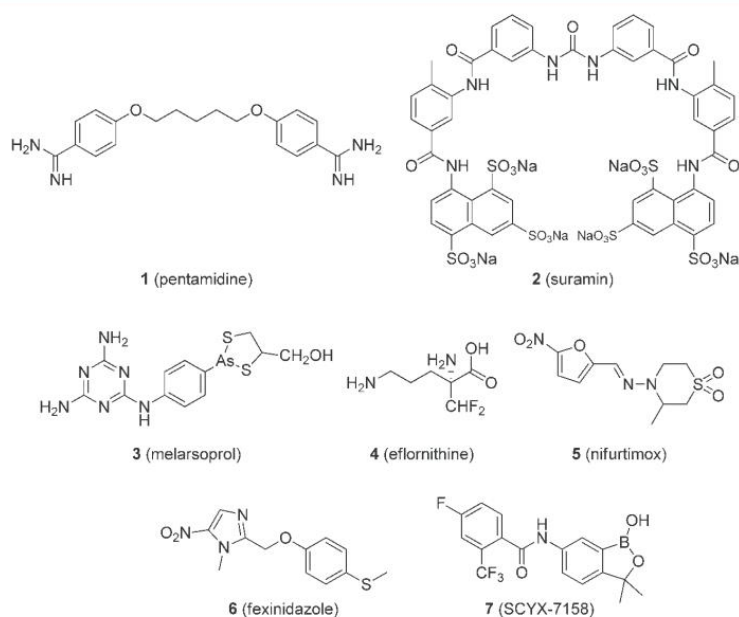


Figure 1. Drugs used for the treatment of human African trypanosomiasis (1–5), fexinidazole (6), now in phase II/III clinical trials, and SCYX-7158 (7) currently in phase I clinical trials.

3–10% of patients.⁷ Eflornithine (4), effective against *T. b. gambiense*,⁷ was registered in 1990 and is less toxic than its predecessor. More recently, a combination therapy of nifurtimox (5) and eflornithine (4) (NECT) was introduced, but it is ineffective against *T. b. rhodesiense* and the need for parenteral administration is a drawback.⁸ A number of compounds have recently entered clinical development for HAT. Pafuramidine, a constrained analogue of pentamidine, entered clinical development in 2005 but was abandoned when liver toxicity and delayed renal insufficiency were identified in an extended phase I trial.⁹ Drugs currently in clinical trials are fexinidazole (6), a nitroheterocycle that is in phase II/III clinical trials,¹⁰ and the oxaborole, SCYX-7158 (7), which entered phase I trials in March 2012. The outcome of these trials is pending.¹¹

Fortunately, with the advent of recent public–private partnerships and related initiatives,¹ it is anticipated that improved treatments will emerge for many of the so-called “neglected” diseases. There are a number of drug discovery avenues currently being utilized in the search for new antitrypanosomal drugs, which we have recently reviewed.¹² We recently conducted high-throughput screening (HTS) against *T. brucei* using a library of 87296 compounds, and discovered several classes with promising activity.¹³ One of these has been progressed to a hit-to-lead medicinal chemistry optimization program.¹⁴ Some inhibitor series were not discussed in the initial HTS publication because they did not meet predefined selection criteria. One of these was a simple pyridyl benzamide (8), which was slightly less active than the other classes with an IC_{50} value of 12 μM , close to the predefined activity cutoff value of <10 μM , and a selectivity index (SI) of 28 relative to HEK 293 cells. However, this compound was attractive to the medicinal chemists as an optimization candidate as its physicochemical properties were deemed to be favorable for development (Figure 2).

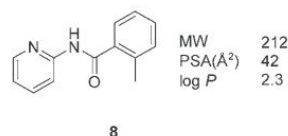


Figure 2. Structure and physicochemical parameters of screening hit 8.

Compound 8 possesses a very low molecular weight of 212 g mol^{-1} , a low polar surface area of 42 \AA^2 suitable for potential CNS penetration to treat stage two HAT, an attractively low lipophilicity (log *P* of 2.3), and would be neutral at physiological pH, aiding BBB penetration. The low molecular weight results in a high ligand efficiency and much scope to optimize; as such, this compound was selected for development of structure–activity relationships (SAR). Herein, we report the results of this investigation.

RESULTS AND DISCUSSION

Mining the HTS database returned 15 compounds, which were broadly related to 8. However, these compounds were not sufficiently similar to develop meaningful SAR. Three parallel approaches were then employed to establish a focused SAR investigation. The first of these involved identification of close analogues in the literature that were associated with previously reported biological activity. Of particular interest were those compounds with demonstrated activity against trypanosomes, or whereby *T. brucei* possesses a target that the compound had reported activity against in other organisms. From this search, it was determined that relatively little was known about the biological activity of 8, although a low level of antifungal activity against a strain of corn-smut has been reported (*Ustilago maydis*).¹⁵ The closely related 2-methylbenzanilide system was reported to have more effective and wide ranging antifungal activity and demonstrated activity against succinate dehydrogenase (Complex II in mitochondria) in corn smut.¹⁵ This

Table 2. *T.b. brucei* Inhibitory Activity of SAR Probes of 8 Focusing on the Pyridine and Amide Moieties

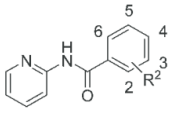
ID	R ¹	IC ₅₀ (μM) ± SEM	percentage inhibition at 10 μM	SI ^a
19-51				
19	3-OCH ₃		<10%	
20	3-CH ₃		34%	
21	3-F		<10%	
22	3-[N] ^b		<10%	
23	4-CN	2.3 ± 0.04		
24	4-[N] ^b		35%	
25	4-CH ₃	2.1 ± 0.1		>37
26	4-Cl	2.1 ± 0.1		>38
27	4-Br	1.8 ± 0.01		>41
28	4-F	0.51 ± 0.13		168
29	4-C≡CPh	1.7 ± 0.4		>51
30	4-C≡CCH ₂ iPr	1.1 ± 0.08		>53
31	4-Ph	2.0 ± 0.002		31
32	5-OCH ₃	3.8 ± 0.4		>22
33	5-CH ₃		<10%	
34	5-F		33%	
35	5-[N] ^b		<10%	
36	5-CN		<10%	
37	5-Cl		<10%	
38	5-Br		<10%	
39	6-OCH ₃		<10%	
40	6-CH ₃		<10%	
41	6-F		<10%	
42	6-CN		11%	
43	6-[N] ^b		<10%	
44	6-Cl		<10%	
45	6-Br		<10%	
46	6-Ph		33%	
47	6-C≡CCH ₂ iPr		<10%	
48	6-CH=CH(CH ₂) ₂ CH ₃	6.0 ± 0.07		>3
49	6-C≡CPh		<10%	
50	6-OH		<10%	
51	6-NH ₂	4.6 ± 0.8		>19
52			<10%	
53			<10%	
54			<10%	
55			<10%	
56			<10%	
57			<10%	
58			<10%	
59			<10%	
60			<10%	
61			<10%	
62			18%	
63			<10%	

^aSelectivity relative to HEK293 cells. ^b[N] = endocyclic nitrogen.

Much more promising were the results from exploring 8 using conventional SAR elaboration. Shown in Table 2 are the data for compounds with a focus on varying substituents around the pyridine ring.

Here it can be seen that at the 3-position, methoxy (19), methyl (20), or fluoro (21) were not well tolerated and neither was an endocyclic nitrogen (22). In the 4-position, a cyano (23) was tolerated, an endocyclic nitrogen (24) less so, but in contrast, good activity accompanied substitution with a range of hydrophobic groups (25–31), particularly with the 4-fluoro

(28). The similar activities for the 4-chloro (26) and very bulky phenylacetylene (29) or phenyl (31) imply this could largely be a favorable transport effect rather than a specific interaction with a hydrophobic pocket in an intracellular target site. In the 5-position, methoxy was favorable for activity (32), but methyl (33), fluoro (34), chloro (37), bromo (38), nitrile (36), or an endocyclic nitrogen (35) were not. As it is hard to envisage that a methoxy would aid transport, this SAR is consistent with the methoxy interacting favorably with its target, whether it be intra- or extracellular. In contrast to substitution at the other

Table 3. *T. b. brucei* Inhibitory Activity of a Number of Analogues of the Tolyl Ring


ID	R ²	IC ₅₀ (μM) ± SEM	percentage inhibition at 10 μM	SI ^a
64	H	9.07 ± 2.2		9.2
65	2-Et	2.74 ± 1.0		30
66	2-F		35%	
67	2-Cl		44%	
68	2-OCF ₃		13%	
69	2-Ph		<10%	
70	2-CH ₃ , 3-F	0.89 ± 0.04		94
71	3-F	7.33 ± 2.1		11
72	2-CH ₃ , 3-Cl	0.63 ± 0.09		132
73	2-CH ₃ , 3-Br	5.7 ± 0.2		15
74	2-CH ₃ , 3-CH ₃	3.5 ± 0.2		24
75	2-CH ₃ , 3-OCH ₃		10%	
76	2-CH ₃ , 3-[N] ^b		21%	
77	2-CH ₃ , 4-F	1.9 ± 0.3		44
78	2-CH ₃ , 4-Cl	1.1 ± 0.09		76
79	2-CH ₃ , 4-Br	1.1 ± 0.06		60
80	2-CH ₃ , 4-OCH ₃		<10%	
81	2-CH ₃ , 4-CH ₃	0.98 ± 0.07		85
82	2-CH ₃ , 4-CH=CH(CH) ₂ CH ₃		24%	
83	2-CH ₃ , 4-Ph		<10%	
84	2-CH ₃ , 5-F		<10%	
85	2-CH ₃ , 5-Br		<10%	
86	2-CH ₃ , 5-CH ₃		22%	
87	2-CH ₃ , 5-OCH ₃		<10%	
88	2-CH ₃ , 5-[N] ^b		<10%	
89	2-CH ₃ , 6-CH ₃		<10%	
90	2-CH ₃ , 6-F		45%	
91	2-CH ₃ , 6-[N] ^b		12%	

^aSelectivity relative to HEK293 cells. ^b[N] = endocyclic nitrogen.

positions, no favorable substitution could be found for the 6-position, even after extensive probing with a variety of diverse groups (39–51). Perhaps the only exception was 51, where an amino group appeared to be tolerated with an IC₅₀ of 4.6 μM. Removal of the pyridyl nitrogen as with the benzanilide (52), and the substitution of the pyridine ring with a range of five-membered heterocycles (54–61), resulted in the complete loss of activity and demonstrated that the pyridine ring was essential for activity. It was thought that replacement of the pyridinyl nitrogen with a nitrile (53) could overcome the observed loss of activity as nitriles are known to replace water-mediated hydrogen-bond bridges involving heterocyclic nitrogens,²⁰ although here such a change resulted in loss of activity. Finally, it was determined through inactivity of the *N*-methyl (62) and reverse amide (63) analogues that the secondary amide was essential for activity.

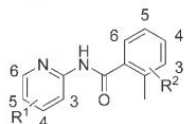
The SAR for the tolyl ring was probed next, and the results are shown in Table 3.

Here, it is observed that the methyl group is important, and its loss (64) led to a 3-fold decrease in activity as compared to 8. Interestingly, extension of the 2-methyl to a 2-ethyl was well tolerated, with 65 having an IC₅₀ of 2.74 μM, although fluoro (66), chloro (67), trifluoromethoxy (68), and phenyl (69) were not tolerated, complementing the results for 14 and 15 in

Table 1. Maintaining the 2-methyl group, other positions were probed, and it can be seen that while a 3-methoxy (75) or endocyclic nitrogen (76) were not tolerated, a 3-fluoro (70) was highly favorable for activity with an IC₅₀ of 0.89 μM. The methyl group was confirmed to be important as its loss from 70 to give des-methyl analogue 71 led to a near 10-fold loss of activity. Substitution with 3-chloro (72) was favorable with an IC₅₀ of 0.63 μM, while the 3-methyl (74) and 3-bromo (73) were significantly less active with respective IC₅₀ values of 3.5 and 5.7 μM. This suggests that a small, electron-withdrawing and hydrophobic group is favorable for activity at the 3-position. In the 4-position, a methoxy (80) was not tolerated; fluorine (77), chlorine (78), bromine (79), and methyl (81) substitution all gave favorable results, with IC₅₀ values of 1.9, 1.1, 1.1, and 0.98 μM, respectively. In the 5-position, substitution of an endocyclic nitrogen (88) led to a loss of activity, and similarly fluorine (84), bromine (85), methyl (86), and methoxy (87) in this position rendered the compounds inactive. It appears as though this position nestles tightly within the target's active site and no manipulation is possible. Likewise, substitution at the 6-position was unfavorable for activity with methyl (89), fluorine (90), and an endocyclic nitrogen (91) leading to a complete loss of activity.

Finally, we looked for evidence of additive SAR to see if further increases in potency could be engineered in a rational way. We saw previously (Table 3) that when R² was 2-methyl, 3-fluoro (70) or 2-methyl, 4-fluoro (77), respective IC₅₀ values of 0.89 and 1.9 μM were obtained, which were better than that for 8 (3.03 μM). Combining the 2-methyl, 3-fluoro, and 4-fluoro in the one molecule gave a further improvement in activity, and 92 (Table 4) returned an IC₅₀ of 0.41 μM. We also

Table 4. *T. b. brucei* Inhibitory Activity of Compounds with a Combination of Favorable Substitution Patterns around the Pyridyl and Phenyl Rings in Search of Additive SAR



ID	R ¹	R ²	IC ₅₀ (μM) ± SEM	SI ^a
92	H	3-F, 4-F	0.41 ± 0.07	205
93	4-CH ₃	3-F	0.83 ± 0.01	100
94	4-CH ₃	3-F, 4-F	0.90 ± 0.44	93
95	4-Cl	3-F	0.47 ± 0.05	177
96	4-Cl	3-F, 4-F	0.53 ± 0.26	160
97	4-F	3-F	0.10 ± 0.04	851
98	4-F	3-F, 4-F	0.19 ± 0.24	450
99	5-OCH ₃	3-F	2.3 ± 0.2	4
100	5-OCH ₃	4-F	2.6 ± 0.2	32

^aSelectivity relative to HEK293 cells.

demonstrated earlier (Table 2) that favorable R¹ substituents comprised 4-methyl (25), 4-chloro (26), 4-fluoro (28), or 5-methoxy (32). When R² was kept constant as 2-methyl, 3-fluoro and combined with these R¹ substituents, compounds 93, 95, 97, and 99 resulted (Table 4). Here, it can be seen that for 95 this combination was beneficial with an IC₅₀ of 0.47 μM and even more so for 97 with an IC₅₀ of 100 nM and an improved selectivity profile as compared to 8, while a neutral effect was observed for 93. Although both 93 and 95 show an improved SI as compared to 8 (27.5), a 16-fold improvement in the SI was obtained when a fluorine was substituted at the 4-position (98), and this compound was significantly more potent than the others, with an IC₅₀ of 190 nM. However, the combination involving the 5-methoxy (99) was detrimental to activity (IC₅₀ 2.3 μM). This detrimental effect of the R¹ 5-methoxy was also observed when R² comprised 2-methyl, 4-fluoro (100, IC₅₀ 2.6 μM).

To investigate activity against the human pathogenic subspecies *T. b. rhodesiense*, the original hit (8) and a selection of analogues were tested against a panel of parasites including *T. b. rhodesiense*, *Trypanosoma cruzi*, *Leishmania donovani*, and *Plasmodium falciparum*, the causative agents of HAT, Chagas disease, leishmania, and malaria, respectively. As shown in Table 5, all of the compounds that were potent against *T. b. rhodesiense* were also potent against *T. b. brucei*. However, there was not a direct correlation, and some compounds, such as 29 and 80, were significantly more potent against the human pathogenic species *T. b. rhodesiense* than might be expected based on their respective activities against *T. b. brucei*. Indeed, the activities of these two compounds against *T. b. rhodesiense* were very promising with respective IC₅₀ values of 61 and 45 nM. In all cases, the compounds were exquisitely selective for

Table 5. Biological Activity Profile of Selected Compounds against a Parasite Panel (IC₅₀, μM)^a

ID	<i>T. b. brucei</i>	<i>T. b. rhod.</i> ^b	<i>T. cruzi</i> ^c	<i>L. don. axe</i> ^d	<i>P. falc. KI</i> ^e	Cytotox. L6 ^f
8	3.03	10	152	48	36	156
25	2.1	0.36	173	>133	124	146
26	2.1	0.61	168	168	88	224
29	1.7	0.061	71	>96	9.7	198
31	2.0	0.97	66	>124	91	70
70	0.89	0.61	198	>131	103	310
79	1.1	0.045	100	>103	48	193
81	0.98	0.24	187	>133	93	283
92	0.41	0.10	176	>121	17	308
94	0.90	0.64	147	>113	72	223

^aValues are means of three experiments, ±50%. ^b*T. b. rhodesiense* strain STIB 900, bloodstream form (trypomastigotes). Melarsoprol was used as a control, IC₅₀ 0.002 μg/mL. ^c*T. cruzi* Tulahaen C4 strain, amastigote stage. Benznidazole was used as a control, EC₅₀ 0.38 μg/mL. ^d*L. donovani* MHOM-ET-67/L82 strain, amastigote stage. Miltefosine was used as a control, EC₅₀ 0.20 μg/mL. ^e*P. falciparum* 3D7 strain, erythrocytic stage. Chloroquine was used as a control, EC₅₀ 0.11 μg/mL. ^fRat skeletal myoblast cell L-6 strain. Podophylotoxin was used as a control, EC₅₀ 0.007 μg/mL.

T. brucei over the other parasites, and they were largely noncytotoxic with respect to the L6 mammalian cell line.

An assessment of drug-likeness was then made, and various physicochemical and metabolic parameters for selected compounds are listed in Table 6. It can be seen that all compounds are of relatively low molecular weight in the range 226–312 gmol⁻¹. Their polar surface areas are low and well within the range where good CNS penetration is plausible.²¹ An in silico prediction model for the potential for CNS exposure was employed to further assess this possibility.²² Of the 14 compounds screened, seven were predicted to have high CNS exposure (nominally defined as a brain to plasma ratio >0.3), and a further two (41 and 93) had values just below the nominal cutoff for high CNS penetration. On the basis of these predictions, this class would be expected to have reasonable CNS exposure, which could potentially lead to the treatment of the CNS stage of HAT. That said, CNS penetration is a very complex phenomenon, given that exposure depends on a number of factors including protein binding, influx and efflux, and metabolism,²³ and an in vivo assessment of these compounds is still required. Likewise, distribution coefficients were favorable in the range 2.3–4.7 at pH 7.4. Aqueous solubility for some compounds was very good; for example, both 42 and 79 had solubilities of greater than 100 μg/mL at both pH 2 and 6.5. This system was strongly influenced by the attached substituents such that 29 was very poorly soluble at 1.6–3.1 μg/mL at pH 2 and <1.6 μg/mL at pH 6.5. Plasma protein binding also varied significantly but was acceptable. Microsomal degradation was moderate to quite high across all compounds tested. Compound 29 was relatively metabolically stable with a predicted E_H value of 0.51. For this compound, the pyridine ring is substituted in the 4-position, and it is possible that the effect is to hinder metabolic oxidation of the adjacent electron-rich 6-position, which is para to the amide group. This hypothesis is supported by the observation that the most metabolically stable compound is 32 with a predicted E_H of 0.47, where the 5-position is blocked by a methoxy group.

The metabolism of compounds 34 and 95 was examined in greater detail in an effort to determine the key sites of

Table 6. Key Physicochemical Parameters and in Vitro Metabolic Stability of Selected Compounds

ID	MW	PSA (Å ²) ^a	log D ^b			cPPB ^d (%)	in vitro CLint (μL/min/mg protein) ^e	microsome-predicted E ₁₁	predicted CNS exposure
			pH 7.4	pH 2	pH 6.5				
22	237	65.8	3.9	6.3–12.5	6.3–12.5	97.6	rapid non-NADPH mediated metabolism	high	
23	237	65.8	2.8	50–100	25–50	64.1	82	0.76	high
25	226	42.0	2.8	>100	25–50	70.1	129	0.83	high
26	247	42.0	3.4	25–50	12.5–50	86.6	128	0.84	high
29	312	42.0	4.7	1.6–3.1	<1.6	98.3	27	0.51	high
32	242	51.2	2.5	>100	12.5–25	60.1	23	0.47	low
34	230	42.0	2.7	25–50	25–50	56.0	43	0.63	low
36	237	65.8	3.9	6.3–12.5	6.3–12.5	97.5	rapid non-NADPH mediated metabolism	high	
41	230	42.0	3.0	>100	>100	67.0	191	0.88	low ^f
70	230	42.0	2.6	50–100	25–50	67.9	58	0.69	low
79	291	42.0	3.2	>100	>100	88.1	97	0.79	low
92	248	42.0	2.8	50–100	25–50	63.9	154	0.86	low
93	244	42.0	3.5	>100	25–50	72.4	237	0.90	low ^f
95	265	42.0	2.3	12.5–25	12.5–25	71.7	254	0.91	high

^aCalculated using ACD/Laboratories software, version 9. ^bMeasured chromatographically. ^cKinetic solubility determined by nephelometry. ^dHuman plasma protein binding estimated using a chromatographic method. ^eIn vitro intrinsic clearance determined in human liver microsomes and predicted hepatic extraction ratio calculated from in vitro data. ^fPredicted B:P values of 0.28, that is, just beneath the nominal cutoff value for high CNS exposure.

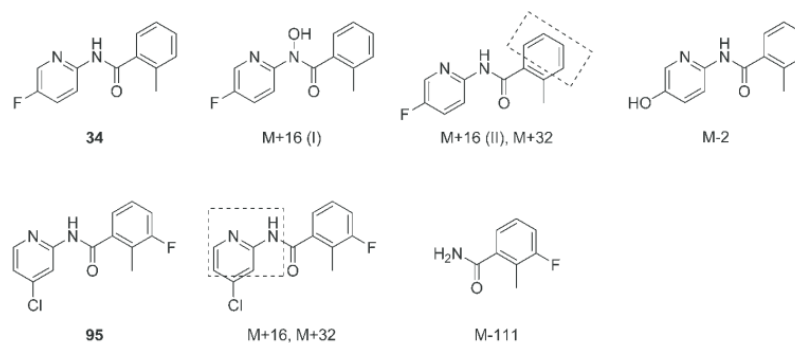


Figure 5. Structures of putative metabolites of 34 and 95. The dotted lines indicate proposed sites of hydroxylation.

metabolism. Metabolism of 34 (Figure 5) in NADPH-supplemented human microsomal incubations revealed two mono-oxygenated metabolites (M+16 (I), *N*-hydroxylation of the amide bond; and M+16 (II), *N*-hydroxylation of the tolyl ring) and one bis-oxygenated metabolite (M+32, dihydroxylation of the tolyl moiety). A putative metabolite with a molecular ion consistent with oxidative defluorination (M–2) was also detected; however, the MS/MS signal was too weak to confirm the structure. In the presence of the dual cofactors, NADPH and UDPGA, limited glucuronidation of M+16 (II) and M+32 was observed, while in an incubation devoid of cofactors, no metabolites were detected, suggesting that NADPH-mediated hydroxylation to M+16 (I) and (II) represents the primary metabolic pathways.

Compound 95 was shown to exhibit a high rate of degradation in NADPH-supplemented human liver microsomes (Table 6), and mono-oxygenated (M+16, oxygenation of the aminopyridine moiety) and bis-oxygenated (M+32, bis-oxygenation of the aminopyridine moiety) species were identified (Figure 5). In addition, a putative metabolite with a molecular ion consistent with *N*-dearylation (M–111) was detected; however, the MS/MS signal was too weak to confirm the structure (Figure 5). In the presence of NADPH and

UDPGA, extensive glucuronidation of the M+16 and M+32 metabolites was observed (i.e., there was a significant decrease in the detection of M+16 and M+32 species in conjunction with the appearance of their respective glucuronide conjugates), while in microsomal samples devoid of cofactors only a very small peak (in terms of peak area response) for the M+16 metabolite was seen, suggesting that this metabolite is likely to be formed via NADPH and, to a lesser extent, non-NADPH-dependent mechanisms. Overall, oxygenation of the aminopyridine region appears to be the major metabolic pathway of 95.

Comparing the metabolite profiles of 34 and 95, the introduction of an aromatic fluorine (as in 95) appeared to reduce the susceptibility of that region to metabolism. However, both compounds were still highly metabolized in the regions without fluorine substitution.

Another important parameter in assessing the therapeutic potential of compounds that inhibit growth of trypanosomes, or indeed any pathogenic parasite, is whether the compounds actually kill the organism or temporarily inhibit their growth. Those that are not cidal are generally viewed with less interest as potential therapeutics. It was therefore determined whether

these compounds were trypanocidal or trypanostatic using cidal assays, and the results are shown in Table 7.

Table 7. Percentage of *T.b. brucei* Trypanosomes Killed Following Exposure to Compounds over a 72 h Period

ID	percentage of cells killed					
	24 h	STDEV	48 h	STDEV	72 h	STDEV
92	92	6.08	99.95	0.07	99.9	0
95	64.23	8.73	83.7	2.40	98.8	0.85
pentamidine	58.1		100		100	
puromycin	100		100		100	
DMSO	0		0		0	

The percentage of *T.b. brucei* trypanosomes killed following 24, 48, and 72 h exposure to the MIC of 92 and 95 as compared to the untreated DMSO control is shown in Table 7. After 24 h incubation with compounds 92 and 95, the number of viable trypanosomes was reduced by >90 and 60%, respectively. Following further 24 h incubation, only a small population of viable trypanosomes remained (<20%), and by 72 h, >98.5% of the trypanosomes had been killed. The continual decrease and almost complete elimination of viable trypanosomes following 72 h exposure to the MIC of 92 and 95 indicates that the compounds are trypanocidal. No viable trypanosomes were detected following 24 and 48 h incubation with puromycin and pentamidine, respectively.

CONCLUSIONS

We have described the discovery of a class of pyridyl benzamides that are novel inhibitors of *T.b. brucei* and *T.b. rhodesiense*. For compound 79, the IC₅₀ value against the human pathogenic subspecies, *T.b. rhodesiense*, was 45 nM. Assessment of predictive ADMET parameters revealed that these very low molecular weight compounds have very favorable properties for further optimization. In particular, they have relatively low log *D* values, good aqueous solubility, and low plasma protein binding. Most of the analogues were predicted to have good CNS penetration, a key feature for the treatment of second stage HAT. These compounds were determined to be cidal and not static in their biological action. Ten compounds have been tested against a panel of parasites, including *T.b. rhodesiense*, alongside *T. cruzi*, *P. falciparum*, and *L. donovani*, and were shown to demonstrate selectivity toward *T. brucei* in comparison to the other trypanosome species. These compounds did not display significant activity against L6 cells. Improvement of the metabolic stability of these compounds will be a key parameter to optimize during the next phase of development.

While an efficacy study for these compounds has not yet been undertaken, it is an important proof of principle experiment. Given the expense associated with using an animal model for HAT and the time required to perform the experiment, further improvement in metabolism is required before these experiments are performed.

The specific biological target or targets of this series of compounds remain unknown. However, for some of the more active compounds, with whole organism IC₅₀ values of less than 100 nM, it is reasonable to assume that target affinity may be in the low nanomolar range. Target identification is warranted to enable the facilitation of the next stage of rational optimization.

EXPERIMENTAL SECTION

General Chemistry Experimental. See the Supporting Information.

Determination of Purity. Purity was determined using high performance liquid chromatography (HPLC) carried out either on a Waters Auto Purification System 3100 with a Waters column (XBridgePrep C18, 5 μm, OBD, 19 × 100 mm) or on a Waters Alliance HT 2795 with a Phenomenex column (Luna, 5 μm, C18, 100 Å, 150 × 10 mm). The purity of all compounds for biological testing was >95% in all cases, except where specified otherwise.

PHYSICOCHEMICAL STUDIES

Solubility Estimates Using Nephelometry. This was obtained as described previously.^{1,24} See the Supporting Information for more information.

Chromatographic Log *D* Measurement. Partition coefficients (log *D*) were estimated as described previously.^{1,25} See the Supporting Information for more information.

Chromatographic Protein Binding Estimation. This was obtained as previously described.^{1,26} See the Supporting Information for more information.

In Vitro Metabolism in Human Liver Microsomes. Data were obtained as described previously.^{1,27,28} See the Supporting Information for more information.

Metabolite ID. Each test compound was incubated at 37 °C with human liver microsomes (XenoTech, lot no. 1210057), and the reaction was initiated by the addition of an NADPH-regenerating system as described above. To maximize the metabolite yield, a high substrate concentration (10 μM) and high microsomal protein concentration (1 mg/mL) were used, and incubations were conducted for up to 60 min. Samples without test compound and without NADPH were included as controls. In addition, a single sample initiated by the addition of the dual cofactor system (containing the NADPH regeneration buffer described and UDPGA (mixture A, BD Gentest) in the presence of 0.025 mg/mL alamethacin) was included (at the 60 min time point) for the qualitative assessment of the potential for glucuronide formation. Reactions were quenched by protein precipitation with an equal volume of ice-cold acetonitrile (containing 0.15 μg/mL diazepam as internal standard), and then centrifuged for 3 min at 10000 rpm. The supernatant was removed and analyzed for parent degradation and metabolite formation by LC/MS (Waters Micromass Xevo G2 QTOF coupled to a Waters Acquity UPLC). The mobile phase consisted of an acetonitrile–water gradient (containing 0.05% formic acid). A Supelco Ascentis Express RP-Amide (50 × 2.1 mm) column was used. MS analyses were conducted in positive mode electrospray ionization under MSE acquisition mode, which allows simultaneous acquisition of MS spectra at low and high collision energies. The identity of putative metabolites was confirmed by accurate mass and MS/MS fragmentation where possible.

In Silico Prediction of CNS Exposure. The partial least-squares projection to latent structures (PLS) model developed for CNS exposure in 2012²² was applied to 14 representative compounds. SMILES strings were submitted to the software Corina 3.0 (Molecular Networks, Erlangen, Germany) to produce the three-dimensional structures. The resulting structures were used to calculate a large number of physicochemical properties and molecular descriptors using DragonX (Talet, Italy). These descriptors were then submitted to the PLS model, and the CNS exposure was predicted. On the basis of the predicted brain to plasma (B:P)

value, the compounds were classified as showing high CNS exposure (B:P > 0.3) or low CNS exposure (B:P < 0.3).

■ BIOLOGICAL ASSAYS

All in vitro assays were carried out at least twice independently in singleton. The IC₅₀ values are the means of two independent assays and vary by less than ±50%.

***P. falciparum* Assay.** This was undertaken as previously described.^{1,29–32} See the Supporting Information for more information.

***L. donovani* Axenic Amastigotes Assay.** This was undertaken as previously described.^{1,32–34} See the Supporting Information for more information.

***T. cruzi* Assay.** Data were obtained as previously described.^{1,32,35} See the Supporting Information for more information.

***T. brucei rhodesiense* Assay.** This was undertaken as previously described.^{1,32,36,37} See the Supporting Information for more information.

Rat Skeletal Myoblast Cytotoxicity Assay. This was undertaken as previously described.^{1,32,38,39} See the Supporting Information for more information.

***T.b. brucei* Assay.** This was undertaken as previously described.^{1,40,41} See the Supporting Information for more information.

HEK293 Cytotoxicity Assay. This was undertaken as previously described.¹ See the Supporting Information for more information.

Cidal Assay. The number of viable trypanosomes remaining following 24, 48, and 72 h exposure to the minimum inhibitory concentration (MIC) of compounds was determined by directly visualizing and counting the number of parasites present at each time point. The assay was performed as described previously in detail by Sykes et al.¹³ Briefly, 55 μL of *T.b. brucei* parasites was added to a black/clear bottomed 384 well microtiter plate and incubated for 24 h at 37 °C/5% CO₂. Compounds were diluted in DMEM medium, and 5 μL of this dilution was added to assay plates to give the MIC. After 24, 48, and 72 h incubation at 37 °C/5% CO₂, wells were directly visualized under a microscope, and the number of parasites remaining was determined by counting a sample of the wells in a hemocytometer. The cell counts were compared to that of the positive control, puromycin (MIC 1.15 μM), and the negative control DMSO (0.4%), and the percentage of trypanosomes killed was subsequently determined. The MIC of each compound was defined as the minimum concentration at which there was a plateau of activity in the Alamar blue assay (>95% activity). The experiment was performed in duplicate.

■ ASSOCIATED CONTENT

Supporting Information

Experimental procedures for compound synthesis and characterization. This material is available free of charge via the Internet at <http://pubs.acs.org>.

■ AUTHOR INFORMATION

Corresponding Author

*Tel.: +61 9903 9044. E-mail: Jonathan.Baell@monash.edu.

Author Contributions

□ L.F. and M.G. contributed equally.

Notes

The authors declare no competing financial interest.

■ ACKNOWLEDGMENTS

This research was supported by the NHMRC (IRIIS grant number 361646; NHMRC Senior Research Fellowship 1020411 (J.B.B.), NHMRC Project Grant 1025581); Victorian State Government OIS grant; the Australian Government for the Australian Postgraduate Award (L.F.); Dr. Jason Dang for his assistance in obtaining some of the analytical data; and DNDi for allowing access to their parasite screening platform at STPHI.

■ ABBREVIATIONS USED

CNS, central nervous system; HAT, human African trypanosomiasis; *T.b. brucei*, *Trypanosoma brucei* *brucei*; *T.b. gambiense*, *Trypanosoma brucei* *gambiense*; *T.b. rhodesiense*, *Trypanosoma brucei* *rhodesiense*

■ REFERENCES

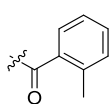
- (1) WHO. Control and surveillance of human African trypanosomiasis. http://apps.who.int/iris/bitstream/10665/95732/1/9789241209847_eng.pdf (accessed, 10th January, 2014).
- (2) Brun, R.; Blum, J.; Chappuis, F.; Burri, C. Human African trypanosomiasis. *Lancet* **2010**, *375*, 148–159.
- (3) WHO. Drugs. http://www.who.int/trypanosomiasis_african/drugs/en/index.html (accessed, July 27, 2012).
- (4) Voogd, T. E.; Vansterkenburg, E. L.; Wilting, J.; Janssen, L. H. Recent research on the biological activity of suramin. *Pharmacol. Rev.* **1993**, *45*, 177–203.
- (5) de Koning, H. P. Transporters in African trypanosomes: role in drug action and resistance. *Int. J. Parasitol.* **2001**, *31*, S12–S22.
- (6) Nok, A. J. Arsenicals (melarsoprol), pentamidine and suramin in the treatment of human African trypanosomiasis. *Parasitol. Res.* **2003**, *90*, 71–79.
- (7) Seebeck, T.; Maser, P. Drug resistance in African Trypanosomiasis. In *Antimicrobial Drug Resistance*; Mayers, D. L., Ed.; Humana Press: Totowa, NJ, 2009; pp 589–604.
- (8) Priotto, G.; Kasparian, S.; Mutombo, W.; Ngouama, D.; Ghorashian, S.; Arnold, U.; Ghabri, S.; Baudin, E.; Buard, V.; Kazadi-Kyanza, S.; Ilunga, M.; Mutangala, W.; Pohl, G.; Schmid, C.; Karunakara, U.; Torrelee, E.; Kande, V. Nifurtimox-eflornithine combination therapy for second-stage African *Trypanosoma brucei gambiense* trypanosomiasis: a multicentre, randomised, phase III, non-inferiority trial. *Lancet* **2009**, *374*, 56–64.
- (9) Barrett, M. P. Potential new drugs for human African trypanosomiasis: some progress at last. *Curr. Opin. Infect. Dis.* **2010**, *23*, 603–608.
- (10) DNDi. New Oral Drug Candidate for African Sleeping Sickness. <http://www.dndi.org/media-centre/press-releases/354-media-centre/press-releases/1505-new-oral-drug-candidate-hat.html> (accessed, 9th July).
- (11) DNDi. Oxaborole SCYX-7158 (HAT). <http://www.dndi.org/portfolio/oxaborole-scyx-7158.html> (accessed, July 27, 2012).
- (12) Ferrins, L.; Rahmani, R.; Baell, J. B. Drug discovery and human African trypanosomiasis: a disease less neglected? *Future Med. Chem.* **2013**, *5*, 1801–1841.
- (13) Sykes, M. L.; Baell, J. B.; Kaiser, M.; Chatelain, E.; Moawad, S. R.; Ganame, D.; Ioset, J.-R.; Avery, V. M. Identification of Compounds with Anti-Proliferative Activity against *Trypanosoma brucei* *brucei* Strain 427 by a Whole Cell Viability Based HTS Campaign. *PLoS Neglected Trop. Dis.* **2012**, *6*, e1896.
- (14) Ferrins, L.; Rahmani, R.; Sykes, M. L.; Jones, A. J.; Avery, V. M.; Teston, E.; Almohaywi, B.; Yin, J.; Smith, J.; Hyland, C.; White, K. L.; Ryan, E.; Campbell, M.; Charman, S. A.; Kaiser, M.; Baell, J. B. 3-(Oxazolo[4,5-*b*]pyridin-2-yl)anilides as a novel class of potent inhibitors for the kinetoplastid *Trypanosoma brucei*, the causative agent for human African trypanosomiasis. *Eur. J. Med. Chem.* **2013**, *66*, 450–465.

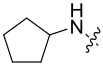
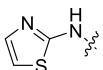
- (15) White, G. A. Substituted benzanilides: Structural variation and inhibition of complex II activity in mitochondria from a wild-type strain and a carboxin-selected mutant strain of *Ustilago maydis*. *Pestic. Biochem. Physiol.* **1987**, *27*, 249–260.
- (16) Turrens, J. F. The role of succinate in the respiratory chain of *Trypanosoma brucei* procyclic trypomastigotes. *Biochem. J.* **1989**, *259*, 363–368.
- (17) Zeiman, E.; Greenblatt, C. L.; Elgavish, S.; Khozin-Goldberg, I.; Golenser, J. Mode of action of fenarimol against *Leishmania* spp. *J. Parasitol.* **2008**, *94*, 280–286.
- (18) Urbina, J. A.; Payares, G.; Molina, J.; Sanoja, C.; et al. Cure of short- and long-term experimental Chagas' disease using D0870. *Science* **1996**, *273*, 969–971.
- (19) Gamon, F.-J.; Sanz, L. M.; Vidal, J.; de Cozar, C.; Alvarez, E.; Lavandera, J.-L.; Vanderwall, D. E.; Green, D. V. S.; Kumar, V.; Hasan, S.; Brown, J. R.; Peishoff, C. E.; Cardon, L. R.; Garcia-Bustos, J. F. Thousands of chemical starting points for antimalarial lead identification. *Nature* **2010**, *465*, 305–310.
- (20) Meanwell, N. A. Synopsis of some recent tactical application of bioisosteres in drug design. *J. Med. Chem.* **2011**, *54*, 2529–2591.
- (21) Pajouhesh, H.; Lenz, G. R. Medicinal chemical properties of successful central nervous system drugs. *NeuroRx* **2005**, *2*, 541–53.
- (22) Bergström, C. S.; Charman, S.; Nicolazzo, J. Computational prediction of CNS drug exposure based on a novel *in vivo* dataset. *Pharm. Res.* **2012**, *29*, 3131–3142.
- (23) Di, L.; Rong, H.; Feng, B. Demystifying brain penetration in central nervous system drug discovery. *J. Med. Chem.* **2012**, *56*, 2–12.
- (24) Bevan, C. D.; Lloyd, R. S. A high-throughput screening method for the determination of aqueous drug solubility using laser nephelometry in microtiter plates. *Anal. Chem.* **2000**, *72*, 1781–1787.
- (25) Lombardo, F.; Shalaeva, M. Y.; Tupper, K. A.; Gao, F. ElogDoct: A tool for lipophilicity determination in drug discovery. 2. Basic and neutral compounds. *J. Med. Chem.* **2001**, *44*, 2490–2497.
- (26) Valko, K.; Nunhuck, S.; Bevan, C.; Abraham, M. H.; Reynolds, D. P. Fast gradient HPLC method to determine compounds binding to human serum albumin. Relationships with octanol/water and immobilized artificial membrane lipophilicity. *J. Pharm. Sci.* **2003**, *92*, 2236–2248.
- (27) Obach, R. S. Prediction of human clearance of twenty-nine drugs from hepatic microsomal intrinsic clearance data: An examination of *in vitro* half-life approach and nonspecific binding to microsomes. *Drug Metab. Dispos.* **1999**, *27*, 1350–1359.
- (28) Davies, B.; Morris, T. Physiological parameters in laboratory animals and humans. *Pharm. Res.* **1993**, *10*, 1093–1095.
- (29) Desjardins, R. E.; Canfield, C. J.; Haynes, J. D.; Chulay, J. D. Quantitative assessment of antimalarial activity *in vitro* by a semiautomated microdilution technique. *Antimicrob. Agents Chemother.* **1979**, *16*, 710–718.
- (30) Matile, H.; Pink, J. R. L. *Plasmodium falciparum* malaria parasite cultures and their use in immunology. In *Immunological Methods*; Lefkovits, I., Pernis, B., Eds.; Academic Press: San Diego, CA, 1990.
- (31) Ponnudurai, T.; Leeuwenberg, A. D.; Meuwissen, J. H. Chloroquine sensitivity of isolates of *Plasmodium falciparum* adapted to *in vitro* culture. *Trop. Geogr. Med.* **1981**, *33*, 50–54.
- (32) Huber, W.; Koella, J. C. A comparison of three methods of estimating EC₅₀ in studies of drug resistance of malaria parasites. *Acta Trop.* **1993**, *55*, 257–261.
- (33) Cunningham, M. L.; Fairlamb, A. H. Trypanothione reductase from *Leishmania donovani*. Purification, characterisation and inhibition by trivalent antimonials. *Eur. J. Biochem.* **1995**, *230*, 460–468.
- (34) Mikus, J.; Steverding, D. A simple colorimetric method to screen drug cytotoxicity against *Leishmania* using the dye Alamar Blue. *Parasitol. Int.* **2000**, *48*, 265–269.
- (35) Buckner, F. S.; Verlinde, C. L.; La Famme, A. C.; CVan Voorhis, W. C. Efficient technique for screening drugs for activity against *Trypanosoma cruzi* using parasites expressing beta-galactosidase. *Antimicrob. Agents Chemother.* **1996**, *40*, 2592–2597.
- (36) Baltz, T.; Baltz, D.; Giroud, C.; Crockett, J. Cultivation in a semi-defined medium of animal infective forms of *Trypanosoma brucei*, *T. equiperdum*, *T. evansi*, *T. rhodesiense* and *T. gambiense*. *EMBO J.* **1985**, *4*, 1273–1277.
- (37) Rätz, B.; Iten, M.; Grether-Bühler, Y.; Kaminsky, R.; Brun, R. The Alamar Blue assay to determine drug sensitivity of African trypanosomes (*T.b. rhodesiense* and *T.b. gambiense*) *in vitro*. *Acta Trop.* **1997**, *68*, 139–147.
- (38) Page, B.; Page, M.; Noel, C. A new fluorometric assay for cytotoxicity measurements *in vitro*. *Int. J. Oncol.* **1993**, *3*, 473–476.
- (39) Ahmed, S. A.; Gogal, R. M.; Walsh, J. E. A new rapid and simple non-radioactive assay to monitor and determine the proliferation of lymphocytes: an alternative to [³H]thymidine incorporation assay. *J. Immunol. Methods* **1994**, *170*, 211–224.
- (40) Sykes, M. L.; Avery, V. M. Development of an Alamar blue viability assay in 384-well format for high throughput whole cell screening of *Trypanosoma brucei brucei* bloodstream form strain 427. *Am. J. Trop. Med. Hyg.* **2009**, *81*, 665–674.
- (41) Hirumi, H.; Hirumi, K. Continuous cultivation of *Trypanosoma brucei* bloodstream forms in a medium containing a low concentration of serum protein without feeder cell layers. *J. Parasitol.* **1989**, *75*, 985–989.

4.6. Post-script: further development of SAR

Throughout the investigations of the pyridine ring a number of analogues with five-membered heterocycles were synthesised, as shown in the preceding published article. In addition to this the cyclopentyl and thiazole analogues were also synthesised, as shown in Table 4.2. Replacement of the pyridine with a cyclopentyl (**4.07**) led to a complete loss of activity in this assay, though this was not unexpected given the loss of activity upon removal of the pyridyl nitrogen as previously shown. Replacement with the thiazole (**4.08**, compound synthesised by Raphaël Rahmani) led to a compound which had an EC₅₀ of 2.19 μM which was comparable to the starting compound, **1.92**.

Table 4.2 Further replacement of the pyridine.



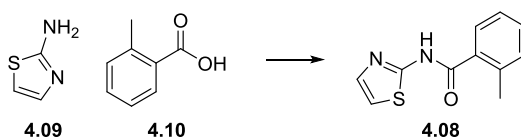
ID	R	EC ₅₀ (μM)	SI ^a
4.07		> 10 ^b	
4.08		2.19 ± 0.02	38

^a Selectivity relative to HEK293 (Human Embryonic Kidney) mammalian cells.

^b Compound exhibited < 50% activity at 10.41 μM.

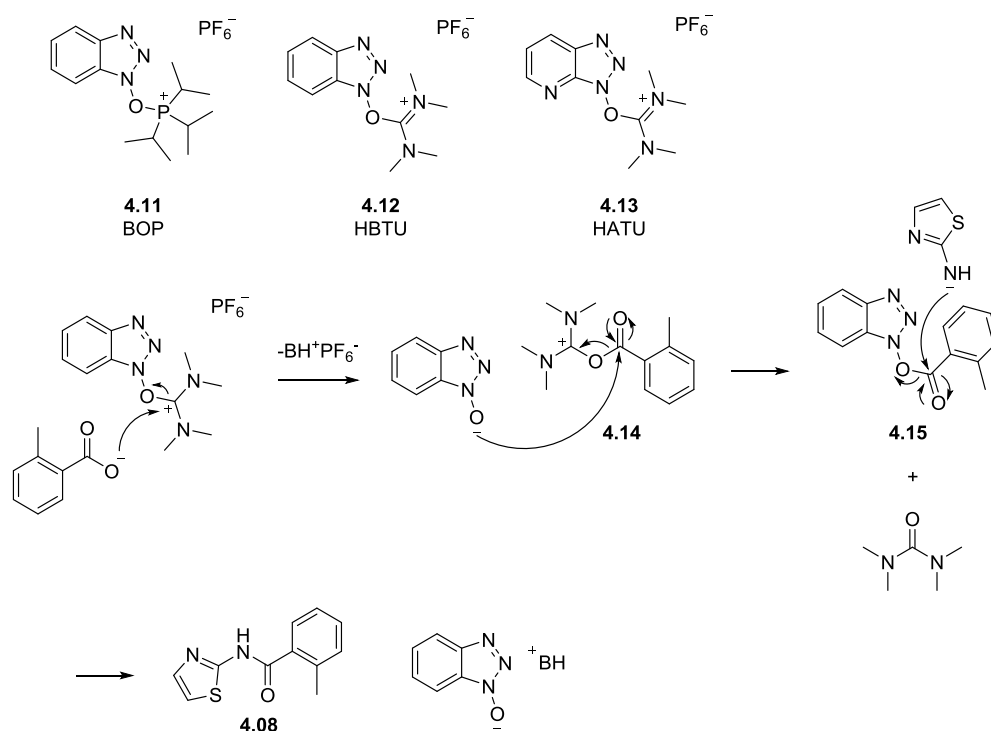
Given the activity of the thiazole analogue new avenues for SAR exploration were opened. In order to explore this new series a number of amide coupling conditions were trialled in order to identify the most suitable conditions for the series. The results of this have been summarised in Table 4.3.

Table 4.3 Optimisation of amide coupling conditions for the thiazole series.



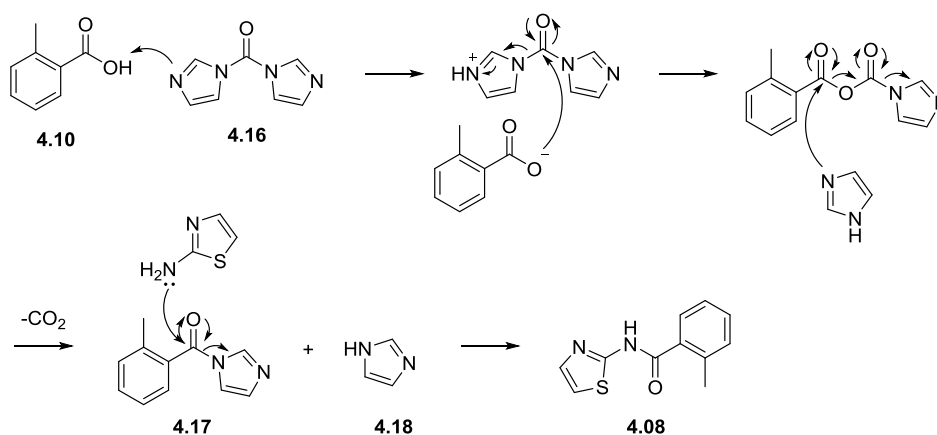
Entry	Reaction conditions	Isolated yield
1	2-aminothiazole (1.1 eq.), <i>o</i> -toluic acid (1 eq.), DIPEA (2 eq.), BOP (1 eq.), DCM	Trace amount of product by LCMS
2	2-aminothiazole (1.2 eq.), <i>o</i> -toluic acid (1 eq.), HATU (1.2 eq.), DIPEA (2 eq.), DMF, rt, 18 h	29%
3	2-aminothiazole (1.2 eq.), <i>o</i> -toluic acid (1 eq.), HBTU (1.2 eq.), DIPEA (2 eq.), DMF, rt, 18 h	62%
4	2-aminothiazole (1 eq.), <i>o</i> -toluic acid (1 eq.), CDI (1 eq.), THF, rt, 18 h	Trace amount of product by LCMS
5	2-aminothiazole (1 eq.), <i>o</i> -toluic acid (1.2 eq.), EDCI (1.2 eq.), DMAP (0.1 eq.), DMF, 45 °C, 18 h	38%
6	2-aminothiazole (1.1 eq.), <i>o</i> -toluic acid (1 eq.), EDCI (1.1 eq.), HOBt (1.1 eq.), DIPEA (2.1 eq.), DMF, rt, 18 h	46%

Initially a range of phosphonium salts, BOP (**4.11**), HBTU (**4.12**) and HATU (**4.13**) were trialled (entries 1-3, Table 4.3). In all of these reactions the acid is first deprotonated by the base before reacting with the phosphonium salt to generate the activated acylphosphonium species (**4.14**) and HOBt (when BOP and HBTU are used) or HOAt (when HATU is used).¹¹⁴ The HOBt/HOAt then readily reacts with the activated acid forming a reactive ester (**4.15**) which then undergoes aminolysis.¹¹⁴ This is summarised in Scheme 4.3. For this series there was a strong preference for HBTU (yield – 62%) with BOP only producing a trace amount of the desired product by LCMS and HATU yielding 29% of the desired product.



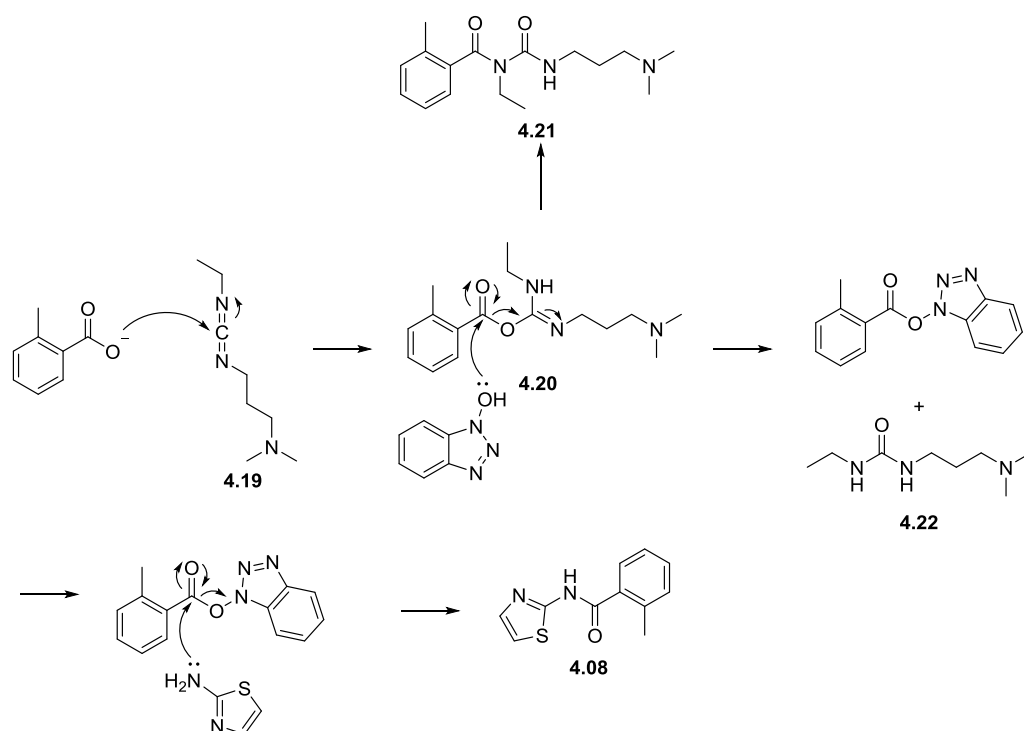
Scheme 4.3 Mechanism for the amide coupling using HBTU. Base initially abstracts the proton from the *o*-toluic acid which can then attack the electron deficient carbon of HBTU. The resulting HOBT anion can then react with the activated benzoic acid intermediate to form an activated ester. The amine then reacts with the activated ester to form the desired product.

Carbonyldiimidazole (CDI; **4.16**) was also utilised (entry 4, Table 4.3) which forms an acylimidazole intermediate (**4.17**) before reacting with the amine, as summarised in Scheme 4.4.¹¹⁵ This route only led to trace amounts of the product being formed by LCMS.



Scheme 4.4 Mechanism for the amide coupling using CDI where imidazole (**4.18**) and carbon dioxide are produced as by-products in the reaction.

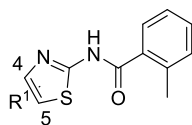
The carbodiimides were further explored utilising solely 1-ethyl-3-(3-dimethylaminopropyl)carbodiimide (EDCI; **4.19**) as in entry 5 (Table 4.3) and EDCI in combination with HOBt as in entry 6 (Table 4.3). In this instance the carbodiimide reacts with the carboxylic acid, forming an *O*-acylisourea mixed anhydride (**4.20**) and the urea by-product **4.22**.¹¹⁴ This activated ester reacts directly with the amine to give the desired product. In the presence of solely EDCI this reaction only yielded 38% of the desired product. However, it is possible to include HOBt in the reaction mixture, which can prevent side reactions from occurring and increase the overall yield of the reaction.¹¹⁴ The main side reaction involves rearrangement of the *O*-acylisourea to the more stable *N*-acylurea (**4.21**). In this instance the addition of the HOBt did lead to an improvement in the yield observed, up to 46%. The mechanism for the amide coupling mediated by EDCI and HOBt is shown in Scheme 4.5.



Scheme 4.5 Mechanism for the amide coupling using EDCI and HOBt. When HOBt is excluded from the reaction mixture it is possible for the O-acylisourea (4.20) to rearrange to the N-acylurea (4.21) which is more stable and results in the termination of the reaction progress at this step. The urea (4.22) and any excess carbodiimide reagent are water soluble so can be easily removed from the reaction.

Overall the most favourable conditions for this transformation involved pre-forming the activated ester with HBTU before reaction with the amine. A number of commercially available analogues were selected in order to probe the SAR around the thiazole system. The results of this preliminary investigation have been summarised in Table 4.4.

Table 4.4 Exploration of the SAR around the thiazole system.



ID	R ¹	Yield	EC ₅₀ (μM)	SI ^a
4.23	4-CH ₃	59%	1.09 ± 0.28	76
4.24	4-COOCH ₃	31%	6.40 ± 1.10	13
4.25	4-COOH	- ^b	> 10 ^c	
4.26	5-CH ₃	48%	> 10 ^d	

^a Selectivity relative to HEK293 (Human Embryonic Kidney) mammalian cells.

^b Compound synthesised by hydrolysis of the ester of **4.24** using lithium hydroxide in a mixture of THF and water.

^c Compound exhibited < 50% activity at 10.41 μM.

^d Compound exhibited 54% activity at 10.41 μM.

Substitution of the 4-position with a methyl group (**4.23**, EC₅₀ 1.09 μM) led to a two-fold improvement in the activity of this series when compared with the unsubstituted thiazole (**4.08**, EC₅₀ 2.19 μM). Substitution with a methyl ester (**4.24**, EC₅₀ 6.40 μM) led to a three-fold loss in activity and the corresponding carboxylic acid derivative (**4.25**, EC₅₀ > 10 μM) was found to lose all activity in these assays. It is possible that this latter result could be as a result of poor membrane permeability rather than a loss of interaction with the putative target of these compounds, though it is not possible to tell at this point. Substitution of the 5-position with a methyl group (**4.26**, EC₅₀ > 10 μM) led to a loss of activity in these assays suggesting that the 5-position is generally unfavourable for substitution. In order to confirm this, a small number of alternative analogues would also need to be synthesised.

4.7. Metabolism analysis

Analysis of the metabolism of these thiazole analogues (Table 4.5) revealed that **4.08** had the superior metabolic profile, with a half-life of 29 min and an *in vitro* hepatic extraction ratio of 0.70. Both of the methylated analogues (**4.23** and **4.26**) were found to have significantly shorter half-lives and higher *in vitro* hepatic extraction ratios than **4.08**.

Table 4.5 Metabolism evaluation of compounds against human and mouse liver microsomes.

ID	Species	Half-life (min)	<i>In vitro</i> CL _{int} (μ l/min/mg protein)	Microsome- predicted E _H	Clearance classification
4.08	Human	29	59	0.70	Intermediate
4.23	Human	4	463	0.95	High
	Mouse	2	959	0.95	Very high
4.26	Human	8 ^a	231	0.90	High
	Mouse	2	845	0.95	High

^a Calculations based on the initial rate of loss (2-30 min), due to apparent deviation from first-order kinetics.

4.8. Biological analysis of compounds against *T. vivax* and *T. congolense*

A selection of compounds were analysed by researchers at the Swiss Tropical and Public Health Institute as part of the GALVmed project. The compounds were tested *ex vivo* against *T. vivax* and *in vivo* against *T. congolense* which are both causative agents for animal trypanosomiasis in Western and Eastern Africa respectively.⁹⁰ Table 4.6 summarises the results of these biological assays.

Table 4.6 *T. vivax* and *T. congolense* inhibitory activity of selected compounds.

ID	<i>T. vivax</i> EC ₅₀ (μM)	<i>T. congolense</i> EC ₅₀ (μM)
1.92	0.81	2.3
29^a	1.5	1.3
92^a	0.044	0.41
97^a	0.072	0.64
4.08	0.51	1.8
Diminazene^b	0.34	0.25
Isometamidium^b	0.0006	0.0006

^a Compound number from the J. Med. Chem. manuscript.

^b Compound included as a standard control.

In general the compounds tested were shown to have nanomolar inhibition against *T. vivax* and low micromolar inhibition against *T. congolense*. Compound **29** is substituted with a phenylacetylene moiety at the 4-position of the pyridyl ring, and this addition leads to a 2-fold drop in activity when compared with **1.92** against *T. vivax*, though there is also a ~two-fold increase in activity when tested against *T. congolense*. Substitution of both the pyridyl and tolyl rings with fluorine (**92** and **97**) led to a significant improvement in the activity against *T. vivax* (20- and 10-fold respectively) and *T. congolense* (6- and 4-fold, respectively). Replacement of the pyridyl ring with the thiazole moiety (**4.08**) also led to a moderate improvement in the activity of the compound against both *T. vivax* and *T. congolense* when compared with **1.92**. In all cases the analogues tested were found to be less potent than the control compounds, diminazene and isometamidium.

4.9. Halonitrobenzamides as inhibitors of *T.b. brucei*

During the course of these investigations data on a related series of halonitrobenzamides was published in the literature (Figure 4.2).¹¹⁶ Compound **4.27** was serendipitously discovered by the researchers during routine testing of compounds for antitrypanosomal activity.¹¹⁶ It was found to have an EC₅₀ of 1.5 μM

against *T.b. brucei*, though selectivity was an issue (HepG2 EC₅₀ 2.5 μM) as was solubility and permeability.¹¹⁶ Replacement of the fluorine with a chlorine and replacement of the hydrophobic chain with a chlorine led to the identification of **4.28**, which still had low micromolar inhibition against *T.b. brucei* (EC₅₀ 1.5 μM) and improved selectivity (EC₅₀ > 50 μM), solubility and permeability.¹¹⁶

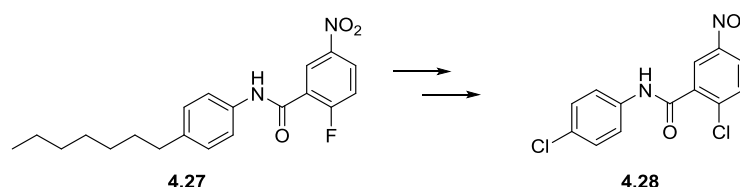


Figure 4.2 Serendipitous discovery of the halonitrobenzamides through routine testing. Compound **4.27** was the initial compound identified and after a series of SAR studies **4.28** was identified with maintained potency and improved selectivity, solubility and permeability.

Further work has since been published that has focused upon elaboration of the SAR around this series of compounds.¹¹⁷ After an extensive SAR investigation **4.29** was identified (Figure 4.3). It was found to have an EC₅₀ of 27 nM against *T.b. brucei* and in further testing against *T.b. rhodesiense* and *T.b. gambiense* it had EC₅₀ values of 7 nM and 2 nM respectively.¹¹⁷ This compound also exhibited excellent selectivity with an EC₅₀ value of > 25 μM against HEK293 and HEPG2 cell lines.¹¹⁷

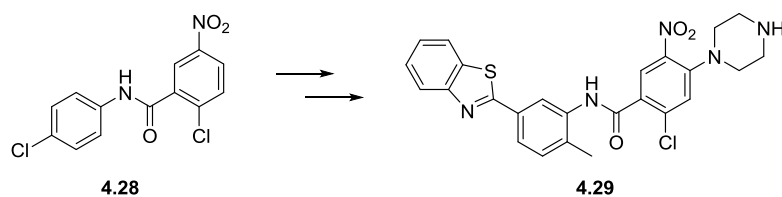


Figure 4.3 Identification of **4.29** after an extensive SAR investigation. Compound **4.29** was found to be a nanomolar inhibitor of *T.b. brucei*, *T.b. rhodesiense* and *T.b. gambiense* it also had good physicochemical properties and microsomal stability for progression into in vivo studies.

Given the overlap between the halonitrobenzamides and the pyridyl benzamides it was decided to test the hypothesis that these series could be related. As such, an analogue was designed with a nitro at the 5-position

of the tolyl ring (**4.30**, Figure 4.4), which would determine if there was the potential for overlapping SAR across this compound series. A number of analogues have already been presented to suggest that these two series were indeed separate with removal of the pyridyl nitrogen leading to an analogue, which had an EC_{50} of $> 10 \mu\text{M}$ against *T.b. brucei* (compound **52**, *J. Med. Chem.* manuscript). However, the nitro substituent appeared to be critical for the activity of the halonitrobenzamides, as such, **4.30** was synthesised and tested against *T.b. brucei*. Compound **4.30** was found to be inactive in the assay, confirming the lack of cross-over activity between the series.

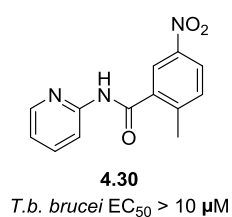


Figure 4.4 Introduction of the nitro group led to a complete loss in activity against *T.b. brucei*.

4.10. Future work

There has been a significant improvement in the inhibitory activity of the compounds in this series, though the ADME analysis revealed that the metabolism of this series is a key factor to address when progressing this series further. Given metabolite identification studies revealed that introduction of an aromatic fluorine at the 5-position of the pyridine ring leads to a reduction in the susceptibility of the region to metabolism, it would be pertinent to further explore this (Figure 4.5). Hydrolysis of the amide and hydroxylation of the amide $-\text{NH}$ were also described in the preceding *J. Med. Chem.* manuscript. Investigation of bulky substituents at the *ortho* positions is required to understand if metabolism can be modulated in this way.

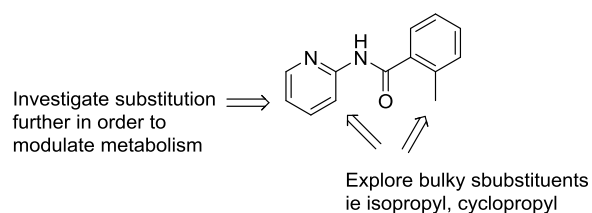


Figure 4.5 Concepts identified for consideration in future synthetic programs.

4.11. Experimental

General Procedure 4-A1: Amide coupling

Relevant benzoic acid (1.0 eq.) was dissolved in dichloromethane (0.5 M final concentration) and catalytic DMF added. The suspension was cooled under nitrogen in an ice bath to 0 °C prior to the gradual addition of oxalyl chloride (1.1 eq.). The reaction was allowed to react until no further effervescence was observed at which point all volatiles were removed under reduced pressure. The residue was again cooled to 0 °C in an ice bath and tetrahydrofuran added (0.5 M final concentration) before gradual addition of the relevant amine (1.0 eq.) and pyridine (2.0 eq.). The reaction mixture was stirred under nitrogen and allowed to warm to ambient temperature and stirred for 18 h. The reaction was acidified with 1.0 M aqueous hydrochloric acid solution and extracted with ethyl acetate. Purification was performed by recrystallisation from cyclohexane and gave the desired pyridyl benzamide.

General Procedure 4-A2: Amide coupling

To a solution of the amine (1.0 eq.) in DMF (0.5 M final concentration) was added the benzoic acid (1.2 eq.), EDCI (1.2 eq.) and DMAP (0.1 eq.). The reaction mixture was stirred at 30 °C for 18 h. Water (approximately 1 ml) was added to the reaction mixture and it was transferred to the fridge overnight. The resulting precipitate was filtered and gave the desired pyridyl benzamide.

General Procedure 4-A3: Amide coupling

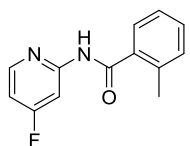
To a solution of the benzoic acid (1.0 eq.) in DMF (0.5 M final concentration) was added HBTU (1.2 eq.), and DIPEA (5.0 eq.). The reaction was allowed to stir at ambient temperature for 10 min before addition of

the amine (2.0 eq.). The reaction mixture was stirred at 60 °C for 18 h. Water (approximately 1 ml) was added to the reaction mixture and it was transferred to the fridge for 18 h. The resulting precipitate was filtered and gave the desired pyridyl benzamide.

General Procedure 4-B1: Suzuki coupling

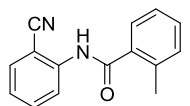
Relevant brominated pyridyl benzamide (1.0 eq.), potassium carbonate (4.0 eq.), relevant phenylboronic acid (or its' pinacol ester as specified) (1.2 eq.), TBAB (0.1 eq.), PdCl₂ (0.05 eq.) and dppf (0.055 eq.) were combined in a microwave reactor vessel with 4:1 dioxane, and water (0.5 M final concentration) were added. The reaction mixture was irradiated in a CEM microwave at 130 °C for the time specified. The reaction was diluted with ethyl acetate and filtered through celite and the filtrate collected. The solvent was removed to give the crude product that was purified by column chromatography, eluting with 10% ethyl acetate/petroleum benzene to give the desired product.

N-(4-Fluoropyridin-2-yl)-2-methylbenzamide (**28**; J. Med. Chem. manuscript)



Title compound prepared according to General Procedure 4-A3 as an off-white solid (54 mg, 13%). HPLC – rt 6.36 min > 98% purity at 254 nm; LRMS [M+H]⁺ 231.0 m/z; HRMS [M+H]⁺ 231.0928 m/z, found 231.0926 m/z; ¹H NMR (400 MHz, DMSO) δ 11.08 (s, 1H), 8.39 (dd, *J* = 9.3, 5.7 Hz, 1H), 8.04 (dd, *J* = 12.0, 2.4 Hz, 1H), 7.51 – 7.43 (m, 1H), 7.39 (td, *J* = 7.5, 1.4 Hz, 1H), 7.34 – 7.22 (m, 2H), 7.10 (ddd, *J* = 8.2, 5.7, 2.4 Hz, 1H), 2.39 (s, 3H); ¹³C NMR (101 MHz, DMSO) δ 168.9, 168.9 (*J*_{C-F} = 258 Hz), 154.4 (*J*_{C-F} = 11 Hz), 150.7 (*J*_{C-F} = 8 Hz), 136.0, 135.5, 130.6, 130.1, 127.6, 125.6, 107.7 (*J*_{C-F} = 17 Hz), 101.3 (*J*_{C-F} = 23 Hz), 19.5.

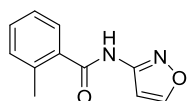
N-(2-Cyanophenyl)-2-methylbenzamide (**53**; J. Med. Chem. manuscript)



Title compound prepared according to General Procedure 4-A1 as a white solid (55%). HPLC – rt 6.68 min > 97% purity at 254 nm; LRMS [M+H]⁺ 237.2 m/z; HRMS [M+H]⁺ 237.1022 m/z, found 237.1022 m/z; ¹H NMR (400 MHz, DMSO) δ 10.58 (s, 1H), 7.88 (dd, *J* = 7.8, 1.3 Hz,

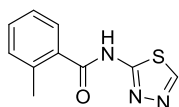
1H), 7.82 – 7.68 (m, 1H), 7.68 – 7.51 (m, 2H), 7.44 (td, $J = 7.7, 1.2$ Hz, 2H), 7.39 – 7.26 (m, 2H), 2.47 (s, 3H); ^{13}C NMR (101 MHz, DMSO) δ 168.0, 140.1, 135.9, 135.8, 133.8, 133.1, 130.7, 130.1, 127.4, 126.5, 126.3, 125.7, 117.0, 109.0, 19.4.

N-(Isoxazol-3-yl)-2-methylbenzamide (**54**; J. Med. Chem. manuscript)



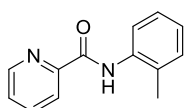
Title compound prepared according to General Procedure 4-A1 as an off-white solid (226 mg, 61%). HPLC – rt 5.82 min > 99% purity at 254 nm; LRMS $[\text{M}+\text{H}]^+$ 203.2 m/z; HRMS $[\text{M}+\text{H}]^+$ 203.0815 m/z, found 203.0813 m/z; ^1H NMR (400 MHz, DMSO) δ 11.35 (s, 1H), 8.83 (d, $J = 1.7$ Hz, 1H), 7.52 – 7.45 (m, 1H), 7.40 (td, $J = 7.5, 1.3$ Hz, 1H), 7.33 – 7.27 (m, 2H), 7.02 (s, 1H), 2.38 (s, 3H); ^{13}C NMR (101 MHz, DMSO) δ 167.9, 160.2, 157.8, 135.9, 135.4, 130.8, 130.4, 127.7, 125.7, 99.6, 19.5.

N-(1,3,4-thiadiazol-2-yl)benzamide (**59**; J. Med. Chem. manuscript)



Title compound prepared according to General Procedure 4-A1 as a pale-yellow solid (108 mg, 27%). HPLC – rt 5.55 min > 99% purity at 254 nm; LRMS $[\text{M}+\text{H}]^+$ 220.1 m/z; HRMS $[\text{M}+\text{H}]^+$ 220.0539 m/z found 220.0534 m/z; ^1H NMR (400 MHz, DMSO) δ 9.24 (s, 1H), 7.68 – 7.53 (m, 1H), 7.46 (td, $J = 7.6, 1.3$ Hz, 1H), 7.33 (ddd, $J = 9.9, 5.3, 0.6$ Hz, 2H), 2.40 (s, 3H); ^{13}C NMR (101 MHz, DMSO) δ 167.5, 158.9, 149.0, 136.6, 133.5, 131.0, 130.9, 128.3, 125.8, 19.6.

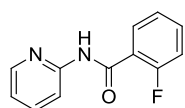
N-(*o*-Tolyl)picolinamide (**63**; J. Med. Chem. manuscript)



Title compound prepared according to General Procedure 4-A2 as a colourless solid (222 mg, 52%). HPLC - rt 7.32 min > 99% purity at 254 nm; LRMS $[\text{M}+\text{H}]^+$ 213.1 m/z; HRMS $[\text{M}+\text{H}]^+$ 213.1022 m/z, found 213.1023 m/z; ^1H NMR (400 MHz, DMSO) δ 10.26 (s, 1H), 8.74 (ddd, $J = 4.8, 1.6, 0.9$ Hz, 1H), 8.17 (dt, $J = 7.8, 1.1$ Hz, 1H), 8.08 (td, $J = 7.7, 1.7$ Hz, 1H), 7.85 (dd, $J = 7.9, 0.8$ Hz, 1H), 7.69 (ddd, $J = 7.5, 4.8, 1.3$ Hz, 1H), 7.26 (dd, $J = 18.1, 7.6$ Hz, 2H), 7.12 (td, $J = 7.4, 1.2$ Hz, 1H), 2.31 (s,

3H); ^{13}C NMR (101 MHz, DMSO) δ 161.9, 149.6, 148.6, 138.3, 136.0, 130.4, 130.3, 127.1, 126.3, 125.0, 123.1, 122.2, 17.5.

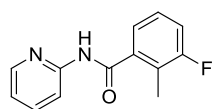
2-Fluoro-N-(pyridin-2-yl)benzamide (**66**; J. Med. Chem. manuscript)



Title compound prepared according to General Procedure 4-A2 as white needles (26%).

HPLC – rt 4.60 min > 99% purity at 254 nm; LRMS $[\text{M}+\text{H}]^+$ 217.2 m/z; HRMS $[\text{M}+\text{H}]^+$ 217.0722 m/z, found 217.0782 m/z; ^1H NMR (400 MHz, DMSO) δ 10.77 (s, 1H), 8.37 (ddd, $J = 4.9, 1.9, 0.9$ Hz, 1H), 8.20 (d, $J = 8.4$ Hz, 1H), 7.86 (ddd, $J = 8.4, 7.5, 1.9$ Hz, 1H), 7.71 (td, $J = 7.5, 1.7$ Hz, 1H), 7.59 (dddd, $J = 8.4, 7.2, 5.3, 1.8$ Hz, 1H), 7.40 – 7.26 (m, 2H), 7.18 (ddd, $J = 7.4, 4.9, 1.0$ Hz, 1H); ^{13}C NMR (101 MHz, CDCl_3) δ 160.6 ($J_{\text{C-F}} = 247$ Hz), 161.8 ($J_{\text{C-F}} = 3$ Hz), 151.4, 148.1, 138.6, 134.3 ($J_{\text{C-F}} = 10$ Hz), 132.2 ($J_{\text{C-F}} = 2$ Hz), 125.2 ($J_{\text{C-F}} = 3$ Hz), 121.3 ($J_{\text{C-F}} = 11$ Hz), 120.3, 116.5 ($J_{\text{C-F}} = 24$ Hz), 114.8.

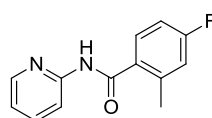
3-Fluoro-2-methyl-N-(pyridin-2-yl)benzamide (**70**; J. Med. Chem. manuscript)



Title compound prepared according to General Procedure 4-A2 as a pale-yellow solid

(20%). LRMS $[\text{M}+\text{H}]^+$ 231.1 m/z; HRMS $[\text{M}+\text{H}]^+$ 231.0928 m/z, found 231.0930 m/z; ^1H NMR (400 MHz, DMSO) δ 10.87 (s, 1H), 8.35 (ddd, $J = 4.9, 1.9, 0.8$ Hz, 1H), 8.18 (d, $J = 8.3$ Hz, 1H), 7.88 – 7.78 (m, 1H), 7.38 – 7.22 (m, 3H), 7.16 (ddd, $J = 7.3, 4.9, 1.0$ Hz, 1H), 2.28 (d, $J = 2.2$ Hz, 3H); ^{13}C NMR (101 MHz, DMSO) δ 167.2 ($J_{\text{C-F}} = 4$ Hz), 160.5 ($J_{\text{C-F}} = 24$ Hz), 151.8, 148.1, 138.9 ($J_{\text{C-F}} = 4$ Hz), 138.1, 127.3 ($J_{\text{C-F}} = 8$ Hz), 123.4 ($J_{\text{C-F}} = 4$ Hz), 122.3 ($J_{\text{C-F}} = 8$ Hz), 119.9, 116.4 ($J_{\text{C-F}} = 23$ Hz), 114.3, 11.3 ($J_{\text{C-F}} = 5$ Hz).

4-Fluoro-2-methyl-N-(pyridin-2-yl)benzamide (**77**; J. Med. Chem. manuscript)

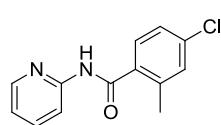


Title compound prepared according to General Procedure 4-A2 as an off-white solid

(24%). HPLC rt 4.97 min > 99% purity at 254 nm; LRMS $[\text{M}+\text{H}]^+$ 231.1 m/z; HRMS $[\text{M}+\text{H}]^+$ 231.0928 m/z, found 231.0937 m/z; ^1H NMR (400 MHz, DMSO) δ 10.78 (s, 1H), 8.34 (ddd, $J =$

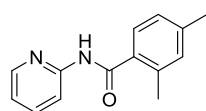
4.9, 1.9, 0.9 Hz, 1H), 8.18 (d, $J = 8.4$ Hz, 1H), 7.93 – 7.73 (m, 1H), 7.54 (dd, $J = 8.5, 6.0$ Hz, 1H), 7.27 – 7.13 (m, 2H), 7.13 – 7.05 (m, 1H), 2.40 (s, 3H); ^{13}C NMR (101 MHz, DMSO) δ 167.6, 162.6 ($J_{\text{C-F}} = 247$ Hz), 152.1, 148.0, 139.1 ($J_{\text{C-F}} = 9$ Hz), 138.1, 132.9 ($J_{\text{C-F}} = 3$ Hz), 130.1 ($J_{\text{C-F}} = 9$ Hz), 119.8, 117.1 ($J_{\text{C-F}} = 21$ Hz), 114.3, 112.3 ($J_{\text{C-F}} = 21$ Hz), 19.5 ($J_{\text{C-F}} = 1$ Hz).

4-Chloro-2-methyl-N-(pyridin-2-yl)benzamide (**78**; J. Med. Chem. manuscript)



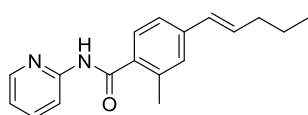
Title compound prepared according to General Procedure 4-A2 as a pale-orange solid (50%). HPLC – rt 6.81 min > 99% purity at 254 nm; LRMS $[\text{M}+\text{H}]^+$ 247.1 m/z; HRMS $[\text{M}+\text{H}]^+$ 247.0633 m/z, found 247.0638 m/z; ^1H NMR (400 MHz, DMSO) δ 10.83 (s, 1H), 8.35 (ddd, $J = 4.9, 1.9, 0.8$ Hz, 1H), 8.17 (d, $J = 8.3$ Hz, 1H), 7.89 – 7.77 (m, 1H), 7.49 (d, $J = 8.2$ Hz, 1H), 7.40 (d, $J = 1.7$ Hz, 1H), 7.33 (dd, $J = 8.2, 1.7$ Hz, 1H), 7.16 (ddd, $J = 7.3, 4.9, 1.0$ Hz, 1H), 2.38 (s, 3H); ^{13}C NMR (101 MHz, DMSO) δ 167.5, 151.9, 148.0, 138.1 (2C), 135.2, 134.2, 130.1, 129.4, 125.4, 119.9, 114.3, 19.1.

2,4-Dimethyl-N-(pyridin-2-yl)benzamide (**81**; J. Med. Chem. manuscript)



Title compound prepared according to General Procedure 4-A3 as a pale-orange solid (25%). HPLC – rt 6.55 min > 97% purity at 254 nm. LRMS $[\text{M}+\text{H}]^+$ 227.2 m/z; HRMS $[\text{M}+\text{H}]^+$ 227.1179 m/z, found 227.1180 m/z; ^1H NMR (400 MHz, DMSO) δ 10.62 (s, 1H), 8.34 (ddd, $J = 4.9, 1.9, 0.8$ Hz, 1H), 8.18 (d, $J = 8.4$ Hz, 1H), 7.86 – 7.75 (m, 1H), 7.39 (d, $J = 7.7$ Hz, 1H), 7.16 – 7.01 (m, 3H), 2.37 (s, 3H), 2.31 (s, 3H); ^{13}C NMR (101 MHz, DMSO) δ 168.4, 152.1, 147.9, 139.5, 138.0, 135.6, 133.4, 131.2, 127.71, 126.0, 119.6, 114.2, 20.8, 19.5.

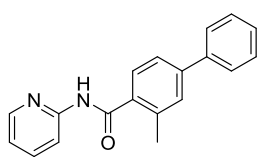
(E)-2-Methyl-4-(3-methylbut-1-en-1-yl)-N-(pyridin-2-yl)benzamide (**82**; J. Med. Chem. manuscript)



Title compound prepared according to General Procedure 4-B1 using the boronic acid pinacol ester as a white solid (37%). LRMS $[\text{M}+\text{H}]^+$ 281.2 m/z;

HRMS $[M+H]^+$ 281.1648 m/z, found 281.1656 m/z; 1H NMR (400 MHz, DMSO) δ 10.68 (s, 1H), 8.43 – 8.27 (m, 1H), 8.19 (d, $J = 8.4$ Hz, 1H), 7.94 – 7.75 (m, 1H), 7.45 (t, $J = 8.6$ Hz, 1H), 7.28 (dd, $J = 17.3, 9.3$ Hz, 2H), 7.21 – 7.08 (m, 1H), 6.50 – 6.32 (m, 2H), 2.39 (s, 3H), 2.29 – 2.10 (m, 2H), 1.58 – 1.43 (m, 2H), 0.94 (q, $J = 7.7$ Hz, 3H); ^{13}C NMR (101 MHz, DMSO) δ 168.3, 152.2, 148.0, 138.9, 138.1, 136.1, 134.5, 132.1, 129.1, 128.1, 128.0, 122.9, 119.7, 114.3, 34.6, 21.9, 19.6, 13.6.

3-Methyl-N-(pyridin-2-yl)-[1,1'-biphenyl]-4-carboxamide (**83**; J. Med. Chem. manuscript)



Title compound prepared according to General Procedure 4-B1 as a white solid (20%). HPLC – rt 6.51 min > 99% purity at 254 nm; LRMS $[M+H]^+$ 289.2 m/z ;

HRMS $[M+H]^+$ 289.1335 m/z, found 289.1342 m/z; 1H NMR (400 MHz, DMSO) δ 10.76 (d, $J = 20.1$ Hz, 2H), 8.37 (d, $J = 3.8$ Hz, 2H), 8.22 (d, $J = 8.3$ Hz, 2H), 7.84 (dt, $J = 23.5, 8.1$ Hz, 2H), 7.70 (t, $J = 12.9$ Hz, 4H), 7.67 – 7.55 (m, 6H), 7.50 (t, $J = 7.6$ Hz, 4H), 7.41 (t, $J = 7.3$ Hz, 2H), 7.16 (dd, $J = 7.0, 5.1$ Hz, 2H), 2.48 (s, 5H); ^{13}C NMR (101 MHz, DMSO) δ 168.3, 152.1, 148.0, 141.5, 139.4, 138.1, 136.3, 135.3, 129.0, 128.8, 128.3, 127.9, 126.8, 123.8, 119.8, 114.3, 19.7.

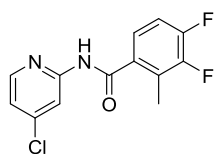
3,4-Difluoro-2-methyl-N-(4-methylpyridin-2-yl)benzamide (**94**; J. Med. Chem. manuscript)



Title compound prepared according to General Procedure 4-A2 which was further purified by recrystallization with cyclohexane to give white needles (26 mg, 5%). HPLC

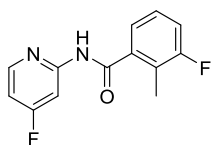
– rt 5.32 min > 99% purity at 254 nm; LRMS $[M+H]^+$ 263.1 m/z; HRMS $[M+H]^+$ 263.0990 m/z, found, 263.0992 m/z; 1H NMR (400 MHz, DMSO) δ 10.82 (s, 1H), 8.31 – 8.13 (m, 1H), 8.03 (s, 1H), 7.46 – 7.22 (m, 2H), 7.01 (ddd, $J = 5.0, 1.4, 0.6$ Hz, 1H), 2.35 (s, 3H), 2.33 (d, $J = 2.6$ Hz, 3H); ^{13}C NMR (101 MHz, DMSO) δ 166.4 ($J_{C-F} = 2$ Hz), 151.9, 150.4 ($J_{C-F} = 233$ Hz), 149.0, 148.0 ($J_{C-F} = 228$ Hz), 134.2, 125.6 ($J_{C-F} = 14$ Hz), 124.1 ($J_{C-F} = 14$ Hz), 121.0, 114.7, 114.4 ($J_{C-F} = 23$ Hz), 20.9, 11.5 ($J_{C-F} = 5$ Hz).

N-(4-Chloropyridin-2-yl)-3,4-difluoro-2-methylbenzamide (**96**; J. Med. Chem. manuscript)



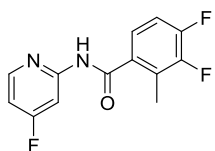
Title compound prepared according to General Procedure 4-A2 with further purification involving dissolution of the crude material in ethyl acetate and washing with saturated sodium bicarbonate solution before a recrystallization from cyclohexane to give the title compound as white needles (26 mg, 5%). HPLC – rt 7.76 min > 95% purity at 254 nm; LRMS [M+H]⁺ 283.1 m/z; HRMS [M+H]⁺ 283.0444 m/z, found 283.0446 m/z; ¹H NMR (400 MHz, DMSO) δ 11.21 (s, 1H), 8.36 (d, *J* = 5.4 Hz, 1H), 8.28 (d, *J* = 1.4 Hz, 1H), 7.47 – 7.23 (m, 3H), 2.33 (d, *J* = 2.4 Hz, 3H); ¹³C NMR (101 MHz, DMSO) δ 166.8 (*J*_{C-F} = 3 Hz), 153.0, 151.8 (*J*_{C-F} = 243 Hz), 149.6, 148.0 (*J*_{C-F} = 238 Hz), 144.0, 133.6 (*J*_{C-F} = 2 Hz), 125.8 (*J*_{C-F} = 14 Hz), 124.4 (*J*_{C-F} = 8 Hz), 120.0, 114.4 (*J*_{C-F} = 17 Hz), 113.8, 11.5 (*J*_{C-F} = 4 Hz).

3-Fluoro-*N*-(4-fluoropyridin-2-yl)-2-methylbenzamide (**97**; J. Med. Chem. manuscript)



Title compound prepared according to General Procedure 4-A2 as a colourless solid (20 mg, 10%). HPLC – rt 6.81 min > 99% purity at 254 nm; LRMS [M+H]⁺ 249.1 m/z; HRMS [M+H]⁺ 249.0834 m/z, found 249.0832 m/z; ¹H NMR (400 MHz, DMSO) δ 11.23 (s, 1H), 8.41 (dd, *J* = 9.3, 5.7 Hz, 1H), 8.04 (dd, *J* = 11.9, 2.4 Hz, 1H), 7.44 – 7.23 (m, 3H), 7.13 (ddd, *J* = 8.2, 5.7, 2.4 Hz, 1H), 2.28 (d, *J* = 2.2 Hz, 3H); ¹³C NMR (101 MHz, DMSO) δ 168.9 (*J*_{C-F} = 259 Hz), 167.6, 160.5 (*J*_{C-F} = 244 Hz), 154.1 (*J*_{C-F} = 12 Hz), 150.8 (*J*_{C-F} = 9 Hz), 138.5 (*J*_{C-F} = 4 Hz), 127.3 (*J*_{C-F} = 9 Hz), 123.6 (*J*_{C-F} = 23 Hz), 122.5 (*J*_{C-F} = 18 Hz), 116.7 (*J*_{C-F} = 23 Hz), 107.9 (*J*_{C-F} = 18 Hz), 101.4 (*J*_{C-F} = 23 Hz), 11.3 (*J*_{C-F} = 5 Hz).

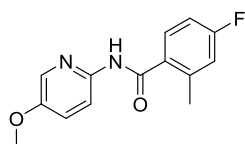
3,4-Difluoro-*N*-(4-fluoropyridin-2-yl)-2-methylbenzamide (**98**; J. Med. Chem. manuscript)



Title compound prepared according to General Procedure 4-A2 with further purification involving dissolution of the crude material in ethyl acetate and washing with saturated

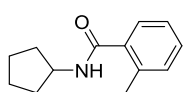
sodium bicarbonate solution before a recrystallisation from cyclohexane to give the title compound as white needles (38 mg, 7%). HPLC – rt 7.07 min > 99% purity at 254 nm; LRMS [M+H]⁺ 267.1 m/z; HRMS [M+H]⁺ 267.0740 m/z, found 267.0742 m/z; ¹H NMR (400 MHz, DMSO) δ 11.25 (s, 1H), 8.41 (dd, *J* = 9.2, 5.7 Hz, 1H), 8.02 (dd, *J* = 11.9, 2.4 Hz, 1H), 7.48 – 7.26 (m, 2H), 7.13 (ddd, *J* = 8.2, 5.7, 2.4 Hz, 1H), 2.34 (d, *J* = 2.6 Hz, 3H); ¹³C NMR (101 MHz, DMSO) δ 170.2, 167.6, 166.8 (*J*_{C-F} = 3 Hz), 152.9 (*J*_{C-F} = 237 Hz), 150.8 (*J*_{C-F} = 8 Hz), 148.1 (*J*_{C-F} = 245 Hz), 133.6, 125.8 (*J*_{C-F} = 14 Hz), 124.4 (*J*_{C-F} = 8 Hz), 114.4 (*J*_{C-F} = 17 Hz), 108.0 (*J*_{C-F} = 17 Hz), 101.4 (*J*_{C-F} = 23 Hz), 11.5 (*J*_{C-F} = 4 Hz).

4-Fluoro-N-(5-methoxypyridin-2-yl)-2-methylbenzamide (**100**; J. Med. Chem. manuscript)



Title compound prepared according to General Procedure 4-A2 as a beige solid (30%). HPLC – rt 5.75 min > 99% purity at 254 nm; LRMS [M+H]⁺ 261.1 m/z; HRMS [M+H]⁺ 261.1034 m/z, found 261.1040 m/z; ¹H NMR (400 MHz, DMSO) δ 10.65 (s, 1H), 8.09 (dd, *J* = 11.0, 6.0 Hz, 2H), 7.50 (ddd, *J* = 12.1, 8.7, 4.6 Hz, 2H), 7.22 – 6.99 (m, 2H), 3.83 (s, 3H), 2.40 (s, 3H); ¹³C NMR (101 MHz, DMSO) δ 167.0, 162.4 (*J*_{C-F} = 247 Hz), 152.4, 145.5, 139.0 (*J*_{C-F} = 9 Hz), 134.4, 133.1, 129.9 (*J*_{C-F} = 9 Hz), 123.1, 117.0 (*J*_{C-F} = 21 Hz), 115.1, 112.2 (*J*_{C-F} = 22 Hz), 55.8, 19.5.

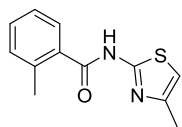
N-Cyclopentyl-2-methylbenzamide (**4.07**)



Title compound prepared according to General Procedure 4-A2 as a colourless solid (83 mg, 20%). HPLC – rt 6.63 min > 99% purity at 254 nm; LRMS [M+H]⁺ 204.2 m/z; HRMS [M+H]⁺ 204.1383 m/z, found 204.1383 m/z; ¹H NMR (400 MHz, DMSO) δ 8.17 (d, *J* = 6.9 Hz, 1H), 7.39 – 7.05 (m, 4H), 4.30 – 4.06 (m, 1H), 2.30 (s, 3H), 1.98 – 1.74 (m, 2H), 1.74 – 1.59 (m, 2H), 1.59 – 1.41 (m, 4H); ¹³C NMR (101 MHz, DMSO) δ 168.6, 137.8, 134.8, 130.2, 128.9, 127.0, 125.4, 50.6, 32.2, 23.6, 19.2.

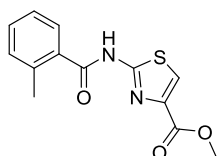
*Note: there are multiple overlapping carbons in the ¹³C NMR.

2-Methyl-N-(4-methylthiazol-2-yl)benzamide (4.23)



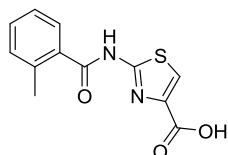
Title compound prepared according to General Procedure 4-A3 as a pale-yellow solid (199 mg, 59%). HPLC – rt 6.69 min > 99% purity at 254 nm; LRMS $[M+H]^+$ 233.1 m/z; HRMS $[M+H]^+$ 233.0743 m/z, found 233.0739 m/z; 1H NMR (400 MHz, $CDCl_3$) δ 7.57 – 7.49 (m, 1H), 7.43 (td, $J = 7.6, 1.4$ Hz, 1H), 7.35 – 7.25 (m, 2H), 5.86 (d, $J = 1.0$ Hz, 1H), 2.46 (s, 3H), 2.25 (d, $J = 1.2$ Hz, 3H); ^{13}C NMR (101 MHz, $CDCl_3$) δ 167.8, 158.5, 137.2, 134.7, 133.4, 131.3, 130.8, 127.9, 126.8, 126.0, 20.0, 11.6. *Note: the –NH peak is missing from the 1H NMR.

Methyl 2-(2-methylbenzamido)thiazole-4-carboxylate (4.24)



Title compound prepared according to General Procedure 4-A3 though the material required further purification by column chromatography, eluting with 2-5% ethyl acetate/dichloromethane to yield the title compound as an off-white solid (311 mg, 31%). HPLC – rt 7.07 min > 98% purity at 254 nm; LRMS $[M+H]^+$ 277.1 m/z; HRMS $[M+H]^+$ 277.0641 m/z, found 277.0637 m/z; 1H NMR (400 MHz, $CDCl_3$) δ 9.99 (s, 1H), 7.86 (s, 1H), 7.42 (ddd, $J = 9.5, 8.8, 4.5$ Hz, 2H), 7.32 – 7.26 (m, 1H), 7.21 (dd, $J = 7.6, 0.5$ Hz, 1H), 3.80 (s, 3H), 2.55 (s, 3H); ^{13}C NMR (101 MHz, $CDCl_3$) δ 167.2, 161.8, 158.5, 141.5, 138.5, 132.5, 132.1, 132.0, 127.2, 126.3, 122.6, 52.4, 20.5.

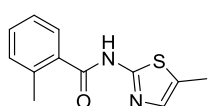
2-(2-Methylbenzamido)thiazole-4-carboxylic acid (4.25)



Methyl 2-(2-methylbenzamido)thiazole-4-carboxylate (95 mg, 0.34 mmol) was dissolved in tetrahydrofuran (0.3 ml) and lithium hydroxide (17 mg, 0.72mmol) was dissolved in water (0.9 ml). The ester solution was added dropwise to the aqueous lithium hydroxide solution. The reaction mixture was stirred for 60 min and LCMS showed complete hydrolysis. The reaction mixture was quenched by addition of an aqueous 1.0 M hydrochloric acid solution to acidic pH and a precipitate was observed. The precipitate was removed by filtration and air dried to yield the title compound as a colourless solid (87 mg, 98%). HPLC – rt 6.31 min > 96% purity at 254 nm; LRMS

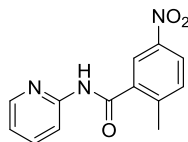
$[M+H]^+$ 263.1 m/z; HRMS $[M+H]^+$ 263.0485 m/z, found 263.0482 m/z; 1H NMR (400 MHz, Acetone) δ 11.21 (s, 1H), 8.00 (s, 1H), 7.74 (d, $J = 7.9$ Hz, 1H), 7.51 – 7.40 (m, 1H), 7.39 – 7.26 (m, 2H), 2.52 (s, 3H); ^{13}C NMR (101 MHz, DMSO) δ 167.8, 162.4, 158.1, 142.2, 136.6, 133.4, 130.9, 128.2, 125.7, 122.5, 19.7. *Note: the –OH peak is missing from the 1H NMR and there is a missing carbon from the ^{13}C NMR which is assumed to be overlapping with another signal.

2-Methyl-N-(5-methylthiazol-2-yl)benzamide (4.26)



Title compound prepared according to General Procedure 4-A3 as an off-white solid (93 mg, 48%). HPLC – rt 6.96 min > 95% purity at 254 nm; LRMS $[M+H]^+$ 233.1 m/z; HRMS $[M+H]^+$ 233.0743 m/z, found 233.0733 m/z; 1H NMR (400 MHz, $CDCl_3$) δ 7.45 (dd, $J = 7.7, 1.2$ Hz, 1H), 7.37 (td, $J = 7.5, 1.3$ Hz, 1H), 7.26 (s, 1H), 7.21 – 7.13 (m, 1H), 6.44 (d, $J = 1.0$ Hz, 1H), 2.50 (s, 3H), 1.72 (d, $J = 1.0$ Hz, 3H); ^{13}C NMR (101 MHz, $CDCl_3$) δ 167.5, 159.2, 147.1, 137.8, 133.7, 131.6, 131.4, 127.9, 126.1, 108.0, 20.2, 15.9. *Note: the –NH peak is missing from the 1H NMR.

2-Methyl-5-nitro-N-(pyridin-2-yl)benzamide (4.30)



Title compound prepared according to General Procedure 4-A1 as colourless needles (13 mg, 2%). HPLC – rt 5.13 min > 98% purity at 254 nm; LRMS $[M+H]^+$ 258.2 m/z; HRMS $[M+H]^+$ 258.0873 m/z, found 258.0875 m/z; 1H NMR (400 MHz, $CDCl_3$) δ 9.11 (s, 1H), 8.37 (d, $J = 2.4$ Hz, 1H), 8.32 (d, $J = 8.3$ Hz, 1H), 8.20 (dd, $J = 8.4, 2.4$ Hz, 1H), 7.98 (d, $J = 4.2$ Hz, 1H), 7.75 (ddd, $J = 8.4, 7.4, 1.9$ Hz, 1H), 7.43 (d, $J = 8.5$ Hz, 1H), 7.02 (ddd, $J = 7.4, 5.0, 1.0$ Hz, 1H), 2.60 (s, 3H); ^{13}C NMR (101 MHz, $CDCl_3$) δ 166.0, 151.3, 147.8, 146.1, 144.7, 138.9, 137.0, 132.5, 125.2, 122.3, 120.6, 114.6, 20.3.

5. Investigation of the structure-activity relationships of the phenylthiazole amide against *T.b. brucei*

5.1. Introduction

The phenylthiazole amide (**130**) was identified with an activity of 0.79 μM against *T.b. brucei* and a selectivity index of > 96 with respect to mammalian HEK293 cells.⁵ Compound **130** possesses a number of desirable properties in addition to its good activity and high selectivity, which make it an ideal compound for further study. It was shown to have a low molecular weight of 306 gmol^{-1} and a highly optimisable structure. Compound **130** also possesses a low PSA of 42 \AA^2 that is indicative of a compound's ability to cross the BBB⁵⁶ and a favourable cLogP of 3.4, which is known to influence the metabolism of compounds.⁵⁶ As a result, **130** was selected for further lead optimisation and entered a hit-to-lead optimisation program.

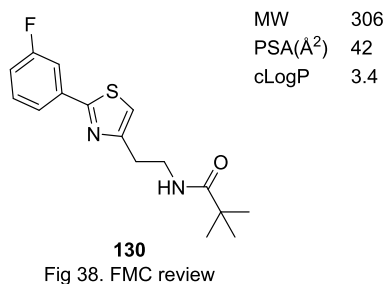


Figure 5.1 Structure and physicochemical properties of **130** with a low cLogP, PSA and MW making it a suitable candidate for lead optimisation.

Testing of this compound against a wider parasite panel showed that it had potent activity against the human infective *T.b. rhodesiense* (EC_{50} 1.47 μM). Compound **130** also showed good activity against the closely related *T. cruzi* (EC_{50} 2.32 μM). The activity was significantly weaker for the unrelated parasites *L. donovani* and *P. falciparum*. These results are summarised in Table 5.1.

Table 5.1 Biological activity profile of **130** against a number of parasites.

Parasite	EC ₅₀ (μM)	SI
<i>T.b. brucei</i>	0.79 ± 0.08	> 96 ^a
<i>T.b. rhodesiense</i>	1.47 ± 0.39	42.3 ^b
<i>T. cruzi</i>	2.32 ± 0.06	26.8 ^b
<i>L. donovani</i> axenic	46.1 ± 22.4	1.35 ^b
<i>P. falciparum</i>	35.4 ± 2.75	1.76 ^b

^a Selectivity relative to HEK293(human embryonic kidney) cells.

^b Selectivity relative to L6 (rat skeletal myoblast) cells.

5.2. Aims

The aim for this section was to investigate modifications of the thiazole core and the ethyl linker region. The work will be presented in a number of sections. Initially, an in depth analysis of the historical work will be presented. This will be followed by a discussion around the design and synthesis of a number of 6-membered heterocyclic core changes, such as a pyridine or pyrimidine ring, before moving on to the methylation of each position of the ethyl linker and the introduction of a cyclopropane group.

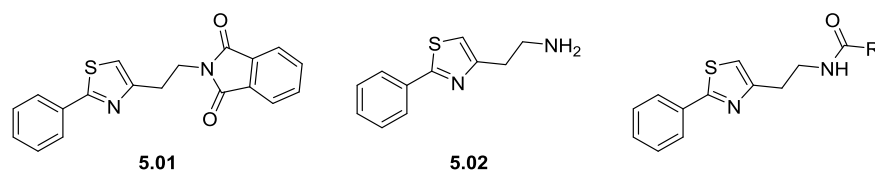
5.3. Historical work completed

A significant number of analogues have already been generated on this class of compound by previous researchers. A summary of this work follows.

Initially investigations centred around the acyl substituent and are summarised in Table 5.2. The synthetic precursors **5.01** and **5.02** were tested and both were found to be inactive, emphasising the importance of the acyl moiety. Replacement of the *tert*-butyl group with either a methyl group (**5.04**), ethyl group (**5.05**), or

complete removal (**5.03**) led to a complete loss in activity whilst the isopropyl group (**5.06**, EC₅₀ 5.3 μM) demonstrated a six-fold decrease in activity against *T.b. brucei*. Compound **5.07** showed a two-fold loss in activity though this was due to the removal of the fluorine from the left hand phenyl ring. Bulkier functional groups such as the phenyl (**5.08**, EC₅₀ 0.55 μM), cyclohexyl (**5.09**, EC₅₀ 0.31 μM) and cyclopentyl (**5.10**, EC₅₀ 0.25 μM) groups were all favourable for activity, suggesting that this region of the molecule is interacting with a hydrophobic pocket. However, there was a ceiling observed to this activity, with the benzyl group (**5.14**) and larger, ring fused analogues (**5.15** – **5.17**) leading to a complete loss of activity. Given the activity of the cyclopentyl group, a range of 5-membered heterocycles were also explored. The 2- and 3-thiophenecarboxamides (**5.18** and **5.27** respectively) maintained activity when compared with **5.08**. The 2- and 3-furans (**5.19** and **5.28** respectively) were also active, though **5.28** was 2-fold more active, indicating that an electronegative or electron withdrawing substituent at this position is favourable. Substitution of the 2-furan with a 5-methyl group (**5.24**) was well tolerated with a further improvement in the activity (EC₅₀ 0.13 μM). Yet, substitution with a 3-methyl group (**5.23**, EC₅₀ 1.9 μM) or 3-bromo group (**5.25**, EC₅₀ 2.5 μM) led to a loss of activity. Introduction of a hydrogen bond donating pyrrole (**5.20**, EC₅₀ 1.6 μM) saw an approximately three-fold decrease in activity when compared with **5.08**, while the thiazole (**5.26**, EC₅₀ 1.2 μM) was two-fold less active. Introduction of the oxazole (**5.21**) led to a complete loss of activity, yet the isoxazole (**5.22**, EC₅₀ 0.74 μM) was well tolerated as expected, given the preference for electronegative atoms at the 2- and 3-positions.

Table 5.2 Replacement of the acyl substituent with alkyl, aromatic and heteroaromatic analogues.



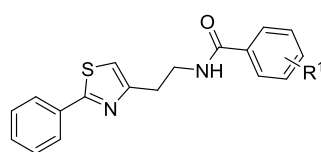
ID	R	EC ₅₀ μM (SI ^a)	ID	R	EC ₅₀ μM (SI ^a)
5.01		> 10 ^b	5.15		> 10 ^b
5.02		> 10 ^b	5.16		> 10 ^b
5.03	-H	> 10 ^b	5.17		> 10 ^b
5.04	-CH ₃	> 10 ^b	5.18		0.35 ± 0.17 (241)
5.05	-CH ₂ CH ₃	> 10 ^b	5.19		0.80 ± 0.11 (77)
5.06		5.3 ± 0.25 (16)	5.20		1.6 ± 0.43 (13)
5.07		1.7 ± 0.09 (50)	5.21		> 10 ^b
5.08		0.55 (151)	5.22		0.74 ± 0.02 (113)
5.09		0.31 ± 0.10 (281)	5.23		1.9 ± 0.25 (22)
5.10		0.25 ± 0.02 (329)	5.24		0.13 ± 0.0 (666)
5.11		5.0 ± 0.24 (17)	5.25		2.5 ± 0.07 (12)
5.12		5.5 ± 0.05 (15)	5.26		1.2 ± 0.02 (68)
5.13		> 10 ^b	5.27		0.23 ± 0.03 (179)
5.14		> 10 ^b	5.28		0.35 ± 0.05 (240)

^a Selectivity relative to HEK293(human embryonic kidney) cells.

^b Compound exhibited < 50% activity at 10.41 μM.

Given the improved potency shown by **5.08**, exploration of the SAR around the right hand side phenyl ring was undertaken (Table 5.3). It was immediately apparent that substitution of the 4-position was generally unfavourable for activity, though the 4-fluoro group was well tolerated (**5.28**, EC₅₀ 0.77 μM). The 3- and 4-positions tolerated substitution though there was a loss of potency when the substituent was electron donating (**5.31-5.33** and **5.38-5.40**) with the most potent substitution shown to be the 3-nitrile (**5.41**, EC₅₀ 0.13 μM) with a four-fold improvement over **5.08**.

Table 5.3 Exploration of the SAR around the phenyl ring of the benzamide.



ID	R ¹	EC ₅₀ μM (SI ^a)	ID	R ¹	EC ₅₀ μM (SI ^a)
5.29	2-F	0.47 ± 0.06 (44)	5.39	3-OH	> 10 ^b
5.30	2-Cl	1.5 ± 0.31 (29)	5.40	3-OCH ₃	1.9 ± 0.30 (26)
5.31	2-CH ₃	3.3 ± 0.8 (2.5)	5.41	3-CN	0.13 ± 0.01 (387)
5.32	2-OH	2.3 ± 0.09 (18)	5.42	3-[N] ^c	0.76 ± 0.28 (110)
5.33	2-OCH ₃	10.6 ± 3.6 (2.0)	5.43	4-F	0.77 ± 0.19 (54)
5.34	2-CN	> 10 ^b	5.44	4-Cl	> 10 ^b
5.35	2-[N] ^c	0.3 ± 0.01 (139)	5.45	4-CH ₃	> 10 ^b
5.36	3-F	0.19 ± 0.01 (444)	5.46	4-OCH ₃	> 10 ^b
5.37	3-Cl	0.42 ± 0.04 (200)	5.47	4-CN	> 10 ^b
5.38	3-CH ₃	3.9 ± 0.81 (21)	5.48	4-[N] ^c	14.1 ± 0.66 (3)

^a Selectivity relative to HEK293 (human embryonic kidney) cells.

^b Compound exhibited < 50% activity at 10.41 μM.

^c Denotes an endocyclic nitrogen.

Given that the thiazole moiety is known to be metabolically labile,⁵³ a range of 5-membered heterocycles were synthesised and combined with some of the active right hand side substituents that were previously

identified. These have been summarised in Table 5.4. Replacement of the thiazole group with a pyrazole group (**5.49–5.51**) was well tolerated, however a range of triazoles (**5.52–5.60**) and the tetrazole (**5.61–5.63**) were found to be inactive against *T. brucei*. Whilst **5.58–5.63** also contain a nitrogen in the same position as both the thiazole and pyrazole cores it is possible that the putative target has both a hydrophilic and hydrophobic face and the additional nitrogen atoms may lead to unfavourable interactions here. Further investigations would be required in order to confirm this.

Table 5.4 Heterocyclic core modifications.



LHS	EC ₅₀ (SI)					
	R=		R=		R=	
	5.49	1.1 ± 0.03 (39)	5.50	0.33 ± 0.12 (125)	5.51	1.6 ± 0.50 (13)
	5.52	> 10 ^b	5.53	> 10 ^b	5.54	> 10 ^b
	5.56	> 10 ^b	5.57	> 10 ^b	5.58	> 10 ^b
	5.59	> 10 ^b	5.60	> 10 ^b	5.61	> 10 ^b
	5.62	> 10 ^b	5.63	> 10 ^b	5.64	> 10 ^b

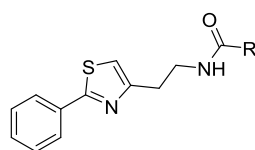
^a Selectivity relative to HEK293(human embryonic kidney) cells.

^b Compound exhibited < 50% activity at 10.41 μM.

A number of carbamates and ureas were also synthesised in place of the right hand side phenyl ring (Table 5.5). Compound **5.64** was a synthetic intermediate and showed no activity against *T.b. brucei*, which is consistent with the previous observations of large acyl substituents losing activity. However, moving from the *tert*-butyl to the isopropyl carbamate (**5.65**, EC₅₀ 0.22 μM) saw restoration of activity of these

compounds. Yet replacement of the isopropyl carbamate (**5.65**) with the *N*-isopropylurea carbamate (**5.66**) saw a four-fold loss in activity. Removal of the hydrogen bond donor with the *N,N*-diethylurea (**5.67**) saw a restoration of the activity, which led to the synthesis of a range of exocyclic ureas. It was found that the piperidine (**5.69**) moiety was highly favoured for both activity and selectivity, the pyrrolidine group (**5.68**) was almost two-fold less active and the azepane group (**5.70**) was three-fold less active. Introduction of the oxygen in the morpholine analogue (**5.71**) again saw a loss in activity.

Table 5.5 Carbamate and urea analogues of the acyl moiety.



ID	R	EC ₅₀ (μM)	SI ^a	ID	R	EC ₅₀ μM	SI ^a
5.64		> 10 ^b		5.68		0.05 ± 0.04	1735
5.65		0.22 ± 0.02	385	5.69		0.028 ± 0.00	2966
5.66		0.90 ± 0.03	93	5.70		0.09 ± 0.02	943
5.67		0.26 ± 0.03	320	5.71		0.69 ± 0.22	127

^a Selectivity relative to HEK293(human embryonic kidney) cells.

^b Compound exhibited < 50% activity at 10.41 μM.

In order to assess the drug-likeness of these compounds a number of physicochemical and metabolic parameters were measured. All of the compounds were of relatively low molecular weight in the range of 291-326 gmol⁻¹. The PSA values were well within the range where good CNS penetration is plausible.⁵⁶ Distribution coefficients at pH 7.4 were also favourable and in the range of 2.8-3.6. The aqueous solubility of some compounds was very good; compound **5.50** in particular had solubilities of greater than 100 μg/ml at both pH 2 and 6.5. In general the thiazole core negatively influenced the solubility of the compounds, such as compounds **5.24** and **5.23**, which were both found to be very poorly soluble at both pH 2 and 6.5. Plasma

protein binding was acceptable for this series in general. The microsomal degradation was quite high for all compounds tested and this was reflected in the *in vitro* clearance and measured degradation half-life for each of the analogues.

Table 5.6 Key physiochemical parameters and *in vitro* metabolic stability of selected compounds.

	MW	PSA (Å ²) ^a	LogD (pH 7.4) ^b	Solubility (µg/ml) ^c		cPPB ^d	Half- life (min)	<i>In vitro</i>	
				pH 2	pH 6.5			CLint (µl/min/mg protein) ^e	Microsome- predicted E _H
5.10	300.42	70.2	3.2	12.5–25.0	12.5–25.0	90.6	6	296	0.92
5.26	315.41	54.9	3.0	25–50	25–50	90.6	27	65	0.72
5.24	312.39	55.1	3.5	6.3–12.5	6.3–12.5	95.1	4	484	0.95
5.36	326.39	42.0	3.6	6.3–12.5	>100	96.1	4	473	0.95
5.23	312.39	55.1	3.4	3.1–6.3	3.1–6.3	94.6	4	446	0.95
5.69	315.43	45.2	3.2	50–100	25–50	90.1	7	244	0.91
5.50	291.35	46.9	3.0	>100	>100	89.1	9	193	0.88
5.68	301.41	45.2	2.8	>100	50–100	85.5	10	177	0.88

^a Calculated using ACD/Laboratories software, version 9.

^b Measured chromatographically.

^c Kinetic solubility determined by nephelometry.

^d Human plasma protein binding estimated using a chromatographic method.

^e *In vitro* intrinsic clearance determined in human liver microsomes and predicted hepatic extraction ratio calculated from *in vitro* data.

Given the rapid metabolism of this class of compounds a study was undertaken to identify the primary metabolites of this series (Figure 5.2). In general both compounds **5.26** and **5.36** were highly susceptible to oxygenation or deamination of the ethylphenylthiazole moiety.

For compound **5.26** two putative mono-oxygenated metabolites were observed and denoted as M+16 (I) and M+16 (II). M+16 (I) was consistent with oxygenation of the phenylthiazole moiety while M+16 (II) was likely derived from hydroxylation of the ethylene bridge. An additional M+32 peak was also observed, however the MS/MS spectrum was too weak to allow for structural confirmation. A peak of M-110 was detected and was consistent with oxidative deamination at the ethylene bridge. Similarly, compound **5.36** exhibited a high rate of degradation with two M+16 metabolites observed. These were again consistent with oxygenation of the phenyl thiazole and ethyl linker. However, an additional metabolite was observed (M+32) that was consistent with the bis-oxygenation of the phenylthiazole moiety. Oxidative deamination was also observed with this compound (M-121) and a further metabolite of M-105 was also observed, which is thought to be the oxygenation of the M-121 metabolite, though the MS/MS spectrum was too weak to confirm this.

Both **5.26** and **5.36** exhibited a high rate of degradation in the presence of NADPH and NADPH combined with UDPGA with approximately 66% and 100% of parent compound lost in 60 min respectively. When the sample was analysed without the presence of cofactors, only 9% and 16% of parent compound was lost respectively over 60 min, suggesting that the ethylphenyl thiazole moiety was most susceptible to NADPH mediated metabolism.

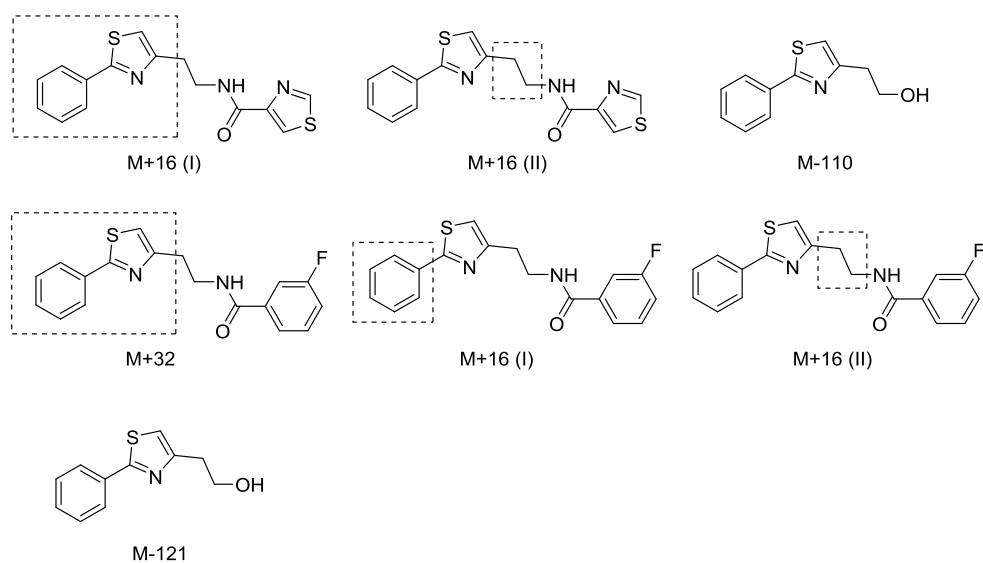
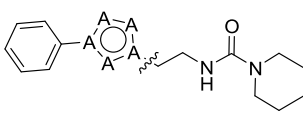
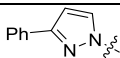
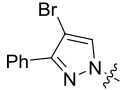
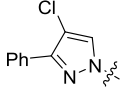
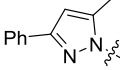
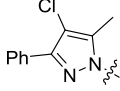
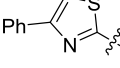
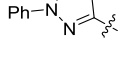


Figure 5.2 Metabolites of **5.26** and **5.36** where the dotted lines denote areas of proposed metabolism.

Given the activity of the pyrazole core (**5.49-5.51**) and the apparent metabolic instability of the thiazole core, a number of substituted pyrazoles were synthesised in combination with the piperidine urea side chain (Table 5.7). Substitution of the 4-position with a bromo (**5.73**) or chloro (**5.74**) led to a significant decrease in the activity. Yet substitution of the 5-position with a methyl (**5.75**) was well tolerated. Combination of the 4-chloro and 5-methyl (**5.76**) led to an overall 6.5-fold decrease in activity. Synthesis of a regioisomer of the thiazole core (**5.77**) led to an analogue that was well tolerated with only a two-fold decrease in activity when compared with **5.69**. The regioisomer of the pyrazole core (**5.78**) exhibited a two-fold improvement in its activity compared with **5.72**.

Table 5.7 Further heterocyclic core modifications

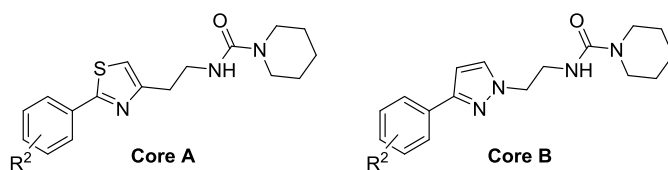


ID	LHS	EC ₅₀ (μM)	SI ^a
5.72		0.12 ± 0.006	680
5.73		2.3 ± 0.08	36
5.74		2.1 ± 0.23	20
5.75		0.16 ± 0.03	520
5.76		1.1 ± 0.20	39
5.77		0.05 ± 0.01	1662
5.78		0.05 ± 0.01	1549

^a Selectivity relative to HEK293(human embryonic kidney) cells.

A variety of substitutions around the right hand side phenyl ring have also been explored on both the thiazole and pyrazole cores (Table 5.8). The 2-position was favourable for substitution with small hydrophobic groups such as a fluorine (5.79, 5.80) and methyl (5.81, 5.82). Whilst substitution with a nitrile and methoxy was tolerated for the thiazole core (5.83 and 5.85) a significant decrease in activity was observed for the pyrazole core (5.84 and 5.86). This was likely caused as a result of the difference in conformation generated by the core change. The 3-position is also favourable for substitution by a small hydrophobic group with both fluorine (5.87 and 5.88) and chlorine groups (5.89 and 5.90) showing increases in potency, with the slightly smaller fluorine being more effective for both cores. Introduction of a nitrile group (5.91) led to a moderate two-fold increase in activity for the thiazole core though there was a corresponding three-fold decrease in the activity for the pyrazole core (5.92). Substitution with a methoxy (5.93 and 5.94) was unfavourable for both cores. The 4-position tolerates substitution with a fluorine (5.95 and 5.96), yet larger substituents such as chlorine (5.99 and 5.100) or methyl groups (5.97 and 5.98) both led to a significant decrease in activity across both cores. Introduction of the nitrile (5.101 and 5.102) and methoxy (5.103 and 5.104) substituents were again generally unfavourable for activity. Combination of the 2-fluoro and 4-fluoro in an effort to gain additive SAR produced mixed results with the thiazole core (5.105) showing no improvement in activity while the pyrazole core (5.106) showed a small improvement in the activity when compared with the singly substituted parents.

Table 5.8 Exploration of the SAR around the left hand side phenyl ring against T.b. brucei.



ID	R ²	Core	EC ₅₀ (μM)	ID	R ²	Core	EC ₅₀ (μM)
5.69	H	A	0.028 ± 0.00	5.93	3-OCH ₃	A	0.67 ± 0.06
5.72		B	0.12 ± 0.006	5.94		B	1.2 ± 0.13
5.79	2-F	A	0.02 ± 0.00	5.95	4-F	A	0.06 ± 0.00
5.80		B	0.10 ± 0.10	5.96		B	0.06 ± 0.00
5.81	2-CH ₃	A	0.19 ± 0.07	5.97	4-CH ₃	A	3.7 ± 0.53
5.82		B	0.35 ± 0.11	5.98		B	5.3 ± 1.45
5.83	2-CN	A	0.56 ± 0.11	5.99	4-Cl	A	1.5 ± 0.21
5.84		B	4.7 ± 0.69	5.100		B	1.2 ± 0.13
5.85	2-OCH ₃	A	0.50 ± 0.07	5.101	4-CN	A	0.33 ± 0.06
5.86		B	2.6 ± 0.58	5.102		B	> 10 ^a
5.87	3-F	A	0.05 ± 0.00	5.103	4-OCH ₃	A	> 10 ^a
5.88		B	0.07 ± 0.03	5.104		B	7.1 ± 1.78
5.89	3-Cl	A	0.16 ± 0.04	5.105	2-F, 4-F	A	0.02 ± 0.00
5.90		B	0.13 ± 0.01	5.106		B	0.045 ± 0.005
5.91	3-CN	A	0.28 ± 0.01				
5.92		B	0.35 ± 0.10				

^a Compound exhibited < 50% activity at 10.41 μM.

Analysis of the metabolism of these analogues (Table 5.9) revealed that no improvement in the metabolic stability had been obtained through altering the thiazole or substituting the phenyl ring. All of the analogues exhibited high to very high rates of degradation in both human and mouse liver microsomes and with these results the compounds would be expected to be subject to rapid hepatic clearance *in vivo*. There was also no

measurable degradation in the control (devoid of cofactors) incubations suggesting that the main mode of metabolism is NADPH mediated.

Table 5.9 Metabolism evaluation of compounds in human and mouse liver microsomes.

ID	Species	Half-life (min)	<i>In vitro</i> CL_{int} (μl/min/mg protein)	Microsome- predicted E_H	Clearance classification
5.37	Human	11	160	0.86	High
	Mouse	1 ^a	1731 ^a	0.97 ^a	Very high
5.69	Human	10	176	0.87	High
	Mouse	1 ^a	2501 ^a	0.98 ^a	Very high
5.64	Human	8	225	0.90	High
	Mouse	1 ^a	2296 ^a	0.98 ^a	Very high
5.29	Human	4	439	0.95	High
	Mouse		Rapid degradation ^b		Very high
5.33	Human	4	445	0.95	High
	Mouse		Rapid degradation ^b		Very high
5.96	Human	20	85	0.77	High
	Mouse	2 ^a	875 ^a	0.95 ^a	High
5.75	Human	16	107	0.81	High
	Mouse		Rapid degradation ^b		Very high
5.21	Human	15	119	0.83	High
	Mouse	1 ^a	1604 ^a	0.97 ^a	Very high
5.24	Human	13	129	0.84	High
	Mouse		Rapid degradation ^b		Very high

^a No measurable concentrations were detected past 5 min, therefore degradation parameters were estimated using the initial two time points (ie 2 and 5 min) only, hence values reported are approximate only.

^b No measurable concentrations were detected past the first time point (ie 2 min) due to rapid NADPH-dependent degradation, hence clearance parameters could not be determined.

5.4. Biological analysis of compounds active against *T. vivax* and *T. congolense*

A selection of compounds were analysed by researchers at the Swiss Tropical and Public Health Institute as part of the GALVmed project. The compounds were tested *ex vivo* against *T. vivax* and *in vivo* against *T. congolense*, which are both causative agents for animal trypanosomiasis in Western and Eastern Africa respectively.⁹⁰ Table 5.10 summarises the results of these biological assays.

Table 5.10 *T. vivax* and *T. congolense* inhibitory activity of selected compounds.

ID	<i>T. vivax</i> EC ₅₀ (µM)	<i>T. congolense</i> EC ₅₀ (µM)
5.75	0.086	0.067
5.24	1.0	0.25
5.10	0.73	0.28
5.72	0.11	0.071
5.37	4.1	44
Diminazene^a	0.34	0.25
Isometamidium^a	0.0006	0.0006

^a Compound included as a standard control.

In general all of the compounds tested exhibited nanomolar inhibition of both *T. vivax* and *T. congolense* with one notable exception. Compound **5.37** (3-Cl-phenyl thiazole) was found to have EC₅₀ values of 4.1 µM and 44 µM against *T. vivax* and *T. congolense*, respectively. Given the activity for the other thiazole core analogues (compounds **5.24** and **5.10**) it would appear that the substituted phenyl is responsible for the loss of activity. The most potent compounds identified against *T. vivax* and *T. congolense* were **5.75** (EC₅₀ of 0.086 µM and 0.067 µM against *T. vivax* and *T. congolense*, respectively) and **5.72** (EC₅₀ of 0.11 µM and 0.071 µM against *T. vivax* and *T. congolense*, respectively). Given the only structural difference between **5.72** and **5.75** is the methyl on the pyrazole core it is unsurprising that these compounds would be equipotent. Both **5.72** and **5.75** were shown to be more potent than diminazene across both parasite subspecies.

Diminazene and isometamidium are routinely used in the treatment of animal trypanosomiasis though both have a multitude of side effects associated with their use.^{91, 92}

5.5. Changes to the thiazole core

Given the poor metabolic stability of this series a number of analogues were envisioned that may lead to an improvement in the overall stability. This consisted of two major areas of work that are discussed below. The first focused on examining alternative core structures, primarily focusing on 6-membered heterocycles. The second area was looking at substituting the linker and constraining it in such a way as to prevent metabolism. These are summarised in Figure 5.3.

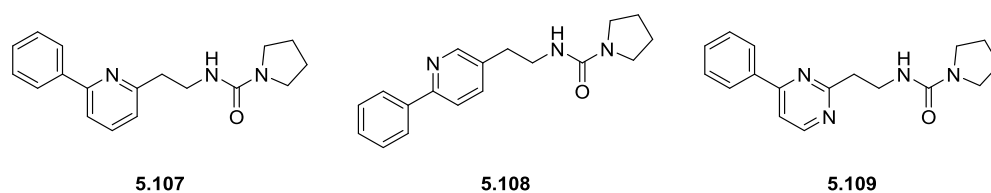
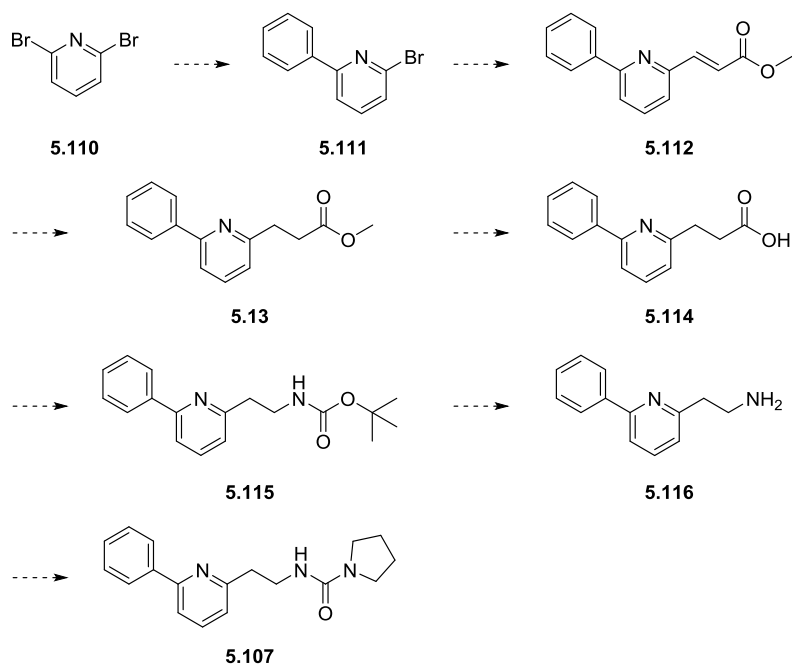


Figure 5.3 Core changes that were identified as replacements for the thiazole moiety.

5.5.1. 2,6-Disubstituted pyridine core

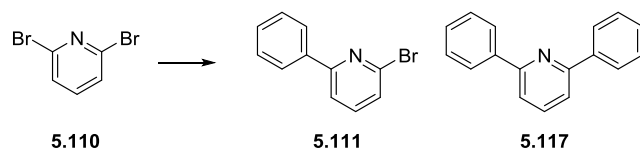
The synthesis of the 2,6-disubstituted pyridine core was initially planned in accordance with Scheme 5.1. The first step was to be a Suzuki coupling between 2,6-dibromopyridine and phenylboronic acid in order to introduce the aromatic group on the left hand side of the compound. A number of possible routes to introduce the side chain were envisaged including the use of a Grignard reagent. The higher reactivity of alkyl magnesium compounds relative to that of other magnesium species (alkenyl, aryl or heteroaryl) along with the known elimination of ethyl linked Grignard species¹¹⁸ meant an alternative route was sought. A Heck coupling was employed utilising methyl acrylate, which could in turn be reduced and the ester hydrolysed. Once the carboxylic acid was obtained it would be possible to perform a Curtius rearrangement

in the presence of *tert*-butanol to give the Boc protected amine. Subsequent Boc deprotection would allow the synthesis of the final product.



Scheme 5.1 Proposed synthesis for the 2,6-disubstituted pyridine core.

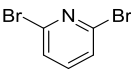
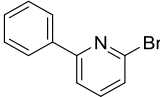
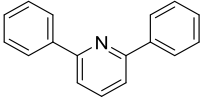
In order to install the aromatic group a Suzuki coupling had initially been planned as the first step. The Suzuki coupling could lead to the desired mono phenyl substituted pyridine (**5.111**) or the disubstituted phenyl product (**5.117**) as shown in Scheme 5.2. After trialling conditions previously reported in the literature it became apparent that optimisation was required in order to minimise the formation of the undesired side product, **5.117**.



Scheme 5.2 Suzuki coupling of 2,6-dibromopyridine with phenylboronic acid led to the isolation of both the desired product (**5.111**) and side-product (**5.117**).

A variety of reaction conditions were trialled in order to minimise the formation of the side-product, as shown in Table 5.11. This was imperative as all three compounds (starting material, product and side-product) were non-polar and had high R_f values when using pure petroleum spirits as the mobile phase, making their separation by column chromatography difficult. Indeed, it was found that the most effective way to separate the desired product from the side-product was through preparative HPLC which was time consuming and resulted in a poor recovery of material. A literature search surrounding the Suzuki coupling of 2,6-dibromopyridine (**5.111**) with phenylboronic acid revealed numerous conditions, though none reported the formation of side-product or purification conditions. The initial conditions involved heating all of the materials in a CEM microwave at 130 °C for 30 mins (entry 1, Table 5.11). However, these conditions were found to be too harsh and a greater percentage of **5.117** was observed. A reduction in the temperature to 70 °C saw the desired product dominate the reaction mixture though there was still 28% of **5.117** by LCMS analysis (entry 2, Table 5.11). A further reduction in the temperature to 40 °C led to an improvement in the ratio of **5.110:5.111:5.117** (entry 3, Table 5.11). Reducing the length of reaction time to 15 min led to 29% of the starting material remaining (entry 4, Table 5.11) though this could be reduced to just 10% after 30 min (entry 4, Table 5.11). These conditions were found to be scalable though a longer reaction time was required in order to minimise the amount of starting material remaining (entry 6, Table 5.11). It was possible to recover the starting material however the product and side-product were not separable and as such, the material was used directly in the next step where the side-product could then be removed by column chromatography.

Table 5.11 Optimisation of the reaction conditions for the initial Suzuki coupling between 2,6-dibromopyridine and phenylboronic acid.

Reaction conditions ^a				Percentage of material ^b		
Eq. phenylboronic acid	Temperature (°C)	Time (min)				
1 ^c	1.2	130	30	0	45	55
2	1.2	70	30	3	69	28
3	1.2	40	30	14	75	11
4	1.0	40	15	29	65	6
5	1.0	40	30	10	75	15
6 ^d	1.0	40	60	21	70	9

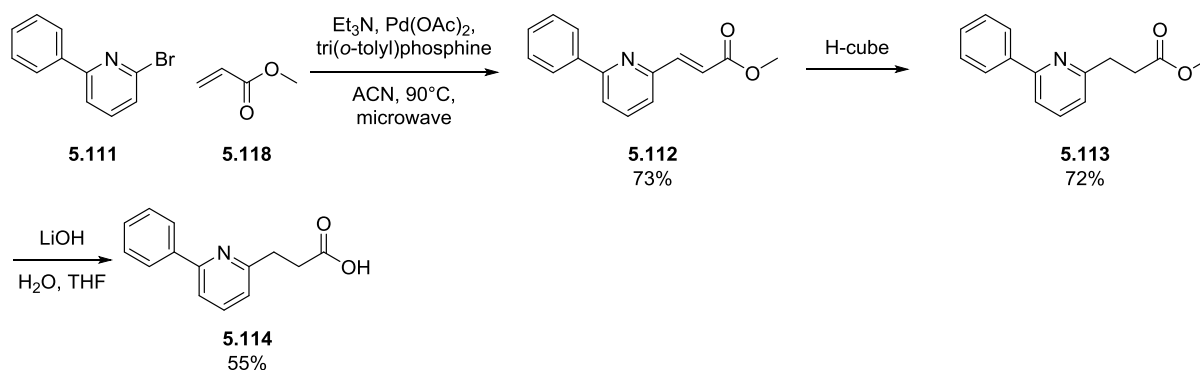
^a 1 eq. 2,6-dibromopyridine (0.21 mmol), 4 eq. potassium carbonate, 0.1 eq. tetra-*n*-butylammonium bromide, 0.05 eq. PdCl₂(dppf), dioxane, water.

^b determined by LCMS analysis.

^c reaction performed in CEM microwave.

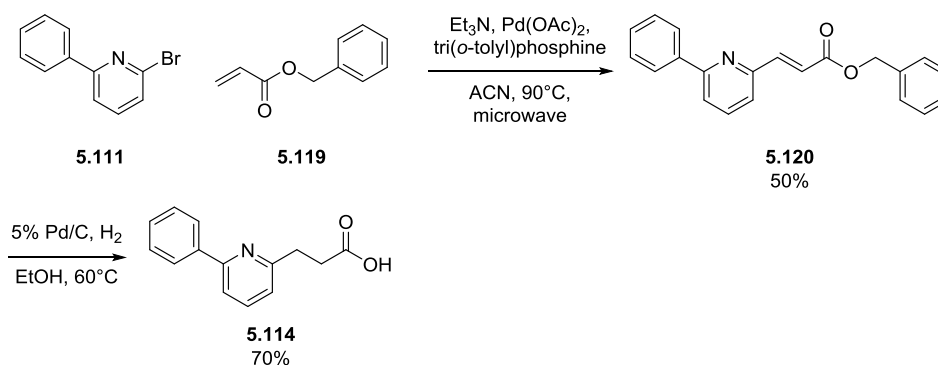
^d reaction performed on 8.44 mmol of 2,6-dibromopyridine.

Reaction between 2-bromo-6-phenylpyridine (**5.111**) and methyl acrylate (**5.118**) was successfully achieved in good yield. It was possible to get either the *cis*- or *trans*-isomer as a result of this reaction, though analysis of the coupling constants in the ¹H NMR revealed a *J* value of 16 Hz, which was consistent with the *trans*-isomer as shown. The subsequent reduction utilising the H-cube[®] with a 10% Pd/C CatCart[®] led to **5.113** in good yield. The ester hydrolysis with lithium hydroxide in water and THF led to the intermediate, **5.114**, though there was a decrease in the yield. It was found that the yield for this reaction was lower than expected as a significant amount of product remained in the aqueous phase and was unable to be extracted despite carefully controlling the pH or varying the solvent used for the extraction. This is likely due to the zwitterionic nature of **5.114** with the basic pyridine and the carboxylic acid.



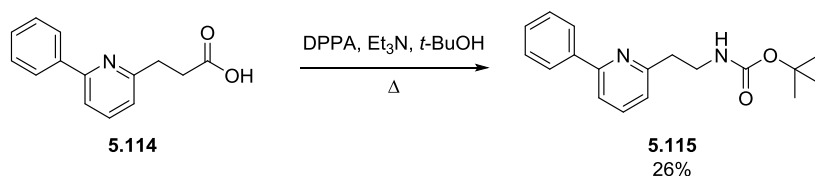
Scheme 5.3 Heck coupling of 2-bromo-6-phenylpyridine with methyl acrylate followed by reduction of the alkene and ester hydrolysis to yield intermediate **5.114**.

In order to overcome the need for an aqueous hydrolysis, 2-bromo-6-phenylpyridine (**5.111**) was reacted with benzyl acrylate (**5.119**) instead to give **5.120**. Analysis of the coupling constants in the ^1H NMR revealed a J value of 16 Hz which is also consistent with the *trans*-isomer as shown (Scheme 5.4). This could then be converted in one step to the desired intermediate, **5.114** through treatment with 5% Pd/C in an atmosphere of hydrogen gas in good yield.



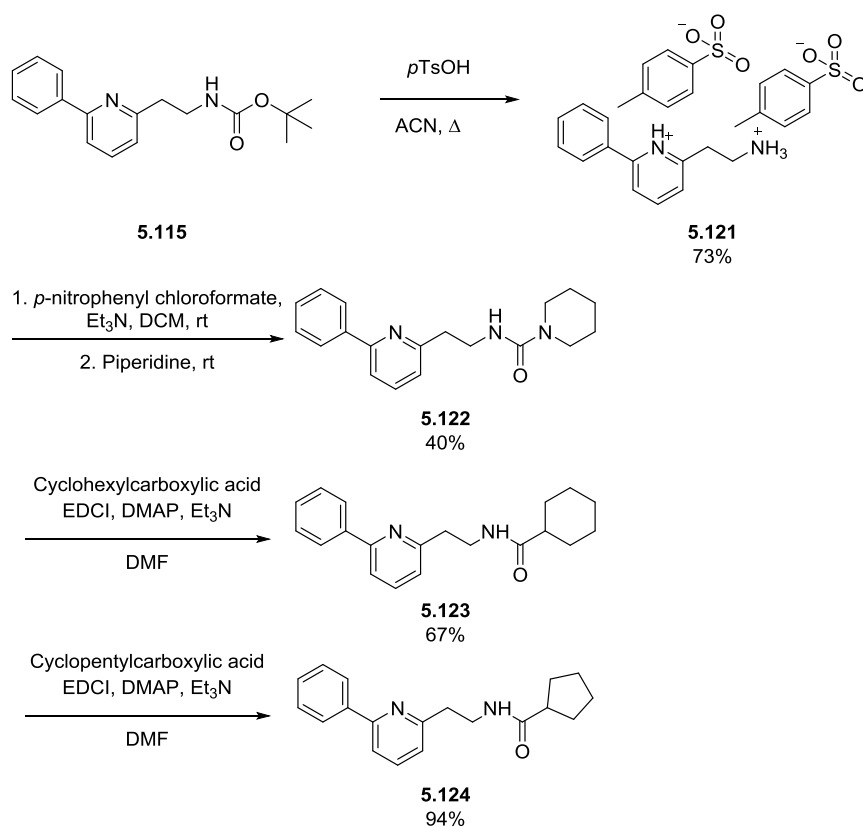
Scheme 5.4 Heck coupling of 2-bromo-6-phenylpyridine with benzyl acrylate followed by simultaneous reduction of the alkene and ester hydrolysis to yield intermediate **5.114**.

The carboxylic acid could then be converted to the *tert*-butyl carbamate (**5.115**) through the Curtius rearrangement with diphenylphosphoryl azide, and triethylamine at reflux in *tert*-butanol (Scheme 5.5).



Scheme 5.5 Curtius rearrangement of **5.114** to give the tert-butyl carbamate, **5.115**.

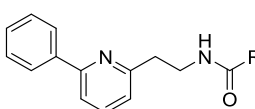
Deprotection of the Boc group was achieved by refluxing **5.115** in acetonitrile with *para*-toluenesulfonic acid. This yielded the desired amine as the salt and by ^1H NMR it was possible to quantify the number of salts that were present. This compound was then utilised to install the piperidine urea (**5.122**), or amide coupled to cyclohexylcarboxylic acid or cyclopentylcarboxylic acid in order to synthesise **5.123** and **5.124**, respectively (Scheme 5.6).



Scheme 5.6 Deprotection of the amine and the subsequent synthesis of analogues **5.122-5.124**.

Table 5.12 summarises the biological activity of the 2,6-disubstituted pyridine core analogues against *T.b. brucei*.

Table 5.12 Biological activity of analogues with a 2,6-disubstituted pyridine core against *T.b. brucei*.



ID	R	EC ₅₀ (μM)	SI ^a
5.115		> 10 ^b	
5.122		0.17 ± 0.06	489
5.123		1.51 ± 0.29	55
5.124		0.81 ± 0.14	103

^a Relative to HEK293 (Human Embryonic Kidney) mammalian cells.

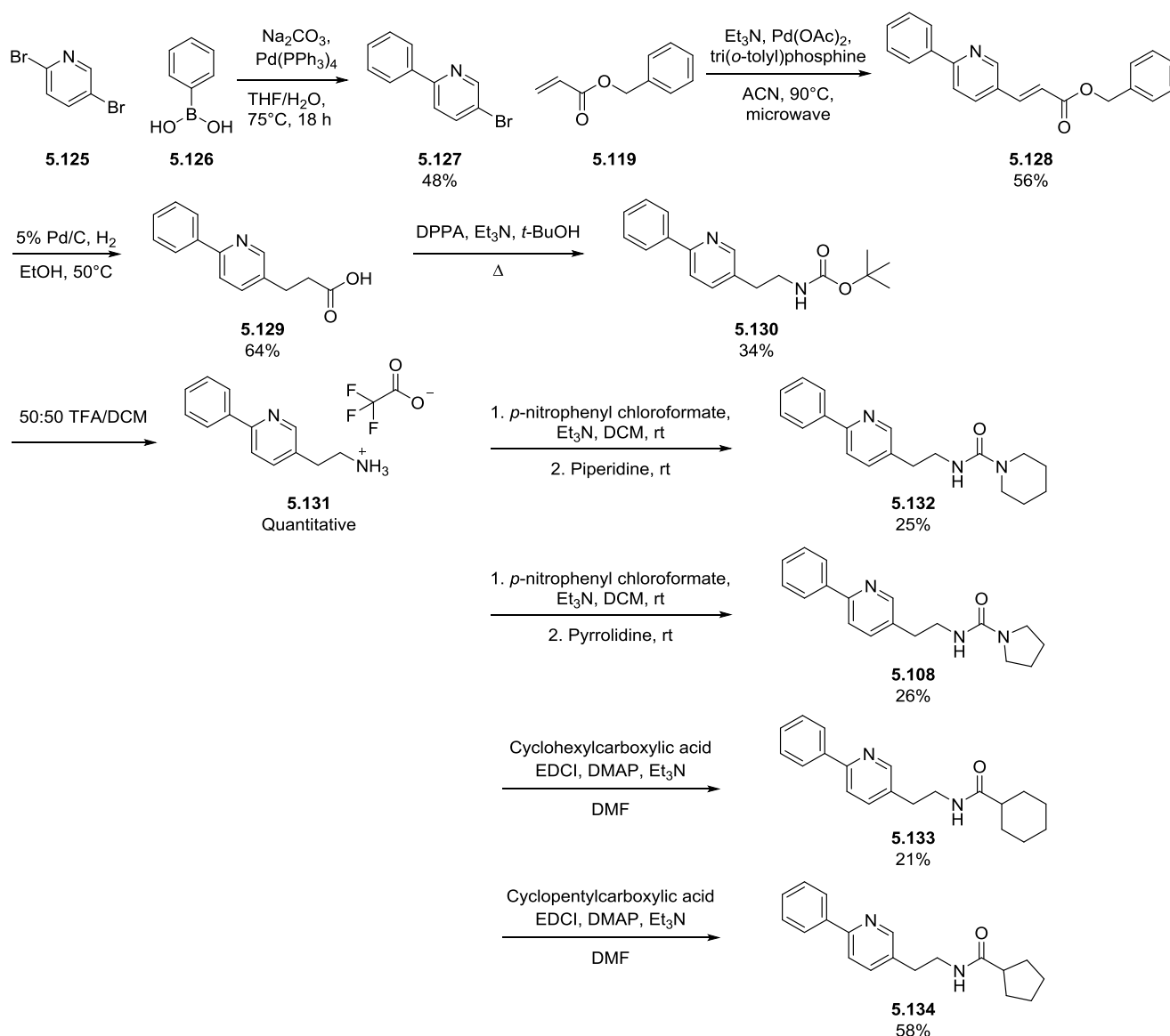
^b Compound exhibited < 50% activity at 10.41 μM.

Combination of the 2,6-disubstituted core and the *tert*-butyl carbamate (**5.115**) led to a complete loss of activity in this assay as it did in combination with the thiazole core (**5.64**; EC₅₀ > 10 μM). In combination with the piperidine (**5.122**) a six-fold decrease in the activity was observed against *T.b. brucei* (**5.69**; EC₅₀ 0.028 μM) whilst a five-fold and three-fold loss in activity was observed when combined with the cyclohexyl (**5.123**) (**5.09**; EC₅₀ 0.31 μM) or cyclopentyl groups (**5.124**) (**5.10**; EC₅₀ 0.25 μM) respectively, when compared with the similarly substituted thiazole core.

5.5.2. 2,5-Disubstituted pyridine core

Synthesis of the 2,5-disubstituted core was achieved following the previously established synthesis for the 2,6-disubstituted analogues as discussed and as summarised in Scheme 5.7. The only variation to the synthetic scheme was with the Suzuki coupling, where previously established literature conditions were employed utilising Pd(PPh₃)₄ in the presence of sodium carbonate and a mixed solvent system of tetrahydrofuran and water.¹¹⁹ This led to the clean isolation of **5.127** with the regiochemistry as shown in

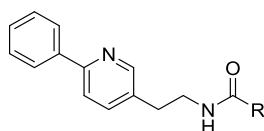
Scheme 5.7, this could then be reacted with benzyl acrylate (**5.119**) in a Heck coupling to give **5.128** in reasonable yields. The subsequent reduction and ester hydrolysis occurred in good yield before the Curtius rearrangement. The yield for this reaction was low though the subsequent Boc deprotection occurred in quantitative yields and the amine could then be reacted with a variety of carboxylic acids to form the amides **5.133-5.134** or the urea could be formed with either pyrrolidine or piperidine as in **5.108** and **5.132**, respectively.



Scheme 5.7 Synthesis for the 2,5-disubstituted pyridine core analogues.

Table 5.13 summarises the biological activity of the 2,5-disubstituted pyridine core analogues against *T.b. brucei*.

Table 5.13 Biological activity of analogues with the 2,5-disubstituted pyridine core against *T.b. brucei*.



ID	R	EC ₅₀ (μM)
5.108		> 10 ^a
5.132		> 10 ^a
5.133		> 10 ^a
5.134		> 10 ^a

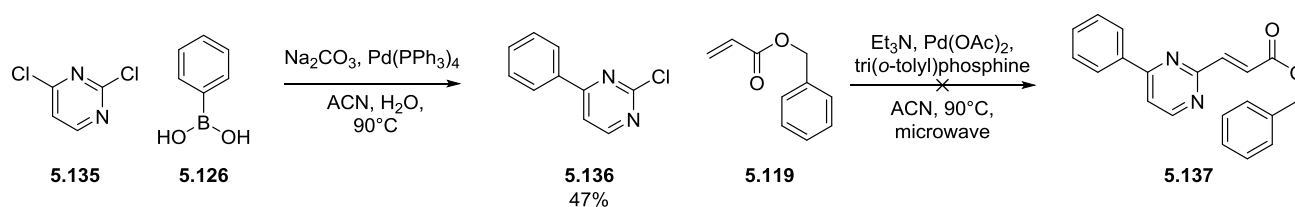
^a Compound found to have < 50% activity at 10.41 μM.

In all cases the 2,5-substitution pattern led to a loss of activity against *T.b. brucei* in this assay. This suggests that the angle of the substituents generated by this substitution pattern renders the analogues unable to interact appropriately with the putative target.

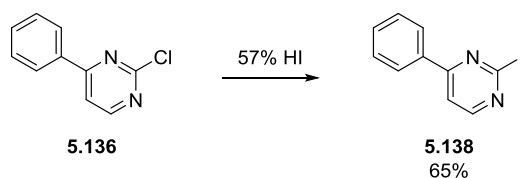
5.5.3. Pyridazine core

The synthesis of the pyridazine core was initially designed to follow the synthetic route developed for the pyridine core. As such a Suzuki coupling was carried out between 2,4-dichloropyrimidine and phenylboronic acid as shown in Scheme 5.8.¹²⁰ Only the desired product with the regiochemistry shown was observed with the 2-chloro being unreactive under these conditions. A Heck coupling with benzyl acrylate was then trialled; however there was no desired product observed by TLC or LCMS and the starting material was recovered from the reaction mixture. Numerous conditions focusing on different acrylates (entries 6-10,

Table 5.14), Sonogashira coupling (entries 1-5, Table 5.14), varying the temperature of the reaction and halogen exchange to the iodo (Scheme 5.9) were employed in order to obtain the desired intermediate. Only once did the *tert*-butyl acrylate successfully couple to give the desired product and in subsequent reactions it proved to be difficult to reproduce the results. As such, an alternative synthesis was sought.

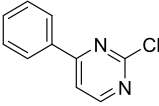
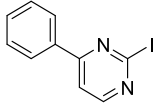


Scheme 5.8 Attempted synthesis of the pyridazine core analogues.



Scheme 5.9 Halogen exchange to produce the more activated iodo intermediate, 5.138.

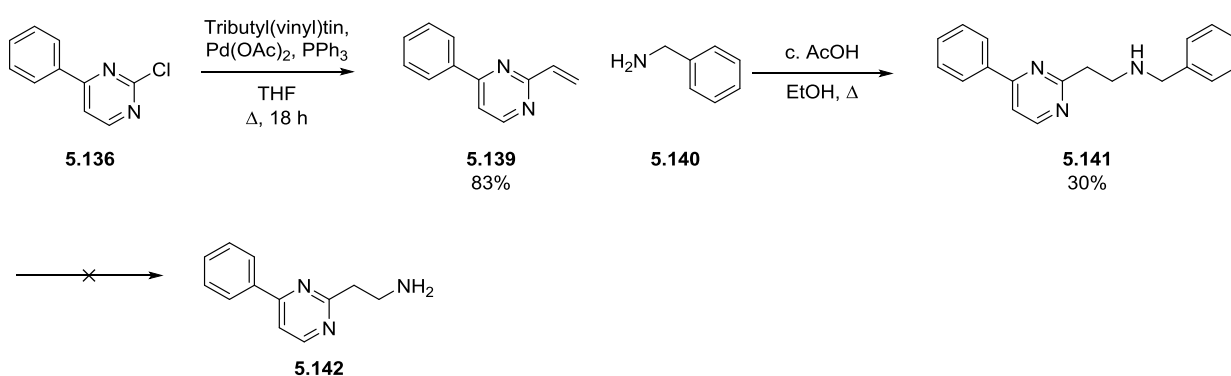
Table 5.14 Reaction conditions for the Sonogashira and Heck coupling reactions attempted on the pyridazine system.

Entry	Reaction conditions	Outcome with starting material	
			
1	Methyl propiolate (1.1 eq.), PdCl ₂ (PPh ₃) ₂ (0.05 eq.), PPh ₃ (0.1 eq.), Et ₃ N (3 eq.), CuI (0.1 eq.), DMF, 90 °C, microwave	No reaction	-
2	Methyl propiolate (1.1 eq.), PdCl ₂ (PPh ₃) ₂ (0.05 eq.), PPh ₃ (0.1 eq.), Et ₃ N (3 eq.), CuI (0.1 eq.), PBu ₃ .BF ₄ (0.1 eq.), DMF, 90 °C, microwave	No reaction	-
3	Methyl propiolate (1.2 eq.), PdCl ₂ (PPh ₃) ₂ (0.05 eq.), PPh ₃ (0.1 eq.), Et ₃ N (3 eq.), PBu ₃ .BF ₄ (0.1 eq.), CuI (0.1 eq.), DMF, rt	-	Decomposition of materials ^b
4	Methyl propiolate (1.2 eq.), PdCl ₂ (PPh ₃) ₂ (0.05 eq.), PPh ₃ (0.1 eq.), DIPEA (5 eq.), PBu ₃ .BF ₄ (0.1 eq.), CuI (0.1 eq.), DMF, rt	-	No reaction
5	Methyl propiolate (1.1 eq.), PdCl ₂ (PPh ₃) ₂ (0.05 eq.), PPh ₃ (0.1 eq.), DIPEA (5 eq.), CuI (0.1 eq.), PBu ₃ .BF ₄ (0.1 eq.), DMF, 90 °C, microwave	-	SM degraded
6	Methyl acrylate (1.2 eq.), Pd(OAc) ₂ (0.1 eq.), tri(<i>o</i> -tolyl)phosphine (0.1 eq.), Et ₃ N (4 eq.), ACN, 90 °C, microwave	No reaction	-
7	Methyl acrylate (1.2 eq.), Pd(OAc) ₂ (0.1 eq.), tri(<i>o</i> -tolyl)phosphine (0.1 eq.), Et ₃ N (4 eq.), PBu ₃ .BF ₄ (0.2 eq.), DMF, 90 °C, microwave	No reaction	-
8	Benzyl acrylate (3 eq.), Pd(OAc) ₂ (0.2 eq.), tri(<i>o</i> -tolyl)phosphine (0.3 eq.), DIPEA (4 eq.), ACN, 90 °C, microwave	No reaction	-
9	<i>Tert</i> -butyl acrylate (1.2 eq.), Pd(OAc) ₂ (0.1 eq.), tri(<i>o</i> -tolyl)phosphine (0.1 eq.), Et ₃ N (4 eq.), PBu ₃ .BF ₄ (0.2 eq.), ACN, 90 °C, microwave	32% of desired product isolated ^a	SM degraded
10	<i>Tert</i> -butyl acrylate (1.2 eq.), Pd(OAc) ₂ (0.1 eq.), tri(<i>o</i> -tolyl)phosphine (0.1 eq.), Et ₃ N (4 eq.), PBu ₃ .BF ₄ (0.2 eq.), ACN, 70 °C, microwave	-	Trace amount of product by LCMS

^a Repetition of these conditions failed to yield the desired product and starting material was recovered.

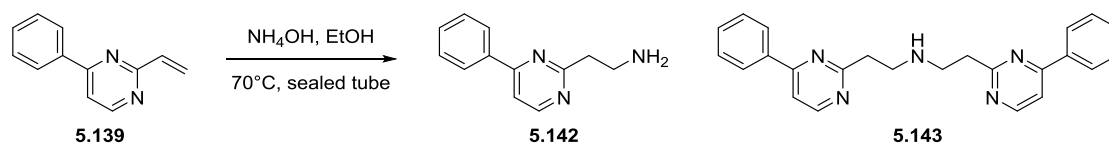
^b Appears to be reaction between methyl propiolate and triethylamine.

As an alternative a Stille coupling was employed with tributyl(vinyl) tin at reflux for 18 h (Scheme 5.10). This led to the isolation of the vinyl pyrimidine intermediate, **5.139**, in excellent yields. A subsequent intermolecular hydroamination could be performed with benzylamine in ethanol with a catalytic amount of acetic acid to give **5.141**. However, at this point numerous conditions were employed in order to try to cleave the benzyl group. This included 5% Pd/C at both ambient temperature and with heat, platinum oxide as the catalyst and the Parr reactor though none of these methods were successful. As a result, an alternative synthetic route was sought in order to install the free amine.



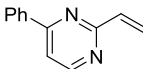
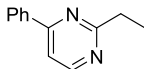
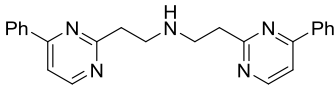
Scheme 5.10 Synthesis of the benzylamine intermediate **5.141** after the Stille coupling of **5.136** with tributyl(vinyl) tin.

In an effort to access the free amine a literature synthesis was adapted that involved combining **5.139** in a sealed tube with ammonium hydroxide and ethanol (Scheme 5.11).¹²¹ However, this led to the formation of significant quantities of the dimer, **5.143**. Through a series of optimisations it was found that the formation of the dimer could be significantly reduced by diluting the reaction mixture to a final concentration of 0.08 M (Table 5.15). Removal of **5.143** from the reaction mixture was readily achieved by precipitating it as the HCl salt upon acidification of the organic phase. Subsequent neutralisation gave ready access to the free amine.



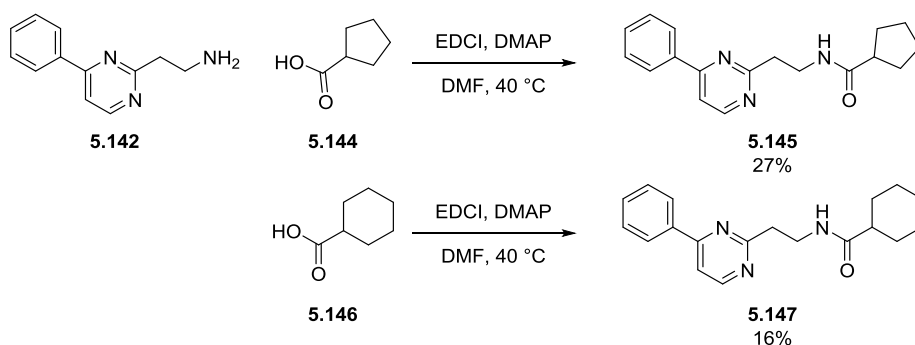
Scheme 5.11 Synthesis of the free amine intermediate (**5.142**) via reaction with ammonium hydroxide and ethanol.

Table 5.15 Optimisation of the reaction conditions for the initial Suzuki coupling.

Reaction conditions	Percentage of material ^a		
			
1 50:50 NH ₄ OH and EtOH Concentration: 0.44 M Time: 48 h Temperature: 70 °C	35	59	5
2 50:50 NH ₄ OH and EtOH concentration: 0.44 M Time: 12 h Temperature: 80 °C	17	74	8
3 50:50 NH ₄ OH and EtOH concentration: 0.77 M Time: 32 h Temperature: 80 °C	37	50	13
4 NH ₄ OH concentration: 0.28 M Time: 8 h Temperature: 80 °C	1	11	88
5 50:50 NH ₄ OH and EtOH concentration: 0.20 M Time: 18 h Temperature: 70 °C	1	68	24
6 50:50 NH ₄ OH and EtOH concentration: 0.08 M Time: 48 h Temperature: 70 °C	72	24	3

^a determined by LCMS analysis

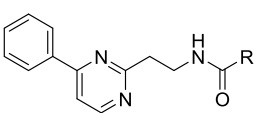
Once the free amine (**5.142**) had been successfully obtained it was possible to then convert it into the amides (**5.145** and **5.147**) shown in Scheme 5.12 in reasonable yields. Synthesis of the urea analogues was also attempted however, the reaction failed to yield any product and further work could not be carried out due to time constraints.



Scheme 5.12 Synthesis for the pyridazine core analogues.

Table 5.16 summarises the biological activity of the pyridazine core analogues against *T.b. brucei*. Both the cyclohexyl (**5.147**) and cyclopentyl (**5.145**) gave analogues that were significantly less active than the thiazole comparators. The cyclopentyl analogue (**5.145**) led to a ~45-fold loss in activity compared with **5.10** (EC_{50} 0.25 μ M). While the cyclohexyl analogue (**5.147**) led to a ~17-fold loss in activity compared with **5.09** (EC_{50} 0.31 μ M). As such, it appears that the addition of the endocyclic nitrogen is largely responsible for the significant decrease in activity when the results are compared with the 2,6-disubstituted pyridine core analogues (**5.124**; cyclopentyl; EC_{50} 0.81 μ M) (**5.125**; cyclohexyl; EC_{50} 1.51 μ M).

Table 5.16 Biological activity of analogues with a pyridazine core against *T.b. brucei*.



ID	R	EC ₅₀ (μM)	SI ^a
5.145		11.2 ± 1.69	7
5.147		5.37 ± 1.50	16

^a Relative to HEK293 (Human Embryonic Kidney) mammalian cells.

5.6. Linker modifications

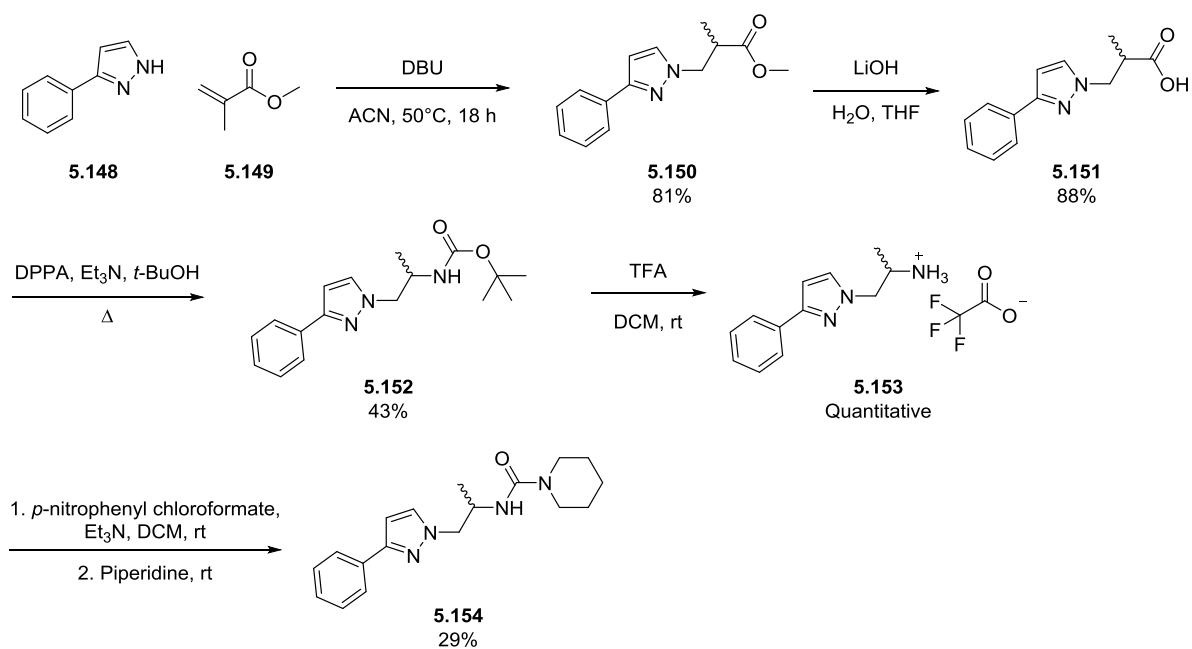
Numerous modifications to the linker were originally envisioned though two were chosen as the focus for this work. Initially methylation of the linker at both of the methylene positions was chosen as well as the introduction of a cyclopropane. A description of this work follows.

5.6.1. Methylation of the ethyl linker

Initially, synthesis of analogues with a methyl at each position of the linker was attempted. The alkylation of a pyrazole has been widely reported in the literature and can proceed via a variety of routes. Such routes involve the reaction between a pyrazole and an aliphatic alcohol either in the presence of triphenylphosphine¹²² or as the activated mesylate¹²³ and are well known. Alternatively, an aliphatic halide can be reacted with a pyrazole in the presence of base to achieve the desired product,^{124, 125} or a Michael addition utilising a variety of Michael acceptors.^{126, 127} In this instance the synthesis of the methylated linker analogues were achieved through a Michael addition.

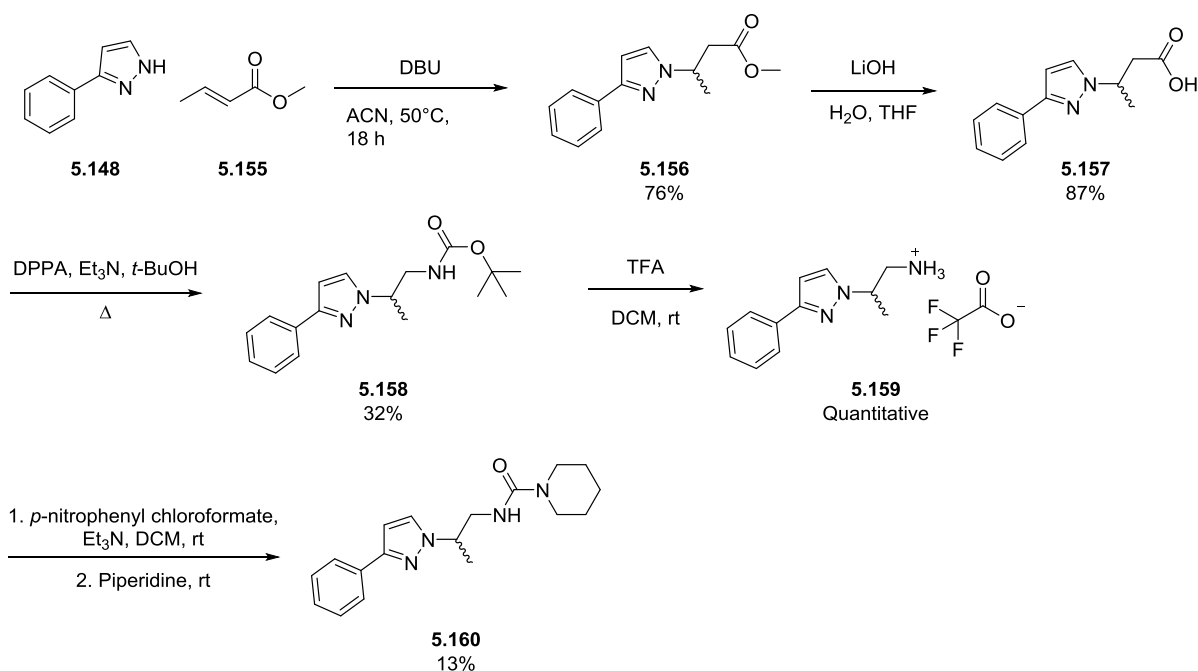
Reaction between 3-phenyl-1*H*-pyrazole (**5.148**) and methyl methacrylate (**5.149**) led to the methyl ester (**5.150**) in good yields as shown in Scheme 5.13. The subsequent ester hydrolysis was accomplished using

lithium hydroxide in water and THF, prior to the Curtius rearrangement in *tert*-butanol to give the Boc protected amine (**5.151**). The Boc group could be removed using TFA in DCM at room temperature for 2 h prior to the urea formation with *para*-nitrophenyl chloroformate in dichloromethane and with triethylamine and piperidine to give the desired product (**5.154**).



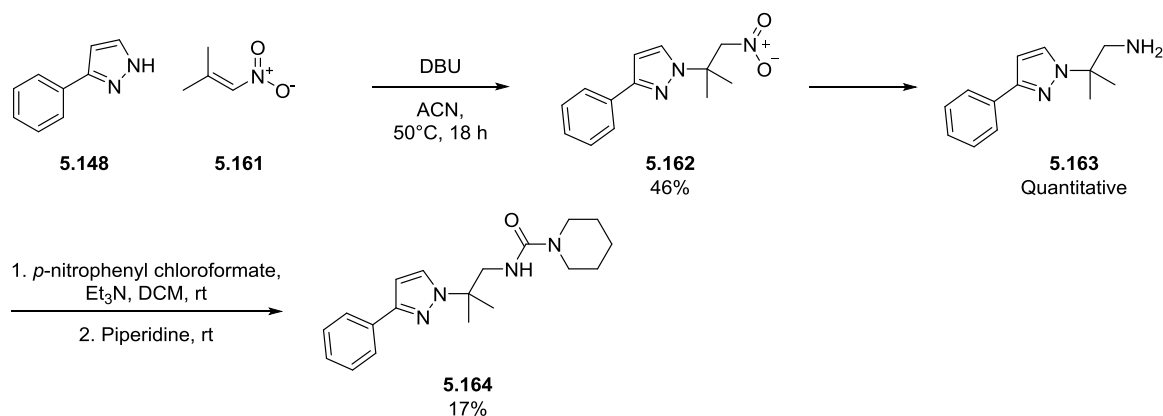
Scheme 5.13 Synthesis of the racemic methylated linker from 3-phenyl-1H-pyrazole and methyl methacrylate.

The same synthetic procedure could be followed in order to obtain the alternate methylated regioisomer (**5.160**) when starting from 3-phenyl-1H-pyrazole (**5.148**) and methyl crotonate (**5.155**) (Scheme 5.14).



Scheme 5.14 Synthesis of the racemic methylated linker from 3-phenyl-1H-pyrazole and methyl crotonate.

Following a similar synthesis to one proposed in the literature¹²⁸ it was possible to access the dimethylated linker analogue (**5.164**) by reacting 3-phenyl-1H-pyrazole (**5.148**) and 2-methyl-1-nitroprop-1-ene (**5.161**) in the presence of DBU to give the nitro intermediate (**5.162**) (Scheme 5.15). Reduction of the nitro to the amine was could be performed utilising 5% Pd/C and hydrogen gas, or using zinc powder in the presence of ammonium chloride. The urea could then be obtained through reaction with *para*-nitrophenyl chloroformate in dichloromethane with triethylamine and piperidine to give **5.164**.



Scheme 5.15 Synthesis of the dimethylated linker from **5.148** and **5.161**.

Table 5.17 summarises the biological activity of compounds **5.154**, **5.160**, and **5.164** against *T.b. brucei*. Compound **5.154** demonstrated a ~five-fold decrease in activity when compared with **5.72** while **5.160** exhibited a ~two-fold loss in activity against *T.b. brucei* when compared with **5.72**. Compound **5.164** exhibited a further 2.5-fold loss in activity compared with **5.160**, which suggested that both of the methyl groups are not equal in terms of interactions within the active site of the putative target.

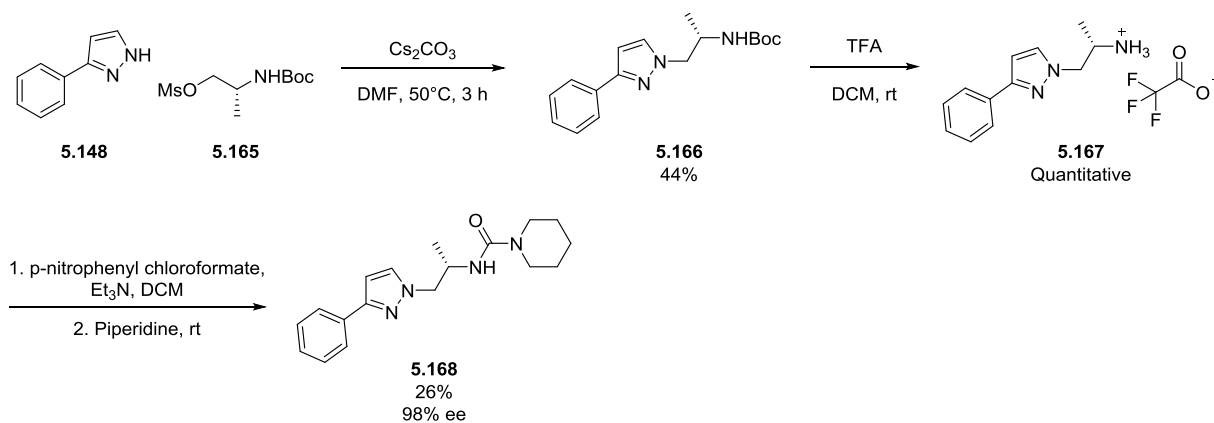
Table 5.17 Biological activity of the racemic methyl and dimethyl linker analogues against *T.b. brucei*.

ID	Structure	EC ₅₀ (μM)	SI ^a
5.72		0.12 ± 0.006	681
5.154		0.64 ± 0.12	131
5.160		0.23 ± 0.04	358
5.164		0.59 ± 0.09	142

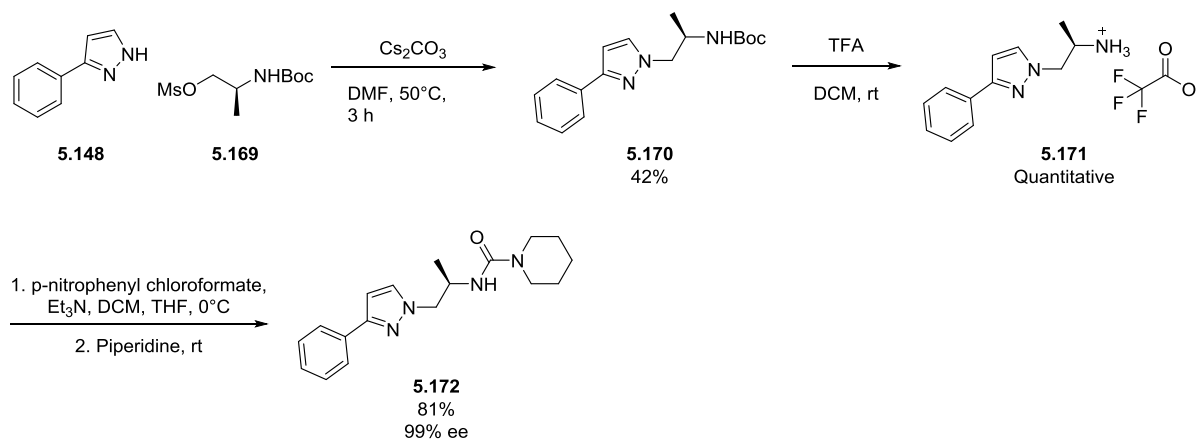
^a Relative to HEK293 (Human Embryonic Kidney) mammalian cells.

Given these results, a synthetic procedure was designed in order to access the four enantiomers of compounds **5.154** and **5.160** utilising enantiopure starting materials. This could be achieved by reacting 3-phenyl-1*H*-pyrazole (**5.148**) with either **5.165** (Scheme 5.16) or **5.169** (Scheme 5.17). This reaction proceeded in relatively low yields, however sufficient material was obtained in order to progress with the synthesis. The Boc group could be cleaved using TFA in DCM in quantitative yields prior to the urea formation. The yield of the reaction between the amine and *p*-nitrophenyl chloroformate could be significantly improved by utilising a 50:50 mixture of dichloromethane and tetrahydrofuran and cooling the

reaction mixture to 0 °C prior to addition and maintaining this temperature until the addition was complete. The resultant products were both found to have an excellent enantiomeric excess of 98% and 99% respectively, as determined by chiral HPLC.

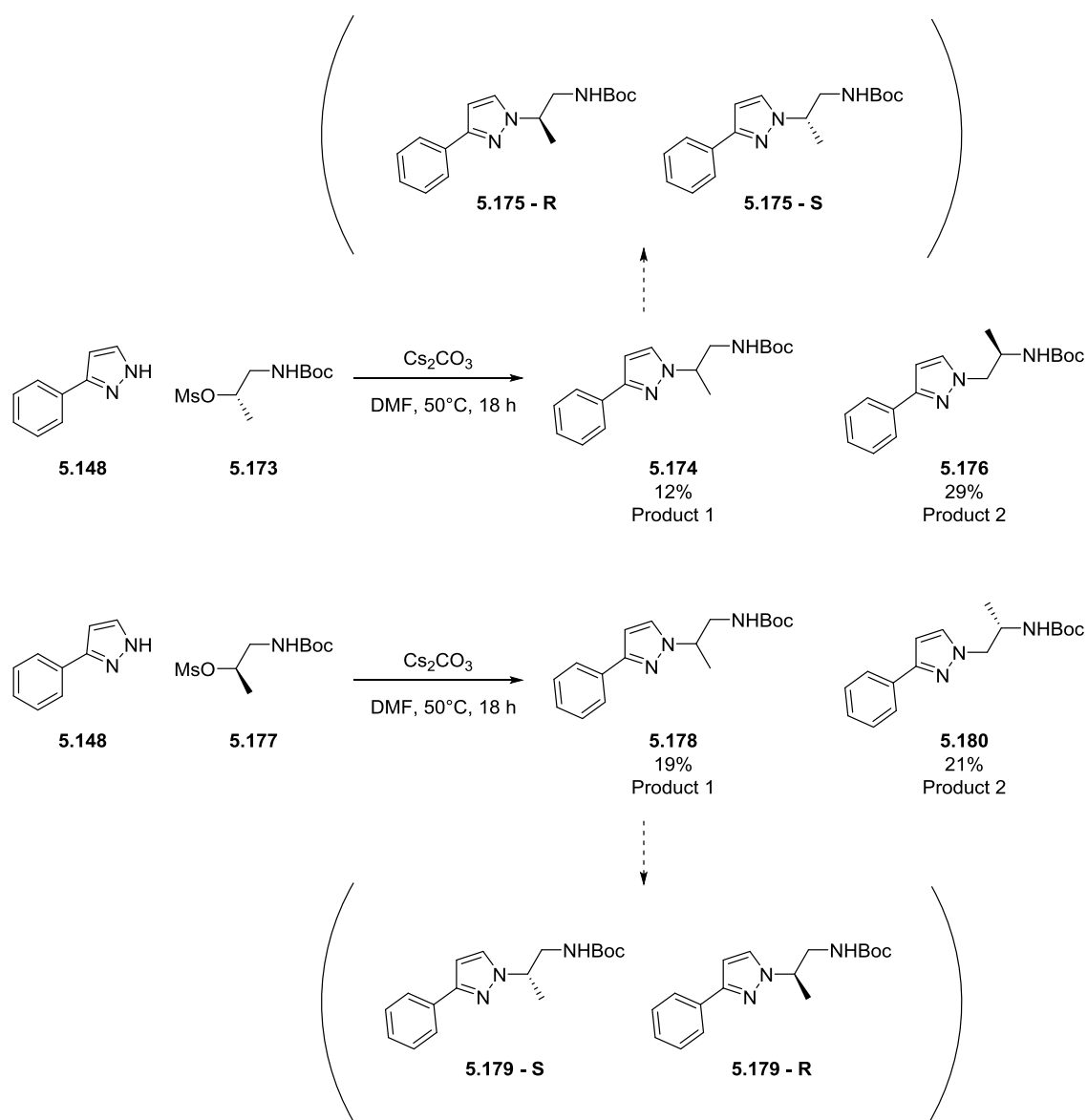


Scheme 5.16 Synthesis of the *S* enantiomer of compound **5.167**



Scheme 5.17 Synthesis of the *R* enantiomer of compound **5.171**

Synthesis of chirally pure forms of the alternative regioisomer was synthetically more challenging. Reaction between 3-phenyl-1*H*-pyrazole (**5.148**) with either (*S*)-1-((*tert*-butoxycarbonyl)amino)propan-2-yl methanesulfonate (**5.173**) or (*R*)-1-((*tert*-butoxycarbonyl)amino)propan-2-yl methanesulfonate (**5.177**), as shown in Scheme 5.18, led in each case to the formation of apparently two products with different R_f values.



Scheme 5.18 Attempted synthesis of chirally pure precursors of **5.160** with unexpected distribution of products and by-products.

Product 1 was later shown to comprise an enantiomeric mixture that matched the expected alkylation product in terms of both mass spectrometry and ¹H NMR analysis. Whilst product 2 also matched the alkylation product by mass spectrometry analysis it differed by ¹H NMR analysis and an analysis of the spectra follows.

In Figure 5.4a the spectra of product 1 is shown. There are cross-peaks present between the –CH and the –CH₃ on the linker (shown in red), and between the –CH and both –CH₂ groups (shown in green) as expected.

Furthermore, there is a cross-peak observed between the -NH and both -CH_2 protons (shown in black), which indicates that the methine and the -NH are adjacent to one another. In Figure 5.4b the spectra of product 2 is shown. Here, a clear cross-peak is observed between both the -CH and the -CH_3 of the linker. There is also an additional cross peak between the -CH and one of the -CH_2 protons but more diagnostically there is a cross peak between the -CH and the -NH protons (shown in purple), which can only occur if the -CH , and consequently the methyl, are adjacent to the -NH . On this basis we assigned product 1 as the desired *N*-alkylated regioisomer and product 2 as the alternative regioisomer.

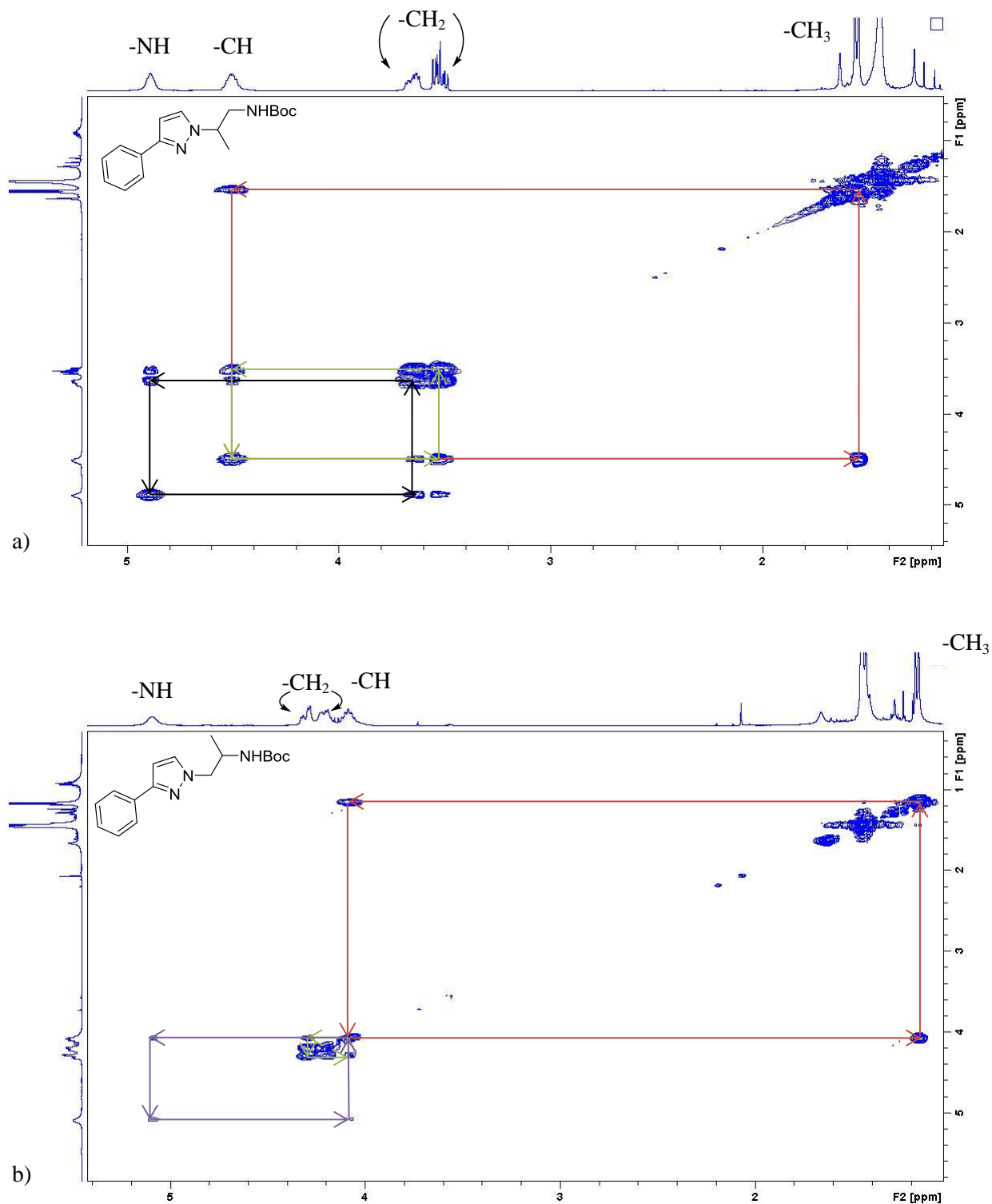
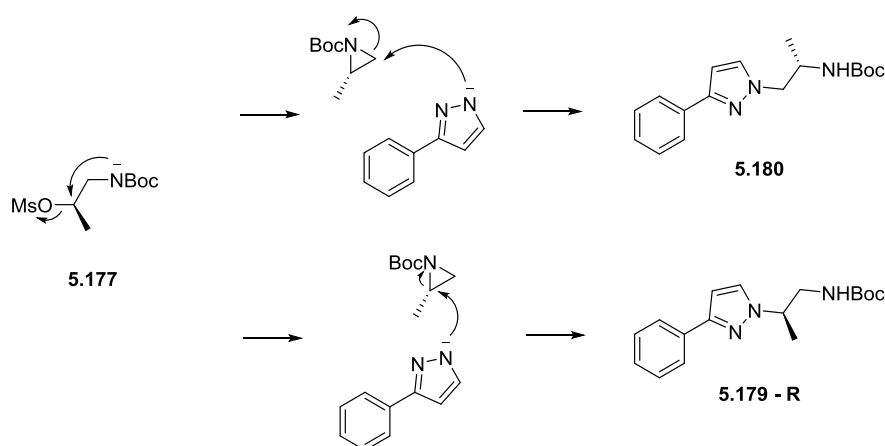


Figure 5.4 COSY spectra of the two products obtained from the reaction of 3-phenyl-1H-pyrazole with (R)-1-((tert-butoxycarbonyl)amino)propan-2-yl methanesulfonate. Red: -CH to -CH₃ cross-coupling; green: -CH to -CH₂ cross-coupling; black: -NH to -CH₂ cross-coupling; purple: -CH to -NH cross-coupling.

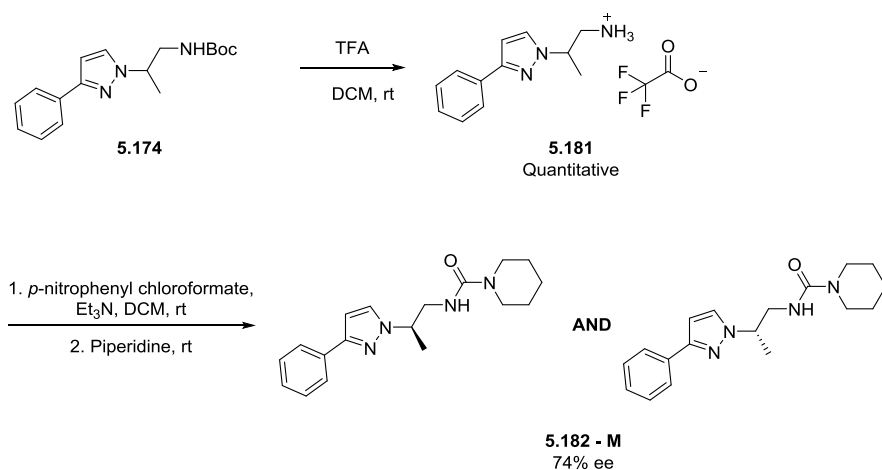
In order for this rearrangement in product 2 to occur we propose a mechanism whereby the amide –NH is deprotonated under the basic conditions and subsequently attacks and eliminates the mesylate group to form an aziridine intermediate (Scheme 5.19). Taking the reaction between **5.148** and **5.177** as an example, this would lead to inversion of the chiral centre to give the *R* aziridine as shown, which upon attack by the pyrazole anion at the less hindered methylene carbon would lead to product **5.180** with retention of the aziridine chirality. This mechanism explains the observation of apparent methyl migration.

It may also be anticipated that some attack of the methine carbon in the aziridine is possible and this would result in chiral re-inversion, which would lead to the expected regioisomer (**5.179 - R**) although of opposite chirality to that expected. If alkylation by the intended mechanism was concomitant with aziridine formation, this would explain the observation of both *R* and *S* enantiomers.

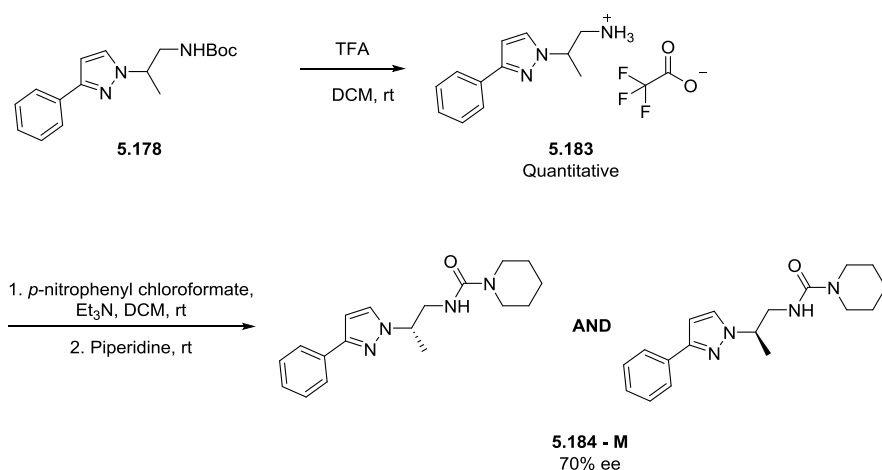


Scheme 5.19 Proposed mechanism of the aziridine formation and subsequent ring opening by the nucleophile from both faces leading to the two products observed.

At this point it was unknown that product 1 was a mixture of enantiomers and it was taken through the remainder of the synthetic procedure where the Boc group could be cleaved using TFA in DCM in quantitative yields. The piperidine urea (**5.182 - M** and **5.184 - M**) could then be formed via reaction with *p*-nitrophenyl chloroformate in DCM with triethylamine and piperidine in reasonable yields (Scheme 5.20 and 5.21 respectively).



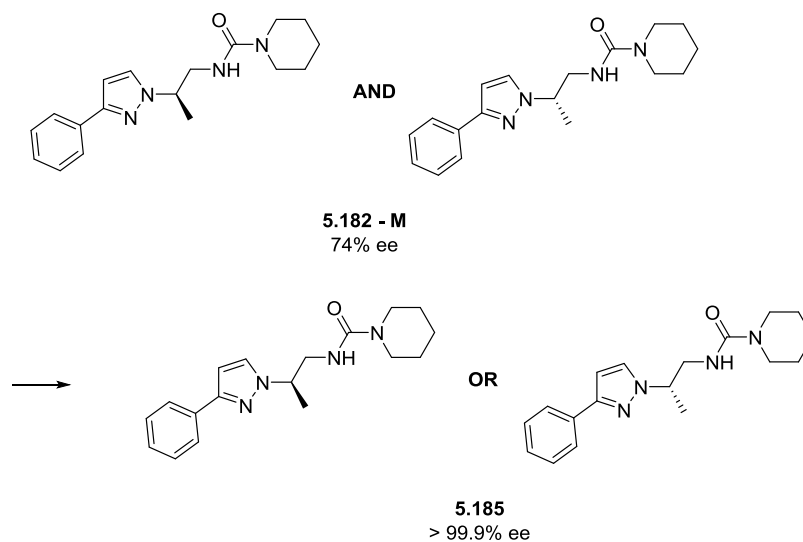
Scheme 5.20 Synthesis of **5.182 – M** which was found to contain a mixture of the *R* and *S* enantiomers by chiral HPLC analysis.



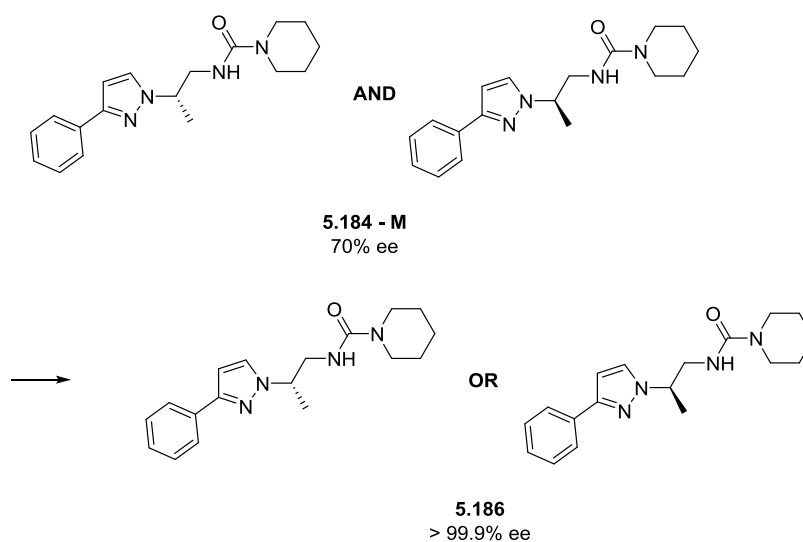
Scheme 5.21 Synthesis of **5.184 – M** which was found to contain a mixture of the *R* and *S* enantiomers by chiral HPLC analysis.

It was at this point that analysis of **5.182 - M** and **5.184 - M** was undertaken by chiral HPLC and this revealed the presence of two compounds of the expected molecular weight. Compound **5.182 - M** was found to have a minor peak with a retention time of 5.59 min and a major peak with a retention time of 6.45 min and the enantiomeric excess (ee) was determined as 74%. By chiral HPLC compound **5.184 - M** was shown to have a major peak at 5.58 min and a minor peak at 6.43 min and it was determined that there was an overall ee of 70%. In order to test both the *R* and *S* enantiomers they were separated by chiral HPLC after

investigating numerous mobile and stationary phases to yield **5.185** and **5.186** each with > 99.9% ee (Scheme 5.22 and 5.23 respectively).



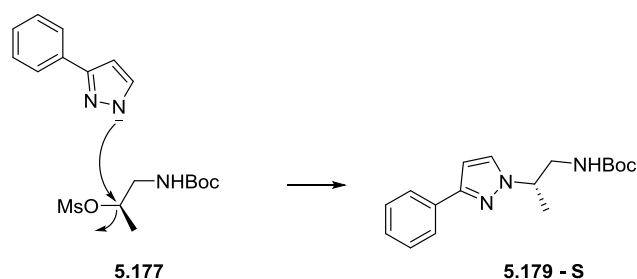
Scheme 5.22 Subsequent purification of **5.182 - M** by chiral HPLC led to the isolation of **5.185** though definitive assignment of the chiral centre as R or S is not possible.



Scheme 5.23 Subsequent purification of **5.184 - M** by chiral HPLC led to the isolation of **5.186** though definitive assignment of the chiral centre as R or S is not possible.

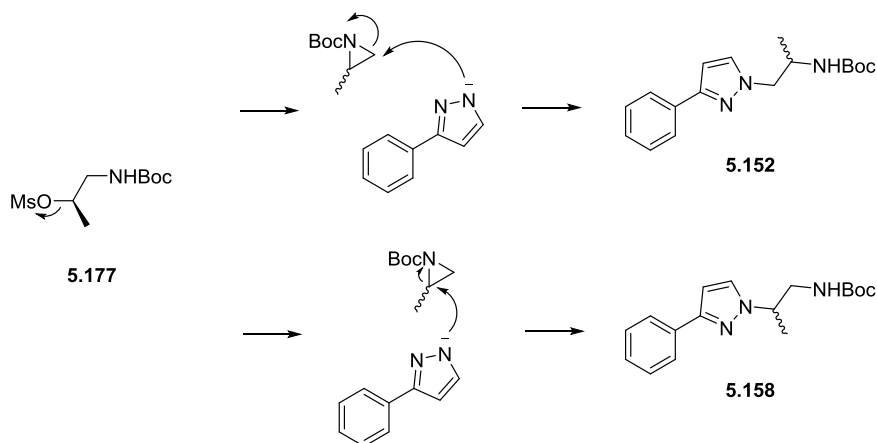
As the rearrangement by-product (**5.176** and **5.180**) was the major product obtained, it has been assumed that the aziridine mechanism predominated. Taking **5.177** by way of example and as shown in Scheme 5.19, this

would furnish the methyl migration product, **5.180** via inversion of the chiral centre. Conversely, the expected regioisomer **5.179** would represent a double inversion and be of *R* chirality. How do we therefore explain the presence of the opposite enantiomer of **5.179**? The most plausible reason is that in addition to aziridine-mediated alkylation, some conventional S_N2 -mediated alkylation took place involving direct attack by the pyrazole anion on **5.177** with single inversion of the chiral centre as shown in Scheme 5.24 to yield **5.179 - S**.



Scheme 5.24 The S_N2 mechanism for the alkylation of the pyrazole -NH by which the racemisation occurs of the methyl group on the linker region.

It cannot be ruled out that the situation is further complicated by participation of an S_N1 -mediated alkylation where the mesylate is eliminated to generate a highly reactive carbocation. As shown in Scheme 5.25, it is likely that this would give rise to the racemic aziridine as the dominant alkylating species that would arise through intramolecular attack rather than a mechanism involving intermolecular attack of the carbocation by anionic pyrazole species. This would then give rise to the racemic **5.152** and **5.158**.

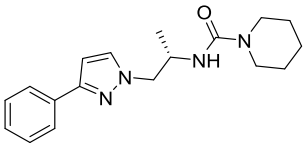
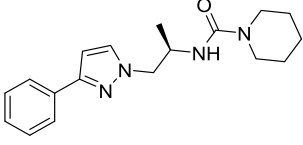
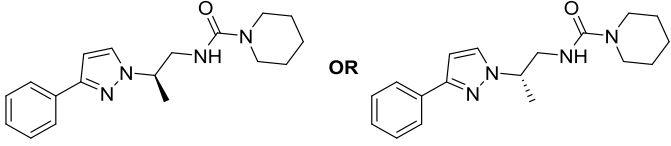
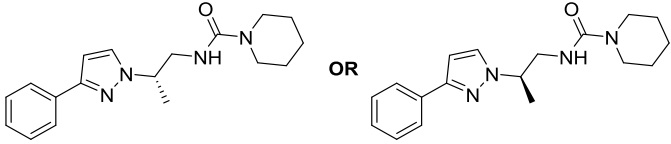


Scheme 5.25 The S_N1 mechanism for the alkylation of the pyrazole -NH by which the racemisation occurs of the methyl group on the linker region.

Further support for the mechanisms that give rise to the observed product distribution could be provided through x-ray crystallographic identification of the chirality of one set of reaction products, such as **5.175 - R**, **5.175 - S** or **5.179 - S**, **5.179 - R** although this has not been undertaken during the course of this thesis.

Table 5.18 summarises the biological activity of the enantiopure methylated analogues against *T.b. brucei*. Compound **5.172** displays only modest activity against *T.b. brucei*, however the corresponding *S* enantiomer (**5.167**) was found to be equipotent with the unmethylated pyrazole **5.72** (EC_{50} 0.12 μ M). Compounds **5.186** and **5.185** were similarly active, however neither analogue was as active as the racemic compound (**5.160**; EC_{50} 0.23 μ M). Whilst it is possible that each of the enantiomers is acting on a unique target and producing an additive effect in the racemate, or this could have arisen due to assay variation though this issue is yet to be fully resolved.

Table 5.18 Biological activity of the enantiopure methylated linker analogues against T.b. brucei.

ID	Structure	EC ₅₀ (μM)	SI ^a
5.168		0.19 ± 0.05	443
5.172		3.44 ± 0.91	24
5.185 ^b		0.57 ± 0.10	147
5.186 ^b		0.66 ± 0.11	127

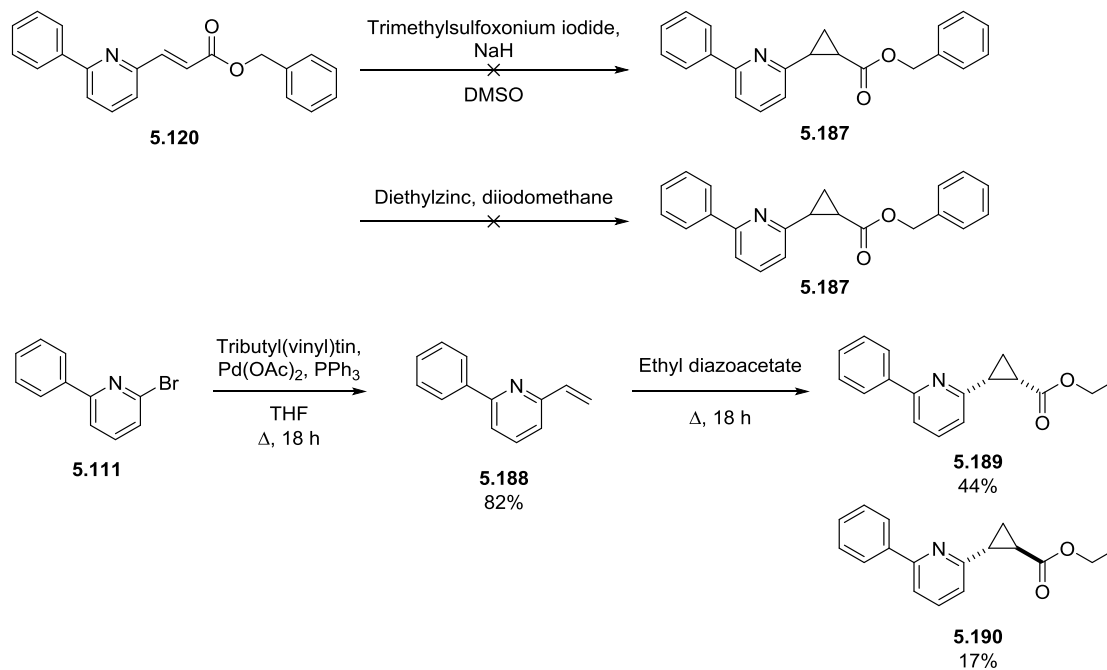
^a Relative to HEK293 (Human Embryonic Kidney) mammalian cells.

^b Definitive structure was unable to be determined.

5.6.2. Cyclopropane linker

Finally, synthesis of a constrained linker was attempted on the pyridine system with the introduction of a cyclopropane. Initially the Corey-Chaykovsky reaction was attempted. Compound **5.120** was treated with trimethylsulfoxonium iodide with sodium hydride in order to generate the sulphur ylide, which is then able to react with an enone to form the cyclopropane. However, this failed to yield the desired product with only starting material recovered. The Simmons-Smith reaction was utilised where **5.120** was treated with a solution of diethylzinc and diiodomethane, however there was no reaction and the starting material was recovered. As an alternative synthesis a Stille coupling between 2-bromo-6-phenylpyridine (**5.111**) and tributyl(vinyl)tin was performed in order to obtain 2-phenyl-6-vinylpyridine (**5.188**). Compound **5.188** was then treated with ethyldiazoacetate at reflux overnight to give the desired product, which could be separated with column chromatography to give both of the stereoisomers, **5.189** and **5.190** (Scheme 5.26). These

isomers could be characterised by ^1H NMR analysis in order to confirm the relative stereochemistry around the cyclopropane.



Scheme 5.26 Synthesis of the cyclopropyl linker via reaction of 2-phenyl-6-vinylpyridine with ethyl diazoacetate.

It has been well documented that it is possible to determine the *cis*- and *trans*- structures of aryl-carboxy disubstituted cyclopropanes via analysis of the ^1H NMR.¹²⁹ It was reported in the literature that the coupling constant of two vicinal protons that are in a *cis*- relationship falls in the range of 8-9 Hz, while two vicinal protons in a *trans*- relationship fall in the range of 4-6 Hz.¹²⁹ It has also been noted that for the *trans*-isomer, the most deshielded signal is observed to be a doublet of doublet of doublets (ddd), while for the *cis*-isomer the most deshielded signal is a quadruplet (q).¹²⁹

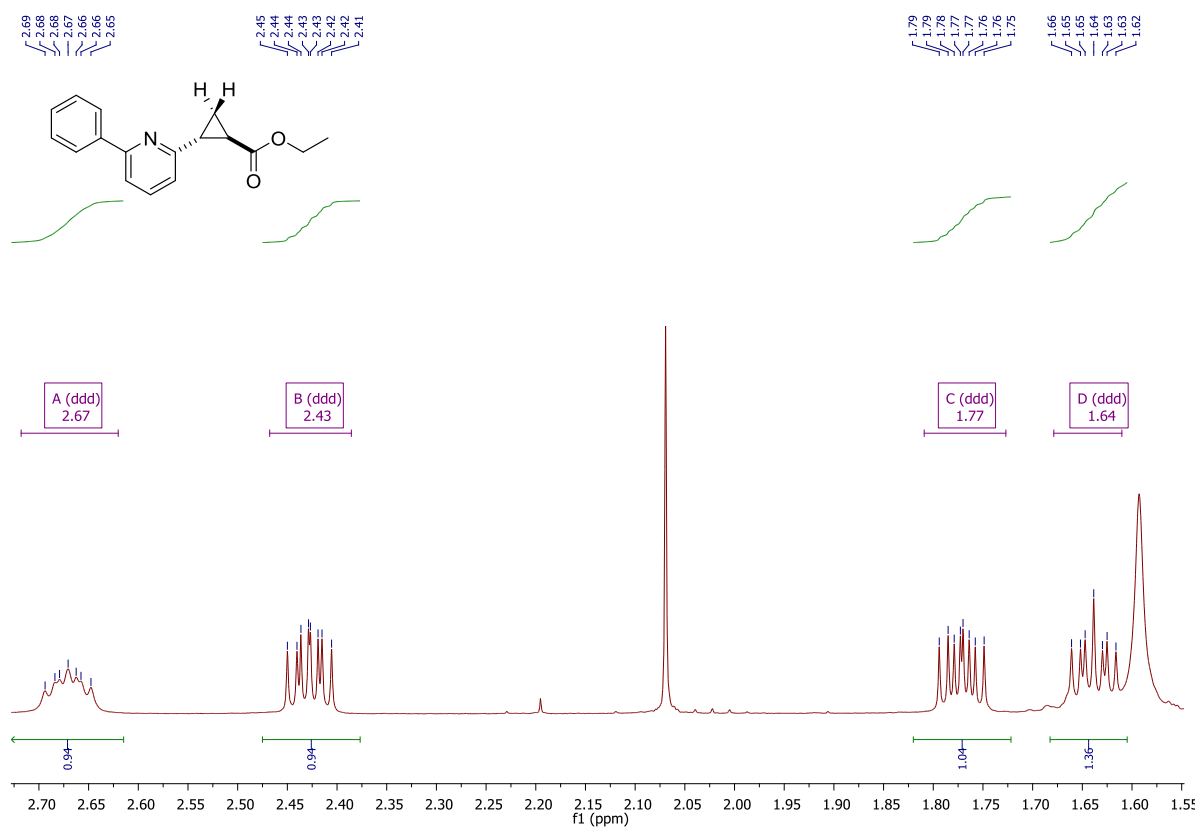


Figure 5.5 ¹H NMR of one of the isolated cyclopropane regioisomers. Through analysis of the ¹H NMR it was determined that it was the *trans*- regioisomer.

Analysis of the ¹H NMR in Figure 5.5 revealed the coupling constants shown in Table 5.19. Upon examination of H₂ (Figure 5.6) it could be seen that there was a coupling constant of 4 Hz, consistent with a *trans*- relationship with H₁. There was also a coupling constant of 9 Hz, representative of the *cis*- relationship with H_{3β} and a coupling constant of 6 Hz, representative of the *trans*- relationship to H_{3α}. Examination of the coupling constants for H₁ also showed two protons in a *trans*- relationship, H₂ and H_{3β}, in addition to displaying a *cis*- relationship with the H_{3α} proton. These previous results were confirmed through analysis of the H_{3α} and H_{3β} coupling constants. H_{3α} was *trans*- with H₂ though it was *cis*- with H₁ and conversely H_{3β} was *cis*- with H₂ and it was *trans*- with H₁. Therefore, H₁ and H₂ were in a *trans*- relationship.

Table 5.19 Coupling values present between the protons in the ^1H NMR of the cyclopropyl intermediate

5.190.

Peak	Proton assignment	J value (Hz)	Coupling
A	H_2	4	Trans
		5	Trans
		9	Cis
B	H_1	4	Trans
		6	Trans
		9	Cis
C	$\text{H}_{3\beta}$	3	Gem
		6	Trans
		9	Cis
D	$\text{H}_{3\alpha}$	3	Gem
		5	Trans
		9	Cis

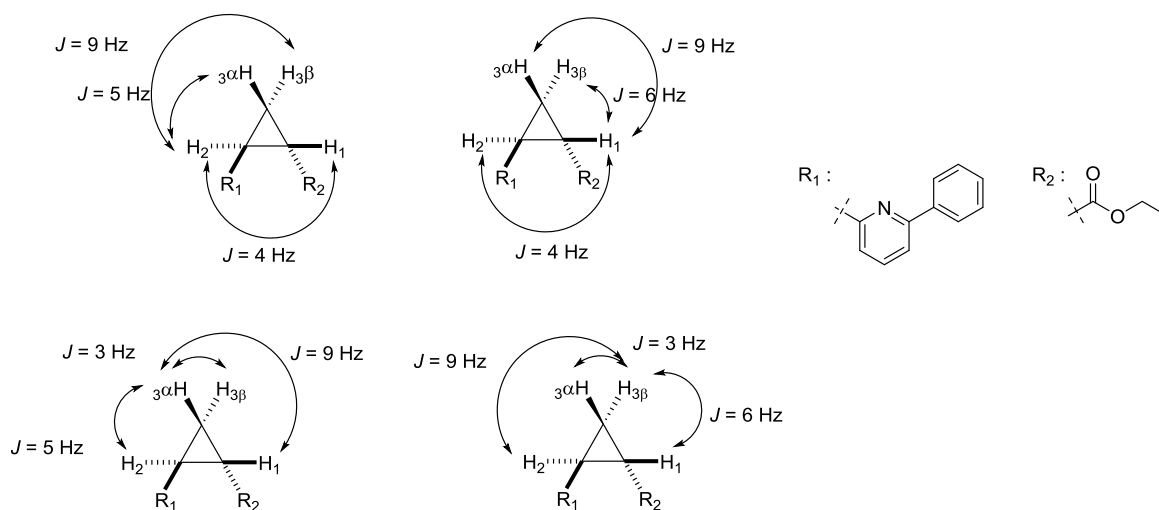


Figure 5.6 The relationship between all protons of the cyclopropyl as determined by the coupling constants from the ^1H NMR showing that the relative stereochemistry of this compound is the trans-isomer.

Further clarification of the structure of this intermediate was obtained when crystals were successfully grown through slow evaporation from a mixture of ethyl acetate and petroleum spirits. The crystals were analysed by Dr. Robert Gable at the University of Melbourne, confirming the *trans*- relationship across the cyclopropyl and showing the planar nature of the phenyl and pyridine rings as shown in Figure 5.7.

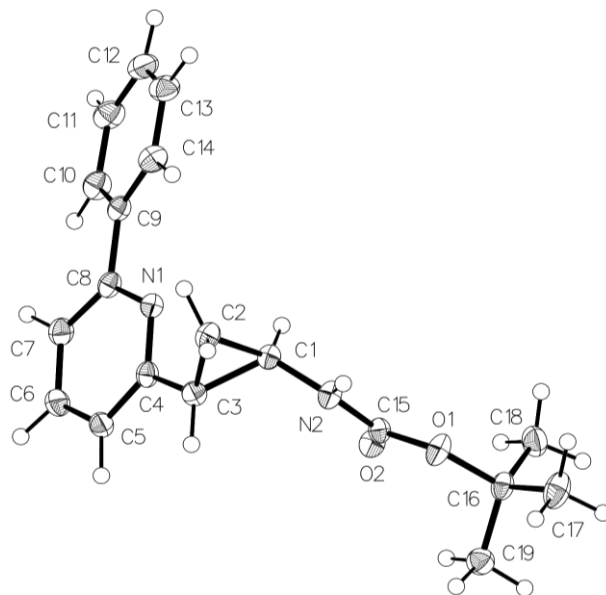


Figure 5.7 Crystal structure of ethyl (1*R*,2*R*)-2-(6-phenylpyridin-2-yl)cyclopropane-1-carboxylate (**5.190**).

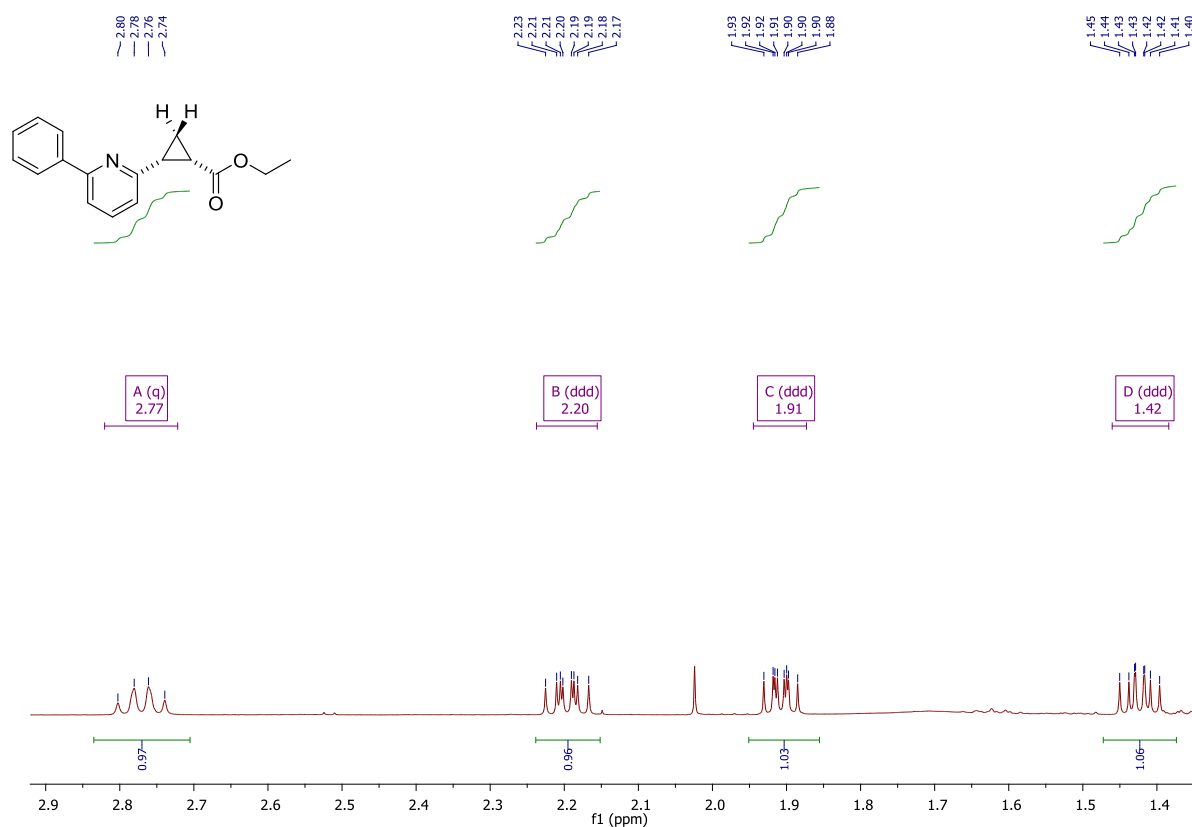


Figure 5.8 ^1H NMR of one of the isolated cyclopropane regioisomers. Through analysis of the ^1H NMR it was determined that it was the *cis*- regioisomer.

Analysis of the ^1H NMR in Figure 5.8 revealed the coupling constants shown in Table 5.20. The coupling constants present in the most deshielded proton, H₂ (Figure 5.9) were not sufficiently different to enable full interpretation of the data. However, it should be noted that the coupling constants observed in the proposed quadruplet were not all equal. Thus highlighting the hidden couplings present between the H₂ proton and the surrounding protons of the cyclopropyl. Examination of the coupling constants for H₁ showed two protons in a *cis*- relationship, H₂ and H_{3 β} , in addition to displaying a *cis*- relationship with the H_{3 α} proton. Analysis of the H_{3 α} and H_{3 β} coupling constants confirmed the relative stereochemistry of the cyclopropyl as H_{3 α} was *trans*- with both H₂ and H₁ and conversely H_{3 β} *cis*- with both H₂ and H₁. Therefore, H₁ and H₂ were in a *cis*- relationship.

Table 5.20 Coupling values present between the protons in the ^1H NMR of the cyclopropyl intermediate

5.189.

Peak	Proton assignment	J value (Hz)	Coupling
		9	
A	H_2	8	
		9	
B	H_1	6	Trans
		8	Cis
		9	Cis
C	$\text{H}_{3\alpha}$	5	Gem
		6	Trans
		7	Trans
D	$\text{H}_{3\beta}$	5	Gem
		8	Cis
		9	Cis

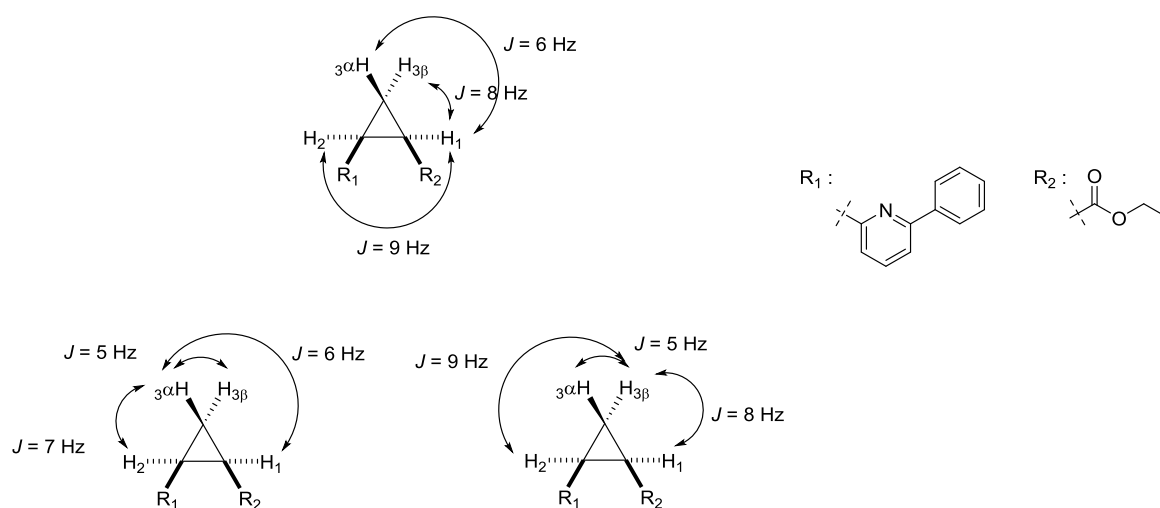
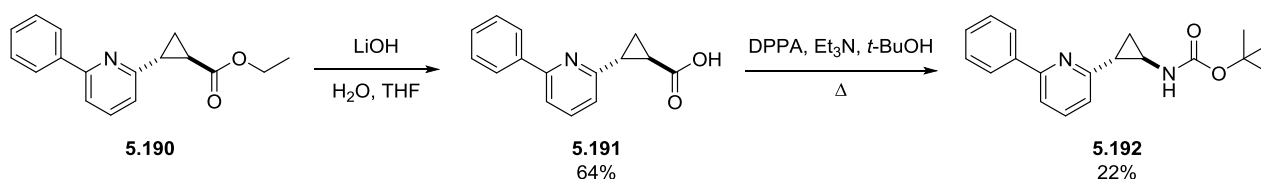


Figure 5.9 The relationship between all protons of the cyclopropyl as determined by the coupling constants from the ^1H NMR showing that the relative stereochemistry of the compound was the cis- isomer.

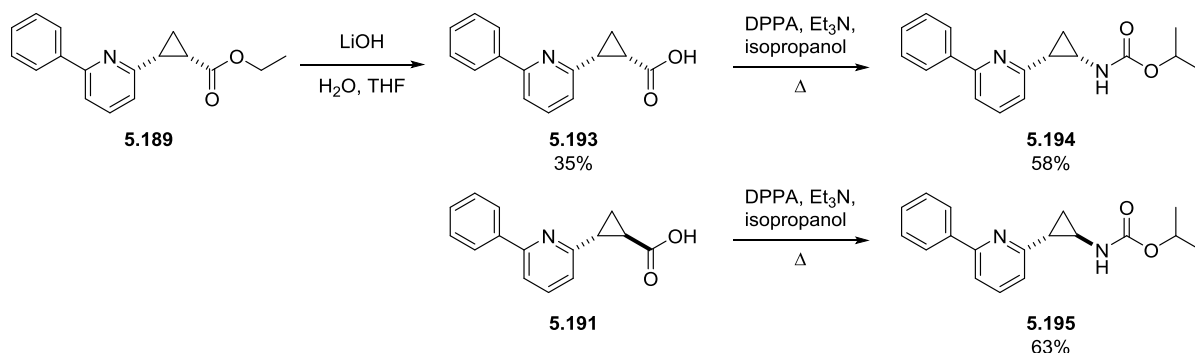
Hydrolysis of the ester could be performed in good yields using lithium hydroxide in water and tetrahydrofuran. Given the presence of the basic pyridine and the carboxylic acid it was not surprising that this intermediate was water soluble and the recovery from the aqueous phase was difficult even with careful control over the pH. The Curtius rearrangement was then performed in order to synthesise the Boc protected amine (**5.192**; Scheme 5.27).



Scheme 5.27 Synthesis of the trans- Boc protected cyclopropyl intermediate.

Subsequent cleavage of the Boc group proved to be difficult. A variety of conditions were trialled and included trifluoroacetic acid in dichloromethane, *p*-toluenesulfonic acid in refluxing acetonitrile, hydrochloric acid in dioxane and hydrochloric acid in ether, however in all cases the product appeared to degrade by LCMS and ¹H NMR analysis.

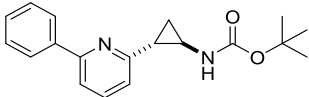
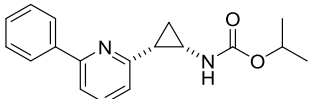
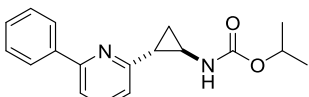
The pyrazole and thiazole cores had all previously been tested with the isopropyl side chain given the activity observed in conjunction with the thiazole core (**5.65**, EC₅₀ 0.22 μM). As such, the isopropyl carbamate analogues (**5.194** and **5.195**) were synthesised via a Curtius rearrangement with distilled isopropanol as the solvent (Scheme 5.28).



Scheme 5.28 Synthesis of the isopropyl analogues, **5.193** and **5.194**.

These analogues were tested for their biological activity against *T.b. brucei* and the results are summarised in Table 5.21.

Table 5.21 Biological activity of the racemic cyclopropyl linker analogues tested against *T.b. brucei*.

ID	Structure	EC ₅₀ (μM)
5.192		> 10 ^a
5.194		> 10 ^a
5.195		> 10 ^a

^a Compound found to have < 50% activity at 10.41 μM.

In all cases the addition of the cyclopropyl to the linker region led to a complete loss of activity. Given the activity of the methylated linker analogues (**5.154**, **5.160** and **5.164**) it is unlikely that the added bulk of the cyclopropyl is compromising the ability of the compound to interact with the putative binding site. It is possible that the conformational restraint, and consequently, the loss of flexibility around the linker is preventing the necessary conformation for potent activity being adopted in the putative binding site.

5.7. Metabolism analysis

Analysis of the metabolism of these analogues (Table 5.22) revealed no improvement in the metabolic stability had been obtained through methylation of the ethyl linker or replacement of the thiazole with the pyridine. All of the analogues exhibited high to very high rates of degradation in both human and mouse liver microsomes and with these results the compounds would be expected to be subject to rapid hepatic clearance *in vivo*. Compounds **5.145** and **5.194** were the exception with microsome predicted E_H ratios in the intermediate range when tested in human liver microsomes, though both of these analogues were found to be

inactive against *T.b. brucei*. In general there was also no measurable degradation in the control (devoid of cofactors) incubations suggesting that the main mode of metabolism is NADPH mediated for this series.

Table 5.22 Metabolism evaluation of compounds using human or mouse liver microsomes

ID	Species	Half-life (min)	<i>In vitro</i> CL_{int} (μl/min/mg protein)	Microsome- predicted E_H	Clearance classification
5.122	Human	11	164	0.87	High
	Mouse		Rapid degradation ^a		Very high
5.133	Human	4	463	0.95	High
	Mouse	< 2	> 875	> 0.95	Very high
5.145	Human	48	36	0.59	Intermediate
	Mouse	< 2 ^{b,c}	> 875	> 0.95	Very high
5.154	Human	9	184	0.88	High
	Mouse	1 ^d	2296	0.98	High
5.160	Human	12	140	0.85	High
	Mouse	2 ^d	971	0.95	High
5.194	Human	49	36	0.59	Intermediate
	Mouse	7	257	0.85	High

^a No measurable concentrations were detected past the first time point (ie 2 min) due to rapid NADPH-dependent degradation, hence clearance parameters could not be determined.

^b Estimate only – calculated metabolism parameters based on first 2-time points (ie 2 and 5 min) due to rapid degradation.

^c Apparent non-NADPH mediated degradation in metabolism control samples. A putative amide hydrolysis product with m/z [M+H] of 200 was detected. A putative mono-oxygenated product with m/z [M+H] of 312 was detected.

^d No measurable concentrations were detected past 5 min, therefore degradation parameters were estimated using the initial two time points (ie 2 and 5 min) only, hence values reported are approximate only.

5.8. *Phenylthiazoles in the literature*

Recently, a high-cell phenotypic assay of the GlaxoSmithKline (GSK) diversity set of 1.8 million compounds was screened against *T.b. brucei*, *T. cruzi* and *L. donovani*.¹³⁰ Activity of the hits was confirmed in intracellular anti-parasitocidal assays and the potential for cytotoxicity was assessed. As a result of these assays three anti-kinetoplastid compound boxes containing ~200 compounds each were compiled. Analysis of the hits revealed a number of compounds with structural similarity to the class of compounds described herein. These compounds have been assigned to both the HAT and Chagas boxes. As such, it is possible that drug discovery efforts could begin by other researchers in the near future.

5.9. *Future work*

Given the activity of **5.168** further modifications to the linker to investigate various substituents is required. It has been well documented that fluorine substitution can induce a conformational change and block metabolism.¹³¹ Whilst the methylated linker analogues didn't generally improve metabolic stability, changing the substituent to fluorine as previously mentioned, trifluoromethyl or extending the substituent to an ethyl or isopropyl may alter this. Given the racemic nature of these analogues the racemic material could initially be tested and then the enantiomers could be isolated and tested individually if interesting activity is observed.

Further modifications to the core thiazole could also be envisaged, whereby a bicyclic system could be introduced. As depicted in Figure 5.10 numerous possibilities are available given the activity of both the pyrazole and pyridine cores. These cores could be coupled to either a 5 or 6 membered ring which could affect interactions within the putative target.

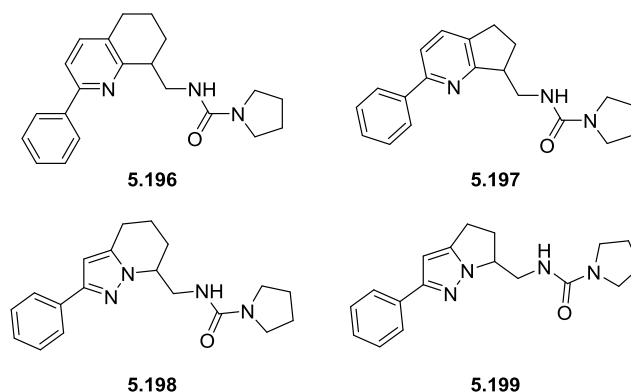
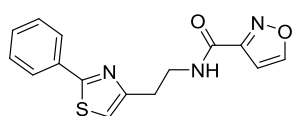


Figure 5.10 Bicyclic analogues which could be targeted in an effort to improve the metabolic stability of this series.

5.10. Experimental

Given the nature of some of the analogues made within this series, variations to the HPLC method were necessary in order to detect the product. These compounds have been denoted with either ‘Hydrophilic HPLC’ or ‘Hydrophobic HPLC’ depending on the variation. For the ‘Hydrophilic HPLC’ method the sample was eluted using a gradient of 5 – 100% of solvent B in solvent D where solvent B: 0.1% formic acid in ACN, and solvent D: 0.1% formic acid in water (5-100% B [7 min], 100% [2 min]; 0.5 ml/min). For the ‘Hydrophobic HPLC’ method the sample was eluted using a gradient of 15 – 100% of solvent B in solvent D (15-80% B [2 min], 80-100% [6 min], 100% [1 min], 100-5% [3 min]; 0.5 ml/min).

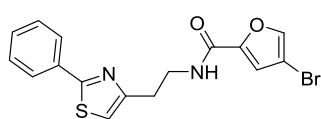
N-(2-(2-Phenylthiazol-4-yl)ethyl)isoxazole-3-carboxamide (**5.22**)



To a solution of the 2-(2-phenylthiazol-4-yl)ethan-1-amine (80 mg, 0.39 mmol) in DMF (1 ml) was added the 1,2-oxazole-3-carboxylic acid (53 mg, 0.47 mmol), EDCI (91 mg, 0.47 mmol) and DMAP (5 mg, 0.04 mmol). The reaction mixture was stirred at 45 °C for 18 h. Water (approximately 2 ml) was added to the reaction mixture and the product extracted with ethyl acetate three times. The organic layers were combined and dried with magnesium sulphate. All of the volatiles were removed *in vacuo* and the crude material was purified by column chromatography, eluting with 10% ethyl

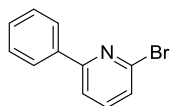
acetate/petroleum spirit to obtain the desired product as a pale-orange oil (17 mg, 15%). LRMS [M+H]⁺ 300.1 m/z; HRMS [M+H]⁺ 300.0801 m/z, found 300.0802 m/z; ¹H NMR (400 MHz, DMSO) δ 9.08 (d, *J* = 1.7 Hz, 1H), 8.94 (t, *J* = 5.6 Hz, 1H), 8.06 – 7.81 (m, 2H), 7.58 – 7.45 (m, 3H), 7.44 (s, 1H), 6.88 (d, *J* = 1.7 Hz, 1H), 3.63 (dd, *J* = 13.1, 7.2 Hz, 2H), 3.03 (t, *J* = 7.2 Hz, 2H).

4-Bromo-N-(2-(2-phenylthiazol-4-yl)ethyl)furan-2-carboxamide (5.25)



To a solution of the 2-(2-phenylthiazol-4-yl)ethan-1-amine (80 mg, 0.39 mmol) in DMF (1 ml) was added the 4-bromo-2-furoic acid (90 mg, 0.47 mmol), EDCI (91 mg, 0.47 mmol) and DMAP (5 mg, 0.04 mmol). The reaction mixture was stirred at 45 °C for 18 h. Water (approximately 2 ml) was added to the reaction mixture and the product extracted with ethyl acetate three times. The organic layers were combined and dried with magnesium sulphate. All of the volatiles were removed *in vacuo* and the crude material was purified by column chromatography, eluting with 10% ethyl acetate/petroleum spirit to obtain the desired product as a colourless solid (13 mg, 9%). LRMS [M+H]⁺ 377.1 m/z (Br⁷⁹), 379.1 m/z (Br⁸¹); HRMS [M+H]⁺ 376.9954 m/z, found 376.9960 m/z (Br⁷⁹), 378.9934 m/z, found 378.9940 m/z (Br⁸¹); ¹H NMR (400 MHz, DMSO) δ 8.62 (t, *J* = 5.7 Hz, 1H), 8.11 (d, *J* = 0.8 Hz, 1H), 7.99 – 7.81 (m, 2H), 7.59 – 7.45 (m, 3H), 7.42 (s, 1H), 7.24 (d, *J* = 0.8 Hz, 1H), 3.58 (dd, *J* = 13.1, 7.1 Hz, 2H), 3.00 (t, *J* = 7.2 Hz, 2H).

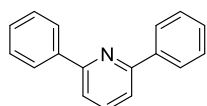
2-Bromo-6-phenylpyridine (5.111)



2,6-Dibromopyridine (2 g, 8.44 mmol), phenylboronic acid (1.03 g, 8.44 mmol), potassium carbonate (4.67 g, 33.77 mmol) and TBAB (271 mg, 0.84 mmol) were combined in a mixture of 1,4-dioxane (16 ml) and water (4 ml). The reaction mixture was degassed by bubbling nitrogen through for 30 min prior to the addition of PdCl₂(dppf) (62 mg, 0.084 mmol). The reaction mixture was stirred at 40 °C for 1 h before being filtered through celite. The filtrate was collected and the solvent removed. The crude material was then purified by column chromatography, eluting with 100% petroleum spirits to give the title compound as a colourless solid (1.85 g, 93%). ¹H NMR (400 MHz, DMSO) δ 8.56

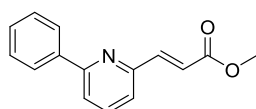
(dd, $J = 6.3, 2.4$ Hz, 1H), 8.36 – 8.18 (m, 2H), 8.16 – 8.00 (m, 2H), 7.61 – 7.53 (m, 2H), 7.53 – 7.45 (m, 1H); ^{13}C NMR (101 MHz, DMSO) δ 155.9, 155.5, 139.0, 138.9, 129.8, 129.3 (2C), 127.1 (2C), 121.0, 119.8.

2,6-Diphenylpyridine (**5.117**)



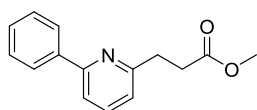
The title compound was isolated as a side product of the previous reaction as a colourless solid. ^1H NMR (400 MHz, DMSO) δ 8.36 – 8.13 (m, 4H), 8.13 – 7.85 (m, 3H), 7.67 – 7.50 (m, 4H), 7.50 – 7.43 (m, 2H).

Methyl (E)-3-(6-phenylpyridin-2-yl)acrylate (**5.112**)



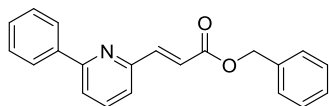
2-Bromo-6-phenylpyridine (300 mg, 1.28 mmol), methyl acrylate (138 μl , 1.54 mmol), triethylamine (680 μl , 5.12 mmol), tri(*o*-tolyl)phosphine (40 mg, 0.13 mmol) and $\text{Pd}(\text{OAc})_2$ (29 mg, 0.13 mmol) were combined in acetonitrile (2.5 ml). Nitrogen was bubbled through the reaction mixture before being placed in a CEM microwave at 90 $^\circ\text{C}$ for 1 h. The reaction was monitored by TLC and once complete it was diluted with ethanol and filtered through celite. The filtrate was collected and all of the volatiles were removed. The crude material was purified by column chromatography, eluting with 0-5% ethyl acetate/petroleum spirit to give the title compound as an off-white solid (223 mg, 73%). HPLC – rt 8.04 min > 99% purity at 254 nm; LRMS $[\text{M}+\text{H}]^+$ 240.2 m/z; HRMS $[\text{M}+\text{H}]^+$ 240.1019 m/z, found 240.1023 m/z; ^1H NMR (400 MHz, DMSO) δ 8.20 – 8.11 (m, 2H), 7.99 (dt, $J = 15.3, 7.4$ Hz, 2H), 7.75 (d, $J = 15.7$ Hz, 1H), 7.71 (dd, $J = 7.4, 0.9$ Hz, 1H), 7.56 – 7.43 (m, 3H), 7.06 (d, $J = 15.7$ Hz, 1H), 3.77 (s, 3H); ^{13}C NMR (101 MHz, DMSO) δ 166.4, 156.1, 151.8, 143.8, 138.4, 138.1, 129.5, 128.9 (2C), 126.7 (2C), 123.6, 121.4, 121.3, 51.7.

Methyl 3-(6-phenylpyridin-2-yl)propanoate (5.113)



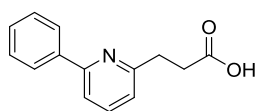
Methyl (*E*)-3-(6-phenylpyridin-2-yl)acrylate (223 mg, 0.93 mmol) was dissolved in a 50% solution of ethyl acetate in ethanol (50 ml). This was loaded on to a ThalesNano H-Cube[®] with a 10% Pd/C CatCart[®]. The reaction was monitored by LCMS until no more starting material was present and the solvent was removed under reduced pressure to give the title compound as a yellow oil (163 mg, 72%). HPLC – rt 4.92 min > 99% purity at 254 nm; LRMS [M+H]⁺ 242.2 m/z; HRMS [M+H]⁺ 242.1176 m/z, found 242.1176 m/z; ¹H NMR (400 MHz, DMSO) δ 8.17 – 7.96 (m, 2H), 7.78 (dd, *J* = 6.4, 2.5 Hz, 2H), 7.57 – 7.36 (m, 3H), 7.32 – 7.15 (m, 1H), 3.60 (s, 3H), 3.10 (t, *J* = 7.1 Hz, 2H), 2.82 (t, *J* = 7.1 Hz, 2H); ¹³C NMR (101 MHz, DMSO) δ 173.1, 159.3, 155.1, 138.7, 137.5, 129.0, 128.7 (2C), 126.5 (2C), 121.6, 117.7, 51.3, 32.0, 32.0.

Benzyl (E)-3-(6-phenylpyridin-2-yl)acrylate (5.120)



2-Bromo-6-phenylpyridine (1.69 g, 7.22 mmol), benzyl acrylate (1.35 ml, 8.66 mmol), tri(*o*-tolyl)phosphine (220 mg, 0.72 mmol) and triethylamine (3.85 ml, 28.88 mmol) were all combined in acetonitrile (5 ml). The reaction mixture was degassed by bubbling nitrogen through it for 2 min prior to the addition of palladium acetate (162 mg, 0.72 mmol). The reaction mixture was transferred to a CEM microwave for 3 h at 90 °C. The reaction was complete by TLC and the reaction mixture was filtered through celite and the filtrate collected. All of the volatiles were removed *in vacuo* and the crude material was purified by column chromatography, eluting with 0-10% ethyl acetate/petroleum spirits to yield the title compound as a yellow oil (1.13 g, 50%). Hydrophobic HPLC – rt 3.77 min > 92% purity at 254 nm; LRMS [M+H]⁺ 316.2 m/z; HRMS [M+H]⁺ 316.1332 m/z, found 316.1336 m/z; ¹H NMR (400 MHz, CDCl₃) δ 8.09 – 8.01 (m, 2H), 7.81 – 7.68 (m, 3H), 7.52 – 7.27 (m, 9H), 7.15 (d, *J* = 15.6 Hz, 1H), 5.27 (s, 2H); ¹³C NMR (101 MHz, CDCl₃) δ 166.9, 157.5, 152.5, 144.2, 138.9, 137.7, 136.1, 129.5, 128.9, 128.8, 128.4, 127.1, 123.0, 122.2, 121.2, 66.6. *Note: there are multiple equivalent carbons in the NMR which are overlapping.

3-(6-Phenylpyridin-2-yl)propanoic acid (5.114)



Methyl 3-(6-phenylpyridin-2-yl)propanoate (160 mg, 0.66 mmol) was dissolved in THF (0.5 ml) and lithium hydroxide (32 mg, 1.32 mmol) was dissolved in water (1.3 ml). The methyl 3-(6-phenylpyridin-2-yl)propanoate solution was added dropwise to the lithium hydroxide solution and the reaction mixture was left to stir for 1 h. The progress of the reaction was monitored by LCMS and, once complete, the reaction was quenched by the gradual addition of an aqueous 1 M hydrochloric acid solution to pH ~ 7. The product was then extracted three times with ethyl acetate and the organic layers were combined and washed with a saturated aqueous solution of sodium chloride and dried with magnesium sulphate. Removal of solvent *in vacuo* yielded the title compound as a pale-yellow oil (83 mg, 55%).

The title compound can also be prepared from benzyl (*E*)-3-(6-phenylpyridin-2-yl)acrylate (1.1 g, 3.49 mmol), which was dissolved in a 50% solution of ethyl acetate in ethanol (40 ml). This was loaded on to a ThalesNano H-Cube[®] with a 10% Pd/C CatCart[®]. The reaction was monitored by LCMS until no more starting material was present and the solvent was removed under reduced pressure to give the title compound as a colourless solid (505 mg, 64%).

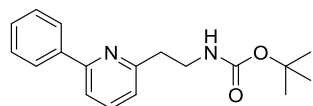
Alternatively, the title compound can be prepared from benzyl (*E*)-3-(6-phenylpyridin-2-yl)acrylate (495 mg, 1.57 mmol), which is dissolved in ethanol (12 ml) and 5% Pd/C (8 mg, 0.8 mmol) was added. The reaction was then placed under an atmosphere of hydrogen. The reaction mixture was stirred at 60 °C for 18 h, at which point both TLC and LCMS confirmed that the reaction was complete. The reaction mixture was then filtered through celite and the solvent removed *in vacuo*. The crude material was then purified by column chromatography, eluting with 40-50% ethyl acetate/petroleum spirits to give the title compound as a colourless solid (248 mg, 70%).

Hydrophobic HPLC – rt 2.02 min > 90% purity at 254 nm; LRMS [M+H]⁺ 228.2 m/z; HRMS [M+H]⁺ 228.1019 m/z, found 228.1020 m/z; ¹H NMR (400 MHz, CDCl₃) δ 7.87 – 7.76 (m, 3H), 7.67 – 7.60 (m, 1H),

7.52 – 7.41 (m, 3H), 7.21 (d, $J = 7.5$ Hz, 1H), 3.32 – 3.14 (m, 2H), 2.97 – 2.82 (m, 2H); ^{13}C NMR (101 MHz, CDCl_3) δ 174.7, 159.6, 157.1, 139.5, 137.4, 130.0, 129.3 (2C), 127.5 (2C), 122.3, 120.4, 34.6, 31.4.

*Note: the –OH peak is missing from the ^1H NMR.

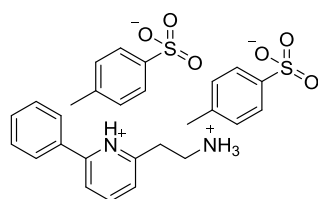
Tert-butyl (2-(6-phenylpyridin-2-yl)ethyl)carbamate (**5.115**)



3-(6-Phenylpyridin-2-yl)propanoic acid (100 mg, 0.44 mmol), diphenylphosphoryl azide (115 μl , 0.53 mmol) and triethylamine (70 μl , 0.53

mmol) were combined in anhydrous *tert*-butanol (1 ml) and the reaction mixture was heated to reflux for 5 h. A saturated aqueous solution of sodium bicarbonate was added and the reaction mixture turned cloudy. The product was extracted with ethyl acetate three times and the organic layers were combined and washed once with a saturated aqueous solution of sodium chloride. The organic phase was then dried with magnesium sulphate before all of the volatiles removed and the crude material purified by column chromatography, eluting with 5-15% ethyl acetate/petroleum spirits. The title compound was obtained as a colourless oil (34 mg, 26%). HPLC – rt 5.81 min > 99% purity at 254 nm; LRMS $[\text{M}+\text{H}]^+$ 299.2 m/z; HRMS $[\text{M}+\text{H}]^+$ 299.1754 m/z, found 299.1756 m/z; ^1H NMR (400 MHz, CDCl_3) δ 7.99 (dd, $J = 5.2, 3.3$ Hz, 2H), 7.66 (t, $J = 7.7$ Hz, 1H), 7.57 (d, $J = 7.5$ Hz, 1H), 7.49 – 7.42 (m, 2H), 7.42 – 7.36 (m, 1H), 7.08 (d, $J = 7.5$ Hz, 1H), 5.50 (s, 1H), 3.60 (dd, $J = 12.2, 6.0$ Hz, 2H), 3.02 (t, $J = 6.3$ Hz, 2H), 1.42 (s, 9H); ^{13}C NMR (101 MHz, CDCl_3) δ 159.6, 156.9, 156.2, 139.5, 137.4, 129.1, 128.9 (2C), 127.0 (2C), 122.0, 118.3, 39.9, 37.6, 28.6 (3C).

2-(2-Ammonioethyl)-6-phenylpyridin-1-ium 4-methylbenzenesulfonate (**5.121**)

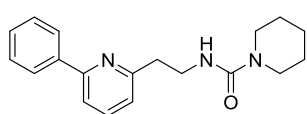


Tert-butyl (2-(6-phenylpyridin-2-yl)ethyl)carbamate (34 mg, 0.11 mmol) was dissolved in acetonitrile (220 μl) and *para*-toluenesulfonic acid (65 mg, 0.34 mmol) was added. The reaction mixture was heated to reflux and the progress

of the reaction was monitored by LRMS. After ~ 2 h the reaction was complete and the reaction mixture was

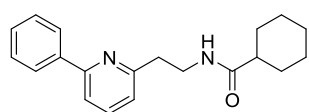
transferred to the fridge. The resultant precipitate was filtered and washed with ether to give the title compound as a colourless solid (41 mg, 73%). LRMS $[M+H]^+$ 199.1 m/z; 1H NMR (400 MHz, DMSO) δ 8.08 (dd, $J = 8.2, 1.2$ Hz, 2H), 7.94 – 7.85 (m, 2H), 7.85 – 7.73 (m, 2H), 7.61 – 7.39 (m, 6H), 7.32 (dd, $J = 6.3, 1.9$ Hz, 1H), 7.11 (d, $J = 7.8$ Hz, 4H), 3.32 (dd, $J = 12.9, 6.8$ Hz, 2H), 3.12 (t, $J = 7.3$ Hz, 2H), 2.29 (s, 6H).

N-(2-(6-Phenylpyridin-2-yl)ethyl)piperidine-1-carboxamide (**5.122**)



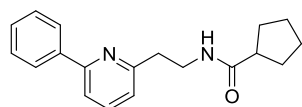
2-(2-Ammonioethyl)-6-phenylpyridin-1-ium 4-methylbenzenesulfonate (41 mg, 0.08 mmol) was dissolved in anhydrous dichloromethane (1 ml) and triethylamine (40 μ l, 0.26 mmol) was added (solution 1). In a separate flask *para*-nitrophenyl chloroformate (24 mg, 0.12 mmol) was dissolved in dichloromethane (1 ml) with stirring (solution 2). Solution 1 was then added dropwise to solution 2 and the reaction mixture was stirred for 2 h at ambient temperature. After 2 h piperidine (20 μ l, 0.16 mmol) was added to the reaction mixture which was allowed to stir at ambient temperature for 18 h. All volatiles were removed *in vacuo* and the crude material was purified by column chromatography, eluting with 30% ethyl acetate/dichloromethane. This yielded the title compound with contaminants, as such the material was further purified by column chromatography, eluting with 25% ethyl acetate/petroleum spirits. This gave the title compound as a colourless oil (10 mg, 40%). LRMS $[M+H]^+$ 310.2 m/z; HRMS $[M+H]^+$ 310.1914 m/z, found 310.1916 m/z; 1H NMR (400 MHz, $CDCl_3$) δ 8.07 – 7.85 (m, 2H), 7.67 (t, $J = 7.7$ Hz, 1H), 7.61 – 7.51 (m, 1H), 7.51 – 7.32 (m, 3H), 7.10 (d, $J = 7.0$ Hz, 1H), 6.11 (s, 1H), 3.64 (dt, $J = 6.0, 5.0$ Hz, 2H), 3.27 – 3.12 (m, 4H), 3.12 – 2.95 (m, 2H), 1.53 – 1.43 (m, 2H), 1.43 – 1.29 (m, 4H); ^{13}C NMR (101 MHz, $CDCl_3$) δ 160.7, 158.1, 156.9, 139.7, 137.6, 129.1, 128.8 (2C), 127.1 (2C), 122.0, 118.5, 44.9 (2C), 40.5, 37.2, 25.6 (2C), 24.6.

N-(2-(6-Phenylpyridin-2-yl)ethyl)cyclohexanecarboxamide (**5.123**)



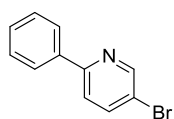
2-(2-Ammonioethyl)-6-phenylpyridin-1-ium 4-methylbenzenesulfonate (21 mg, 0.11 mmol) was dissolved in anhydrous *N,N*-dimethylformamide (0.5 ml) and cyclohexanecarboxylic acid (15 μ l, 0.13 mmol), triethylamine (150 μ l, 1.06 mmol), EDCI (20 mg, 0.13 mmol) and DMAP (2 mg, 0.01 mmol) were added. The resulting mixture was then heated to 40 °C for 18 h. The reaction mixture was concentrated *in vacuo* and the crude material purified by column chromatography, eluting with 0-15% ethyl acetate/dichloromethane. The title compound was obtained as an off-white solid (22 mg, 67%). LRMS $[M+H]^+$ 309.2 m/z; HRMS $[M+H]^+$ 309.1961 m/z, found 309.1961 m/z; ^1H NMR (400 MHz, CDCl_3) δ 7.99 – 7.93 (m, 2H), 7.68 (t, $J = 7.7$ Hz, 1H), 7.58 (dd, $J = 7.9, 0.8$ Hz, 1H), 7.50 – 7.36 (m, 3H), 7.10 (d, $J = 7.6$ Hz, 1H), 6.95 (s, 1H), 3.75 – 3.64 (m, 2H), 3.07 – 2.98 (m, 2H), 2.02 (tt, $J = 11.8, 3.5$ Hz, 1H), 1.92 – 1.86 (m, 1H), 1.84 – 1.53 (m, 7H), 1.50 – 1.34 (m, 2H); ^{13}C NMR (101 MHz, CDCl_3) δ 180.9, 176.3, 159.9, 156.9, 137.8, 129.2, 128.9 (2C), 127.1 (2C), 122.1, 118.7, 45.8, 43.0, 38.7, 36.7, 29.8, 29.0, 25.9, 25.5.

N-(2-(6-Phenylpyridin-2-yl)ethyl)cyclopentanecarboxamide (**5.124**)



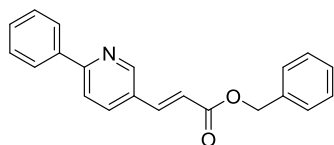
2-(2-Ammonioethyl)-6-phenylpyridin-1-ium 4-methylbenzenesulfonate (21 mg, 0.11 mmol) was dissolved in anhydrous *N,N*-dimethylformamide (0.5 ml) and cyclopentanecarboxylic acid (14 μ l, 0.13 mmol), triethylamine (150 μ l, 1.06 mmol), EDCI (20 mg, 0.13 mmol) and DMAP (2 mg, 0.01 mmol) were added. The resulting mixture was then heated to 40 °C for 18 h. The reaction mixture was concentrated *in vacuo* and the crude material purified by column chromatography, eluting with 0-15% ethyl acetate/dichloromethane. The title compound was obtained as a colourless solid (29 mg, 94%). LRMS $[M+H]^+$ 295.2 m/z; HRMS $[M+H]^+$ 295.1805 m/z, found 295.1807 m/z; ^1H NMR (400 MHz, CDCl_3) δ 8.05 – 7.91 (m, 2H), 7.69 (t, $J = 7.7$ Hz, 1H), 7.63 – 7.55 (m, 1H), 7.51 – 7.37 (m, 3H), 7.11 (d, $J = 7.5$ Hz, 1H), 6.78 (s, 1H), 3.81 – 3.64 (m, 2H), 3.14 – 3.01 (m, 2H), 2.55 – 2.37 (m, 1H), 1.87 – 1.53 (m, 8H); ^{13}C NMR (101 MHz, CDCl_3) δ 176.2, 159.9, 156.8, 139.5, 137.6, 129.2, 128.9 (2C), 127.0 (2C), 122.0, 118.4, 46.2, 38.7, 36.9, 30.5 (2C), 25.9 (2C).

5-Bromo-2-phenylpyridine¹¹⁹ (5.127)



2,5-Dibromopyridine (2 g, 8.44 mmol), phenyl boronic acid (1.03 g, 8.44 mmol) and sodium carbonate (1.79 g, 16.88 mmol) were added to a mixture of tetrahydrofuran (12 ml) and water (12 ml). The reaction mixture was degassed by bubbling nitrogen through it for 10 min prior to the addition of Pd(PPh₃)₄ (178 mg, 0.17 mmol). The reaction mixture was heated to 75 °C for 18 h. The reaction mixture was then filtered through celite and the filtrate was collected and all volatiles were removed. The residue was dissolved in a mixture of water and dichloromethane. The dichloromethane layer was isolated and the aqueous phase was then re-extracted with dichloromethane. The organic layers were combined and dried with magnesium sulphate. All of the volatiles were removed and the crude material was purified by column chromatography, eluting with 10-20% ethyl acetate/petroleum spirits. The title compound was obtained as a colourless solid (446 mg, 48%). LRMS [M+H]⁺ 234.1 m/z (Br⁷⁹), 236.1 m/z (Br⁸¹); ¹H NMR (400 MHz, CDCl₃) δ 8.72 (dd, *J* = 2.4, 0.7 Hz, 1H), 8.02 – 7.89 (m, 2H), 7.85 (dd, *J* = 8.5, 2.4 Hz, 1H), 7.61 (dd, *J* = 8.5, 0.7 Hz, 1H), 7.54 – 7.32 (m, 3H); ¹³C NMR (101 MHz, CDCl₃) δ 156.1, 150.8, 139.5, 138.3, 129.5, 129.0 (2C), 126.9 (2C), 121.8, 119.5.

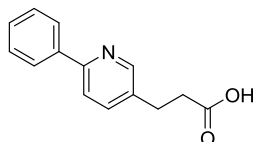
Benzyl (E)-3-(6-phenylpyridin-3-yl)acrylate (5.128)



5-Bromo-2-phenylpyridine (1 g, 4.27 mmol), benzyl acrylate (785 μl, 5.13 mmol), tri(*o*-tolyl)phosphine (131 mg, 0.43 mmol) and triethylamine (2.25 ml, 17.09 mmol) were combined in acetonitrile (8 ml). The reaction mixture was thoroughly degassed by bubbling nitrogen through for 5 min prior to the addition of palladium acetate (97 mg, 0.43 mmol). The reaction mixture was transferred to a CEM microwave for 3 h at 90 °C. The reaction mixture was filtered through celite and the filtrate was collected and all of the volatiles were removed. The crude material was purified by column chromatography, eluting with 5-10% ethyl acetate/petroleum spirits to yield the title compound as a colourless solid (756 mg, 56%). HPLC – rt 7.92 min > 92% purity at 254 nm; LRMS [M+H]⁺ 316.2 m/z; HRMS [M+H]⁺ 316.1332 m/z, found 316.1336 m/z; ¹H NMR (400 MHz, CDCl₃) δ 8.78 (d, *J* = 2.1 Hz, 1H), 8.12 – 7.95 (m, 2H), 7.88 (dd, *J* = 8.3, 2.3 Hz, 1H), 7.82 – 7.66 (m, 2H),

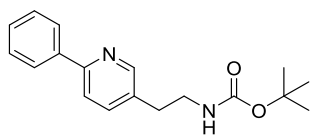
7.54 – 7.28 (m, 8H), 6.56 (d, $J = 16.1$ Hz, 1H), 5.26 (s, 2H); ^{13}C NMR (101 MHz, CDCl_3) δ 166.4, 158.8, 150.0, 141.5, 138.6, 136.0, 135.1, 129.8, 129.0, 128.8, 128.6, 128.5, 127.1, 120.5, 119.5, 66.8. *Note: there are multiple carbons overlapping in the NMR.

3-(6-Phenylpyridin-3-yl)propanoic acid (**5.129**)



Benzyl (*E*)-3-(6-phenylpyridin-3-yl)acrylate (1 g, 3.17 mmol) was dissolved in ethanol (25 ml) and 5% Pd/C (17 mg, 0.16 mmol) was added prior to the reaction being flushed with hydrogen gas. The reaction mixture was stirred at 50 °C and monitored by TLC and LCMS. Once completed, the reaction mixture was filtered through celite and the solvent removed *in vacuo*. The crude material was purified by column chromatography, eluting with 25-40% ethyl acetate/petroleum spirits + 1% acetic acid. The appropriate fractions were collected and washed three times with an aqueous saturated sodium bicarbonate solution. All of the volatiles were removed *in vacuo* to give the title compound as a cloudy oil (462 mg, 64%). Hydrophilic HPLC – rt 8.05 min > 99% purity at 254 nm; LRMS $[\text{M}+\text{H}]^+$ 228.2 m/z; HRMS $[\text{M}+\text{H}]^+$ 228.1019 m/z, found 228.1019 m/z; ^1H NMR (400 MHz, CDCl_3) δ 8.60 (s, 1H), 8.00 – 7.81 (m, 2H), 7.65 (dd, $J = 3.9, 1.9$ Hz, 2H), 7.53 – 7.31 (m, 3H), 3.00 (t, $J = 7.4$ Hz, 2H), 2.71 (dd, $J = 8.6, 6.2$ Hz, 2H); ^{13}C NMR (101 MHz, CDCl_3) δ 177.0, 155.6, 149.0, 138.5, 137.9, 134.8, 129.3, 129.0 (2C), 127.2 (2C), 121.2, 35.2, 27.7. *Note: carboxylic acid proton not visible by ^1H NMR.

Tert-butyl (2-(6-phenylpyridin-3-yl)ethyl)carbamate (**5.130**)



3-(6-Phenylpyridin-3-yl)propanoic acid (462 mg, 2.03 mmol), diphenylphosphoryl azide (525 μl , 2.44 mmol) and triethylamine (325 μl , 2.44 mmol) were combined in anhydrous *tert*-butanol (5 ml) and the reaction mixture was heated to reflux for 18 h. A saturated aqueous solution of sodium bicarbonate was added and the product was extracted with ethyl acetate twice. The organic layers were combined and washed once with a saturated aqueous solution of sodium chloride. The organic phase was then dried with magnesium sulphate before all

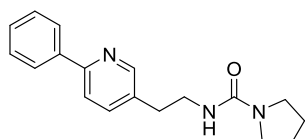
of the volatiles were removed and the crude material purified by column chromatography, eluting with 5-10% ethyl acetate/petroleum spirits. The title compound was obtained as a colourless solid (205 mg, 34%). Hydrophobic HPLC – rt 2.17 min > 88% purity at 254 nm; LRMS $[M+H]^+$ 299.2 m/z; HRMS $[M+H]^+$ 299.1754 m/z, found 299.1715 m/z; 1H NMR (400 MHz, $CDCl_3$) δ 8.50 (d, J = 1.8 Hz, 1H), 8.06 – 7.86 (m, 2H), 7.66 (dd, J = 8.1, 0.5 Hz, 1H), 7.57 (dd, J = 8.0, 1.6 Hz, 1H), 7.49 – 7.41 (m, 2H), 7.41 – 7.34 (m, 1H), 4.63 (s, 1H), 3.51 – 3.22 (m, 2H), 2.82 (t, J = 6.9 Hz, 2H), 1.41 (s, 9H); ^{13}C NMR (101 MHz, $CDCl_3$) δ 156.0, 155.9, 150.1, 139.2, 137.3, 133.0, 129.0, 128.9 (2C), 126.9 (2C), 120.5, 41.6, 33.3, 28.5 (3C).

2-(6-Phenylpyridin-3-yl)ethan-1-amine (5.131)



Tert-butyl (2-(6-phenylpyridin-3-yl)ethyl)carbamate (205 mg, 0.69 mmol) was added to a 50:50 mixture of trifluoroacetic acid:dichloromethane (4 ml). The reaction mixture was stirred at ambient temperature for 18 h and TLC showed complete disappearance of starting material. All of the volatiles were removed and the residue was washed with toluene three times. This gave the title compound as a dark yellow oil which was used directly. LRMS $[M+H]^+$ 199.2 m/z; 1H NMR (400 MHz, $CDCl_3$) δ 8.83 (s, 1H), 8.34 (dd, J = 8.4, 1.8 Hz, 1H), 8.01 (d, J = 8.4 Hz, 2H), 7.91 – 7.73 (m, 2H), 7.71 – 7.45 (m, 2H), 3.42 (d, J = 1.3 Hz, 2H), 3.28 – 3.19 (m, 2H), 3.13 (d, J = 25.1 Hz, 2H).

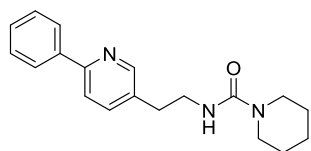
N-(2-(6-Phenylpyridin-3-yl)ethyl)pyrrolidine-1-carboxamide (5.108)



2-(6-Phenylpyridin-3-yl)ethan-1-amine (35 mg, 0.17 mmol) was dissolved in anhydrous dichloromethane (0.5 ml) and triethylamine (125 μ l, 1.70 mmol) added (solution 1). In a separate flask *para*-nitrophenyl chloroformate (69 mg, 0.34 mmol) was dissolved in dichloromethane (1 ml) with stirring (solution 2). Solution 1 was then added dropwise to solution 2 and the reaction mixture was stirred for 2 h at ambient temperature. After 2 h pyrrolidine (30 μ l, 0.34 mmol) was added to the reaction mixture which was allowed to stir at ambient temperature for 18 h. All of the volatiles were removed *in vacuo* and the crude material was purified by

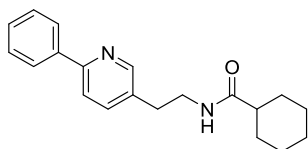
column chromatography, eluting with 0-60% ethyl acetate/dichloromethane. The title compound was obtained as a colourless solid (13 mg, 26%). HPLC – rt 5.02 min > 96% purity at 254 nm; LRMS [M+H]⁺ 296.2 m/z; HRMS [M+H]⁺ 296.1757 m/z, found 296.1761 m/z; ¹H NMR (400 MHz, CDCl₃) δ 8.51 (d, *J* = 1.7 Hz, 1H), 8.04 – 7.83 (m, 2H), 7.73 – 7.53 (m, 2H), 7.51 – 7.30 (m, 3H), 4.27 (s, 1H), 3.50 (dd, *J* = 12.9, 6.8 Hz, 2H), 3.26 (t, *J* = 6.3 Hz, 4H), 2.86 (t, *J* = 6.9 Hz, 2H), 1.93 – 1.75 (m, 4H); ¹³C NMR (101 MHz, CDCl₃) δ 156.8, 155.7, 150.0, 139.2, 137.5, 133.6, 129.0, 128.9 (2C), 126.9 (2C), 120.6, 45.6, 41.7, 33.7, 25.7. *Note: there are multiple equivalent carbons which are overlapping in the ¹³C NMR.

N-(2-(6-Phenylpyridin-3-yl)ethyl)piperidine-1-carboxamide (**5.132**)



2-(6-Phenylpyridin-3-yl)ethan-1-amine (35 mg, 0.17 mmol) was dissolved in anhydrous dichloromethane (0.5 ml) and triethylamine (125 μl, 1.70 mmol) was added (solution 1). In a separate flask *para*-nitrophenyl chloroformate (69 mg, 0.34 mmol) was dissolved in dichloromethane (1 ml) with stirring (solution 2). Solution 1 was then added dropwise to solution 2 and the reaction mixture was stirred for 2 h at ambient temperature. After 2 h piperidine (35 μl, 0.34 mmol) was added to the reaction mixture which was allowed to stir at ambient temperature for 18 h. All of the volatiles were removed *in vacuo* and the crude material was purified by column chromatography, eluting with 0-60% ethyl acetate/dichloromethane. The title compound was obtained as a colourless solid (13 mg, 26%). HPLC – rt 5.01 min > 97% purity at 254 nm; LRMS [M+H]⁺ 310.2 m/z; HRMS [M+H]⁺ 310.1914 m/z, found 310.1913 m/z; ¹H NMR (400 MHz, CDCl₃) δ 8.51 (d, *J* = 1.7 Hz, 1H), 8.03 – 7.88 (m, 2H), 7.67 (dd, *J* = 8.1, 0.6 Hz, 1H), 7.60 (dd, *J* = 8.1, 2.3 Hz, 1H), 7.49 – 7.42 (m, 2H), 7.41 – 7.35 (m, 1H), 4.51 (s, 1H), 3.49 (dd, *J* = 12.8, 6.9 Hz, 2H), 3.33 – 3.22 (m, 4H), 2.86 (t, *J* = 6.9 Hz, 2H), 1.68 – 1.42 (m, 6H); ¹³C NMR (101 MHz, CDCl₃) δ 157.6, 155.7, 150.0, 139.1, 137.6, 133.7, 129.0, 128.9 (2C), 126.9 (2C), 120.6, 45.0, 42.0, 33.5, 25.7, 24.5. *Note: there are multiple equivalent carbons which are overlapping in the ¹³C NMR.

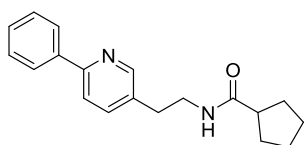
N-(2-(6-Phenylpyridin-3-yl)ethyl)cyclohexanecarboxamide (**5.133**)



2-(6-Phenylpyridin-3-yl)ethan-1-amine (35 mg, 0.17 mmol) and triethylamine (125 μ l, 1.70 mmol) were combined in DMF (500 μ l) and pre-stirred for 2 min.

The cyclohexanecarboxylic acid (25 μ l, 0.20 mmol), EDCI (32 mg, 0.20 mmol), and DMAP (2 mg, 0.02 mmol) were then added. The reaction mixture was heated to 40 °C and monitored by TLC and LCMS analysis. After 18 h the reaction was complete and all of the volatiles were removed. The crude material was purified by column chromatography, eluting with 0-15% ethyl acetate/dichloromethane to give the title compound as a colourless solid (11 mg, 21%). HPLC – rt 5.40 min > 99% purity at 254 nm; LRMS $[M+H]^+$ 309.2 m/z; HRMS $[M+H]^+$ 309.1961 m/z, found 309.1961 m/z; ^1H NMR (400 MHz, CDCl_3) δ 8.50 (d, $J = 1.7$ Hz, 1H), 8.03 – 7.87 (m, 2H), 7.69 (d, $J = 8.0$ Hz, 1H), 7.60 (dd, $J = 8.1, 2.2$ Hz, 1H), 7.53 – 7.35 (m, 3H), 5.52 (s, 1H), 3.52 (q, $J = 6.8$ Hz, 2H), 2.85 (t, $J = 6.8$ Hz, 2H), 2.09 – 1.94 (m, 1H), 1.94 – 1.68 (m, 5H), 1.48 – 1.28 (m, 2H), 1.28 – 1.06 (m, 3H); ^{13}C NMR (101 MHz, CDCl_3) δ 176.4, 155.9, 149.9, 139.0, 137.6, 133.2, 129.1, 129.0 (2C), 127.0 (2C), 120.7, 45.7, 40.3, 32.8, 25.8. *Note: there are multiple equivalent carbons which are overlapping in the ^{13}C NMR.

N-(2-(6-Phenylpyridin-3-yl)ethyl)cyclopentanecarboxamide (**5.134**)

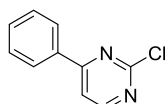


2-(6-Phenylpyridin-3-yl)ethan-1-amine (35 mg, 0.17 mmol) and triethylamine (125 μ l, 1.70 mmol) were combined in DMF (500 μ l) and pre-stirred for 2 min.

The cyclopentanecarboxylic acid (25 μ l, 0.20 mmol), EDCI (32 mg, 0.20 mmol), and DMAP (2 mg, 0.02 mmol) were then added. The reaction mixture was heated to 40 °C and monitored by TLC and LCMS analysis. After 18 h the reaction was complete and all of the volatiles were removed. The crude material was purified by column chromatography, eluting with 0-15% ethyl acetate/dichloromethane to give the title compound as a colourless solid (29 mg, 58%). HPLC – rt 5.08 min > 99% purity at 254 nm; LRMS $[M+H]^+$ 295.2 m/z; HRMS $[M+H]^+$ 295.1805 m/z, found 295.1803 m/z; ^1H NMR (400 MHz, CDCl_3) δ 8.51 (d, $J = 1.7$ Hz, 1H), 8.03 – 7.87 (m, 2H), 7.69 (dd, $J = 8.1, 0.6$ Hz, 1H), 7.62 (dd, $J = 8.1, 2.2$ Hz, 1H), 7.51 – 7.43 (m, 2H), 7.41 (dt, $J = 9.6, 4.3$ Hz, 1H), 5.53 (s, 1H), 3.53 (q, $J = 6.8$ Hz, 2H), 2.86 (t, $J = 6.9$ Hz,

2H), 2.55 – 2.31 (m, 1H), 1.99 – 1.61 (m, 6H), 1.53 (tdd, $J = 6.9, 4.2, 1.7$ Hz, 2H); ^{13}C NMR (101 MHz, CDCl_3) δ 176.5, 155.9, 149.9, 139.1, 137.5, 133.1, 129.1, 128.9 (2C), 126.9 (2C), 120.6, 46.0, 40.4, 32.8, 30.6, 26.0.

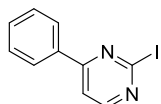
2-Chloro-4-phenylpyrimidine (**5.136**)



Synthesis was based upon a procedure by Brown *et al.*¹²⁰

2,4-Dichloropyrimidine (5.0 g, 33.57 mmol) was dissolved in acetonitrile (60 ml) prior to the addition of water (15 ml). To this was added phenylboronic acid (4.09 g, 33.57 mmol) and sodium carbonate (14.23 g, 134.28 mmol). The reaction mixture was degassed for 10 min by bubbling nitrogen through it before addition of $\text{Pd}(\text{PPh}_3)_4$ (354 mg, 0.34 mmol). The reaction mixture was stirred under nitrogen at 90 °C for 18 h. The reaction mixture was then filtered through celite and the filtrate collected. The solvent was removed *in vacuo* and the crude material was purified by column chromatography, eluting with 10-15% ethyl acetate/petroleum spirits to give the title compound as a colourless solid (2.98 g, 47%). LRMS $[\text{M}+\text{H}]^+$ 191.1 m/z; ^1H NMR (400 MHz, CDCl_3) δ 8.62 (d, $J = 5.3$ Hz, 1H), 8.16 – 7.99 (m, 2H), 7.63 (d, $J = 5.3$ Hz, 1H), 7.50 (qdd, $J = 6.0, 3.2, 1.4$ Hz, 3H); ^{13}C NMR (101 MHz, CDCl_3) δ 167.3, 160.0, 135.2, 132.1, 129.3 (2C), 127.6 (2C), 115.3. *Note: there are multiple equivalent carbons which are overlapping in the ^{13}C NMR.

2-Iodo-4-phenylpyrimidine (**5.138**)

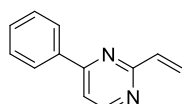


Synthesis adapted from Giblin *et al.*¹³²

Hydroiodic acid (5 ml) was cooled to 0 °C prior to the addition of 2-chloro-4-phenylpyrimidine (500 mg, 2.62 mmol). The reaction mixture was maintained at 0 °C and the reaction was monitored by LRMS. After ~ 6 h there was no further decrease in the amount of starting material though a by-product was observed. The reaction mixture was added dropwise to an aqueous 10% solution of sodium carbonate and was then decolourised by addition of potassium thiosulphate. The product was extracted with ethyl acetate (three times) and the organic layers combined, dried with magnesium sulphate and all volatiles removed *in vacuo*. The crude material was then purified by column chromatography, eluting 10% ethyl

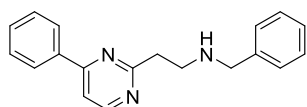
acetate/petroleum spirits to give the title compound as a pale-orange solid (478 mg, 65%). LRMS $[M+H]^+$ 283.1 m/z; 1H NMR (400 MHz, $CDCl_3$) δ 8.43 (d, $J = 5.3$ Hz, 1H), 8.11 – 7.97 (m, 2H), 7.66 (d, $J = 5.3$ Hz, 1H), 7.57 – 7.42 (m, 3H).

4-Phenyl-2-vinylpyrimidine (5.139)



2-Chloro-4-phenylpyrimidine (400 mg, 2.10 mmol), tributyl(vinyl)tin (1.3 ml, 4.62 mmol), palladium acetate (71 mg, 0.32 mmol) and triphenylphosphine (165 mg, 0.63 mmol) were combined in tetrahydrofuran (4 ml) and the reaction mixture was heated to reflux for 18 h. The reaction mixture was filtered through celite and the filtrate was collected. All of the volatiles were removed *in vacuo* and the crude material was purified by column chromatography, eluting with 50-75% ethyl acetate/petroleum spirits. The title compound was obtained as an orange oil (316 mg, 83%). HPLC – rt 7.28 min > 97% purity at 254 nm; LRMS $[M+H]^+$ 183.2 m/z; HRMS $[M+H]^+$ 183.0917 m/z, found 183.0919 m/z; 1H NMR (400 MHz, $CDCl_3$) δ 8.71 (d, $J = 5.3$ Hz, 1H), 8.18 – 8.02 (m, 2H), 7.60 – 7.42 (m, 4H), 6.95 (dd, $J = 17.3, 10.5$ Hz, 1H), 6.72 (dd, $J = 17.3, 1.8$ Hz, 1H), 5.75 (dd, $J = 10.5, 1.8$ Hz, 1H); ^{13}C NMR (101 MHz, $CDCl_3$) δ 164.5, 164.0, 157.7, 137.0, 137.0, 131.1, 129.1 (2C), 127.3 (2C), 123.9, 114.9.

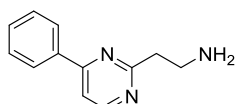
N-Benzyl-2-(4-phenylpyrimidin-2-yl)ethan-1-amine (5.141)



4-Phenyl-2-vinylpyrimidine (200 mg, 1.10 mmol) was dissolved in ethanol (2.5 ml). Acetic acid (150 μ l, 2.64 mmol) and benzylamine (240 μ l, 2.20 mmol) were added to the reaction mixture and the resulting solution was heated to reflux. The reaction was followed by TLC until complete (~36 h), at which point all of the volatiles were removed. The residue was re-dissolved in ethyl acetate and washed once with a 5 M aqueous sodium hydroxide solution. The volatiles were removed *in vacuo* and the crude material purified by column chromatography, eluting with 0-10% methanol/dichloromethane. The title compound was obtained as an orange oil (95 mg, 30%). 1H NMR (400 MHz, $CDCl_3$) δ 8.66 (d, $J = 5.3$ Hz, 1H), 8.08 – 7.96 (m, 2H), 7.59 – 7.39 (m, 4H), 7.36 – 7.25 (m, 4H), 3.90 (s, 2H), 3.33 – 3.26 (m, 2H), 3.25 – 3.17 (m, 2H); ^{13}C NMR (101 MHz, $CDCl_3$) δ 169.8, 164.2, 157.7, 139.4,

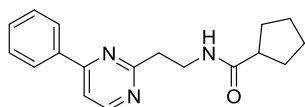
136.8, 131.1, 129.1 (2C), 128.6 (2C), 128.5 (2C), 127.3 (2C), 114.5, 53.7, 47.3, 38.7. *Note: there are two aromatic protons missing from the ^1H NMR spectrum. There are multiple equivalent carbons which are overlapping in the ^{13}C NMR.

2-(4-Phenylpyrimidin-2-yl)ethan-1-amine (5.142)



4-Phenyl-2-vinylpyrimidine (86 mg, 0.47 mmol) was added to a solution of ammonium hydroxide (3 ml) and ethanol (3 ml) in a sealed tube. The resulting reaction mixture was heated to 70 °C and monitored by LCMS. After 48 h there was minimal starting material remaining and mostly the desired product present. The reaction mixture was diluted with ethyl acetate and washed with an aqueous 2 M solution of hydrochloric acid. Any precipitate was filtered off at this stage. The aqueous phase was then collected and basified with an aqueous 5 M solution of sodium hydroxide and the product was extracted with ethyl acetate three times. The organic layers were combined and dried with magnesium sulphate to yield the title compound as a brown oil (71 mg, 76%) which was used without further purification. LRMS $[\text{M}+\text{H}]^+$ 200.1 m/z; ^1H NMR (400 MHz, DMSO) δ 8.74 (dd, $J = 25.6, 5.3$ Hz, 1H), 8.23 – 8.13 (m, 2H), 7.85 (dd, $J = 27.7, 5.4$ Hz, 1H), 7.61 – 7.46 (m, 3H), 3.33 (bs, 2H), 3.20 – 2.93 (m, 4H); ^{13}C NMR (101 MHz, DMSO) δ 169.5, 162.4, 158.1, 136.3, 131.0, 129.0 (2C), 127.0 (2C), 114.3, 56.0 (2C). *Note: there are multiple equivalent carbons which are overlapping in the ^{13}C NMR.

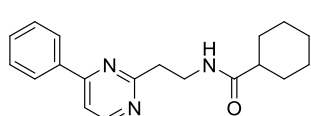
N-(2-(4-Phenylpyrimidin-2-yl)ethyl)cyclopentanecarboxamide (5.145)



2-(4-Phenylpyrimidin-2-yl)ethan-1-amine (20 mg, 0.10 mmol), cyclopentanecarboxylic acid (13 μl , 0.12 mmol), EDCI (19 mg, 0.12 mmol) and DMAP (1 mg, 0.01 mmol) were combined in DMF (500 μl). The reaction mixture was heated to 40 °C and monitored by TLC and LCMS analysis. After 18 h the reaction was complete and all of the volatiles were removed. The crude material was purified by column chromatography, eluting with 10% ethyl acetate/petroleum spirits to give the title compound as an off-white solid (8 mg, 27%). HPLC – rt 5.97 min > 98 % purity at 254 nm; LRMS $[\text{M}+\text{H}]^+$ 296.2 m/z; HRMS $[\text{M}+\text{H}]^+$ 296.1757 m/z, found 296.1758 m/z; ^1H

NMR (400 MHz, CDCl₃) δ 8.69 (d, *J* = 5.4 Hz, 1H), 8.15 – 7.98 (m, 2H), 7.56 (d, *J* = 5.4 Hz, 1H), 7.53 – 7.43 (m, 3H), 6.60 (s, 1H), 3.80 (dd, *J* = 12.0, 5.8 Hz, 2H), 3.28 – 3.14 (m, 2H), 2.56 – 2.39 (m, 1H), 1.86 – 1.53 (m, 8H); ¹³C NMR (101 MHz, CDCl₃) δ 176.2, 169.6, 164.2, 157.7, 136.7, 131.3, 129.2 (2C), 127.3 (2C), 114.7, 46.2, 38.6, 37.4, 30.5 (2C), 26.0 (2C).

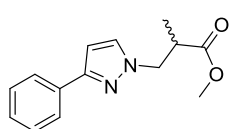
N-(2-(4-Phenylpyrimidin-2-yl)ethyl)cyclohexanecarboxamide (**5.147**)



2-(4-Phenylpyrimidin-2-yl)ethan-1-amine (20 mg, 0.10 mmol), cyclohexanecarboxylic acid (15 μl, 0.12 mmol), EDCI (19 mg, 0.12 mmol) and

DMAP (1 mg, 0.01 mmol) were combined in DMF (500 μl). The reaction mixture was heated to 40 °C and monitored by TLC and LCMS analysis. After 18 h the reaction was complete and all of the volatiles were removed. The crude material was purified by column chromatography, eluting with 10% ethyl acetate/petroleum spirits to give the title compound as an off-white solid (5 mg, 16%). HPLC – rt 6.37 min > 95 % purity at 254 nm; LRMS [M+H]⁺ 310.1 m/z; HRMS [M+H]⁺ 310.1914 m/z, found 310.1916 m/z; ¹H NMR (400 MHz, CDCl₃) δ 8.70 (d, *J* = 5.4 Hz, 1H), 8.14 – 7.96 (m, 2H), 7.56 (d, *J* = 5.4 Hz, 1H), 7.54 – 7.47 (m, 3H), 6.75 – 6.56 (m, 1H), 3.88 – 3.69 (m, 2H), 3.28 – 3.13 (m, 2H), 2.08 – 1.97 (m, 1H), 1.85 – 1.53 (m, 7H), 1.47 – 1.28 (m, 3H); ¹³C NMR (101 MHz, CDCl₃) δ 176.1, 169.6, 164.2, 157.8, 136.7, 131.3, 129.2 (2C), 127.3 (2C), 114.7, 45.8, 38.6, 37.3, 29.8 (2C), 25.9 (2C). *Note: the amide –NH is missing from the ¹H NMR. There is one CH₂ missing from the ¹³C NMR spectrum.

Methyl 2-methyl-3-(3-phenyl-1H-pyrazol-1-yl)propanoate (**5.150**)

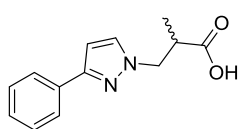


3-Phenyl-1H-pyrazole (250 mg, 1.73 mmol), methyl methacrylate (280 μl, 2.60 mmol) and DBU (130 μl, 0.87 mmol) were combined in acetonitrile (3.5 ml), under nitrogen.

The reaction was stirred at 50 °C for 18 h, though by TLC there was only a 50% conversion of the starting material to product. Additional methyl methacrylate (280 μl, 2.60 mmol) was added to the reaction, and returned to heat at 50 °C for an additional 2 h. By TLC the reaction was complete and all of the volatiles were removed *in vacuo* and the crude material was purified by column

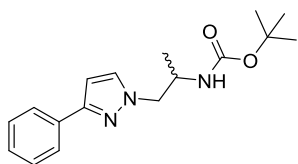
chromatography, eluting with 15-25% ethyl acetate/petroleum spirits. The title compound was obtained as a colourless oil (342 mg, 81%). HPLC – rt 7.42 min > 97% purity at 254 nm; LRMS [M+H]⁺ 245.2 m/z; HRMS [M+H]⁺ 245.1285 m/z, found 245.1284 m/z; ¹H NMR (400 MHz, DMSO) δ 7.76 (ddd, *J* = 9.8, 6.3, 1.8 Hz, 3H), 7.44 – 7.33 (m, 2H), 7.29 (dt, *J* = 9.3, 4.3 Hz, 1H), 6.68 (d, *J* = 2.3 Hz, 1H), 4.37 (dd, *J* = 13.6, 7.1 Hz, 1H), 4.25 (dd, *J* = 13.6, 6.4 Hz, 1H), 3.61 (s, 3H), 3.06 (dd, *J* = 13.7, 7.0 Hz, 1H), 1.06 (d, *J* = 7.1 Hz, 3H); ¹³C NMR (101 MHz, DMSO) δ 174.0, 150.3, 133.4, 132.4, 128.6 (2C), 127.4, 125.0 (2C), 102.3, 53.6, 51.7, 40.0, 14.3.

2-Methyl-3-(3-phenyl-1H-pyrazol-1-yl)propanoic acid (5.151)



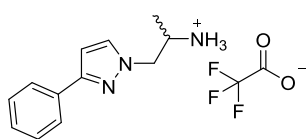
Methyl 2-methyl-3-(3-phenyl-1H-pyrazol-1-yl)propanoate (300 mg, 1.23 mmol) was dissolved in tetrahydrofuran (1 ml) and lithium hydroxide (59 mg, 2.46 mmol) was dissolved in water (2.6 ml). The ester solution was added dropwise to the aqueous lithium hydroxide solution. The reaction mixture was stirred for 90 min and LCMS showed complete hydrolysis. The reaction mixture was quenched by addition of an aqueous 1 M hydrochloric acid solution to acidic pH. The product was extracted with ethyl acetate three times and the subsequent organic layers were combined, washed once with a saturated aqueous solution of sodium chloride and dried with magnesium sulphate. All of the volatiles were removed to yield the title compound as a pale-yellow oil (249 mg, 88%). HPLC – rt 6.27 min > 93% purity at 254 nm; LRMS [M+H]⁺ 231.1 m/z; HRMS [M+H]⁺ 231.1128 m/z, found 231.1127 m/z; ¹H NMR (400 MHz, DMSO) δ 12.47 (s, 1H), 7.88 – 7.65 (m, 3H), 7.45 – 7.33 (m, 2H), 7.33 – 7.17 (m, 1H), 6.68 (d, *J* = 2.3 Hz, 1H), 4.38 (dd, *J* = 13.6, 7.0 Hz, 1H), 4.17 (dd, *J* = 13.6, 7.0 Hz, 1H), 2.98 (h, *J* = 7.1 Hz, 1H), 1.06 (d, *J* = 7.1 Hz, 3H); ¹³C NMR (101 MHz, CDCl₃) δ 179.1, 152.1, 133.1, 131.9, 128.8 (2C), 128.0, 125.9 (2C), 103.0, 53.9, 40.8, 15.0.

Tert-butyl (1-(3-phenyl-1H-pyrazol-1-yl)propan-2-yl)carbamate (5.152)



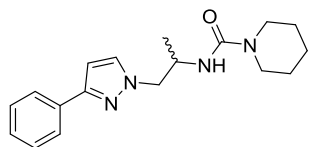
2-Methyl-3-(3-phenyl-1H-pyrazol-1-yl)propanoic acid (200 mg, 0.87 mmol), diphenylphosphoryl azide (225 μ l, 1.04 mmol) and triethylamine (140 μ l, 1.04 mmol) were combined in anhydrous *tert*-butanol (2 ml). The reaction mixture was heated to reflux for 4 h and the reactions progress was monitored by LCMS. A saturated aqueous solution of sodium bicarbonate was added and the product was extracted with ethyl acetate three times. The organic layers were combined and washed once with a saturated aqueous solution of sodium chloride and dried with magnesium sulphate. All of the volatiles were removed *in vacuo* and the crude material was purified by column chromatography, eluting with 0-15% ethyl acetate/petroleum spirit. The title compound was obtained as a colourless solid (113 mg, 43%). LRMS $[M+H]^+$ 302.2 m/z, $[M-^tBu]^+$ 246.2 m/z; 1H NMR (400 MHz, DMSO) δ 7.86 – 7.73 (m, 2H), 7.69 (d, J = 1.9 Hz, 1H), 7.39 (dd, J = 10.5, 4.7 Hz, 2H), 7.33 – 7.21 (m, 1H), 6.90 (d, J = 8.2 Hz, 1H), 6.68 (d, J = 2.3 Hz, 1H), 4.09 (qd, J = 13.9, 7.2 Hz, 2H), 3.91 (dt, J = 14.1, 6.9 Hz, 1H), 1.35 (s, 9H), 1.01 (d, J = 6.6 Hz, 3H); ^{13}C NMR (101 MHz, DMSO) δ 155.3, 150.5, 134.0, 132.6, 129.0, 127.8, 125.5, 102.8, 78.2, 56.3, 47.0, 28.7, 18.5. *Note: there are multiple equivalent carbons which are overlapping in the ^{13}C NMR.

1-(3-Phenyl-1H-pyrazol-1-yl)propan-2-amine (5.153)



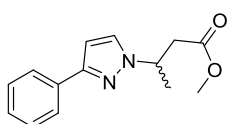
Tert-butyl (1-(3-phenyl-1H-pyrazol-1-yl)propan-2-yl)carbamate (50 mg, 0.17 mmol) was added to a 50:50 mixture of trifluoroacetic acid:dichloromethane (1 ml). The reaction mixture was stirred at ambient temperature for 2 h and TLC showed complete disappearance of starting material. All of the volatiles were removed and the residue was washed with toluene three times. This gave the title compound as a colourless solid which was used directly. LRMS $[M+H]^+$ 202.2 m/z; 1H NMR (400 MHz, $CDCl_3$) δ 7.77 – 7.62 (m, 2H), 7.41 – 7.32 (m, 3H), 7.30 (dt, J = 9.6, 4.3 Hz, 1H), 6.52 (d, J = 2.4 Hz, 1H), 5.10 (s, 2H), 4.25 (qd, J = 14.6, 5.1 Hz, 2H), 3.82 (s, 1H), 1.27 (d, J = 6.7 Hz, 3H).

N-(1-(3-Phenyl-1*H*-pyrazol-1-yl)propan-2-yl)piperidine-1-carboxamide (**5.154**)



1-(3-Phenyl-1*H*-pyrazol-1-yl)propan-2-amine (60 mg, 0.30 mmol) was dissolved in anhydrous dichloromethane (1 ml) and triethylamine (420 μ l, 2.97 mmol) was added (solution 1). In a separate flask *para*-nitrophenyl chloroformate (90 mg, 0.45 mmol) was dissolved in dichloromethane (1 ml) with stirring (solution 2). Solution 1 was then added dropwise to solution 2 and the reaction mixture was stirred for 2 h at ambient temperature. After 2 h piperidine (60 μ l, 0.60 mmol) was added to the reaction mixture which was allowed to stir at ambient temperature for 18 h. All of the volatiles were removed *in vacuo* and the crude material was purified by column chromatography, eluting with 40-60% ethyl acetate/dichloromethane. This yielded the title compound with contaminants so the material was further purified by column chromatography, eluting with 25-50% ethyl acetate/petroleum spirits to 40% ethyl acetate/dichloromethane. This gave the title compound as a colourless oil (27 mg, 29%). HPLC – rt 6.92 min > 98% purity at 254 nm; LRMS [M+H]⁺ 313.3 m/z; HRMS [M+H]⁺ 313.2023 m/z, found 313.2027 m/z; ¹H NMR (400 MHz, CDCl₃) δ 7.77 (dd, *J* = 5.2, 3.2 Hz, 2H), 7.41 (d, *J* = 2.3 Hz, 1H), 7.39 – 7.32 (m, 2H), 7.30 – 7.24 (m, 1H), 6.52 (d, *J* = 2.3 Hz, 1H), 5.35 (t, *J* = 4.9 Hz, 1H), 4.62 – 4.37 (m, 1H), 3.72 (dd, *J* = 6.1, 3.6 Hz, 1H), 3.46 (ddd, *J* = 13.7, 8.5, 5.1 Hz, 1H), 1.53 (d, *J* = 6.8 Hz, 6H), 1.45 (d, *J* = 4.4 Hz, 4H), 1.20 (t, *J* = 7.0 Hz, 3H); ¹³C NMR (101 MHz, CDCl₃) δ 157.7, 151.6, 133.6, 130.0, 128.7 (2C), 127.7, 125.5 (2C), 102.3, 57.7, 46.6, 45.0 (2C), 25.6 (2C), 24.5, 18.3.

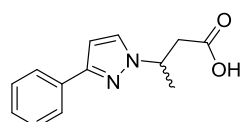
Methyl 3-(3-phenyl-1*H*-pyrazol-1-yl)butanoate (**5.156**)



3-Phenyl-1*H*-pyrazole (250 mg, 1.73 mmol), methyl crotonate (275 μ l, 2.60 mmol) and DBU (130 μ l, 0.87 mmol) were combined in acetonitrile (3.5 ml), under nitrogen. The reaction was stirred at 50 °C for 18 h and by TLC the reaction was complete. All of the volatiles were removed *in vacuo* and the crude material was purified by column chromatography, eluting with 15-25% ethyl acetate/petroleum spirits. The title compound was obtained as a colourless oil (321 mg, 76%). HPLC – rt 7.48 min > 98% purity at 254 nm; LRMS [M+H]⁺ 245.2 m/z; HRMS [M+H]⁺ 245.1285 m/z, found 245.1284 m/z; ¹H NMR (400 MHz, DMSO) δ 7.87 – 7.70 (m, 3H), 7.44 – 7.33 (m, 2H), 7.33 –

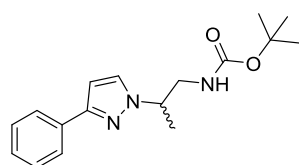
7.19 (m, 1H), 6.66 (d, $J = 2.3$ Hz, 1H), 4.93 – 4.62 (m, 1H), 3.56 (s, 3H), 2.93 (ddd, $J = 22.0, 16.0, 7.0$ Hz, 2H), 1.48 (d, $J = 6.8$ Hz, 3H); ^{13}C NMR (101 MHz, DMSO) δ 170.8, 149.7, 133.5, 130.3, 128.6 (2C), 127.3, 125.0 (2C), 102.2, 54.0, 51.5, 40.5, 20.9.

3-(3-Phenyl-1H-pyrazol-1-yl)butanoic acid (5.157)



Methyl 3-(3-phenyl-1H-pyrazol-1-yl)butanoate (300 mg, 1.23 mmol) was dissolved in tetrahydrofuran (1 ml) and lithium hydroxide (59 mg, 2.46 mmol) was dissolved in water (2.6 ml). The ester solution was added dropwise to the aqueous lithium hydroxide solution. The reaction mixture was stirred for 90 min and LCMS showed complete hydrolysis. The reaction mixture was quenched by addition of an aqueous 1 M hydrochloric acid solution to acidic pH. The product was extracted with ethyl acetate three times and the subsequent organic layers were combined, washed once with a saturated aqueous solution of sodium chloride and dried with magnesium sulphate. All volatiles were removed to yield the title compound as a pale-yellow oil (251 mg, 87%). HPLC – rt 6.35 min > 99% purity at 254 nm; LRMS $[\text{M}+\text{H}]^+$ 231.2 m/z; HRMS $[\text{M}+\text{H}]^+$ 231.1128 m/z, found 231.1128 m/z; ^1H NMR (400 MHz, DMSO) δ 7.95 – 7.64 (m, 3H), 7.38 (t, $J = 7.6$ Hz, 2H), 7.27 (t, $J = 7.3$ Hz, 1H), 6.66 (d, $J = 2.3$ Hz, 1H), 4.75 (dd, $J = 14.1, 6.7$ Hz, 1H), 2.92 (dd, $J = 16.2, 7.9$ Hz, 1H), 2.77 (dd, $J = 16.2, 6.2$ Hz, 1H), 1.46 (d, $J = 6.7$ Hz, 3H); ^{13}C NMR (101 MHz, DMSO) δ 171.8, 149.7, 133.6, 130.3, 128.6 (2C), 127.3, 125.0 (2C), 102.1, 54.1, 40.8, 21.1. *Note: the –OH peak is missing from the ^1H NMR.

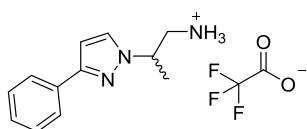
Tert-butyl (2-(3-phenyl-1H-pyrazol-1-yl)propyl)carbamate (5.158)



3-(3-Phenyl-1H-pyrazol-1-yl)butanoic acid (100 mg, 0.43 mmol), diphenylphosphoryl azide (115 μl , 0.52 mmol) and triethylamine (70 μl , 0.52 mmol) were combined in anhydrous *tert*-butanol (1 ml). The reaction mixture was heated to reflux for 12 h and the reaction progress was monitored by LCMS. Upon completion a saturated aqueous solution of sodium bicarbonate was added and the product was extracted with ethyl acetate three times. The organic layers were combined and washed once with a saturated aqueous solution of sodium

chloride and dried with magnesium sulphate. All of the volatiles were removed *in vacuo* and the crude material was purified by column chromatography, eluting with 0-15% ethyl acetate/petroleum spirit. The title compound was obtained as a colourless solid (42 mg, 32%). LRMS $[M+H]^+$ 302.2 m/z, $[M-^t\text{Bu}]^+$ 246.1 m/z; ^1H NMR (400 MHz, CDCl_3) δ 7.88 – 7.75 (m, 2H), 7.46 – 7.35 (m, 3H), 7.30 (ddd, $J = 7.4, 3.9, 1.3$ Hz, 1H), 6.55 (d, $J = 2.3$ Hz, 1H), 5.00 – 4.75 (m, 1H), 4.59 – 4.38 (m, $J = 10.8, 7.9$ Hz, 1H), 3.72 – 3.56 (m, 1H), 3.50 (ddd, $J = 14.1, 8.4, 5.6$ Hz, 1H), 1.53 (d, $J = 6.8$ Hz, 3H), 1.42 (s, 9H); ^{13}C NMR (101 MHz, DMSO) δ 155.7, 149.7, 133.7, 130.2, 128.6, 127.3, 125.1, 102.2, 77.8, 56.9, 45.5, 28.2, 18.4.

2-(3-Phenyl-1H-pyrazol-1-yl)propan-1-amine (5.159)

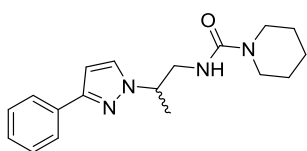


Tert-butyl (2-(3-phenyl-1H-pyrazol-1-yl)propyl)carbamate (50 mg, 0.17 mmol)

was added to a 50:50 mixture of trifluoroacetic acid:dichloromethane (1 ml).

The reaction mixture was stirred at ambient temperature for 2 h and TLC showed complete disappearance of starting material. All of the volatiles were removed and the residue was washed with toluene three times. This gave the title compound as a colourless solid which was used directly. LRMS $[M+H]^+$ 202.2 m/z; ^1H NMR (400 MHz, DMSO) δ 8.37 (d, $J = 0.8$ Hz, 2H), 8.33 (d, $J = 2.4$ Hz, 1H), 8.29 (dd, $J = 8.3, 1.2$ Hz, 2H), 7.96 – 7.82 (m, 2H), 7.82 – 7.71 (m, 1H), 5.19 – 5.02 (m, 1H), 3.92 – 3.62 (m, 2H), 2.96 (dt, $J = 3.6, 1.8$ Hz, 3H). *Note: there is one aromatic proton missing from the ^1H NMR spectrum.

N-(2-(3-Phenyl-1H-pyrazol-1-yl)propyl)piperidine-1-carboxamide (5.160)



1-(3-Phenyl-1H-pyrazol-1-yl)propan-2-amine (80 mg, 0.40 mmol) was

dissolved in anhydrous dichloromethane (1 ml) and triethylamine (555 μl , 3.97

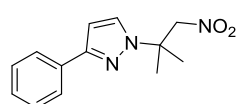
mmol) was added (solution 1). In a separate flask *para*-nitrophenyl

chloroformate (120 mg, 0.60 mmol) was dissolved in dichloromethane (1 ml) with stirring (solution 2).

Solution 1 was then added dropwise to solution 2 and the reaction mixture was stirred for 2 h at ambient temperature. After 2 h piperidine (80 μl , 0.80 mmol) was added to the reaction mixture which was allowed to stir at ambient temperature for 18 h. All volatiles were removed *in vacuo* and the crude material was purified

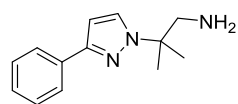
by column chromatography, eluting with 40-60% ethyl acetate/dichloromethane. This yielded the title compound with contaminants so the material was further purified by column chromatography, eluting with 25-50% ethyl acetate/petroleum spirits to 40% ethyl acetate/dichloromethane. This gave the title compound as a colourless oil (16 mg, 13%). HPLC – rt 6.93 min > 96% purity at 254 nm; LRMS [M+H]⁺ 313.3 m/z; HRMS [M+H]⁺ 313.2023 m/z, found 313.2028 m/z; ¹H NMR (400 MHz, CDCl₃) δ 7.89 – 7.65 (m, 2H), 7.49 – 7.31 (m, 3H), 7.31 – 7.25 (m, 1H), 6.55 (d, *J* = 2.3 Hz, 1H), 5.88 (d, *J* = 7.1 Hz, 1H), 4.32 (dd, *J* = 13.7, 3.6 Hz, 1H), 4.29 – 4.17 (m, 1H), 4.10 (dd, *J* = 13.7, 4.8 Hz, 1H), 3.31 (h, *J* = 8.6 Hz, 4H), 1.67 – 1.41 (m, 6H), 1.08 (d, *J* = 6.6 Hz, 3H); ¹³C NMR (101 MHz, CDCl₃) δ 157.2, 151.9, 133.4, 132.5, 128.7 (2C), 127.9, 125.5 (2C), 102.6, 56.6, 47.0, 44.9 (2C), 25.7 (2C), 24.6, 18.7.

1-(2-Methyl-1-nitropropan-2-yl)-3-phenyl-1H-pyrazole (5.162)



3-Phenyl-1*H*-pyrazole (250 mg, 1.73 mmol), 2-methyl-1-nitroprop-1-ene (351 mg, 3.47 mmol) and DBU (20 μl, 0.87 mmol) were combined in acetonitrile (3.5 ml), under nitrogen. The reaction was stirred at 50 °C for 18 h and LCMS showed ~ 60 % conversion of the starting material. All of the volatiles were removed *in vacuo* and the crude material was purified by column chromatography, eluting with 10-20% ethyl acetate/petroleum spirits. The title compound was obtained as a pale-yellow oil (197 mg, 46%). HPLC – rt 7.94 min > 99% purity at 254 nm; LRMS [M+H]⁺ 246.2 m/z; HRMS [M+H]⁺ 246.1237 m/z, found 246.1235 m/z; ¹H NMR (400 MHz, DMSO) δ 7.92 (d, *J* = 2.5 Hz, 1H), 7.86 – 7.71 (m, 2H), 7.49 – 7.35 (m, 2H), 7.30 (dt, *J* = 9.3, 4.3 Hz, 1H), 6.72 (d, *J* = 2.5 Hz, 1H), 5.05 (s, 2H), 1.71 (s, 6H); ¹³C NMR (101 MHz, DMSO) δ 150.1, 133.4, 129.5, 128.6 (2C), 127.5, 125.2 (2C), 102.6, 83.2, 59.7, 25.3 (2C).

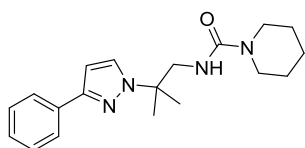
2-Methyl-2-(3-phenyl-1H-pyrazol-1-yl)propan-1-amine (5.163)



A 0.05 M solution of **5.162** (197 mg, 0.80 mmol) was made up in 50:50 ethyl acetate/ethanol (10 ml). This was loaded on to a ThalesNano H-Cube[®] with a 10% Pd/C CatCart[®]. The reaction was monitored by LCMS until no more starting material was present and the

solvent was removed under reduced pressure to give the amine as a yellow oil, which was used directly in the next reaction. LRMS $[M+H]^+$ 216.1 m/z; ^1H NMR (400 MHz, CDCl_3) δ 7.80 (dd, $J = 5.1, 3.3$ Hz, 1H), 7.77 – 7.71 (m, 1H), 7.51 (dd, $J = 6.1, 2.4$ Hz, 1H), 7.41 – 7.30 (m, 3H), 7.27 (dd, $J = 7.4, 1.5$ Hz, 1H), 1.78 (s, 2H), 1.59 (dd, $J = 13.1, 9.7$ Hz, 6H).

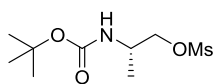
N-(2-Methyl-2-(3-phenyl-1H-pyrazol-1-yl)propyl)piperidine-1-carboxamide **5.164**)



Compound **5.163** (50 mg, 0.23 mmol) was dissolved in anhydrous dichloromethane (1 ml) and triethylamine (100 μl , 0.74 mmol) was added (solution 1). In a separate flask *para*-nitrophenyl chloroformate (70 mg, 0.35

mmol) was dissolved in dichloromethane (1 ml) with stirring (solution 2). Solution 1 was then added dropwise to solution 2 and the reaction mixture was stirred for 2 h at ambient temperature. After 2 h piperidine (65 μl , 0.46 mmol) was added to the reaction mixture which was allowed to stir at ambient temperature for 18 h. All volatiles were removed *in vacuo* and the crude material was purified by column chromatography, eluting with 25-75% ethyl acetate/petroleum spirits. The material contained some contaminants and was further purified by column chromatography, eluting with 5-10% ethyl acetate/dichloromethane. This yielded the title compound was obtained as a colourless oil (13 mg, 17%). LRMS $[M+H]^+$ 327.2 m/z; ^1H NMR (400 MHz, CDCl_3) δ 7.81 – 7.75 (m, 2H), 7.52 (d, $J = 2.4$ Hz, 1H), 7.40 – 7.33 (m, 2H), 7.31 – 7.25 (m, 1H), 6.55 (d, $J = 2.4$ Hz, 1H), 6.00 (s, 1H), 3.62 (d, $J = 5.6$ Hz, 2H), 3.38 – 3.24 (m, 4H), 1.59 (s, 6H), 1.51 (ddd, $J = 9.9, 7.4, 2.8$ Hz, 6H); ^{13}C NMR (101 MHz, CDCl_3) δ 157.9, 151.1, 133.7, 128.7 (2C), 128.1, 127.8, 125.5 (2C), 102.3, 51.0, 45.1 (2C), 25.9 (2C), 25.8 (2C), 24.7. *Note: there is a quaternary carbon missing from the ^{13}C NMR.

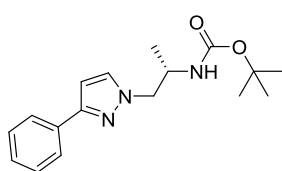
(*S*)-2-((Tert-butoxycarbonyl)amino)propyl methanesulfonate (**5.165**)



Boc-L-alaninol (1 g, 5.71 mmol) was dissolved in anhydrous dichloromethane (11.5 ml) under nitrogen and cooled to 0 °C. To this triethylamine (795 μl , 5.71 mmol) and methanesulfonyl chloride (440 μl , 5.71 mmol) were added. The resulting mixture was stirred at 0 °C for 30

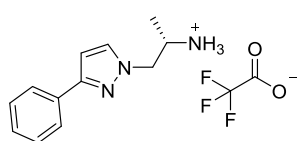
min before the being gradually warmed to ambient temperature. After 30 min the reaction was quenched by addition of water and the organic layer was collected and washed with water three more times. The organic layer was dried with magnesium sulphate before all volatiles were removed *in vacuo* to yield the title compound as a colourless solid (1.32 g, 91%). ^1H NMR (400 MHz, DMSO) δ 6.95 (d, $J = 7.8$ Hz, 1H), 4.03 (d, $J = 5.8$ Hz, 2H), 3.73 (dd, $J = 13.6, 6.8$ Hz, 1H), 3.16 (s, 3H), 1.38 (s, 9H), 1.05 (d, $J = 6.8$ Hz, 3H); ^{13}C NMR (101 MHz, DMSO) δ 155.0, 78.0, 72.0, 45.1, 39.5, 36.7, 28.2, 16.7.

Tert-butyl (S)-1-(3-phenyl-1H-pyrazol-1-yl)propan-2-yl)carbamate (5.166)



3-Phenyl-1H-pyrazole (200 mg, 1.39 mmol), cesium carbonate (4.52 g, 13.90 mmol) and **5.165** (704 mg, 2.78 mmol) were combined in anhydrous *N,N*-dimethylformamide (4 ml). The resulting suspension was heated to 50 °C and the progress of the reaction was monitored by TLC. Once the reaction was complete (~ 3 h) the reaction mixture was quenched by addition of water and the product was extracted with ethyl acetate three times. The organic layers were combined and washed with a saturated aqueous solution of sodium chloride. The crude material was purified by column chromatography, eluting with 20% ethyl acetate/petroleum spirits to give the title compound as a colourless solid (183 mg, 44%). HPLC – rt 7.55 min > 92% purity at 254 nm; LRMS $[\text{M}+\text{H}]^+$ 302.2 m/z; HRMS $[\text{M}+\text{H}]^+$ 302.1863 m/z, found 302.1867 m/z; ^1H NMR (400 MHz, CDCl_3) δ 7.87 – 7.70 (m, 2H), 7.41 – 7.34 (m, 3H), 7.31 – 7.25 (m, 1H), 6.54 (d, $J = 2.3$ Hz, 1H), 5.06 (d, $J = 1.1$ Hz, 1H), 4.25 (dd, $J = 13.8, 4.5$ Hz, 1H), 4.20 – 4.10 (m, 1H), 4.04 (dt, $J = 12.4, 6.0$ Hz, 1H), 1.41 (s, 9H), 1.12 (d, $J = 6.8$ Hz, 3H).

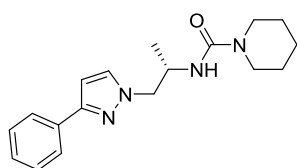
(S)-1-(3-Phenyl-1H-pyrazol-1-yl)propan-2-amine (5.167)



Compound **5.156** (50 mg, 0.17 mmol) was added to a 50:50 mixture of trifluoroacetic acid:dichloromethane (1 ml). The reaction mixture was stirred at ambient temperature for 2 h and TLC showed complete disappearance of starting material. All of the volatiles were removed and the residue was washed with toluene three times. This gave

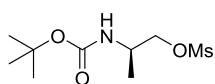
the title compound as a colourless solid which was used directly. LRMS $[M+H]^+$ 202.1 m/z; ^1H NMR (400 MHz, CDCl_3) δ 7.71 (d, $J = 8.0$ Hz, 2H), 7.37 (dddd, $J = 12.8, 11.3, 5.7, 3.0$ Hz, 3H), 7.19 – 7.10 (m, 1H), 6.64 – 6.51 (m, 1H), 4.46 – 4.31 (m, 1H), 4.26 (ddd, $J = 11.9, 6.6, 4.8$ Hz, 1H), 2.99 (s, 2H), 2.34 (s, 1H), 1.34 (dd, $J = 12.6, 6.4$ Hz, 3H).

(S)-N-(1-(3-Phenyl-1H-pyrazol-1-yl)propan-2-yl)piperidine-1-carboxamide (**5.168**)



Compound **5.157** (67 mg, 0.33 mmol) was dissolved in anhydrous dichloromethane (1 ml) and triethylamine (464 μl , 3.33 mmol) was added (solution 1). In a separate flask *para*-nitrophenyl chloroformate (100 mg, 0.50 mmol) was dissolved in dichloromethane (1 ml) with stirring (solution 2). Solution 1 was then added dropwise to solution 2 and the reaction mixture was stirred for 2 h at ambient temperature. After 2 h piperidine (65 μl , 0.66 mmol) was added to the reaction mixture which was allowed to stir at ambient temperature for 18 h. All volatiles were removed *in vacuo* and the crude material was purified by column chromatography, eluting with 5% ethyl acetate/dichloromethane. This yielded the title compound as a pale-yellow oil (27 mg, 26%). LRMS $[M+H]^+$ 313.3 m/z; ^1H NMR (400 MHz, CDCl_3) δ 7.87 – 7.67 (m, 2H), 7.41 – 7.33 (m, 3H), 7.31 – 7.25 (m, 1H), 6.55 (d, $J = 2.3$ Hz, 1H), 6.06 – 5.90 (m, 1H), 4.32 (dd, $J = 13.7, 3.6$ Hz, 1H), 4.28 – 4.19 (m, 1H), 4.12 – 4.02 (m, 1H), 3.32 (dd, $J = 9.0, 4.4$ Hz, 4H), 1.64 – 1.42 (m, 6H), 1.09 (t, $J = 6.2$ Hz, 3H); ^{13}C NMR (101 MHz, CDCl_3) δ 157.3, 152.0, 133.3, 132.5, 128.8 (2C), 127.9, 125.5 (2C), 102.7, 56.6, 47.0, 44.9 (2C), 25.7 (2C), 24.5, 18.6.

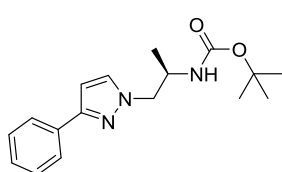
(R)-2-((Tert-butoxycarbonyl)amino)propyl methanesulfonate (**5.169**)



Boc-D-alaninol (1 g, 5.71 mmol) was dissolved in anhydrous dichloromethane (11.5 ml) under nitrogen and cooled to 0 °C. To this triethylamine (795 μl , 5.71 mmol) and methanesulfonyl chloride (440 μl , 5.71 mmol) was added. The resulting mixture was stirred at 0 °C for 30 min before the being gradually warmed to ambient temperature. After 30 min the reaction was quenched by addition of water and the organic layer was collected and washed with water three more times. The organic

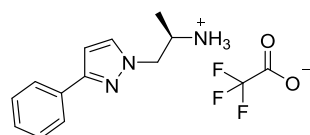
layer was dried with magnesium sulphate before all volatiles were removed *in vacuo* to yield the title compound as a colourless solid (1.05 g, 72%). ¹H NMR (400 MHz, DMSO) δ 6.95 (d, *J* = 7.7 Hz, 1H), 4.05 (dd, *J* = 10.0, 5.9 Hz, 3H), 3.96 (dd, *J* = 21.9, 10.2 Hz, 2H), 3.74 (dt, *J* = 12.9, 6.4 Hz, 1H), 1.38 (s, 9H), 1.05 (d, *J* = 6.8 Hz, 3H); ¹³C NMR (101 MHz, DMSO) δ 155.0, 72.0, 45.1, 36.7, 28.2, 16.8. *Note: there is a carbon missing from the ¹³C NMR.

Tert-butyl (R)-(1-(3-phenyl-1H-pyrazol-1-yl)propan-2-yl)carbamate (5.170)



3-Phenyl-1H-pyrazole (200 mg, 1.39 mmol), cesium carbonate (4.52 g, 13.90 mmol) and **5.169** (704 mg, 2.78 mmol) were combined in anhydrous *N,N*-dimethylformamide (4 ml). The resulting suspension was heated to 50 °C and the progress of the reaction was monitored by TLC. Once the reaction was complete (~ 3 h) the reaction mixture was quenched by addition of water and the product was extracted with ethyl acetate three times. The organic layers were combined and washed with a saturated aqueous solution of sodium chloride. The crude material was purified by column chromatography, eluting with 20% ethyl acetate/petroleum spirits to give the title compound as a colourless solid (177 mg, 42%). LRMS [M+H]⁺ 302.2 m/z; HRMS [M+H]⁺ 302.1863 m/z found 302.1864 m/z; ¹H NMR (400 MHz, CDCl₃) δ 7.86 – 7.73 (m, 2H), 7.43 – 7.35 (m, 3H), 7.33 – 7.27 (m, 1H), 6.55 (d, *J* = 2.3 Hz, 1H), 5.08 (s, 1H), 4.27 (dd, *J* = 13.7, 4.5 Hz, 1H), 4.23 – 4.13 (m, 1H), 4.05 (dd, *J* = 12.7, 5.8 Hz, 1H), 1.43 (s, 9H), 1.14 (d, *J* = 6.8 Hz, 3H).

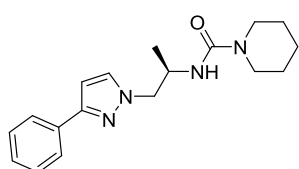
(R)-1-(3-Phenyl-1H-pyrazol-1-yl)propan-2-amine (5.171)



Tert-butyl (R)-(1-(3-phenyl-1H-pyrazol-1-yl)propan-2-yl)carbamate (239 mg, 0.79 mmol) was added to a 50:50 mixture of trifluoroacetic acid:dichloromethane (1 ml). The reaction mixture was stirred at ambient temperature for 18 h and TLC showed complete disappearance of starting material. All of the volatiles were removed and the residue was washed with toluene three times. This gave the title compound as a yellow oil which was used directly. LRMS [M+H]⁺ 202.2 m/z; ¹H NMR (400 MHz, CDCl₃) δ 7.70 (d, *J* = 8.0 Hz, 2H),

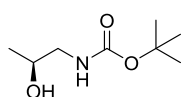
7.37 (dddd, $J = 12.8, 11.3, 5.7, 3.0$ Hz, 3H), 7.17 – 7.09 (m, 1H), 6.64 – 6.51 (m, 1H), 4.46 – 4.31 (m, 1H), 4.26 (ddd, $J = 11.9, 6.6, 4.8$ Hz, 1H), 2.99 (s, 2H), 2.35 (s, 1H), 1.30 (dd, $J = 12.6, 6.4$ Hz, 3H).

(R)-N-(1-(3-Phenyl-1H-pyrazol-1-yl)propan-2-yl)piperidine-1-carboxamide (**5.172**)



Compound **5.171** (159 mg, 0.79 mmol) was dissolved in a 50:50 solution of anhydrous dichloromethane and tetrahydrofuran (2 ml) and triethylamine (1.1 ml, 7.90 mmol) was then added (solution 1). In a separate flask *para*-nitrophenyl chloroformate (796 mg, 3.95 mmol) was dissolved in dichloromethane (1 ml) and tetrahydrofuran (2 ml) with stirring (solution 2). Solution 2 was cooled to 0 °C prior to dropwise addition of solution 1. The reaction was allowed to warm to ambient temperature and stirred for 2 h. After 2 h piperidine (160 μ l, 1.58 mmol) was added to the reaction mixture which was allowed to stir at ambient temperature for 18 h. All volatiles were removed *in vacuo* and the crude material was purified by column chromatography, eluting with 0-30% ethyl acetate/dichloromethane. This yielded the title compound as a pale-yellow oil (135 mg, 55%). HPLC – rt 6.93 min > 96% purity at 254 nm; LRMS $[M+H]^+$ 313.2 m/z; HRMS $[M+H]^+$ 313.2023 m/z, found 313.2027 m/z; ^1H NMR (400 MHz, CDCl_3) δ 7.86 – 7.67 (m, 2H), 7.48 – 7.34 (m, 3H), 7.29 (dt, $J = 9.4, 4.3$ Hz, 1H), 6.56 (d, $J = 2.3$ Hz, 1H), 5.99 (s, 1H), 4.34 (dd, $J = 13.8, 3.5$ Hz, 1H), 4.30 – 4.19 (m, 1H), 4.10 (dd, $J = 13.8, 4.8$ Hz, 1H), 3.42 – 3.22 (m, 4H), 1.53 (ddd, $J = 16.0, 9.0, 4.4$ Hz, 6H), 1.09 (d, $J = 6.6$ Hz, 3H); ^{13}C NMR (101 MHz, CDCl_3) δ 157.3, 152.0, 133.4, 132.6, 128.8 (2C), 127.9, 125.5 (2C), 102.7, 56.6, 47.0, 45.0 (2C), 25.7 (2C), 24.6, 18.7.

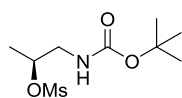
Tert-butyl (S)-(2-hydroxypropyl)carbamate (**5.200**)



Boc-anhydride (2.77 g, 12.70 mmol) was dissolved in tetrahydrofuran (50 ml). This was added dropwise to a solution of (*S*)-(+)-1-amino-2-propanol (1 ml, 12.70 mmol) and sodium bicarbonate (5.34 g, 63.5 mmol) in water (50 ml). The reaction mixture was then stirred at ambient temperature for 18 h after which all volatiles were removed *in vacuo*. The product was extracted twice with dichloromethane, the organic layers were then combined and dried with magnesium sulphate. All volatiles

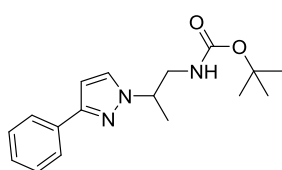
were removed *in vacuo* to yield the title compound as a colourless oil (2.01 g, 90%). ^1H NMR (400 MHz, CDCl_3) δ 5.26 (s, 1H), 3.77 (s, 1H), 3.64 (s, 1H), 3.14 (dd, $J = 10.7, 3.1$ Hz, 1H), 2.99 – 2.78 (m, 1H), 1.35 (s, 9H), 1.07 (d, $J = 6.3$ Hz, 3H); ^{13}C NMR (101 MHz, CDCl_3) δ 156.8, 79.5, 67.3, 47.9, 28.4 (3C), 20.5.

(S)-1-((Tert-butoxycarbonyl)amino)propan-2-yl methanesulfonate (**5.173**)



Compound **5.200** (1.95 g, 11.13 mmol) was dissolved in anhydrous dichloromethane (20 ml) under nitrogen and cooled to 0 °C. To this triethylamine (1.55 ml, 11.13 mmol) and methanesulfonyl chloride (860 μl , 11.13 mmol) was added. The resulting mixture was stirred at 0 °C for 30 min before being gradually warmed to ambient temperature. After 30 min the reaction was quenched by addition of water and the organic layer was collected and washed with water three more times. The organic layer was dried with magnesium sulphate before all volatiles were removed *in vacuo* to yield the title compound as a colourless solid (2.57 g, 91%). ^1H NMR (400 MHz, DMSO) δ 7.40 (s, 1H), 4.88 (ddd, $J = 7.9, 6.4, 3.5$ Hz, 1H), 4.63 (ddq, $J = 12.5, 8.1, 6.2$ Hz, 1H), 3.80 (dd, $J = 10.6, 4.5$ Hz, 1H), 3.26 (s, 3H), 2.36 (s, 9H), 1.38 (d, $J = 6.4$ Hz, 3H); ^{13}C NMR (101 MHz, CDCl_3) δ 160.6, 73.6, 47.5, 39.3, 28.4, 20.5. *Note: there are multiple equivalent carbons in the ^{13}C NMR spectrum.

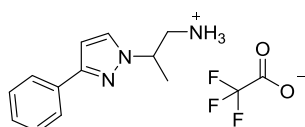
Tert-butyl (R)-(2-(3-phenyl-1H-pyrazol-1-yl)propyl)carbamate (**5.174**)



3-Phenyl-1H-pyrazole (250 mg, 1.73 mmol), cesium carbonate (5.65 g, 17.30 mmol) and **5.173** (876 mg, 3.46 mmol) were combined in anhydrous *N,N*-dimethylformamide (10 ml). The resulting suspension was heated to 50 °C and the progress of the reaction was monitored by TLC. Once the reaction was complete (~ 18 h) the reaction mixture was quenched by addition of water and the product was extracted with ethyl acetate three times. The organic layers were combined and washed with a saturated aqueous solution of sodium chloride. All of the volatiles were removed *in vacuo*. The crude material was purified by column chromatography, eluting with 5-10% ethyl acetate/petroleum spirits to give the title compound as a colourless solid (60 mg, 12%). HPLC – rt 7.56 min > 91% purity at 254 nm; LRMS $[\text{M}+\text{H}]^+$ 302.2 m/z; HRMS $[\text{M}+\text{H}]^+$ 302.1863 m/z, found

302.1867 m/z; $^1\text{H NMR}$ (400 MHz, CDCl_3) δ 7.85 – 7.72 (m, 2H), 7.41 – 7.33 (m, 3H), 7.31 – 7.25 (m, 1H), 6.54 (d, $J = 2.3$ Hz, 1H), 5.05 (d, $J = 1.1$ Hz, 1H), 4.26 (dd, $J = 13.8, 4.5$ Hz, 1H), 4.21 – 4.10 (m, 1H), 4.05 (dd, $J = 12.6, 6.7$ Hz, 1H), 1.41 (s, 9H), 1.12 (d, $J = 6.8$ Hz, 3H).

(R)-2-(3-Phenyl-1H-pyrazol-1-yl)propan-1-amine (5.181)

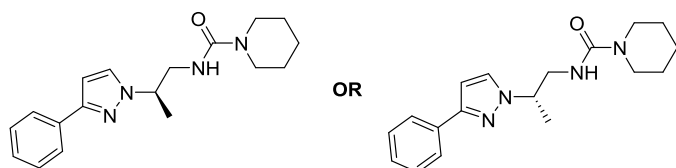


Compound **5.174** (239 mg, 0.79 mmol) was added to a 50:50 mixture of trifluoroacetic acid:dichloromethane (1 ml). The reaction mixture was stirred at ambient temperature for 18 h and TLC showed complete disappearance of

starting material. All of the volatiles were removed and the residue was washed with toluene three times.

This gave the title compound as a brown oil which was used directly. LRMS $[\text{M}+\text{H}]^+$ 202.2 m/z; $^1\text{H NMR}$ (400 MHz, CDCl_3) δ 7.79 – 7.63 (m, 2H), 7.48 (d, $J = 2.4$ Hz, 1H), 7.38 (t, $J = 7.4$ Hz, 2H), 7.34 – 7.26 (m, 1H), 6.57 (d, $J = 2.4$ Hz, 1H), 4.65 (dd, $J = 12.3, 6.1$ Hz, 1H), 3.40 (d, $J = 5.7$ Hz, 2H), 2.66 (s, 2H), 1.58 (d, $J = 6.8$ Hz, 3H).

(R)-N-(2-(3-Phenyl-1H-pyrazol-1-yl)propyl)piperidine-1-carboxamide (5.185)

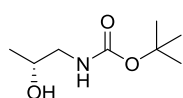


Compound **5.181** (35 mg, 0.17 mmol) was dissolved in anhydrous dichloromethane (0.5 ml) and triethylamine (125 μl , 1.70 mmol) was added

(solution 1). In a separate flask *para*-nitrophenyl chloroformate (69 mg, 0.34 mmol) was dissolved in dichloromethane (1 ml) with stirring (solution 2). Solution 1 was then added dropwise to solution 2 and the reaction mixture was stirred for 2 h at ambient temperature. After 2 h piperidine (35 μl , 0.34 mmol) was added to the reaction mixture which was allowed to stir at ambient temperature for 18 h. All of the volatiles were removed *in vacuo* and the crude material was purified by column chromatography, eluting with 10-50% ethyl acetate/dichloromethane (32 mg, 60%). A portion of the material was further purified by chiral HPLC using a ChiralPAK[®] column and eluting with 10% ethanol/petroleum spirits to ensure > 99.9% e.e. This yielded the title compound as a clear oil. HPLC – t_r 7.15 min > 99% purity at 254 nm; cHPLC – 8.63 min,

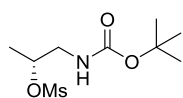
100% ee; LRMS $[M+H]^+$ 313.3 m/z; HRMS $[M+H]^+$ 313.2023 m/z, found 313.2025 m/z; ^1H NMR (400 MHz, CDCl_3) δ 7.85 – 7.71 (m, 2H), 7.41 (d, $J = 2.3$ Hz, 1H), 7.40 – 7.32 (m, 2H), 7.31 – 7.24 (m, 1H), 6.53 (d, $J = 2.3$ Hz, 1H), 5.32 (s, 1H), 4.50 (dq, $J = 8.3, 6.8, 3.5$ Hz, 1H), 3.71 (d, $J = 13.7$ Hz, 1H), 3.47 (dd, $J = 13.5, 8.6$ Hz, 1H), 3.33 – 3.19 (m, 4H), 1.51 (t, $J = 15.5$ Hz, 6H); ^{13}C NMR (101 MHz, CDCl_3) δ 157.7, 151.6, 133.6, 129.9, 128.7 (2C), 127.7, 125.5 (2C), 102.3, 57.7, 46.6, 45.0 (2C), 25.7 (2C), 24.5, 18.3.

Tert-butyl (R)-(2-hydroxypropyl)carbamate (5.201)



Boc-anhydride (2.77 g, 12.70 mmol) was dissolved in tetrahydrofuran (50 ml). This was added dropwise to a solution of (R)-(-)-1-amino-2-propanol (1 ml, 12.70 mmol) and sodium bicarbonate (5.34 g, 63.5 mmol) in water (50 ml). The reaction mixture was then stirred at ambient temperature for 18 h after which all volatiles were removed *in vacuo*. The product was extracted twice with dichloromethane, the organic layers were then combined and dried with magnesium sulphate. All volatiles were removed *in vacuo* to yield the title compound as a colourless oil (2.06 g, 92%). ^1H NMR (400 MHz, CDCl_3) δ 5.19 (s, 1H), 3.81 (s, 1H), 3.38 (s, 1H), 3.27 – 3.11 (m, 1H), 3.02 – 2.85 (m, 1H), 1.37 (s, 9H), 1.10 (d, $J = 6.3$ Hz, 3H); ^{13}C NMR (101 MHz, CDCl_3) δ 156.9, 79.6, 67.4, 47.9, 28.4 (3C), 20.6.

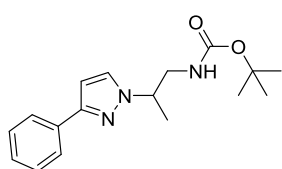
(R)-1-((Tert-butoxycarbonyl)amino)propan-2-yl methanesulfonate (5.177)



Compound **5.201** (2.06 g, 11.76 mmol) was dissolved in anhydrous dichloromethane (20 ml) under nitrogen and cooled to 0 °C. To this was added triethylamine (1.64 ml, 11.76 mmol) and methanesulfonyl chloride (910 μl , 11.76 mmol). The resulting mixture was stirred at 0 °C for 30 min before the being gradually warmed to ambient temperature. After 30 min the reaction was quenched by addition of water and the organic layer was collected and washed with water three times. The organic layer was dried with magnesium sulphate before all of the volatiles were removed *in vacuo* to yield the title compound as a colourless solid (2.38 g, 80%). ^1H NMR (400 MHz, DMSO) δ 7.40 (s, 1H), 4.87 (dtd, $J = 9.2, 6.4, 3.1$ Hz, 1H), 4.64 (dp, $J = 8.1, 6.3$ Hz, 1H), 3.90 – 3.68 (m, 1H), 3.26 (s, 3H), 2.34 (s, 9H), 1.39 (d, $J =$

6.4 Hz, 3H); ^{13}C NMR (101 MHz, CDCl_3) δ 160.5, 73.6, 47.5, 39.3, 28.5, 20.6. *Note: there are multiple equivalent carbons in the ^{13}C NMR.

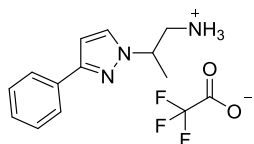
Tert-butyl (S)-2-(3-phenyl-1H-pyrazol-1-yl)propyl)carbamate (5.178)



3-Phenyl-1H-pyrazole (250 mg, 1.73 mmol), cesium carbonate (5.65 g, 17.30 mmol) and (*R*)-1-((*tert*-butoxycarbonyl)amino)propan-2-yl methanesulfonate (876 mg, 3.46 mmol) were combined in anhydrous *N,N*-dimethylformamide (10 ml).

The resulting suspension was heated to 50 °C and the progress of the reaction was monitored by TLC. Once the reaction was complete (~ 18 h) the reaction mixture was quenched by addition of water and the product was extracted with ethyl acetate three times. The organic layers were combined and washed with a saturated aqueous solution of sodium chloride. All of the volatiles were removed *in vacuo*. The crude material was purified by column chromatography, eluting with 5-10% ethyl acetate/petroleum spirits to give the title compound as a colourless solid (97 mg, 19%). LRMS $[\text{M}+\text{H}]^+$ 302.2 m/z; HRMS $[\text{M}+\text{H}]^+$ 302.1863 m/z, found m/z 302.1864 m/z; ^1H NMR (400 MHz, CDCl_3) δ 7.87 – 7.71 (m, 2H), 7.38 (dd, $J = 13.0, 5.1$ Hz, 3H), 7.31 – 7.25 (m, 1H), 6.53 (d, $J = 2.3$ Hz, 1H), 4.87 (s, 1H), 4.56 – 4.37 (m, 1H), 3.60 (ddd, $J = 13.6, 6.6, 4.1$ Hz, 1H), 3.47 (ddd, $J = 14.1, 8.5, 5.6$ Hz, 1H), 1.51 (d, $J = 6.8$ Hz, 3H), 1.40 (s, 9H); ^{13}C NMR (101 MHz, CDCl_3) δ 156.2, 151.6, 133.8, 129.9, 128.7 (2C), 127.7, 125.7 (2C), 102.5, 79.6, 57.8, 45.9, 28.5 (3C), 18.6.

(S)-2-(3-Phenyl-1H-pyrazol-1-yl)propan-1-amine (5.183)

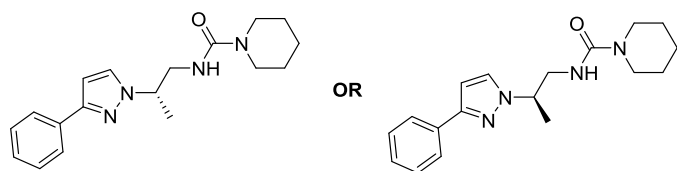


Compound **5.178** (239 mg, 0.79 mmol) was added to a 50:50 mixture of trifluoroacetic acid:dichloromethane (1 ml). The reaction mixture was stirred at ambient temperature for 18 h and TLC showed complete disappearance of starting

material. All of the volatiles were removed and the residue was washed with toluene three times. This gave the title compound as a brown oil which was used directly. LRMS $[\text{M}+\text{H}]^+$ 202.2 m/z; ^1H NMR (400 MHz, CDCl_3) δ 7.78 – 7.62 (m, 2H), 7.49 (d, $J = 2.4$ Hz, 1H), 7.41 – 7.34 (m, 2H), 7.31 (dt, $J = 9.6, 4.3$ Hz, 1H),

6.58 (d, $J = 2.4$ Hz, 1H), 4.64 (dd, $J = 12.7, 6.2$ Hz, 1H), 4.48 (s, 2H), 3.41 (d, $J = 5.7$ Hz, 2H), 1.58 (d, $J = 6.9$ Hz, 3H).

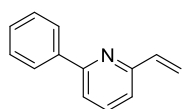
(S)-N-(2-(3-Phenyl-1H-pyrazol-1-yl)propyl)piperidine-1-carboxamide (**5.186**)



Compound **5.183** (35 mg, 0.17 mmol) was dissolved in anhydrous dichloromethane (0.5 ml) and triethylamine (125 μ l, 1.70 mmol) was added

(solution 1). In a separate flask *para*-nitrophenyl chloroformate (69 mg, 0.34 mmol) was dissolved in dichloromethane (1 ml) with stirring (solution 2). Solution 1 was then added dropwise to solution 2 and the reaction mixture was stirred for 2 h at ambient temperature. After 2 h piperidine (35 μ l, 0.34 mmol) was added to the reaction mixture which was allowed to stir at ambient temperature for 18 h. All volatiles were removed *in vacuo* and the crude material was purified by column chromatography, eluting 10-50% ethyl acetate/dichloromethane (40 mg, 75%). A portion of the material was further purified by chiral HPLC using a ChiralPAK[®] column and eluting with 10% ethanol/petroleum spirits to ensure > 99.9% e.e. This yielded the title compound as a clear oil. HPLC – rt 7.13 min > 99% purity at 254 nm; cHPLC – rt 9.84 min, 100% ee; LRMS $[M+H]^+$ 313.2 m/z; HRMS $[M+H]^+$ 313.2023 m/z, found 313.2025 m/z; ¹H NMR (400 MHz, CDCl₃) δ 7.87 – 7.70 (m, 2H), 7.41 (d, $J = 2.3$ Hz, 1H), 7.40 – 7.33 (m, 2H), 7.30 – 7.25 (m, 1H), 6.53 (d, $J = 2.3$ Hz, 1H), 5.34 (s, 1H), 4.50 (dq, $J = 8.4, 6.8, 3.5$ Hz, 1H), 3.71 (d, $J = 13.6$ Hz, 1H), 3.47 (dd, $J = 13.6, 8.5$ Hz, 1H), 3.32 – 3.15 (m, 3H), 1.50 (dd, $J = 29.9, 5.6$ Hz, 10H); ¹³C NMR (101 MHz, CDCl₃) δ 157.7, 151.6, 133.6, 129.9, 128.7 (2C), 127.7, 125.5 (2C), 102.3, 57.7, 46.6, 45.0 (2C), 25.7 (2C), 24.5, 18.3.

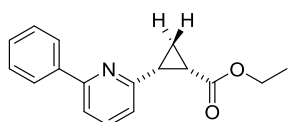
2-Phenyl-6-vinylpyridine¹³³ (**5.188**)



2-Bromo-6-phenylpyridine (959 mg, 4.10 mmol), tributyl(vinyl) tin (2.40 ml, 8.20 mmol), palladium acetate (138 mg, 0.62 mmol) and triphenylphosphine (323 mg, 1.23 mmol) were combined in tetrahydrofuran (8.2 ml) and the reaction mixture was thoroughly degassed. The reaction mixture was refluxed for 48 h and monitored for completion. Once complete, the reaction mixture was

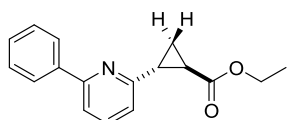
filtered through celite and the filtrate concentrated. The crude material was purified by column chromatography, eluting with 0-5% ethyl acetate/petroleum spirits to give the title compound as a clear oil (713 mg, 96%). LRMS $[M+H]^+$ 182.1 m/z; 1H NMR (400 MHz, $CDCl_3$) δ 8.08 – 8.01 (m, 2H), 7.69 (t, J = 7.8 Hz, 1H), 7.63 – 7.55 (m, 1H), 7.51 – 7.42 (m, 2H), 7.42 – 7.35 (m, 1H), 6.88 (dd, J = 17.4, 10.7 Hz, 1H), 6.34 (dd, J = 17.4, 1.4 Hz, 1H), 5.48 (td, J = 10.9, 1.4 Hz, 2H); ^{13}C NMR (101 MHz, $CDCl_3$) δ 157.0, 155.6, 139.6, 137.3, 129.1, 128.8 (2C), 127.1 (2C), 120.1, 119.8, 119.3, 118.4.

Ethyl (1S,2R)-2-(6-phenylpyridin-2-yl)cyclopropane-1-carboxylate (5.189)



The title compound was isolated as a product of the previous reaction as a colourless oil which crystallised on standing (137 mg, 13%). HPLC – rt 5.89 min > 98% purity at 254 nm; LRMS $[M+H]^+$ 268.2 m/z; HRMS $[M+H]^+$ 268.1332 m/z, found 268.1334 m/z; 1H NMR (400 MHz, $CDCl_3$) δ 7.96 (ddd, J = 4.2, 3.5, 1.8 Hz, 2H), 7.64 (t, J = 7.8 Hz, 1H), 7.53 (dd, J = 7.8, 0.5 Hz, 1H), 7.47 – 7.40 (m, 2H), 7.39 – 7.34 (m, 1H), 7.20 (d, J = 7.6 Hz, 1H), 3.87 (q, J = 7.1 Hz, 2H), 2.77 (q, J = 16.5, 8.8 Hz, 1H), 2.20 (ddd, J = 9.3, 8.0, 6.0 Hz, 1H), 1.91 (ddd, J = 7.3, 6.0, 5.0 Hz, 1H), 1.42 (ddd, J = 8.6, 8.0, 5.0 Hz, 1H), 0.95 (t, J = 7.1 Hz, 3H); ^{13}C NMR (101 MHz, $CDCl_3$) δ 171.2, 156.9, 156.5, 136.8, 128.9, 128.8 (2C), 127.1 (2C), 122.1, 118.5, 60.4, 27.3, 22.4, 14.1, 12.1.*Note: there is one quaternary carbon missing from the ^{13}C NMR.

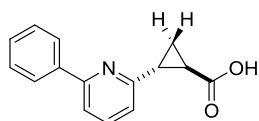
Ethyl (1R,2R)-2-(6-phenylpyridin-2-yl)cyclopropane-1-carboxylate (5.190)



2-Phenyl-6-vinylpyridine (710 mg, 3.92 mmol) was added to ethyl diazoacetate (8 ml) and the reaction mixture was refluxed for 18 h. The reaction mixture was then concentrated *in vacuo* and the crude material was purified by column chromatography, eluting with 0-10% ethyl acetate/petroleum spirits. The title compound was obtained as a colourless solid (310 mg, 30%). HPLC – rt 7.74 min > 99% purity at 254 nm; LRMS $[M+H]^+$ 268.2 m/z; HRMS $[M+H]^+$ 268.1332 m/z, found 268.1334 m/z; 1H NMR (400 MHz, $CDCl_3$) δ 8.06 – 7.97 (m, 2H), 7.65 (t, J = 7.7 Hz, 1H), 7.60 – 7.55 (m, 1H), 7.51 – 7.44 (m, 2H), 7.44 – 7.38 (m, 1H), 7.20 (dt, J = 4.0, 3.3 Hz, 1H), 4.20 (qd, J = 7.1, 1.2 Hz, 2H),

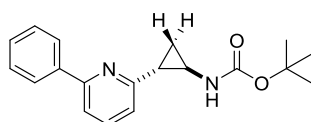
2.67 (ddd, $J = 8.0, 4.0$ Hz, 1H), 2.43 (ddd, $J = 8.5, 5.5, 3.9$ Hz, 1H), 1.77 (ddd, $J = 8.5, 6.0, 3.6$ Hz, 1H), 1.64 (ddd, $J = 8.9, 5.5, 3.6$ Hz, 1H), 1.30 (t, $J = 8.0$ Hz, 3H); ^{13}C NMR (101 MHz, CDCl_3) δ 173.7, 158.7, 156.6, 136.9, 129.1, 128.8 (2C), 126.9 (2C), 121.0, 117.9, 60.8, 27.5, 24.6, 17.8, 14.4. *Note: there is one quaternary carbon missing from the ^{13}C NMR.

(1R,2R)-2-(6-Phenylpyridin-2-yl)cyclopropane-1-carboxylic acid (**5.191**)



Ethyl (*1R,2R*)-2-(6-phenylpyridin-2-yl)cyclopropane-1-carboxylate (310 mg, 1.16 mmol) was dissolved in tetrahydrofuran (0.8 ml) and this solution was added dropwise to an solution of lithium hydroxide (56 mg, 2.32 mmol) in water (1 ml). The reaction mixture was stirred at 50 °C and monitored by LCMS and TLC for completion. Once complete (~ 2 h) the reaction mixture was neutralised by addition of an aqueous solution of 1 M hydrochloric acid. The product could then be extracted with ethyl acetate to give the title compound as an off-white solid (141 mg, 51%). HPLC – rt 6.16 min > 99% purity at 254 nm; LRMS $[\text{M}+\text{H}]^+$ 240.2 m/z; HRMS $[\text{M}+\text{H}]^+$ 240.1019 m/z, found 240.1019 m/z; ^1H NMR (400 MHz, CDCl_3) δ 8.00 – 7.94 (m, 2H), 7.62 (t, $J = 7.7$ Hz, 1H), 7.54 (dd, $J = 7.9, 1.0$ Hz, 1H), 7.47 – 7.35 (m, 3H), 7.17 (dd, $J = 7.5, 0.9$ Hz, 1H), 2.71 (ddd, $J = 8.9, 6.2, 3.8$ Hz, 1H), 2.39 (ddd, $J = 8.5, 5.4, 3.8$ Hz, 1H), 1.83 (ddd, $J = 8.4, 6.2, 3.7$ Hz, 1H), 1.66 (ddd, $J = 9.0, 5.4, 3.7$ Hz, 1H); ^{13}C NMR (101 MHz, CDCl_3) δ 179.5, 158.1, 156.7, 139.2, 137.0, 129.2, 128.8 (2C), 126.9 (2C), 121.1, 118.2, 28.2, 24.4, 18.2. *Note: the –OH peak is missing from the ^1H NMR.

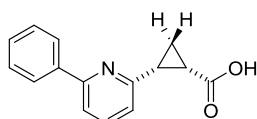
Tert-butyl ((1R,2R)-2-(6-phenylpyridin-2-yl)cyclopropyl)carbamate (**5.192**)



(1R,2R)-2-(6-phenylpyridin-2-yl)cyclopropane-1-carboxylic acid (141 mg, 0.59 mmol), diphenylphosphoryl azide (150 μl , 0.71 mmol), and triethylamine (99 μl , 0.71 mmol) were combined in anhydrous *tert*-butanol (2 ml). The reaction mixture was heated to reflux for 5 h and the progress monitored by TLC. Once complete, all of the volatiles were removed *in vacuo* and the crude material was purified by column chromatography, eluting with 0-25% ethyl acetate/petroleum spirits. The title compound was obtained as an off-white solid (75 mg, 41%). LRMS $[\text{M}+\text{H}]^+$ 311.2 m/z; HRMS

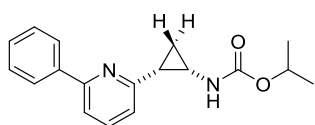
$[M+H]^+$ 311.1754 m/z, found 311.1754 m/z; $^1\text{H NMR}$ (400 MHz, CDCl_3) δ 8.01 – 7.93 (m, 2H), 7.58 (t, $J = 7.7$ Hz, 1H), 7.48 (dd, $J = 7.8, 0.8$ Hz, 1H), 7.45 – 7.38 (m, 2H), 7.38 – 7.32 (m, 1H), 7.14 (d, $J = 7.5$ Hz, 1H), 4.88 (s, 1H), 3.15 (s, 1H), 2.18 (s, 1H), 1.64 (ddd, $J = 7.4, 5.8, 5.0$ Hz, 2H), 1.42 (s, 9H).

(1S,2R)-2-(6-Phenylpyridin-2-yl)cyclopropane-1-carboxylic acid (5.193)



Ethyl (1S,2R)-2-(6-phenylpyridin-2-yl)cyclopropane-1-carboxylate (137 mg, 0.51 mmol) was dissolved in tetrahydrofuran (0.3 ml) and this solution was added dropwise to a solution of lithium hydroxide (25 mg, 1.02 mmol) in water (0.5 ml). The reaction mixture was stirred at 50 °C and monitored by LCMS and TLC for completion. Once complete (~ 2 h) the reaction mixture was neutralised by addition of an aqueous solution of 1 M hydrochloric acid. The product was extracted with ethyl acetate to give the title compound as an off-white solid (43 mg, 35%). LRMS $[M+H]^+$ 240.2 m/z; $^1\text{H NMR}$ (400 MHz, CDCl_3) δ 7.85 (t, $J = 7.9$ Hz, 1H), 7.78 (ddd, $J = 5.8, 4.2, 2.4$ Hz, 2H), 7.60 (dd, $J = 8.0, 0.9$ Hz, 1H), 7.52 – 7.44 (m, 3H), 7.41 (dd, $J = 7.8, 0.9$ Hz, 1H), 2.54 (dd, $J = 16.1, 8.4$ Hz, 1H), 2.38 (ddd, $J = 15.7, 8.4, 7.3$ Hz, 1H), 1.85 (dt, $J = 9.1, 4.6$ Hz, 1H), 1.77 (td, $J = 7.3, 5.1$ Hz, 1H). *Note: the –OH peak is missing from the $^1\text{H NMR}$.

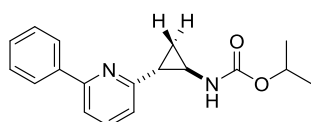
Isopropyl ((1S,2R)-2-(6-phenylpyridin-2-yl)cyclopropyl)carbamate (5.194)



(1S,2R)-2-(6-phenylpyridin-2-yl)cyclopropane-1-carboxylic acid (75 mg, 0.31 mmol), diphenylphosphoryl azide (81 μl , 0.38 mmol), and triethylamine (52 μl , 0.38 mmol) were combined in anhydrous isopropanol (5 ml). The reaction mixture was heated to reflux for 2 h and the progress monitored by TLC. Once complete, all of the volatiles were removed *in vacuo* and the crude material was purified by column chromatography, eluting with 0-25% ethyl acetate/petroleum spirits. This gave the title compound as a pale-yellow solid (53 mg, 58%) though further purification was required. A small amount of material (~12 mg) was purified by preparative TLC with 10% ethyl acetate/petroleum spirits as the eluent. This led to the isolation of the title compound as an off-white solid. LRMS $[M+H]^+$ 297.2 m/z; HRMS $[M+H]^+$ 297.1598 m/z, found 297.1600 m/z; $^1\text{H NMR}$

(400 MHz, CDCl₃) δ 8.03 – 7.96 (m, 2H), 7.61 (t, *J* = 7.7 Hz, 1H), 7.52 (dd, *J* = 7.8, 0.7 Hz, 1H), 7.48 – 7.34 (m, 3H), 7.17 (d, *J* = 7.5 Hz, 1H), 4.93 (dt, *J* = 12.5, 6.2 Hz, 2H), 3.17 (s, 1H), 2.22 (s, 1H), 1.23 (dd, *J* = 6.2, 3.4 Hz, 6H); ¹³C NMR (101 MHz, CDCl₃) δ 159.3, 156.3, 139.4, 136.6, 128.8, 128.6, 126.8, 120.6, 117.3, 77.0, 22.2, 17.2. *Note: there are two protons missing from the ¹H NMR spectrum, one from the –NH and the other is believed to be from the cyclopropane. There are multiple equivalent carbons in the ¹³C NMR spectrum.

Isopropyl ((1R,2R)-2-(6-phenylpyridin-2-yl)cyclopropyl)carbamate (5.195)



(1*R*,2*R*)-2-(6-phenylpyridin-2-yl)cyclopropane-1-carboxylic acid (75 mg, 0.31 mmol), diphenylphosphoryl azide (81 μl, 0.38 mmol), and triethylamine (52 μl, 0.38 mmol) were combined in anhydrous isopropanol (5 ml). The reaction mixture was heated to reflux for 2 h and the progress monitored by TLC. Once complete, all of the volatiles were removed *in vacuo* and the crude material was purified by column chromatography, eluting with 0-25% ethyl acetate/petroleum spirits. This gave the title compound as a pale-yellow solid (58 mg, 63%) though further purification was required. A small amount of material (~12 mg) was purified by preparative TLC with 10% ethyl acetate/petroleum spirits as the eluent. This gave the title compound as an off-white solid. LRMS [M+H]⁺ 297.2 m/z; HRMS [M+H]⁺ 297.1598 m/z, found 297.1597 m/z; ¹H NMR (400 MHz, CDCl₃) δ 8.01 – 7.92 (m, 2H), 7.59 (t, *J* = 7.7 Hz, 1H), 7.52 – 7.47 (m, 1H), 7.45 – 7.39 (m, 2H), 7.36 (dt, *J* = 9.7, 4.3 Hz, 1H), 7.15 (d, *J* = 7.4 Hz, 1H), 4.90 (dt, *J* = 12.5, 6.3 Hz, 2H), 3.14 (s, 1H), 2.20 (s, 1H), 1.68 (ddd, *J* = 7.3, 5.8, 5.1 Hz, 1H), 1.21 (dd, *J* = 6.2, 3.4 Hz, 6H). *Note: the –NH is missing from the ¹H NMR spectrum.

6. References

1. Brimacombe, K. R.; Walsh, M. J.; Liu, L.; Vásquez-Valdivieso, M. G.; Morgan, H. P.; McNae, I.; Fothergill-Gilmore, L. A.; Michels, P. A. M.; Auld, D. S.; Simeonov, A.; Walkinshaw, M. D.; Shen, M.; Boxer, M. B. Identification of ML251, a potent inhibitor of *T. brucei* and *T. cruzi* Phosphofructokinase. *ACS Med. Chem. Lett.* **2013**, 5, 12-17.
2. Nathan, H. C.; Bacchi, C. J.; Nichol, C. A.; Duch, D. S.; Mullaney, E. A.; Hutner, S. H. Antitumor phthalanilides active in acute and chronic *Trypanosoma brucei brucei* murine infections. *Am. J. Trop. Med. Hyg.* **1984**, 33, 845-850.
3. Dong, Y.; Wang, X.; Cal, M.; Kaiser, M.; Vennerstrom, J. L. Activity of diimidazoline amides against African trypanosomiasis. *Bioorg. Med. Chem. Lett.* **2014**, 24, 944-948.
4. Tatipaka, H. B.; Gillespie, J. R.; Chatterjee, A. K.; Norcross, N. R.; Hulverson, M. A.; Ranade, R. M.; Nagendar, P.; Creason, S. A.; McQueen, J.; Duster, N. A.; Nagle, A.; Supek, F.; Molteni, V.; Wenzler, T.; Brun, R.; Glynne, R.; Buckner, F. S.; Gelb, M. H. Substituted 2-phenylimidazopyridines: A new class of drug leads for human African trypanosomiasis. *J. Med. Chem.* **2013**, 57, 828-835.
5. Sykes, M. L.; Baell, J. B.; Kaiser, M.; Chatelain, E.; Moawad, S. R.; Ganame, D.; Ioset, J.-R.; Avery, V. M. Identification of compounds with anti-proliferative activity against *Trypanosoma brucei brucei* strain 427 by a whole cell viability based HTS campaign. *PLoS Negl Trop Dis* **2012**, 6, e1896.
6. Gelb, M. H. (2014), personal communication.
7. Chatterjee, A. K.; Nagle, A. S.; Paraselli, P.; Kondreddi, R. R.; Leong, S. Y.; Mishra, P. K.; Moreau, R. J.; Roland, J. T.; Sim, W. L. S.; Simon, O.; Tan, L. J.; Yeung, B. K.; Zou, B.; Bollu, V. Compounds and compositions for the treatment of parasitic diseases. WO2014078802 A1, 22/05/2014, 2014.
8. Chatterjee, A. K.; Nagle, A.; Wu, T.; Tully, D.; Kuhen, K. L. Compounds and compositions for the treatment of parasitic diseases. WO2011006143 A2, 09/07/2010, 2010.
9. Ochsenreiter, T.; Hajduk, S. The function of RNA editing in trypanosomes. In *RNA Editing*, Göringer, H. U., Ed. Springer Berlin Heidelberg: 2008; Vol. 20, pp 181-197.
10. Simpson, L.; Thiemann, O. H.; Savill, N. J.; Alfonzo, J. D.; Maslov, D. A. Evolution of RNA editing in trypanosome mitochondria. *PNAS* **2000**, 97, 6986-6993.
11. Demir, Ö.; Labaied, M.; Merritt, C.; Stuart, K.; Amaro, R. E. Computer-aided discovery of *Trypanosoma brucei* RNA-editing Terminal Uridylyl Transferase 2 inhibitors. *Chem. Biol. Drug Des.* **2014**, 84, 131-139.
12. Ferrins, L.; Rahmani, R.; Baell, J. B. Drug discovery and human African trypanosomiasis: a disease less neglected? *Future Med. Chem.* **2013**, 5, 1801-1841.
13. Wu, P.; Zhang, J.; Meng, Q.; Nare, B.; Jacobs, R. T.; Zhou, H. Novel pyrrolobenzoxaboroles: Design, synthesis, and biological evaluation against *Trypanosoma brucei*. *Euro. J. Med. Chem.* **2014**, 81, 59-75.
14. Tulloch, L. B.; Martini, V. P.; Iulek, J.; Huggan, J. K.; Lee, J. H.; Gibson, C. L.; Smith, T. K.; Suckling, C. J.; Hunter, W. N. Structure-based design of Pteridine Reductase inhibitors targeting African sleeping sickness and the Leishmaniases. *J. Med. Chem.* **2009**, 53, 221-229.

15. Spinks, D.; Ong, H. B.; Mpamhanga, C. P.; Shanks, E. J.; Robinson, D. A.; Collie, I. T.; Read, K. D.; Frearson, J. A.; Wyatt, P. G.; Brenk, R.; Fairlamb, A. H.; Gilbert, I. H. Design, synthesis and biological evaluation of novel inhibitors of *Trypanosoma brucei* Pteridine Reductase 1. *ChemMedChem* **2011**, 6, 302-308.
16. Barrett, M. P.; Fairlamb, A. H. The biochemical basis of arsenical–diamidine crossresistance in African Trypanosomes. *Parasitol. Today* **1999**, 15, 136-140.
17. Carter, N. S.; Berger, B. J.; Fairlamb, A. H. Uptake of diamidine drugs by the P2 Nucleoside transporter in Melarsen-sensitive and -resistant *Trypanosoma brucei brucei*. *J. Biol. Chem.* **1995**, 270, 28153-28157.
18. Khalaf, A. I.; Huggan, J. K.; Suckling, C. J.; Gibson, C. L.; Stewart, K.; Giordani, F.; Barrett, M. P.; Wong, P. E.; Barrack, K. L.; Hunter, W. N. Structure-based design and synthesis of antiparasitic pyrrolopyrimidines targeting Pteridine Reductase 1. *J. Med. Chem.* **2014**, 57, 6479-6494.
19. Dube, D.; Sharma, S.; Singh, T. P.; Kaur, P. Pharmacophore mapping, *in silico* screening and molecular docking to identify selective *Trypanosoma brucei* Pteridine Reductase inhibitors. *Mol. Inform.* **2014**, 33, 124-134.
20. Roussaki, M.; Hall, B.; Lima, S. C.; da Silva, A. C.; Wilkinson, S.; Detsi, A. Synthesis and anti-parasitic activity of a novel quinolinone–chalcone series. *Bioorg. Med. Chem. Lett.* **2013**, 23, 6436-6441.
21. Diaz, R.; Luengo-Arratta, S. A.; Seixas, J. D.; Amata, E.; Devine, W.; Cordon-Obras, C.; Rojas-Barros, D. I.; Jimenez, E.; Ortega, F.; Crouch, S.; Colmenarejo, G.; Fiandor, J. M.; Martin, J. J.; Berlanga, M.; Gonzalez, S.; Manzano, P.; Navarro, M.; Pollastri, M. P. Identification and characterization of hundreds of potent and selective inhibitors of *Trypanosoma brucei* growth from a kinase-targeted library screening campaign. *PLoS Negl Trop Dis* **2014**, 8, e3253.
22. Hata, Y.; Ebrahimi, S. N.; De Mieri, M.; Zimmermann, S.; Mokoka, T.; Naidoo, D.; Fouche, G.; Maharaj, V.; Kaiser, M.; Brun, R.; Potterat, O.; Hamburger, M. Antitrypanosomal isoflavan quinones from *Abrus precatorius*. *Fitoterapia* **2014**, 93, 81-87.
23. Baell, J. B.; Holloway, G. A. New substructure filters for removal of Pan Assay Interference Compounds (PAINS) from screening libraries and for their exclusion in bioassays. *J. Med. Chem.* **2010**, 53, 2719-2740.
24. Frederiksen, S.; Mallng, H.; Klenow, H. Isolation of 3'-deoxyadenosine (cordycepin) from the liquid medium of *Cordyceps militaris* (L. ex Fr.) Link. *BBA - Nucleic Acids and Protein Synthesis* **1965**, 95, 189-193.
25. Vodnala, S. K.; Lundbäck, T.; Yeheskieli, E.; Sjöberg, B.; Gustavsson, A.-L.; Svensson, R.; Olivera, G. C.; Eze, A. A.; de Koning, H. P.; Hammarström, L. G. J.; Rottenberg, M. E. Structure–activity relationships of synthetic cordycepin analogues as experimental therapeutics for African trypanosomiasis. *J. Med. Chem.* **2013**, 56, 9861-9873.
26. Rottenberg, Martin E.; Masocha, W.; Ferella, M.; Petitto-Assis, F.; Goto, H.; Kristensson, K.; McCaffrey, R.; Wigzell, H. Treatment of African trypanosomiasis with cordycepin and Adenosine Deaminase inhibitors in a mouse model. *J. Infect. Dis.* **2005**, 192, 1658-1665.
27. Vodnala, S. K.; Ferella, M.; Lundén-Miguel, H.; Betha, E.; van Reet, N.; Amin, D. N.; Öberg, B.; Andersson, B.; Kristensson, K.; Wigzell, H.; Rottenberg, M. E. Preclinical assessment of the treatment of second-stage African trypanosomiasis with cordycepin and deoxycoformycin. *PLoS Negl Trop Dis* **2009**, 3, e495.

28. Dickinson, M. J.; Holly, F. W.; Walton, E.; Zimmerman, M. 3'-Deoxynucleosides. V. 3'-Deoxy-2-fluoroadenosine. *J. Med. Chem.* **1967**, 10, 1165-1166.
29. Davis, R. A.; Sykes, M.; Avery, V. M.; Camp, D.; Quinn, R. J. Convolutamines I and J, antitrypanosomal alkaloids from the bryozoan *Amathia tortusa*. *Bioorg. Med. Chem.* **2011**, 19, 6615-6619.
30. Pham, N. B.; Deydier, S.; Labaied, M.; Monnerat, S.; Stuart, K.; Quinn, R. J. N^1, N^1 -Dimethyl- N^3 -(3-(trifluoromethyl)phenethyl)propane-1,3-diamine, a new lead for the treatment of human African trypanosomiasis. *Euro. J. Med. Chem.* **2014**, 74, 541-551.
31. Filler, R.; Saha, R. Fluorine in medicinal chemistry: a century of progress and a 60-year retrospective of selected highlights. *Future Med. Chem.* **2009**, 1, 777-791.
32. Ochiana, S. O.; Pandarinath, V.; Wang, Z.; Kapoor, R.; Ondrechen, M. J.; Ruben, L.; Pollastri, M. P. The human Aurora kinase inhibitor danusertib is a lead compound for anti-trypanosomal drug discovery via target repurposing. *Euro. J. Med. Chem.* **2013**, 62, 777-784.
33. Behera, R.; Thomas, S. M.; Mensa-Wilmot, K. New chemical scaffolds for human African trypanosomiasis lead discovery from a screen of Tyrosine Kinase inhibitor drugs. *Antimicrob. Agents Chemother.* **2014**, 58, 2202-2210.
34. Patel, G.; Roncal, N. E.; Lee, P. J.; Leed, S. E.; Erath, J.; Rodriguez, A.; Sciotti, R. J.; Pollastri, M. P. Repurposing human Aurora kinase inhibitors as leads for anti-protozoan drug discovery. *MedChemComm* **2014**, 5, 655-658.
35. Parsons, M.; Worthey, E.; Ward, P.; Mottram, J. Comparative analysis of the kinomes of three pathogenic trypanosomatids: *Leishmania major*, *Trypanosoma brucei* and *Trypanosoma cruzi*. *BMC Genomics* **2005**, 6, 1-19.
36. Tu, X.; Kumar, P.; Li, Z.; Wang, C. C. An Aurora kinase homologue is involved in regulating both mitosis and cytokinesis in *Trypanosoma brucei*. *J. Biol. Chem.* **2006**, 281, 9677-9687.
37. Li, Z.; Wang, C. C. Changing roles of Aurora-B kinase in two life cycle stages of *Trypanosoma brucei*. *Eukaryot. Cell* **2006**, 5, 1026-1035.
38. Jetton, N.; Rothberg, K. G.; Hubbard, J. G.; Wise, J.; Li, Y.; Ball, H. L.; Ruben, L. The cell cycle as a therapeutic target against *Trypanosoma brucei*: Hesperadin inhibits Aurora kinase-1 and blocks mitotic progression in bloodstream forms. *Mol. Microbiol.* **2009**, 72, 442-458.
39. Li, Z.; Umeyama, T.; Wang, C. C. The Aurora Kinase in *Trypanosoma brucei* plays distinctive roles in metaphase-anaphase transition and cytokinetic initiation. *PLoS Pathog* **2009**, 5, e1000575.
40. Fancelli, D.; Moll, J.; Varasi, M.; Bravo, R.; Artico, R.; Berta, D.; Bindi, S.; Cameron, A.; Candiani, I.; Cappella, P.; Carpinelli, P.; Croci, W.; Forte, B.; Giorgini, M. L.; Klapwijk, J.; Marsiglio, A.; Pesenti, E.; Rocchetti, M.; Roletto, F.; Severino, D.; Soncini, C.; Storici, P.; Tonani, R.; Zugnoni, P.; Vianello, P. 1,4,5,6-Tetrahydropyrrolo[3,4-c]pyrazoles: Identification of a potent Aurora kinase inhibitor with a favorable antitumor kinase inhibition profile. *J. Med. Chem.* **2006**, 49, 7247-7251.
41. Ikezoe, T.; Yang, J.; Nishioka, C.; Tasaka, T.; Taniguchi, A.; Kuwayama, Y.; Komatsu, N.; Bandobashi, K.; Togitani, K.; Koeffler, H. P.; Taguchi, H. A novel treatment strategy targeting Aurora kinases in acute myelogenous leukemia. *Mol. Cancer Ther.* **2007**, 6, 1851-1857.
42. Diaz-Gonzalez, R.; Kuhlmann, F. M.; Galan-Rodriguez, C.; da Silva, L. M.; Saldivia, M.; Karver, C. E.; Rodriguez, A.; Beverley, S. M.; Navarro, M.; Pollastri, M. P. The susceptibility of trypanosomatid pathogens to PI3/mTOR kinase inhibitors affords a new opportunity for drug repurposing. *PLoS Negl Trop Dis* **2011**, 5, e1297.

43. Novartis Pharmaceuticals. BEZ235 in patients with advanced renal cell carcinoma (RCC). <http://www.cancer.gov/clinicaltrials> (accessed Nov 10, 2014).
44. Novartis Pharmaceuticals. A Phase I/II Study of BEZ235 in patients with advanced solid malignancies enriched by patients with advanced breast cancer. <http://www.cancer.gov/clinicaltrials> (accessed Nov 10, 2014).
45. Novartis Pharmaceuticals. A Study of BEZ235 in adult Japanese patients with advanced solid tumors. <http://www.cancer.gov/clinicaltrials> (accessed Nov 10, 2014).
46. Novartis Pharmaceuticals. Study of PI3 Kinase/mTOR inhibitor BEZ235 twice daily for advanced solid tumors. <http://www.cancer.gov/clinicaltrials> (accessed Nov 10, 2014).
47. Seixas, J. D.; Luengo-Arratta, S. A.; Diaz, R.; Saldivia, M.; Rojas-Barros, D. I.; Manzano, P.; Gonzalez, S.; Berlanga, M.; Smith, T. K.; Navarro, M.; Pollastri, M. P. Establishment of a structure–activity relationship of 1*H*-imidazo[4,5-*c*]quinoline-based kinase inhibitor NVP-BEZ235 as a lead for African sleeping sickness. *J. Med. Chem.* **2014**, *57*, 4834-4848.
48. Maira, S.-M.; Stauffer, F.; Brueggen, J.; Furet, P.; Schnell, C.; Fritsch, C.; Brachmann, S.; Chène, P.; De Pover, A.; Schoemaker, K.; Fabbro, D.; Gabriel, D.; Simonen, M.; Murphy, L.; Finan, P.; Sellers, W.; García-Echeverría, C. Identification and characterization of NVP-BEZ235, a new orally available dual phosphatidylinositol 3-kinase/mammalian target of rapamycin inhibitor with potent *in vivo* antitumor activity. *Mol. Cancer Ther.* **2008**, *7*, 1851-1863.
49. Subramanya, S.; Mensa-Wilmot, K. Diacylglycerol-stimulated endocytosis of Transferrin in trypanosomatids is dependent on Tyrosine kinase activity. *PLoS ONE* **2010**, *5*, e8538.
50. Subramanya, S.; Hardin, C. F.; Steverding, D.; Mensa-Wilmot, K. Glycosylphosphatidylinositol-specific phospholipase C regulates transferrin endocytosis in the African trypanosome. *Biochem J* **2009**, *417*, 685-94.
51. Steverding, D. The transferrin receptor of *Trypanosoma brucei*. *Parasitol. Int.* **2000**, *48*, 191-198.
52. Patel, G.; Karver, C. E.; Behera, R.; Guyett, P. J.; Sullenberger, C.; Edwards, P.; Roncal, N. E.; Mensa-Wilmot, K.; Pollastri, M. P. Kinase scaffold repurposing for neglected disease drug discovery: Discovery of an efficacious, lapatanib-derived lead compound for trypanosomiasis. *J. Med. Chem.* **2013**, *56*, 3820-3832.
53. Kalgutkar, A. S.; Gardner, I.; Obach, R. S.; Shaffer, C. L.; Callegari, E.; Henne, K. R.; Mutlib, A. E.; Dalvie, D. K.; Lee, J. S.; Nakai, Y.; O'Donnell, J. P.; Boer, J.; Harriman, S. P. A comprehensive listing of bioactivation pathways of organic functional groups. *Curr. Drug Metab.* **2005**, *6*, 161-225.
54. Ioset, J.-R. Natural products for neglected diseases: A review. *Curr. Org. Chem.* **2008**, *12*, 643-666.
55. Hansch, C.; Leo, A. *Exploring QSAR: Fundamentals and applications in chemistry and biology*. American Chemical Society: Washington D.C., 1995.
56. Pajouhesh, H.; Lenz, G. R. Medicinal chemical properties of successful central nervous system drugs. *NeuroRx* **2005**, *2*, 541-53.
57. Deborggraeve, S.; Koffi, M.; Jamonneau, V.; Bonsu, F. A.; Queyson, R.; Simarro, P. P.; Herdewijn, P.; Büscher, P. Molecular analysis of archived blood slides reveals an atypical human *Trypanosoma* infection. *Diagn. Micr. Infec. Dis.* **2008**, *61*, 428-433.
58. Wager, T. T.; Hou, X.; Verhoest, P. R.; Villalobos, A. Moving beyond rules: The development of a central nervous system multiparameter optimization (CNS MPO) approach to enable alignment of druglike properties. *ACS Chem. Neurosci.* **2010**, *1*, 435-449.

59. Savjani, K. T.; Gajjar, A. K.; Savjani, J. K. Drug solubility: Importance and enhancement techniques. *ISRN Pharm.* **2012**, 2012, 10.
60. Fournier, T.; Medjoubi-N, N.; Porquet, D. Alpha-1-acid glycoprotein. *BBA - Protein Structure and Molecular Enzymology* **2000**, 1482, 157-171.
61. Kremer, J. M.; Wilting, J.; Janssen, L. H. Drug binding to human alpha-1-acid glycoprotein in health and disease. *Pharmacol. Rev.* **1988**, 40, 1-47.
62. Sykes, M. L.; Avery, V. M. Development of an Alamar Blue™ viability assay in 384-well format for high throughput whole cell screening of *Trypanosoma brucei brucei* bloodstream form strain 427. *Am. J. Trop. Med. Hyg.* **2009**, 81, 665-674.
63. Hirumi, H.; Hirumi, K. Continuous cultivation of *Trypanosoma brucei* blood stream forms in a medium containing a low concentration of serum protein without feeder cell layers. *J. Parasitol.* **1989**, 75, 985-989.
64. Desjardins, R. E.; Canfield, C. J.; Haynes, J. D.; Chulay, J. D. Quantitative assessment of antimalarial activity *in vitro* by a semiautomated microdilution technique. *Antimicrob. Agents Chemother.* **1979**, 16, 710-718.
65. Matile, H.; Pink, J. R. L. *Plasmodium falciparum* malaria parasite cultures and their use in immunology. In *Immunological Methods*, Lefkovits, I.; Pernis, B., Eds. Academic Press: San Diego, 1990.
66. Ponnudurai, T.; Leeuwenberg, A. D.; Meuwissen, J. H. Chloroquine sensitivity of isolates of *Plasmodium falciparum* adapted to *in vitro* culture. *Trop. Geogr. Med.* **1981**, 33, 50-54.
67. Huber, W.; Koella, J. C. A comparison of three methods of estimating EC₅₀ in studies of drug resistance of malaria parasites. *Acta Trop.* **1993**, 55, 257-261.
68. Cunningham, M. L.; Fairlamb, A. H. Trypanothione reductase from *Leishmania donovani*. Purification, characterisation and inhibition by trivalent antimonials. *Eur. J. Biochem.* **1995**, 230, 460-468.
69. Mikus, J.; Steverding, D. A simple colorimetric method to screen drug cytotoxicity against *Leishmania* using the dye Alamar Blue®. *Parasitol Int* **2000**, 48, 265-269.
70. Buckner, F. S.; Verlinde, C. L.; La Famme, A. C.; CVan Voorhis, W. C. Efficient technique for screening drugs for activity against *Trypanosoma cruzi* using parasites expressing beta-galactosidase. *Antimicrob. Agents Chemother.* **1996**, 40, 2592-2597.
71. Baltz, T.; Baltz, D.; Giroud, C.; Crockett, J. Cultivation in a semi-defined medium of animal infective forms of *Trypanosoma brucei*, *T. equiperdum*, *T. evansi*, *T. rhodesiense* and *T. gambiense*. *EMBO J.* **1985**, 4, 1273-1277.
72. Rüz, B.; Iten, M.; Grether-Bühler, Y.; Kaminsky, R.; Brun, R. The Alamar Blue® assay to determine drug sensitivity of African trypanosomes (*T.b. rhodesiense* and *T.b. gambiense*) *in vitro*. *Acta Trop.* **1997**, 68, 139-147.
73. Page, B.; Page, M.; Noel, C. A new fluorometric assay for cytotoxicity measurements *in vitro*. *Int. J. Oncol.* **1993**, 3, 473-476.
74. Ahmed, S. A.; Gogal, R. M.; Walsh, J. E. A new rapid and simple non-radioactive assay to monitor and determine the proliferation of lymphocytes: an alternative to [³H]thymidine incorporation assay. *J. Immunol. Methods* **1994**, 170, 211-224.

75. Bevan, C. D.; Lloyd, R. S. A high-throughput screening method for the determination of aqueous drug solubility using laser nephelometry in microtiter plates. *Anal. Chem.* **2000**, 72, 1781-1787.
76. Lombardo, F.; Shalaeva, M. Y.; Tupper, K. A.; Gao, F. ElogDoct: A tool for lipophilicity determination in drug discovery. 2. Basic and neutral compounds. *J. Med. Chem.* **2001**, 44, 2490-2497.
77. Valko, K.; Nunhuck, S.; Bevan, C.; Abraham, M. H.; Reynolds, D. P. Fast gradient HPLC method to determine compounds binding to human serum albumin. Relationships with octanol/water and immobilized artificial membrane lipophilicity. *J. Pharm. Sci.* **2003**, 92, 2236-2248.
78. Obach, R. S. Prediction of human clearance of twenty-nine drugs from hepatic microsomal intrinsic clearance data: An examination of *in vitro* half-life approach and nonspecific binding to microsomes. *Drug Metab Dispos* **1999**, 27, 1350-1359.
79. Davies, B.; Morris, T. Physiological parameters in laboratory animals and humans. *Pharm. Res.* **1993**, 10, 1093-1095.
80. Hansch, C.; Steward, A. R.; Anderson, S. M.; Bentley, D. L. Parabolic dependence of drug action upon lipophilic character as revealed by a study of hypnotics. *J. Med. Chem.* **1968**, 11, 1-11.
81. Nunes, J. J.; Milne, J.; Bernis, J.; Xie, R.; Vu, C. B.; Ng, P. Y.; Disch, J. S. Imidazopyridine derivatives as sirtuin modulating agents. WO2007019345 A1, 2007.
82. Milburn, M.; Milne, J.; Bemis, J.; Nunes, J. J.; Xie, R.; Normington, K. D.; Vu, C. B. *N*-Phenyl benzamide derivatives as sirtuin modulators. WO2006094236, 2006.
83. Bonham, L.; Leung, D. W.; Hollenback, D. M.; Klein, J. P.; Finney, R. E.; White, T., H.; Shaffer, S. A.; Tang, N. M. Benzoxazole LPAAT-beta inhibitors and uses thereof. WO2002036580 A9, 2002.
84. Huber, J. L.; McDonagh, T. E. Therapeutic compounds and related methods of use. EP2521549 A1, 2009.
85. Bemis, J. E.; Vu, C. B.; Xie, R.; Nunes, J. J.; Ng, P. Y.; Disch, J. S.; Milne, J. C.; Carney, D. P.; Lynch, A. V.; Jin, L.; Smith, J. J.; Lavu, S.; Iffland, A.; Jirousek, M. R.; Perni, R. B. Discovery of oxazolo[4,5-*b*]pyridines and related heterocyclic analogs as novel SIRT1 activators. *Bioorg. Med. Chem. Lett.* **2009**, 19, 2350-2353.
86. Kowieski, T. M.; Lee, S.; Denu, J. M. Acetylation-dependent ADP-ribosylation by *Trypanosoma brucei* Sir2. *J. Biol. Chem.* **2008**, 283, 5317-5326.
87. Alsford, S.; Kawahara, T.; Isamah, C.; Horn, D. A sirtuin in the African trypanosome is involved in both DNA repair and telomeric gene silencing but is not required for antigenic variation. *Mol. Microbiol.* **2007**, 63, 724-736.
88. Tsukinoki, T.; Tsuzuki, H. Organic reaction in water. Part 5. Novel synthesis of anilines by zinc metal-mediated chemoselective reduction of nitroarenes. *Green Chem.* **2001**, 3, 37-38.
89. Niemczyk, H. J. Ribonucleoside-tribose. US6518254 B1, 2002.
90. Losos, G. J.; Ikede, B. O. Review of pathology of diseases in domestic and laboratory animals caused by *Trypanosoma congolense*, *T. vivax*, *T. brucei*, *T. rhodesiense* and *T. gambiense*. *Vet. Pathol.* **1972**, 9, 1-79.
91. Peregrine, A. S.; Mamman, M. Pharmacology of diminazene: a review. *Acta Trop.* **1993**, 54, 185-203.

92. Kinabo, L. D. B. Pharmacology of existing drugs for animal trypanosomiasis. *Acta Trop.* **1993**, *54*, 169-183.
93. Picard, J. A.; Roark, W. H.; Sliskovic, D. R. 6,5-Fused bicyclic heterocycles. WO2001096336 A3, 2000.
94. Chai, Y.; Paul, A.; Rettig, M.; Wilson, W. D.; Boykin, D. W. Design and synthesis of heterocyclic cations for specific DNA recognition: From AT-rich to mixed-base-pair DNA sequences. *J. Org. Chem.* **2014**, *79*, 852-866.
95. van de Waterbeemd, H.; Camenisch, G.; Folkers, G.; Chretien, J. R.; Raevsky, O. A. Estimation of blood-brain barrier crossing of drugs using molecular size and shape, and H-bonding descriptors. *J. Drug Target.* **1998**, *6*, 151-165.
96. Fichert, T.; Yazdaniyan, M.; Proudfoot, J. R. A structure-permeability study of small drug-like molecules. *Bioorg. Med. Chem. Lett.* **2003**, *13*, 719-722.
97. Lovering, F.; Bikker, J.; Humblet, C. Escape from flatland: Increasing saturation as an approach to improving clinical success. *J. Med. Chem.* **2009**, *52*, 6752-6756.
98. Bordwell, F. G.; Harrelson, J. A.; Lynch, T.-Y. Homolytic bond dissociation energies for the cleavage of alpha-N-H bonds in carboxamides, sulfonamides, and their derivatives. The question of synergism in nitrogen-centered radicals. *J. Org. Chem.* **1990**, *55*, 3337-3341.
99. Bordwell, F. G.; Algrim, D. J. Acidities of anilines in dimethyl sulfoxide solution. *J. Am. Chem. Soc.* **1988**, *110*, 2964-2968.
100. Falco, J. L.; Palomer, A.; Guglietta, A. Imidazo[1,2-a]pyridine compounds, compositions, uses and methods related thereto. WO2006051063 A1, 2006.
101. Blurton, P.; Fletcher, S.; Hamblett, C.; Harrison, T.; Munoz, B.; Otte, K.; Rivkin, A.; Siliphaivanh, P.; Teall, M. Piperazine derivatives for treatment of AD and related conditions. WO2008099210 A3, 2008.
102. Jeanjot, P.; Bruyneel, F.; Arrault, A.; Gharbi, S.; Cavalier, J.-F.; Abels, A.; Marchand, C.; Touillaux, R.; Rees, J.-F.; Marchand-Brynaert, J. *N*-(Alkyl)-2-amino-1,4-pyrazine derivatives: Synthesis and antioxidative properties of 3- and 3,5-*p*-hydroxyphenyl-substituted compounds. *Synthesis* **2003**, *4*, 0513-0522.
103. Chatterjee, A. K.; Nagle, A. S.; Paraselli, P.; Leong, S. Y.; Roland, J. T.; Mishra, P. K.; Yeung, B. K.; Zou, B. Compounds and compositions for the treatment of parasitic diseases. WO2014078813 A1, 2014.
104. Chan, T. Y.; Hong, L.; Mccoy, M. A.; Mckittrick, B.; Prongay, A.; Pu, H.; Xiao, L. Kinase inhibitors. WO2007126964 A3, 2007.
105. Valeur, E.; Bradley, M. Amide bond formation: Beyond the myth of coupling reagents. *Chem. Soc. Rev.* **2009**, *38*, 606-631.
106. Meanwell, N. A. Synopsis of some recent tactical application of bioisosteres in drug design. *J. Med. Chem.* **2011**, *54*, 2529-2591.
107. Bell, M. G.; Cao, G.; Escribano, A. M.; Fernandez, M. C.; Mantlo, N. B.; Martin, D. L. N. E. M.; Mateo, H. A. I.; Mayhugh, D. R.; Wang, X. Composés et procédés destinés au traitement de la dyslipidémie. WO2005097805 A1, 2005.
108. Burger, M.; Lindvall, M.; Han, W.; Lan, J.; Nishiguchi, G.; Shafer, C.; Bellamacina, C.; Huh, K.; Atallah, G.; McBride, C. Pim kinase inhibitors and methods of their use. US20140249135 A1, 2008.

109. White, G. A. Substituted benzanilides: Structural variation and inhibition of complex II activity in mitochondria from a wild-type strain and a carboxin-selected mutant strain of *Ustilago maydis*. *Pest. Biochem. Phys.* **1987**, 27, 249-260.
110. Morales, J.; Mogi, T.; Mineki, S.; Takashima, E.; Mineki, R.; Hirawake, H.; Sakamoto, K.; Omura, S.; Kita, K. Novel mitochondrial complex II isolated from *Trypanosoma cruzi* is composed of 12 peptides including a heterodimeric Ip subunit. *J. Biol. Chem.* **2009**, 284, 7255-7263.
111. Zeiman, E.; Greenblatt, C.L.; Elgavish, S.; Khozin-Goldberg, I.; Golenser, J. Mode of action of fenarimol against *Leishmania* spp. *J Parasitol* **2008**, 94, 280-286.
112. Urbina, J. A.; Payares, G.; Molina, J.; Sanoja, C.; Liendo, A.; Lazard, K.; Piras, M. M.; Piras, R.; Perez, N.; Wincker, P.; Ryley, J. F. Cure of short- and long-term experimental Chagas' disease using D0870. *Science* **1996**, 273, 969-971.
113. Gamo, F.-J.; Sanz, L. M.; Vidal, J.; de Cozar, C.; Alvarez, E.; Lavandera, J.-L.; Vanderwall, D. E.; Green, D. V. S.; Kumar, V.; Hasan, S.; Brown, J. R.; Peishoff, C. E.; Cardon, L. R.; Garcia-Bustos, J. F. Thousands of chemical starting points for antimalarial lead identification. *Nature* **2010**, 465, 305-310.
114. Montalbetti, C. A. G. N.; Falque, V. Amide bond formation and peptide coupling. *Tetrahedron* **2005**, 61, 10827-10852.
115. Valeur, E.; Bradley, M. Amide bond formation: beyond the myth of coupling reagents. *Chem. Soc. Rev.* **2009**, 38, 606-631.
116. Hwang, J. Y.; Smithson, D.; Connelly, M.; Maier, J.; Zhu, F.; Guy, K. R. Discovery of halonitrobenzamides with potential application against human African trypanosomiasis. *Bioorg. Med. Chem. Lett.* **2010**, 20, 149-152.
117. Hwang, J. Y.; Smithson, D.; Zhu, F.; Holbrook, G.; Connelly, M. C.; Kaiser, M.; Brun, R.; Guy, R. K. Optimization of chloronitrobenzamides (CNBs) as therapeutic leads for human African trypanosomiasis (HAT). *J. Med. Chem.* **2013**, 56, 2850-2860.
118. Knochel, P.; Dohle, W.; Gommermann, N.; Kneisel, F. F.; Kopp, F.; Korn, T.; Sapountzis, I.; Vu, V. A. highly functionalized organomagnesium reagents prepared through halogen-metal exchange. *Angew. Chem. Int. Ed.* **2003**, 42, 4302-4320.
119. Zhou, Q.; Zhang, B.; Su, L.; Jiang, T.; Chen, R.; Du, T.; Ye, Y.; Shen, J.; Dai, G.; Han, D.; Jiang, H. Palladium-catalyzed highly regioselective 2-arylation of 2,x-dibromopyridines and its application in the efficient synthesis of a 17 β -HSD1 inhibitor. *Tetrahedron* **2013**, 69, 10996-11003.
120. Brown, M. L.; Aaron, W.; Austin, R. J.; Chong, A.; Huang, T.; Jiang, B.; Kaizerman, J. A.; Lee, G.; Lucas, B. S.; McMinn, D. L.; Orf, J.; Rong, M.; Toteva, M. M.; Xu, G.; Ye, Q.; Zhong, W.; DeGraffenreid, M. R.; Wickramasinghe, D.; Powers, J. P.; Hungate, R.; Johnson, M. G. Discovery of amide replacements that improve activity and metabolic stability of a bis-amide smoothed antagonist hit. *Bioorg. Med. Chem. Lett.* **2011**, 21, 5206-5209.
121. Wang, G.; Beigelman, L.; Truong, A.; Napolitano, C.; Andreotti, D.; He, H. Compounds for the treatment of paramyxovirus viral infections. WO2014031784 A1, 2014.
122. Wohlfahrt, G.; Törmäkangas, O.; Salo, H.; Höglund, L.; Karjalainen, A.; Knuutila, P.; Holm, P.; Rasku, S.; Vesalainen, A. Androgen receptor modulating compounds. WO2011051540 A8, 2010.
123. Nozawa, D.; Suzuki, R.; Futamura, A.; Shimono, R.; Abe, M.; Ohta, H.; Araki, Y. Pyrazole derivative. US20130281465 A1, 2013.

124. Dombroski, M. A.; Duplantier, A. J.; Subramanyam, C. Benzamide inhibitors of the P2X7 receptor. US7186742 B2, 2004.
125. Bialy, L.; Lorenz, K.; Wirth, K.; Steinmeyer, K.; Hessler, G.; Pernerstorfer, J.; Brendel, J. Substituted 4,5,6,7-tetrahydro-1*H*-pyrazolo[4,3-*c*]pyridines, their use as medicament, and pharmaceutical preparations comprising them. CA2845473 A1, 2013.
126. Crew, A. P.; Dong, H.; Ferraro, C.; Sherman, D.; Siu, K. W. Macrocyclic kinase inhibitors. US20130261086 A1, 2012.
127. Boys, M. L.; Burgess, L. E.; Groneberg, R. D.; Harvey, D. M.; Huang, L.; Kercher, T.; Kraser, C. F.; Laird, E.; Tarlton, E.; Zhao, Q. 5,7-Substituted-imidazo[1,2-*c*]pyrimidines as inhibitors of Jak kinases. WO2011130146 A1, 2011.
128. Baell, J. B.; Burgess, A. W.; Lessene, G. L.; Maruta, H. Protein kinase inhibitors and methods of treatment. WO2012003544 A1, 2012.
129. Solladié-Cavallo, A.; Isarno, T. Unambiguous and rapid cis/trans assignment of aryl-carboxy disubstituted cyclopropanes using NMR. *Tetrahedron Lett.* **1999**, 40, 1579-1582.
130. Pena, I.; Pilar Manzano, M.; Cantizani, J.; Kessler, A.; Alonso-Padilla, J.; Bardera, A. I.; Alvarez, E.; Colmenarejo, G.; Cotillo, I.; Roquero, I.; de Dios-Anton, F.; Barroso, V.; Rodriguez, A.; Gray, D. W.; Navarro, M.; Kumar, V.; Sherstnev, A.; Drewry, D. H.; Brown, J. R.; Fiandor, J. M.; Julio Martin, J. New compound sets identified from high throughput phenotypic screening against three kinetoplastid parasites: An open resource. *Sci. Rep.* **2015**, 5.
131. Park, B. K.; Kitteringham, N. R.; O'Neill, P. M. Metabolism of fluorine-containing drugs. *Annu. Rev. Pharmacol.* **2001**, 41, 443-470.
132. Giblin, G. M. P.; Macpherson, D. T.; Witty, D. R.; Stanway, S. J. Novel compounds. WO2013175206, 2013.
133. Komanduri, V.; Grant, C. D.; Krische, M. J. Branch-selective reductive coupling of 2-vinyl pyridines and imines via Rhodium catalyzed C-C bond forming hydrogenation. *J. Am. Chem. Soc.* **2008**, 130, 12592-12593.

7. Appendix

Supporting Information

Pyridyl benzamides as a novel class of potent inhibitors for the kinetoplastid *Trypanosoma brucei*

Lori Ferrins,^{1,†} Michelle Gazdik,^{2,3,†} Raphaël Rahmani,¹ Swapna Varghese,² Melissa L. Sykes,⁴ Amy J. Jones,⁴ Vicky M. Avery,⁴ Karen L. White,⁵ Eileen Ryan,⁵ Susan A. Charman,^{1,5} Marcel Kaiser,^{6,7} Christel A. S. Bergström,^{8,9} Jonathan B. Baell.^{1,3,10} *

¹ Medicinal Chemistry, Monash Institute of Pharmaceutical Sciences, Monash University, Parkville, Victoria, 3052, Australia.

² Department of Chemistry, La Trobe Institute for Molecular Science, La Trobe University, Melbourne, Victoria 3086, Australia.

³ The Walter and Eliza Hall Institute, 1G Royal Parade, Parkville, Victoria, 3052, Australia.

⁴ Eskitis Institute for Drug Discovery, Griffith University, Brisbane Innovation Park, Don Young Road, Nathan, Queensland, 4111, Australia.

⁵ Centre for Drug Candidate Optimisation, Monash University, Parkville, Victoria, 3052, Australia.

⁶ Swiss Tropical and Public Health Institute, Socinstrasse 57, Basel, 4051, Switzerland.

⁷ University of Basel, Petersplatz 1, Basel, 4003, Switzerland.

⁸ Drug Delivery, Disposition and Dynamics, Monash Institute of Pharmaceutical Sciences, Monash University, Parkville, Victoria, 3052, Australia.

⁹ Department of Pharmacy, Uppsala University, Biomedical Center P.O. Box 580, SE-751 23 Uppsala, Sweden

¹⁰ Department of Medical Biology, University of Melbourne, Parkville, Victoria, 3010, Australia

*Corresponding Author: Prof. Jonathan Baell, 

Table of contents

Physicochemical Experimental	S2
Biological Experimental	S2
General Chemistry Experimental	S4
General Chemistry Procedures	S5
Compound Characterization	S6
References	S21

Physicochemical studies

Solubility Estimates using Nephelometry Stock solutions of compound (10 mg/mL) prepared in DMSO were spiked into either pH 6.5 phosphate buffer or 0.01 M HCl (approximately pH 2.0) with the final DMSO concentration being 1% (v/v). Samples were then analysed by nephelometry to determine the solubility range as described previously.²⁴

Chromatographic LogD Measurement Partition coefficients (LogD) were estimated by comparing the chromatographic retention properties of each compound at pH 7.4 to the retention characteristics of a series of standard compounds with known partition coefficients. Data were collected using a Waters 2795 HPLC instrument with a Waters 2487 dual channel UV detector with a Synergy Hydro-RP 4 μm (30 mm x 2 mm) column. The mobile phase consisted of aqueous buffer (50 mM ammonium acetate, pH 7.4) and acetonitrile, with an acetonitrile gradient of 0 – 100% over 10 min. Compound elution was monitored at 220 and 254 nm. This method is a gradient HPLC method based on that originally described by Lombardo.²⁵

Chromatographic Protein Binding Estimation Plasma protein binding values were estimated using a chromatographic method whereby the retention characteristics on a human albumin column (Chromtech Chiral-HSA 50 mm x 3.0 mm, 5 μm , Sigma-Aldrich) were compared to the retention characteristics of a series of compounds with known human protein binding values. The method is a modification of a previously published method.²⁶ A Waters 2795 HPLC system equipped with a Waters 2487 dual channel UV detector (monitored at 220 and 254 nm) was used with a mobile phase comprised of aqueous buffer (25 mM ammonium acetate buffer, pH 7.4) and 30% isopropyl alcohol in the same buffer. The isopropanol concentration gradient varied over 10 min and the column was reconditioned prior to the next injection.

In Vitro Metabolism in Human Liver Microsomes A 10 mg/mL stock solution was prepared in DMSO and diluted in 50% acetonitrile/water to a spiking concentration of 500 μM . This solution was then diluted 1 in 500 to give a final compound concentration of 1 μM and incubated at 37°C in the presence of human liver microsomes (XenoTech LLC, Lenexa, Kansas City) suspended in 0.1 M phosphate buffer (pH 7.4) at a final protein concentration of 0.4 mg/mL. An NADPH-regenerating system (1 mg/mL NADP, 1 mg/mL glucose-6-phosphate, 1 U/mL glucose-6-phosphate dehydrogenase and 0.67 mg/mL MgCl_2) were added to initiate the metabolic reactions, which were subsequently quenched with ice-cold acetonitrile at various time points over 60 min. Samples were centrifuged for 3 min at 10,000 rpm and the amount of parent compound remaining in the supernatant quantified by LC-MS using a Waters Micromass ZQ coupled to a Waters Alliance 2975 HPLC. The first order rate constant for substrate depletion was determined by fitting the data to an exponential decay function and these values were used to calculate the in vitro intrinsic clearance (CL_{int}) and the predicted in vivo intrinsic clearance value ($\text{CL}_{\text{int vivo}}$) as described previously.²⁷ The predicted in vivo hepatic extraction ratio (E_{H}) was calculated using the following relationship: $E_{\text{H}} = \text{CL}_{\text{int vivo}} / (\text{Q} + \text{CL}_{\text{int vivo}})$ where Q is human liver blood flow (20.7 mL/min/kg).²⁸

Biological Assays

All *in vitro* assays were carried out *at least* twice independently in singleton. The IC_{50} values are the means of two independent assays and vary by less than $\pm 50\%$.

***P. falciparum* assay** In vitro activity against erythrocytic stages of *P. falciparum* was determined using a ³H-hypoxanthine incorporation assay,^{29, 30} using the drug sensitive NF54 strain³¹ and the standard drug chloroquine (Sigma C6628). Compounds were dissolved in DMSO at 10 mg/mL and added to parasite cultures incubated in RPMI 1640 medium without hypoxanthine, supplemented with HEPES (5.94 g/L), NaHCO_3 (2.1 g/L), neomycin (100 U/mL), Albumax^R (5 g/L) and washed human red cells (type A⁺) at 2.5% haematocrit (0.3% parasitaemia). Serial drug dilutions of eleven 3-fold dilution steps covering a range from 100 to 0.002 $\mu\text{g/mL}$ were prepared. The 96-well plates were incubated in a humidified atmosphere at 37°C; 4% CO_2 , 3% O_2 , 93% N_2 . After 48 h, 50 μL of ³H-hypoxanthine (0.5 μCi) was added to each well of the plate. The plates were incubated for a further 24 h under the same conditions. The plates were then harvested with a BetaplateTM cell harvester (Wallac, Zurich, Switzerland), and the red blood cells transferred onto a glass fibre filter and washed with distilled water. The dried filters were inserted into a plastic foil with 10 mL of scintillation fluid, and counted in a BetaplateTM liquid scintillation counter (Wallac, Zurich, Switzerland). IC_{50} values were calculated from sigmoidal inhibition curves by linear regression³² using Microsoft Excel. Chloroquine and artemisinin we used as controls.

***L. donovani* axenic amastigotes assay** Amastigotes of *L. donovani* strain MHOM/ET/67/L82 were grown in axenic culture at 37°C in SM medium³³ at pH 5.4 supplemented with 10% heat-inactivated fetal bovine serum under an atmosphere of 5% CO_2 in air. 100 μL of culture medium with 10^5 amastigotes from axenic culture with or without a serial drug dilution were seeded in 96-well microtitre plates. Serial drug dilutions of eleven 3-fold dilution steps covering a range from 100 to 0.002 $\mu\text{g/mL}$ were prepared. After 70 h of incubation the plates were inspected under an inverted microscope to assure growth of the controls and sterile conditions. 10 μL of Alamar Blue (12.5 mg resazurin dissolved in 100 mL distilled water)³⁴ were then added to each well and the plates incubated for another 2 h. The plates were read with a Spectramax Gemini XS microplate fluorometer (Molecular Devices Cooperation, Sunnyvale, CA,

USA) using an excitation wavelength of 536 nm and an emission wavelength of 588 nm. Data were analyzed using the software Softmax Pro (Molecular Devices Cooperation, Sunnyvale, CA, USA). Decrease of fluorescence (i.e. inhibition) was expressed as percentage of the fluorescence of control cultures and plotted against the drug concentrations. From the sigmoidal inhibition curves the IC₅₀ values were calculated by linear regression.³² Miltefosine was used as a control.

***T. cruzi* assay** Rat skeletal myoblasts (L-6 cells) were seeded in 96-well microtitre plates at 2000 cells/well in 100 µL RPMI 1640 medium with 10% FBS and 2 mM l-glutamine. After 24 h, the medium was removed and replaced by 100 µL per well containing 5000 trypomastigote forms of *T. cruzi* Tulahuen strain C2C4 containing the β-galactosidase (Lac Z) gene.³⁵ After 48 h the medium was removed from the wells and replaced by 100 µL fresh medium with or without a serial drug dilution of eleven 3-fold dilution steps covering a range from 100 to 0.002 µg/mL. After 96 h of incubation the plates were inspected under an inverted microscope to assure growth of the controls and sterility and the substrate CPRG/Nonidet (50 µL) was added to all wells. A color reaction developed within 2–6 h and could be read photometrically at 540 nm. Data were analyzed with the graphic programme Softmax Pro (Molecular Devices), which calculated IC₅₀ values by linear regression³² from the sigmoidal dose inhibition curves. Benznidazole was used as a control.

***T. brucei rhodesiense* assay** This parasite stock was isolated in 1982 from a human patient in Tanzania and after several mouse passages cloned and adapted to axenic culture conditions.³⁶ Minimum Essential Medium (50 µL) supplemented with 25 mM HEPES, 1 g/L additional glucose, 1% MEM non-essential amino acids (100x), 0.2 mM 2-mercaptoethanol, 1 mM Na-pyruvate and 15% heat inactivated horse serum was added to each well of a 96-well microtiter plate. Serial drug dilutions of eleven 3-fold dilution steps covering a range from 100 to 0.002 µg/mL were prepared. Then 4x10³ bloodstream forms of *T.b. rhodesiense* STIB 900 in 50 µL was added to each well and the plate incubated at 37°C under a 5% CO₂ atmosphere for 70 h. 10 µL Alamar Blue (resazurin, 12.5 mg in 100 mL double-distilled water) was then added to each well and incubation continued for a further 2–4 h.³⁷ Then the plates were read with a Spectramax Gemini XS microplate fluorometer (Molecular Devices Cooperation, Sunnyvale, CA, USA) using an excitation wavelength of 536 nm and an emission wavelength of 588 nm. The IC₅₀ values were calculated by linear regression³² from the sigmoidal dose inhibition curves using SoftmaxPro software (Molecular Devices Cooperation, Sunnyvale, CA, USA). Melarsoprol was used as a control.

Rat skeletal myoblast cytotoxicity assay Assays were performed in 96-well microtiter plates, each well containing 100 µL of RPMI 1640 medium supplemented with 1% L-glutamine (200 mM) and 10% fetal bovine serum, and 4000 L-6 cells (a primary cell line derived from rat skeletal myoblasts).^{38, 39} Serial drug dilutions of eleven 3-fold dilution steps covering a range from 100 to 0.002 µg/mL were prepared. After 70 h of incubation the plates were inspected under an inverted microscope to assure growth of the controls and sterile conditions. 10 µL of Alamar Blue was then added to each well and the plates incubated for another 2 h. The plates were then read with a Spectramax Gemini XS microplate fluorometer (Molecular Devices Cooperation, Sunnyvale, CA, USA) using an excitation wavelength of 536 nm and an emission wavelength of 588 nm. The IC₅₀ values were calculated by linear regression³² from the sigmoidal dose inhibition curves using SoftmaxPro software (Molecular Devices Cooperation, Sunnyvale, CA, USA). Podophyllotoxine was used as a control.

***T.b. brucei* assay** Compound activity against *T.b. brucei* was assessed in an Alamar blue® viability assay as previously described by Sykes and Avery.⁴⁰ Briefly, 55 µL of HMI-9 media +10% FCS⁴¹ containing 1200 cells/mL of logarithmic phase *T.b. brucei* 427 bloodstream parasites were added to a 384-well microtiter plate (BD biosciences) and incubated for 24 h at 37°C/5% CO₂. Serial drug concentrations were prepared in 100% DMSO and diluted 1:21 in DMEM media. 5 µL of this dilution was subsequently added to assay plates to give final compound concentrations ranging from 41.67 to 0.0004 µM. Plates were incubated for 48 h at 37°C/5% CO₂. 10 µL of 70% Alamar Blue® (Invitrogen) prepared in HMI-9 media +10% FCS was added to assay plates and plates incubated for a further 2 h at 37°C/5% CO₂ followed by 22 h at room temperature. Assay plates were read at 535 nm excitation/590 nm emission on an Envision® multiplate reader (PerkinElmer, Massachusetts, USA). Data was analysed and IC₅₀ values calculated using the software GraphPad Prism 5. Pentamidine and suramin are used as controls.

HEK293 cytotoxicity assay 55 µL of DMEM +10% FCS media (Gibco) containing 72727 cells/mL of confluent HEK293 cells was added to a 384-well microtiter plate (BD biosciences) and incubated for 24 h at 37°C/5% CO₂. Serial compound concentrations were prepared in 100% DMSO and diluted 1:21 in DMEM media. 5 µL of this dilution was subsequently added to assay plates to give final compound concentrations ranging from 83.34 to 0.0004 µM. Plates were incubated for 48 h at 37°C/5% CO₂. 10 µL of 70% Alamar Blue® (Invitrogen) prepared in DMEM media +10% FCS was added to assay plates and plates incubated for a further 5 h at 37°C/5% CO₂ followed by 19 h at room temperature. Assay plates were read at 535 nm excitation/590 nm emission on an En vision® multiplate reader (PerkinElmer, Massachusetts, USA). Data was analysed and IC₅₀ values calculated using the software GraphPad Prism 5. Puromycin is used as a control.

General Chemistry Experimental

Analytical thin-layer chromatography was performed on silica gel 60 F₂₅₄ pre-coated aluminium sheets (0.25 mm, Merck) and visualized at 254 nm or by chemical staining with a solution ceric sulfate/phosphomolybdic acid followed by heating. Flash column chromatography was carried out using Merck silica gel 60, 0.63 – 0.20 mm (70-230 mesh). The purity of all compounds for biological testing was > 95% in all cases, except where specified otherwise.

Experimental conditions (Exp1): All non-aqueous reactions were performed under an atmosphere of dry nitrogen, unless otherwise specified. Melting points were recorded on an 'OptiMelt' automated melting point system and are uncorrected. The solvent for recrystallisations for melting point is noted in brackets. Automated flash chromatography was performed on the Biotage Flash Master II, while manual flash chromatography was carried out with silica gel supplied by Merck chemicals. NMR spectra were recorded on a Bruker UltraShield 300 with the solvents indicated (¹H NMR at 300 MHz; ¹³C NMR at 75 MHz). Chemical shifts are recorded as δ values in parts per million (ppm) values, referenced to the appropriate solvent peak (ie. CHCl₃ = 7.26 and 77.16, MeOH = 3.31 and 49.00, DMSO = 2.50 and 39.52) and coupling constants (*J*) were recorded in Hz. Infrared spectra were obtained on a Bruker Tensor 27 FT-IR spectrometer at a resolution of 4cm⁻¹ and absorptions are given in wavenumbers (cm⁻¹). Liquid Chromatography-Mass spectrometry (LCMS) was performed on two different instruments, a Finnigan LCQ Advantage MAX carried out on a Phenomenex column (Gemini, 3 μ m, 110Å, 20 x 4mm) and a Waters Auto Purification System 3100 carried out with a Waters column (XBridge, 4 μ m, 100Å, 4.6 x 100mm). High Performance Liquid Chromatography (HPLC) was also carried out on two different instruments, the Waters Auto Purification System 3100 with a Waters column (XBridgePrep C18, 5 μ m, OBD, 19 x 100mm) and the Waters Alliance HT 2795 with a Phenomenex column (Luna, 5 μ m, C18, 100 Å, 150 x 10mm). Compounds purified via this method are noted. Some compounds occasionally gave a shoulder and this is denoted by an asterisk (*). This can be attributed to overloading but has not definitively identified to be the cause.

Experimental conditions (Exp2): Microwave reactions were performed on a CEM discovery fitted with an intellivent explorer unit. The temperature range of the unit is -80°C to 300°C, a pressure range of 0 – 27 bar, power range of 0 - 300 W and no pre stirring was required. Analytical reverse-phase HPLC was carried out on a Waters Millennium 2690 system, fitted with a Phenomenex Luna C8 100 Å, 5 μ m (150 x 4.6 mm I.D.) column. A binary solvent system was used (solvent A: 0.1% aqueous TFA, solvent B: 0.1% TFA/ 19.9% H₂O/80% ACN), with UV detection at 214 nm. A gradient of 0-80% buffer B over 10 min for a 20 min run time was used, with a flow rate of 1 mL/min. ¹H and ¹³C NMR spectra were recorded at 400.13 and 100.62 MHz, respectively, on a Bruker Avance III Nanobay spectrometer with BACS 60 sample changer, using solvents from Cambridge Isotope Laboratories. Chemical shifts (δ , ppm) are reported relative to the solvent peak (CDCl₃: 7.26 [¹H] or 77.16 [¹³C]; DMSO-d₆: 2.50 [¹H] or 39.52 [¹³C]). Proton resonances are annotated as: chemical shift (δ), multiplicity (s, singlet; d, doublet; t, triplet; q, quartet; m, multiplet; br, broad), coupling constant (*J*, Hz), and number of protons. Low resolution mass spectrometry was performed on an Agilent 6100 Series Single Quad LC/MS coupled with an Agilent 1200 Series HPLC, G1311A quaternary pump, G1329A thermostatted autosampler, and G1314B variable wavelength detector (214 and 254 nm). LC conditions: Phenomenex Luna C8(2) column (100 Å, 5 mm, 50 x 4.6 mm), 30°C; sample (5 mL) was eluted using a binary gradient (solvent A: 0.1% aq. HCO₂H; solvent B: 0.1% HCO₂H in CH₃CN; 5 to 100% B [10 min], 100% B [10 min]; 0.5 mL/min). MS conditions: quadrupole ion source with multimode-ESI; drying gas temperature, 300°C; vaporizer temperature, 200°C; capillary voltage, 2000 V (positive mode) or 4000 V (negative mode); scan range, 100–1000 m/z; step size, 0.1 s over 10 min. High resolution MS was performed on an Agilent 6224 TOF LC/MS coupled to an Agilent 1290 Infinity LC. All data were acquired and reference mass corrected via a dual-spray electrospray ionisation (ESI) source. Each scan or data point on the total ion chromatogram (TIC) is an average of 13,700 transients, producing a spectrum every second. Mass spectra were created by averaging the scans across each peak and subtracting the background from first 10 sec of the TIC. Acquisition was performed using the Agilent Mass Hunter Data Acquisition software ver. B.05.00 Build 5.0.5042.2 and analysis was performed using Mass Hunter Qualitative Analysis ver. B.05.00 Build 5.0.519.13. Acquisition parameters: mode, ESI; drying gas flow, 11 L/min; nebuliser pressure, 45 psi; drying gas temperature, 325°C; voltages: capillary, 4000 V; fragmentor, 160 V; skimmer, 65 V; octapole RF, 750 V; scan range, 100–1500 m/z; positive ion mode internal reference ions, m/z 121.050873 and 922.009798. LC conditions: Agilent Zorbax SB-C18 Rapid Resolution HT (2.1 x 50 mm, 1.8 mm column), 30°C; sample (5 mL) was eluted using a binary gradient (solvent A: 0.1% aq. HCO₂H; solvent B: 0.1% HCO₂H in CH₃CN; 5 to 100% B [3.5 min], 0.5 mL/min).

General Chemistry Procedures

General Procedure A1: Amide Coupling

To a stirred solution of a benzoic acid (0.734 mmol) in DMF (0.5 M final concentration) was added HBTU (0.881 mmol) and DIPEA (3.67 mmol). The reaction mixture was stirred for 10 mins at room temperature. An excess of an aminopyridine (1.47 mmol) was added and the resulting suspension was stirred overnight at 60°C. The progression of

the reaction was monitored via TLC. The reaction mixture was quenched with water and washed with ethyl acetate, aqueous NaHCO₃, 10% w/v aqueous citric acid and brine. The organic layer was dried with Na₂SO₄ and the solvent was removed under reduced pressure to afford the crude residue, which was subjected to column chromatography to give the desired product.

General Procedure A2: Amide Coupling

Thionyl chloride (12.10 mmol) was added dropwise to a stirred solution of a benzoic acid (1.21 mmol) in DMF (3 mL) and heated at 70°C for 2 h. The solvent was removed under reduced pressure. A small amount of toluene was then added to the reaction mixture to remove any remaining SOCl₂ which was concentrated to give the desired benzoyl chloride. To a stirred solution of an aminopyridine (1.16 mmol) in DCE (0.5 M final concentration) was added DIPEA (1.39 mmol) and dropwise a benzoyl chloride (1.16 mmol) and heated at 65°C for 2 h. The progression of the reaction was monitored via TLC. The reaction mixture was diluted with ethyl acetate and the organic layer was washed with aqueous NaHCO₃, 10% w/v aqueous citric acid and brine. The organic layer was dried with Na₂SO₄ and the solvent was removed under reduced pressure to leave the crude product, which was subjected to column chromatography to yield the desired product.

General Procedure A3: Amide Coupling

o-Toluoyl chloride (1.00 mmol) was added dropwise to pyridine (1 mL). The amine (1.10 mmol) was predissolved in pyridine (1 mL) before adding it to the reaction mixture and stirred overnight at room temperature. Upon completion, 10% w/v aqueous citric acid was added to the reaction mixture until a pH of 3 to 4 was reached and refrigerated until a sufficient amount of solid formed. The solid was filtered and vacuum dried to give the desired product.

General Procedure A4: Amide Coupling

To a solution of the amine (1.0 eq) in DMF (0.5 M final concentration) was added the benzoic acid (1.2 eq), EDCI (1.2 eq) and DMAP (0.1 eq). The reaction mixture was stirred at 30°C overnight. Water (approximately 2 mL) was added to the reaction mixture and it was transferred to the fridge overnight. The resulting precipitate was filtered and gave the desired pyridyl benzamide.

General Procedure A5: Amide Coupling

Relevant benzoic acid (1.0 eq) dissolved in DCM (0.5 M final concentration) and catalytic DMF added. The suspension was cooled under nitrogen in an ice bath to 0°C prior to the gradual addition of 1.1 eq oxalyl chloride. The reaction was allowed to react until no further effervescence was observed at which point all volatiles were removed under reduced pressure. The residue was again cooled to 0°C in an ice bath before gradual addition of the relevant amine (1.0 eq) and pyridine (2.0 eq) as a 0.5 M solution in THF. The reaction mixture was stirred under nitrogen and allowed to warm to room temperature overnight. Reaction was acidified with 1.0 M aqueous hydrochloric acid solution and extracted with ethyl acetate. Purification performed by recrystallisation from cyclohexane to give the desired pyridyl benzamide.

General Procedure A6: Amide Coupling

Oxalyl chloride (1.1 eq) was added dropwise to a cooled solution of a benzoic acid (1.0 eq) in DMF (0.5 M final concentration) and DCM (catalytic) and stirred until no further effervescence observed. All volatiles were removed under reduced pressure to give the desired benzoyl chloride. The residue was then dissolved in THF (0.5 M final concentration) before addition of the relevant amine (1.0 eq) and pyridine (2.0 eq). The reaction was allowed to warm to room temperature slowly and stirred for 12 h. The reaction mixture was neutralized with saturated aq NH₄Cl and extracted with EtOAc three times. The organic layers were combined, washed with brine, dried and the solvent removed under reduced pressure. The crude material was subject to column chromatography to yield the desired product.

General Procedure B: N-Alkylation

To a stirred solution of **8** (0.353 mmol), K₂CO₃ (0.530 mmol) and TBAB (0.035 mmol) in acetone (3 mL) was added after 10 minutes the alkylating agent (1.06 mmol). After stirring overnight, the solvent was removed under reduced pressure and the mixture was partitioned between ether (4 mL) and water (3 mL). The separated organic layer was washed with saturated aqueous KHSO₄ (3 x 1 mL), dried with Na₂SO₄ and concentrated to give the crude product, which was subjected to column chromatography to yield to desired product.

General Procedure C: Suzuki Coupling Reactions

A bromo pyridyl benzamide (0.687 mmol) was dissolved in 1,4-dioxane (2 mL) and water (0.5 mL), along with the boronic acid (0.721 mmol), K₂CO₃ (2.75 mmol), TBAB (0.069 mmol) and Pd(PPh₃)₂Cl₂ (0.034 mmol). The mixture was stirred in the microwave while heating at 130°C for 15 mins. The reaction mixture was dried with Na₂SO₄ and filtered through a plug of silica/celite with ethyl acetate. The solvent was removed under reduced pressure to give the crude product, which was subjected to column chromatography to yield the desired product.

General Procedure D: Sonogashira Coupling Reactions

To a solution of a bromo pyridyl benzamide (0.687 mmol) in DMF (1.5 mL) and Et₃N (0.28 mL) was added the alkyne (1.37 mmol), Pd(PPh₃)₂Cl₂ or Pd(PPh₃)₄ (0.034 mmol), CuI (0.069 mmol) and PPh₃ (0.069 mmol). The reaction mixture was heated under microwave irradiation at 120°C whilst stirring for 10 to 40 mins. The reaction mixture was diluted with 60% ethyl acetate/petroleum ether and filtered through a plug of celite/silica. The solvent was concentrated and dried to give the crude product, which was subjected to column chromatography to yield the desired product.

Compound Characterization

2-Methyl-N-(pyridin-2-yl)benzamide (8) (Exp1)

Title compound prepared according to General Procedure A1 to give a white crystalline solid (65%), mp 119-122°C. LCMS (Waters) - rt 5.33 min 98% purity at 254 nm; [M+H]⁺ 213.2 m/z; ¹H NMR (300 MHz, DMSO) δ 10.68 (s, 1H), 8.34-8.32 (m, 1H), 8.17 (dd, *J* = 8.3 and 0.9 Hz, 1H), 7.84-7.78 (m, 1H), 7.45 (d, *J* = 7.5 Hz, 1H), 7.39-7.34 (m, 1H), 7.28-7.23 (m, 2H), 7.16-7.13 (m, 1H), 2.38 (s, 3H); ¹³C NMR (75 MHz, DMSO) δ 168.5, 152.0, 148.0, 138.0, 136.4, 135.4, 130.4, 129.8, 127.5, 125.5, 119.7, 114.3, 19.4; IR (cm⁻¹) ν 3168.98 (NH), 2974.32 (CH), 1672.49 (C=O), 1629.65, 1520.68, 1429.90, 1308.15, 766.72.

2-Methyl-N-(5-(4-methylpent-1-yn-1-yl)pyridin-2-yl)benzamide (9) (Exp1)

Title compound prepared according to General Procedure D to give a yellow solid (50%), mp (cx) 110-112°C. LCMS (Finnigan) - rt 6.06 min 98% purity at 254 nm; [M+H]⁺ 293.1 m/z; ¹H NMR (300 MHz, CDCl₃) δ 9.27 (s, 1H), 8.44 (s, 1H), 7.80 (d, *J* = 8.1 Hz, 1H), 7.57 (d, *J* = 7.2 Hz, 1H), 7.42-7.38 (m, 1H), 7.30-7.25 (m, 3H), 2.53 (s, 3H), 2.35 (d, *J* = 6.5 Hz, 2H), 1.95 (sep, *J* = 6.6 Hz, 1H), 1.08 (d, *J* = 6.6 Hz, 6H); IR (cm⁻¹) ν 3174.58 (NH), 2958.73-2870.66 (CH), 1683.01 (C=O), 1583.89, 1516.22, 1373.17, 1303.39, 735.79.

(E)-2-Methyl-N-(5-(pent-1-en-1-yl)pyridin-2-yl)benzamide (10) (Exp1)

Title compound prepared according to General Procedure C to give a light yellow solid (26%), mp (cx) 94-96°C. LCMS (Finnigan) - rt 5.76 min 99% purity at 254 nm; [M+H]⁺ 281.1 m/z; ¹H NMR (300 MHz, CDCl₃) δ 9.33 (s, 1H), 8.27 (d, *J* = 8.7 Hz, 1H), 7.73 (s, 1H), 7.67 (dd, *J* = 8.7 and 1.8 Hz, 1H), 7.45 (d, *J* = 7.9 Hz, 1H), 7.25-7.20 (m, 1H), 7.14-7.10 (m, 2H), 6.10-6.06 (m, 2H), 2.37 (s, 3H), 2.05 (q, *J* = 7.2 Hz, 2H), 1.36 (sex, *J* = 7.3 Hz, 2H), 0.81 (t, *J* = 7.3 Hz, 3H); ¹³C NMR (75 MHz, CDCl₃) δ 168.1, 149.6, 143.1, 137.0, 136.5, 135.2, 133.3, 131.4, 130.9, 130.3, 127.2, 126.1, 125.1, 114.4, 35.2, 22.3, 20.1, 13.7; IR (cm⁻¹) ν 3153.82 (NH), 2952.37-2867.85 (CH), 1681.10 (C=O), 1582.83, 1513.53, 1388.67, 1301.35, 740.24.

2-Methyl-N-(5-phenylpyridin-2-yl)benzamide (11) (Exp1)

Title compound prepared according to General Procedure A1 to give a white crystalline solid (28%), mp 145-150°C. LCMS (Waters) - rt 7.68 min 99% purity at 254 nm; [M+H]⁺ 289.2 m/z; ¹H NMR (300 MHz, CDCl₃) δ 9.44 (s, 1H), 8.52 (d, *J* = 8.7 Hz, 1H), 8.13 (s, 1H), 7.99 (dd, *J* = 8.7 and 2.4 Hz, 1H), 7.61-7.58 (m, 1H), 7.52-7.32 (m, 6H), 7.28-7.24 (m, 2H), 2.55 (s, 3H); ¹³C NMR (75 MHz, CDCl₃) δ 168.4, 150.6, 144.9, 137.5, 137.0, 136.8, 135.7, 133.0, 131.4, 130.8, 129.1, 128.0, 127.1, 126.8, 126.0, 114.3, 20.0; IR (cm⁻¹) ν 3221.94 (NH), 2965.54 (CH), 1673.97 (C=O), 1586.38, 1490.70, 1447.33, 1372.79, 732.25.

6-Isobutoxyppyridin-2-amine (101) (Exp1)

2-Methyl-1-propanol (0.086g, 1.16mmol) was heated in a sealed tube with 2-amino-6-bromopyridine (0.578mmol) and NaH (0.047g, 1.17mmol) in DME (0.8 mL) for 19 hours at 190°C. The tube was cooled and opened carefully. The supernatant was removed and concentrated to give the crude product mixture, which was subjected to column chromatography to give **101** as a brown amorphous solid (0.079g, 82%). LCMS (Waters) - rt 4.10 min 95% purity at 254 nm; [M+H]⁺ 167.2 m/z; ¹H NMR (300 MHz, CDCl₃) δ 7.38 (t, *J* = 7.9 Hz, 1H), 6.13 (d, *J* = 7.9 Hz, 1H), 6.06 (d, *J* = 8.0 Hz, 1H), 5.10 (s, 2H), 3.93 (d, *J* = 6.6 Hz, 2H), 2.12-2.03 (m, 1H), 1.00 (d, *J* = 6.7 Hz, 6H); ¹³C NMR (75 MHz, CDCl₃) δ 162.7, 156.7, 141.2, 100.4, 97.4, 73.1, 28.0, 19.2; IR (cm⁻¹) ν 3332.07 (NH), 2959.66 (CH), 1664.00, 1613.74, 1443.00, 1256.40 (CN), 1027.71, 784.82.

N-(6-Isobutoxyppyridin-2-yl)-2-methylbenzamide (12) (Exp1)

Compound **101** was involved in General Procedure A1 to give the title compound as a light yellow crystalline solid (18%), mp 51-55°C. LCMS (Waters) - rt 8.58 min 70% purity at 254 nm; [M+H]⁺ 285.2 m/z; ¹H NMR (300 MHz,

CDCl₃) δ 8.31 (s, 1H), 7.92 (d, *J* = 7.9 Hz, 1H), 7.68 (t, *J* = 8.0 Hz, 1H), 7.56 (d, *J* = 7.3 Hz, 1H), 7.41-7.28 (m, 1H), 7.30-7.26 (m, 2H), 6.53 (d, *J* = 8.1 Hz, 1H), 3.97 (d, *J* = 6.7 Hz, 2H), 2.53 (s, 3H), 2.07 (m, 1H), 1.01 (d, *J* = 6.7 Hz, 6H); ¹³C NMR (75 MHz, CDCl₃) δ 168.0, 161.8, 148.8, 142.7, 137.1, 135.1, 131.5, 130.9, 127.2, 126.0, 105.9, 105.2, 73.8, 28.0, 20.1, 19.1; IR (cm⁻¹) ν 3291.87 (NH), 2962.41 (CH), 1683.45 (C=O), 1579.11, 1520.94, 1445.15, 1274.45, 1245.59.

N-Butyl-2-methyl-*N*-(pyridin-2-yl)benzamide (**13a**) (Exp1)

Title compound prepared according to General Procedure B to give a yellow oil (20%). LCMS (Finnigan) - rt 5.31 min 98% purity at 254 nm; [M+H]⁺ 269.1 m/z; ¹H NMR (300 MHz, MeOD) δ 8.37 (d, *J* = 4.7 Hz, 1H), 7.58 (t, *J* = 7.6 Hz, 1H), 7.31-7.23 (m, 2H), 7.17-7.13 (m, 2H), 7.06-7.00 (m, 2H), 2.33-2.29 (m, 3H), 1.62-1.54 (m, 2H), 1.40-1.29 (m, 2H), 1.18-1.10 (m, 2H), 0.90 (t, *J* = 7.3 Hz, 3H); ¹³C NMR (75 MHz, MeOD) δ 210.0, 149.9, 139.3, 137.8, 136.4, 131.6, 131.4, 130.3, 128.2, 126.4, 124.0, 123.4, 31.3, 30.7, 21.1, 19.5, 14.0. IR (cm⁻¹) ν 3058.76 (NH), 2957.98-2871.64 (CH), 1651.10 (C=O), 1601.49, 1467.63, 1433.96, 1379.11, 742.74.

2-Methyl-*N*-pentyl-*N*-(pyridin-2-yl)benzamide (**13b**) (Exp1)

Title compound prepared according to General Procedure B to give a colorless oil (18%). LCMS (Waters) - rt 7.73 min 90% purity at 254 nm; [M+H]⁺ 283.3 m/z; ¹H NMR (300 MHz, MeOD) δ 8.37 (d, *J* = 3.3 Hz, 1H), 7.59 (t, *J* = 7.8 Hz, 1H), 7.19-7.10 (m, 3H), 7.06-7.00 (m, 3H), 4.02 (t, *J* = 7.4 Hz, 2H), 2.33 (s, 3H), 1.64 (m, 2H), 1.32-1.30 (m, 4H), 0.90-0.85 (m, 3H); ¹³C NMR (75 MHz, MeOD) δ 173.3, 156.0, 149.9, 139.3, 137.8, 136.4, 131.4, 130.3, 128.2, 126.4, 124.0, 123.4, 30.7, 30.1, 28.8, 23.3, 19.5, 14.3; IR (cm⁻¹) ν 3057.81 (NH), 2955.74-2859.52 (CH), 1649.98 (C=O), 1585.86, 1467.35, 1433.89, 1381.05, 741.81.

2-Iodo-*N*-(pyridin-2-yl)benzamide (**14**) (Exp1)

2-Iodobenzoyl chloride was obtained according to General Procedure A2 to give the title compound as a light yellow solid (7%), mp (ex) 175-178°C. LCMS (Finnigan) - rt 4.75 min 92% purity at 254 nm; [M+H]⁺ 325.0 m/z; ¹H NMR (300 MHz, CDCl₃) δ 9.51 (s, 1H), 8.44 (d, *J* = 8.3 Hz, 1H), 7.95-7.90 (m, 2H), 7.84-7.77 (m, 1H), 7.59-7.54 (m, 1H), 7.43 (dt, *J* = 7.5 and 1.1 Hz, 1H), 7.16 (dt, *J* = 7.7 and 1.7 Hz, 1H), 7.06-7.02 (m, 1H); ¹³C NMR (75 MHz, CDCl₃) δ 167.6, 151.0, 145.9, 141.1, 140.4, 139.9, 131.8, 128.5, 128.4, 120.0, 115.0, 92.6; IR (cm⁻¹) ν 2976.39 (NH), 1680.92 (C=O), 1577.86, 1524.27, 1432.36, 1312.24, 773.56-736.11 (CI).

N-(Pyridin-2-yl)-2-(trifluoromethyl)benzamide (**15**) (Exp1)

Title compound prepared according to General Procedure A1 to give a dull yellow crystalline solid (55%), mp 130-132°C. LCMS (Finnigan) - rt 4.81 min 98% purity at 254 nm; [M+H]⁺ 267.0 m/z; ¹H NMR (300 MHz, DMSO) δ 11.09 (s, 1H), 8.35 (d, *J* = 4.2 Hz, 1H), 8.17 (d, *J* = 8.1 Hz, 1H), 7.88-7.67 (m, 5H), 7.19-7.17 (m, 1H); IR (cm⁻¹) ν 2979.59 (NH), 1684.91 (C=O), 1633.69, 1431.43, 1312.64, 1124.48, 767.26.

N-(5-Bromo-6-methylpyridin-2-yl)-2-methylbenzamide (**16**) (Exp1)

To a solution of 2-amino-6-picoline (2.77 mmol) in methanol (8.5 mL) was slowly added NBS (2.83 mmol) portion-wise as a solid. The resulting mixture was stirred at room temperature for 30 mins and the solvent removed under reduced pressure. The reaction mixture was quenched with water, diluted with ethyl acetate and washed with aqueous NaHCO₃ and brine. The organic layer was dried with Na₂SO₄ and the solvent concentrated to give 6-amino-3-bromo-2-picoline⁴² as a light brown solid (82%). Title compound was then prepared according to General Procedure C to give a brown crystalline solid (93%), mp 91-94°C. LCMS (Finnigan) - rt 5.63 min 95% purity at 254 nm; [M+H]⁺ 305.3 m/z (⁷⁹Br), 307.0 m/z (⁸¹Br); ¹H NMR (300 MHz, CDCl₃) δ 8.31 (s, 1H), 8.12 (d, *J* = 8.7 Hz, 1H), 7.83 (d, *J* = 8.7 Hz, 1H), 7.51 (d, *J* = 7.5 Hz, 1H), 7.40-7.35 (m, 1H), 7.28-7.22 (m, 2H), 2.53 (d, *J* = 6.0 Hz, 6H); ¹³C NMR (75 MHz, CDCl₃) δ 168.0, 155.3, 149.6, 142.3, 136.9, 135.3, 131.5, 130.8, 126.8, 126.0, 115.3, 112.8, 24.2, 20.0; IR (cm⁻¹) ν 3168.85 (NH), 2964.18-2926.46 (CH), 1684.22 (C=O), 1511.66, 1432.25, 1300.39, 999.19, 740.03 (CBr).

5-(*N*-(*t*-Butyl)sulfamoyl)-2-methyl-*N*-(5-methylpyridin-2-yl)benzamide (**17**) (Exp2)

Title compound prepared according to General Procedure A4 to give a white solid (35%). HPLC - rt 5.79 min > 95% purity at 254 nm; LRMS [M+H]⁺ 362.3 m/z; ¹H NMR (400 MHz, CDCl₃) δ 9.34 (s, 1H), 8.31 (d, *J* = 8.3 Hz, 1H), 8.12 (d, *J* = 1.9 Hz, 1H), 7.97 (d, *J* = 24.8 Hz, 1H), 7.88 (dd, *J* = 8.1, 2.0 Hz, 1H), 7.65 (dd, *J* = 8.5, 1.8 Hz, 1H), 7.39 (d, *J* = 8.1 Hz, 1H), 4.84 (s, 1H), 2.59 (s, 3H), 2.33 (s, 3H), 1.29 - 1.20 (s, 9H); ¹³C NMR (101 MHz, CDCl₃) δ 166.6, 148.9, 146.3, 146.3, 141.8, 141.4, 140.2, 131.9, 130.0, 128.8, 125.7, 114.3, 55.0, 30.2 (3C), 20.2, 17.9.

N-(*Quinolin-2-yl*)-[*1,1'*-*biphenyl*]-*2-carboxamide* (**18**) (**Exp1**)

Title compound prepared according to General Procedure A1 to give a light yellow solid (71%), mp (cx) 132-135°C. LCMS (Waters) - rt 7.58 min 98% purity at 254 nm; [M+H]⁺ 325.2 m/z; ¹H NMR (300 MHz, CDCl₃) δ 8.86 (s, 1H), 8.47 (d, *J* = 8.7 Hz, 1H), 8.15 (d, *J* = 9.0 Hz, 1H), 7.73 (d, *J* = 8.0 Hz, 1H), 7.61-7.52 (m, 3H), 7.45-7.28 (m, 9H); ¹³C NMR (75 MHz, CDCl₃) δ 168.7, 151.1, 146.1, 140.2, 139.8, 138.7, 135.3, 130.7, 130.5, 129.9, 128.7, 128.7, 128.5, 127.9, 127.4, 127.4, 127.0, 126.2, 125.1, 114.3; IR (cm⁻¹) ν 3053.34 (NH), 1672.26 (C=O), 1597.34, 1498.29, 1424.69, 1318.85, 741.15.

N-(*3-Methoxypyridin-2-yl*)-*2-methylbenzamide* (**19**) (**Exp1**)

Title compound prepared according to General Procedure A1 to give a colorless oil (22%). LCMS (Waters) - rt 4.32 min > 97% purity at 254 nm; [M+H]⁺ 243.2 m/z; ¹H NMR (300 MHz, MeOD) δ 8.02 (s, 1H), 7.64-7.56 (m, 2H), 7.44-7.28 (m, 4H), 3.96 (s, 3H), 2.53 (s, 3H); ¹³C NMR (75 MHz, CDCl₃) δ 171.8, 150.4, 142.1, 138.4, 137.7, 137.1, 132.0, 131.6, 128.6, 126.8, 123.7, 121.7, 56.7, 19.9; IR (cm⁻¹) ν 3411.61 (NH), 2927.17 (CH), 1680.67 (C=O), 1601.71, 1502.38, 1455.96, 1421.24, 836.77.

2-Methyl-N-(*3-methylpyridin-2-yl*)*benzamide* (**20**) (**Exp1**)

Title compound prepared according to General Procedure A1 to give a yellow solid (42%), mp (cx) 109-111°C. LCMS (Waters) - rt 4.70 min 95% purity at 254 nm; [M+H]⁺ 227.2 m/z; ¹H NMR (300 MHz, MeOD) δ 8.29 (d, *J* = 4.5 Hz, 1H), 7.77 (d, *J* = 7.6 Hz, 1H), 7.60 (d, *J* = 7.4 Hz, 1H), 7.41-7.36 (m, 1H), 7.31-7.27 (m, 3H), 2.51 (s, 3H), 2.37 (s, 3H); ¹³C NMR (75 MHz, MeOD) δ 171.9, 150.6, 147.1, 141.6, 137.5, 137.1, 132.0, 132.0, 131.5, 128.5, 126.9, 124.1, 20.0, 18.0; IR (cm⁻¹) ν 3167.43 (NH), 2976.24 (CH), 1666.61 (C=O), 1579.47, 1445.55, 1367.81, 1284.10, 747.15.

N-(*3-Fluoropyridin-2-yl*)-*2-methylbenzamide* (**21**) (**Exp1**)

Title compound prepared according to General Procedure A3 to give a white solid (80%), mp (cx) 123-125°C. LCMS (Finnigan) - rt 4.44 min 98% purity at 254 nm; [M+H]⁺ 231.0 m/z; ¹H NMR (300 MHz, CDCl₃) δ 8.45 (s, 1H), 8.15-8.09 (m, 1H), 7.62 (d, *J* = 7.8 Hz, 1H), 7.58-7.50 (m, 1H), 7.43-7.38 (m, 1H), 7.30-7.25 (m, 2H), 7.21-7.16 (m, 1H), 2.55 (s, 3H); IR (cm⁻¹) ν 3389.77 (NH), 2915.09 (CH), 1654.86 (C=O), 1514.62, 1463.55, 1314.29, 802.47, 740.56.

2-Methyl-N-(*pyrimidin-2-yl*)*benzamide* (**22**) (**Exp2**)

Title compound prepared according to General Procedure A4 as a white solid (24%). HPLC - rt 4.54 min > 95% purity at 254 nm; LRMS [M+H]⁺ 214.0 m/z; ¹H NMR (400 MHz, CDCl₃) δ 9.32 (s, 1H), 8.35 (d, *J* = 5.9 Hz, 1H), 7.86 (d, *J* = 8.1 Hz, 1H), 7.34 (m, 1H), 7.54 (d, *J* = 7.6 Hz, 1H), 7.31 (d, *J* = 7.6 Hz, 1H), 7.26 - 7.10 (m, 2H), 2.53 (s, 3H); ¹³C NMR (101 MHz, CDCl₃) δ 165.1, 157.3 (2C), 154.2, 138.3, 132.8, 131.6, 131.4, 127.6, 127.1, 114.3, 19.2.

N-(*4-Cyanopyridin-2-yl*)-*2-methylbenzamide* (**23**) (**Exp1**)

Title compound prepared according to General Procedure A1 to give a dull yellow crystalline solid (15%), mp 150-153°C. LCMS (Waters) - rt 6.57 min 99% purity at 254 nm; [M+H]⁺ 238.2 m/z; ¹H NMR (300 MHz, CDCl₃) δ 9.29 (s, 1H), 8.76 (s, 1H), 8.10-8.08 (m, 1H), 7.56-7.54 (m, 1H), 7.45-7.41 (m, 1H), 7.32-7.28 (m, 2H), 7.24-7.22 (m, 1H), 2.54 (s, 3H); ¹³C NMR (75 MHz, CDCl₃) δ 168.4, 152.4, 148.6, 137.1, 134.8, 131.6, 131.2, 127.0, 126.1, 122.9, 121.1, 116.3, 116.3, 20.0; IR (cm⁻¹) ν 3191.96 (NH), 2977.79 (CH), 2243.52 (CN), 1688.37 (C=O), 1559.47, 1405.30, 1224.68, 967.48, 746.08.

2-Methyl-N-(*pyrazin-2-yl*)*benzamide* (**24**) (**Exp1**)

Title compound prepared according to General Procedure A1 to give a light yellow solid (50%), mp (cx) 114-116°C. LCMS (Waters) - rt 5.40 min 98% purity at 254 nm; [M+H]⁺ 214.2 m/z; ¹H NMR (300 MHz, MeOD) δ 9.51 (d, *J* = 1.5 Hz, 1H), 8.40-8.38 (m, 1H), 8.34 (d, *J* = 2.4 Hz, 1H), 7.53 (d, *J* = 7.7 Hz, 1H), 7.44-7.38 (m, 1H), 7.33-7.28 (m, 2H), 2.48 (s, 3H); ¹³C NMR (75 MHz, MeOD) δ 171.3, 150.7, 144.3, 140.9, 138.0, 137.5, 137.0, 132.1, 131.7, 128.4, 126.9, 19.8; IR (cm⁻¹) ν 3167.49 (NH), 3095.12 (CH), 1688.62 (C=O), 1526.92, 1409.57, 1298.00, 1268.65, 729.37.

2-Methyl-N-(*4-methylpyridin-2-yl*)*benzamide* (**25**) (**Exp1**)

Title compound prepared according to General Procedure A1 to give a white solid (61%), mp (cx) 120-123°C. LCMS (Waters) - rt 4.68 + 4.93 min 98% purity at 254 nm; [M+H]⁺ 227.2 m/z; ¹H NMR (300 MHz, CDCl₃) δ 10.54 (s, 1H),

8.24 (s, 1H), 7.44 (d, $J = 7.6$ Hz, 1H), 7.33-7.28 (m, 1H), 7.20-7.13 (m, 2H), 6.99 (d, $J = 5.2$ Hz, 1H), 6.58 (d, $J = 5.2$ Hz, 1H), 2.45 (s, 3H), 2.31 (s, 3H); ^{13}C NMR (75 MHz, CDCl_3) δ 169.2, 152.1, 150.0, 146.7, 136.7, 136.0, 131.0, 130.2, 127.2, 125.9, 120.7, 115.0, 21.4, 19.7; IR (cm^{-1}) ν 3181.15 (NH), 2978.23 (CH), 1679.51 (C=O), 1613.92, 1572.61, 1527.05, 1408.90, 1299.12.

N-(4-Chloropyridin-2-yl)-2-methylbenzamide (**26**) (Exp1)

Title compound prepared according to General Procedure A1 to give a yellow crystalline solid (37%), mp 84-87°C. LCMS (Waters) - rt 7.32 min 90% purity at 254 nm; $[\text{M}+\text{H}]^+$ 247.2 (^{35}Cl), 249.1 (^{37}Cl) m/z; ^1H NMR (300 MHz, DMSO, rotamers) δ 11.03 (s, 1H), 8.36-8.32 (m, 2H), 7.82 (d, $J = 7.8$ Hz, 1H), 7.49 (d, $J = 7.7$ Hz, 1H), 7.44-7.37 (m, 2H), 7.31-7.26 (m, 5H), 2.40 (s, 3H); ^{13}C NMR (75 MHz, DMSO, rotamers) δ 168.8, 168.6, 153.2, 149.4, 143.9, 138.9, 136.0, 135.5, 131.6, 131.4, 130.5, 130.1, 130.0, 127.6, 125.8, 125.5, 119.7, 113.7, 21.2, 19.4; IR (cm^{-1}) ν 3222.31 (NH), 2970.27 (CH), 1683.80 (C=O), 1567.06, 1402.41, 1265.72, 1033.32, 831.60, 721.93 (C-Cl).

N-(4-Bromopyridin-2-yl)-2-methylbenzamide (**27**) (Exp1)

Title compound prepared according to General Procedure A3 to give a white solid (75%). LCMS (Finnigan) - rt 5.37 min 98% purity at 254 nm; $[\text{M}+\text{H}]^+$ 291.4 m/z (^{79}Br), 293.0 m/z (^{81}Br); ^1H NMR (300 MHz, CDCl_3) δ 9.63 (s, 1H), 8.87 (s, 1H), 7.68 (d, $J = 8.0$ Hz, 1H), 7.47-7.42 (m, 1H), 7.35-7.28 (m, 4H), 2.57 (s, 3H); ^{13}C NMR (75 MHz, CDCl_3) δ 168.0, 151.3, 144.6, 137.7, 134.0, 131.7, 131.5, 127.4, 126.2, 123.2, 120.3, 118.2, 20.2; IR (cm^{-1}) ν 3217.90 (NH) 3058.26 (CH), 1684.75 (C=O), 1564.11, 1509.45, 1396.93, 1266.59, 1082.22, 735.89 (C-Br).

N-(4-Fluoropyridin-2-yl)-2-methylbenzamide (**28**) (Exp2)

Title compound prepared according to General Procedure A1 as an off-white solid (13%). HPLC - rt 6.36 min > 98% purity at 254 nm; LRMS $[\text{M}+\text{H}]^+$ 231.0 m/z; HRMS $[\text{M}+\text{H}]^+$ 231.0928 m/z, found 231.0926 m/z; ^1H NMR (400 MHz, DMSO) δ 11.08 (s, 1H), 8.39 (dd, $J = 9.3, 5.7$ Hz, 1H), 8.04 (dd, $J = 12.0, 2.4$ Hz, 1H), 7.51 - 7.43 (m, 1H), 7.39 (td, $J = 7.5, 1.4$ Hz, 1H), 7.34 - 7.22 (m, 2H), 7.10 (ddd, $J = 8.2, 5.7, 2.4$ Hz, 1H), 2.39 (s, 3H); ^{13}C NMR (101 MHz, DMSO) δ 168.9, 168.9 ($J_{\text{C-F}} = 258$ Hz), 154.4 ($J_{\text{C-F}} = 11$ Hz), 150.7 ($J_{\text{C-F}} = 8$ Hz), 136.0, 135.5, 130.6, 130.1, 127.6, 125.6, 107.7 ($J_{\text{C-F}} = 17$ Hz), 101.3 ($J_{\text{C-F}} = 23$ Hz), 19.5.

2-Methyl-N-(4-(phenylethynyl)pyridin-2-yl)benzamide (**29**) (Exp1)

Title compound prepared according to General Procedure D to give a yellow crystalline solid (93%), mp 157-160°C. LCMS (Finnigan) - rt 5.89 min 95% purity at 254 nm; $[\text{M}+\text{H}]^+$ 313.1 m/z; ^1H NMR (300 MHz, DMSO) δ 10.89 (s, 1H), 8.40 (s, 1H), 8.32 (s, 1H), 7.66-7.63 (m, 2H), 7.49-7.46 (m, 4H), 7.37 (d, $J = 7.2$ Hz, 1H), 7.28 (d, $J = 7.2$ Hz, 3H), 2.39 (s, 3H); IR (cm^{-1}) ν 3183.06 (NH), 3031.34 (CH), 2360.26 (C \equiv C-), 1678.21 (C=O), 1551.25, 1411.62, 1298.00, 1277.49, 752.01.

2-Methyl-N-(4-(4-methylpent-1-yn-1-yl)pyridin-2-yl)benzamide (**30**) (Exp1)

Title compound prepared according to General Procedure D to give a yellow solid (44%), mp (cx) 134-136°C. LCMS (Finnigan) - rt 6.01 min > 98% purity at 254 nm; $[\text{M}+\text{H}]^+$ 293.1 m/z; ^1H NMR (300 MHz, CDCl_3) δ 9.29 (s, 1H), 8.54 (s, 1H), 7.56 (d, $J = 7.2$ Hz, 1H), 7.42-7.37 (m, 1H), 7.30-7.25 (m, 3H), 7.06 (s, 1H), 2.54 (s, 3H), 2.34 (d, $J = 6.5$ Hz, 2H), 1.95 (sep, $J = 6.6$ Hz, 1H), 1.07 (d, $J = 6.6$ Hz, 6H); IR (cm^{-1}) ν 3182.16 (NH), 2958.42 (CH), 2236.62 (C \equiv C-), 1673.88 (C=O), 1603.32, 1550.71, 1410.72, 1301.66, 1275.84.

2-Methyl-N-(4-phenylpyridin-2-yl)benzamide (**31**) (Exp1)

Title compound prepared according to General Procedure C to give a light yellow crystalline solid (99%), mp 160-163°C. LCMS (Finnigan) - rt 5.37 min 98% purity at 254 nm; $[\text{M}+\text{H}]^+$ 289.1 m/z; ^1H NMR (300 MHz, CDCl_3) δ 9.69 (s, 1H), 8.77 (s, 1H), 7.85 (d, $J = 5.1$ Hz, 1H), 7.76-7.73 (m, 2H), 7.61 (d, $J = 7.8$ Hz, 1H), 7.52-7.39 (m, 4H), 7.31-7.23 (m, 3H), 2.57 (s, 3H); ^{13}C NMR (75 MHz, CDCl_3) δ 168.6, 152.2, 151.8, 146.9, 137.9, 136.7, 135.8, 131.4, 130.7, 129.5, 129.1, 127.3, 127.2, 126.0, 117.9, 112.2, 20.0; IR (cm^{-1}) ν 3183.97 (NH), 3056.67 (CH), 1676.60 (C=O), 1491.20, 1275.69, 1211.86, 761.46, 693.54.

N-(5-Methoxy-pyridin-2-yl)-2-methylbenzamide (**32**) (Exp1)

Title compound prepared according to General Procedure A1 to give a brown solid (99%), mp (cx) 100-103°C. LCMS (Finnigan) - rt 4.84 min 98% purity at 254 nm; [M+H]⁺ 243.1 m/z; ¹H NMR (300 MHz, CDCl₃) δ 9.46 (s, 1H), 8.37 (d, *J* = 9.1 Hz, 1H), 9.57-7.54 (m, 2H), 7.39-7.35 (m, 2H), 7.28-7.25 (m, 2H), 3.81 (s, 3H), 2.52 (s, 3H); ¹³C NMR (75 MHz, CDCl₃) δ 168.3, 152.9, 145.2, 136.7, 135.7, 132.2, 131.3, 130.6, 127.2, 125.9, 125.2, 115.3, 56.1, 19.9; IR (cm⁻¹) ν 3165.66 (NH), 2971.43 (CH), 1668.71 (C=O), 1528.37, 1398.58, 1253.69, 1016.34, 831.41.

2-Methyl-N-(5-methylpyridin-2-yl)benzamide (**33**) (Exp1)

Title compound prepared according to General Procedure A1 to give a white crystalline solid (56%), mp 122-124°C. LCMS (Finnigan) - rt 4.27 min > 99% purity at 254 nm; [M+H]⁺ 227.1 m/z; ¹H NMR (300 MHz, MeOD) δ 8.12 (d, *J* = 8.4 Hz, 1H), 7.91 (s, 1H), 7.66 (d, *J* = 8.4 Hz, 1H), 7.49 (d, *J* = 7.2 Hz, 1H), 7.43-7.38 (m, 1H), 7.32-7.27 (m, 2H), 2.46 (s, 3H), 2.29 (s, 3H); ¹³C NMR (75 MHz, MeOD) δ 171.3, 150.9, 148.9, 140.1, 137.9, 137.1, 132.0, 131.4, 131.1, 128.2, 127.0, 115.7, 19.7, 17.8; IR (cm⁻¹) ν 3168.26 (NH), 2988.17 (CH), 1677.45 (C=O), 1592.34, 1521.80, 1388.31, 1307.71, 736.25.

N-(5-Fluoro-pyridin-2-yl)-2-methylbenzamide (**34**) (Exp1)

Title compound prepared according to General Procedure A2 (20%) and D (81%) to give a dull yellow crystalline solid, mp 140-143°C. LCMS (Finnigan) - rt 5.09 min 99% purity at 254 nm; [M+H]⁺ 231.1 m/z; ¹H NMR (300 MHz, CDCl₃) δ 9.08 (s, 1H), 8.47 (dd, *J* = 9.2, 4.1 Hz, 1H), 7.77-7.76 (m, 1H), 7.56-7.49 (m, 2H), 7.44-7.39 (m, 1H), 7.31-7.26 (m, 2H), 2.53 (s, 3H); ¹³C NMR (75 MHz, CDCl₃) δ 168.3, 156.4 (*J*_{C-F} = 250 Hz), 148.0, 136.8, 135.7, 134.8 (*J*_{C-F} = 26 Hz), 131.6, 130.9, 127.1, 126.2, 126.0 (*J*_{C-F} = 20 Hz), 115.3 (*J*_{C-F} = 4 Hz), 20.0; IR (cm⁻¹) ν 3174.67 (NH), 3067.80 (CH), 1670.14 (C=O), 1518.38, 1388.38, 1305.89, 1234.27, 747.23.

2-Methyl-N-(pyrimidin-4-yl)benzamide (**35**) (Exp2)

Title compound prepared according to General Procedure A4 as a white solid (59%). HPLC - rt 4.59 min > 95% purity at 254 nm; LRMS [M+H]⁺ 214.2 m/z; ¹H NMR (400 MHz, CDCl₃) δ 9.32 (s, 1H), 8.66 (d, *J* = 5.7 Hz, 1H), 8.43 (d, *J* = 15.1 Hz, 1H), 8.36 (t, *J* = 6.6 Hz, 1H), 7.54 (d, *J* = 7.6 Hz, 1H), 7.45 (t, *J* = 7.6 Hz, 1H), 7.35 - 7.20 (m, 2H), 2.50 (s, 3H); ¹³C NMR (101 MHz, CDCl₃) δ 169.2, 158.7, 158.2, 157.6, 137.1, 134.9, 131.8, 131.4, 127.2, 126.3, 110.6, 20.2.

N-(5-Cyano-pyridin-2-yl)-2-methylbenzamide (**36**) (Exp1)

Title compound prepared according to General Procedure A1 to give a dull yellow crystalline solid (10%), mp 112-114°C. LCMS (Waters) - rt 7.70 min 99% purity at 254 nm; [M+H]⁺ 238.2 m/z; ¹H NMR (300 MHz, CDCl₃) δ 8.34 (d, *J* = 8.3 Hz, 1H), 8.09 (d, *J* = 8.3 Hz, 1H), 7.65 (t, *J* = 7.7 Hz, 1H), 7.56 (d, *J* = 7.7 Hz, 1H), 7.52 - 7.40 (m, 2H), 7.30 (d, *J* = 8.6 Hz, 2H), 2.37 (s, 3H); ¹³C NMR (75 MHz, CDCl₃) δ 168.3, 146.2, 138.0, 132.3, 131.8, 131.8, 131.1, 130.4, 130.0, 126.4, 125.5, 120.3, 114.6, 20.1; IR (cm⁻¹) ν 2929.90 (NH/CH), 2362.83 (CN), 1705.19 (C=O), 1359.38, 1287.95, 1234.52, 934.32, 731.56.

N-(5-Chloro-pyridin-2-yl)-2-methylbenzamide (**37**) (Exp1)

Title compound prepared according to General Procedure A2 and was purified via HPLC to give a white crystalline solid (10%), mp 129-131°C. LCMS (Finnigan) - rt 5.38 min 99% purity at 254 nm; [M+H]⁺ 247.1 (³⁵Cl), 249.0 (³⁷Cl) m/z; ¹H NMR (300 MHz, CDCl₃) δ 8.69 (s, 1H), 8.42 (s, 1H), 8.03 (s, 1H), 7.75 (d, *J* = 8.9 Hz, 1H), 7.55 (d, *J* = 7.6 Hz, 1H), 7.45-7.40 (m, 1H), 7.32-7.28 (m, 2H), 2.54 (s, 3H); IR (cm⁻¹) ν 3149.57 (NH), 2956.59-2919.21 (CH), 1678.40 (C=O), 1578.18, 1517.71, 1460.12, 1376.38, 1298.24, 739.08 (CCI).

N-(5-Bromo-pyridin-2-yl)-2-methylbenzamide (**38**) (Exp1)

Title compound prepared according to General Procedure A3 to give a white solid (79%), mp (cx) 129-131°C. LCMS (Finnigan) - rt 5.44 min 99% purity at 254 nm; [M+H]⁺, 291.3 (⁷⁹Br), 293.0 (⁸¹Br) m/z; ¹H NMR (300 MHz, CDCl₃) δ 9.42 (s, 1H), 8.53 (s, 1H), 8.24 (s, 1H), 7.98 (d, *J* = 8.9 Hz, 1H), 7.64 (d, *J* = 7.4 Hz, 1H), 7.44-7.39 (m, 1H), 7.33-7.28 (m, 2H), 2.54 (s, 3H); ¹³C NMR (75 MHz, CDCl₃) δ 168.0, 149.7, 145.2, 143.4, 137.5, 134.3, 131.7, 131.4, 127.3, 126.2, 116.6, 116.3, 20.2; IR (cm⁻¹) ν 3155.49 (NH), 2980.99 (CH), 1678.99 (C=O), 1572.03, 1516.29, 1370.72, 1298.57, 738.26 (CBr).

N-(6-Methoxypyridin-2-yl)-2-methylbenzamide (**39**) (**Exp1**)

Title compound prepared according to General Procedure A1 to give a yellow oil (39%). LCMS (Finnigan) - rt 5.33 + 5.57 min 98% purity at 254 nm; [M+H]⁺ 243.1 m/z; ¹H NMR (300 MHz, CDCl₃, rotamers) δ 8.06 – 7.94 (m, 1H), 7.80 (d, *J* = 7.8 Hz, 1H), 7.56 – 7.46 (m, 1H), 7.45 – 7.38 (m, 2H), 7.37 – 7.21 (m, 2H), 7.20 – 7.10 (m, 2H), 6.41 (d, *J* = 8.1 Hz, 1H), 3.73 (s, 3H), 2.42 (s, 3H); ¹³C NMR (75 MHz, CDCl₃, rotamers) δ 168.0, 162.9, 149.2, 140.9, 136.6, 135.9, 134.7, 132.4, 131.4, 131.4, 130.5, 128.7, 126.7, 126.5, 125.9, 124.8, 120.5, 108.4, 106.1, 105.5, 53.4, 19.9; IR (cm⁻¹) ν 3274.15 (NH), 2946.93 (CH), 1677.11 (C=O), 1518.83, 1455.58, 1397.94, 1243.86, 732.34.

2-Methyl-N-(6-methylpyridin-2-yl)benzamide (**40**) (**Exp1**)

Title compound prepared according to General Procedure A1 to give a brown amorphous solid (99%). LCMS (Finnigan) - rt 4.40 min 90% purity at 254 nm; [M+H]⁺ 227.1 m/z; ¹H NMR (300 MHz, CDCl₃) δ 8.81 (s, 1H), 8.22 (d, *J* = 8.4 Hz, 1H), 7.77 (t, *J* = 7.9 Hz, 1H), 7.61 (d, *J* = 7.1 Hz, 1H), 7.43-7.38 (m, 1H), 7.31-7.27 (m, 2H), 7.02 (d, *J* = 7.5 Hz, 1H), 2.55 (d, *J* = 4.8 Hz, 6H); ¹³C NMR (75 MHz, CDCl₃) δ 167.1, 154.6, 149.1, 138.1, 135.3, 133.9, 129.9, 129.3, 125.4, 124.4, 118.1, 109.6, 22.1, 18.4; IR (cm⁻¹) ν 3183.36 (NH), 2927.27 (CH), 1676.72 (C=O), 1522.50, 1451.84, 1300.94, 839.02, 735.31.

N-(6-Fluoropyridin-2-yl)-2-methylbenzamide (**41**) (**Exp1**)

Title compound prepared according to General Procedure A3 to give a colorless oil (69%). LCMS (Finnigan) - rt 5.23 min 99% purity at 254 nm; [M+H]⁺ 231.0 m/z; ¹H NMR (300 MHz, CDCl₃) δ 8.44 (s, 1H), 8.25 (d, *J* = 8.0 Hz, 1H), 7.82 (q, *J* = 8.1 Hz, 1H), 7.47 (d, *J* = 7.5 Hz, 1H), 7.38-7.33 (m, 1H), 7.26-7.19 (m, 2H), 6.65 (d, *J* = 8.0 Hz, 1H), 2.50 (s, 3H); ¹³C NMR (75 MHz, CDCl₃) δ 168.1, 161.9 (*J*_{C-F} = 240 Hz), 149.8 (*J*_{C-F} = 14 Hz), 143.3 (*J*_{C-F} = 8 Hz), 136.8, 135.2, 131.4, 130.8, 126.8, 125.9, 110.5 (*J*_{C-F} = 4 Hz), 104.4 (*J*_{C-F} = 35 Hz), 19.9; IR (cm⁻¹) ν 3260.29 (NH), 2928.92 (CH), 1675.55 (C=O), 1584.74, 1514.41, 1443.07, 1405.39, 1233.62.

N-(6-Cyanopyridin-2-yl)-2-methylbenzamide (**42**) (**Exp1**)

Title compound prepared according to General Procedure A2 to give a white solid (44%), mp (cx) 95-98°C. LCMS (Finnigan) - rt 5.22 min 99% purity at 254 nm; [M+H]⁺ 238.0 m/z; ¹H NMR (300 MHz, MeOD) δ 7.10-7.06 (m, 1H), 6.53-6.48 (m, 1H), 6.13-6.10 (m, 1H), 6.04-6.02 (m, 1H), 5.92-5.90 (m, 1H), 5.84-5.81 (m, 2H), 0.99 (s, 3H); ¹³C NMR (75 MHz, MeOD) δ 171.5, 154.5, 140.7, 137.4, 137.1, 132.9, 132.1, 131.7, 128.1, 127.0, 125.8, 119.6, 118.0, 19.9; IR (cm⁻¹) ν 3226.44 (NH), 2965.74 (CH), 2237.44 (CN), 1650.76 (C=O), 1444.74, 1376.26, 1301.34, 811.78, 736.76.

2-Methyl-N-(pyridazin-3-yl)benzamide (**43**) (**Exp1**)

Title compound prepared according to General Procedure A1 to give a brown oil (96%). LCMS (Waters) - rt 5.15 min > 98% purity at 254 nm; [M+H]⁺ 214.2 m/z; ¹H NMR (300 MHz, CDCl₃) δ 9.01 (d, *J* = 9.4 Hz, 1H), 8.94 (s, 1H), 7.82 (d, *J* = 7.7 Hz, 2H), 7.48-7.44 (m, 1H), 7.38-7.31 (m, 2H), 2.57 (s, 3H); ¹³C NMR (75 MHz, CDCl₃) δ 168.6, 155.3, 148.6, 137.1, 134.7, 131.6, 131.2, 128.3, 126.9, 126.1, 118.7, 19.9; IR (cm⁻¹) ν 3222.45 (NH), 2932.35 (CH), 1679.54 (C=O), 1578.54, 1513.01, 1439.95, 1288.68, 840.34. Note: amide peak is missing from the NMR.

N-(6-Chloropyridin-2-yl)-2-methylbenzamide (**44**) (**Exp1**)

Title compound prepared according to General Procedure A2 to give a dull yellow oil (76%). LCMS (Finnigan) - rt 5.42 min 99% purity at 254 nm; [M+H]⁺ 247.2 (³⁵Cl), 249.0 (³⁷Cl) m/z; ¹H NMR (300 MHz, CDCl₃) δ 8.39 (s, 1H), 8.29 (d, *J* = 8.2 Hz, 1H), 7.68 (t, *J* = 8.0 Hz, 1H), 7.47 (d, *J* = 7.7 Hz, 1H), 7.37-7.32 (m, 1H), 7.25-7.18 (m, 2H), 7.05 (d, *J* = 7.7 Hz, 1H), 2.49 (s, 3H); ¹³C NMR (75 MHz, CDCl₃) δ 168.1, 151.3, 149.0, 141.0, 136.9, 135.1, 131.5, 130.9, 126.8, 125.9, 119.9, 112.0, 19.9; IR (cm⁻¹) ν 3244.83 (NH), 3068.05 (CH), 1676.47 (C=O), 1568.31, 1507.66, 1431.75, 1384.36, 786.16 (CCl).

N-(6-Bromopyridin-2-yl)-2-methylbenzamide (**45**) (**Exp1**)

Title compound prepared according to General Procedure A3 to give a white solid (78%), mp (cx) 80-83°C. LCMS (Finnigan) - rt 5.46 min 97% purity at 254 nm; [M+H]⁺ 291.0 (⁷⁹Br), 292.9 (⁸¹Br) m/z; ¹H NMR (300 MHz, CDCl₃) δ 8.33 (d, *J* = 8.1 Hz, 1H), 8.29 (s, 1H), 7.59 (t, *J* = 7.9 Hz, 1H), 7.49 (d, *J* = 7.7 Hz, 1H), 7.39-7.34 (m, 1H), 7.28-7.21 (m, 3H), 2.51 (s, 3H); ¹³C NMR (75 MHz, CDCl₃) δ 168.0, 151.6, 140.7, 139.3, 136.9, 135.0, 131.5, 130.9, 126.8, 125.9, 123.7, 112.4, 20.0; IR (cm⁻¹) ν 3249.19 (NH), 3067.96 (CH), 1675.90 (C=O), 1562.00, 1508.41, 1427.19, 1380.37, 783.59 (CBr).

2-Methyl-N-(6-phenylpyridin-2-yl)benzamide (46) (Exp1)

Title compound prepared according to General Procedure C to give a yellow solid (76%), mp (cx) 120-123°C. LCMS (Finnigan) - rt 5.80 min 93% purity at 254 nm; [M+H]⁺ 289.1 m/z; ¹H NMR (300 MHz, CDCl₃) δ 8.70 (s, 1H), 8.34 (d, *J* = 8.2 Hz, 1H), 7.92 (dd, *J* = 8.2 and 1.7 Hz, 2H), 7.83 (t, *J* = 8.0 Hz, 1H), 7.50-7.33 (m, 6H), 7.25-7.17 (m, 2H), 2.49 (s, 3H); ¹³C NMR (75 MHz, CDCl₃) δ 168.5, 151.4, 139.4, 136.7, 135.7, 131.3, 130.5, 129.5, 129.2, 128.7, 126.8, 126.7, 125.9, 116.6, 115.4, 112.4, 19.9; IR (cm⁻¹) ν 3172.10 (NH), 2927.06 (CH), 1676.38 (C=O), 1568.23, 1442.85, 1277.63, 737.10, 696.00.

2-Methyl-N-(6-(4-methylpent-1-yn-1-yl)pyridin-2-yl)benzamide (47) (Exp1)

Title compound prepared according to General Procedure D and was purified via HPLC to give a light yellow oil (17%). LCMS (Finnigan) - rt 6.01 min 99% purity at 254 nm; [M+H]⁺ 293.1 m/z; ¹H NMR (300 MHz, CDCl₃) δ 8.59 (s, 1H), 8.35 (d, *J* = 8.2 Hz, 1H), 7.73 (dt, *J* = 8.1 and 1.7 Hz, 1H), 7.55 (d, *J* = 7.6 Hz, 1H), 7.40-7.35 (m, 1H), 7.28-7.18 (m, 3H), 2.54 (s, 3H), 2.35 (dd, *J* = 6.6 and 1.8 Hz, 2H), 1.96 (sep, *J* = 6.6 Hz, 1H), 1.06 (dd, *J* = 6.7 and 1.9 Hz, 6H); ¹³C NMR (75 MHz, CDCl₃) δ 168.1, 151.1, 141.3, 139.0, 137.0, 135.2, 131.5, 130.8, 126.8, 125.9, 123.0, 113.1, 91.3, 80.1, 28.5, 28.0, 22.1, 20.0; IR (cm⁻¹) ν 3233.82 (NH), 2957.95-2870.03 (CH), 2229.05 (C≡C-), 1678.56 (C=O), 1567.78, 1443.31, 1381.44, 1277.82, 733.12.

(E)-2-Methyl-N-(6-(pent-1-en-1-yl)pyridin-2-yl)benzamide (48) (Exp1)

Title compound prepared according to General Procedure C and was purified via HPLC to give a colorless oil (6%). LCMS (Finnigan) - rt 5.89 min 99% purity at 254 nm; [M+H]⁺ 281.1 m/z; ¹H NMR (300 MHz, CDCl₃) δ 8.41 (br s, 1H), 8.21 (d, *J* = 8.1 Hz, 1H), 7.70 (t, *J* = 7.9 Hz, 1H), 7.56 (d, *J* = 7.3 Hz, 1H), 7.44 – 7.33 (m, 1H), 7.31 – 7.26 (m, 2H), 7.03 (d, *J* = 7.6 Hz, 1H), 6.82 – 6.66 (m, 1H), 6.38 (d, *J* = 15.7 Hz, 1H), 2.53 (s, 3H), 2.23 (q, *J* = 7.2 Hz, 2H), 1.55 (sex, *J* = 7.2 Hz, 2H), 0.96 (t, *J* = 7.4 Hz, 3H); IR (cm⁻¹) ν 3244.32 (NH), 2958.72-2871.57 (CH), 1678.57 (C=O), 1568.72, 1515.49, 1446.46, 1295.27, 734.67.

2-Methyl-N-(6-(phenylethynyl)pyridin-2-yl)benzamide (49) (Exp1)

Title compound prepared according to General Procedure D to give a brown oil (84%). LCMS (Finnigan) - rt 5.92 min 98% purity at 254 nm; [M+H]⁺ 313.1 m/z; ¹H NMR (300 MHz, CDCl₃) δ 8.51 (s, 1H), 8.40 (d, *J* = 8.4 Hz, 1H), 7.78 (t, *J* = 7.6 Hz, 1H), 7.62-7.55 (m, 3H), 7.42-7.27 (m, 7H), 2.55 (s, 3H); ¹³C NMR (75 MHz, CDCl₃) δ 168.2, 151.5, 141.3, 138.9, 136.9, 135.3, 132.1, 131.5, 130.8, 129.2, 128.4, 126.8, 126.0, 123.5, 121.9, 113.6, 89.8, 87.7, 20.0; IR (cm⁻¹) ν 3246.96 (NH), 3057.39 (CH), 2216.71 (C≡C-), 1734.69 (C=O), 1566.94, 1441.41, 1380.94, 1281.58, 1238.25.

N-(6-Hydroxypyridin-2-yl)-2-methylbenzamide (50) (Exp1)

Title compound prepared according to General Procedure A1 to give a white solid (61%), mp (cx) 150-152°C. LCMS (Finnigan) - rt 5.05 min 99% purity at 254 nm; [M+H]⁺ 228.9 m/z; ¹H NMR (300 MHz, CDCl₃) δ 8.30 – 8.16 (m, 1H), 7.72 – 7.57 (m, 1H), 7.55 – 7.42 (m, 1H), 7.40 – 7.28 (m, 2H), 6.67 – 6.55 (m, 2H), 5.62 (br s, 1H), 2.68 (d, *J* = 4.4 Hz, 3H); ¹³C NMR (75 MHz, CDCl₃): δ 165.3, 158.1, 156.9, 141.7, 140.9, 132.9, 131.9, 131.5, 128.1, 125.9, 106.3, 104.9, 21.9; IR (cm⁻¹) ν 3411.97 (OH), 3311.49 (NH), 3202.45 (CH), 1723.46 (C=O), 1481.78, 1439.12, 1246.53, 1201.43, 1042.04 (CO). Note: amide peak is missing from the NMR.

N-(6-Aminopyridin-2-yl)-2-methylbenzamide (51) (Exp1)

Title compound prepared according to General Procedure A1 to give a dull yellow crystalline solid (80%), mp 100-103°C. LCMS (Waters) - rt 4.42 min 98% purity at 254 nm; [M+H]⁺ 228.2 m/z; ¹H NMR (300 MHz, MeOD) δ 7.46-7.41 (m, 3H), 7.36-7.31 (m, 1H), 7.25-7.19 (m, 2H), 6.32-6.29 (m, 1H), 2.43 (s, 3H); ¹³C NMR (75 MHz, MeOD) δ 171.0, 160.1, 151.4, 140.9, 137.8, 137.2, 132.1, 131.4, 128.1, 127.0, 106.1, 104.0, 20.1; IR (cm⁻¹) ν 3443.92-3361.58 (NH), 2927.50 (CH), 1611.25 (C=O), 1536.42, 1449.39, 1303.18, 788.49, 733.65.

2-Methyl-N-phenylbenzamide (52) (Exp1)

Title compound prepared according to General Procedure A1 to give a brown solid (99%), mp (cx) 127-129°C. LCMS (Finnigan) - rt 5.14 min 99% purity at 254 nm; [M+H]⁺ 212.1 m/z; ¹H NMR (300 MHz, DMSO) δ 10.28 (s, 1H), 7.76 (d, *J* = 8.0 Hz, 2H), 7.47-7.28 (m, 6H), 7.14-7.07 (m, 1H), 2.39 (s, 3H); ¹³C NMR (75 MHz, DMSO) δ 167.8, 139.3, 137.3, 135.1, 130.5, 129.5, 129.0, 128.6, 127.1, 125.6, 123.5, 119.6, 119.56, 19.2; IR (cm⁻¹) ν 3233.87 (NH), 3018.10 (CH), 1634.78 (C=O), 1595.72, 1498.03, 1404.45, 841.91, 741.26.

N-(2-Cyanophenyl)-2-methylbenzamide (**53**) (Exp2)

Title compound prepared according to General Procedure A1 as a white solid (55%). HPLC – rt 6.68 min > 97% purity at 254 nm; LRMS [M+H]⁺ 237.2 m/z; HRMS [M+H]⁺ 237.1022 m/z, found 237.1022 m/z; ¹H NMR (400 MHz, DMSO) δ 10.58 (s, 1H), 7.88 (dd, *J* = 7.8, 1.3 Hz, 1H), 7.82 – 7.68 (m, 1H), 7.68 – 7.51 (m, 2H), 7.44 (td, *J* = 7.7, 1.2 Hz, 2H), 7.39 – 7.26 (m, 2H), 2.47 (s, 3H); ¹³C NMR (101 MHz, DMSO) δ 168.0, 140.1, 135.9, 135.8, 133.8, 133.1, 130.7, 130.1, 127.4, 126.5, 126.3, 125.7, 117.0, 109.0, 19.4.

N-(Isoxazol-3-yl)-2-methylbenzamide (**54**) (Exp2)

Title compound prepared according to General Procedure A6 as an off-white solid (61%). HPLC – rt 5.82 min > 99% purity at 254 nm; LRMS [M+H]⁺ 203.2 m/z; HRMS [M+H]⁺ 203.0815 m/z, found 203.0813 m/z; ¹H NMR (400 MHz, DMSO) δ 11.35 (s, 1H), 8.83 (d, *J* = 1.7 Hz, 1H), 7.52 – 7.45 (m, 1H), 7.40 (td, *J* = 7.5, 1.3 Hz, 1H), 7.33 – 7.27 (m, 2H), 7.02 (s, 1H), 2.38 (s, 3H); ¹³C NMR (101 MHz, DMSO) δ 167.9, 160.2, 157.8, 135.9, 135.4, 130.8, 130.4, 127.7, 125.7, 99.6, 19.5.

2-Methyl-N-(5-methylisoxazol-3-yl)benzamide (**55**) (Exp2)

Title compound prepared according to General Procedure A6 as a white solid (55%). HPLC – rt 6.34 min > 97% purity at 254 nm; LRMS [M+H]⁺ 217.1 m/z; HRMS [M+H]⁺ 217.0972 m/z, found 217.0972 m/z; ¹H NMR (400 MHz, CDCl₃) δ 8.61 (s, 1H), 7.53 (d, *J* = 7.9 Hz, 1H), 7.44 – 7.36 (m, 1H), 7.28 (d, *J* = 7.5 Hz, 2H), 6.85 (s, 1H), 2.51 (s, 3H), 2.42 (d, *J* = 0.8 Hz, 3H); ¹³C NMR (101 MHz, CDCl₃) δ 170.3, 167.4, 158.3, 137.4, 134.6, 131.7, 131.2, 127.1, 126.2, 96.6, 20.2, 12.8.

2-Methyl-N-(oxazol-2-yl)benzamide (**56**) (Exp2)

Title compound prepared according to General Procedure A6 as a pink solid (55%). HPLC –rt 4.735 min > 97% purity at 254 nm; LRMS [M+H]⁺ 203.1 m/z; HRMS [M+H]⁺ 203.0815 m/z, found 203.0815 m/z; ¹H NMR (400 MHz, CDCl₃) δ 7.49 (d, *J* = 7.5 Hz, 1H), 7.35 (ddd, *J* = 7.3, 6.8, 1.1 Hz, 2H), 7.27 – 7.20 (m, 2H), 6.18 (s, 1H), 2.45 (s, 3H); ¹³C NMR (101 MHz, CDCl₃) δ 167.0, 155.1, 137.3, 135.2, 134.9, 131.4, 131.0, 127.7, 125.9, 124.9, 20.0. Note: amide peak is missing from the NMR.

2-Methyl-N-(1H-pyrazol-3-yl)benzamide (**57**) (Exp2)

Title compound prepared according to General Procedure A4 as a white solid (48%). HPLC – rt 5.34 min > 97% purity at 254 nm; LRMS [M+Na]⁺ 224.2 m/z; ¹H NMR (400 MHz, DMSO) δ 8.09 (s, 1H), 7.39 (m, 2H), 7.32 – 7.22 (m, 2H), 6.01 (d, *J* = 3.0 Hz, 1H), 5.68 (m, 2H), 2.20 (s, 3H); ¹³C NMR (101 MHz, DMSO) δ 166.2, 159.5, 135.2, 134.6, 130.5, 130.0, 129.9, 127.8, 125.2, 102.7, 19.1.

2-Methyl-N-(4H-1,2,4-triazol-3-yl)benzamide (**58**) (Exp2)

Title compound prepared according to General Procedure A6 as white solid (32%). HPLC –rt 5.331 min > 83% purity at 254 nm; LRMS [M+H]⁺ 203.1 m/z; HRMS [M+H]⁺ 203.0927 m/z, found 203.0927 m/z; ¹H NMR (400 MHz, CDCl₃) δ 7.53 (dd, *J* = 8.0, 1.3 Hz, 1H), 7.46 (s, 1H), 7.43 (dd, *J* = 7.6, 1.4 Hz, 1H), 7.31 (ddd, *J* = 7.2, 3.4, 2.8 Hz, 2H), 6.69 (s, 2H), 2.39 (s, 3H); ¹³C NMR (101 MHz, CDCl₃) δ 170.7, 157.8, 151.3, 136.9, 132.5, 131.6, 131.0, 128.7, 125.5, 20.0.

2-Methyl-N-(1,3,4-thiadiazol-2-yl)benzamide (**59**) (Exp2)

Title compound prepared according to General Procedure A6 as a pale yellow solid (27%). HPLC – rt 5.55 min > 99% purity at 254 nm; LRMS [M+H]⁺ 220.1 m/z; HRMS [M+H]⁺ 220.0539 m/z found 220.0534 m/z; ¹H NMR (400 MHz, DMSO) δ 9.24 (s, 1H), 7.68 – 7.53 (m, 1H), 7.46 (td, *J* = 7.6, 1.3 Hz, 1H), 7.33 (ddd, *J* = 9.9, 5.3, 0.6 Hz, 2H), 2.40 (s, 3H); ¹³C NMR (101 MHz, DMSO) δ 167.5, 158.9, 149.0, 136.6, 133.5, 131.0, 130.9, 128.3, 125.8, 19.6.

2-Methyl-N-(1,2,4-thiadiazol-5-yl)benzamide (60) (Exp2)

Title compound prepared according to General Procedure **A1**, with one exception, the reaction was stirred at 30°C overnight, as a white solid (33%). HPLC –rt 6.23 min > 95% purity at 254 nm; LRMS [M+H]⁺ 220.1 m/z; HRMS [M+H]⁺ 220.0539 m/z, found 220.0539 m/z; ¹H NMR (400 MHz, CDCl₃) δ 7.80 (s, 1H), 7.64 (d, *J* = 7.7 Hz, 1H), 7.57 – 7.48 (m, 1H), 7.43 – 7.33 (m, 1H), 2.57 (s, 3H); ¹³C NMR (101 MHz, DMSO) δ 175.3, 168.7, 158.6, 137.1, 132.2, 131.5, 131.1, 128.5, 125.8, 19.7 Note: amide peak is missing from the NMR.

2-Methyl-N-(thiophen-3-yl)benzamide (61) (Exp2)

Title compound prepared according to General Procedure **A1**, with one exception, the reaction was stirred at 30°C overnight, as a brown oil (15%). HPLC –rt 6.92 min > 99% purity at 254 nm; LRMS [M+H]⁺ 218.1 m/z; HRMS [M+H]⁺ 218.0634 m/z, found 218.0634 m/z; ¹H NMR (400 MHz, DMSO) δ 10.69 (s, 1H), 7.71 (dd, *J* = 3.2, 1.3 Hz, 1H), 7.50 – 7.43 (m, 2H), 7.42 – 7.35 (m, 1H), 7.33 – 7.26 (m, 2H), 7.20 (dd, *J* = 5.2, 1.3 Hz, 1H), 2.38 (s, 3H); ¹³C NMR (101 MHz, DMSO) δ 166.8, 137.0, 136.7, 135.4, 130.6, 129.7, 127.2, 125.7, 124.6, 121.8, 109.1, 19.4.

N-2-Dimethyl-N-(pyridin-2-yl)benzamide (62) (Exp1)

Title compound prepared according to General Procedure B to give a yellow oil (16%). LCMS (Finnigan) - rt 4.61 min 87% purity at 254 nm; [M+H]⁺ 227.0 m/z; ¹H NMR (300 MHz, MeOD) δ 8.41 (d, *J* = 4.8 Hz, 1H), 7.65 (t, *J* = 7.6 Hz, 1H), 7.33-7.15 (m, 6H), 3.52 (s, 3H), 2.35 (s, 3H); ¹³C NMR (75 MHz, MeOD) δ 210.6, 157.0, 149.7, 139.4, 137.7, 131.6, 131.5, 130.5, 128.2, 126.5, 123.2, 122.9, 36.0, 19.4; IR (cm⁻¹) ν 3055.62 (NH), 2927.82-2855.38 (CH), 1656.79 (C=O), 1588.71, 1470.82, 1357.04, 777.20, 744.88.

N-(o-Tolyl)picolinamide (63) (Exp2)

Title compound prepared according to General Procedure A4 to give an off-white solid (64%). HPLC - rt 7.32 min > 99% purity at 254 nm; LRMS [M+H]⁺ 213.1 m/z; HRMS [M+H]⁺ 213.1022 m/z, found 213.1023 m/z; ¹H NMR (400 MHz, DMSO) δ 10.26 (s, 1H), 8.74 (ddd, *J* = 4.8, 1.6, 0.9 Hz, 1H), 8.17 (dt, *J* = 7.8, 1.1 Hz, 1H), 8.08 (td, *J* = 7.7, 1.7 Hz, 1H), 7.85 (dd, *J* = 7.9, 0.8 Hz, 1H), 7.69 (ddd, *J* = 7.5, 4.8, 1.3 Hz, 1H), 7.26 (dd, *J* = 18.1, 7.6 Hz, 2H), 7.12 (td, *J* = 7.4, 1.2 Hz, 1H), 2.31 (s, 3H); ¹³C NMR (101 MHz, DMSO) δ 161.9, 149.6, 148.6, 138.3, 136.0, 130.4, 130.3, 127.1, 126.3, 125.0, 123.1, 122.2, 17.5.

N-(Pyridin-2-yl)benzamide (64) (Exp1)

Title compound prepared according to General Procedure A1 to give a light brown crystalline solid (65%), mp 75-80°C. LCMS (Waters) - rt 4.80 min 98% purity at 254 nm; [M+H]⁺ 199.2 m/z; ¹H NMR (300 MHz, MeOD) δ 8.24-8.21 (m, 2H), 7.96-7.92 (m, 2H), 7.77-7.71 (m, 1H), 7.53-7.44 (m, 3H), 7.08-7.04 (m, 1H); ¹³C NMR (75 MHz, MeOD) δ 168.6, 153.3, 149.1, 139.6, 135.7, 133.3, 129.8, 128.7, 121.3, 116.3; IR (cm⁻¹) ν 3168.84 (NH), 1670.47 (C=O), 1576.65, 1524.78, 1429.87, 1301.87, 774.37.

2-Ethyl-N-(pyridin-2-yl)benzamide (65) (Exp1)

Title compound prepared according to General Procedure A1 to give a white solid (56%), mp (cx) 70-73°C. LCMS (Finnigan) –rt 4.62 min 99% purity at 254 nm; [M+H]⁺ 227.1 m/z; ¹H NMR (300 MHz, CDCl₃) δ 9.56 (s, 1H), 8.43 (d, *J* = 8.4 Hz, 1H), 7.78-7.76 (m, 2H), 7.55-7.50 (m, 1H), 7.41 (t, *J* = 7.6 Hz, 1H), 7.35-7.22 (m, 2H), 6.98-6.94 (m, 1H), 2.86 (q, *J* = 7.6 Hz, 2H), 1.25 (t, *J* = 7.6 Hz, 3H); ¹³C NMR (75 MHz, CDCl₃) δ 174.0, 155.8, 151.5, 145.9, 142.2, 140.1, 134.1, 133.1, 130.8, 129.6, 123.7, 118.5, 29.9, 18.8; IR (cm⁻¹) ν 3169.40 (NH), 2963.80 (CH), 1673.21 (C=O), 1578.01, 1524.31, 1432.59, 1302.77, 751.53.

2-Fluoro-N-(pyridin-2-yl)benzamide (66) (Exp2)

Title compound prepared according to General Procedure A4 as white needles (26%). HPLC –rt 4.60 min > 99% purity at 254 nm; LRMS [M+H]⁺ 217.2 m/z; HRMS [M+H]⁺ 217.0722 m/z, found 217.0782 m/z; ¹H NMR (400 MHz, DMSO) δ 10.77 (s, 1H), 8.37 (ddd, *J* = 4.9, 1.9, 0.9 Hz, 1H), 8.20 (d, *J* = 8.4 Hz, 1H), 7.86 (ddd, *J* = 8.4, 7.5, 1.9 Hz, 1H), 7.71 (td, *J* = 7.5, 1.7 Hz, 1H), 7.59 (dddd, *J* = 8.4, 7.2, 5.3, 1.8 Hz, 1H), 7.40 – 7.26 (m, 2H), 7.18 (ddd, *J* = 7.4, 4.9, 1.0 Hz, 1H); ¹³C NMR (101 MHz, CDCl₃) δ 160.6 (*J*_{C-F} = 247 Hz), 161.8 (*J*_{C-F} = 3 Hz), 151.4, 148.1, 138.6, 134.3 (*J*_{C-F} = 10 Hz), 132.2 (*J*_{C-F} = 2 Hz), 125.2 (*J*_{C-F} = 3 Hz), 121.3 (*J*_{C-F} = 11 Hz), 120.3, 116.5 (*J*_{C-F} = 24 Hz), 114.8.

2-Chloro-N-(pyridin-2-yl)benzamide (67) (Exp1)

2-Chlorobenzoyl chloride was obtained according to General Procedure A2 and utilised to give the title compound as a yellow crystalline solid (10%), mp 136-139°C. LCMS (Finnigan) - rt 4.52 min 98% purity at 254 nm; [M+H]⁺ 233.1 (³⁵Cl), 235.0 (³⁷Cl) m/z; ¹H NMR (300 MHz, CDCl₃) δ 9.62 (s, 1H), 8.40 (d, *J* = 8.4 Hz, 1H), 7.90 (d, *J* = 4.7 Hz, 1H), 7.78-7.73 (m, 1H), 7.69 (d, *J* = 7.8 Hz, 1H), 7.43-7.34 (m, 3H), 7.01-6.97 (m, 1H); ¹³C NMR (75 MHz, CDCl₃) δ 165.2, 151.4, 147.2, 138.8, 135.2, 131.7, 131.1, 130.4, 129.8, 127.2, 120.0, 114.7; IR (cm⁻¹) ν 2986.52 (NH), 1681.66 (C=O), 1577.76, 1533.84, 1433.28, 1310.49, 764.70-735.96 (CCl).

N-(Pyridin-2-yl)-2-(trifluoromethoxy)benzamide (68) (Exp1)

Title compound prepared according to General Procedure A1 as a yellow crystalline solid (50%), mp 75-80°C. LCMS (Waters) - rt 6.60 min 99% purity at 254 nm; [M+H]⁺ 283.2 m/z; ¹H NMR (300 MHz, MeOD) δ 8.25-8.18 (m, 2H), 7.84-7.74 (m, 2H), 7.64-7.59 (m, 1H), 7.50-7.40 (m, 2H), 7.13-7.09 (m, 1H); IR (cm⁻¹) ν 2981.00 (NH), 1681.78 (C=O), 1578.87, 1536.35, 1433.58, 1212.89, 1160.27.

N-(Pyridin-2-yl)-[1,1'-biphenyl]-2-carboxamide (69) (Exp1)

Title compound prepared according to General Procedure A1 as a white solid (27%), mp (cx) 169-171°C. LCMS (Finnigan) - rt 5.17 min 99% purity at 254 nm; [M+H]⁺ 275.1 m/z; ¹H NMR (300 MHz, CDCl₃) δ 9.69 (s, 1H), 8.28 (d, *J* = 8.4 Hz, 1H), 7.68-7.62 (m, 1H), 7.56-7.49 (m, 2 H), 7.40-7.33 (m, 8 H), 6.83-6.79 (m, 1H); ¹³C NMR (75 MHz, CDCl₃) δ 168.7, 151.7, 146.8, 140.2, 139.8, 138.7, 135.8, 130.5, 130.5, 128.6, 128.6, 128.5, 127.8, 127.4, 119.4, 114.3; IR (cm⁻¹) ν 2977.89 (NH), 1675.28 (C=O), 1578.05, 1527.26, 1460.08, 1306.14, 746.11.

3-Fluoro-2-methyl-N-(pyridin-2-yl)benzamide (70) (Exp2)

Title compound prepared according to General Procedure A4 as a pale-yellow solid (20%). LRMS [M+H]⁺ 231.1 m/z; HRMS [M+H]⁺ 231.0928 m/z, found 231.0930 m/z; ¹H NMR (400 MHz, DMSO) δ 10.87 (s, 1H), 8.35 (ddd, *J* = 4.9, 1.9, 0.8 Hz, 1H), 8.18 (d, *J* = 8.3 Hz, 1H), 7.88 – 7.78 (m, 1H), 7.38 – 7.22 (m, 3H), 7.16 (ddd, *J* = 7.3, 4.9, 1.0 Hz, 1H), 2.28 (d, *J* = 2.2 Hz, 3H); ¹³C NMR (101 MHz, DMSO) δ 167.2 (*J*_{C-F} = 4 Hz), 160.5 (*J*_{C-F} = 24 Hz), 151.8, 148.1, 138.9 (*J*_{C-F} = 4 Hz), 138.1, 127.3 (*J*_{C-F} = 8 Hz), 123.4 (*J*_{C-F} = 4 Hz), 122.3 (*J*_{C-F} = 8 Hz), 119.9, 116.4 (*J*_{C-F} = 23 Hz), 114.3, 11.3 (*J*_{C-F} = 5 Hz).

3-Fluoro-N-(pyridin-2-yl)benzamide (71) (Exp2)

Title compound prepared according to General Procedure A4 as a white solid (12%). HPLC – rt 4.63 min > 99% purity at 254 nm; LRMS [M+H]⁺ 217.1 m/z; HRMS [M+H]⁺ 217.0772 m/z, found 217.0769 m/z; ¹H NMR (400 MHz, DMSO) δ 10.90 (s, 1H), 8.48-8.31 (m, 1H), 8.18 (dd, *J* = 8.4, 0.8 Hz, 1H), 7.95-7.77 (m, 3H), 7.57 (td, *J* = 8.0, 5.9 Hz, 1H), 7.45 (td, *J* = 8.3, 2.2 Hz, 1H), 7.26-7.08 (m, 1H); ¹³C NMR (101 MHz, DMSO) δ 164.7, 161.9 (*J*_{C-F} = 245 Hz), 152.0, 148.0, 138.2, 136.4 (*J*_{C-F} = 6 Hz), 130.5 (*J*_{C-F} = 8 Hz), 124.2 (*J*_{C-F} = 3 Hz), 120.0, 118.8 (*J*_{C-F} = 21 Hz), 114.8 (*J*_{C-F} = 23 Hz), 114.8.

3-Chloro-2-methyl-N-(pyridin-2-yl)benzamide (72) (Exp2)

Title compound prepared according to General Procedure A4 as a white solid (71%). HPLC – rt 4.81 min > 95% purity at 254 nm; LRMS [M+H]⁺ 247.1 m/z; ¹H NMR (400 MHz, CDCl₃) δ 9.74 (s, 1H), 8.38 (d, *J* = 8.3 Hz, 1H), 7.78 – 7.69 (m, 1H), 7.60 (ddd, *J* = 5.0, 1.8, 0.7 Hz, 1H), 7.46 (dd, *J* = 8.0, 0.9 Hz, 1H), 7.37 (dd, *J* = 7.6, 0.9 Hz, 1H), 7.17 (t, *J* = 7.8 Hz, 1H), 6.93 (ddd, *J* = 7.3, 5.0, 0.9 Hz, 1H), 2.45 (s, 3H); ¹³C NMR (101 MHz, CDCl₃) δ 168.0, 151.7, 147.4, 138.9, 138.6, 136.1, 134.2, 131.2, 127.1, 125.4, 120.1, 114.6, 17.2.

3-Bromo-2-methyl-N-(pyridin-2-yl)benzamide (73) (Exp1)

Title compound prepared according to General Procedure A1 to give a brown oil (94%). LCMS (Waters) - rt 6.52 min 90% purity at 254 nm; [M+H]⁺ 291.1 (⁷⁹Br), 293.1 (⁸¹Br) m/z; ¹H NMR (300 MHz, MeOD) δ 8.34-8.23 (m, 1H), 8.02 (s, 1H), 7.91-7.85 (m, 1H), 7.74 (d, *J* = 7.8 Hz, 1H), 7.51-7.45 (m, 1H), 7.27-7.19 (m, 1H), 6.63-6.59 (m, 1H), 2.85 (s, 3H); ¹³C NMR (75 MHz, MeOD) δ 164.9, 149.3, 147.7, 139.6, 139.4, 135.3, 128.6, 127.4, 121.5, 116.1, 114.0, 110.4, 20.3; IR (cm⁻¹) ν 3170.77 (NH), 2916.38 (CH), 1671.98 (C=O), 1518.57, 1431.39, 1307.90, 1149.57, 839.03 (CBr).

2,3-Dimethyl-N-(pyridin-2-yl)benzamide (74) (Exp2)

Title compound prepared according to General procedure A4 as a white solid (69%). HPLC – rt 5.03 min > 95% purity at 254 nm; LRMS [M+H]⁺ 227.2 m/z; ¹H NMR (400 MHz, CDCl₃) δ 9.09 (s, 1H), 8.42 (d, *J* = 8.3 Hz, 1H), 7.89 (d, *J* = 4.7 Hz, 1H), 7.85 – 7.66 (m, 1H), 7.33 (t, *J* = 9.2 Hz, 1H), 7.30 – 7.20 (m, 1H), 7.16 (t, *J* = 7.6 Hz, 1H), 7.06 – 6.93 (m, 1H), 2.36 (s, 3H), 2.30 (s, 3H); ¹³C NMR (101 MHz, CDCl₃) δ 169.4, 151.7, 147.4, 138.9, 138.4, 136.9, 134.6, 131.9, 125.9, 124.6, 119.9, 114.4, 20.4, 16.5.

3-Methoxy-2-methyl-N-(pyridin-2-yl)benzamide (75) (Exp1)

Title compound prepared according to General Procedure A1 as a white crystalline solid (65%), mp 159-161°C. LCMS (Waters) - rt 5.50 min 99% purity at 254 nm; [M+H]⁺ 243.2 m/z; ¹H NMR (300 MHz, CDCl₃) δ 9.08 (s, 1H), 8.48 (d, *J* = 8.5 Hz, 1H), 8.13 (dd, *J* = 5.1, 0.1 Hz, 1H), 7.86-7.80 (m, 1H), 7.26 (d, *J* = 7.7 Hz, 1H), 7.16 (dd, *J* = 7.7 and 0.1 Hz, 1H), 7.09 (ddd, *J* = 7.3, 5.1 and 0.9 Hz, 1H), 6.96 (d, *J* = 7.5 Hz, 1H), 3.86 (s, 3H), 2.36 (s, 3H); ¹³C NMR (75 MHz, CDCl₃) δ 168.3, 158.2, 151.2, 145.8, 139.8, 136.9, 126.9, 125.5, 119.7, 118.9, 114.7, 112.4, 55.7, 12.6; IR (cm⁻¹) ν 3166.51 (NH), 2967.01 (CH), 1677.50 (C=O), 1578.38, 1433.79, 1315.33, 1257.99, 1071.71.

2-Methyl-N-(pyridin-2-yl)nicotinamide (76) (Exp1)

Title compound prepared according to General Procedure A1 as a brown crystalline solid (77%), mp 125-128°C. LCMS (Waters) - rt 1.17* + 1.67 min 98% purity at 254 nm; [M+H]⁺ 214.2 m/z; ¹H NMR (300 MHz, MeOD) δ 8.54 (d, *J* = 5.1 Hz, 1H), 8.31 (d, *J* = 4.2 Hz, 1H), 8.24 (d, *J* = 8.1 Hz, 1H), 7.96 (d, *J* = 7.5 Hz, 1H), 7.88-7.82 (m, 1H), 7.38 (t, *J* = 6.3 Hz, 1H), 7.20-7.15 (m, 1H), 2.69 (s, 3H); ¹³C NMR (75 MHz, MeOD, rotamers) δ 169.2, 157.0, 153.0, 150.9, 149.3, 147.3, 139.6, 139.6, 137.2, 133.7, 122.6, 121.6, 116.1, 114.0, 110.6, 22.5; IR (cm⁻¹) ν 3181.59 (NH), 2980.41 (CH), 1680.62 (C=O), 1571.18, 1433.22, 1306.46, 838.82, 778.24.

4-Fluoro-2-methyl-N-(pyridin-2-yl)benzamide (77) (Exp2)

Title compound prepared according to General Procedure A4 as an off-white solid (24%). HPLC rt 4.97 min > 99% purity at 254 nm; LRMS [M+H]⁺ 231.1 m/z; HRMS [M+H]⁺ 231.0928 m/z, found 231.0937 m/z; ¹H NMR (400 MHz, DMSO) δ 10.78 (s, 1H), 8.34 (ddd, *J* = 4.9, 1.9, 0.9 Hz, 1H), 8.18 (d, *J* = 8.4 Hz, 1H), 7.93 – 7.73 (m, 1H), 7.54 (dd, *J* = 8.5, 6.0 Hz, 1H), 7.27 – 7.13 (m, 2H), 7.13 – 7.05 (m, 1H), 2.40 (s, 3H); ¹³C NMR (101 MHz, DMSO) δ 167.6, 162.6 (*J*_{C-F} = 247 Hz), 152.1, 148.0, 139.1 (*J*_{C-F} = 9 Hz), 138.1, 132.9 (*J*_{C-F} = 3 Hz), 130.1 (*J*_{C-F} = 9 Hz), 119.8, 117.1 (*J*_{C-F} = 21 Hz), 114.3, 112.3 (*J*_{C-F} = 21 Hz), 19.5 (*J*_{C-F} = 1 Hz).

4-Chloro-2-methyl-N-(pyridin-2-yl)benzamide (78) (Exp2)

Title compound prepared according to General Procedure A4 as a pale-orange solid (50%). HPLC – rt 6.81 min > 99% purity at 254 nm; LRMS [M+H]⁺ 247.1 m/z; HRMS [M+H]⁺ 247.0633 m/z, found 247.0638 m/z; ¹H NMR (400 MHz, DMSO) δ 10.83 (s, 1H), 8.35 (ddd, *J* = 4.9, 1.9, 0.8 Hz, 1H), 8.17 (d, *J* = 8.3 Hz, 1H), 7.89 – 7.77 (m, 1H), 7.49 (d, *J* = 8.2 Hz, 1H), 7.40 (d, *J* = 1.7 Hz, 1H), 7.33 (dd, *J* = 8.2, 1.7 Hz, 1H), 7.16 (ddd, *J* = 7.3, 4.9, 1.0 Hz, 1H), 2.38 (s, 3H); ¹³C NMR (101 MHz, DMSO) δ 167.5, 151.9, 148.0, 138.1 (2C), 135.2, 134.2, 130.1, 129.4, 125.4, 119.9, 114.3, 19.1.

4-Bromo-2-methyl-N-(pyridin-2-yl)benzamide (79) (Exp1)

Title compound prepared according to General Procedure A1 as a white crystalline solid (62%), mp 140-143°C. LCMS (Waters) - rt 6.48 min 99% purity at 254 nm; [M+H]⁺ 291.1 (⁷⁹Br), 293.1 (⁸¹Br) m/z; ¹H NMR (300 MHz, MeOD) δ 8.36-8.34 (m, 1H), 8.23 (d, *J* = 8.4 Hz, 1H), 7.90-7.84 (m, 1H), 7.55-7.44 (m, 3H), 7.20 (ddd, *J* = 7.3, 4.9 and 0.9 Hz, 1H), 2.50 (s, 3H); ¹³C NMR (75 MHz, MeOD) δ 170.26, 153.05, 149.22, 139.85, 139.56, 136.72, 134.77, 130.03, 130.01, 125.29, 121.42, 116.08, 19.57; IR (cm⁻¹) ν 3246.82 (NH), 2983.89 (CH), 1682.62 (C=O), 1576.67, 1527.64, 1436.68, 1303.30, 784.87 (CBr).

4-Methoxy-2-methyl-N-(pyridin-2-yl)benzamide (80) (Exp1)

Title compound prepared according to General Procedure A1 as a white crystalline solid (47%), mp 144-146°C. LCMS (Waters) - rt 7.65 min 98% purity at 254 nm; [M+H]⁺ + CH₃CN] 284.2 m/z; ¹H NMR (300 MHz, DMSO) δ 8.35 (d, *J* = 8.6 Hz, 1H), 8.15 (d, *J* = 8.4 Hz, 1H), 7.88 (d, *J* = 0.8 Hz, 1H), 7.65 (t, *J* = 7.6 Hz, 1H), 7.52 (t, *J* = 7.8 Hz, 1H), 7.10-7.05 (m, 2H), 3.90 (s, 3H), 2.57 (s, 3H); ¹³C NMR (75 MHz, DMSO) δ 168.0, 161.7, 142.1, 132.7, 127.8, 127.3, 124.5, 122.1, 119.1, 116.7, 111.1, 109.6, 55.2, 21.8; IR (cm⁻¹) ν 2972.63 (NH), 2838.09 (CH), 1778.14 (C=O), 1606.55, 1446.95, 1226.11, 961.31, 750.28. Note: amide peak is missing from the NMR.

2,4-Dimethyl-N-(pyridin-2-yl)benzamide (81) (Exp2)

Title compound prepared according to General Procedure A1 as a pale-orange solid (25%). HPLC – rt 6.55 min > 97% purity at 254 nm; LRMS [M+H]⁺ 227.2 m/z; HRMS [M+H]⁺ 227.1179 m/z, found 227.1180 m/z; ¹H NMR (400 MHz, DMSO) δ 10.62 (s, 1H), 8.34 (ddd, *J* = 4.9, 1.9, 0.8 Hz, 1H), 8.18 (d, *J* = 8.4 Hz, 1H), 7.86 – 7.75 (m, 1H), 7.39 (d, *J* = 7.7 Hz, 1H), 7.16 – 7.01 (m, 3H), 2.37 (s, 3H), 2.31 (s, 3H); ¹³C NMR (101 MHz, DMSO) δ 168.4, 152.1, 147.9, 139.5, 138.0, 135.6, 133.4, 131.2, 127.7, 126.0, 119.6, 114.2, 20.8, 19.5.

(E)-2-methyl-4-(pent-1-en-1-yl)-N-(pyridin-2-yl)benzamide (82) (Exp2)

Title compound prepared according to General Procedure C using the boronic acid pinacol ester as a white solid (37%). LRMS [M+H]⁺ 281.2 m/z; HRMS [M+H]⁺ 281.1648 m/z, found 281.1656 m/z; ¹H NMR (400 MHz, DMSO) δ 10.68 (s, 1H), 8.43 – 8.27 (m, 1H), 8.19 (d, *J* = 8.4 Hz, 1H), 7.94 – 7.75 (m, 1H), 7.45 (t, *J* = 8.6 Hz, 1H), 7.28 (dd, *J* = 17.3, 9.3 Hz, 2H), 7.21 – 7.08 (m, 1H), 6.50 – 6.32 (m, 2H), 2.39 (s, 3H), 2.29 – 2.10 (m, 2H), 1.58 – 1.43 (m, 2H), 0.94 (q, *J* = 7.7 Hz, 3H); ¹³C NMR (101 MHz, DMSO) δ 168.3, 152.2, 148.0, 138.9, 138.1, 136.1, 134.5, 132.1, 129.1, 128.1, 128.0, 122.9, 119.7, 114.3, 34.6, 21.9, 19.6, 13.6.

3-Methyl-N-(pyridin-2-yl)-[1,1'-biphenyl]-4-carboxamide (83) (Exp2)

Title compound prepared according to General Procedure C as a white solid (20%). HPLC – rt 6.51 min > 99% purity at 254 nm; LRMS [M+H]⁺ 289.2 m/z; HRMS [M+H]⁺ 289.1335 m/z, found 289.1342 m/z; ¹H NMR (400 MHz, DMSO) δ 10.76 (d, *J* = 20.1 Hz, 2H), 8.37 (d, *J* = 3.8 Hz, 2H), 8.22 (d, *J* = 8.3 Hz, 2H), 7.84 (dt, *J* = 23.5, 8.1 Hz, 2H), 7.70 (t, *J* = 12.9 Hz, 4H), 7.67 – 7.55 (m, 6H), 7.50 (t, *J* = 7.6 Hz, 4H), 7.41 (t, *J* = 7.3 Hz, 2H), 7.16 (dd, *J* = 7.0, 5.1 Hz, 2H), 2.48 (s, 5H); ¹³C NMR (101 MHz, DMSO) δ 168.3, 152.1, 148.0, 141.5, 139.4, 138.1, 136.3, 135.3, 129.0, 128.8, 128.3, 127.9, 126.8, 123.8, 119.8, 114.3, 19.7.

5-Fluoro-2-methyl-N-(pyridin-2-yl)benzamide (84) (Exp2)

Title compound prepared according to General Procedure A4 as a beige solid (68%). HPLC – rt 5.00 min > 95% purity at 254 nm; LRMS [M+H]⁺ 231.2 m/z; ¹H NMR (400 MHz, CDCl₃) δ 9.01 (s, 1H), 8.38 (d, *J* = 8.4 Hz, 1H), 8.01 (d, *J* = 4.6 Hz, 1H), 7.84 – 7.68 (m, 1H), 7.34 – 7.16 (m, 2H), 7.15 – 6.95 (m, 1H), 2.47 (s, 3H); ¹³C NMR (101 MHz, CDCl₃) δ 161.94, 160.7 (*J*_{C-F} = 241.4 Hz), 159.5, 151.3, 147.3, 143.5, 138.9, 132.9 (*J*_{C-F} = 7.7 Hz), 120.1, 117.5 (*J*_{C-F} = 20.6 Hz), 114.0 (*J*_{C-F} = 22.9 Hz), 113.9, 19.2.

5-Bromo-2-methyl-N-(pyridin-2-yl)benzamide (85) (Exp1)

Title compound prepared according to General Procedure A1 as a brown oil (99%). LCMS (Waters) - rt 6.52 min 90% purity at 254 nm; [M+H]⁺ 291.1 m/z (⁷⁹Br), 293.1 m/z (⁸¹Br); ¹H NMR (300 MHz, MeOD) δ 8.37-8.22 (m, 1H), 8.02 (s, 1H), 7.91-7.85 (m, 1H), 7.58 (dd, *J* = 8.2 and 1.9 Hz, 1H), 7.52-7.46 (m, 1H), 7.29-7.20 (m, 1H), 6.65-6.60 (m, 1H), 2.85 (s, 3H); ¹³C NMR (75 MHz, MeOD) δ 164.9, 149.3, 147.6, 139.6, 139.4, 134.2, 133.9, 131.0, 121.5, 116.2, 114.0, 110.4, 19.3; IR (cm⁻¹) ν 3198.85 (NH), 2916.81 (CH), 1665.06 (C=O), 1601.46, 1433.05, 1385.58, 1305.23, 838.18 (CBr).

2,5-Dimethyl-N-(pyridin-2-yl)benzamide (86) (Exp2)

Title compound prepared according to General Procedure A4 as a beige solid (76%). HPLC – rt 5.25 min > 95% purity at 254 nm; LRMS [M+H]⁺ 227.1 m/z; ¹H NMR (400 MHz, CDCl₃) δ 9.39 (s, 1H), 8.42 (d, *J* = 8.4 Hz, 1H), 7.89 (ddd, *J* = 5.0, 1.8, 0.8 Hz, 1H), 7.75 (ddd, *J* = 8.5, 7.4, 1.9 Hz, 1H), 7.33 (d, *J* = 15.8 Hz, 1H), 7.20 – 7.11 (m, 2H), 7.01 – 6.95 (m, 1H), 2.47 (s, 3H), 2.31 (s, 3H); ¹³C NMR (101 MHz, CDCl₃) δ 168.9, 151.9, 147.4, 138.9, 135.8, 135.7, 133.6, 131.4, 131.3, 127.8, 119.8, 114.5, 20.9, 19.6.

5-Methoxy-2-methyl-N-(pyridin-2-yl)benzamide (87) (Exp2)

Title compound prepared according to General Procedure A4 as a beige solid (74%). HPLC – rt 4.89 min > 95% purity at 254 nm; LRMS [M+H]⁺ 243.0 m/z; ¹H NMR (400 MHz, CDCl₃) δ 9.86 (br s, 1H), 8.38 (d, *J* = 8.3 Hz, 1H), 7.70 (dd, *J* = 10.6, 5.0 Hz, 1H), 7.52 (t, *J* = 14.9 Hz, 1H), 7.12 (dd, *J* = 8.3, 2.8 Hz, 1H), 7.04 – 6.96 (m, 1H), 6.94 – 6.85 (m, 2H), 3.74 (d, *J* = 4.2 Hz, 3H), 2.39 (d, *J* = 2.7 Hz, 3H); ¹³C NMR (101 MHz, CDCl₃) δ 168.8, 157.7, 152.0, 147.6, 138.6, 137.1, 132.3, 127.9, 119.8, 116.5, 114.4, 112.3, 55.5, 18.9.

4-Methyl-N-(pyridin-2-yl)nicotinamide (88) (Exp1)

Title compound prepared according to General Procedure A1 as a brown crystalline solid (55%), mp 131-134°C. LCMS (Waters) - rt 1.78* + 2.22 min 90% purity at 254 nm; [M+H]⁺ 214.2 m/z; ¹H NMR (300 MHz, MeOD) δ 8.63 (s, 1H), 8.48 (d, *J* = 5.2 Hz, 1H), 8.31-8.29 (m, 1H), 8.21 (d, *J* = 8.4 Hz, 1H), 7.86-7.80 (m, 1H), 7.37 (d, *J* = 5.2 Hz, 1H), 7.16 (ddd, *J* = 7.3, 4.9 and 1.0 Hz, 1H), 2.51 (s, 3H); ¹³C NMR (75 MHz, MeOD, rotamers) δ 168.2, 153.0, 151.3, 149.3, 148.3, 148.3, 147.2, 139.7, 139.6, 134.5, 127.5, 121.6, 116.2, 114.0, 110.6, 19.4; IR (cm⁻¹) ν 3216.63 (NH), 2978.34 (CH), 1667.16 (C=O), 1593.45, 1432.27, 1316.31, 837.72, 774.98.

2,6-Dimethyl-N-(pyridin-2-yl)benzamide (89) (Exp2)

Title compound prepared according to General Procedure A4 as a beige solid (15%). HPLC - rt 5.24 min > 95% purity at 254 nm; LRMS [M+H]⁺ 227.1 m/z; ¹H NMR (400 MHz, CDCl₃) δ 9.73 (br s, 1H), 8.14 (d, *J* = 7.9 Hz, 1H), 7.75 (t, *J* = 7.3 Hz, 1H), 7.53 (m, 1H), 7.36 (d, *J* = 8.1 Hz, 1H), 7.26 - 7.10 (m, 1H), 7.04 - 6.96 (m, 1H), 6.94 - 6.85 (m, 1H), 3.74 (d, *J* = 4.2 Hz, 3H), 2.39 (d, *J* = 2.7 Hz, 3H); ¹³C NMR (101 MHz, CDCl₃) δ 167.3, 153.1, 150.9, 140.2, 137.6, 136.3 (2C), 129.1, 127.9 (2C), 117.9, 113.9, 19.3 (2C).

2-Fluoro-6-methyl-N-(pyridin-2-yl)benzamide (90) (Exp2)

Title compound prepared according to General Procedure A4 as a beige solid (21%). HPLC - rt 4.79 min > 95% purity at 254 nm; LRMS [M+H]⁺ 231.1 m/z; ¹H NMR (400 MHz, CDCl₃) δ 9.65 (br s, 1H), 8.23 (d, *J* = 7.7 Hz, 1H), 7.64 - 7.53 (m, 2H), 7.35 (d, *J* = 8.4 Hz, 1H), 7.24 - 7.10 (m, 2H), 6.99 (m, 1H), 2.43 (s, 3H); ¹³C NMR (101 MHz, CDCl₃) δ 165.3, 159.6 (*J*_{C-F} = 245.9 Hz), 153.0, 146.5, 139.6 (*J*_{C-F} = 7.8 Hz), 137.6, 131.6 (*J*_{C-F} = 9.4 Hz), 129.3 (*J*_{C-F} = 5.1 Hz), 124.3 (*J*_{C-F} = 20.3 Hz), 116.1, 114.6, 110.3 (*J*_{C-F} = 16.6 Hz), 19.3 (*J*_{C-F} = 4.6 Hz).

3-Methyl-N-(pyridin-2-yl)picolinamide (91) (Exp1)

Title compound prepared according to General Procedure A1 as a brown amorphous solid (75%). LCMS (Waters) - rt 5.55 min 99% purity at 254 nm; [M+H]⁺ 214.2 m/z; ¹H NMR (300 MHz, DMSO) δ 10.62 (s, 1H), 8.55 (d, *J* = 4.2 Hz, 1H), 8.36 (d, *J* = 4.5 Hz, 1H), 8.24 (d, *J* = 8.4 Hz, 1H), 7.88-7.83 (m, 2H), 7.58-7.54 (m, 1H), 7.18-7.14 (m, 1H), 2.67 (s, 3H); ¹³C NMR (75 MHz, DMSO, rotamers) δ 163.9, 151.0, 148.4, 146.7, 146.6, 146.0, 141.1, 138.4, 137.5, 134.9, 126.6, 119.9, 113.0, 113.0, 111.8, 108.4, 108.3, 19.7; IR (cm⁻¹) ν 3336.78 (NH), 2916.54 (CH), 1687.12 (C=O), 1514.17, 1435.56, 1303.62, 838.24, 777.85.

3,4-Difluoro-2-methyl-N-(pyridin-2-yl)benzamide (92) (Exp2)

Title compound prepared according to General Procedure A4 as a beige solid (51%). HPLC - rt 5.13 min > 95% purity at 254 nm; LRMS [M+H]⁺ 249.1 m/z; ¹H NMR (400 MHz, CDCl₃) δ 9.50 - 8.91 (m, 1H), 8.35 (d, *J* = 8.4 Hz, 1H), 8.09 - 7.83 (m, 1H), 7.84 - 7.69 (m, 1H), 7.36 - 7.21 (m, 1H), 7.13 - 6.95 (m, 2H), 2.45 (s, 3H); ¹³C NMR (101 MHz, CDCl₃) δ 166.4, 159.4 (*J*_{C-F} = 243.6 Hz), 151.4, 150.6, 147.5 (*J*_{C-F} = 242.5 Hz), 138.8 (*J*_{C-F} = 4.9 Hz), 133.1 (*J*_{C-F} = 13.4 Hz), 130.9, 127.8, 122.9 (*J*_{C-F} = 4.8 Hz), 122.8 (*J*_{C-F} = 5.2 Hz), 114.5 (*J*_{C-F} = 17.6 Hz), 11.7.

3-Fluoro-2-methyl-N-(4-methylpyridin-2-yl)benzamide (93) (Exp2)

Title compound prepared according to General Procedure A4 as a beige solid (49%). HPLC - rt 5.02 min > 95% purity at 254 nm; LRMS [M+H]⁺ 245.2 m/z; ¹H NMR (400 MHz, CDCl₃) δ 9.82 (s, 1H), 8.22 (s, 1H), 7.43 (d, *J* = 5.1 Hz, 1H), 7.26 (s, 1H), 7.19 (td, *J* = 7.8, 5.4 Hz, 1H), 7.15 - 7.08 (m, 1H), 6.74 (dd, *J* = 5.1, 0.7 Hz, 1H), 2.52 - 2.29 (m, 6H); ¹³C NMR (101 MHz, CDCl₃) δ 167.6 (*J*_{C-F} = 3.3 Hz), 161.6 (*J*_{C-F} = 246.1 Hz), 151.8, 150.3, 147.1, 138.7 (*J*_{C-F} = 4.2 Hz), 127.3 (*J*_{C-F} = 8.6 Hz), 123.9 (*J*_{C-F} = 18.3 Hz), 122.7 (*J*_{C-F} = 3.5 Hz), 121.2, 117.1 (*J*_{C-F} = 23.2 Hz), 115.0, 21.5, 11.6 (*J*_{C-F} = 5.0 Hz).

3,4-Difluoro-2-methyl-N-(4-methylpyridin-2-yl)benzamide (94) (Exp2)

Title compound prepared according to General Procedure A2 which was further purified by recrystallization with cyclohexane to give white needles (5%). HPLC - rt 5.32 min > 99% purity at 254 nm; LRMS [M+H]⁺ 263.1 m/z; HRMS [M+H]⁺ 263.0990 m/z, found, 263.0992 m/z; ¹H NMR (400 MHz, DMSO) δ 10.82 (s, 1H), 8.31 - 8.13 (m, 1H), 8.03 (s, 1H), 7.46 - 7.22 (m, 2H), 7.01 (ddd, *J* = 5.0, 1.4, 0.6 Hz, 1H), 2.35 (s, 3H), 2.33 (d, *J* = 2.6 Hz, 3H); ¹³C NMR (101 MHz, DMSO) δ 166.4 (*J*_{C-F} = 2 Hz), 151.9, 150.4 (*J*_{C-F} = 233 Hz), 149.0, 148.0 (*J*_{C-F} = 228 Hz), 134.2, 125.6 (*J*_{C-F} = 14 Hz), 124.1 (*J*_{C-F} = 14 Hz), 121.0, 114.7, 114.4 (*J*_{C-F} = 23 Hz), 20.9, 11.5 (*J*_{C-F} = 5 Hz).

N-(4-Chloropyridin-2-yl)-3-fluoro-2-methylbenzamide (**95**) (Exp2)

Title compound prepared according to General Procedure A4 as white needles (5%). HPLC – rt 7.12 min > 97% purity at 254 nm; LRMS [M+H]⁺ 265.1 m/z; HRMS [M+H]⁺ 265.0539 m/z, found 265.0545 m/z; ¹H NMR (400 MHz, DMSO) δ 11.18 (s, 1H), 8.35 (d, *J* = 5.4 Hz, 1H), 8.29 (d, *J* = 1.7 Hz, 1H), 7.42 – 7.20 (m, 4H), 2.27 (d, *J* = 2.1 Hz, 3H); ¹³C NMR (101 MHz, DMSO) δ 167.6 (*J*_{C-F} = 3 Hz), 160.5 (*J*_{C-F} = 244 Hz), 153.0, 149.5, 144.0, 138.4 (*J*_{C-F} = 5 Hz), 127.3 (*J*_{C-F} = 8 Hz), 123.6 (*J*_{C-F} = 3 Hz), 122.5 (*J*_{C-F} = 18 Hz), 120.0, 116.6 (*J*_{C-F} = 23 Hz), 113.8, 11.3 (*J*_{C-F} = 5 Hz).

N-(4-Chloropyridin-2-yl)-3,4-difluoro-2-methylbenzamide (**96**) (Exp2)

Title compound prepared according to General Procedure A2 with further purification involving dissolution of the crude material in ethyl acetate and washing with saturated sodium bicarbonate solution before a recrystallization from cyclohexane to give the title compound as white needles (5%). HPLC – rt 7.76 min > 95% purity at 254 nm; LRMS [M+H]⁺ 283.1 m/z; HRMS [M+H]⁺ 283.0444 m/z, found 283.0446 m/z; ¹H NMR (400 MHz, DMSO) δ 11.21 (s, 1H), 8.36 (d, *J* = 5.4 Hz, 1H), 8.28 (d, *J* = 1.4 Hz, 1H), 7.47 – 7.23 (m, 3H), 2.33 (d, *J* = 2.4 Hz, 3H); ¹³C NMR (101 MHz, DMSO) δ 166.8 (*J*_{C-F} = 3 Hz), 153.0, 151.8 (*J*_{C-F} = 243 Hz), 149.6, 148.0 (*J*_{C-F} = 238 Hz), 144.0, 133.6 (*J*_{C-F} = 2 Hz), 125.8 (*J*_{C-F} = 14 Hz), 124.4 (*J*_{C-F} = 8 Hz), 120.0, 114.4 (*J*_{C-F} = 17 Hz), 113.8, 11.5 (*J*_{C-F} = 4 Hz).

3-Fluoro-*N*-(4-fluoropyridin-2-yl)-2-methylbenzamide (**97**) (Exp2)

Title compound prepared according to General Procedure A4 as a white solid (9%). HPLC – rt 6.81 min > 99% purity at 254 nm; LRMS [M+H]⁺ 249.1 m/z; HRMS [M+H]⁺ 249.0834 m/z, found 249.0832 m/z; ¹H NMR (400 MHz, DMSO) δ 11.23 (s, 1H), 8.41 (dd, *J* = 9.3, 5.7 Hz, 1H), 8.04 (dd, *J* = 11.9, 2.4 Hz, 1H), 7.44 – 7.23 (m, 3H), 7.13 (ddd, *J* = 8.2, 5.7, 2.4 Hz, 1H), 2.28 (d, *J* = 2.2 Hz, 3H); ¹³C NMR (101 MHz, DMSO) δ 168.9 (*J*_{C-F} = 259 Hz), 167.6, 160.5 (*J*_{C-F} = 244 Hz), 154.1 (*J*_{C-F} = 12 Hz), 150.8 (*J*_{C-F} = 9 Hz), 138.5 (*J*_{C-F} = 4 Hz), 127.3 (*J*_{C-F} = 9 Hz), 123.6 (*J*_{C-F} = 23 Hz), 122.5 (*J*_{C-F} = 18 Hz), 116.7 (*J*_{C-F} = 23 Hz), 107.9 (*J*_{C-F} = 18 Hz), 101.4 (*J*_{C-F} = 23 Hz), 11.3 (*J*_{C-F} = 5 Hz).

3,4-Difluoro-*N*-(4-fluoropyridin-2-yl)-2-methylbenzamide (**98**) (Exp2)

Title compound prepared according to General Procedure A2 with further purification involving dissolution of the crude material in ethyl acetate and washing with saturated sodium bicarbonate solution before a recrystallization from cyclohexane to give the title compound as white needles (7%). HPLC – rt 7.07 min > 99% purity at 254 nm; LRMS [M+H]⁺ 267.1 m/z; HRMS [M+H]⁺ 267.0740 m/z, found 267.0742 m/z; ¹H NMR (400 MHz, DMSO) δ 11.25 (s, 1H), 8.41 (dd, *J* = 9.2, 5.7 Hz, 1H), 8.02 (dd, *J* = 11.9, 2.4 Hz, 1H), 7.48 – 7.26 (m, 2H), 7.13 (ddd, *J* = 8.2, 5.7, 2.4 Hz, 1H), 2.34 (d, *J* = 2.6 Hz, 3H); ¹³C NMR (101 MHz, DMSO) δ 170.2, 167.6, 166.8 (*J*_{C-F} = 3 Hz), 152.9 (*J*_{C-F} = 237 Hz), 150.8 (*J*_{C-F} = 8 Hz), 148.1 (*J*_{C-F} = 245 Hz), 133.6, 125.8 (*J*_{C-F} = 14 Hz), 124.4 (*J*_{C-F} = 8 Hz), 114.4 (*J*_{C-F} = 17 Hz), 108.0 (*J*_{C-F} = 17 Hz), 101.4 (*J*_{C-F} = 23 Hz), 11.5 (*J*_{C-F} = 4 Hz).

3-Fluoro-*N*-(5-methoxypyridin-2-yl)-2-methylbenzamide (**99**) (Exp2)

Title compound prepared according to General Procedure A4 as a beige solid (43%). HPLC – rt 4.96 min > 95% purity at 254 nm; LRMS [M+H]⁺ 261.2 m/z; ¹H NMR (400 MHz, CDCl₃) δ 8.95 (s, 1H), 8.33 (d, *J* = 9.0 Hz, 1H), 7.67 (d, *J* = 2.7 Hz, 1H), 7.36 – 7.28 (m, 2H), 7.25 – 7.19 (m, 1H), 7.18 – 7.07 (m, 1H), 3.82 (s, 3H), 2.40 (d, *J* = 2.2 Hz, 3H); ¹³C NMR (101 MHz, CDCl₃) δ 166.7 (*J*_{C-F} = 3.3 Hz), 161.5 (*J*_{C-F} = 246.0 Hz), 153.0, 144.9, 138.2, 133.5, 127.3 (*J*_{C-F} = 8.6 Hz), 124.1, 123.9, 122.5 (*J*_{C-F} = 3.5 Hz), 117.2 (*J*_{C-F} = 23.2 Hz), 114.9, 56.0, 11.5 (*J*_{C-F} = 5.2 Hz).

4-Fluoro-*N*-(5-methoxypyridin-2-yl)-2-methylbenzamide (**100**) (Exp2)

Title compound prepared according to General Procedure A2 as a beige solid (30%). HPLC – rt 5.75 min > 99% purity at 254 nm; LRMS [M+H]⁺ 261.1 m/z; HRMS [M+H]⁺ 261.1034 m/z, found 261.1040 m/z; ¹H NMR (400 MHz, DMSO) δ 10.65 (s, 1H), 8.09 (dd, *J* = 11.0, 6.0 Hz, 2H), 7.50 (ddd, *J* = 12.1, 8.7, 4.6 Hz, 2H), 7.22 – 6.99 (m, 2H), 3.83 (s, 3H), 2.40 (s, 3H); ¹³C NMR (101 MHz, DMSO) δ 167.0, 162.4 (*J*_{C-F} = 247 Hz), 152.4, 145.5, 139.0 (*J*_{C-F} = 9 Hz), 134.4, 133.1, 129.9 (*J*_{C-F} = 9 Hz), 123.1, 117.0 (*J*_{C-F} = 21 Hz), 115.1, 112.2 (*J*_{C-F} = 22 Hz), 55.8, 19.5.

References

- (24) Bevan, C. D.; Lloyd, R. S. A High-Throughput Screening Method for the Determination of Aqueous Drug Solubility Using Laser Nephelometry in Microtiter Plates. *Anal. Chem.* **2000**, *72*, 1781-1787.
- (25) Lombardo, F.; Shalaeva, M. Y.; Tupper, K. A.; Gao, F. ElogDoct: A Tool for Lipophilicity Determination in Drug Discovery. 2. Basic and Neutral Compounds. *Journal of Medicinal Chemistry* **2001**, *44*, 2490-2497.
- (26) Valko, K.; Nunhuck, S.; Bevan, C.; Abraham, M. H.; Reynolds, D. P. Fast gradient HPLC method to determine compounds binding to human serum albumin. Relationships with octanol/water and immobilized artificial membrane lipophilicity. *J. Pharm. Sci.* **2003**, *92*, 2236-2248.
- (27) Obach, R. S. Prediction of Human Clearance of Twenty-Nine Drugs from Hepatic Microsomal Intrinsic Clearance Data: An Examination of *In Vitro* Half-Life Approach and Nonspecific Binding to Microsomes. *Drug Metab Dispos* **1999**, *27*, 1350-1359.
- (28) Davies, B.; Morris, T. Physiological Parameters in Laboratory Animals and Humans. *Pharmaceutical Research* **1993**, *10*, 1093-1095.
- (29) Desjardins, R. E.; Canfield, C. J.; Haynes, J. D.; Chulay, J. D. Quantitative assessment of antimalarial activity *in vitro* by a semiautomated microdilution technique. *Antimicrob. Agents Chemother.* **1979**, *16*, 710-718.
- (30) Matile, H.; Pink, J. R. L. *Plasmodium falciparum* malaria parasite cultures and their use in immunology. In *Immunological Methods*, Lefkovits, I.; Pernis, B., Eds. Academic Press: San Diego, 1990.
- (31) Ponnudurai, T.; Leeuwenberg, A. D.; Meuwissen, J. H. Chloroquine sensitivity of isolates of *Plasmodium falciparum* adapted to *in vitro* culture. *Trop. Geogr. Med.* **1981**, *33*, 50-54.
- (32) Huber, W.; Koella, J. C. A comparison of three methods of estimating EC₅₀ in studies of drug resistance of malaria parasites. *Acta Trop.* **1993**, *55*, 257-261.
- (33) Cunningham, M. L.; Fairlamb, A. H. Trypanothione reductase from *Leishmania donovani*. Purification, characterisation and inhibition by trivalent antimonials. *Eur. J. Biochem.* **1995**, *230*, 460-468.
- (34) Mikus, J.; Steverding, D. A simple colorimetric method to screen drug cytotoxicity against *Leishmania* using the dye Alamar Blue®. *Parasitol Int* **2000**, *48*, 265-269.
- (35) Buckner, F. S.; Verlinde, C. L.; La Famme, A. C.; CVan Voorhis, W. C. Efficient technique for screening drugs for activity against *Trypanosoma cruzi* using parasites expressing beta-galactosidase. *Antimicrob. Agents Chemother.* **1996**, *40*, 2592-2597.
- (36) Baltz, T.; Baltz, D.; Giroud, C.; Crockett, J. Cultivation in a semi-defined medium of animal infective forms of *Trypanosoma brucei*, *T. equiperdum*, *T. evansi*, *T. rhodesiense* and *T. gambiense*. *EMBO J.* **1985**, *4*, 1273-1277.
- (37) Rüz, B.; Iten, M.; Grether-Bühler, Y.; Kaminsky, R.; Brun, R. The Alamar Blue® assay to determine drug sensitivity of African trypanosomes (*T.b. rhodesiense* and *T.b. gambiense*) *in vitro*. *Acta Trop.* **1997**, *68*, 139-147.
- (38) Page, B.; Page, M.; Noel, C. A new fluorometric assay for cytotoxicity measurements *in vitro*. *Int. J. Oncol.* **1993**, *3*, 473-476.
- (39) Ahmed, S. A.; Gogal, R. M.; Walsh, J. E. A new rapid and simple non-radioactive assay to monitor and determine the proliferation of lymphocytes: an alternative to [³H]thymidine incorporation assay. *J. Immunol. Methods* **1994**, *170*, 211-224.
- (40) Sykes, M. L.; Avery, V. M. Development of an Alamar Blue™ Viability Assay in 384-Well Format for High Throughput Whole Cell Screening of *Trypanosoma brucei brucei* Bloodstream Form Strain 427. *Am. J. Trop. Med. Hyg.* **2009**, *81*, 665-674.
- (41) Hirumi, H.; Hirumi, K. Continuous cultivation of *Trypanosoma brucei* blood stream forms in a medium containing a low concentration of serum protein without feeder cell layers. *J. Parasitol.* **1989**, *75*, 985-989.
- (42) Zhou, Y. Substituted imidazolidinones and related compounds as chemokine receptor binding compounds and their preparation, pharmaceutical compositions and the use in the treatment of infection of target cells by human immunodeficiency virus. *PCT Int. Appl.* **2007**.